PHILIPPINES-AUSTRALIA MARINE SEISMIC SURVEY PROJECT

GEOLOGY AND PETROLEUM POTENTIAL OF RAGAY GULF, TAYABAS BAY, NORTHEAST PALAWAN SHELF AND CUYO PLATFORM, PHILIPPINES

VOLUME 1: TEXT

AGSO RECORD 1994/41

PREPARED BY:
AUSTRALIAN GEOLOGICAL SURVEY ORGANISATION
PHILIPPINE DEPARTMENT OF ENERGY

FUNDED BY:
AUSTRALIAN INTERNATIONAL DEVELOPMENT ASSISTANCE BUREAU

1994

FOREWORD

AN INVITATION TO INVEST IN THE PHILIPPINE EXPLORATION INDUSTRY

As the country moves towards economic industrialisation, the necessity of being energy self-reliant becomes all the more crucial. We must tap all our indigenous resources that will sustain the growth and progress of our economy.

In the long-forgotten past, the idea of our country as self-sufficient in its petroleum requirements had been dismissed as wishful thinking. However, recent developments have proven that this lofty goal is not as remote as it seemed in the past.

This report which is the consummation of the Philippines - Australia Marine Seismic Survey Project funded by the Australian International Development Assistance Bureau, through the cooperative efforts of the Department of Energy and the Australian Geological Survey Organisation, endeavours to explore the frontier areas of the country using new ideas and concepts together with cutting-edge technology. The Project has covered four (4) areas, namely, Ragay Gulf, Tayabas Bay, Northeast Palawan Shelf and Cuyo Platform. The seismic, geochemical, and geological data generated by the Project has spawned new exploration plays contributing to the prospectivity of the areas.

With this report, we invite the private sector to actively participate in the exploration of these frontier areas. Together, our efforts will provide the needed impetus to the continued development of the Philippine petroleum industry.

DELFIN L. LAZARO
Secretary of Energy

CONTENTS OF VOLUMES

VOLUME 1 **TEXT**

Executive Summary
Acknowledgements
Part 1: Geology and Petroleum Potential of Ragay Gulf
Part 2: Geology and Petroleum Potential of Tayabas Bay
Part 3: Geology and Petroleum Potential of Northeast Palawan Shelf
Part 4: Geology and Petroleum Potential of Cuyo Platform

VOLUME 2 **APPENDICES**

Appendix 1: Evaluation of Reservoirs, Bondoc Peninsula
Appendix 2: Geohistory Modelling of Ragay Gulf and Tayabas Bay
Appendix 3: Geohistory Modelling of Northeast Palawan Shelf and Cuyo Platform
Appendix 4: New Hydrocarbon Geochemistry of Oil and Gas Seeps from Bondoc and Bicol Peninsulas, Southeast Luzon
Appendix 5: Direct Hydrocarbon Detection in Bottom Waters with Application to Offshore Petroleum Exploration in the Philippines
Appendix 6: Palynological Analysis of San Francisco-1 and Katumbo Creek-1 Wells, Southeast Luzon

VOLUME 3 **MAPS**

Maps R-1 to R-11: Ragay Gulf
Maps T-1 to T-5: Tayabas Bay
Maps P-1 to P-15: Northeast Palawan Shelf
Maps C-1 to C-4: Cuyo Platform

VOLUME 4 **PLATES**

Plates R-1 to R-13: Ragay Gulf
Plates T-1 to T-6: Tayabas Bay
Plates P-1 to P-8: Northeast Palawan Shelf
Plates C-1 to C-3: Cuyo Platform

ISSN 1039-0073
ISBN 0 642 21253 8

EXECUTIVE SUMMARY

The Philippines is currently energy deficient and there is a continuing dependence on imported petroleum for many industries, especially in the transport sector. The Government of the Philippines has therefore decided to actively promote oil and gas exploration in the country, encouraged by recent studies and exploration results suggesting that potential oil and gas reserves exist in offshore Philippine basins. The Department of Energy (DOE) has identified tectonic complexity and lack of geoscientific information as contributing to the low level of petroleum exploration in the majority of the thirteen identified offshore basins. The Government has therefore requested Australian assistance in the form of a comprehensive offshore seismic survey in selected, potentially oil-bearing, basins.

The survey project undertaken from September 1991 to June 1994 had two main objectives:

- to upgrade the knowledge of petroleum prospectivity of selected areas in the Philippines and to promote potential opportunities for future Philippines - Australia joint venture exploration; and
- to assist the Philippines Government in acquiring the skills necessary to acquire and interpret seismic data and other petroleum-related information, and use these to focus future petroleum exploration in Philippine waters.

The project was funded by the Australian International Development Assistance Bureau (AIDAB), and involved staff of the Australian Geological Survey Organisation (AGSO) working in co-operation with staff from the Philippine DOE. Data were acquired using the Australian geoscientific research vessel, *Rig Seismic,* during a forty-five day cruise from late March to early May, 1992. The survey resulted in 2750 line km of new seismic and magnetic data, and nearly 5000 km of geochemical, gravity and bathymetric profiling data. The work was undertaken in four areas: Ragay Gulf and Tayabas Bay (offshore southeast Luzon), and the Northeast Palawan Shelf and Cuyo Platform (northeast of Palawan).

Interpretation of the survey data has indicated that the survey was successful in its main objectives. The new seismic shooting achieved penetration to depths greater than those previously reached, thus allowing improved definition of key horizons and structural features. In the Ragay Gulf, major fault systems controlling the distribution of hydrocarbon traps are now better understood and have been mapped more accurately. An important limestone formation containing possible petroleum source and reservoir rocks, the Late Oligocene to Early Miocene Panaon Limestone, was shown to be much more extensive than was thought of before. The formation also included reefal deposits which may provide attractive targets for future exploration by oil companies. Three separate source 'kitchens' where petroleum source rocks are sufficiently deeply buried for oil and gas generation to be occurring, were identified in the Ragay Gulf area. Structural leads containing potentially commercial quantities of hydrocarbons were identified in eight areas of the basin. These were mapped with sufficient accuracy to estimate likely reserves.

Offshore geochemical sampling involved the use of a towed 'fish' to measure the concentration of hydrocarbons dissolved in sea-water a few metres above the seabed. Hydrocarbons collected in this way were analysed to determine whether they are 'thermogenic' hydrocarbons such as oil, gas or condensate escaping from sub-surface rocks, or are the product of recent biological activity in the water column or bottom

oozes. The analysis indicated that most of the hydrocarbons collected in the Ragay Gulf are of fossil origin, thus demonstrating that source rocks for petroleum generation are abundantly present in the sub-surface. Zones with anomalously high hydrocarbon concentration mark the sites where hydrocarbons are escaping from the seabed. By examining these zones in relation to the seismic data, it was possible to identify faults providing pathways for hydrocarbons to migrate from deeply buried source rocks into reservoir rocks, and structural traps where hydrocarbons are likely to be accumulating.

Seismic interpretation of the Tayabas Bay area has resulted in a new tectonic model which gives a better understanding of the structurally complex basin. Geochemistry data, both offshore and onshore, have confirmed the presence of mature source rocks from which generated hydrocarbons are currently migrating to the surface. The present study suggests that there is a prolific source rock in the Middle Miocene Vigo Formation and/or the Late Oligocene to Early Miocene Panaon Limestone, and that oil and gas generation is occurring in the Bondoc Sub-basin, which is roughly coincident with the southern part of the Bondoc Peninsula. Several play types are envisaged in which hydrocarbons could be sourced from a 'kitchen' area in the Bondoc Sub-basin.

Two groups of reservoirs have been identified or proposed. The older group consists of shelf carbonates of the Panaon Formation beneath the shales of the Vigo Formation on the Marinduque Platform. The second group consists of early Middle Miocene carbonates and basin-floor clastics near the base of the Vigo Formation. Traps were formed when Late Oligocene to Early Miocene carbonate reefs and shelf deposits of the Panaon Limestone were buried by the Middle Miocene clastics of the Vigo Formation. A later set of traps was formed (and sometimes superimposed) by intense deformation associated with movement on the Philippine strike-slip fault system which has continued from the Late Pliocene up to the present .

Seismic interpretation in the Northeast Palawan Shelf was tied to three exploration wells drilled between 1979 and 1981. The best potential reservoirs encountered in wells are well developed intervals of clean sandstone within a Middle Miocene prograding sequence. This sequence subcrops a Middle Miocene unconformity under the outer shelf and slope along most of the northeast Palawan margin. Possible reef buildups on the edge of the Middle Miocene paleo-shelf may also have good potential as reservoirs. No source rocks were penetrated in wells, but their existence in the basin is confirmed by the presence of a gas accumulation and dead oil traces in a 1000 metre thick section of non-reservoir conglomerates in the Dumaran-1 well.

Three lead areas and the Dumaran gas accumulation were evaluated for potential hydrocarbon reserves. The leads are closed structural highs at Middle Miocene unconformity and Top Cretaceous levels. The Dumaran gas accumulation is not structurally closed and must be limited to the northwest and northeast by intra-formational permeability barriers. The accumulation may be of significant size if it encompasses good reservoir sandstones of the Middle Miocene prograding sequence three kilometres to the southeast of the well. This sequence is interposed between the well and a probable source 'kitchen' area to the southeast. The accumulation may include oil as well as gas if dead oil traces, observed over a 300 metre interval in the well, are remnants of an oil column displaced down dip by gas.

Seismic data from the Cuyo Platform show deeper horizons which were not mapped from previous seismic surveys. The new interpretation was used to infer the possible existence of source and reservoir rocks deeper than the Middle Miocene unconformity. With a

relatively wide seismic line spacing, only one lead was delineated sufficiently for hydrocarbon evaluation. It is an anticlinal structure bounded by normal faults. Potential reservoir rocks may be present in the form of sandstones in the Jurassic interval, and calcarenites in the Oligocene to Early Miocene interval. Offshore geochemical sampling data, and reports of onshore hydrocarbon seepages and shows in exploration wells, were used to evaluate the source potential of the area. Possible source rocks are believed to exist in carbonaceous clastic sequences both in the Jurassic and Oligocene-Early Miocene intervals. Weak geochemical anomalies are coincident with mapped structural highs.

ACKNOWLEDGEMENTS

The project is supported under an Australian aid development fund from AIDAB. AGSO and DOE would like to express our thanks to AIDAB, the National Economic and Development Authority of the Philippines, the Australian Embassy in Manila and the Philippine Embassy in Canberra for their administrative support through the life of the project.

We would like to express our sincere thanks to Attorney W. de la Paz, the former Philippine Presidential Adviser on Energy Affairs, and Dr. D. Falvey, the Associate Director of AGSO for their initiation of the project and unceasing support throughout all stages of this project. The enthusiasm, skill, and cooperation of the masters and crew of the *Rig Seismic* and *African Queen* are gratefully acknowledged. We would also like to thank our colleaques in AGSO; this include Mr. F. Brassil and his staff for data processing, Mr. J. Creasey and his staff for Landsat image data processing, Dr. R. Summons and his staff for geochemistry data analysis, and Mr. L Hollands and his staff for figure preparation.

The project involved a number of private companyies and consultants for various activities. Mr. V. Robinson of Robertson Australia Pty. Ltd., Mr. I. Hawkshaw of Bellbird Geophysical Consultancy, and Mr. J. Allender helped to monitor the progress of the project. Project Design Management Pty. Ltd. assisted in the initial project design, and Supply Oil Field in the Philippines arranged the ship logistics during the data acquisition phase. Petrosys Pty. Ltd. provided the hardware, software and training for the Petrosys seismic mapping and database system, Encom Technology Pty. Ltd. recovered the deteriorating World Bank seismic tapes, and Petroconsultants Pty. Ltd. scanned the CITCO seismic sections. Kestrel Information Management Pty. Ltd. managed the data copying, and Corporate Electronic Publishing prepared the montages. Professor P. Davies of University of Sydney and Dr. M. Etheridge of Etheridge & Henley Geoscience Consultants provided training in Manila. We would like to extend our thanks to all these groups and individuals.

We greatly appreciate the valuable technical inputs, and workshop participation of the 34 Australian and Philippine consultative oil companies.

To replace

Volume 1

Page xi

ACKNOWLEDGEMENTS

The project is supported under an Australian aid development fund from AIDAB. AGSO and DOE would like to express our thanks to AIDAB, the National Economic and Development Authority of the Philippines, the Australian Embassy in Manila and the Philippine Embassy in Canberra for their administrative support through the life of the project.

The enthusiasm, skill, and cooperation of the masters and crew of the *Rig Seismic* and *African Queen* are gratefully acknowledged. We would also like to thank our colleaques in AGSO; this include Mr. F. Brassil and his staff for data processing, Mr. J. Creasey and his staff for Landsat image data processing, Dr. R. Summons and his staff for geochemistry data analysis, and Mr. L Hollands and his staff for figure preparation.

The project involved a number of private companyies and consultants for various activities. Mr. V. Robinson of Robertson Australia Pty. Ltd., Mr. I. Hawkshaw of Bellbird Geophysical Consultancy, and Mr. J. Allender helped to monitor the progress of the project. Project Design Management Pty. Ltd. assisted in the initial project design, and Supply Oil Field in the Philippines arranged the ship logistics during the data acquisition phase. Petrosys Pty. Ltd. provided the hardware, software and training for the Petrosys seismic mapping and database system, Encom Technology Pty. Ltd. recovered the deteriorating World Bank seismic tapes, and Petroconsultants Pty. Ltd. scanned the CITCO seismic sections. Kestrel Information Management Pty. Ltd. managed the data copying, and Corporate Electronic Publishing prepared the montages. Professor P. Davies of University of Sydney and Dr. M. Etheridge of Etheridge & Henley Geoscience Consultants provided training in Manila. We would like to extend our thanks to all these groups and individuals.

We greatly appreciate the valuable technical inputs, and workshop participation of the 34 Australian and Philippine consultative oil companies.

PART 1

GEOLOGY AND PETROLEUM POTENTIAL OF RAGAY GULF

by

C. S. Lee[1], M. C. Galloway[1], J. B. Willcox[1], A. R. Fraser[1], A. M. G. Moore[1], J. R. L. Apostol[2], N. D. Trinidad[2], R. P. Abando[2], D. V. Panganiban[2], and E. B. Guazon[2]

1 Australian Geological Survey Organisation, Canberra, ACT, Australia
2 Department of Energy, Makati, Metro Manila, Philippines

ABSTRACT

From March to May 1992, the Australian Geological Survey Organisation and the Philippine Department of Energy conducted a co-operative marine seismic, gravity, magnetic, bathymetry and geochemical 'direct hydrocarbon detection' survey in four offshore Philippine basins which included Ragay Gulf. The project was funded by the Australian International Development Assistance Bureau. The survey work was conducted using the Australian Government's geoscientific vessel, *Rig Seismic*.

The 950 km of newly acquired seismic data and 280 km of reprocessed data from Ragay Gulf show a significant improvement in penetration and stratigraphic resolution over the pre-existing seismic data. The improved density and distribution of seismic coverage allowed more confident definition of leads, many of which could not be detected with the former seismic coverage. Seismic interpretation revealed the existence of five sedimentary sub-basins with 2.5 to 6 seconds of Eocene to Recent sediments. Potential traps in eight areas were evaluated for hydrocarbon reserves.

No well has been drilled in the Ragay Gulf. Onshore well information and stratigraphy have assisted in the correlation and interpretation of offshore seismic data and allowed potential carbonate and clastic reservoirs to be recognised. The primary reservoir targets are carbonate sequences of both Early and Late Miocene age. Widespread volcanogenic sands may be cleaner beneath Ragay Gulf than onshore, and are an important secondary target, especially as gas reservoirs.

The geochemical data, both from the water bottom sampling and from sampling of onshore seeps and leaking exploration wells have confirmed the presence of mature source rocks from which generated hydrocarbons are currently migrating to the surface both onshore and offshore. This indicates the widespread occurrence of mature source rocks and the presence of migration pathways to the surface and, by inference, to reservoirs en route to the surface.

A wide diversity of play types is recognised which could have been sourced from three separate source kitchens in the Bondoc, Burias and Ragay Sub-basins. Both sandstone and carbonate reservoirs are believed to be present in a variety of traps formed during an early, pre-Middle Miocene phase of structuring (e.g. Arena) and a later phase which has in some cases has continued up to the present (e.g. Anima Sola). Specific entrapment possibilities are:

(1) Compressional fault-dependent traps (e.g. Anima Sola).

(2) Compressional anticlinal fault independent traps (Alibijaban and Palad).

(3) Late Miocene carbonate reefal buildups (Apud and Gorda).

(4) Early Miocene carbonate reservoirs in drape over highs (San Narciso and Bagulaya).

CONTENTS

INTRODUCTION **9**

REGIONAL STRUCTURE **12**

STRATIGRAPHY **14**

EXPLORATION HISTORY **20**
- License History
- Seismic Surveys
- Exploration Wells

SEISMIC INTERPRETATION **21**
- Data Description
- Seismic Horizons
- Seismic Sequences
- Structural Interpretation

PETROLEUM GEOLOGY **26**
- Reservoirs
- Geochemical Studies
- Source Rocks and Maturation
- Migration and Timing
- Evaluation of Leads

CONCLUSIONS **40**

REFERENCES **41**

TABLES

Table 1 Parameters for Alibijaban Lead.
Table 2 Parameters for Anima Sola Lead.
Table 3 Parameters for Apud Lead.
Table 4 Parameters for Arena Lead.
Table 5 Parameters for Bagulaya Lead.
Table 6 Parameters for Gorda Lead.
Table 7 Parameters for Palad Lead.
Table 8 Parameters for San Narciso Lead.

FIGURES

Figure 1 Survey areas of the Philippines - Australia Marine Seismic Survey Project.
Figure 2 Ship track location of new AGSO/DOE/AIDAB and previous industry seismic lines in Ragay Gulf.
Figure 3 Tectonic map of Ragay Gulf.
Figure 4 Stratigraphy of Bondoc Peninsula.
Figure 5 Major seismic horizons in Ragay Gulf, seismic section 109-58.
Figure 6 Simplified east-west cross section model of Ragay Gulf.
Figure 7 Strain ellipse for the Philippine Fault System. After Harding, 1974.
Figure 8 Bathymetry and location of leads in Ragay Gulf.

ENCLOSURES

Maps (see Volume 3)

Map R-1 Bathymetry of Ragay Gulf from seismic survey data. This map has not been integrated with the nautical chart data especially in shallow water where obvious errors are present. Scale 1:100,000.
Map R-2 Time structure map at top of Late Oligocene-lower Panaon Limestone (Brown Horizon) Sheet 4. Scale 1:50,000.
Map R-3 Time structure map at top of Late Oligocene to Early Miocene Panaon Limestone (Green Horizon) Sheet 2. Scale 1:50,000.
Map R-4 Time structure map at top of Late Oligocene to Early Miocene Panaon Limestone (Green Horizon) Sheet 4. Scale 1:50,000.
Map R-5 Time structure map at top of Late Oligocene to Early Miocene Panaon Limestone (Green Horizon) Sheet 7. Scale 1:50,000.
Map R-6 Time structure map at top of Middle Miocene Vigo Formation (Red Horizon) Sheet 2. Scale 1:50,000.
Map R-7 Time structure map at top of Middle Miocene Vigo Formation (Red Horizon) Sheet 4. Scale 1:50,000.
Map R-8 Time structure map at top of Middle Miocene Vigo Formation (Red Horizon) Sheet 7. Scale 1:50,000.
Map R-9 Time structure map at top of Late Miocene Lower Canguinsa Formation (Yellow Horizon) Sheet 2. Scale 1:50,000.
Map R-10 Time structure map at top of Late Miocene Lower Canguinsa Formation (Yellow Horizon) Sheet 4. Scale 1:50,000.
Map R-11 Time structure map at top of Late Miocene Lower Canguinsa Formation (Yellow Horizon) Sheet 7. Scale 1:50,000.

Plates (see Volume 4)

Plate R-1	Tectonic Elements of Ragay Gulf - Tayabas Bay, Southeast Luzon. Scale 1:250,000.
Plate R-2	Geological Map of Bondoc Peninsula. Scale 1:50,000.
Plate R-3	Time structure map at top of Late Oligocene to Early Miocene Panaon Limestone (Green Horizon). Scale 1:150,000.
Plate R-4	Time structure map at top of Middle Miocene Vigo Formation (Red Horizon). Scale 1:150,000.
Plate R-5	Time structure map at top of Late Miocene Lower Canguinsa Formation (Yellow Horizon). Scale 1:150,000.
Plate R-6	Montage for Alibijaban Leads.
Plate R-7	Montage for Anima Sola Leads.
Plate R-8	Montage for Apud Leads.
Plate R-9	Montage for Arena Lead.
Plate R-10	Montage for Bagulaya Leads.
Plate R-11	Montage for Gorda Leads.
Plate R-12	Montage for Palad Leads.
Plate R-13	Montage for San Narciso Leads.

INTRODUCTION

The Philippines is currently energy deficient but recent studies and exploration results (ie. the discoveries of West Linapacan, Malampaya and Octon oil/gas fields) indicate that potential oil and gas reserves exist in offshore Philippine basins. The Government of the Philippines has decided to actively promote oil and gas exploration activity in the country. It identified tectonic complexity and lack of geoscientific information as contributing to the low level of petroleum exploration in most of the thirteen identified offshore basins (BED, 1986). As a result, the Philippine Government requested the Australian Government to assist by conducting a comprehensive offshore geophysical and geochemical survey in selected, potentially oil-bearing, basins.

The Philippines-Australia Marine Seismic Survey Project was conducted co-operatively by the Australian Geological Survey Organisation (AGSO) and the Philippine Department of Energy (DOE) with funding from the Australian International Development Assistance Bureau (AIDAB). A joint consultative group consisting of seventeen Australian and seventeen Philippine oil companies was formed to provide the project with technical advice.The project had two main objectives:

> (1) to upgrade knowledge of petroleum prospectivity in selected areas of the Philippines and thus identify potential opportunities for future Philippine-Australian joint venture exploration; and
>
> (2) to assist the Philippine Government to acquire the skills necessary to obtain and interpret seismic and other geoscientific data and use these to focus future petroleum exploration in Philippine waters.

From March to May 1992, AGSO in conjunction with DOE conducted a geophysical and geochemical survey in Philippine waters using the Australian research vessel, *Rig Seismic*. This ship has a unique capability to simultaneously collect seismic, gravity, magnetic, bathymetric and bottom-water geochemical Direct Hydrocarbon Detection (DHD) data. About 2750 kms of seismic and magnetic data was obtained during a 45 day cruise in the Philippines. In addition, more than 5000 km of geochemical, gravity and bathymetric data were obtained. The work was undertaken in four areas: Ragay Gulf, Tayabas Bay, Northeast Palawan Shelf and Cuyo Platform (Fig. 1).

Of the four survey areas, the Ragay Gulf is of particular interest, with complex structures, multi-phase tectonism and up to 6 seconds two-way time (TWT) of thick sedimentary infill. The gulf is underlain by a northwest-southeast aligned Tertiary basin which formed in response to left-lateral strike-slip movement along the major Philippine Fault System as a result of collision between the Pacific and Southeast Asian Plates (Aurelio et al., 1991). The basin is about 150 kms long and 50 kms across, with the bulk of it offshore. There are numerous onshore oil and gas seeps on both sides of the basin, and some exploration wells had initial flows of up to 200 barrels/day (Bureau of Energy Development; BED, 1986). The seismic grid in Ragay Gulf has a spacing of 2 to 5 km and consists of 950 kms of new AGSO data, 280 kms of data reprocessed by AGSO, and some 2000 kms of previous exploration data (Fig. 2). The seismic interpretation confirmed the existence of five sedimentary sub-basins with 2.5 to 6 seconds TWT of Eocene to Recent sediments (Lee and Ramsay, 1992). Several types of potential hydrocarbon trap were identified, the most prospective probably being buried carbonate buildups, buried atolls and wrench-related structures (Lee et al., 1992; Galloway et al., 1992). Many geochemical DHD anomalies were located in the gulf (Bishop et al., 1992; Evans et al., 1992). These are

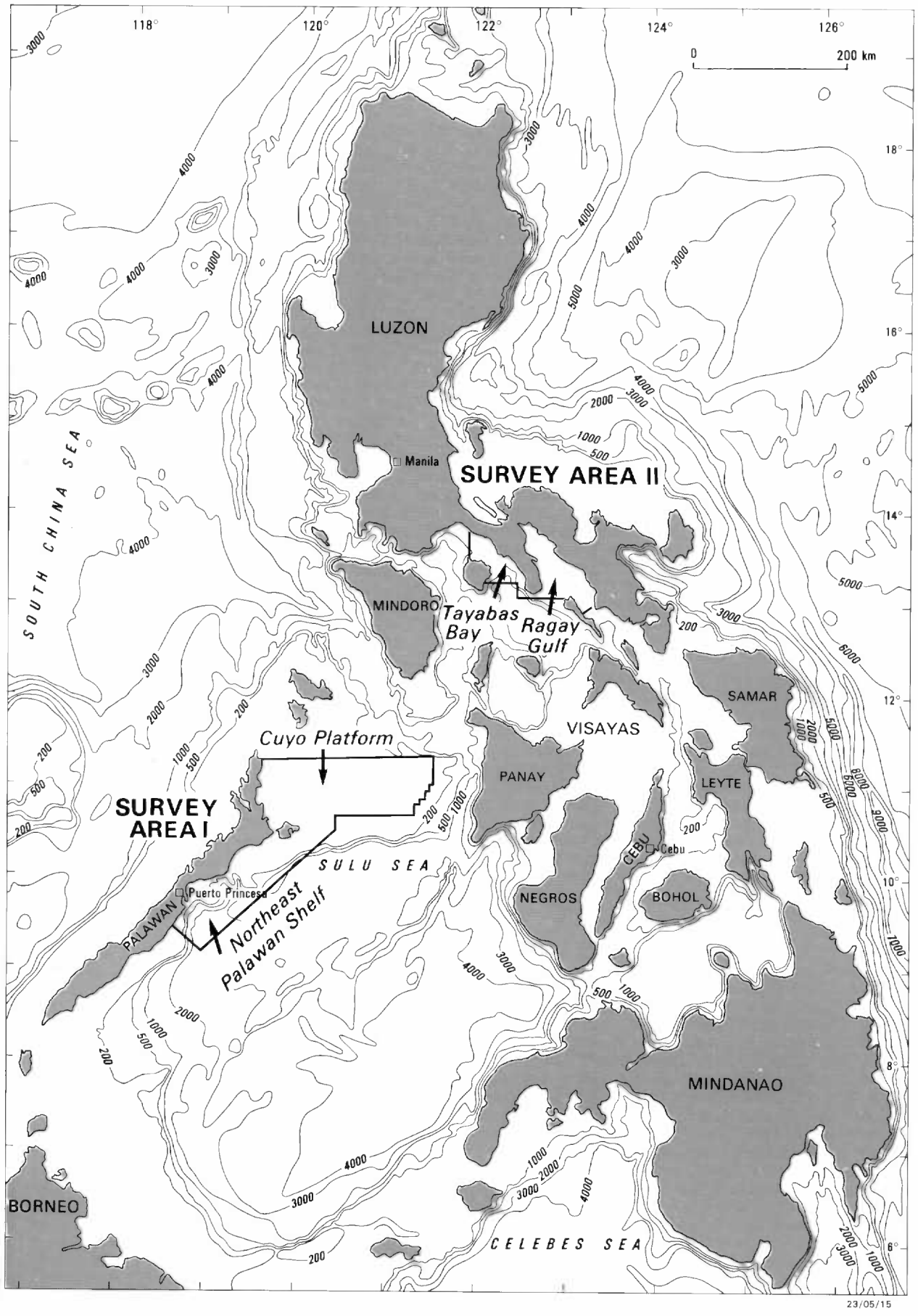

Figure 1 Survey areas of the Philippines - Australia Marine Seismic Survey Project.

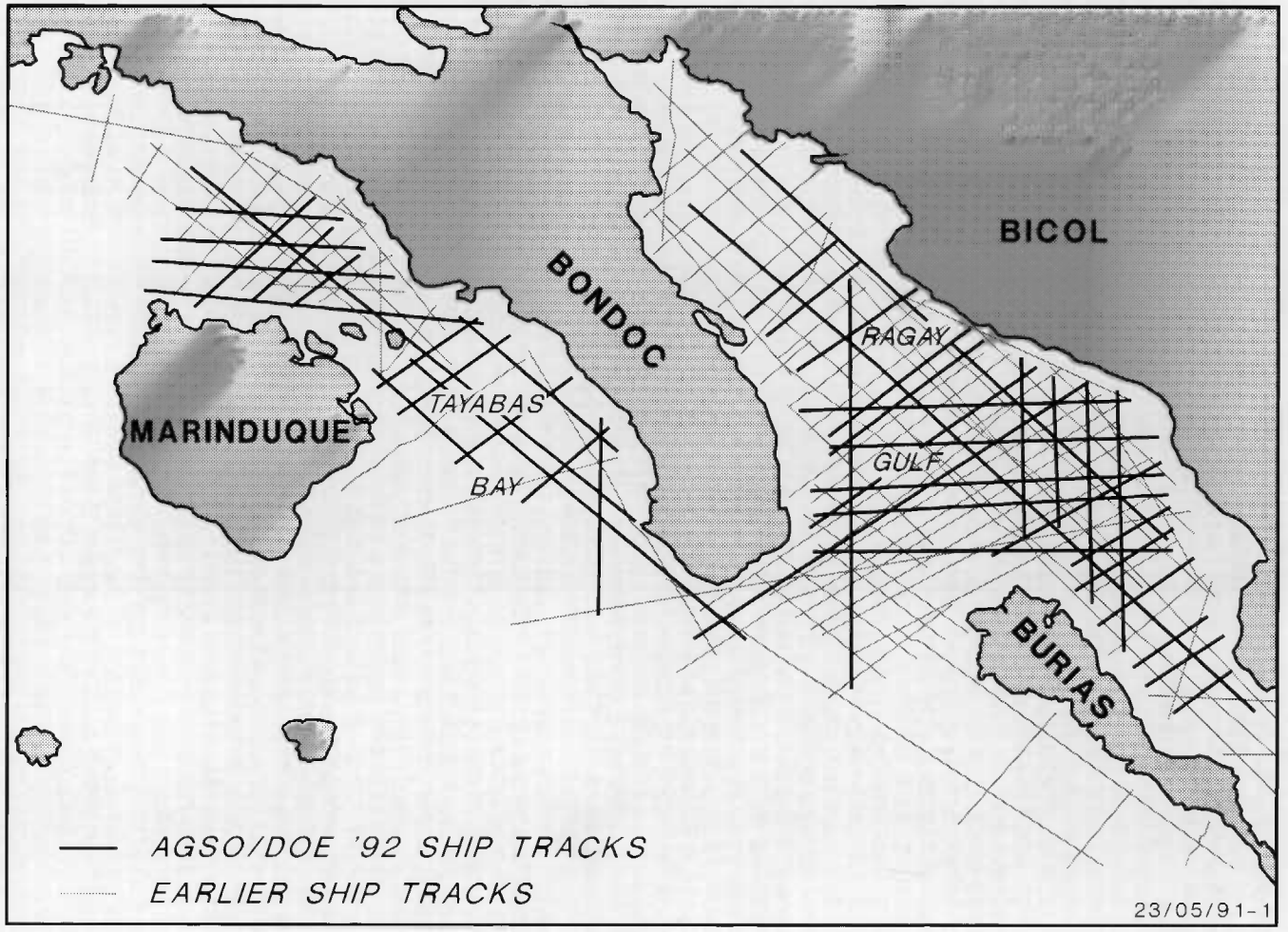

Figure 2 Ship track location of new AGSO/DOE/AIDAB and previous industry seismic lines in Ragay Gulf.

thermogenic in origin, indicating the presence of mature source rocks. In addition, the DOE collected seven samples from oil and gas seeps in the Bondoc and Bicol Peninsulas in March 1993 (Trinidad et al., 1993). Analyses of these samples at the AGSO geochemistry laboratory provided further evidence for mature source rocks (Cortez and Murray, 1993).

All the new data were integrated with previous seismic and well data, and interpreted and analysed to assess the petroleum potential of the survey area. This report describes the structure, stratigraphy and petroleum potential of Ragay Gulf. Overall, the Ragay Gulf has encouraging oil and gas potential and the exploration rights are being made available to private oil companies.

REGIONAL STRUCTURE

Previous seismic interpretations (BED, 1986) have shown that the Ragay Gulf can be subdivided into five sedimentary sub-basins (Fig. 3; Plate R-1) which are briefly described as follows:

The Ragay Sub-Basin extends for about 80 km along the eastern edge of Ragay Gulf. It is bounded in the northeast by the Legaspi Lineament and in the west by the Alabat-Burias High as far as the Anima Sola Fault. To the south it connects via a saddle to the Burias Sub-basin. Sediments thicken to a maximum of about 5 seconds TWT in the middle of the sub-basin.

The Bondoc Sub-basin is bounded by the Alabat-Burias High in the east and by the Mompog-San Miguel Disruption in the north. It extends to the west beneath the Bondoc Peninsula (Plate R-2). The basin was primarily developed during the Middle Miocene, with 4700 metres of sediment being recorded in outcrop onshore, and up to two seconds of section identified from seismic south and east of Bondoc Peninsula. During the Late Miocene a further 1500 metres of sediments were deposited onshore as evident from measured sections and wells. The sub-basin is believed to have been a major depocentre at least until the end of the Middle Miocene, and probably to the end of the Miocene. Seismic data indicates that the sub-basin has its greatest thickness beneath the area drilled by the Bondoc 1-7 wells.

Major deformation and uplift occurred at the end of the Middle Miocene and during the Late Miocene and Pliocene, but probably with decreasing severity after the end of the Middle Miocene. Pleistocene marine carbonates are found at an elevation of 300 metres or more in southern Bondoc Peninsula showing that major uplift has continued, probably until the present. The basin was subject to a major inversion along the axis of Bondoc Peninsula, but with major synclinal areas remaining on either side of it. This was probably driven by compressive wrenching along the Central Bondoc Fault. Unlike the East Bondoc Fault, which seismic indicates has been inactive since the end of the Middle Miocene, the Central Bondoc Fault has probably been active until the present.

The Burias Sub-basin extends southeastwards from the saddle at the southern end of the Ragay Sub-basin. In the east it onlaps the basement high east of the Nagas Fault and in the west is bounded by the Alabat-Burias High. It has at least 4 seconds TWT of layered section as shown on seismic lines and probably contains the "kitchen" area for the oil seeps of southern Burias Island.

The Capuluan Sub-basin is located in the northeast of Ragay Gulf. It is bounded in the west by the Alabat-Burias High and in the east by the Bicol Terrace. It extends onshore

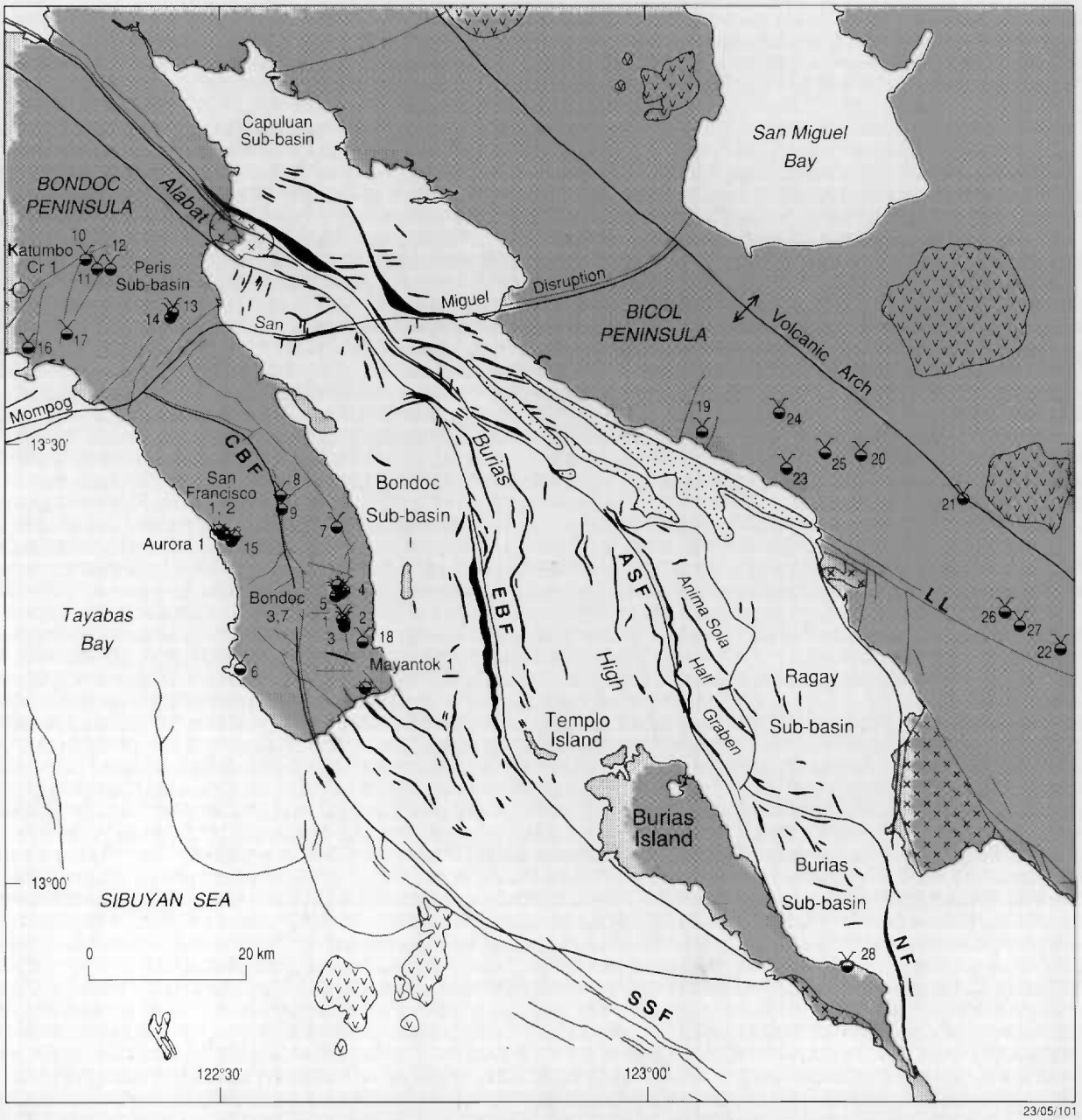

Figure 3 Tectonic map of Ragay Gulf.

toward the northwest and is closed to the southeast by a rise associated with the Mompog-San Miguel Disruption. It forms a half graben against the Legaspi Lineament with up to 3.4 second TWT of section evident on seismic lines.

The Peris Sub-basin is located in the northwest Ragay Gulf and the adjacent part of the Bondoc Peninsula. It is bounded in the northeast by the Alabat-Burias High and in the south by the Mompog-San Miguel Disruption.

STRATIGRAPHY

Stratigraphic knowledge is based on a limited number of maps and reports from oil and mining companies, as well as data from wells drilled in the Bondoc Peninsula. Of 25 wells drilled on the peninsula, 16 are less than 1000 m deep, only five exceed 1500 m and two exceed 2000 m. Just six wells, Katumbo Creek-1, Aurora-1 and -2, San Francisco-1 and -2 and Mayantok-1 (Fig. 3), have a complete suite of logs. From the lithological descriptions of field outcrops (Antonio, 1961; Yap, 1972; Poblete & Ferrer, 1990) and information from the World Bank Report (BED, 1986), a brief description of stratigraphy is given in Figure 4. An example of a seismic section and an idealised cross-section are shown in Figure 5 and 6 (Lee et al., 1993).

Basement

Basement comprises the oldest rocks known on the Bondoc Peninsula (Figs. 4, 5 and 6). In the northwest, basement crops out in the vicinity of Lian Point near Peris Bay and the Unisan township. The rocks consists of locally foliated hornblende schists with scattered quartz veins. Alteration of chlorite and epidote is common. No estimation of thickness has been possible. On Burias Island, similar rocks of Eocene or older age occur on the southwest coast near Malapingan Point. To the north of Burias Island basement crops out on the east coast of Templo Island as volcanics and intrusive serpentinites, with subordinate amounts of limestone and conglomerate. Tanguingi Island, north of Burias, is composed of black, scoriaceous extrusive basalt porphyry; a small outcrop of serpentine occurs on nearby Busing Island. On Marinduque Island, located west of Bondoc Peninsula, basement consists of metamorphosed greenstone facies and ophiolitic lava flows with intercalated greywackes and siltstones (BED, 1986). In a minor limestone member *Globotruncana sp,* indicative of Cretaceous age, was identified. Basement on Bicol Peninsula is exposed to the east of the Nagas Fault in the form of a 5 by 9 km quartz diorite stock of Miocene age, and at Balatan between the Legaspi Lineament and the coast where a hornblende diorite body is present.

Unisan Formation

Unconformably overlying basement schists is the Unisan Formation (Figs. 4, 5 and 6) consisting of volcanoclastic and carbonate breccia composed of fine-grained porphyritic volcanics and tuffs together with penecontemporaneous, tuffaceous, silty carbonates containing rich foraminifera. The thickness of the unit is unknown. In Katumbo Creek-1 well, the sediments show close petrographic affinities in composition, texture and alteration to outcrop samples from the northern Bondoc Peninsula (BED, 1986). The age is late Eocene to late Oligocene, probably in the range P15 to P19. On the northwest coast of Burias Island (Aurelio et al., 1991) are very limited exposures of highly indurated volcanic wackes, siltstones and shales of late Eocene to early Oligocene age (NP22). These may be equivalents of the Unisan Formation.

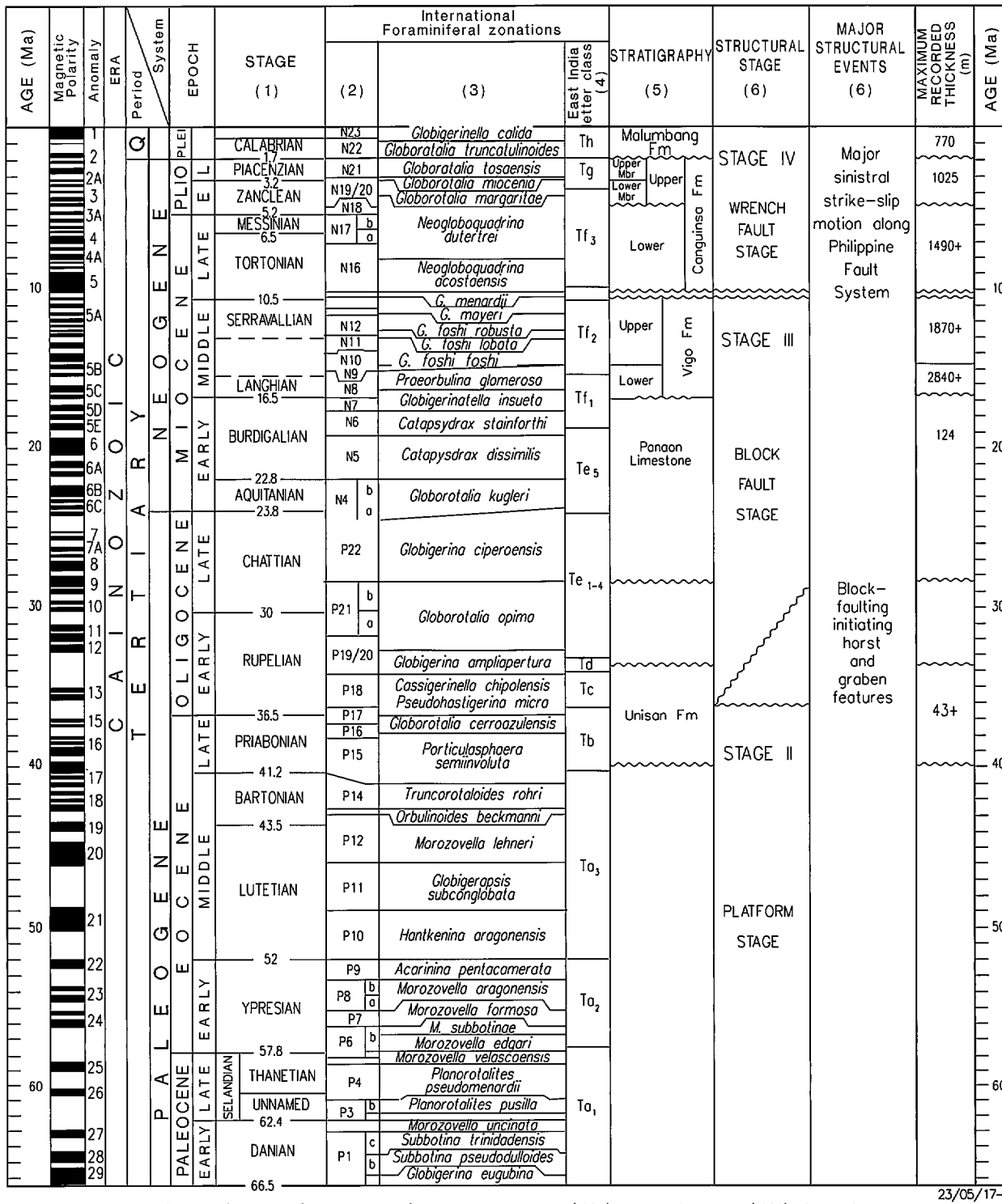

1 Berggren & others, (1985a, b). Burger, (in prep. a & b)
2 Blow (1969, 1979), Berggren (1969)
3 Bolli (1957, 1966), Stainforth & others, (1975), Bolli & Premoli-Silva (1973), Caron (1985)
4 Adams (1984), Adams & others, (1986), Chaproniere (1981), (1983), Jenkins & others, (1985)
5 Antonio 1961 Yap 1972, OEA 1988
6 BED 1986

Figure 4 Stratigraphy of Bondoc Peninsula.

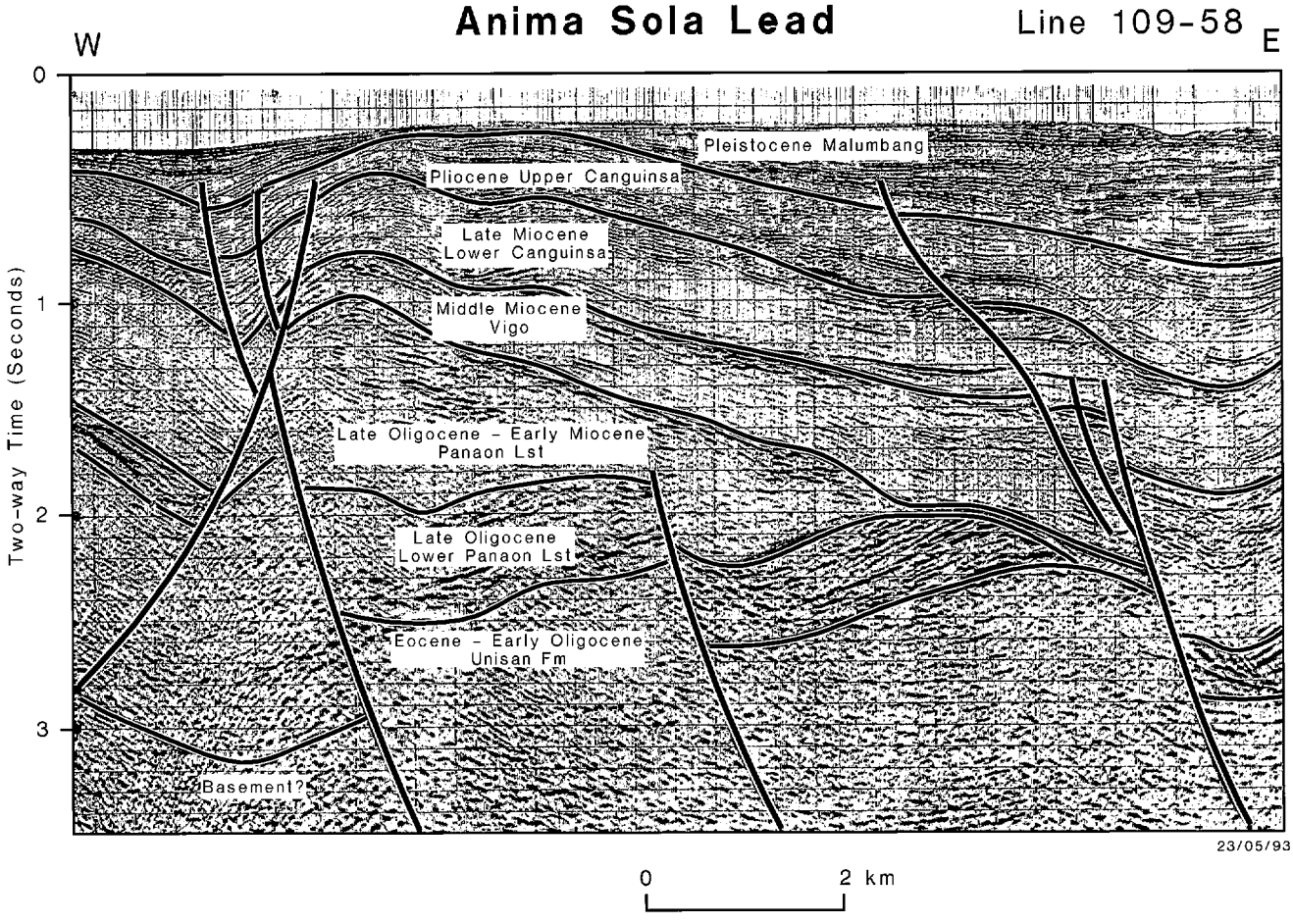

Figure 5 Major seismic horizons in Ragay Gulf, seismic section 109-58.

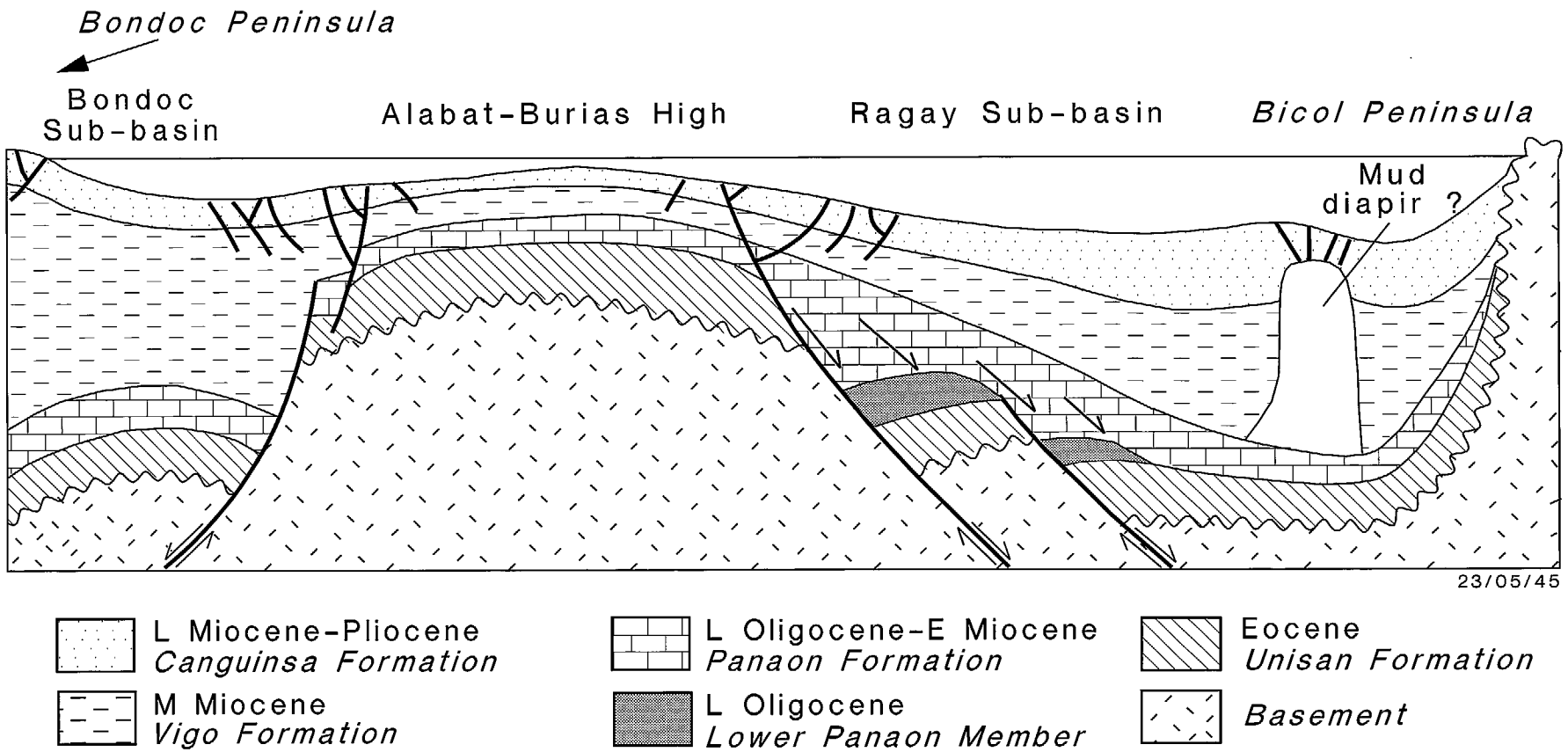

Figure 6 **Simplified east-west cross section model of Ragay Gulf.**

Panaon Limestone

The Panaon Limestone unconformably overlies the Unisan Formation (Figs. 4, 5 and 6). It consists of limestone which varies from dense crystalline with coralline relics to completely recrystallised limestone. The recrystallisation is believed to be due to surface alteration and may not indicate lack of porosity at depth. Maximum thickness on Bondoc Peninsula is estimated to vary from 500 to 1000 m. It is thought to be highly variable in thickness and locally lenticular. It was deposited in shallow marine conditions in the Late Oligocene to Early Miocene (N3/P22 to N7). Seismic data indicate that the formation is buried below economically drillable depths in the southern part of the Bondoc Peninsula

Its age equivalent, the Makalawang Limestone, crops out over Templo Island, located northwest of Burias Island, and in a limited area on Burias Island (BED, 1986). Its estimated thickness is 1200 to 1300 m and it consists of coarsely crystalline limestone, varicoloured limestone and grit, together with hard, white, thin bedded limestone. It is highly probable that the Panaon-Makalawang Limestone extends beneath the Alabat-Burias High at economically drillable depths. It is the target for a number of leads identified offshore and is the age equivalent of the Nido Limestone of northwest Palawan, which is the Philippines major producing horizon.

The Siramag Marble crops out immediately east of the Legaspi Lineament on the west coast of Bicol Peninsula, adjacent to Ragay Gulf. Fauna is sparse in the 300 m thick unit and no age dating has been possible. The Pantao Limestone, farther south and adjacent to the Nagas Fault, is regarded as of Eocene age by the World Bank (BED, 1986). It is possible however that the age is actually Oligocene and if so the Panaon, Makalawang, Siramag and Pantao facies could be age equivalent and extend continuously throughout the area beneath Bondoc Peninsula and Ragay Gulf as suggested by the seismic interpretation.

Vigo Formation

The Vigo Formation (Antonio, 1961; Yap, 1972) crops out along the length of the Bondoc Peninsula (Figs. 4, 5 and 6). It has been subdivided into upper and lower parts. Relations with the underlying Panaon Limestone vary from conformable to unconformable. According to the World Bank Report (BED, 1986), the Vigo unconformably overlies the Panaon Limestone but Antonio (1961) believes they are conformable as evident from the presence of numerous limestone lenses up to 10 m thick at the base of the Lower Vigo, predominantly in the Pitago-Gumaca area, suggesting a facies transition from clastic-poor sedimentation of the Panaon to clastic-dominated sedimentation of the Vigo Formation. Geochemical analyses of well cuttings and outcrop samples show the Vigo to have significant hydrocarbon source potential (BED, 1986).

The Lower Vigo Formation consists predominantly of alternating coarse to very fine sandstone and sandy to silty shale. Where the base of the formation can be observed in the far northwest of Bondoc Peninsula, lenses of limestone up to 10 m thick with conglomerates and volcanic interbeds occur in up to five separate horizons. Locally, carbonaceous silts, shales and coal seams occur. The conglomerates contain pebbles of schist, volcanic rock and limestone. Thickness of the unit in its incomplete section is 2840 m, but a total thickness of 3000-4000 m has been estimated (Antonio, 1961). The formation was deposited in an environment that varied from shallow marine, as evident from the common limestone throughout, to coastal paludal coal swamps, as is evident

from the common thin coal seams and carbonaceous silts and shales. Age is earliest Middle Miocene (N8 to N9).

The Upper Vigo Formation shows a marked increase in the proportion of conglomerates and sandstones as compared to sandstones and shales of the Lower Vigo Formation. Individual conglomerate/sandstone beds are commonly over 1 m thick. Limestone lenses are scattered throughout the section. Volcanic interbeds are known at several locations, all in the northwest, near Pitago-Unisan. In the southern Bondoc Peninsula, the formation is less sandy and has been termed the Vigo Shale (Corby, 1951; Hashimoto, 1981). Maximum thickness of the Upper Vigo Formation was measured to be 1870 m. It was deposited in similar conditions to the Lower Vigo Formation in the Middle Miocene (N10 to N14).

Canguinsa Formation

The Canguinsa Formation overlies the Vigo Formation with a marked angular unconformity (Figs. 4, 5 and 6). It is subdivided into an upper and lower part (Antonio, 1961; Yap, 1972). The lower part of the Lower Canguinsa Formation consists of cross-bedded sandstones and poorly sorted conglomerates with interbedded grey shales, siltstones and dark-coloured sandstones. Carbonaceous streaks occur throughout. The conglomerate contains pebbles of quartz, schists, igneous rocks, limestone, hard siltstone and sandstone with finer grains of quartz schist and igneous rock fragments. In the upper part, the conglomerates are lighter in colour and calcareous; they contain mica flakes but little carbonaceous material. Maximum recorded thickness is 1490 m in Bondoc-3 and similar thicknesses have been measured in the field in northern Bondoc. As with the Vigo Formation the presence of limestones and thin coals and carbonaceous silts and shales indicate an environment varying from shallow marine to littoral-paralic. Age is Miocene (N16 to N17).

The Upper Canguinsa Formation overlies the Lower Canguinsa with no angular unconformity. An hiatus, however, is suggested by the absence of thin shelled mega-fossils in the Lower Canguinsa and their common occurrence in Upper Canguinsa. Faunal changes in the cuttings have been recorded in Katumbo Creek-1, San Francisco-1, -2 and Mayantok-1, as well as dipmeter changes in San Francisco-1 and -2. Poblete and Ferrer (1990) believe the provenance of the Canguinsa Formation was the Tayabas-Marinduque area. Lithologically it consists predominantly of indistinctly bedded calcareous and micaceous, buff coloured, siltstone interbedded with thin mudstone layers and some limestone. There are conspicuous thin-shelled megafossils throughout. The maximum thickness claimed by Antonio (1961) exceeds 1025 m but the formation is believed to thicken to the southeast. The unit appears to have been deposited exclusively in shallow marine conditions during the Pliocene (N18 to N21).

Malumbang Formation

The Malumbang Formation (Antonio, 1961; Yap, 1972) unconformably overlies the Canguinsa and all older units as a relatively flat drape (Figs. 4, 5 and 6). In the north it consists predominantly, in the lower part, of chalky white, porous, dense, crystalline megafossiliferous limestone; in the middle part, of silty to shaly calcareous sandstone with limestone interbeds and; in the upper part, of porous, gently dipping limestone. In the south, this three-fold subdivision is not evident. The Malumbang Formation is generally a very shallow marine carbonate complex including reefal limestones, detrital carbonates

and some clastic facies. Maximum recorded thickness is about 770 m and age is Pleistocene (N22 to N23).

Diapirs

Diapirs have been identified on seismic sections in the deeper parts of the Ragay Sub-basin (BED, 1986). Velocity analyses carried out during seismic processing suggests that the diapirs are composed of very low velocity materials such as clay or mud, rather than salt or salt mixture which would have a much higher velocity. Whether or not diapirs are present onshore has yet to be resolved. The World Bank Report (BED, 1986) shows a wide zone of diapiric structures down the centre of Bondoc Peninsula in an area where the Vigo Formation crops out. In a radar imagery interpretation report by the Arkansas Research Consultant Inc. (ARCI, 1988), some isolated diapirs, mostly east of the Central Bondoc Fault, were recognised. Antonio (1961) does not refer to diapirs and his detailed maps at 1:50000 scale show complex dip patterns indicative of shale flowage under compression, but not of diapirism. While it is possible that the restricted diapirs referred to in the radar imagery report may be present, we have seen no evidence to support the wide belt of diapirs shown in the World Bank Report.

EXPLORATION HISTORY

License History

In the past, the contract blocks on the Bondoc Peninsula have included the adjacent portions of the offshore Tayabas Bay and Ragay Gulf. The Geophysical Service and Exploration Contract (GSEC) No. 12, awarded in 1976 to SEDCO Inc., covered large areas of northern Ragay Gulf and Tayabas Bay in which seismic surveys were shot in 1979. The block was relinquished in 1980 after drilling of the onshore well Katumbo Creek-1. The GSEC 46 was held by Ran Ricks (name later changed to Far East Resources) between 1988 and 1990. The block extended over part of southwest Ragay Gulf, but onshore seismic work was only carried out prior to the drilling of Mayantok-1 well on the Bondoc Peninsula.

Seismic Surveys

Since 1979 a total of approximately 2900 line km of seismic data have been recorded in the Ragay Gulf area by different organisations. Seismic surveys are listed below:

Recorded By	Lines	Location	Km
Seiscom Delta	R-*-79*	Northwest Ragay Gulf	267
GSI	80-B-**	Central Ragay-Burias Pass	347
GSI	81-**	Burias Pass	82
BED \ Seiscom Delta	RG-83-8**	Central Ragay Gulf	274
Petro-Canada	98**-86	Central Ragay Gulf	975
AGSO/DOE/AIDAB	109-**	Ragay Gulf and Burias Pass	950
		Total Line-km	**2895**

The R-*-79 lines were shot by Seiscom Delta under contract to SEDCO Inc. during exploration of block GSEC 12. Lines 80-B-** and 81-** are speculative survey lines shot by Geophysical Service International (GSI). The remaining three seismic surveys were designed to promote further exploration activity by improving regional coverage and

delineating large scale prospects and leads in the Ragay Gulf. The BED survey in 1983 was funded by the World Bank, the Petro-Canada survey in 1986 by the Canadian Government and the AGSO/DOE/AIDAB survey in 1992 by the Australian Government.

Exploration Wells

Twenty-one wells were drilled on the Bondoc Peninsula between 1906 and 1972, when the Petroleum Exploration Concession system was replaced by the Service Contract system. Nineteen of these wells encountered oil or gas shows, testifying to the petroliferous nature of the Bondoc Peninsula. Over the same period, twenty-three wells were drilled on the Bicol Peninsula on the eastern side of Ragay Gulf, of which six encountered oil or gas shows. Promising flow rates were recorded in several of these early wells. Pina-1 drilled in the 1920's to a depth of 1565 m, produced gas at a rate of 92 Mcfd. Bondoc-2, drilled in the 1940's, flowed 250 BOPD on a 36 hour test until the perforations became plugged. A strong flow of gas was recorded in Aurora-2 in 1971, but the well had to be abandoned due to inability to control the pressure.

Four wells have been drilled since implementation of the Service Contract system in 1972. All of these are located on the Bondoc Peninsula -no offshore well has yet been drilled. San Francisco-1 and -2 were drilled in 1977 on the Aurora structure, to the northwest of the Aurora wells. Only weak gas flows were recorded from very coarse sandstones, comprising poorly to moderately sorted volcanic and feldspathic rock fragments in the Vigo and Lower Canguinsa Formations. Reservoir was thought to be degraded by the presence of argillaceous matrix filling voids. The Katumbo Creek-1 well was drilled in 1980 to test a possible reef facies developed within the Panaon Limestone. The target horizon proved to be the top of a thick accumulation of quartz and volcanic sands and conglomerates, representing a fan build-up at the base of a major fault. There was no good development of reservoirs, the sandstones being mainly feldspathic with little or no porosity. Mayantok-1 was drilled in 1989 to test sandstone and/or conglomerate intervals within the Upper Member of the Lower Canguinsa Formation. The well penetrated only 220m of the Canguinsa Formation, followed by Upper and Lower parts of the Vigo Formation to TD. A repeat section of Upper Vigo occurred near the bottom of the well, below a major reverse fault with an estimated throw of 500 m. The Vigo Formation comprises predominantly siltstone and sandstone with several interbeds of limestone and claystone. The sandstones are fine-grained, moderately sorted with calcareous cement and argillaceous matrix. No good reservoirs could be identified and no tests were carried out despite the presence of gas-saturated zones and oil shows .

SEISMIC INTERPRETATION

Data Description

Seismic data (see above list) were processed by the acquiring contractor except for the BED data which were recorded by Seiscom Delta and processed in Manila by the Philippine National Oil Company using the Seismograph Services Corporation Phoenix VAX system; and the Petro-Canada data which were processed by Western Geophysical Corporation. Migrated sections are available for most lines exceptions being the R-*-79* lines, shot for SEDCO Inc., and BED lines RG-86-802, 810 and 814. Vertical scales vary from 5 cm per second for the SEDCO R-*-79* lines to 3 3/4 " per second for the GSI 80 and 81 lines, Petro-Canada and most of the BED lines. Some BED lines and all AGSO/DOE/AIDAB lines are displayed at 10 cm per second. Horizontal scales generally range from 1:20,000 to 1:25,000 and are mostly consistent within each survey

All data were used but quality, definition and penetration vary between surveys. The GSI data has good resolution but limited penetration. The BED data is limited with respect to both resolution and penetration. The Petro-Canada and AGSO data are of the best overall quality and provided the regional interpretation framework into which other lines were tied.

As there are no offshore wells in the area, horizons were identified by character correlation from onshore to offshore, and from one area to another across major structures, based on gross seismic reflection characteristics of sequences. For Ragay Gulf this was done using the Mayantok-1 well and onshore seismic data from a survey by Ran Ricks of the Philippines Inc. Outcrop information was plotted on seismic sections as a check on the validity of the interpretation.

Seismic Horizons

Seven horizons corresponding to major sequence boundaries were picked on seismic sections, of which five were mapped. From oldest to youngest, the five mapped horizons are Top Lower Panaon Member (Map R-2), Top Panaon Limestone (Maps R-3 to R-5; Plate R-3), Top Vigo Formation (Maps R-6 to R-8; Plate R-4), Top Lower Canguinsa Formation (Maps R-9 to R-11; Plate R-5), and Water Bottom (Map R-1)

Intra-Unisan Formation (purple horizon) is recognisable only on the new data and lies below the previous lowest mappable horizon (Figs. 5 and 6). It is a high amplitude, low frequency event conformable with reflections above and below, which presumably corresponds to a high velocity layer within the Unisan Formation. Nowhere does the event 'ring' in a manner suggestive of high velocity acoustic basement.

Top Unisan Formation (blue horizon) is a high amplitude, moderately continuous, low frequency reflection (Figs. 5 and 6) evident on the AGSO and Petro-Canada data and to a lesser extent on the BED data. Although generally mappable throughout the gulf area, it is barely recognisable in reflection-free diapir zones in the eastern Ragay Gulf. The horizon is generally conformable with the reflections above and below. It probably represents the lateral equivalent of the top of the Unisan Formation of Late Eocene to Early Oligocene age.

Top Lower Panaon Member (brown horizon) marks the top of a series of moderately high amplitude events about 200 to 400 ms above the Unisan Formation (Figs. 5 and 6) in a restricted area east of the Anima Sola Fault, northeast of Burias Island. The horizon is conformable with the sequence below and represents the base of a prograding sequence. It is terminated in the west by the Anima Sola Fault system and in the east by erosional truncation at the Top Panaon unconformity.

Top Panaon Limestone (green horizon) corresponds to an unconformity at the top of the Late Oligocene to early Miocene Panaon Limestone, equivalent to the formation encountered in the onshore Katumbo Creek-1 well of western Bondoc Peninsula (Figs. 5 and 6). It is a wide spread continuous event, characterised by high to moderately high amplitudes, recognisable on all seismic lines. It is probably the most characteristic and continuous event in Ragay Gulf.

Top Vigo Formation (red horizon) separates the Middle Miocene Upper Vigo from the overlying Late Miocene Lower Canguinsa Formation. It marks an unconformity between two sequences which show similar internal stratal configurations. The underlying

sequence onlaps the basement in the Alabat-Burias High especially northwest and west of Burias Island.

Top Lower Canguinsa Formation (yellow horizon) represents the internal boundary between the upper and lower parts of the Canguinsa Formation but there is little distinction between the two sequences. Both are characterised by very continuous, high amplitude, and medium to high frequency reflections although the lower sequence appears to have less continuous reflections in some areas. This sequence subcrops over restricted areas of the Alabat Burias High especially north and northwest of Burias Island at the southern end of the Bondoc Sub-basin.

Seismic Sequences

The lower part of the Unisan Formation (pre-purple horizon) is characterised by parallel to mildly divergent reflections with poor to fair continuity and medium to low amplitude.
Age: Possibly Eocene to Oligocene.
Lithology: Unknown.
Reservoir potential: Unknown but assumed to be minimal.

The upper part of the Unisan Formation (purple to blue interval) is represented by parallel to mildly divergent reflections with fair continuity and medium amplitude.
Age: Oligocene to earliest Early Miocene.
Lithology: Volcanoclastic shales, sands conglomerates tuffs and minor limestones where encountered in outcrop and in Katumbo Creek-1 of western Bondoc Peninsula. Lateral equivalents under Ragay Gulf could contain fluvio-deltaic source rocks.
Reservoir potential: Appears minimal from outcrop and Katumbo Creek-1 but lateral equivalents may have potential.

The Lower Panaon Member (blue to brown interval) is characterised by subparallel reflections with moderate continuity and high to medium amplitude. Seismic definition varies from quite distinct to poor. The sequence is terminated in the west by the Anima Sola Fault system and in the east by erosional truncation.
Age: Early Miocene.
Lithology: unknown.
Reservoir potential: unknown.

The Panaon Limestone (brown to green interval) generally has high to moderately high amplitude events in the top 300 milliseconds. Reflections are characterised by a number of high to moderately high amplitude events that vary from parallel with high continuity to chaotic or contorted events in the central ridge. Towards the deep troughs there is a moderately divergent pattern associated with progressive thickening. High amplitude reflections are suggestive of bedded carbonates, but the characteristic, mounded, reef-like structures as seen in northwest Palawan are not observed. Below the upper 300 milliseconds, reflections vary from subparallel to strongly divergent, with medium to low amplitude and moderate continuity. While this section may have a significant carbonate content it is possibly dominated by shale, siltstone and sand.
Age: Early Miocene.
Lithology: Limestone, with shale ,siltstone and sand likely to be present.
Reservoir potential: Outcrop on Bondoc Peninsula and Templo Island, and data from Katumbo Creek-1 show the Panaon Limestone to be recrystallised and tight, but its stratigraphic equivalent, the Nido Limestone of north-west Palawan, is the major reservoir

for Philippine discoveries. The formation could include a major reservoir beneath Ragay Gulf.

The Vigo Formation (green to red interval) is represented by low amplitude, subparallel reflections of fair to moderate continuity on AGSO lines south of Bondoc Peninsula in the Bondoc Sub-basin. On the Petro-Canada, BED and GSI lines however, the interval is chaotic and largely reflection free, characteristic of a relatively homogeneous shale sequence. The presence of weak reflections on AGSO lines indicate that some siltstones and sandstones are present. The unconformity separating the Upper and Lower Vigo Formations onshore could not be systematically picked or mapped offshore.
Age: Middle Miocene.
Lithology: Predominantly shale with volcanoclastic silts and sands that grade to conglomerates. Quartzose intervals were encountered in San Francisco-1 well in the western Bondoc Peninsula. Outcrop data suggests the formation has seal and source potential.
Reservoir potential: Most Bondoc Peninsula wells had oil and gas shows with Bondoc-2 reported as producing 250 barrels/day. No sustained production was achieved from any of the Bondoc wells but some seeps and leaking wells were successfully sampled for oil and gas in March 1993 by DOE staff (Trinidad et al., 1993). If drilled with muds that minimised formation damage, the formation could prove to be productive, especially of gas.

The Lower Canguinsa Formation (red to yellow interval) is characterised by parallel reflectors with high continuity and high to medium amplitude. The sequence is bounded below by a major unconformity and above by an angular unconformity or disconformity. At the top of the interval in the southeast Ragay Gulf-Burias Pass area there appear to be several carbonate buildups. These are up to 40 sq km in area; smaller ones may be present elsewhere in Ragay Gulf. No similar reefal structures have been described onshore.
Age: Late Miocene.
Lithology: Carbonate buildups, limey shales, carbonate sands, conglomerates and local thin limestones.
Reservoir potential: Onshore limestones have porosity; some shows were encountered in onshore Bondoc wells. Offshore carbonate buildups would be of particular interest

The Upper Canguinsa, Malumbang and younger formations (post-yellow horizon) have similar seismic characteristics to the Lower Canguinsa Formation though carbonate buildups no carbonate buildups have been recognised.
Age: Pliocene, Pleistocene and Holocene.
Lithology. Calcareous silts and sands with local limestones.
Reservoir potential: Good visual porosity seen in unweathered sands and limestones. Sequence however is unlikely to be sealed anywhere.

Structural Interpretation

The Ragay Gulf is located within the Philippine Fault System (Fig. 3). The new seismic mapping has shown that basin structures are dominated by left lateral strike-slip movement along the main fault and its various splays. The predominant tectonic grain is northwest oriented. The left lateral strain ellipse model (Harding, 1974) explains the majority of the faults and folds observed in Ragay Gulf and surrounding areas (Fig. 7). Faults fall into three main categories: primary wrench faults with significant amounts of left lateral movement; secondary wrench faults that appear to form links between the primary faults; and antithetic strike-slip faults, exhibiting a complex combination of right lateral and normal fault movement.

There are two primary wrench faults in the region. The Legaspi Lineament is a through-going splay of the Philippine Fault System passing through the survey area (Fig. 3). Using the new seismic data it can now be mapped confidently for the first time beneath Ragay Gulf, extending from near Panto township on Bicol Peninsula north-westwards across Ragay Gulf to near Lian Point on Bondoc Peninsula. The Sibuyan Sea Fault is also a splay of the Philippine Fault System (Fig. 3), splitting off from the Philippine Fault near Masbate Island, and passing west of Ticao and southern Burias Island (Aurelio et al., 1991). It is considered by Sarewitz and Lewis (1991) to terminate south of Bondoc Peninsula. However, from the seismic interpretation and from the careful mapping of the onshore geology of Bondoc Peninsula, this fault is now interpreted to horsetail northwards into the Central Bondoc Fault.

There are four secondary wrench faults, all believed to be north-south, horsetail splays off the Sibuyan Sea Fault: the Central Bondoc Fault is a compressive wrench fault that has been mapped from the southernmost tip of Bondoc Peninsula northwards for about 35 km (Fig. 3). It is associated with a series of flower structures indicating shear. Several seeps occur along the fault system and petroleum exploration wells drilled on flower structures have encountered oil and gas shows. Outcrop geology and the limited poor quality seismic data indicate that major regional movements took place at the end of the Middle Miocene, in Late Miocene, and in the Pliocene. Early Miocene and older movements may have taken place but are difficult to confirm except locally. The East Bondoc Fault is a compressive wrench located east of Bondoc Peninsula and marks the eastern limit of the Bondoc Sub-basin (Fig. 3). The Middle Miocene section thickens greatly west of the fault, but seismic data show no displacement of the post-Middle Miocene section indicating that movement on the fault ceased at the end of the Middle Miocene. The Anima Sola Fault is located on the eastern edge of the Alabat-Burias High (Fig. 3). The fault shows significant compression and the section thickens on its east side especially in the Early Miocene and older section. All seismic horizons including the water bottom are displaced and all seismic intervals show growth to the east indicating that the fault has been active from 40 million years to the present. In the north the fault appears to terminate against or merge with the Legaspi Lineament. Tracing it to the south is uncertain but it is interpreted to extend parallel the eastern coast of Burias Island, then continue southeastwards along the coast of Burias Island to join the Sibuyan Sea Fault. The Nagas Fault is shown as a series of relay faults which extends from the Legaspi Lineament at Lake Bato on Bicol Peninsula, southwards along the western edge of the quartz diorite body adjacent to Nagas, thence offshore to near Taguilid on Burias Island (Fig. 3). From there it probably cuts across Burias Island to join the Sibuyan Sea Fault.

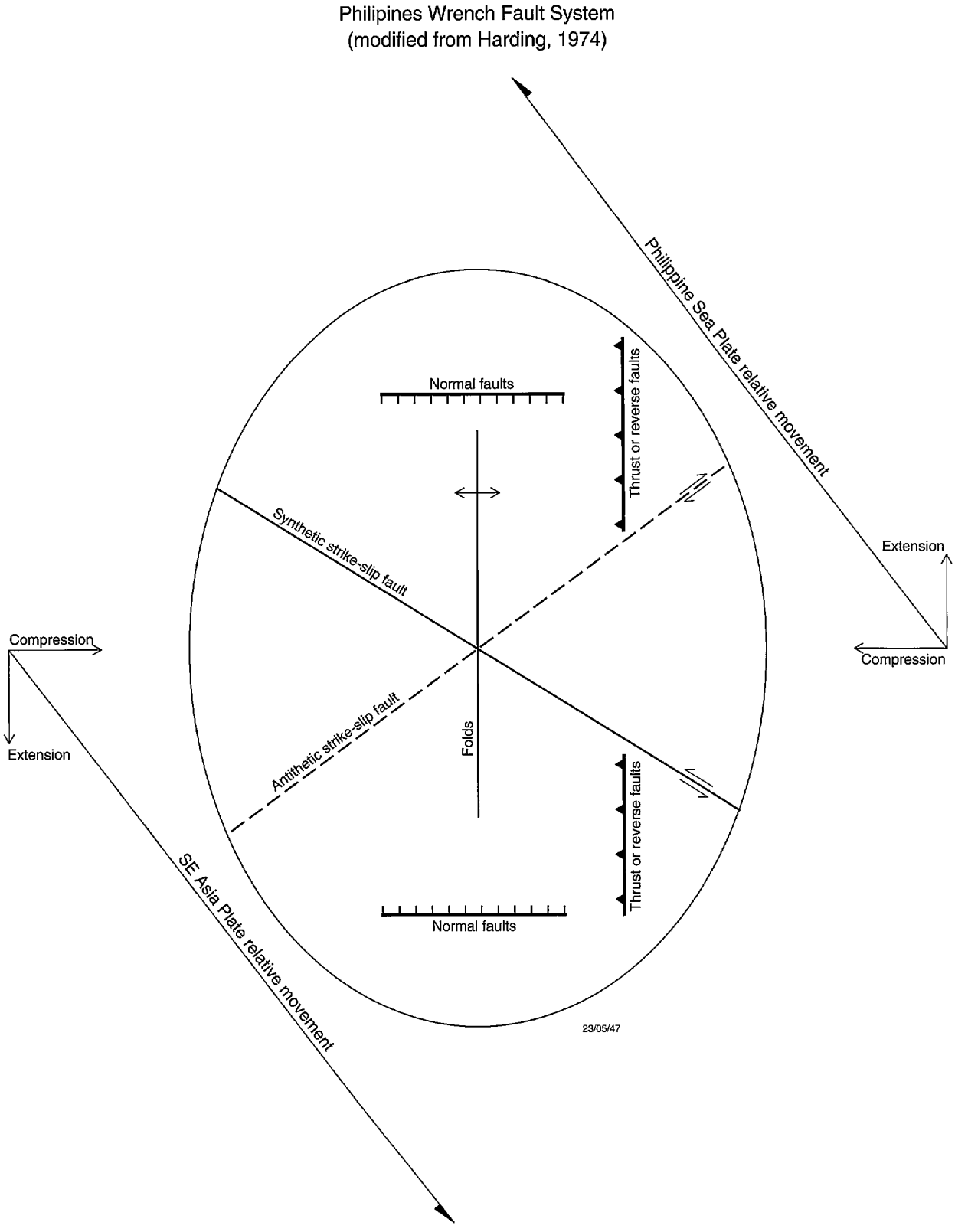

Figure 7 Strain ellipse for the Philippine Fault System. After Harding, 1974.

The Mompog-San Miguel Disruption is an antithetic wrench fault system that extends in an east-northeast direction from the vicinity of Mompog Island, located between Marinduque Island and Bondoc Peninsula, across Bondoc Peninsula, Ragay Gulf and Bicol Peninsula to the southwest corner of San Miguel Bay (Fig. 3). From east to west the feature is represented by: a down-to-south fault mapped from San Miguel Bay to Ragay Gulf near the southeast end of Caima Bay on Bicol Peninsula; the northwest termination of the Ragay Sub-basin and a 2 km wide east-west oriented graben in the Ragay Gulf; a series of right lateral faults mapped across Bondoc Peninsula; and down-to-south faults mapped across the southern end of Mompog Pass of Tayabas Bay. The nature of this "disruption" is uncertain. It seems to be a simple down-to-south fault in much of Bicol Peninsula, a more complex one in Ragay Gulf and Mompog Pass, yet on Bondoc Peninsula it coincides with four mapped right lateral faults that show only minor throw. Its orientation would coincide with the expected direction for right lateral faults in the strain ellipsoid model of the Philippine Fault System. It is perhaps best described as a combination of a right lateral fault with additional and highly variable down-to-south movement.

PETROLEUM GEOLOGY

Reservoirs

Both carbonate and clastic reservoirs may be present beneath Ragay Gulf. This can be predicted on the basis of an evaluation of reservoirs encountered in wells on the Bondoc Peninsula (Appendix 1) and from surface outcrop on Bondoc Peninsula showing that carbonate sequences of significant thickness are present in the Panaon Limestone, near the base of the Lower Vigo Formation and in the Malumbang Formation. Thinner carbonates are present in the Vigo and Canguinsa Formations. Clastic reservoirs are possible in the Lower Canguinsa and Lower Vigo Formations.

The Panaon Limestone overlying basement is seen in outcrops near Lian Point of the northeast Ragay Gulf and north of Unisan township in northwest Bondoc Peninsula. The Panaon equivalent, the Makalawang Limestone, occurs on Burias and Templo Islands where its base is not seen. On Bicol Peninsula the Siramag Marble and Pantao Limestone are probable time and environment equivalents of the Panaon and Makalawang Limestones. Seismic evidence shows a high amplitude event at shallow to moderate depth along the length of the Alabat-Burias High and adjacent areas. This interpreted Panaon-Makalawang-Pantao-Siramag Limestone event can be followed throughout much of Ragay Gulf where it is characterised by a high amplitude reflection beneath the comparatively reflection-free Vigo interval (Fig. 5). The Panaon interval is variable in thickness but is consistently characterised by high amplitudes. It is found at 0.8 to 1.0 seconds TWT along the crest and 1.0 to 1.5 seconds TWT down the flanks of the Alabat-Burias High. Careful analysis of the seismic, including specialised processing, may allow porosity variations within the carbonate to be detected. The Vigo Formation carbonates, around 10 m thick in outcrop, may also occur offshore but have not yet been identified on seismic. The Upper Canguinsa Formation carbonates, although very young, and not overlain by potentially sealing formations onshore, may provide sealed reservoirs offshore where the formation increases in thickness and is overlain by up to half a second of sediments. The formation therefore has optimum prospectivity in deep troughs where the thickness of cover is greatest.

From the outcrop geology and well data, clastic reservoirs are most likely to be found in the Lower Canguinsa and Lower Vigo Formations. Despite outcrop descriptions of sands as quartz-rich, well data indicates that sandstones are generally volcanoclastic, Fe-Mg rich, and contain only 10 to 15% quartz. Furthermore where encountered in the San Francisco wells, they are mostly carbonate cemented and of low permeability. Mayantok-1 well intersected a repeat section of Upper Vigo beneath a major reverse fault, and thus did not fully test the clastic reservoir potential of the Lower Vigo Formation. If the source of the Vigo and Canguinsa clastic sediments was from the Marinduque area in the west, as claimed by Poblete and Ferrer (1990), then cleaner sands may be present beneath Ragay Gulf. From the presence of numerous seeps and oil shows in wells, it would seem highly likely that any porous sand with an effective seal would be oil or gas filled. Any drilling should be done with muds that are least likely to react with unstable minerals in the clastic sands so that porosity is not occluded.

Geochemical Studies

Twenty-eight oil and gas seeps have been reported from Bondoc and Bicol Peninsulas, and from Burias Island (BED, 1986). In March 1993, DOE staff collected seven samples from seeps and leaking, abandoned, exploration wells on Bondoc and Bicol Peninsulas (Trinidad et al., 1993). These were analysed at the AGSO laboratories in Canberra as part of the Philippines Project (Cortez and Murray, 1993; Appendix 4). The main conclusions are:

1. The source rocks for all five sampled oils are rich in resinous, terrestrial, organic material and were deposited as hydrogen-rich shales in oxic or sub-oxic conditions, probably in a lower delta plain or inner neritic "fluvio-deltaic" setting. The age of the source rocks is Cainozoic, probably Oligocene or younger.
2. The Bondoc Peninsula oils were generated from early mature source rocks while those from the Bicol Peninsula appear to have come from a more mature source.
3. The isotopic composition of the Bondoc-3 gas well sample indicated that it came from a similar source to oils from the same area, and to water bottom DHD samples from beneath Ragay Gulf.

The geochemical DHD system was used concurrently with seismic shooting from R/V *Rig Seismic* and at night, on DHD only lines, when seismic shooting could not proceed due to the presence of fish traps. The DHD system utilises a submerged tow fish beneath the vessel which detects light hydrocarbons in bottom waters through continuous water sampling. Field observations of the DHD program on board the R/V *Rig Seismic* showed major oil/gas seeps in Ragay Gulf (Lee & Ramsay, 1992; Evans et al., 1992).

Two types of geochemical anomalies were observed (Bishop et al., 1992). Type I is characterised by high concentrations of methane, ethane and propane with traces of butane and pentane. Hydrocarbon wetness values (% wetness = $(C_2+C_3+C_4)/(C_1+C_2+C_3+C_4)$ x 100) are 1 to 1.5%. These are referred to as 'wet gas' anomalies. Type II or 'dry gas' anomalies, are characterised by high concentrations of methane, with only traces of ethane. Hydrocarbon wetness values are less than 0.5%. The difference between these two types of anomalies is believed to indicate the likely origin of the hydrocarbons (Heggie et al., 1993; Appendix 5; Evans et al., 1992). Type I anomalies show increasing wetness with increasing methane, suggesting that the hydrocarbons originate from gas-condensate rocks or accumulations. Type II anomalies show

decreasing wetness with increasing methane and originate from either dry thermogenic gas or biogenic hydrocarbons.

In order to help clarify the origin of DHD anomalies, whether thermogenic or biogenic, twenty-five gas samples were sent to the New Zealand National Institute of Water and Atmospheric Research Limited for C-13 isotopic analyses (Heggie et al., 1993; Evans et al., 1992). Subsequently eight of them were selected for additional C-14 analyses. The C-13 analyses showed that most samples are of a thermogenic origin, ranging from -57 to -38 °/oo (Evans et al., 1992). According to the Bernard model (Bernard et al., 1977; Rice & Claypool 1981; Claypool & Kvenvolden, 1983), all eight Type I anomalies samples were found to be of thermogenic origin; the Type II anomalies were thermogenic (7 samples), mixed thermogenic-biogenic (9 samples) and biogenic (1 sample). The C-14 measurements further supported the evidence for a fossil hydrocarbon source.

According to the Tissot and Welte model (1984), both the molecular and isotopic data suggest that the geochemical anomalies may be sourced from gas or condensate-prone source rocks (Heggie et al., 1993; Evans et al., 1992). It is interesting to note that the analyses of samples from onshore wells, San Francisco-1 and Bondoc-3, indicated a terrestrially derived, waxy kerogen source (BED, 1986). Further analyses of probable source rocks would help to clarify the actual kerogen type and composition of the source.

Source Rocks and Maturation

Little is known directly about source rocks in the Ragay Gulf area. No wells have been drilled in the gulf, and there are no records of source rocks from wells drilled on the Bondoc Peninsula. The Ragay and Burias Sub-basins are undrilled, and more than half of the prospective succession in the main part of the Bondoc Sub-basin, including the lower Vigo and Panaon Formations, remains untested. Furthermore, the zone of maturity for hydrocarbons is virtually undrilled as most wells terminated at depths less than two kilometres, which is above the oil generation window for this area. However, the widespread oil shows and seeps on the Bondoc Peninsula indicate that oil and gas are being generated in the Bondoc Sub-basin. The geochemical data, obtained from analyses of oil samples taken during field expeditions to the Bondoc Peninsula by DOE geologists, has confirmed the presence of mature sources from which generated hydrocarbons are currently migrating to the surface. Sampling of bottom waters by *Rig Seismic* in Ragay Gulf detected strong anomalous concentrations of hydrocarbons indicating that mature source rocks also exist in the Ragay and Burias Sub-basins, and on parts of the Alabat-Burias High.

Geohistory and maturation studies of the onshore wells (Appendix 2) suggest that the lower part of the Middle Miocene Vigo Formation, and probably the underlying Panaon Formation, are mature for hydrocarbon generation. This is confirmed by geohistory modelling of 'kitchen areas' near depocentres. In the Ragay 'kitchen', the whole of the Vigo Formation and half of the Lower Canguinsa are mature, and the oil generation 'window' is more than two kilometres thick. In the Burias Sub-basin, most of the Vigo Formation is mature, and the underlying succession is at optimum maturity. In the Bondoc East 'kitchen', near the Alabat-Burias High, most of the Vigo Formation is mature for oil generation and the Panaon Formation is mature for gas generation. This may account for the 'dry' anomalies and gas-condensate signatures of some offshore bottom water samples collected in the Ragay Gulf.

Because of the very moderate heat flows (1.5 HFU and less) and thermal gradients (35°C/km or less), the oil window begins at depths greater than 2000 m subsurface, definitely not at the shallower depths referred to in some of the literature (e.g. Yap, 1977, p.13). On the other hand, there is some evidence for suppression of vitrinite reflectance in the Vigo Formation (e.g. at San Francisco-1), which makes maturity appear less than it really is. This suppression is known to occur in very oil prone or oil-saturated sediments (Jeffrey et al., 1991, Snowdon and Powell, 1982). It has been taken into account in determining the depth of onset of maturity.

Migration and Timing

The succession in most of the Ragay Gulf, and especially in the depocentres, is more deeply buried now than at any previous time. Subsidence is continuing. Generation commenced within the deep synclinal areas of the Ragay and Bondoc Sub-basins in the Middle Miocene and is continuing on the flanks of these areas to the present day. It follows that traps of any age, even Recent, are in a position to intercept migrating hydrocarbons. In the west of the gulf, the leads on the Alabat-Burias High are situated between two 'kitchen' areas. They are therefore in a position to be charged by hydrocarbons from both east (the Ragay kitchen) and west (the Bondoc East kitchen).

Evaluation of Leads

There is a wide diversity of play types in the area arising from a multiplicity of source rocks, reservoirs and trapping mechanisms (Lee et al., 1993). There are three potential source areas: Bondoc, Ragay and Burias Sub-basins in all of which hydrocarbon seeps are documented. Traps include compressional fault dependent (Anima Sola) and fault independent closures (Alibijaban, Palad). Structuring of traps varies from an earlier pre-Middle Miocene phase (Arena), to a later phase from Miocene to Recent (Anima Sola). Over the Alabat-Burias High, drape structures occur that could be sourced from the Bondoc Sub-basin (San Narciso, Gorda), or from the Ragay Sub-basin (Bagulaya). Numerous similar but smaller structures are apparent in the Alabat-Burias High south of 13° 25' north. Late Miocene carbonate reefal buildups occur in the Burias Sub-basin (Apud) and the Bondoc Sub-basin (Gorda South). Potential traps associated with the diapirs of the Ragay Sub-basin, though not assessed, are a significant play and are worthy of exploration.

Leads were identified in eight areas (Fig. 8). They are described in the montages in Volume 4 (Plates R-6 to R-13) and summarised in Tables 1 to 8. All leads are located in fairly shallow water depths: five in less than 200 m, and three in between 200 and 400 m (Fig. 8). Due to the very limited data available on reservoir parameters and fluid properties, as well as the varying density and quality of seismic coverage, rigorous assessment of prospective structures was not possible. Consequently all prospective structures are termed leads rather than prospects. Despite this, it is hoped that the conservative parameters used in these assessments, which are based on the best guesses from the available data, will afford a basis for comparing the leads.

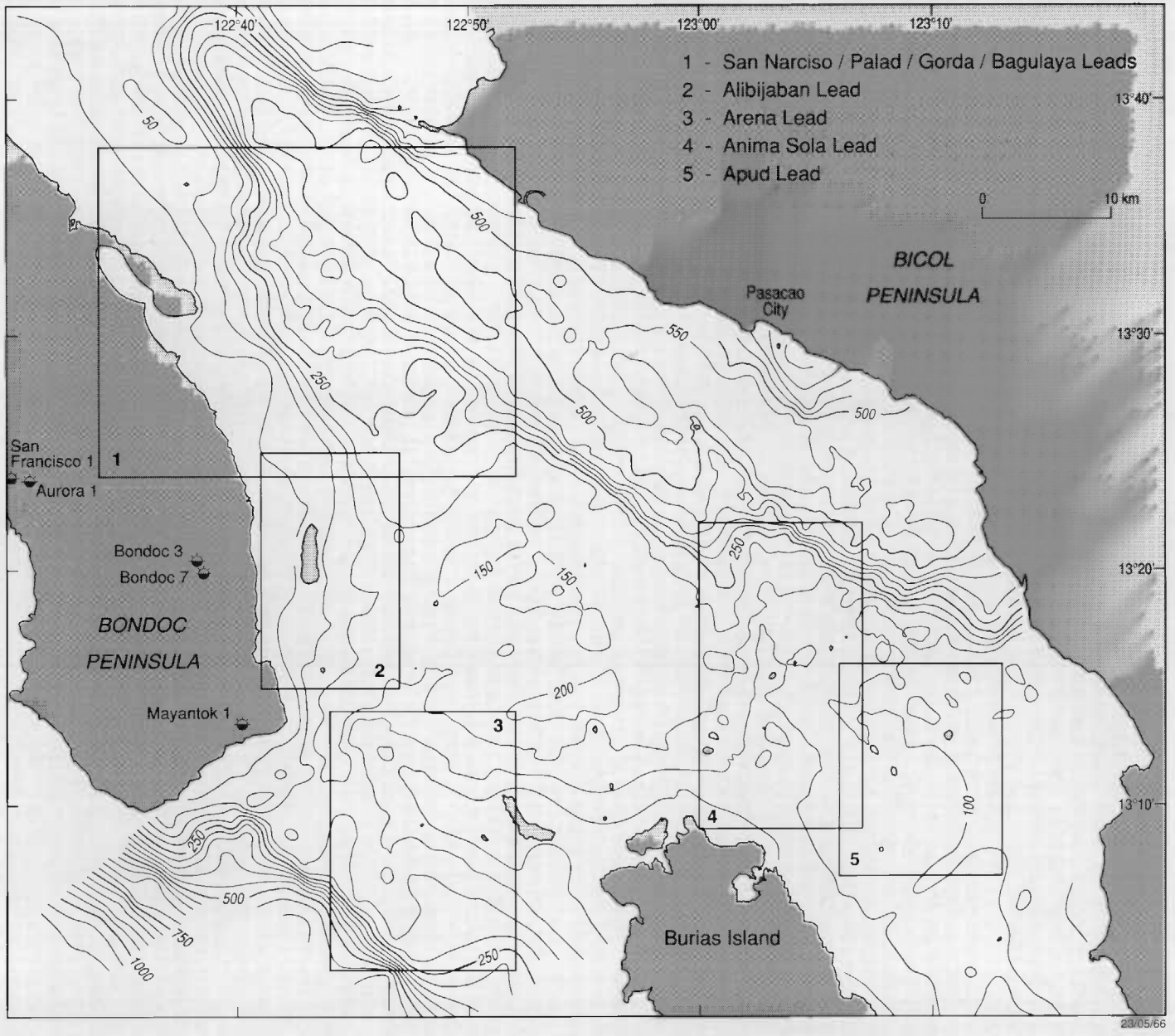

Figure 8 Bathymetry and location of leads in Ragay Gulf.

Table 1. Parameters for Alibijaban Lead

PLAY DESCRIPTION

HORIZONS	**: Top Lower Canguinsa (yellow horizon), Top Vigo (red)**
RESERVOIRS	**: Sandstones of the Lower Canguinsa and Lower Vigo Formations.**
SOURCE ROCKS	**: Shales of the Bondoc Sub-basin to the west**
TRAP AND SEAL	**: Major compressional structure of high to moderate relief with reservoirs sealed by interbedded shales**
MIGRATION	**: Migration up dip from the west and via faults from the underlying section**

RESERVE ESTIMATE

LOCATION	**: Line 9863-86, SP1960**
WATER DEPTH	**: 90 m**
WATER SATURATION	**: 30%**
RECOVERY FACTOR	**: 30%**
FORM. VOL. FACTOR	**: 1.4**

HORIZON	Yellow	Red
Top (ms)	≈100	≈320
Base (ms)	420	640
Area (Ha)	3878	3900
Reservoir type	sand	sand
Potential Res. Int.(m)	100	100
Gross/Potential	0.45	0.2
Net/Gross	0.4	0.5
Net Res. Thickness(m)	18	10
Net Res. Vol.(Ha.m)	69804	39000
Porosity	20%	15%
Reserves(MMBO)	132	55

Table 2. Parameters for Anima Sola Lead

PLAY DESCRIPTION

HORIZONS	**: Top Lower Canguinsa (yellow horizon), Top Vigo (red), Top Panaon Limestone (green), Intra-Panaon Limestone (brown)**
RESERVOIR	**: Sandstones of the Lower Canguinsa and Lower Vigo Formations, carbonates of the Panaon Limestone**
SOURCE ROCKS	**: Shales in the underlying Anima Sola Half Graben and the Ragay Sub-basin 10 km to the east**
TRAP AND SEAL	**: Major compressional structure with fault dependent closure east of Anima Sola Fault. Reservoirs at four levels are sealed by shales**

RESERVE ESTIMATE

LOCATION	**: Line 109-58, SP 860**
WATER DEPTH	**: 158m**
WATER SATURATION	**: 30%**
RECOVERY FACTOR	**: 30%**
FORM. VOL. FACTOR	**: 1.4**

HORIZON	Yellow	Red	Green	Brown
Top (ms)	≈290	≈480	≈835	≈1893
Base (ms)	500	750	1500	2200
Area (Ha)	1705	1097	5669	1234
Reservoir type	sand	sand	limestone	limestone
Potential Res. Int.(m)	100	100	100	100
Gross/Potential	0.45	0.2	0.75	0.75
Net/Gross	0.5	0.5	0.5	0.5
Net Res. Thckns(m)	22.5	10	37.5	37.5
Net Res. Vol.(Ha.m)	38362	10970	212588	46275
Porosity	20%	17%	15%	10%
Reserves(MMBO)	73.4	17.6	300	44

Table 3. Parameters for Apud Lead

PLAY DESCRIPTION

HORIZON	**: Top Lower Canguinsa (yellow horizon) and Top Vigo Formation (red horizon)**
RESERVOIRS	**: Carbonate reefal build-up of Late Miocene age and sandstones of the Lower Vigo Formation**
SOURCE ROCKS	**: Middle Miocene shales of the Vigo Formation and Oligocene-Early Miocene coaly sediments within the underlying Burias Sub-basin**
TRAP AND SEAL	**: Reefal build-up (yellow) and anticlines (red) sealed by shales**
MIGRATION	**: Migration up dip and via faults from the underlying section**

RESERVE ESTIMATE

LOCATION	**: Line 109-32, SP 1160**
WATER DEPTH	**: 90 m**
WATER SATURATION	**: 30%**
RECOVERY FACTOR	**: 30%**
FORM. VOL. FACTOR	**: 1.4**

HORIZON	Yellow	Red	
		North	South
Top (ms)	192	338	285
Base (ms)	400	400	500
Area (Ha)	5305	2506	2304
Reservoir type	carbonate	sandst	sandst
Potential Res. Int.(m)	75	50	50
Gross/Potential	0.75	0.2	0.2
Net/Gross	0.8	0.5	0.5
Net Res. Thickness(m)	45	5	5
Net Res. Vol.(Ha.m)	238725	12530	11520
Porosity	20%	15%	15%
Reserves(MMBO)	450	17.7	16.3

to replace
Volume I
Part I
p. 34 Thanks.

Table 3. Parameters for Apud Lead

PLAY DESCRIPTION

HORIZON	**: Top Lower Canguinsa (yellow horizon)**
RESERVOIRS	**: Carbonate reefal build-up of Late Miocene age**
SOURCE ROCKS	**: Middle Miocene shales of the Vigo Formation and Oligocene-Early Miocene coaly sediments within the underlying Burias Sub-basin**
TRAP AND SEAL	**: Reefal build-up sealed by shales**
MIGRATION	**: Migration up dip and via faults from the underlying section**

RESERVE ESTIMATE

LOCATION	**: Line 109-32, SP 1160**
WATER DEPTH	**: 90 m**
WATER SATURATION	**: 30%**
RECOVERY FACTOR	**: 30%**
FORM. VOL. FACTOR	**: 1.4**

HORIZON	**Yellow**
Top (ms)	**192**
Base (ms)	**400**
Area (Ha)	**5305**
Reservoir type	**carbonate**
Potential Res. Int.(m)	**75**
Gross/Potential	**0.75**
Net/Gross	**0.8**
Net Res. Thickness(m)	**45**
Net Res. Vol.(Ha.m)	**238725**
Porosity	**20%**
Reserves(MMBO)	**450**

Table 4. Parameters for Arena Lead

PLAY DESCRIPTION

HORIZONS : Top Panaon limestone (green horizon)

RESERVOIRS : Carbonates of the Panaon limestone

SOURCE ROCKS : Panaon and older sediments beneath and in the Bondoc Sub-basin to the north

TRAP AND SEAL : Structural high and possible carbonate buildup of Early Miocene Panaon Limestone sealed by shales in the overlying Middle Miocene section

MIGRATION : Migration up dip and via faults from the underlying section

RESERVE ESTIMATE

LOCATION : Line 9862-86, SP 460

WATER DEPTH : 90 m

WATER SATURATION : 30%

RECOVERY FACTOR : 30%

FORM. VOL. FACTOR : 1.4

HORIZON			Green		
TRAP	1 SW	1 NE	2	3	4
Top (ms)	500	780	430	517	200
Base (ms)	900	900	650	650	600
Area (Ha)	427	154	802	728	1664
Reservoir type	carb.	carb	carb	carb	carb
Pot'l Res. Int.(m)	100	50	50	50	100
Gross/Potential	0.75	0.75	0.75	0.75	0.75
Net/Gross	0.5	0.5	0.5	0.5	0.5
Net Res.Thckns(m)	37.5	18.8	18.8	18.8	37.5
Net Res.Vol.(Ha.m)	16013	2888	15038	13650	62400
Porosity	0.15	0.15	0.15	0.15	0.15
Reserves(MMBO)	22	4	21	19	88.3

Table 5. Parameters for Bagulaya Lead

PLAY DESCRIPTION

HORIZONS : Top Vigo (red horizon), Top Panaon Limestone (green)

RESERVOIRS : Sandstones of the Lower Vigo Formation, carbonates of the Panaon Limestone

SOURCE ROCKS : Shales of the Ragay Sub-basin to the northeast

TRAP AND SEAL : Structural high of moderate relief with reservoirs sealed by interbedded shales

MIGRATION : Migration up dip from the northeast and via faults from the underlying section

RESERVE ESTIMATE

LOCATION : Line 109-38, SP 692

WATER DEPTH : 315 m

WATER SATURATION : 30%

RECOVERY FACTOR : 30%

FORM. VOL. FACTOR : 1.4

HORIZON	Red	Green	
TRAP		West	East
Top (ms)	542	500	1000
Base (ms)	700	1000	1150
Area (Ha)	1714	1600	298
Reservoir type	sand	carb.	carb.
Potential Res. Int.(m)	50	50	50
Gross/Potential	0.2	0.75	0.75
Net/Gross	0.5	0.5	0.5
Net Res. Thickness(m)	5	18.75	18.75
Net Res. Vol.(Ha.m)	8570	30 000	5588
Porosity	15%	15%	15%
Reserves(MMBO)	12	42	8

Table 6. Parameters for Gorda Lead

PLAY DESCRIPTION

HORIZONS : Top Vigo (red horizon), Top Panaon Limestone (green)

RESERVOIRS : Sandstones of the Lower Vigo Formation, carbonates of the Panaon Limestone

SOURCE ROCKS : Shales of the Bondoc Sub-basin to the west

TRAP AND SEAL : Structural high of low to moderate relief with reservoirs sealed by interbedded shales

MIGRATION : Migration up dip from the west and via faults from the underlying section

RESERVE ESTIMATE

LOCATION : Line 109-34, SP 325

WATER DEPTH : 300 m

WATER SATURATION : 30%

RECOVERY FACTOR : 30%

FORM. VOL. FACTOR : 1.4

HORIZON	Red	Green		
TRAP		North	Central	South
Top (ms)	≈640	≈695	795	900
Base (ms)	700	900	900	1000
Area (Ha)	432	3340	272	190
Reservoir type	sand	carb.	carb.	carb.
Pot'l.Res. Int.(m)	50	75	50	50
Gross/Potential	0.2	0.75	0.75	0.75
Net/Gross	0.5	0.5	0.5	0.5
Net Res. Thckns(m)	5	28.13	18.75	18.75
Net Res. Vol.(Ha.m)	864	93938	5100	3563
Porosity	0.15	0.15	0.15	0.15
Reserves(MMBO)	7.6	133	7	5

Table 7. Parameters for Palad Lead

PLAY DESCRIPTION

HORIZONS	**: Top Vigo (red horizon), Top Panaon Limestone (green)**
RESERVOIRS	**: Sandstones of the Lower Vigo Formation, carbonates of the Panaon Limestone**
SOURCE ROCKS	**: Shales of the Bondoc Sub-basin to the west**
TRAP AND SEAL	**: High relief compressional structure with reservoirs at two levels sealed by interbedded shales**
MIGRATION	**: Migration up dip from the west and via faults from the underlying section**

RESERVE ESTIMATE

LOCATION	**: Line RG-83-801, SP 275**
WATER DEPTH	**: 73 m**
WATER SATURATION	**: 30%**
RECOVERY FACTOR	**: 30%**
FORM. VOL. FACTOR	**: 1.4**

HORIZON	Red	Green
Top (ms)	≈290	≈370
Base (ms)	700	900
Area (Ha)	2327	2323
Reservoir type	sand	limestone
Potential Res. Int.(m)	100	100
Gross/Potential	0.2	0.75
Net/Gross	0.5	0.5
Net Res. Thickness(m)	10	37.5
Net Res. Vol.(Ha.m)	23270	87113
Porosity	15%	15%
Reserves(MMBO)	33	123

Table 8. Parameters for San Narciso Lead

PLAY DESCRIPTION

HORIZONS	**: Top Vigo (red horizon), Top Panaon Limestone (green)**
RESERVOIRS	**: Sandstones of the Lower Vigo Formation, carbonates of the Panaon Limestone**
SOURCE ROCKS	**: Shales of the Bondoc Sub-basin to the southwest**
TRAP AND SEAL	**: Extensive low relief closure on the southwestern flank of the Alabat-Burias High. Reservoirs sealed by interbedded shales**
MIGRATION	**: Migration up dip from the southwest**

RESERVE ESTIMATE

LOCATION	**: Line 109-60, SP 780**
WATER DEPTH	**: 120 m**
WATER SATURATION	**: 30%**
RECOVERY FACTOR	**: 30%**
FORM. VOL. FACTOR	**: 1.4**

HORIZON	Red	Green
Top (ms)	580	705
Base (ms)	750	900
Area (Ha)	411	5964
Reservoir type	sand	carbonate
Potential Res. Int.(m)	100	50
Gross/Potential	0.2	0.75
Net/Gross	0.5	0.75
Net Res. Thickness(m)	10	28.13
Net Res. Vol.(Ha.m)	4110	167738
Porosity	15%	15%
Reserves(MMBO)	5.8	237

CONCLUSIONS

The 950 km of newly acquired seismic data and 280 km of reprocessed data (RG-83-8** lines) show a significant improvement in penetration and resolution over the pre-existing seismic data. The density and distribution of seismic coverage over the Ragay Gulf has also been improved allowing more confident definition of leads, many of which could not be detected with the former seismic coverage. Geochemical results, based on analyses of water bottom samples and samples collected from onshore seeps and leaking exploration wells, have confirmed the presence of mature source rocks from which generated hydrocarbons are currently migrating to the surface. The main conclusions are:

(1) The oil and gas potential in the Ragay Gulf area looks encouraging, with most of the petroleum occurrence criteria having been satisfied.

(2) Geochemical DHD results confirm onshore evidence indicating:

- the presence of widespread, mature source rocks,
- the existence of migration pathways to the surface and, by inference, to reservoirs.

(3) From onshore well and outcrop information the main potential reservoir rocks appear to be:

- carbonate sequences of both Early and Late Miocene age.
- volcanogenic clastic sands which may be cleaner beneath Ragay Gulf and are important secondary targets, especially as gas reservoirs.

(4) A wide diversity in play types is recognised. Hydrocarbons are probably being generated in three separate source kitchens in the Bondoc, Burias and Ragay Sub-basins. Both sandstone and carbonate reservoirs are believed to be present in a variety of traps formed during an early, pre-Middle Miocene phase of structuring (e.g. Arena) and a later phase which has in some cases continued up to the present (e.g. Anima Sola). Specific entrapment possibilities are:

- Compressional fault-dependent traps (e.g. Anima Sola).
- Compressional anticline with fault independent traps (e.g. Alibijaban and Palad).
- Late Miocene carbonate reefal buildups sourced from the Burias Sub-basin (e.g. Apud), or the Bondoc Sub-basin (e.g. South Gorda).
- Early Miocene carbonate reservoirs in drape over highs sourced from the Bondoc Sub-basin (e.g. San Narciso).
- Early Miocene carbonate reservoirs in drape over highs sourced from the Ragay Sub-basin (e.g. Bagulaya).

REFERENCES

ANTONIO, I.S., 1961 -- Geological report on PEC 68, 73, and 102 Northern Bondoc Peninsula Quezon Province, Luzon Island, Philippines, Fourth Calendar Year. Maremco Mineral Corp. and Republic Resources and Development Corp.Report, 53p. (unpublished).

ARCI, 1988 -- Radar image interpretation to assess the hydrocarbon potential of four sites in the Philippines. Arkansas Research Consultants Inc. Report, 3 volumes, 99p. (unpublished).

AURELIO, M.A., BARRIER, E., RANGIN, C., & MULLER, C., 1991 -- The Philippine fault in the Late Cenozoic tectonic evolution of the Bondoc-Masbate-N. Leyte area, central Philippines. *Journal of Southeast Asian Earth Sciences*, 6, 221-238.

BED, 1986 -- Sedimentary Basins of the Philippines - their Geology and Hydrocarbon Potential. World Bank financed Petroleum Exploration Promotion Project, prepared by the Bureau of Energy Development Office of the President, under the supervision of Robertson Research, Australia and Flower Doery and Buchan Pty Ltd., 12 volumes.

BERNARD, B., BROOKS, J.M. & SACKETT, W.H., 1977 -- A geochemical model for characterisation of hydrocarbon gas sources in marine sediments. *9th Annual Offshore Technology Conference*, Houston Texas, 435-438.

BISHOP, J.H., HEGGIE, D.T., LEE, C.S. & EVANS, D., 1992 -- New Clues to Petroleum Prospectivity of Offshore Philippine Basins with AGSO Surface Geochemical (DHD.) Techniques. *Australian Geological Survey Organisation Newsletter*, 17, 1-2.

CLAYPOOL, G. E. & KVENVOLDEN, K. A., 1983 -- Methane and other hydrocarbon gases in marine sediment. *Annual Review Earth Planet Science*, 11, 299-327.

CORBY, G.W. *et al.*, 1951 -- Geology and Oil possibilities of the Philippines. *Department of Agriculture and Natural Resources, Technical Bulletin.*, 21, 359 p.

CORTEZ, E.E. & MURRAY A.P., 1993 -- New Hydrocarbon Geochemistry of Oil and Gas Seeps from Bondoc and Bicol, SE Luzon Basin. *Interim Report of the Philippine Marine Seismic Survey Project*, Chapter 3, 69p., (unpublished).

EVANS, D., HEGGIE, D.T., BISHOP, J.H., REYES, E.N. & LEE, C.S., 1992 -- Light Hydrocarbon Geochemistry in Bottom Waters of the Philippines Continental shelf, Part A: Ragay Gulf and Tayabas Bay. *Australian Geological Survey Organisation Record*, 1992/92, 350p.

GALLOWAY, M.C., LEE, C.S. & RILLERA, F.G., 1992 -- Australian RV *Rig Seismic* Survey of Philippines - A Precursor To Renewed Exploration? *Proceeding of Offshore Southeast Asia Conference & Exhibition*, Singapore, 715-719.

HARDING, T.P., 1974 -- Petroleum Traps Associated with Wrench Faults. *American Association of Petroleum Geologists Bulletin*, 58-7, 1290-1304.

HASHIMOTO, W. & MATSUMARU, K., 1981 -- Geological significance of the discovery of Nummulites fichteli (Michelotti) from the Sagada Plateau, Bontoc, Mountain Province, Northern Luzon, Philippines: *Contributions to the Geology and Paleontology of Southeast Asia, CCXVI*, University of Tokyo Press, 75-192.

HEGGIE, D.T., EVANS, D., REYES, E.N., BISHOP, J.H., LEE, C.S., GALLOWAY, M.C. & LOWE, D., 1993 -- A Synthesis of Direct Hydrocarbon Detection (DHD) data from the Ragay Gulf, Philippines, with Implications for Hydrocarbon Exploration. *Interim Report of the Philippine Marine Seismic Survey Project*, Chapter 2, 82p. (unpublished).

JEFFREY, A.W.A., ALIMI, H.M., and JENDEN, P.D., 1991 -- Geochemistry of Los Angeles Basin Oil and Gas Systems. *In* BIDDLE, K.T., Active Margin Basins; *AAPG Memoir* 52, 197-219.

LEE, C.S. & RAMSAY, D., 1992 -- Philippines Marine Seismic Survey Project Cruise Report. *Bureau of Mineral Resources, Australia, Record*, 1992/49, 69p.

LEE. C.S., TRINIDAD, N.D., & GALLOWAY, M.C., 1992 -- A Preliminary Result of the Ragay Gulf Survey: Stratigraphy, Seismic and Geochemistry. *Geocon 1992. 5th Annual Convention of the Geological Society of the Philippines*, Plenary Session on Geo-energy, 23p.

LEE, C.S, GALLOWAY, M.C., MOORE, A., WEST, P., APOSTOL, J.R.L., ABANDO, R.P., PANGANIBAN, D.V., & GUAZON, E.B., 1993 -- Structure, Stratigraphy and Petroleum Potential of Ragay Gulf, Southeast Luzon, Philippines., *Interim Report of the Philippine Marine Seismic Survey Project,* Chapter 1, 148p. (unpublished).

POBLETE R.G. Jr., & FERRER, A.P., 1990 -- Regional geological study of the total Canguinsa section. Internal report, Logistic/Marketing Philippines Inc., 12p. (unpublished).

RICE, D.D. & CLAYPOOL, G.E., 1981 -- Generation, accumulation and source potential of biogenic gas. *American Association Petroleum Geology Bulletin,* 65, 5-25.

SAREWITZ, D.R. & LEWIS, S.D., 1991 -- The Marinduque intra-arc basin, Philippines: Basin genesis and *in situ* development in a strike-slip setting. *Geological Society of America Bulletin,* 103, 597-614.

SNOWDON, L.R., and Powell, T.G. 1982. -- Immature oil and condensates-modification of hydrocarbon generation model for terrestrial organic matter; *AAPG Bulletin,* 66, 775-588.

TISSOT, B.P. & WELTE, D.H., 1984 -- Petroleum formation and occurrence. Springer Verlag, Berlin, 2nd ed., 210p.

TRINIDAD, N.D., GUAZON, E.B., & ANICETO, A.G., 1993 -- Geological and Geochemical Field Trip Report of Bondoc and Bicol Peninsulas, Philippines. *Interim Report of the Philippine Marine Seismic Survey Project, 50p.* (unpublished).

YAP, A.L., 1972 -- Geological Report on PEC 68 Bondoc Peninsula, Quezon Province. Maremco Mineral Corp., 14p. (unpublished).

PART 2

GEOLOGY AND PETROLEUM POTENTIAL OF TAYABAS BAY

by

A. M. G. Moore[1] and J. Bacud[2]

1 Australian Geological Survey Organisation, Canberra, ACT, Australia
2 Department of Energy, Makati, Metro Manila, Philippines

ABSTRACT

Tayabas Bay is one of four offshore Philippine areas where the Australian Geological Survey Organisation and the Philippine Department of Energy conducted a cooperative marine seismic, gravity, magnetic, bathymetry and geochemical survey. The Australian International Development Assistance Bureau funded the project.

The project acquired 490 km of new seismic data in Tayabas Bay, and reprocessed 200 km of older data. A new seismic interpretation has revealed the structure of this tectonically active and geologically complex area. Evaluation for hydrocarbon reserves of several possible traps has identified three significant leads, namely, Yuni in the south, Mulanay in the central area, and Mabio in the north.

Geochemistry data, both offshore and onshore, have confirmed the presence of mature source rocks from which generated hydrocarbons are currently migrating to the surface both onshore and offshore. The present study suggests that there is a prolific source rock in the Middle Miocene Vigo Formation and/or the Late Oligocene-Early Miocene Panaon Limestone, and that oil and gas are being generated in the Bondoc Sub-basin, which is roughly coincident with the southern part of the Bondoc Peninsula. Several play types are envisaged in which hydrocarbons could be sourced from a 'kitchen' area in the Bondoc Sub-basin.

Two groups of reservoirs have been identified or proposed. The older group consists of shelf carbonates of the Early Miocene Panaon Formation beneath the mid-Miocene shales of the Vigo Formation on the Marinduque Platform. The second group consists of early Middle Miocene carbonates and basin-floor clastics near the base of the Vigo Formation.

Traps were formed when the Late Oligocene-Early Miocene carbonate reefs and shelf deposits of the Panaon Limestone were buried by the Middle Miocene clastics of the Vigo Formation. A later set of traps was formed (and sometimes superimposed) by intense deformation associated with the Philippine strike-slip fault system which has continued from the Late Pliocene up to the present. Specific entrapment possibilities are:

1. Fault-dependent traps, e.g. the structural closures against the Tayabas Bay Fault and the Bondoc Point Flower Structure in the Mulanay and Yuni lead areas.
2. Anticlinal fault independent traps, e.g. the Tuquian Anticline in the Mabio area, and the Mulanay Lead.
3. Pre-Middle Miocene carbonate reefal buildups containing hydrocarbons sourced from the Bondoc Sub-basin and sealed by the Vigo Formation, e.g. the mound underlying a fault-dependent closure against the Bondoc Point Flower Structure in the Yuni area.
4. Early Middle Miocene sands and carbonates in basin floor complexes, sourced from the Bondoc Sub-basin and sealed by the Vigo Formation, e.g. the extensive mound in the west of the Mulanay area, and the equally extensive complex in the western Yuni area.

This report deals with the geology and petroleum potential of Tayabas Bay and adjacent onshore areas. It is concluded that the Bondoc Peninsula is an active 'kitchen' area where hydrocarbons are now being generated.

CONTENTS

INTRODUCTION 7

TECTONIC SETTING 7

BATHYMETRY 10

STRATIGRAPHY 14

EXPLORATION HISTORY 17
- Licence History
- Seismic Surveys
- Exploration Wells

SEISMIC INTERPRETATION 18
- Data Description
- Well Ties
- Seismic Horizons
- Seismic Sequences
- Seismic Time Structure Maps
- Structural Interpretation
- Disturbed Structure
- Geologic History

PETROLEUM GEOLOGY 32
- Reservoirs
- Traps and Seals
- Onshore Geochemical Sampling
- Offshore Geochemical Sampling
- Source Rocks and Maturation
- Migration and Timing
- Lead Description and Evaluation
- The Effects of Faulting on Traps

CONCLUSIONS 41

REFERENCES 42

TABLES

Table 1 Parameters for Mabio Lead.
Table 2 Parameters for Mulanay Lead.
Table 3 Parameters for Yuni Lead.

FIGURES

Figure 1 Survey areas of the Philippines - Australia Marine Seismic Survey Project.
Figure 2 Tayabas Bay and Ragay Gulf showing location of AGSO/DOE/AIDAB survey and previous seismic lines.
Figure 3 Stratigraphy of Bondoc Peninsula.
Figure 4 Simplified cross section diagram of southern Tayabas Bay area.
Figure 5 Tectonic element map of Tayabas Bay area.
Figure 6 Seismic section 109-65 showing key horizons and Tayabas Bay Fault.
Figure 7 Mabio Lead at green horizon. Two-way time structure map.
Figure 8 Seismic section 109-66 showing Mabio Lead.
Figure 9 Mulanay Lead at green horizon (compensated for water depth variations).
Figure 10 Seismic section RG-83-808 showing Mulanay Lead.
Figure 11 Yuni Lead at green horizon (compensated for water depth variations).
Figure 12 Seismic section RG-83-807 showing Yuni Lead.

ENCLOSURES

Maps (see Volume 3)

Map T-1 Bathymetry of Tayabas Bay from seismic survey data. Scale 1:100,000.
Map T-2 Time structure map at top of Late Oligocene to Early Miocene Panaon Limestone (green horizon). Scale 1:100,000.
Map T-3 Time structure map of Mabio area at top of Late Oligocene to Early Miocene Panaon Limestone (green horizon) Sheet 1. Scale 1:50,000.
Map T-4 Time structure map at top of Middle Miocene Vigo Formation (red horizon) Scale 1:100,000.
Map T-5 Time structure map at top of Late Miocene Lower Canguinsa Formation (yellow horizon). Scale 1:100,000.

Plates (see Volume 4)

Plate T-1 Time structure map at top of Late Oligocene to Early Miocene Panaon Limestone (green horizon). Scale 1:150,000.
Plate T-2 Time structure map at top of Middle Miocene Vigo Formation (red horizon). Scale 1:150,000.
Plate T-3 Time structure map at top of Late Miocene Lower Canguinsa Formation (yellow horizon). Scale 1:150,000.
Plate T-4 Montage for Mabio Lead.
Plate T-5 Montage for Mulanay Lead.
Plate T-6 Montage for Yuni Lead.

INTRODUCTION

From March to May 1992, The Australian Geological Survey Organisation (AGSO), in conjunction with the Philippine Department of Energy (DOE), conducted a geophysical and geochemical survey in the Philippines using the Australian research vessel, *Rig Seismic* (Figure 1), under funding from the Australian International Development Assistance Bureau (AIDAB). As part of this survey, 490 kms of new seismic reflection data were obtained in Tayabas Bay (Figure 2).

Tayabas Bay lies to the west of the Bondoc Peninsula, and is the western part of the Southeast Luzon Basin. The basin is very complex, with major strike-slip and compressive faults, multi-phase tectonism and thick sedimentary infill (maximum more than 8 kms). It is about 200 kms long and 80 kms across, with the bulk of it offshore. It trends northwest-southeast, and is clearly a Tertiary basin, formed within an active Pacific margin volcanic island-arc system. It is dominated today by left-lateral strike-slip movement along the major Philippine Fault System, a result of the collision of the Pacific and Southeast Asia Plates. It is classified as a back-arc basin modified by wrenching (Bureau of Energy Development, BED, 1986). There are numerous onshore seeps of oil, and some exploration wells had initial flows of up to 200 barrels/day. Most of the wells with hydrocarbon shows are on the Bondoc Peninsula which borders Tayabas Bay on the east. There are no offshore wells.

The seismic data grid in Tayabas Bay consists of 490 kms of AGSO/DOE/AIDAB new data, 202 kms of recovered and re-processed data, and some 414 kms of previous exploration company data offshore, with a grid spacing of 2-5 kms (Figure 2). There is a sparse distribution of seismic profiles of older vintage onshore on the Bondoc Peninsula where there are gaps of up to 20 kilometres between data sets.

In March 1993, DOE staff collected 29 samples from oil and gas seeps in the Bondoc and Bicol Peninsulas. Analysis of these samples at the AGSO geochemistry laboratory provided further evidence for mature source rocks (Appendix 4).

An integrated interpretation of the new seismic and geochemical data with previous seismic and well data, has been undertaken for this study with the aim of assessing the petroleum potential. This report deals with the structure, stratigraphy and petroleum potential of Tayabas Bay and makes some reference to the adjacent Bondoc Peninsula. Overall, the Tayabas Bay area has encouraging oil and gas potential and the exploration rights are being made available to private oil companies.

TECTONIC SETTING

The regional tectonic and structural setting is shown on Plate R-1 (see Volume 4), which is based on the current study together with the radar image interpretation of the structure of the Bondoc Peninsula (ARCI, 1988) and geologic reports to the Republic of the Philippines Department of Energy.

The Tayabas Bay area is located within the Philippine Mobile Belt (Rangin, 1991) and is dominated by the left lateral Philippine Fault System. The Sibuyan Sea Fault (Forster et al, 1990, Aurelio et al, 1991), splits off from the Philippine Fault near Masbate Island, passing west of Ticao and southern Burias Island. It is considered by Sarewitz and Lewis (1991) to terminate south of the Bondoc Peninsula. The predominant tectonic grain is northwest oriented. The area is bordered to the east and north by the thick Bondoc Sub-basin and the Alabat Trough (BED 1986). To the west is the basement outcrop and the

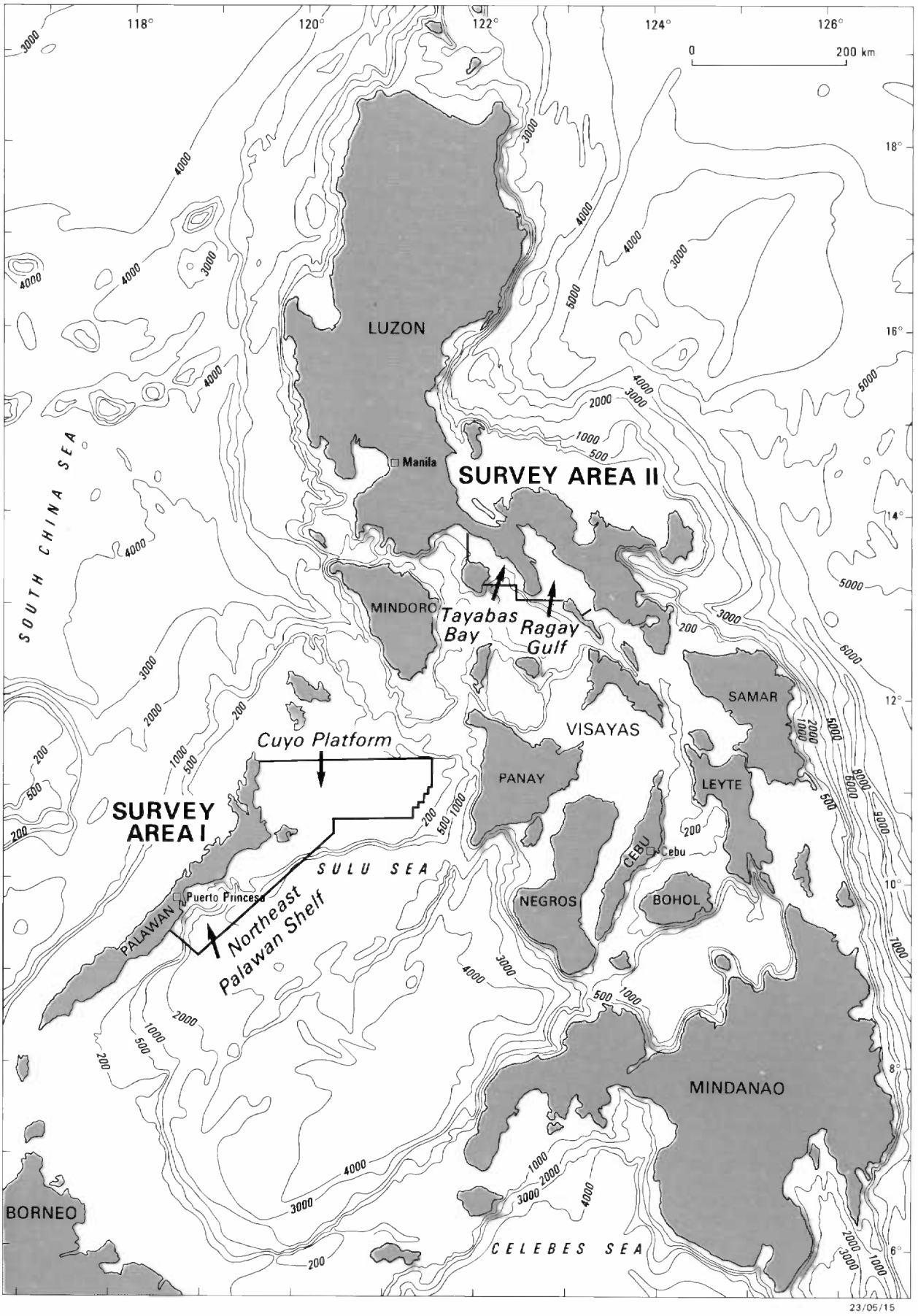

Figure 1 Survey areas of the Philippines - Australia Marine Seismic Survey Project.

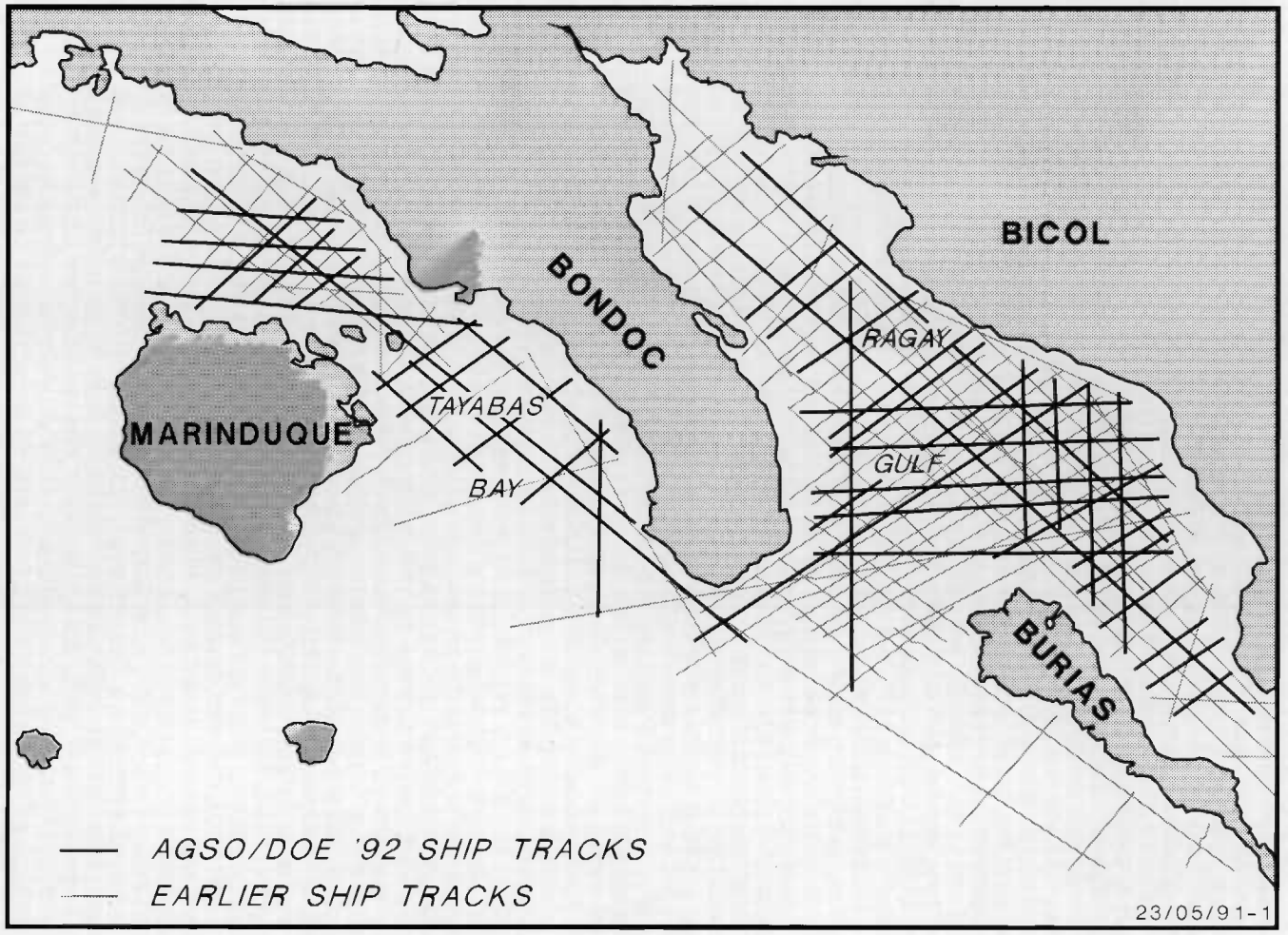

Figure 2 Tayabas Bay and Ragay Gulf showing location of AGSO/DOE/AIDAB survey and previous seismic lines.

modern volcanoes of Marinduque Island. To the south is a marine intra-arc basin (the Marinduque Basin), a small pull-apart feature with a central volcanic ridge and floored with oceanic crust (Sarewitz and Lewis, 1991).

The Tayabas Bay area is dominated by the following structural elements:

The Marinduque Platform occupies the northern and western parts of Tayabas Bay and outcrops on Marinduque Island. It is characterized by the absence of thick Miocene or younger sediments. In outcrop on Marinduque Island the mainly Oligocene Unisan Formation overlies Cretaceous basement. Outliers of Late Oligocene to Early Miocene Panaon Limestone occur on the island and probably underlie an Early Miocene unconformity (the green horizon of this study) offshore in Tayabas Bay. The seismic succession underlying the unconformity offshore is several hundreds of metres thick on many lines (e.g. lines RG-83-808A, 109-65). Carbonates and clastics, including some volcanogenics, may occur under the Middle Miocene shales offshore on the Marinduque Platform, east of the island.

The Bondoc Sub-basin is a deep linear trough underlying the southern half of the Bondoc Peninsula and nearby areas offshore. It is filled with up to 8 kilometres of sediments of Miocene to Pleistocene, but mainly mid-Miocene, age (Figure 3). This study has defined the western boundary of the sub-basin, offshore to the west of the Bondoc Peninsula where it onlaps the older rocks of the Marinduque Platform. There is seismic evidence that it not only onlaps, but may be thrust onto, the platform, with decollement at the base of and within the Middle Miocene Vigo Formation. A simplified cross section is shown is Figure 4.

A large strike-slip fault, mapped by this study (Figure 5)and named the Tayabas Bay Fault (new name), traverses the area from southeast to northwest, cutting across the other two elements and apparently post-dating them. It may be a continuation of the Sibuyan Sea Fault. An area of disturbed structure near the southern tip of the Bondoc Peninsula has been named herein the Bondoc Point Flower Structure (new name). These elements are further described and explained below in the sections on seismic interpretation and structure.

BATHYMETRY

The most detailed bathymetry of the area is available on nautical chart No. 4218, Ragay Gulf to Tayabas Bay at 1:200,000 scale, published by the Philippines Coasts and Geodetic Survey and the similar nautical chart No. 91340 published by the Defense Mapping Agency, Hydrographic/ Topographic Centre Washington D. C. These maps show good detail in the shallow areas (<40 m), but in the deeper areas, they become progressively less reliable owing to reduced density of data. The seismic, on the other hand, is most reliable in water depths greater than about 60 m, and becomes less so in shallow water owing to the muting of the water bottom reflection during processing. Using the PETROSEIS mapping system, a water depth contour map (Map T-1) was made from the digitised water bottom reflection times of the seismic sections. These data were converted to depth using a water velocity of 1500 metres per second. Data from all surveys in the Tayabas Bay were used and there was remarkably good agreement at line intersections. The map shows good agreement with the nautical charts beyond the 20 fathom line (~40 m) and far more detail than the nautical charts in deeper water. Note that Map T-1 has not been integrated with the nautical chart, though it has been visually compared. North of Mompog Island, the water depth is uniformly shallow (100 m or

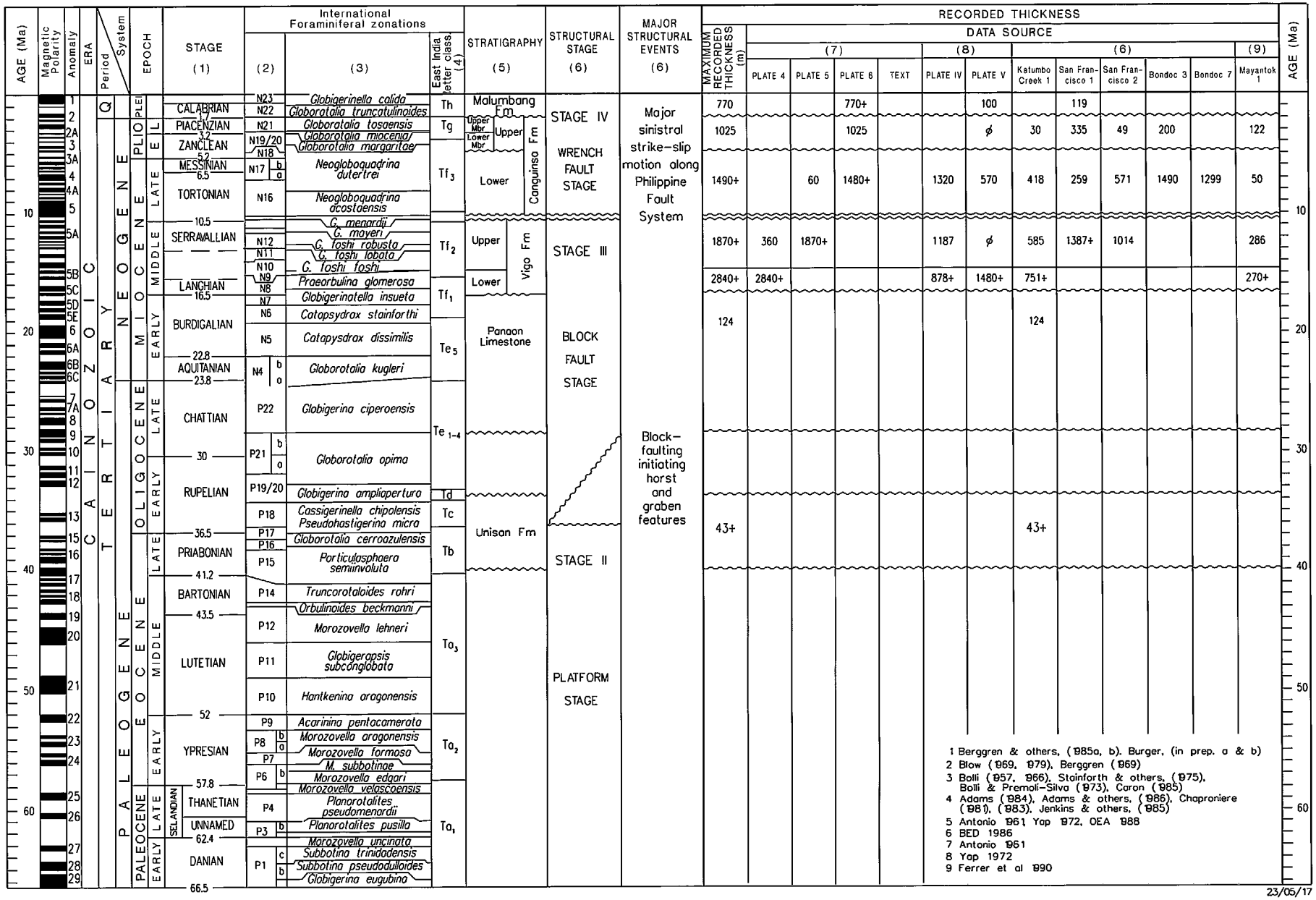

Figure 3 Stratigraphy of Bondoc Peninsula.

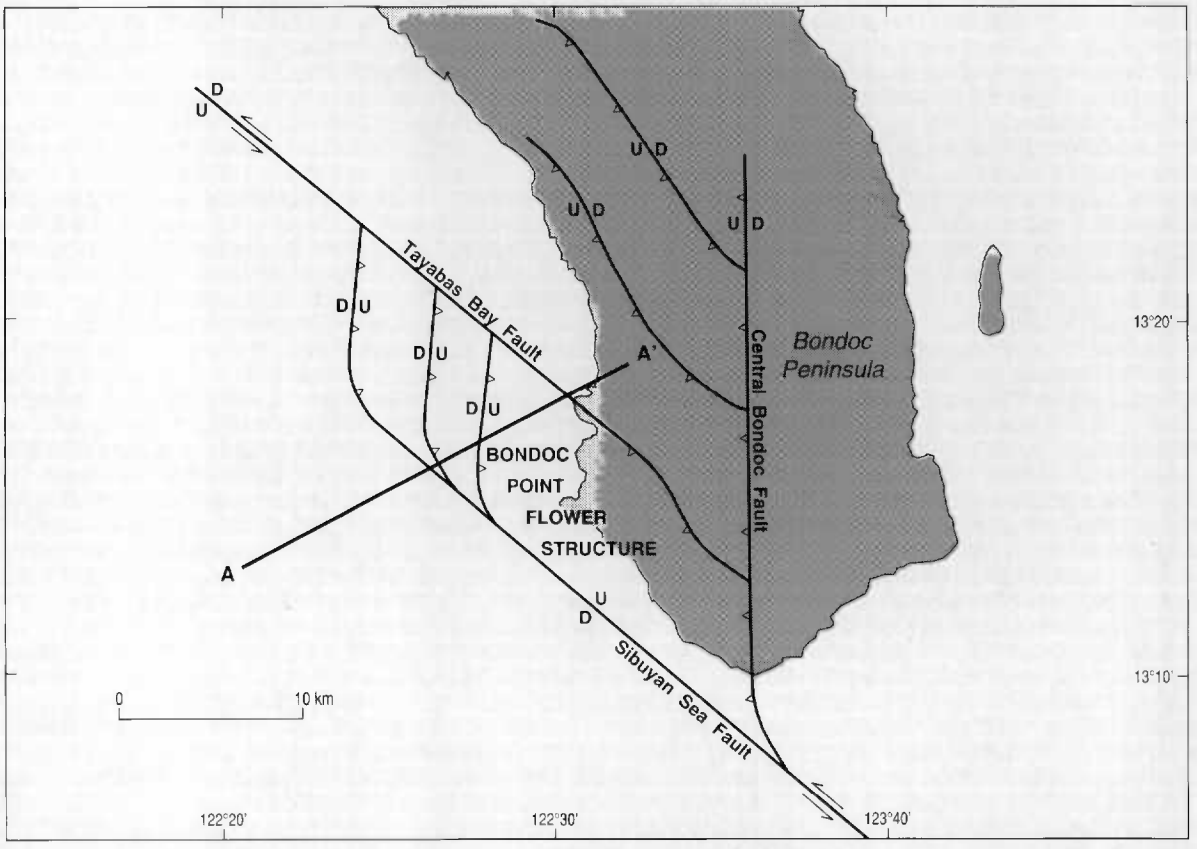

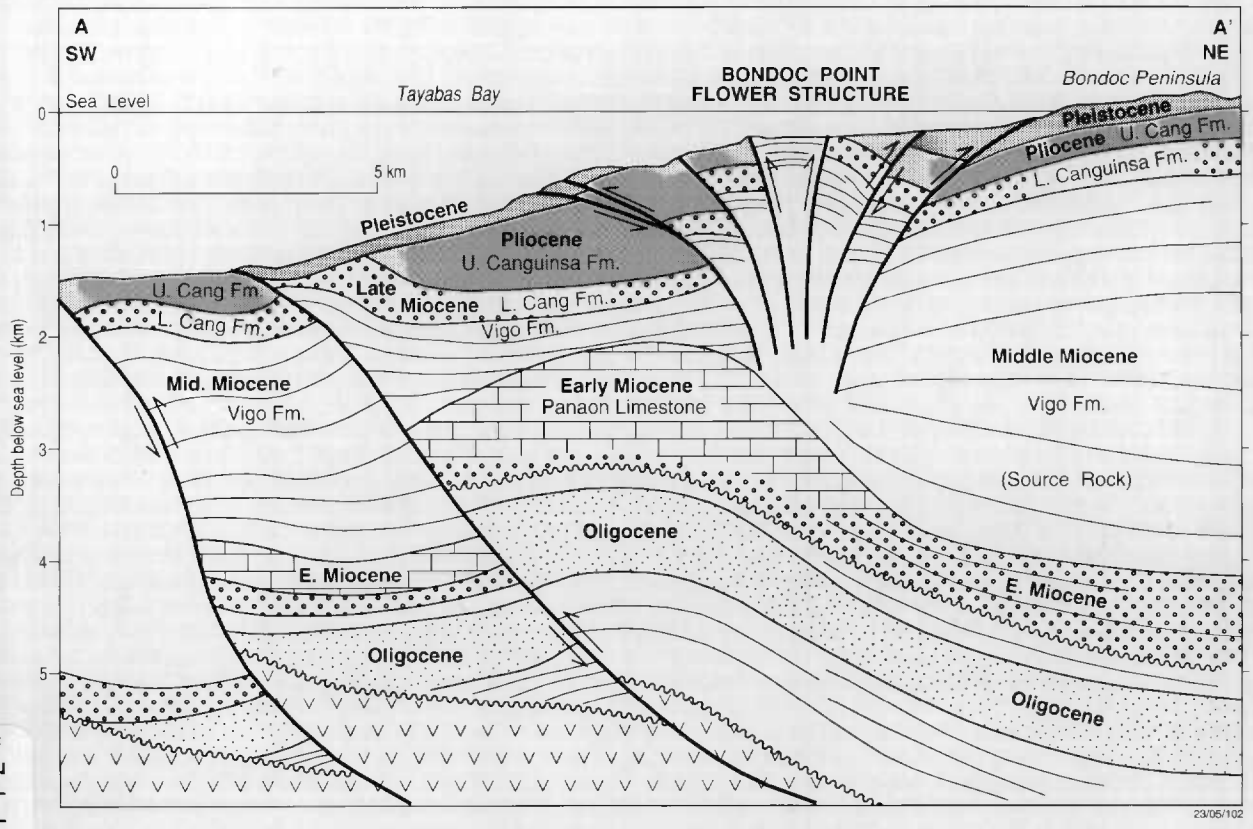

Figure 4 Simplified cross section diagram of southern Tayabas Bay area.

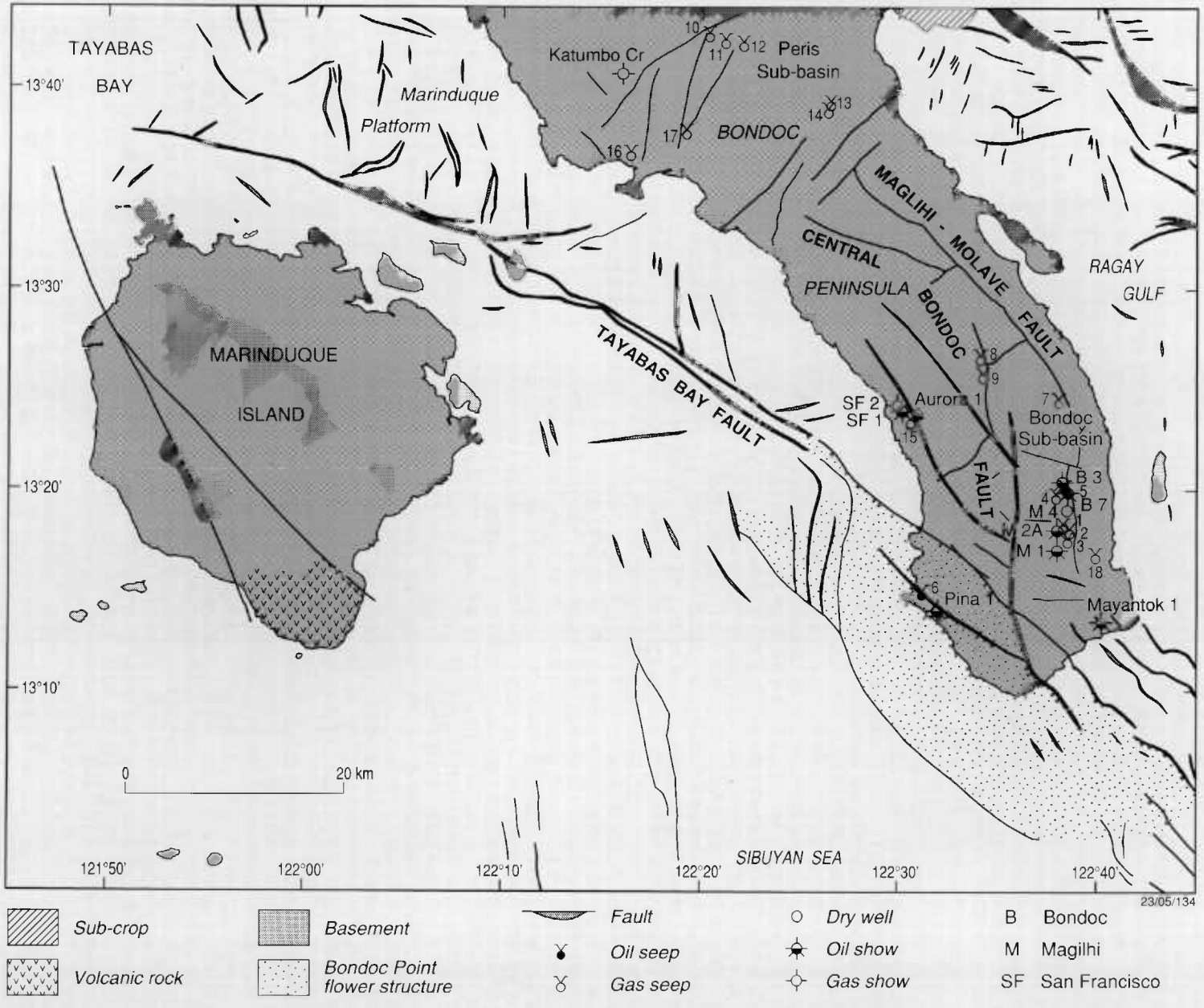

Figure 5 Tectonic element map of Tayabas Bay area.

less) over the Marinduque Platform. South of Mompog, it deepens to more than 2000 m as a result of the development of the Marinduque Basin. Offshore from the southern Bondoc Peninsula, the northeastern flank of the basin is currently undergoing shallowing as a result of westerly thrusting from the peninsula.

STRATIGRAPHY

Tayabas Bay is bounded to the east by the Bondoc Peninsula and to the west by Marinduque Island. The sequence interpreted to underlie Tayabas Bay has been correlated with the stratigraphy of Bondoc Peninsula (Figure 3).

Several maps and reports from oil and mineral companies, and data from the wells, provided the information regarding the stratigraphy of the Bondoc Peninsula. Of 25 wells drilled on the peninsula, 15 are less than 1000 m deep, three range between 1000 m and 1500 m, four exceed 1500 m and only two exceed 2000 m. Just four wells, Katumbo Creek-1, San Francisco-1 and-2 and Mayantok-1, have a complete suite of logs. Two wells, Aurora-1 (2088 m) and Aurora-2 (1103 m), 1970, have only sp-resistivity logs, which were only run over a limited depth range. The absence of sonic, gamma ray, neutron or density logs seriously limits the usefulness of these wells for correlation purposes.

Lithological descriptions of field outcrops (Antonio, 1961; Yap, 1972; Poblete and Ferrer, 1990) and information from the World Bank Report (BED, 1986), provided information for the rock description below. The stratigraphy and a simplified cross section diagram are given in Figures 3 and 4.

Basement

On Marinduque Island, in the west of the study area, basement consists of metamorphosed greenschist facies, ophiolitic lava flows with intercalated greywackes, and siltstones. In a minor limestone member, *Globotruncana sp,* characteristic of Cretaceous age, was identified (BED, 1986).

The oldest rocks known on the Bondoc Peninsula outcrop in the northwest, about 2 to 3 km northeast of Unisan town. Locally, the foliated hornblende schists with scattered quartz veins comprise the lithology. Alteration of chlorite and epidote is common. Estimation of their thickness, however, was not possible.

Unisan Formation

Unconformably overlying the basement schists is the Unisan Formation. It consists of volcanoclastic carbonate breccia composed of fine-grained porphyritic volcanics and tuffs, together with penecontemporaneous tuffaceous silty carbonates containing rich foraminifera. The thickness of the unit is unknown. The age is late Eocene to late Oligocene, probably in the range P15-P19. In Katumbo Creek well, it shows close petrographic affinities in composition, texture and alteration to the outcrop samples from northern Bondoc Peninsula (BED, 1986).

Panaon Limestone

The Panaon Limestone unconformably overlies the Unisan Formation. It consists of limestone which varies from dense crystalline with coralline relics to completely recrystallised. The recrystallisation is believed to be due to surface alteration and may not indicate lack of porosity at depth. It was deposited in shallow marine conditions in the Late Oligocene to Early Miocene (N3/P22-N7). It is the target for a number of leads

identified offshore and is the age equivalent of the Nido Limestone of northwest Palawan which is the Philippines' major producing horizon.

Toward the south of the Bondoc Peninsula, both onshore and adjacent to it offshore, the seismic data indicate that this carbonate unit is deeply buried. It is thought to be highly variable in thickness and locally lenticular. The maximum thickness on Bondoc Peninsula is estimated to be about 1000 m.

Vigo Formation

The Vigo Formation (Vigo Shale of Pratt & Smith, 1913; Gumaca Formation of Antonio, 1961; Yap, 1972) outcrops along the length of Bondoc Peninsula. It varies from conformable to unconformable relative to the underlying Panaon Limestone. According to BED (1986), the Vigo Formation unconformably overlies the Panaon Limestone, but Antonio (1961) believes that the two formations are conformable, as evident from the presence of numerous limestone lenses up to 10 m thick near the base of the Lower Vigo, predominantly in the Pitago-Gumaca area. This suggests a facies transition from the clastic-poor sedimentation of the Panaon Limestone to the clastic-dominated sedimentation of the Vigo Formation. Geochemical analyses (BED, 1986) of well cuttings and outcrop samples show the Vigo Formation to have significant hydrocarbon source potential. It has been subdivided into upper and lower parts.

The Lower Vigo Formation consists predominantly of alternating coarse to very fine grained sandstone, and sandy to silty shale. Where the base of the formation can be observed in the far northwest of the Bondoc Peninsula, lenses of limestone up to 10 m thick with conglomerates and volcanic interbeds occur in up to five separate horizons. Local occurences of carbonaceous silts, shales and coal seams are noted. The conglomerates contain pebbles of schists, volcanic rocks and limestone. The thickness of the unit in its incomplete section is 2840 m but the total thickness was estimated to be 3000-4000 m (Antonio, 1961). It was deposited in an environment that varied from shallow marine, as evident from the common limestone throughout, to coastal paludal coal swamps, as is evident from the common though thin coal seams and carbonaceous silts and shales. Age is earliest Middle Miocene (N8-N9).

The Upper Vigo Formation shows a conspicuous increase in the ratio of conglomerate and sandstone as compared to sandstone and shale over the Lower Vigo Formation. Individual conglomerate-sandstone beds are usually over 1 m thick. Limestone lenses are scattered throughout the section. Volcanic interbeds are known from several locations, all in the northwest, near Pitago-Unisan. In the southern Bondoc Peninsula, the formation is less sandy and has been termed the Vigo Shale (Corby, 1937; Hashimoto and Matsumaru, 1981). Maximum thickness of the Upper Vigo Formation was measured to be 1870 m. It was deposited in similar conditions to the Lower Vigo Formation in the Middle Miocene (N10-N14).

Canguinsa Formation

The Canguinsa Formation overlies the Vigo Formation with a marked angular unconformity in places. It is subdivided into an upper and lower part (Lopez and Hondagua Formations respectively of Antonio 1961; Yap 1972).

The lower part of the Lower Canguinsa Formation consists of cross-bedded sandstone and poorly sorted conglomerate with interbedded grey shale, siltstone and dark-coloured sandstone. Carbonaceous streaks appear throughout the section. The conglomerate

contains pebbles of quartz, schists, igneous rocks, limestone, some hard siltstone and sandstone with finer grains of quartz schist and igneous rock fragments. The conglomerate in the upper part is lighter in colour, calcareous and contains mica flakes but with minor carbonaceous materials. Maximum recorded thickness is 1490 m in Bondoc 3 well and similar thicknesses have been measured in the field in northern Bondoc. The presence of limestones and thin coals and carbonaceous silts and shales indicate a varying depositional environment ranging from shallow marine to littoral-paralic, the same as with the Vigo Formation. Age is Miocene (N16-N17).

In general, southeast of Peris Bay-Catanauan, the Lower Canguinsa can be subdivided into lower and upper members. This subdivision is not readily recognisable in the west but is clearly evident in the southeast. The Lower Member consists predominantly of siltstone and claystone with minor interbeds of fine grained sandstone and rare conglomeratic lenses. It was deposited in an outer neritic to bathyal marine environment. The Upper Member shows an increase in coarse materials which is evident both in well cuttings and surface outcrops. The sandstones are volcanic wackes, fine to medium grained, with clasts made up of metavolcanics, andesite and polycrystalline quartz with various bioclasts in a clay-carbonate matrix.

The Lower Canguinsa Formation in the west cannot be subdivided. Sandstones are predominant as medium to coarse grained volcano-feldspathic wacke which are made up of lithic fragments, poly-crystalline quartz, plagioclase and planktonic foraminifera with abundant plant debris.

The Upper Canguinsa Formation conformably overlies the Lower Canguinsa north of Peris Bay-Catanauan. A time break disconformity is suggested by the absence of thin shelled mega-fossils in the Lower Canguinsa and their common occurrence in the Upper Canguinsa. South of Peris Bay-Catanauan, on the east side of the Peninsula, there is an obvious angular unconformity in the field and in San Francisco-1 and -2. Faunal changes in the cuttings have been recorded in Katumbo Creek-1, San Francisco-1, -2 and Mayantok-1, as well as dipmeter changes in San Francisco-1 and -2. Poblete and Ferrer (1990) believe the provenance of the Canguinsa Formation was the Tayabas-Marinduque area. Lithologically, it consists predominantly of indistinctly bedded calcareous and micaceous, buff-coloured siltstone interbedded with thin mudstone layers and some limestone. There are conspicuous thin shelled megafossils throughout. The maximum thickness claimed by Antonio (1961) exceeds 1025 m but the formation is believed to thicken to the southeast. The unit appears to have been deposited exclusively in shallow marine conditions during the Pliocene (N18-N21).

Malumbang Formation

The Malumbang Formation (Catanauan Limestone of Antonio, 1961; Yap, 1972) unconformably overlies the Canguinsa Formation. It forms a relatively flat blanket on all older units. A three-fold subdivision is evident in the north: a lower part, consisting of chalky white, porous, dense, crystalline megafossiliferous limestone; a middle part, which is a sequence of silty to shaley calcareous sandstone with limestone interbeds and; an upper part, consisting of porous, gently dipping limestone. In contrast, this subdivision is not recognised in the south. The Malumbang Formation is generally a very shallow marine carbonate complex with the lithology varying from reefal limestone to detrital carbonates and some clastic facies. Maximum recorded thickness is about 770 m and its age is Pleistocene (N22-N23).

EXPLORATION HISTORY

Licence History

Several petroleum contracts have been awarded in the area, but they were mostly on the Bondoc Peninsula and covered only small portions of Tayabas Bay. Among the recent contracts were those of SEDCO, PODCO and Ran Ricks (Far East Resources). The Geophysical Survey and Exploration Contract (GSEC) No. 12 of 280,000 hectares, including about 38,000 hectares of northern Tayabas Bay, was awarded to SEDCO in February,1976 and was relinquished in August,1980. SEDCO acquired the T-*-79 series of seismic lines offshore and drilled the Katumbo Creek-1 well in Bondoc Peninsula. PODCO's Service Contract No.20 covered about 100,000 hectares and ran from August,1976 to relinquishment in December,1979. Two wells were drilled, namely, San Francisco-1 and -2. GSEC No.46 of Ran Ricks/Far East Resources covered 368,000 hectares and was effective from January,1988 to July,1990. Ran Ricks drilled the Mayantok-1 well. Both PODCO and Ran Ricks restricted their seismic acquisition to portions of the Bondoc Peninsula.

Seismic Surveys

Since 1979 a total of approximately 1300 line km of seismic data have been recorded in the Tayabas Bay area and on Bondoc Peninsula by different organisations. The distribution is as listed below:

RECORDED BY	LINE NAME	LOCATION	LINE-KMS
BED-Seiscom Delta	RG-83-8**	Tayabas Bay	202
SEDCO	T-*-79	Northern Tayabas Bay	414
PODCO	B-*-79	Central Bondoc Peninsula	111
Ran Ricks	B-10*	Southern Bondoc Peninsula	70
AGSO/DOE/AIDAB	109-*	Tayabas Bay/Ragay Gulf	490
		TOTAL LINE-KMS	1287

Exploration Wells

There are no wells in Tayabas Bay. Of the twenty five wells drilled on the Bondoc Peninsula, many are very shallow and poorly documented. Of the pre-1940 wells, Richmond's Pina-1 in 1924, drilled to 1565 m within the Bondoc Point Flower Structure, produced gas at the rate of 2600 m^3/day. Most others had hydrocarbon shows. Of the wells drilled since World War 2, the most significant are Bondoc-3 and -7, Aurora-1, San Francisco-1 and -2, Katumbo Creek-1, and Mayantok-1. The deepest well is San Francisco-1, drilled to 2088 m. Only four have significant log suites. Again, most had hydrocarbon shows.

Most of the Bondoc Peninsula wells were drilled near seeps or on surface anticlines. There was very little subsurface information prior to drilling. The interpretation of seismic for this study suggests that the surface anticlines on the Bondoc Peninsula, especially in the south, may be de-coupled from the subsurface. Hence, wells located on surface anticlines may not have been located on the same feature at depth. Katumbo Creek, for example, one of the few wells without shows, was drilled low on the flank of the central Bondoc anticline, and penetrated a major fault-plane. Mayantok-1, and

probably San Francisco-1, drilled through unexpected thrust planes. The discussion of structure by Nicolai et al (1973, p. 28) summarises possible reasons for the failure of many of these wells.

Since only about 2 km of the 7 km of Miocene sediments in the southern Bondoc Peninsula have been drilled, the hydrocarbon source rock has probably not been penetrated.

SEISMIC INTERPRETATION

Data Description

This study used migrated seismic sections which were available for all lines, except the T series lines offshore and the B series onshore. All lines are displayed at a vertical scale of 10 cm per second. Horizontal scales are generally about 1:20,000 to 1:25,000. The onshore lines were too far apart to enable mapping of the Bondoc Peninsula. Some lines (e.g.the 1979 B-series acquired onshore by PODCO) also showed shadow zones which are attributed to disturbed structure and severe reverse faulting. The 109-series data acquired in 1992 are of very good quality. Considerable processing effort was applied to problem areas of incoherent reflections. These are now considered to be areas of distorted structure caused by compression, with complex thrust and reverse faulting and probable shale flowage. The BED data (RG-83-series), reprocessed on AGSO's in-house system, generally are of very good quality.

The AGSO/DOE/AIDAB lines (109-series) and the BED reprocessed lines provided the interpretation framework to which the T-series lines were tied. The B series onshore lines and lines south and east of Bondoc Peninsula were 'jump-correlated' with the Tayabas Bay interpretation, because there are no direct ties across the coast and across the reflection-free zone of the Bondoc Point Flower Structure.

Well ties

The San Francisco-1 well on Bondoc Peninsula provided an approximate tie of the top of the Middle Miocene Vigo Formation to the red horizon on the PODCO line B-2-79. This seismic horizon tie was carried to the western part of the Bondoc Sub-basin offshore in Tayabas Bay by character correlation across a coastal gap of five kilometres. Correlation from the offshore Bondoc Sub-basin to the Marinduque Platform was across the disturbed stratigraphy and thrust faulting of the Bondoc Point Flower Structure. The green horizon, the main regional unconformity, was below TD of the San Francisco-1 well but, from regional considerations, is thought to correlate with the base of the Vigo Formation.

The Mayantok-1 well was tied through the northeast-southwest seismic Line B-105 to Lines B-109, 8, 7, and 6 that run northwest. The Katumbo Creek-1 well was tied to the onshore PODCO Line B-8-79 through the wellsite, and jump-correlated to the nearby offshore lines. This is the only well that penetrated the mid-Miocene shales, the Panaon Limestone and the basement, but its reliability as a tie is dubious owing to the proximity of a major fault-plane.

Using the above ties, and the interpretations in BED (1986), six horizons and their associated sequences were picked in Tayabas Bay and tentatively correlated with the onshore stratigraphy.

Seismic Horizons

Of the six horizons identified, most are major sequence boundaries. Three of these (the green, red and yellow horizons) are widespread, while others (blue, orange and pink horizons) have limited extent or could not be identified on some lines.

The blue horizon appears as a high amplitude, moderately continuous, low frequency reflection which is generally mappable in the shallower northern Tayabas Bay. It is evident on the AGSO lines and to a lesser extent on the SEDCO (T-series) lines. In the offshore area south of the Mompog-San Miguel Disruption, the horizon often is not recognisable because of the intense structuring and disturbed stratigraphy in much of the area. On the Marinduque Platform, it is generally conformable with the sequence above and below. It is believed to be derived from a lateral equivalent of the top of Unisan Formation of Late Eocene to Early Oligocene age. A contour map of this horizon has not been produced.

The green horizon in Tayabas Bay is not tied directly to any well, because of intervening faults and structures, and the gap in seismic coverage at the coast. Besides, it is believed that none of the wells on the Bondoc Peninsula penetrated this stratigraphic level except Katumbo Creek-1. It is identified by its character on seismic (e.g. line 109-65, Figure 6), and is the most widespread and visible major deep unconformity in the region. From considerations of regional geology, the green horizon is believed to correspond with the unconformity at the top of the Panaon Limestone Formation of Late Oligocene and Early Miocene age, and the base of the Vigo Formation shales of Middle Miocene age. The presence of the Panaon Limestone beneath the unconformity is inferred. To the west, it is mapped in outcrop on Marinduque Island, where it overlies volcanoclastics and Cretaceous basement. To the east, in Katumbo Creek-1, an interval of 124 m below the Middle Miocene shales was identified as Panaon Limestone. It is reasonable therefore to assume that between these two occurrences, the Marinduque Platform and the margins of the later Bondoc Sub-basin were shallow marine shelf areas dominated by carbonate deposition, before downwarping of the southern Bondoc area, and deepwater clastic sedimentation within the resulting restricted basin, began in the Middle Miocene. Maps T-2 and T-3 show the present-day structure of the area at this stratigraphic level. It is an important objective horizon in the play assessments discussed below.

The overlying orange horizon outlines the top of mound-like structures which rest on the green horizon on the Marinduque Platform (e.g. on Line RG-83-807). This horizon occurs too locally to be separately mapped and contoured, but the positions of the mounds are noted on the green horizon structure maps (e.g. Maps T-2, T-3 and Plate T-1).

The red horizon is characterised (e.g. on Line 109-65, Figure 6), as a channel-incised surface at the top of a thick, often-transparent or disturbed sequence in the Bondoc Sub-basin. It is tied to the top of the mid-Miocene Vigo Formation in San Francisco 1 well. It represents the top of what is considered to be one of the regional seals in the area, but at this level the Vigo Formation has sandy intervals intercalated with the shales, and the overlying Canguinsa Formation is of variable lithology. The horizon therefore is an objective that may be associated with reservoirs. Map T-4 and Plate T-2 show the structure at this level.

The yellow horizon is confined largely to the structurally deeper parts of the study area and does not occur in the shallower northern portion. It represents the internal boundary

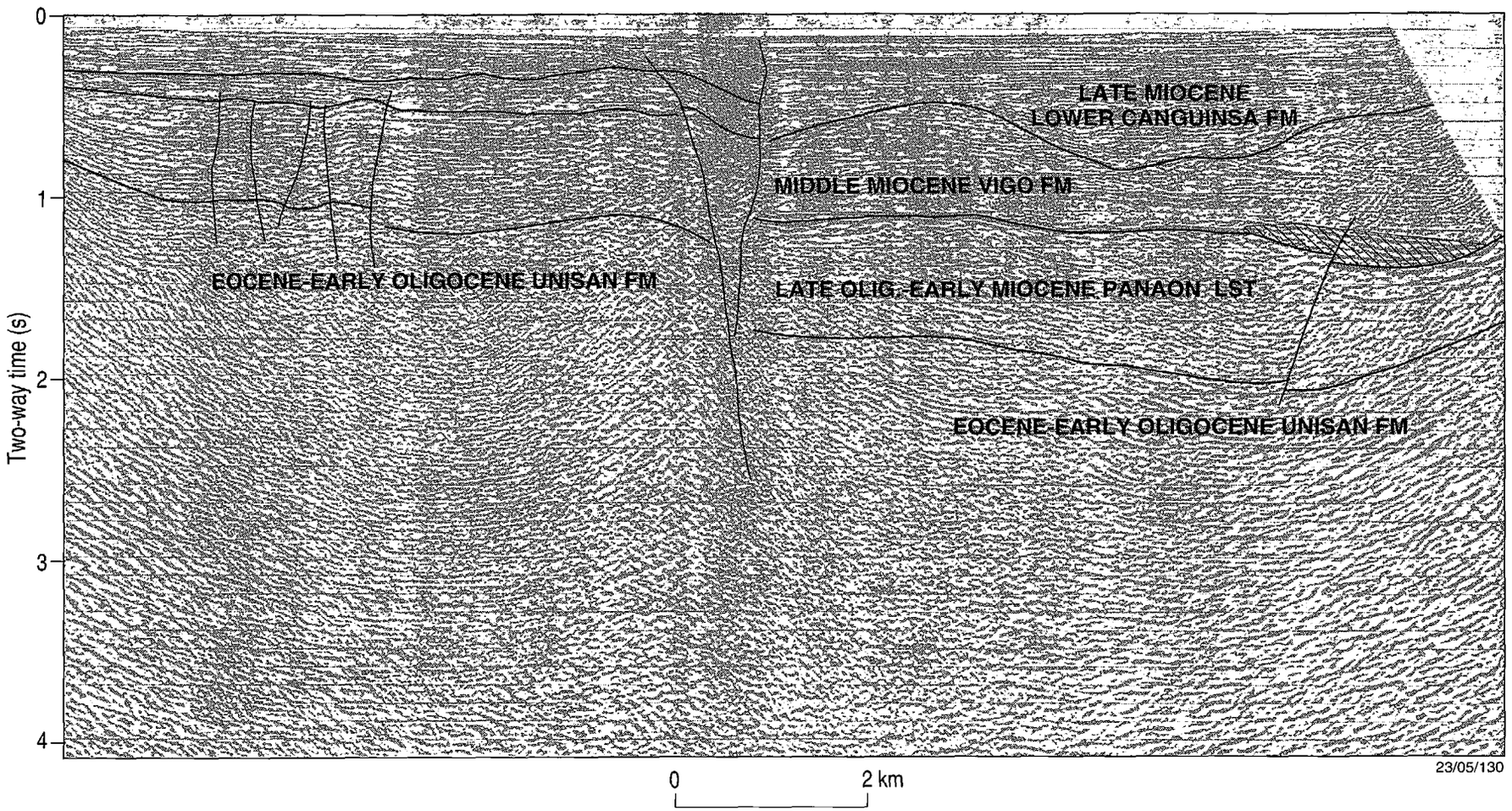

Figure 6 Seismic section 109/65 showing key horizons and Tayabas Bay Fault.

between the Upper (Pliocene) and Lower (Late Miocene) members of the Canguinsa Formation, which are geologically similar. The horizon is identified on seismic (e.g. Line 109-22) as top of the Late Miocene Lower Canguinsa Formation. Map T-5 and Plate T-3 show the structure of the area at this level.

The pink horizon is confined to the structurally deep parts of the Bondoc Sub-basin and other synclinal areas. It separates the Upper Canguinsa Formation from the overlying Pleistocene Malumbang Formation. It is easily recognised as a surface of downlap or onlap except in structurally high areas. No map has been produced for this horizon.

Seismic Sequences

The Pre-Blue Interval is characterised by sparse reflections with poor continuity and low amplitude.
Age: Possibly Mesozoic.
Lithology: Unknown, could be a basement complex, similar to that outcropping on Marinduque Island.
Trap size and potential: Not defined.

The Blue-Green Interval is hard to characterise over large parts of the area because of subsequent structural disturbance and disruption of the overlying sequences. Where it is more easily visible, mainly in the north, the interval below green in places has high to moderately high amplitude events for the top 300-400 ms. Reflections are characterised by a number of high to moderately high amplitude events that vary from parallel with good continuity, to hummocky, contorted and chaotic. Its high amplitude suggests that it may be bedded to mounded carbonate. Below this upper interval the events vary from subparallel to strongly divergent, with medium to low amplitude and moderate continuity. While this lower section may have a carbonate content it appears to be dominated by shale and siltstone.
Age: Early Miocene to Oligocene.
Lithology: Panaon Limestone and earlier clastics. Volcanogenic sediments possible in places.
Trap size and potential: Encouraging features include the Tuquian Anticline in the Mabio area, and mounds in the Mulanay and Yuni areas.

On many lines the Green-Red Interval is largely reflection free. This is characteristic of a relatively homogeneous shale sequence. However on some lines there are parallel reflections with high continuity and amplitude toward the top of the interval, indicating variation of lithology with sands or limestones. Large regions show evidence of chaotic, contorted or intensively-faulted bedding, indicating movement of these sediments after deposition, under the influence of gravity and/or compression and faulting. Near the base, there are local occurrences of an additional sequence. The green to orange interval consists of locally high-amplitude divergent or hummocky reflections within the green to red interval. Examples can be seen on Lines RG-83-807 and RG-83-808. They are probably basin floor fan complexes and, in some locations, carbonate bioherms and associated clastics. They have been shown on the green horizon structure maps (Maps T-2 and T-3) as 'mounds'.
Age: Early Middle Miocene, Vigo Formation.
Lithology from outcrop and wells: The green-red interval is equated with the Vigo Formation. This formation is only partly known from outcrop and wells. The basal part has been seen only near the basin edge. The bottom four thousand metres have not been drilled in the main part of the Bondoc Sub-basin, that is, south of the Mompog-San

Miguel Disruption. Limestone intervals are common near the base in outcrop, and in the Katumbo Creek-1 well north of the disruption. In these thinner parts the formation is predominantly shale with volcanoclastic silts, and sands that grade to conglomerates. San Francisco-1 well on western Bondoc Peninsula intersected several quite quartzose intervals of about 10 m thickness, as shown on the gamma log, but although it is the deepest well in the Bondoc Sub-basin, it terminated more than a kilometre short of the base of the formation.

Source potential: Most eastern and western Bondoc Peninsula wells had extensive oil and gas shows, and many plugged and abandoned wells are today leaking oil and gas to the surface. The widespread occurrence of these shows in Bondoc wells, and of seeps on the surface elsewhere, indicate that a prolific and mature source exists either within the lower parts of the Vigo Formation or immediately beneath it. Outcrop data suggests the formation has very good seal and source potential. Some seeps and leaking wells were successfully sampled for oil and gas in March 1993 by DOE staff.

Trap size and potential: The Bondoc Sub-basin and parts of the Marinduque Platform are highly deformed, both on and offshore, so there is a wide variety of structures, many of them associated with the large-scale faulting. They are discussed more fully below, grouped into areas of interest under the names Mabio, Mulanay and Yuni. At levels between the green and red horizons, these structures are not considered susceptible to fault leak because of the high shale content of the Vigo Formation, which is likely to preserve seal on almost all faults. The red horizon is missing over the crest of the Bondoc Point Flower Structure, hence part of the green to red interval (the uppermost Vigo formation) is exposed on the Bondoc Peninsula and offshore.

The Red-Yellow Interval, corresponding to the Lower Canguinsa sequence, is characterised by parallel reflectors with good continuity and high to medium amplitude. It is bounded below by a major unconformity and above by either an angular unconformity or a disconformity.

Age: Late Miocene.

Lithology: Lower Canguinsa Formation limy shales, carbonate sands, conglomerates and local thin limestones.

Structure size and potential: Several interesting structures are associated with the Tayabas Bay Fault. The yellow horizon is missing over the Bondoc Point Flower Structure, and the red-to-yellow interval (the Lower Canguinsa formation) outcrops on its flanks both on and offshore.

The Post Yellow Interval is thin, and present only as pockets in later depocentres. It is characterised by continuous high frequency reflections, sometimes with downlap against the yellow horizon. The interval represents the Upper Canguinsa and Malumbang formations onshore. It is similar to the red - yellow interval with sequence boundaries at the yellow and pink (base Pleistocene) horizons and seabed.

Age: Pliocene, Pleistocene and Holocene.

Lithology: Calcareous silts and sands with local limestones.

Seismic Time Structure Maps

Seismic two-way time structure maps are presented for three horizons, namely, the Early Miocene Unconformity (green horizon, Maps T-2 and T-3), the top of the Middle Miocene Vigo Formation (red horizon, Map T-4) and the top of the Late Miocene Lower Canguinsa Formation (yellow horizon, Map T-5). The times represent sea-level corrected times as seen on processed seismic sections, but they are not compensated for variable

water depth offshore. The scale is 1:100,000 but, for the green horizon, an additional map of the northern area at 1:50,000 is presented. Maps and an example of seismic sections of each lead are also presented in Figures 7, 8, 9,10, 11 and 12. These cover the areas around the leads, and all except Figure 7 have been compensated for variable water depth. Because of geological complexity, some smoothing of the contours was applied on small complicated features (e.g. in the Yuni area), and only the more significant faults are included.

The maps were made by digitising horizons from the interpreted seismic sections into the PETROSEIS mapping system. Computer posted and contoured time structure maps were produced. The posted map of the main regional unconformity at the base of the Vigo Formation (the green horizon) was hand contoured as a quality-control check on the computer contoured version. Faults were correlated and drawn manually on maps at each horizon level. The manual fault correlation map of each horizon was digitised and used to control the computer-contoured maps. Because of the high relief, especially in the vicinity of the Bondoc Point Flower Structure, a 100 millisecond contour interval was used for most maps. This represents a contour depth interval of 110 to 125 m. A 50 millisecond interval was used in some areas of low dip (e.g. on the 1:50,000 scale map T-3 of the Mabio area). This represents a depth contour interval of 55 to 62 m.

The maps with compensation for water depth (Figures 9 and 11; Plates T-4 to T-6) were constructed because the leads in the southern part of Tayabas Bay (the Mulanay and Yuni areas) are distorted by variable water depths. Water at the velocity of 1500 m/sec was replaced with sediment at 2000 m/sec for this calculation. Figure 7 was not compensated, because the water depth in the Mabio area is uniformly shallow (<100 m). The water depth compensated maps were used for calculation of trap parameters such as area and volume.

Because there are no wells offshore, there is no database of reliable velocity information for use in depth conversion of the seismic times, the only source being the seismic processing velocities. These are unmodified 'stacking velocities', and their relationship to vertical velocities in the subsurface is complex. They sometimes vary greatly between the different vintages of lines over the one structure. Therefore, they were not considered suitable for depth conversion, and depth maps are not presented. For prognosed depths given in the montages (Plates T-4 to T-6) average interval velocities from onshore wells were used.

Structural Interpretation

The Philippines Fault System, which extends across the whole region from the south (Mindanao) to the north (Luzon Island) on a north to northwest trend, is considered responsible for the major structural lineaments in the Tayabas area. It has a primary splay, observed mainly south of Tayabas Bay, called the Sibuyan Sea Fault (Forster, 1990; Aurelio et al, 1991).

Our seismic interpretation and mapping of the Tayabas Bay area reveals the effects of a convex-eastward, 'restraining bend' on the Sibuyan Sea Fault. Off the southern end of the Bondoc Peninsula, the fault is transformed locally into a series of north-south trending compressive faults. It steps northward along the peninsula and the near offshore, and then resumes its northwest orientation offshore in Tayabas Bay, passing through or very near Mompog Island, and continuing north of Marinduque Island to the northwestern limit of

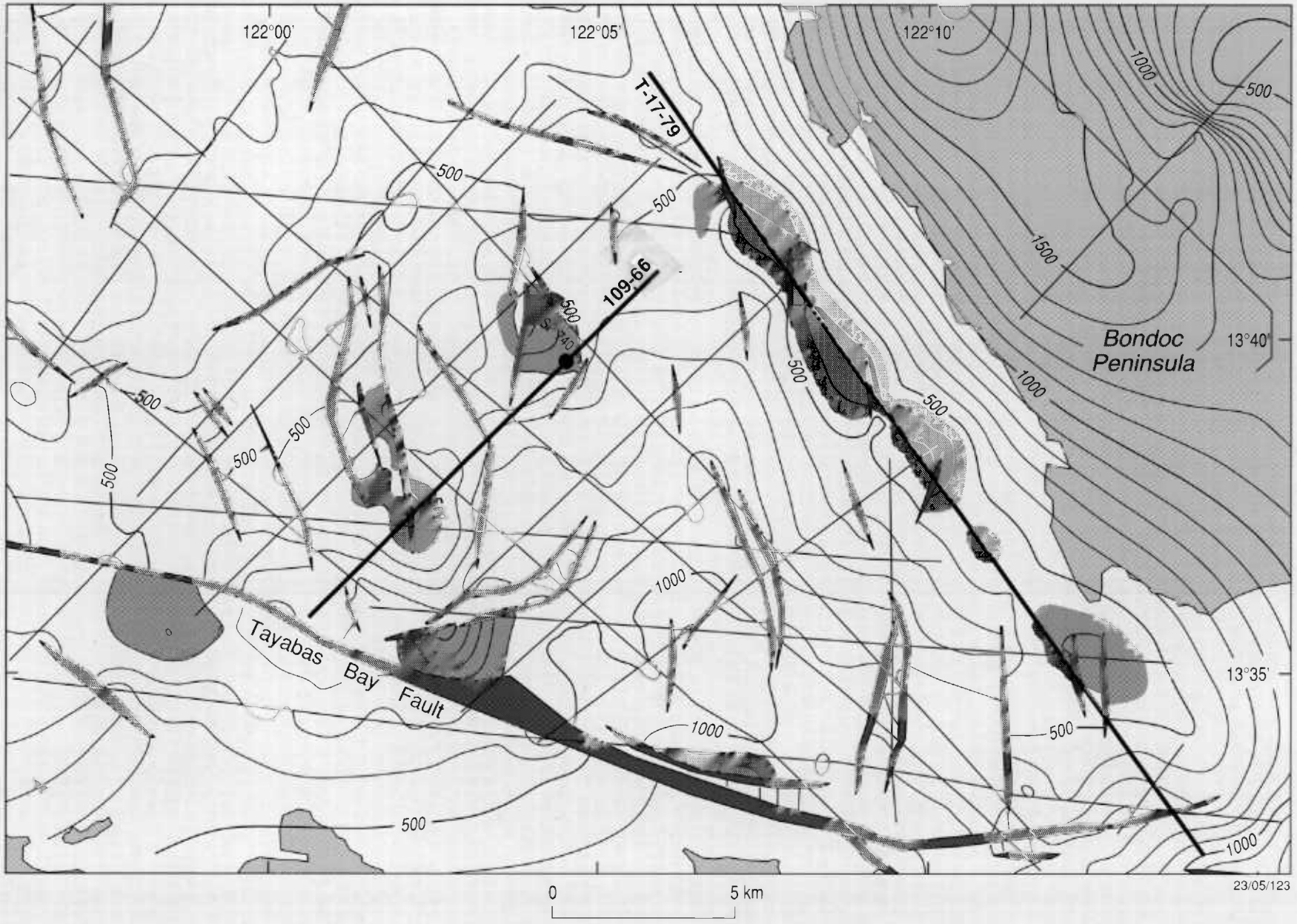

Figure 7 Mabio Lead at green horizon. Two-way time structure map.

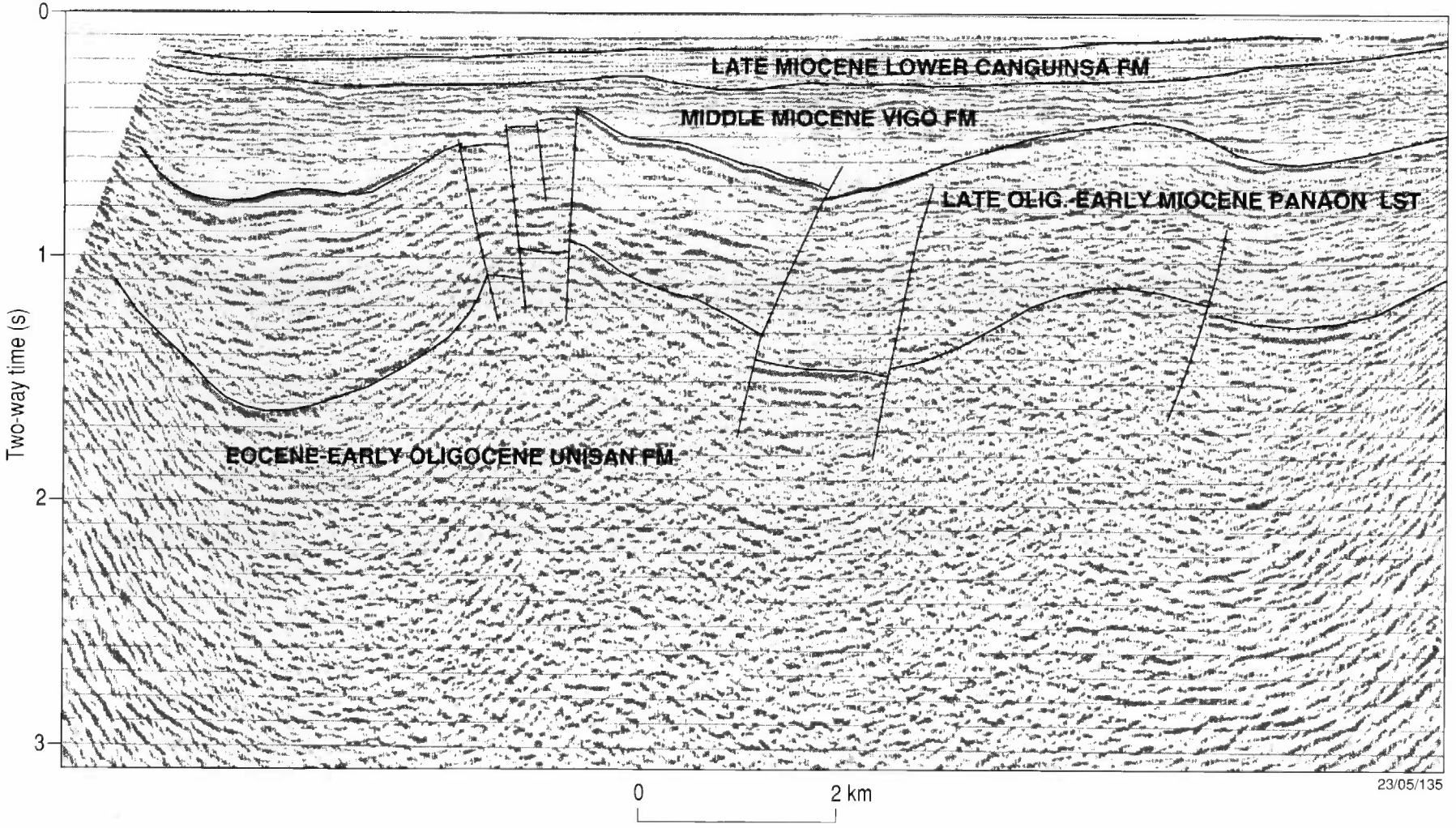

Figure 8 Seismic section 109/66 showing Mabio Lead.

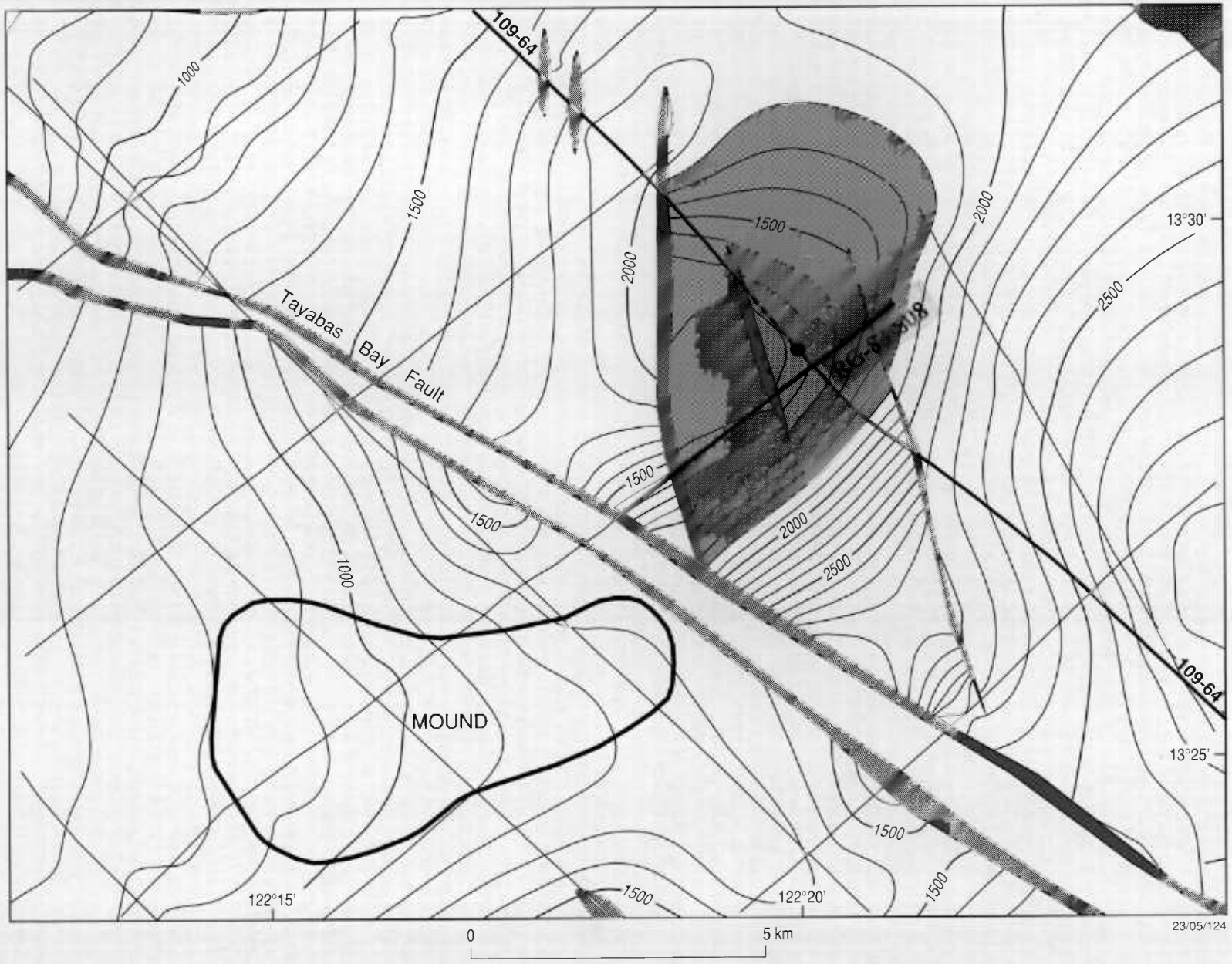

Figure 9 Mulanay Lead at green horizon (compensated for water depth variations).

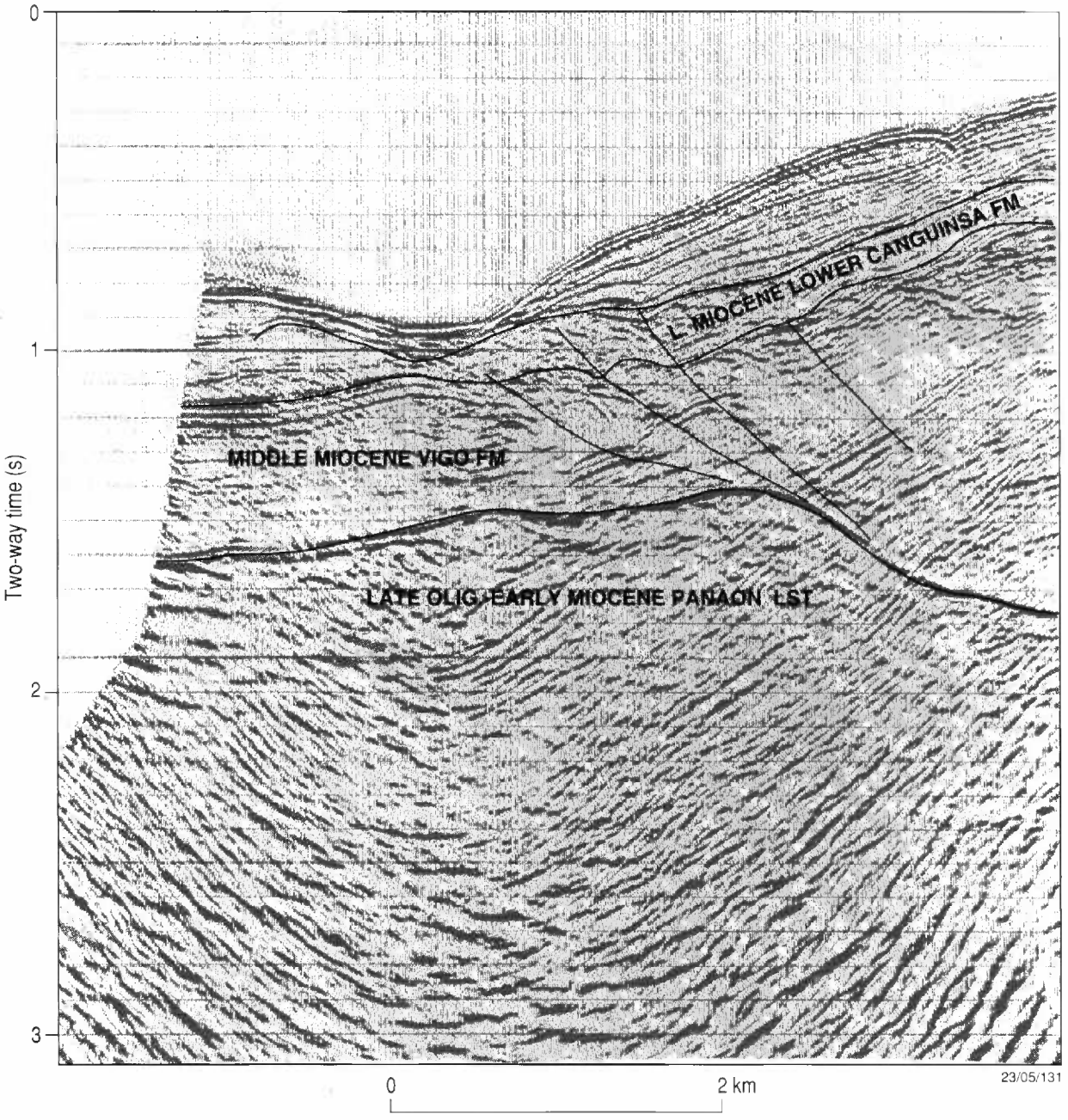

Figure 10 Seismic section RG-83-808 showing Mulanay Lead.

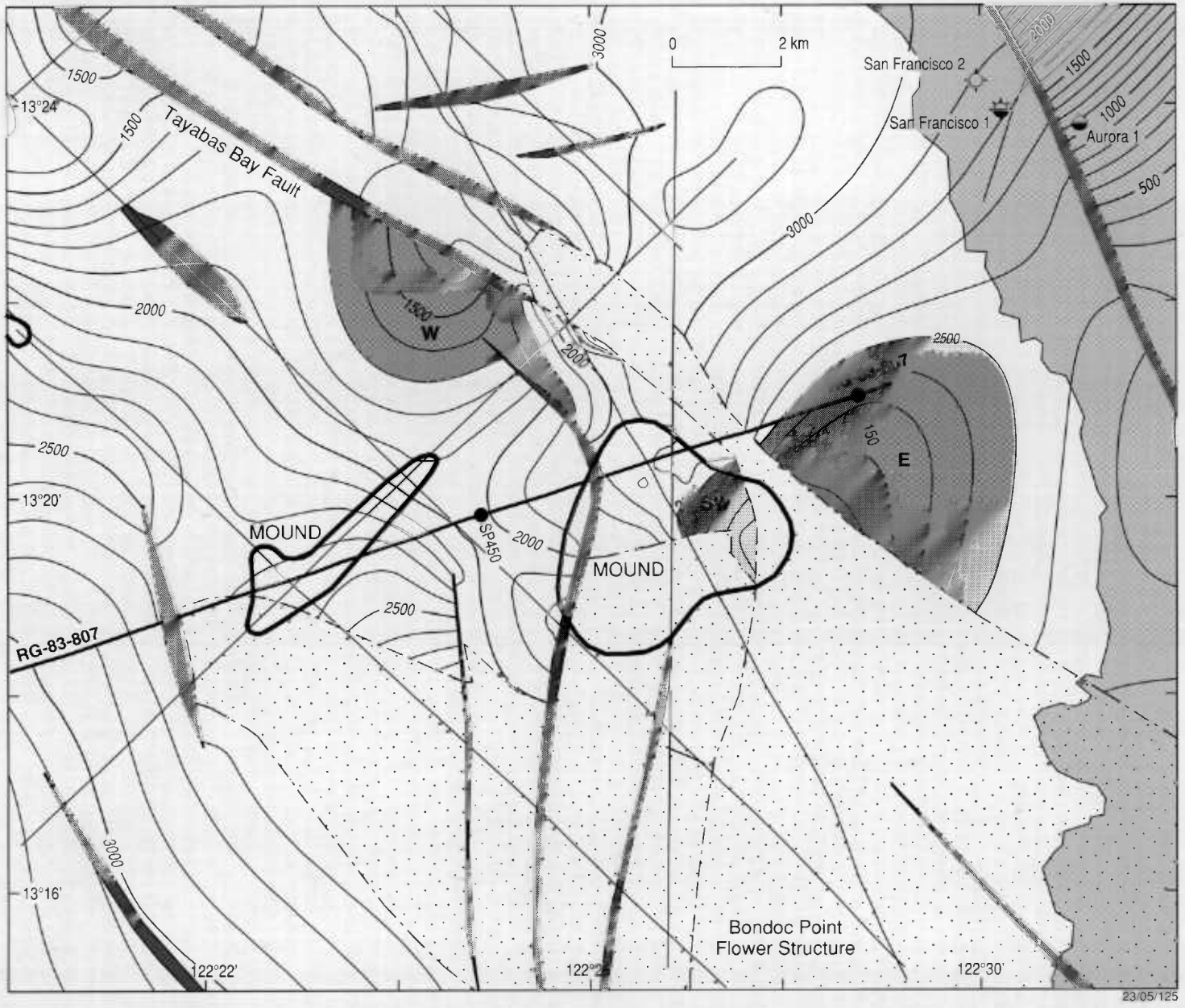

Figure 11 Yuni Lead at green horizon (compensated for water depth variations).

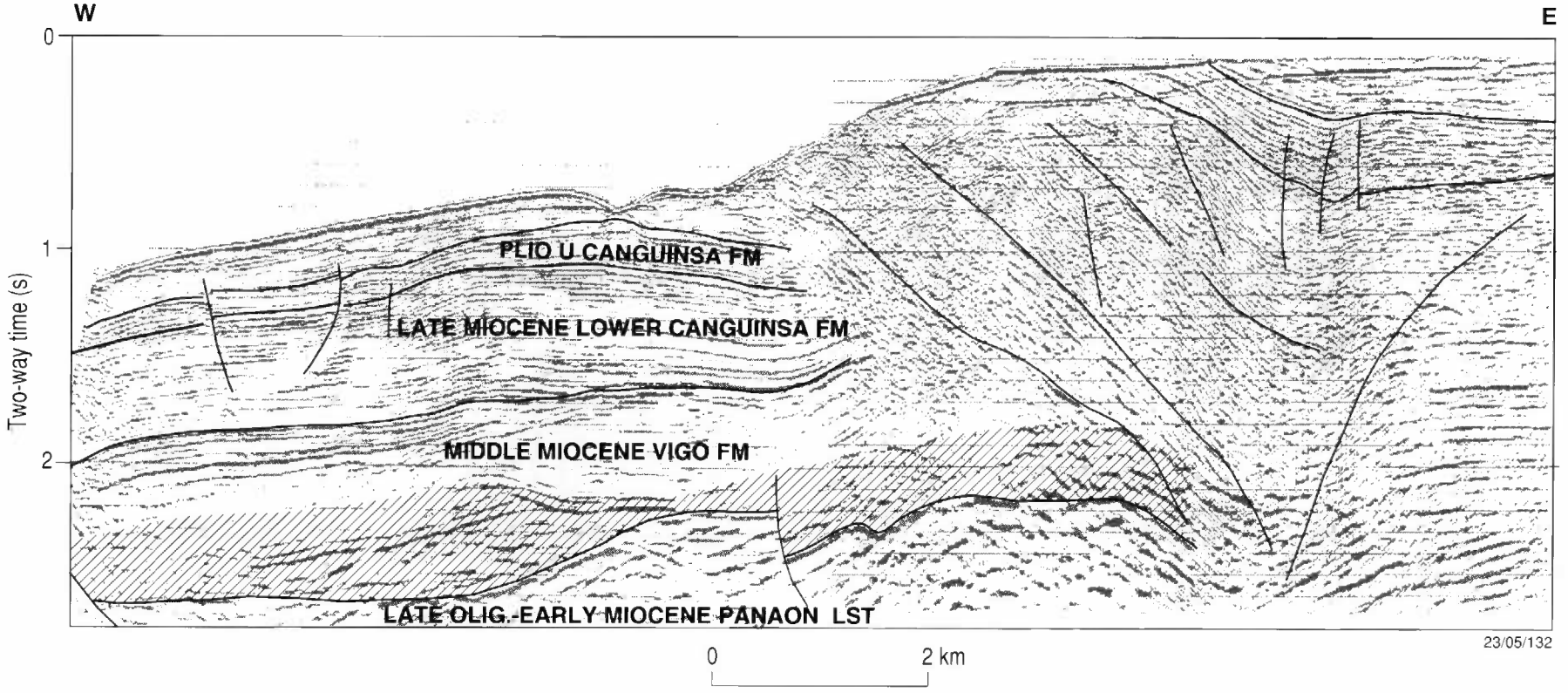

Figure 12 Seismic section RG-83-807 showing Yuni Lead.

this study as shown in Forster et al (1990). It is shown on Plate R-1 and Figure 5, where we have named it the Tayabas Bay Fault.

The northwest-trending Tayabas Bay Fault dominates the Tayabas Bay area. On seismic it shows the typical features of a strike-slip fault and, because of its association with the Philippine Fault, is assumed to be left-lateral. Where the Tayabas Bay Fault crosses the Marinduque Platform in the northwest, it is a narrow fault zone, generally throwing down toward the northeast.

To the southeast, in the deep Middle Miocene trough of the Bondoc Sub-basin, near and on the southern tip of the Bondoc Peninsula, it is a broad fault zone, up to fifteen kilometres wide, and very complex. Its western side is defined by several reverse faults trending north-south and thrusting westward. A large positive 'flower' structure occupies the zone between the Central Bondoc Fault and these western thrusts.

The Bondoc Point Flower Structure is located within the Bondoc Sub-basin at the southern end of the Bondoc Peninsula and offshore to the west (Figures 4 and 5, Plate R-1, Maps T-2 and T-4). It is a positive (compressive) trapezoid-shaped feature bounded by outward-facing thrusts on its northeastern, southern, southwestern and western flanks. Offshore on its western and southwestern flanks, it is seen on seismic to thrust westward and southwestward respectively (Figures 10, 12, Plates T-5, T-6). Onshore on its northeasterly flank, it is documented (Nicolai et al, 1973, p.19) as thrusting from the southwest (i.e. toward the northeast). The 'broad submarine rise' referred to in the above report is probably the expression of the Bondoc Point Flower Structure on earlier seismic data. At its widest, this compressive feature almost assumes the proportions of a 'duplex' structure, being about 15 kilometres wide, although there is no central area of undisturbed terrain such as would be expected in the interior of a duplex. Attempts to correlate seismic sequences within it have not yielded mappable results. The seismic is either reflection-free or saturated with fault planes (seismic section 109-30, panel 2), indicating heavy imbrication by thrusting. The seismically incoherent basin margin described by Sarewitz and Lewis (1991) is located on the southernmost part of the structure, in an area where seismic control is sparse, and those authors ascribed the morphological features they detected on the side-scan sonar to reverse faulting. The 'uplifted basin fill' on their Figure 16-C is the body of the Bondoc Point Flower Structure. It is a very young feature, thought to be the result of movement along the Sibuyan Sea Fault during the last 2 million years. The cause is likely to be compression on a constraining (rightward-stepping) bend in the left-lateral strike-slip fault system. It may, like salt diapirs in other parts of the world, act as a focus for oil accumulation.

In this study, the Mompog-San Miguel Disruption is mapped as an eastward-trending splay fault at a bend in the Tayabas Bay Fault. It appears to be not as large nor as prominent as in areas to the east, although there does appear to be a change in the pre-Middle Miocene stratigraphy across it. It may be an old feature, mildly reactivated by the Philippine Fault System.

Disturbed Structure

In the Bondoc Point Flower Structure, the thick argillaceous Middle Miocene Vigo Formation, the main stratigraphic unit incorporated in the structure, has been finely imbricated and may even have begun to deform in a plastic manner. The current interpretation places it in the setting of a westward-thrusting fault zone. We believe that the lack of internal reflections within the structure e.g. on Line 109-30 south, Line RG -

83-815A north, is due to disruption of bedding-planes by reverse faulting on an extensive scale, possibly leading to 'smearing' or flowage of the Middle Miocene shales. We believe that this is a cause of poor seismic data zones in both the onshore and offshore areas.

The Central Bondoc High, an anticlinal complex along the spine of the Peninsula in the central part of the Bondoc Sub-basin, is characterised on seismic by a border of very disturbed reflections and a wide no-reflection zone. The feature may be a thrusted anticlinal complex, de-coupled from the underlying structure and moving westward. It is independent of the structural elements described above, lying between them and the Alabat-Burias High.

Diapirs have been identified on the seismic sections in the deeper parts of the Ragay Sub-basin. They appear to be composed of very low velocity materials (i.e. clay or mud) as is evident from the velocity analyses carried out in conjunction with the seismic processing.

The Central Bondoc High is shown as a wide zone of diapirs on some maps (e.g. BED, 1986, Plate II AF9). Additional diapirs are shown offshore on that map in the location where the Bondoc Point Flower Structure is now mapped. In the ARCI (1988) radar imagery interpretation report, some isolated diapirs were recognised, primarily east of the Central Bondoc Wrench Fault. Our inspection of the satellite imagery has not enabled recognition of either the central zone of diapirs or the individual diapirs, but this may be due to the masking effect of the dense vegetation cover. Antonio (1961) does not recognize diapirs, but his detailed 1:50,000 scale maps show complex dip patterns indicative of shale flowage under compression. The widely-separated onshore seismic lines do show well-defined, reflection-free zones in what appears to be a line of highs (the Central Bondoc High) or thrusts down the centre of the Bondoc Peninsula, but there is not enough evidence to determine whether they are diapirs, or compressive features with possible shale flowage like the Bondoc Point Flower Structure. The World Bank report (BED, 1986) makes the point that they are not basement-involved, and we agree.

Slumping occurs on some seismic lines. At the western end of Line RG-83-809 there is evidence of olistostromes on steep submarine slopes off the southern end of the Bondoc Peninsula. A toe thrust in Miocene sediments at the base of the slope, even affects Pliocene sediments. This is on the flank of the flower structure, and complicates the task of interpretation. This slumped mass may be the result of complete expulsion of shale from the core of the flower structure itself. At least one of the 'arcuate side-scan features' mentioned by Sarewitz and Lewis (1991) may be the surface expression of a slumped mass of Miocene shale expelled from the structure. Such a hypothesis is easily testable by dredging.

Geologic History

The following account is based on the seismic interpretation, supplemented with reference to Sarewitz et al, (1991), Aurelio et al, (1991) and the onshore geology.

Deposition in the Tayabas Bay area began in the latest Eocene or earliest Oligocene, when the volcaniclastics of the Unisan Formation were laid down on a basement of oceanic, possibly ophiolitic origin in an intra-arc setting. This was followed in the Late Oligocene/Early Miocene by deposition of the carbonates of the Panaon Formation on parts of what was probably an inshore area.

The Late Oligocene to early Middle Miocene succession has not been drilled in the area. The seismic interpretation indicates development of a deep trough, the Bondoc Sub-basin,

in the southern Bondoc Peninsula and adjacent parts of southern Tayabas Bay, with the accumulation of several kilometres of turbidites and shallow-marine sediments of the Vigo Formation during the Middle Miocene. This scenario is consistent with the extensional basin and paleostress map of Aurelio et al (1991, figure 6). The extension was in a NW-SE direction. The western and northern areas of Tayabas Bay were less affected by subsidence and deposition, and were only gradually covered by the Vigo Formation siltstones and shales. Mounds underlying the Vigo Formation near the edge of the Marinduque Platform may well be carbonate reefs of early Middle Miocene age which were later drowned by the clastics of the developing Bondoc Sub-basin. Other mounds of post-Early Miocene unconformity age may be basin-floor complexes. Deposition slowed gradually during the Late Miocene and Pliocene deposition of the neritic clastics of the Canguinsa Formation.

A change in the stress regime occurred in the latest Pliocene and Pleistocene, with superposition of intense, left-lateral, strike-slip movement in a northwest-southeast direction, cutting across the older tectonic elements of the Bondoc Sub-basin and the Marinduque Platform. This strike-slip movement persists to the present, and is accompanied by compression along an east-west axis. The southern end of the Bondoc Peninsula is being rotated clockwise, compressed and thrust westward on to the margins of the Marinduque Basin and Platform, and the Bondoc Point Flower Structure continues to develop at the overstep of the Sibuyan Sea and Tayabas Bay Faults.

PETROLEUM GEOLOGY

Reservoirs

The reservoir properties of the formations are summarised as follows, in order from oldest to youngest:

Basement and Unisan Formation - Unknown but assumed to be minimal. Could form a reservoir locally if deeply weathered and fractured. This could occur on the Marinduque Platform.

Panaon Limestone - Outcrop on Bondoc Peninsula and Templo Island and data from Katumbo Creek 1 show it to be recrystallised and tight. That may be a local condition not widely reflected in the subsurface. The stratigraphic equivalent, the Nido Limestone of northwest Palawan, is the major reservoir for Philippine discoveries.

Vigo Formation - In San Francisco-1 sandy intervals around 10m thick are interpreted. Sandstone interbeds northeast of Aurora township were described by Yap (1977) as seeping oil. Bondoc-2 well was reported as producing 250 BOPD. Formation damage appears to have affected drill stem testing. If drilled with a mud system that minimised such damage the formation could prove to be productive, especially of gas but also of oil.

Lower Canguinsa - Onshore limestones have porosity; some shows were encountered in Bondoc wells.

Upper Canguinsa and Malumbang Formations - Good visual porosity in sands and limestones that have not suffered surface alteration. Sequence is unlikely to be sealed anywhere.

From onshore well and outcrop information and the interpretation of onshore and offshore seismic data, two main groups of reservoirs are proposed as objectives for exploration wells. One lies below, and one above the Early Miocene unconformity (the

green horizon). The older group consists of shelf carbonates of the Early Miocene Panaon Formation beneath the mid-Miocene Vigo Formation on the Marinduque Platform. The second group consists of early Middle Miocene carbonates and basin-floor clastics within and near the base of the Vigo Formation.

The sonic, density and neutron logs in three onshore wells were used to evaluate reservoir properties in the succession drilled by those wells. The evaluation is presented as Appendix 1. Note that because these wells were drilled in the deeper part of the Bondoc Sub-basin, none of them reached either of the two groups of postulated reservoirs mentioned above, except for Katumbo Creek-1, in which section may have been missing because of faulting.

Traps and Seals

The seismic has indicated a number of potential traps in Tayabas Bay, arising from a variety of trapping mechanisms. Traps include closures dependent on compressional faults (the Mulanay, Yuni areas) and fault independent closures (the Tuquian Anticline, and other closures in the Mabio area). Because of the continuing deformation of the area, most of the leads are affected by faulting, and structuring has generally continued to Pliocene or Recent times. Neither of these circumstances are detrimental to the prospects of the area, as the discussion below on timing and maturation, and the later section on faulting and traps, makes clear. The Bondoc Point Flower Structure, in particular, with its overthrusted or deformed shales, though it is a very young feature, is capable of providing a lateral seal against sands in the Vigo and Canguinsa Formations that abut its flanks (Figure 4).

Onshore Geochemical Sampling

Many oil and gas seeps have been reported from Bondoc Peninsula. They are so numerous that they have attracted the attention of oil explorationists from the earliest days. The latest sampling of seeps and leaking oil exploration wells was done in March 1993 by DOE staff. These samples were analysed at the AGSO laboratories in Canberra as part of this project and the details of the analyses are in Appendix 4 (Cortez and Murray). Because of its direct relevance to the assessment of Tayabas Bay, a summary of the information on seeps is given below. Seep numbers are those accompanying the diamond shaped markers on Plate R-1.

1) Corby (1937), p6. "Irwin River No 1 now stands with oil in the hole; the top of the fluid level is within 50 feet of the surface".

2) Corby (1937), p6. The seep is located near Banco "at the bottom of Canilbo Creek and the sides of the creek are saturated with oil. The oil is light in gravity ... Gas bubbles are present."

3) Corby (1937), p6. The seep is located near Banco, "a short distance south of Maalat Creek." A sample (AGSO no 794) was collected from near the junction of Maalat and Canilbo creeks. Oil was collected from mud in creek. Creek was dry but during rainy season there is a strong odour of hydrocarbon and staining occurs.

4) Bondoc-2. The cement floor of the derrick is still intact with oil and gas strongly seeping out of the now unplugged drill hole. (Martin and Espiritu 1968). Sample (AGSO no 793) of oil in mud collected by DOE in March 1993 and analysed at AGSO.

4a) Bondoc-3. Gas sample (BP-GS-01) and oil sample (BP-OS-02, AGSO no 792) collected from uncemented well with bubbles coming from borehole, believed to be Bondoc-3 well. Sample collected March 1993 by DOE and analysed at AGSO.

5) Bondoc-4. The concrete floor of the derrick used in drilling still exists. Drill hole is marked by the presence of oil soaked mud on the surface. Sizzling sound of gas emanates around or from the hole with its plug now probably destroyed." (Martin and Espiritu, 1968).

6) Pina-1. The site is now marked by a small depression about 10 metres in diameter with a strong emission of gas from the cracked ground surface. (Martin and Espiritu 1968). This is within the Bondoc Point Flower Structure.

7) Bahay-1. The first well on Bondoc Peninsula was hand dug as Bahay-1, and was sited on an oil seep from a fault (Domingo 1976).

8) Seep about 10 km northeast of San Francisco (Aurora) township, identified on map of Yap (1977) and described as being from sandstone interbeds in the Vigo Formation.

9) Seep about 9 km northeast of San Francisco (Aurora) township and 2 km south of seep 8, identified on map of Yap (1977) and described as being from sandstone interbeds in the Vigo Formation.

10 to 14) Seeps east of General Luna from map in Yap (1972).

15) Seep in vicinity of San Francisco-1 and -2. Location not known precisely.

16, 17) Oil and gas seeps north of Catanauan and shown on Plate II A. F. 1 of BED (1986). This is in the San Isidro Syncline adjacent to the Tuquian Anticline on the Mabio Lead.

18) Mangero seep sample (BP-0S-01, AGSO no 791), collected by DOE March 1993 and analysed at AGSO. Sample came from a shallow dug-out along a relatively shallow ravine near splay of the Philippine fault, 5.5 km south of San Andreas and 2 km northwest of Pandanan.

The results of the seep analyses indicated the following:

1) The source rocks for the sampled oils (from locations 3, 4, the Bondoc-2 and-3 wells) were rich in resinous terrestrial organic material and were deposited in oxic or sub-oxic conditions, probably in an inner neritic or lower delta plain "fluvio deltaic" setting containing hydrogen-rich shales. This points to the terrestrial clastics of the lower Vigo Formation rather than the marine Panaon Limestone. There were subsidiary features pointing to either co-sourcing from, or migration through a carbonate facies (Panaon Limestone or lowermost Vigo Formation carbonate beds?).

2) The age of the source rocks is Late Oligocene, Miocene or younger. This is compatible with the Miocene age of the Vigo and Panaon Formations.

3) Bondoc Peninsula oils were generated from early mature source rocks. Again, this points to a lower Vigo Formation source (Appendix 2).

4) The isotopic composition of the Bondoc-3 gas well sample indicated that it came from a source similar to the oils from the same area, and to water bottom DHD samples from beneath Ragay Gulf.

Offshore Geochemical Sampling

An offshore geochemical Direct Hydrocarbon Detection (DHD) survey was conducted simultaneously with the seismic recording aboard R/V *Rig Seismic*. A total of 490 kms was recorded along 16 lines in Tayabas Bay. The DHD system uses a submerged tow-fish beneath the vessel which detects light hydrocarbons in bottom waters through continuous water sampling. The findings are presented in Appendix 5.

Hydrocarbon anomalies were detected in Tayabas Bay but were fewer than in Ragay Gulf. The anomalies were also considered as generally weak and are of Type II (dry) molecular compositions. In addition, many of the anomalies were believed to be related to variations in the bathymetry and tow-fish depth as shown by changes in the ethylene and propylene concentrations. The great variation in water depths in Tayabas Bay (Map T-1), and the generally greater depth of water compared with the Ragay Gulf, which caused the towfish distance above the sea floor to vary markedly, make the interpretation of the geochemistry results less certain. Nevertheless, bottom water sources of hydrocarbons were not ruled out, and it was noted that the higher levels of hydrocarbon in the area were concentrated near the Tayabas Bay Fault, and around the margins of the Bondoc Point Flower Structure. Typical background values for hydrocarbons throughout the survey areas were: total hydrocarbon content 8 to 10 ppm; methane 3 to 5 ppm; C_2 and C_3 hydrocarbons less than 0.05 ppm. Butane levels were generally below the detection limit of 0.005 ppm.

According to the Tissot and Welte model (1984), both the molecular and isotopic data suggest that the geochemical anomalies may be sourced from gas or condensate-prone source rocks (Evans et al, 1992, Appendix 5). It is interesting to note that the seeps from adjacent onshore wells, San Francisco-1 and Bondoc-3, have indicated a terrestrially derived, waxy kerogen source (BED, 1986). Further analyses of probable source rocks would help to clarify the actual kerogen type and composition of the source.

Source Rocks and Maturation

There are no wells offshore in Tayabas Bay. Onshore, more than half of the prospective succession, including the lower Vigo and Panaon Formations, remains unexplored in the main part of the Bondoc Sub-basin. Because the area does not have a high geothermal gradient, and because most of the wells terminated at depths less than two kilometres, the zone of maturity for hydrocarbons is almost undrilled. However, the widespread oil shows and seeps on the Bondoc Peninsula indicate that oil and gas generation have been and are occurring in the Bondoc Sub-basin. The geochemistry data, from analysis of oil samples taken during field expeditions by DOE geologists, has confirmed the presence of mature sources, from which generated hydrocarbons are currently migrating to the surface, both onshore and offshore.

Maturation studies (Appendix 2) point to the lower part of the Middle Miocene Vigo Formation mainly, and possibly the underlying Panaon Formation, as providing a source that is presently active in the 'Tayabas Kitchen' area of the Sub-basin. Because of the very moderate heatflows (1.5 HFU and less) and thermal gradients (35°C/km or less), the 'oil window' is considered to begin at burial depths greater than 2000 m, definitely not at the shallower depths referred to in some of the literature (e.g. Yap,1977, page 13). On the other hand there is some evidence (e.g. at San Francisco-1) of suppression of vitrinite reflectance in the Vigo Formation. This suppression is known to occur in very oil prone

or oil-saturated sediments (Jeffrey et al, 1991, Snowdon and Powell, 1982) and has been taken account of in determining the above figure for the depth of onset of maturity.

Migration and Timing

The onset of generation in Tayabas Bay is late and has continued to the present (Appendix 2). It follows that traps of any age, even Recent, are in a position to intercept migrating hydrocarbons. Migration from the active kitchen area under the Bondoc Peninsula could be toward the east (the Alabat-Burias High in the Ragay Gulf), the west (the Yuni Lead), the north (the Mulanay and Mabio areas), and/or the south (the Arena Lead in the Ragay Gulf).

Lead Description and Evaluation

A number of leads have been identified, but the assessment is limited by the sparsity of data on reservoir and fluid parameters, as well as the variable distribution and quality of seismic coverage. Despite this, it is considered that the conservative parameters used in the reserve estimates, will afford a basis for comparing potential field sizes through the Bondoc and Ragay Gulf regions. To this end, the parameters chosen are similar to those used for Ragay Gulf leads.

Gross Trap Volume was calculated using PETROSEIS software and the digitised time-structure maps. Estimation of the ratio Gross reservoir/volume (the fraction of trap volume that could be reservoir rock) was based on outcrop information from Bondoc Peninsula. Net/gross reservoir thickness refers to the assumed amount of effective reservoir above the lower porosity cutoff. Net pore volume is the result of the multiplication of these factors, and represents the available space within the reservoir.

Oil saturation (So) of the reservoir has been taken as 70%, with water occupying the remaining 30%. The recovery factor of oil has been set at 30%, and the volume of recoverable reserves reduced accordingly. Formation volume factor (Bo) has been taken as constant for all reservoirs regardless of depth. Seeps and Bondoc wells suggest that any oil will be saturated with gas. Consequently a value of 1.4 has been used, the volume of oil has been divided by this factor, and estimated recoverable oil reserves reduced accordingly. No estimate of the amount of wet gas has been made but clearly a significant quantity would be produced during any oil production.

Three main areas of interest containing leads have been identified. From north to south, they are named Mabio (Table 1; Figures 7 & 8; Map T-3, Plate T-4), Mulanay (Table 2; Figures 9 & 10; Map T-2; and Plate T-5) and Yuni (Table 3; Figures 11 to 1&12; Maps T-2, T-4 and T-5 and Plate T-6).

Mabio is located between the north of Marinduque Island and Bondoc Peninsula, north of the Mompog-San Miguel Disruption. The largest lead in the Mabio area is the Tuquian Anticline, which trends NW-SE, adjacent to the coast. It is a compressional anticline of Middle Miocene age. There may be a small component of velocity 'pullup' due to present-day reefs in the area. The potential reserves have been calculated for the anticline. In addition there are several small separate culminations to the west. The Tuquian Anticline is defined by several seismic lines on the southwest flank up to the crest, a line along the crest, and three dip lines and one strike line on land near the Katumbo Creek-1 well. There is a gap in seismic coverage on the northeastern flank, at the coast. Both the offshore and onshore data are old and of poor quality. There is no seismic line clearly defining both flanks of the anticline, so the seismic line on the montage (Line RG-83-66)

Table 1. Parameters for Mabio Lead

PLAY DESCRIPTION

HORIZONS	: Top Panaon Limestone (green horizon)
RESERVOIRS	: Limestones of the Panaon Formation and sandstones and limestones of the lowermost Vigo Formation.
SOURCE ROCKS	: Shales and carbonates of the Bondoc Sub-basin to the east
TRAP AND SEAL	: Several compressional (?) features, sealed by interbedded shales
MIGRATION	: Short-range migration up dip from the San Isidro Syncline
DISPLAYS	: Map T-3, Plate T-4, Figures 7 and 8

RESERVE ESTIMATE

LOCATION	: Line T-19-79, SP 415
WATER DEPTH	: 29 m
WATER SATURATION	: 30%
RECOVERY FACTOR	: 30%
FORM. VOL. FACTOR	: 1.4

HORIZON	Green
Top (ms)	350
Base (ms)	450
Area (Ha)	2913
Gross trap volume (ha-m)	141500
Reservoir (Res.) type	limestone
Potential Res.Int.(m)	125
Gross/Potential Res.	0.5
Net/Gross Res.	0.5
Net Res. Thickness (m)	31
Net Pore Vol.(Ha.m)	5306
Porosity	15%
Oil Saturation	70%
Recoverable Reserves	50 MMBO

Table 2. Parameters for Mulanay Lead

PLAY DESCRIPTION

HORIZONS	**: Top Panaon Limestone (green horizon)**
RESERVOIRS	**: Limestones of the Panaon Formation and sandstones and limestones of the lowermost Vigo Formation.**
SOURCE ROCKS	**: Shales and carbonates of the Bondoc Sub-basin to the east**
TRAP AND SEAL	**: An anticline, sealed by interbedded shales of the Vigo Formation**
MIGRATION	**: Short-range migration up dip from the Bondoc Sub-basin (Tayabas kitchen area nearby to the east)**
DISPLAYS	**: Map T-2, Plate T-5, Figures 9 and 10**

RESERVE ESTIMATE

LOCATION	**: Line 109-64, SP 1000**
WATER DEPTH	**: 415 m**
WATER SATURATION	**: 30%**
RECOVERY FACTOR	**: 30%**
FORM. VOL. FACTOR	**: 1.4**

HORIZON	**Green**
Top (ms)	**1400**
Base (ms)	**1900**
Area (Ha)	**2431**
Gross trap volume (ha-m)	**892125**
Reservoir (Res.) type	**carbonate**
Potential Res.Int.(m)	**600**
Gross/Potential	**0.5**
Net/Gross	**0.5**
Net Res. Thickness (m)	**150**
Net Pore Vol.(ha-m)	**33455**
Porosity	**15%**
Oil Saturation	**70%**
Recoverable Reserves	**316 MMBO**

Table 3. Parameters for Yuni Lead

PLAY DESCRIPTION

HORIZONS	**: Top Panaon Limestone (green)**
RESERVOIR	**: Sandstones of the Lower Vigo Formation. Carbonates of the Panaon Limestone**
SOURCE ROCKS	**: Shales in the Bondoc Sub-basin (Tayabas kitchen) 6 km to the north**
TRAP AND SEAL	**: Major compressional structures with fault dependent closure east and west of the Tayabas Bay Fault. Reservoirs sealed by interbedded shales of the Vigo Formation**
MIGRATION	**: Yuni East - short range from below. Yuni West: - Short range across the Tayabas Bay Fault.**
DISPLAYS	**; Maps T-2, T-4, and T-5; Plate T-6; Figures 11to 14**

RESERVE ESTIMATE

LOCATION	**: Line RG-83-807, SP 150 (east) : Line RG-83-807, SP 450 (west**
WATER DEPTH	**: 10m (east), 315m (west)**
WATER SATURATION	**: 30%**
RECOVERY FACTOR	**: 30%**
FORM. VOL. FACTOR	**: 1.4**

HORIZON	East	West
Top (ms) (wd comp.map)	2100	1400
Base (ms)	2500	1700
Area (Ha)	1520	7600
Reservoir type	sandst	limestone
Potential Res.(m)	500	400
Gross/Potential Res.:	0.5	0.5
Net/Gross Res.	0.5	0.5
Net Res. Thckns (m)	125	100
Porosity	15%	15%
Net Pore Vol.(Ha.m)	9923	4158
Recoverable Reserves	93.6MMBO	39.2 MMBO

is located on an adjacent anticline, one of the smaller Mabio leads, with a history similar to the Tuquian Anticline, but lying 7 km to the west. More seismic should be done on land and across the coastal gap to confirm the Tuquian Anticline as a prospect and to discover others onshore. The southerly culmination could be drilled from the land.

The main lead in the Mulanay area is a faulted culmination located offshore in the Bondoc Sub-basin west of Bondoc Peninsula and east of the Tayabas Bay Fault. The trap is defined by 3 dip lines and 2 strike lines. A large mound, probably a basin-floor complex with sand reservoirs, is shown 10 km southwest of the main lead in deep water (~500 m). The volume has not been calculated, but could be larger than the main anticlinal lead.

The Yuni area is located west of the Bondoc Peninsula on the western side of the Tayabas Bay Fault and on the northern and western flanks of the Bondoc Point Flower Structure. There are at least ten potential traps in theYuni area. The two best defined of these, Yuni East and Yuni West, occur at green horizon level (base of Vigo Formation) and are displayed on the montage(Plate T-6). They are fault-closed culminations, probably of Middle Miocene age, though modified by later deformation along the Tayabas Bay Fault. The inferred culminations are not crossed by any seismic lines.

Other potential traps visible on the maps are a small closure against the Bondoc Point Flower Structure on the green horizon (Yuni SW, Figure 11) and a mound associated with it, interpreted to be an Early Middle Miocene reef, in a similar setting to that portrayed in the diagram in Figure 4. Another mound above the green horizon, interpreted as a basin-floor complex possibly including carbonate talus, lies to the southwest in deeper water on line RG-83-807 (Figure 12). Other possible traps can be discerned at younger stratigraphic levels (Maps T-4 and T-5), with Canguinsa Formation reservoirs sealed laterally by shales of the Vigo Formation in the Bondoc Point Flower Structure. Very large volumes and potential reserves can been calculated for these, but such estimates are likely to be inaccurate because of the complex structure in this area, and they are not presented here. The traps at green horizon level are defined by two dip lines and two strike lines.

The Effects of Faulting on Traps

Because of the thick regional seal provided by the Middle Miocene Vigo formation, traps at the base of the formation (the green horizon) will not necessarily be breached by faulting. Fault-dependent closures on the uplifted side of faults, such as those in the Yuni area (Yuni West and SW) and the main Mulanay Lead, will juxtapose basal Middle Miocene sands or carbonates, or Late Oligocene to Early Miocene carbonates (the objectives) against the middle parts of the Vigo Formation, which are thought to be largely sealing shales. Fault-dependent closures on the downthrown side of faults will have the basal parts of the Middle Miocene (the objective) thrown against the Oligocene. Thus the effectiveness of seal will depend on the lithology of these older rocks. The Oligocene rocks are postulated to contain reservoirs, hence fluids could migrate across the faults from the downthrown to the upthrown side. An exception to this may be the Bondoc Point Flower Structure. In this case, Canguinsa Formation or uppermost Vigo Formation reservoirs near the yellow or red horizons may be overthrust by deformed Miocene shale, providing both a lateral and a partial top seal. Thus, very large accumulations may occur around the flower structure (e.g. in the Yuni area).

CONCLUSIONS

A number of play types are recognised which could be sourced from the hydrocarbon kitchen in the Bondoc Sub-basin. Both sandstone and carbonate reservoirs are postulated to be present in a variety of traps formed on the Marinduque Platform during the Early and early Middle Miocene. The oldest traps are the closures in the Mabio area, and the mounds in the Mulanay and Yuni areas. Many structures, however, like the closures at green horizon level adjacent to the Tayabas Bay Fault and the Bondoc Point Flower Structure, may have been formed or modified in a later phase of structuring which began in the later Middle Miocene and has in general continued up to the present.

The main types of traps are:

- Compressional anticlines with fault independent closure such as the Tuquian Anticline and some possible smaller closures at Early Miocene unconformity (green horizon) level in the Mabio area.
- Compressional fault-dependent traps such as the main Mulanay closure on the Tayabas Bay Fault and its offshoots, possible large closures at top of Middle Miocene (red) and base of Pliocene (yellow) level against the Bondoc Point Flower Structure in the Yuni area.
- Late Early Miocene and early Middle Miocene carbonate reefal buildups along the edge of the developing Bondoc Sub-basin such as the Yuni mounds above and below the green horizon.
- Early Middle Miocene basin floor fans such as the Mulanay mound above the green horizon on line RG-83-808, and a mound in the Yuni area in deeper water.

If reservoirs are present, there is potential for large oil reserves within the structures, amounting to some 50 million barrels in very shallow water in the Mabio area in the north, more than 300 million barrels in the Mulanay area in just one of several traps, and over 100 million barrels at the base of Middle Miocene (green horizon) level in the Yuni area. Large additional reserves at shallower levels in the Yuni area can be hypothesised if a lateral seal is provided by Miocene shales in the Bondoc Point Flower Structure, and top seal by the Canguinsa Formation.

The large potential traps in the Mulanay and Yuni areas lie largely in water depths exceeding 200 m, but deviated drilling could be carried out from a water depth of 200 m. It should be possible to drill one of the Mabio culminations from onshore.

REFERENCES

ADAMS, C.G., 1984. Neogene larger foraminifera, evolutionary and geological events in the context of datum planes. In: N. Ikebe and R. Tsuchi (Ed.), Pacific Neogene Datum Planes: *Contributions to Biostratigraphy and Chronology*, Univ. of Tokyo Press, 47-67.

ADAMS, C.G., BUTTERLIN, J., and SAMANTA, B.K., 1986: Larger Foraminiferida and events at the Eocene/Oligocene boundary in the Indo-West Pacific region. In: C. Pomerol and I. Premoli Silva (Eds), *Terminal Eocene Events*. 237-252. Elsevier, Amsterdam.

ANTONIO I. S., 1961. Geological report on PEC 68, 73, and 102 Northern Bondoc Peninsula Quezon Province, Luzon Island, Philippines, Fourth Calendar Year. Maremco Mineral Corp. and Republic Resources and Development Corp. 53p. (unpublished).

ARCI, 1988. Radar image interpretation to assess the hydrocarbon potential of four sites in the Philippines. Arkansas Research Consultants Inc., 3 volumes, pp 77-99. (unpublished).

AURELIO, M. A., BARRIER, E., RANGIN, C., and MULLER, C., 1991. The Philippine fault in the Late Cenozoic tectonic evolution of the Bondoc-Masbate-N. Leyte area, central Philippines. *Journal of Southeast Asian Earth Sciences*, 6, (3/4), pp 221-238.

BED, 1986. Sedimentary Basins of the Philippines - their Geology and Hydrocarbon Potential. World Bank financed Petroleum Exploration Promotion Project, prepared by the Bureau of Energy Development Office of the President, under the supervision of Robertson Research (Australia) and Flower Doery and Buchan Pty Ltd.

BERGGREN, W.A., 1969. Cainozoic chronostratigraphy, planktonic foraminiferal zonation and the radiometric time scale. *Nature*, 224, 1072-1075.

BERGGREN, W.A., KENT, D.V., & FLYNN, J.J., 1985a. Palaeogene geochronology and chronostratigraphy. In: N.J. Snelling (Ed.). The Chronology of the Geological Record. *Geological Society of London, Memoir*, 10, 141-195.

BERGGREN, W.A., KENT, D.V., & VAN COUVERING, J.A., 1985b. The Neogene: Part II. Neogene geochronology and chronostratigraphy. In: N.J. Snelling (Ed.). The Chronology of the Geological Record. *Geol. Soc. of London, Memoir*, 10, 211-250.

BLOW, W.H., 1969. Late Middle Eocene to Recent planktonic foraminiferal biostratigraphy. In: P. Bronniman & H.H. Renz (Eds.), *Proceedings of the 1st International Conference on Planktonic Micro fossils*, Geneva, 1967, I, 199-422.

BLOW, W.H., 1979. The Cainozoic Globigerinida. A study of the morphology, taxonomy, evolutionary relationships and the stratigraphical distribution of some Globigerinida (mainly Globigerinacea). *E.J. Brill, Leiden.*

BOLLI, H.M., 1957a. The genera *Globigerina* and *Globorotalia* in the Paleocene- lower Eocene Lizard Springs Formation of Trinidad, B.W.I. In: Studies in Foraminifera. *United States National Museum Bulletin*, 215, 61-81.

BOLLI, H.M., 1957b. Planktonic foraminiferids from the Oligocene - Miocene Cipero and Lengua Formations of Trinidad, B.W.I. In: Studies in Foraminifera. *United States National Museum Bulletin*, 215, 97-123.

BOLLI, H.M., 1966. Zonation of Cretaceous to Pliocene marine sediments based on planktonic foraminifera. *Boletin Informativo, Associacion Venezolan de Geologia, Mineria y Petroleo*, 9, 3-32.

BOLLI, H.M., & PREMOLI SILVA, I., 1973. Late Cretaceous to Eocene planktonic foraminifera and stratigraphy of the Leg 15 sites in the Caribbean Sea. In: N.T. Edgar, J.B. Saunders, et al., *Initial Reports of the Deep Sea Drilling Project*, 15, 475-497. U.S. Government Printing Office, Washington.

BUREAU OF MINES, 1963. 1:1,000,000 Geological Map Series, *City of Manila (ND-51)*, Bureau of Mines, Manila, Philippines.

CARON, M, 1985. Cretaceous planktonic foramnifera. In: H. M. Bolli, J. B. Saunders and K. Perch-Neilson, eds, *Planktonic Stratigraphy*, 17-86. Canterbury University Press.

CHAPRONIERE, G.C.H., 1981. Australian mid-Tertiary larger foraminiferal associations and their bearing on the East Indian letter Classification. *BMR Journal of Australian Geology and Geophysics*, 6, 145-151.

CHAPRONIERE, G.C.H., 1983. Tertiary larger foraminiferids from the northwestern margin of the Queensland Plateau, Australia. *Bureau of Mineral Resources Australia*, Bulletin 217, 31-57.

CORBY, G. W. 1937. A preliminary report of the Maglihi-Molove area, Bondoc Peninsula Tayabas. Far East Oil Development Corporation, 10p.

CORBY, G. W. *et al*, 1951. Geology and Oil possibilities of the Philippines, *Department of Agriculture and Natural Resources, Technical Bulletin* 21, 359 pp.

DOE, 1988. Petroleum potential of the Philippines. Office of Energy Affairs, Republic of the Philippines, 88p. (unpublished).

DOMINGO, C. G., 1976. Oil and gas possibilities on Southern Part of the Bondoc Peninsula, Quezon Province for Bondoc Service Contract No 20, Report to Department of Energy, Philippines, 26p. (unpublished).

EVANS, D., HEGGIE, D.T., BISHOP, J.H., REYES, E.N. & LEE, C.S., 1992. Light Hydrocarbon Geochemistry in Bottom Waters of the Philippines Continental shelf, Part A: Ragay Gulf and Tayabas Bay. *Australian Geological Survey Organisation, Record* 1992/92, 350.

FORSTER , Hg., OLES, D., KNITTEL, U., DEFANT, M. and TORRES, R., 1990. The Macolod Corridor: A rift crossing the Philippine island arc. Tectonophysics, 183, 265-271. Elsevier Science Publishers BIV., Amsterdam.

HASHIMOTO, W. and MATSUMARU, K., 1981. Geological significance of the discovery of Nummulites *fichteli* (*Michelotti*) from the Sagada Plateau, Bontoc, Mountain Province, Northern Luzon, Philippines: *Contributions to the Geology and Paleontology of Southeast Asia*, CCXVI, University of Tokyo Press, 75-192.

JEFFREY, A.W.A., ALIMI, H.M., and JENDEN, P.D., 1991 -- Geochemistry of Los Angeles Basin Oil and Gas Systems. *In* BIDDLE, K.T., Active Margin Basins; *AAPG Memoir* 52, 197-219.

JENKINS, D.G., BOWEN, D.Q., ADAMS, C.G., SHACKLETON, N.J., & BRASSIL, S.C., 1985. The Neogene: Part 1. In: N.J. Snelling (Ed.), The Chronology of the Geological Record. *Geological Society of London, Memoir* 10, 199-210.

LEE, C.S. and RAMSAY, D., 1992. Philippines Marine Seismic Survey Project Cruise Report. *Bureau of Mineral Resources, Australia, Record*, 1992/49, 69p.

MARTIN, S. G. and ESPIRITU, E. A., 1968. Report on the Geology and section measurements on Bondoc Peninsula, Quezon Province. Report for Petroleum Division Bureau of Mines, 88p. Unpublished.

MITCHUM, R.M., VAIL, P.R. and SANGREE, J.B., 1977. Seismic Stratigraphy and Global Changes of Sea Level, Part 6: Stratigraphic Interpretation of Seismic Reflection Patterns in Depositional Sequences. in Seismic Stratigraphy -applications to hydrocarbon exploration. *American Association of Petroleum Geologists Memoir* 26, 117-133.

NICOLAI, E.O., OLIVARES, N.D. AND SCOTT, H.S., 1973. Oil and Gas Possibilities in Part of the Bondoc Peninsula, Quezon Province, Philippines. White Eagle Overseas Oil Company Inc.

PRATT, W. E. and SMITH, W. D., 1913. The Geology and Petroleum Resources of the Southern part of the Bondoc Peninsula, Tayabas Province, Philippine Islands. *Philippines Journal of Science*, 8, (4).

POBLETE R.G. Jr., & FERRER, A.P., 1990. Regional geological study of the total Canguinsa section. Internal report, Lomar Logistic/Marketing Philippines Inc., 12p. (unpublished).

RANGIN C., 1991. The Philippine Mobile Belt: a complex plate boundary. *Journal of Southeast Asian Earth Sciences*, 6 (3/4), pp 209-220.

SAREWITZ, D.R. & LEWIS, S.D., 1991. The Marinduque intra-arc basin, Philippines: Basin genesis and *in situ* development in a strike-slip setting. *Geological Society of America Bulletin*, 103, 597-614.

SNOWDON, L.R., and Powell, T.G. 1982. -- Immature oil and condensates-modification of hydrocarbon generation model for terrestrial organic matter; *AAPG Bulletin*, 66, 775-588.

STAINFORTH, R.M., LAMB, J.L., LUTERBACHER, H., BEARD, J.H., & JEFFORDS, R.M., 1975. Cainozoic planktonic foraminiferal zonation and characteristics of index forms. *University of Kansas Paleontological Contributions*, Article 62, 1-425.

TISSOT, B.P. & WELTE, D.H., 1984. Petroleum formation and occurrence. *Springer Verlag*, Berlin, 2nd Ed., Figure. 11.6.7, p. 210.

YAP, A.L., 1972. Geological Report on PEC 68 Bondoc Peninsula, Quezon Province. Maremco Mineral Corporation. 14p. (unpublished).

YAP, A.L., 1977. Geological Evaluation of the Service Contract No 20 Area, Bondoc Peninsula, Quezon Province, Philippines. For Philippines Oil Development Co Inc, 7p.

PART 3

GEOLOGY AND PETROLEUM POTENTIAL OF NORTHEAST PALAWAN SHELF

by

A. R. Fraser[1] and E. B. Guazon[2]

1 Australian Geological Survey Organisation, Canberra, ACT, Australia
2 Department of Energy, Makati, Metro Manila, Philippines

ABSTRACT

This report assesses the geology and petroleum potential of the continental shelf of northeast Palawan based on an interpretation of 2076 kilometres of seismic data acquired in 1978 and 1979 by CITCO Philippines Petroleum Corporation, and 580 kilometres of seismic and geochemical data acquired in 1992 by the Australian Geological Survey Organisation in conjunction with the Philippine Department of Energy, under funding from the Australian International Development Assistance Bureau. The seismic interpretation was tied to three exploration wells drilled by CITCO: Roxas-1 drilled in 1979 to a depth of 2030 metres; Dumaran-1 drilled in 1979 to a depth of 2186 metres; and Paly-1 drilled in 1981 to a depth of 2098 metres.

Four major sequences were recognised seismically and correlated to wells. These are a Cretaceous rift sequence deposited in terrestrial to marginal marine environments when the area was attached to the China craton; an Oligocene to Middle Miocene, mainly transgressive sequence of clastics deposited in inner to middle sublittoral environments while the Palawan microcontinent drifted southwards as a result of opening of the South China Sea; a Middle Miocene prograding sequence deposited during a regressive phase which probably marked the onset of collision tectonics; and a Late Middle Miocene to Pleistocene sequence of clastics and limestones deposited on the shelf and slope after the collision-induced Middle Miocene phase of uplift and erosion.

The best potential reservoirs encountered in exploration wells are well developed intervals of clean sandstone within the Middle Miocene prograding sequence. This sequence subcrops the Middle Miocene unconformity under the outer shelf and slope along most of the northeast Palawan margin. Possible reef buildups on the edge of the Middle Miocene paleo-shelf may also have good potential as reservoirs. The potential of the Oligocene to Middle Miocene and Cretaceous sequences is rated as moderate.

No source rocks were penetrated in wells, but their existence in the basin is confirmed by the presence of a gas accumulation and dead oil traces in a 1000 metre thick section of non-reservoir conglomerates in the Dumaran-1 well. Measurements of vitrinite reflectance and spore coloration indicate maturity levels ranging from early to middle mature for oil in the pre-unconformity section. These levels were attained prior to Middle Miocene uplift however, and are not indicative of present-day generative capacity at the well locations.

Traps were seismically defined at the Middle Miocene unconformity and Top Cretaceous levels. Middle Miocene anticlinal and (?)reef traps may be sealed by shales in the post-unconformity section, and charged by hydrocarbons generated from Cretaceous sources beneath the traps, or from sources in a thick wedge of Oligo-Miocene sediments under the continental slope 15 to 30 kilometres away. Traps defined at Top Cretaceous level may be sealed intra-formationally or by shales in the overlying Oligo-Miocene section. The traps had formed by the Oligocene and could have been charged by hydrocarbons generated from Cretaceous sources or from Oligo-Miocene shales prior to Middle Miocene uplift. Early charging of traps could have helped preserve porosity by inhibiting calcite cementation.

Three lead areas and the Dumaran gas accumulation were evaluated for potential hydrocarbon reserves. The leads are closed structural highs at Middle Miocene unconformity and Top Cretaceous levels. The Dumaran gas accumulation is not structurally closed and must be limited to the northwest and northeast by intra-formational

permeability barriers. The accumulation may be of significant size if it encompasses good reservoir sandstones of the Middle Miocene prograding sequence three kilometres to the southeast of the well. This sequence is interposed between the well and a probable source 'kitchen' area to the southeast. The accumulation may include oil as well as gas if dead oil traces, observed over a 300 metre interval in the well, are remnants of an oil column displaced down dip by gas.

CONTENTS

INTRODUCTION **9**

TECTONIC SETTING **12**

EXPLORATION HISTORY **12**
- Licence History
- Seismic Surveys
- Exploration Wells

SEISMIC INTERPRETATION **19**
- Data Description
- Seismic Horizons
- Seismic Sequences
- Structural Divisions
- Synthesis

PETROLEUM GEOLOGY **30**
- Reservoirs
- Traps and Seals
- Geochemical Sampling
- Source Rocks and Maturation
- Migration and Timing
- Drilling Analysis
- Evaluation of Leads

CONCLUSIONS **41**

REFERENCES **47**

TABLES

Table 1 Depths and travel times to horizons identified in wells.
Table 2 Seismic horizons and sequences.
Table 3 Parameters for Dumaran Lead.
Table 4 Parameters for Roxas Lead.
Table 5 Parameters for Pasig Lead.
Table 6 Parameters for Honda Bay Lead.

FIGURES

Figure 1 Survey areas for the Philippines - Australia Marine Seismic Survey Project.
Figure 2 Location map.
Figure 3 Tectonic elements of the Eurasian Plate.
Figure 4 Former contract areas.
Figure 5 Seismic coverage and location of sample seismic lines.
Figure 6 Generalised stratigraphic column.
Figure 7 Well lithologies and seismic horizons.
Figure 8 Seismic line 109/02 showing Middle Miocene prograding sequence.
Figure 9 Seismic line 109/02 showing basement high.
Figure 10 Seismic line 78-52 showing seismic sequences.
Figure 11 Seismic line 78-78 showing reverse fault in Dumaran area.
Figure 12 Roxas-1 logs and calculated porosities.
Figure 13 Paly-1 logs and calculated porosities.
Figure 14 Dumaran-1 logs and calculated porosities.
Figure 15 Seismic line 78-67 showing possible Middle Miocene reef.
Figure 16 Paly-Dumaran area total hydrocarbon content.
Figure 17 Roxas area total hydrocarbon content.
Figure 18 Honda Bay area total hydrocarbon content.
Figure 19 Seismic line 78-95 through Paly-1.

ENCLOSURES

Maps (see Volume 3)

Map P-1 Bathymetry map of Paly-Dumaran area. Scale 1:50,000.
Map P-2 Time structure map of Paly-Dumaran area at Middle Miocene Unconformity. Scale 1:50,000.
Map P-3 Time structure map of Paly-Dumaran area at base of Middle Miocene Prograding Sequence. Scale 1:50,000.
Map P-4 Time structure map of Paly-Dumaran area at top Oligocene(?). Scale 1:50,000.
Map P-5 Time structure map of Paly-Dumaran area at base Tertiary. Scale 1:50,000.
Map P-6 Bathymetry map of Roxas area. Scale 1:50,000.
Map P-7 Time structure map of Roxas area at Middle Miocene Unconformity. Scale 1:50,000.
Map P-8 Time structure map of Roxas area at Middle Miocene Unconformity (Water Compensated). Scale 1:50,000.

Map P-9	Time structure map of Roxas area at base of Middle Miocene Prograding Sequence. Scale 1:50,000.
Map P-10	Time structure map of Roxas area at top Cretaceous. Scale 1:50,000.
Map P-11	Time structure map of Roxas area at top Cretaceous (Water Compensated). Scale 1:50,000.
Map P-12	Bathymetry map of Honda Bay area. Scale 1:50,000.
Map P-13	Time structure map of Honda Bay area at top Cretaceous. Scale 1:50,000.
Map P-14	Time structure map of Honda Bay area at top Cretaceous (Water Compensated). Scale 1:50,000.
Map P-15	Regional geology map of Northeast Palawan Shelf. Scale 1:150,000.

Plates (see Volume 4)

Plate P-1	Time structure map of Paly-Dumaran area at Middle Miocene Unconformity. Scale 1:75,000.
Plate P-2	Time structure map of Roxas area at Middle Miocene Unconformity (Water Compensated). Scale 1:75,000.
Plate P-3	Time structure map of Roxas area at top Cretaceous (Water Compensated). Scale 1:75,000.
Plate P-4	Time structure map of Honda Bay area at top Cretaceous (Water Compensated). Scale 1:75,000.
Plate P-5	Montage for Dumaran Lead.
Plate P-6	Montage for Roxas Lead.
Plate P-7	Montage for Pasig Leads.
Plate P-8	Montage for Honda Bay Lead.

INTRODUCTION

The continental shelf of northeast Palawan is one of four areas of the offshore Philippines (Fig. 1) over which combined geophysical/geochemical surveys were conducted in 1992 by the Australian Geological Survey Organisation (AGSO), in conjunction with the Philippine Department of Energy (DOE), under funding from the Australian International Development Assistance Bureau (AIDAB). The shelf extends for about 180 kilometres in a northeasterly direction and is up to 40 kilometres wide (Fig. 2). It varies from a gently deepening surface with no well defined shelf break in the north; a broad flat surface with a well-defined shelf break in the central portion; to a deeply dissected surface cut by submarine canyons in the south.

The area was previously explored for hydrocarbons by CITCO Philippines Petroleum Corporation, a subsidiary of the former independent American oil company, Cities Service Inc. CITCO conducted seismic surveys in 1978 and 1979 prior to the drilling of three exploration wells: Roxas-1, drilled in 1979 to a depth of 2030 metres; Dumaran-1, also drilled in 1979 to a depth of 2186 metres, with a sidetrack drilled to 2088 metres; and Paly-1, drilled in 1981 to a depth of 2098 metres. No significant hydrocarbon shows were recorded in Roxas-1 or Paly-1, but Dumaran-1 encountered gas shows over the interval 1000 metres to 2040 metres and traces of dead oil between 1660 metres and 1970 metres. Four drill stem tests in the sidetrack hole produced only minor flows and the well was plugged and abandoned. CITCO relinquished the Northeast Palawan Contract Area in 1981.

This report assesses the geology and petroleum potential of the Northeast Palawan Shelf. Seismic data were interpreted and mapped in an effort to locate structural traps of potentially economic size and, in combination with well results, to predict a possible distribution of source and reservoir rocks. The seismic data comprises 2076 kilometres of data acquired by CITCO in 1978 and 1979, and 580 kilometres acquired by AGSO in 1992. The two data sets are complementary. The CITCO lines form a 1 to 2 kilometre grid concentrated over portions of the shelf with thickest sedimentary development, whereas the AGSO lines, spaced at 6 to 10 kilometre intervals, tie the wells and extend over deeper water areas including the canyon-incised Honda Bay area in the south. Hence, the CITCO lines are important for the structural delineation of leads and prospects, while the AGSO lines are important for stratigraphic correlation between and beyond areas of closely spaced seismic lines.

Concurrently with seismic acquisition, AGSO carried out geochemical, gravity and magnetic surveys. Gravity and magnetic profiles were plotted on seismic sections. The geochemical survey utilised a submerged towfish to detect light hydrocarbons dissolved in bottom waters through continuous water sampling. Direct hydrocarbon detection (DHD) anomalies may indicate the presence of mature source rocks in an area, and the existence of migration pathways extending from source beds into reservoirs en route to the surface. The DHD results were prepared in a form suitable for comparison with the seismic interpretation.

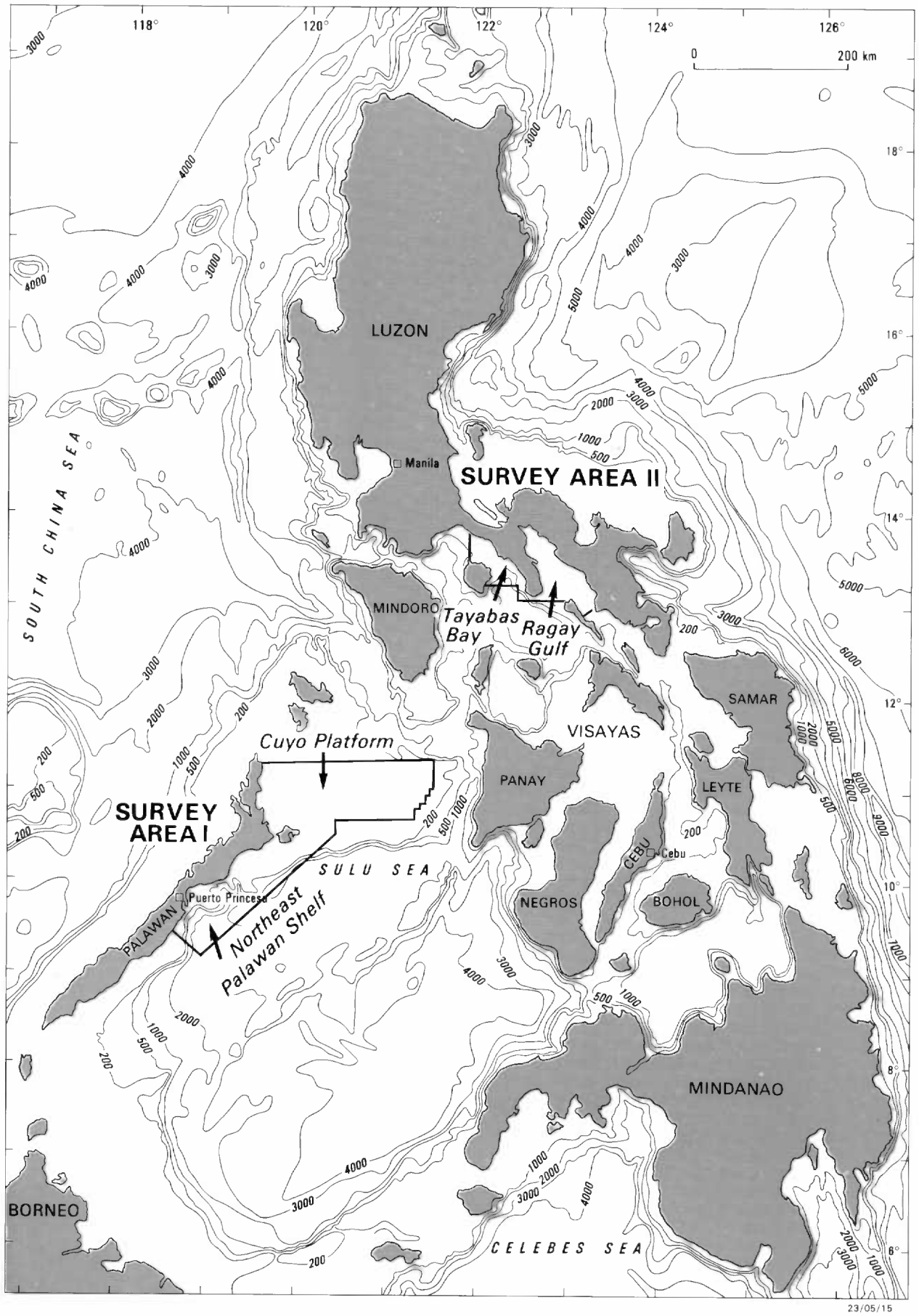

Figure 1 Survey areas of the Philippines - Australia Marine Seismic Survey Project.

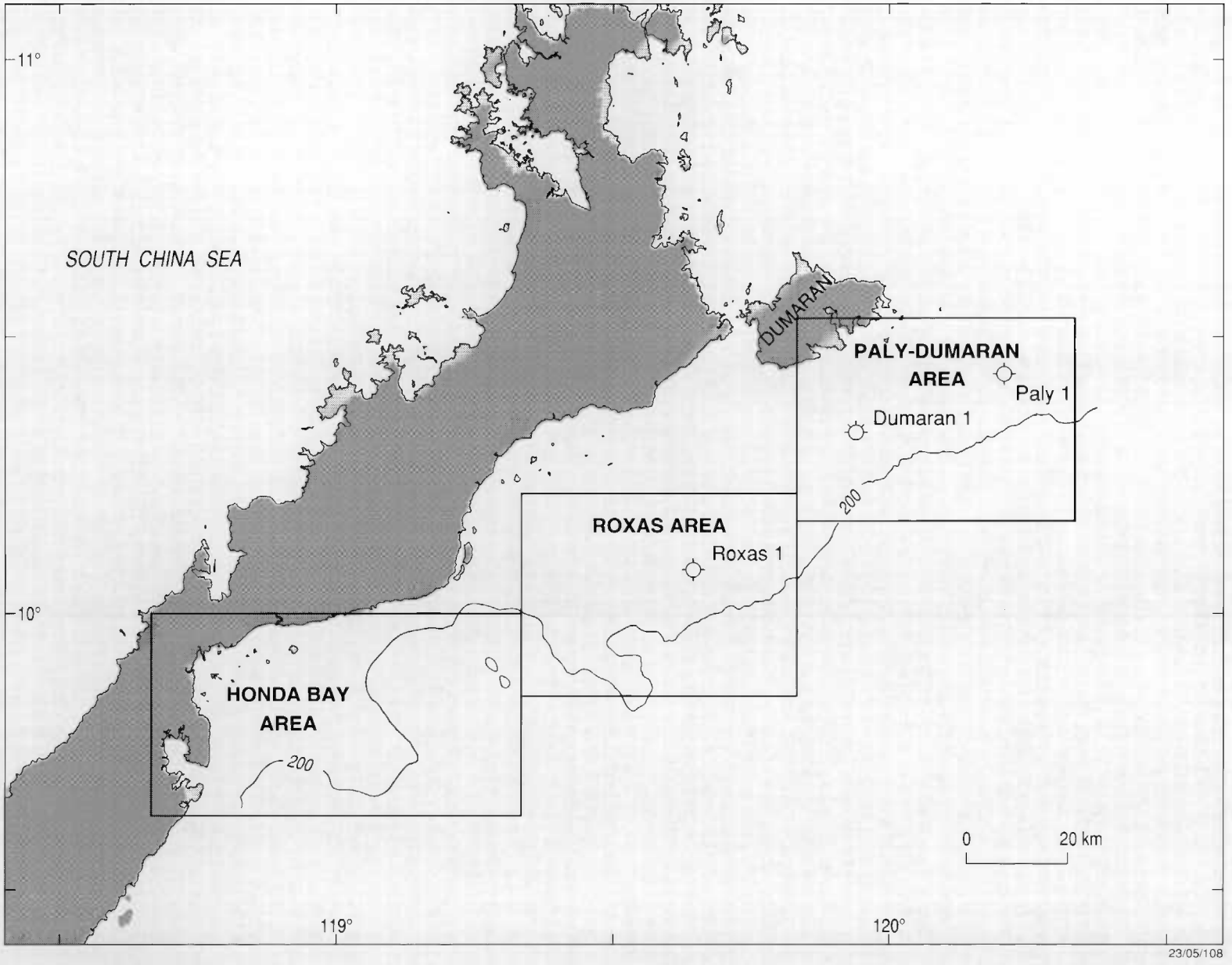

Figure 2 Location map.

Bathymetric and seismic maps are presented at 1:50 000 scale in three sheet areas. From northeast to southwest these are named the Paly-Dumaran, Roxas and Honda Bay areas (Fig. 2). Colour maps at 100 000 scale and montages are presented for prospective horizons and lead areas respectively.

TECTONIC SETTING

The island of Palawan lies in the southeastern part of the Kalayaan-Calamian microplate which is regarded as a continental fragment that separated from the southern margin of China in Oligocene times (Bureau of Energy Development, 1986). This separation was preceded by a prolonged period of extension tectonics culminating in continental breakup and opening of the South China Sea in a north-south direction (Fig. 3). Oceanic magnetic anomalies in the South China Sea strike east-west and range in age from Oligocene (32 My) to Early Miocene (17 My).

Seafloor spreading was terminated in Middle Miocene times by the collision of the Kalayaan-Calamian microplate with the southern end of the Philippine island arc complex. This collisional event led to widespread uplift and erosion and is marked by a regional unconformity in most parts of the Philippines.

The Kalayaan-Calamian microplate may consist of two or more microcontinental fragments, originally separated by oceanic or highly stretched continental crust, but sutured as a result of collision. Palawan and the zone of intermediate crust (i.e. highly extended continental crust) to its southeast formed the leading microcontinent which collided with the Cagayan Ridge, a volcanic arc in the Sulu Sea corresponding to an old subduction zone (Rangin, 1991; Holloway, 1982). Collision was followed by short-lived subduction of oceanic crust to the northwest of Palawan, forming the Palawan Trench. Subduction here was terminated by collision, with Palawan, of a fragment of stretched continental crust including Reed Bank.

EXPLORATION HISTORY

Licence History

CITCO Philippines Petroleum Corporation was awarded the Northeast Palawan Geophysical Contract Area (Fig. 4), covering most of the continental shelf and slope of northeast Palawan in September 1978. In November 1978, after completion of an 1899 kilometre seismic survey, 337,300 hectares of the original area on the outer shelf was retained by CITCO as the Northeast Palawan Service Contract Area, while the remaining area was relinquished. After the drilling of Roxas-1 and Dumaran-1 wells in 1979 and Paly-1 well in 1981, the service contract area was relinquished in November 1981.

Seismic Surveys (Fig. 5)

The 1978 survey was conducted by Western Geophysical of America under contract to CITCO (CITCO, 1978). A 48 group, 33 1/3 metre group interval, 1600 metre length streamer was employed during the survey and, with shot interval every 16 2/3 metres, coverage was 48 fold. The energy source was Western's Aqua Pulse gas gun array. Data were acquired along 100 lines with a total length of 1899 kilometres. Line spacing in areas of thickest sedimentary development on the shelf was generally 1 or 2 kilometres. The survey benefited from excellent weather for the most part, resulting in data of fair to good quality.

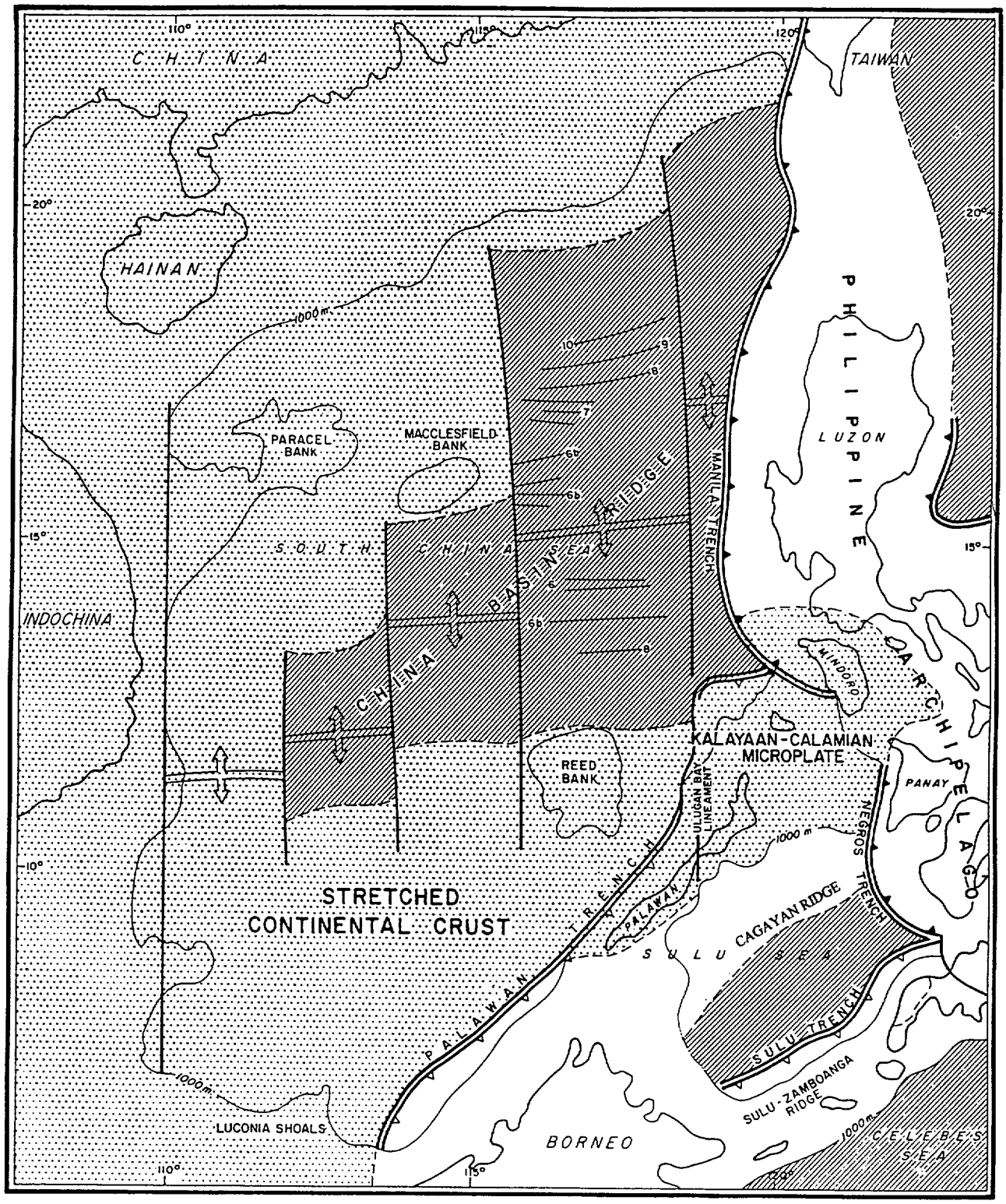

Figure 3 Tectonic elements of the Eurasian Plate.

(After Bureau of Energy Development, 1986)

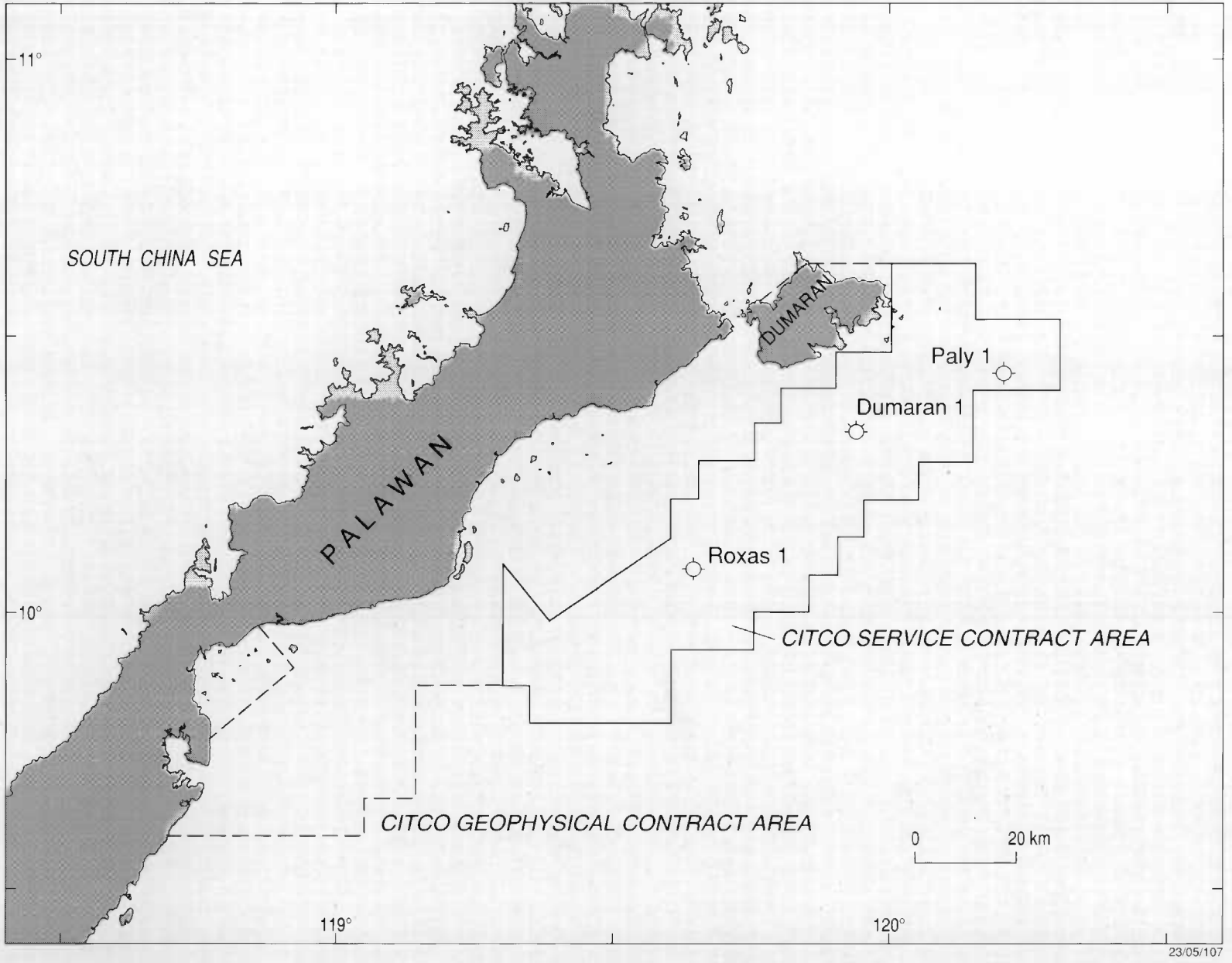

Figure 4 Former contract areas.

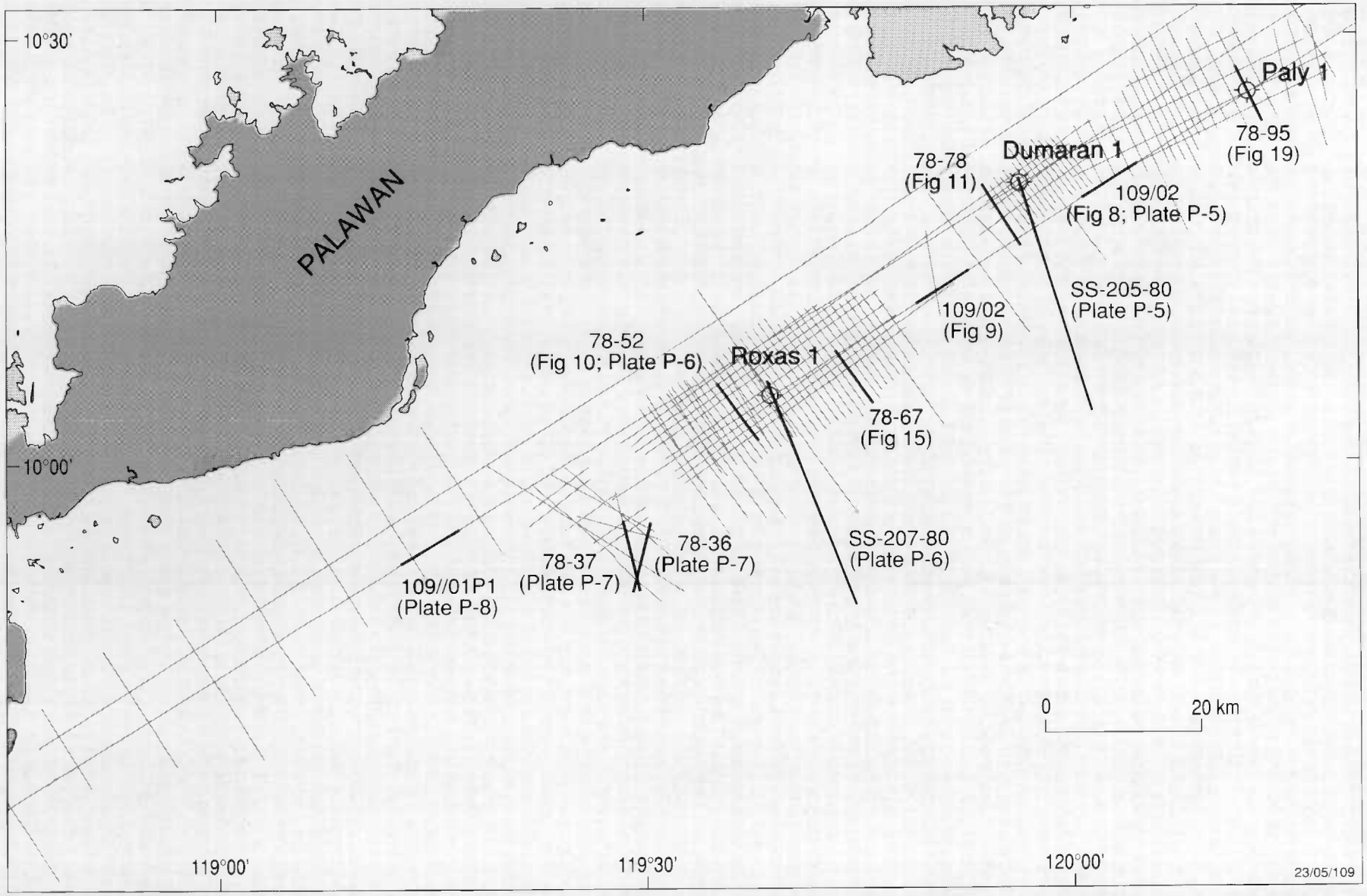

Figure 5 Seismic coverage and location of sample seismic lines.

The 1979 survey was conducted by Geophysical Exploration Company (GECO) of Norway under contract to CITCO (CITCO, 1979a). A 48 group, 50 metre group interval, 2400 metre streamer cable was employed during the survey and, with shot interval every 25 metres, coverage was 48 fold. The energy source was GECO's 2450 cu. in. conventional airgun array. The programme consisted of 15 NW-SE lines at 750 metre spacing and 3 NE-SW lines, totalling 177 kilometres. Bad weather and/or heavy seas during the survey were probably the main reasons for the poor quality of seismic data.

Exploration Wells

Roxas-1 was drilled in 1979 to evaluate a prognosed carbonate build-up or erosional feature thought to be of Lower Miocene age (CITCO, 1979b). The well penetrated some 460 metres of Plio-Pleistocene limestone overlying a Plio-Middle Miocene conglomerate down to 820 metres where a Middle Miocene unconformity was intersected (Figs. 6 and 7). Several moderately clean sands of probable Middle Miocene age were penetrated between 820 and 1200 metres, but the bulk of the sequence was a poorly sorted conglomerate. The section from 1200 to 1850 metres was an argillaceous sandy section with interbedded red clays of unknown age. The seismic objective was reached at 1850 metres and turned out to be an erosional surface on a tight sand-shale sequence of Upper Cretaceous age. The well penetrated 170 metres of this section before reaching TD at 2030 metres.

No oil or gas shows were recorded in Roxas-1 and no tests were run. However, encouragement was seen in the presence of clean sands in the Middle Miocene section, and geochemistry results suggesting that maturity is high enough for hydrocarbons to have been generated.

Dumaran-1 was drilled in 1979 to test a seismic anomaly that was considered to be either a carbonate build-up or a basement high, possibly overlain by draping sand or reef growth (CITCO, 1980). The sequence down to the Middle Miocene unconformity (952 metres) was similar to that encountered in Roxas-1; an upper limestone overlying a dirty conglomeratic sequence (Plio-Pleistocene-Middle Miocene) which had no shows. Similarities between the two wells end here, however, as gas shows were recorded in the well from about 1000 metres, with C1 through C3 down to 1080 metres and C1 through C4 from 1080 to 2040 metres. The section was a sandy, but non-reservoir, dirty conglomerate, and was essentially undifferentiated from the unconformity to the top of the objective (2048 metres). Traces of dead oil were seen between about 1660 and 1970 metres. The objective turned out to be serpentinized peridotite, of probable igneous origin. The well was terminated in basement at 2186 metres.

Four drill stem tests were conducted in a sidetrack hole drilled to 2088 metres. DST 1 (1935-1954 metres) was designed as a water test, but the formation was extremely tight and nothing was recovered. DST 2 (1722-1734 metres), DST 3 (1649-1658 metres), and DST 4 (1399-1417 metres) all produced small gas flows. Analyses of gas samples from DSTs 3 and 4 indicate that the two gases have a common source. Organic carbon values of cuttings from the well are very low (average 0.17 percent), indicating that gas must have migrated up dip from a source deeper in the basin.

The pre-Middle Miocene unconformity sediments were assigned an Upper Cretaceous age by the operator. The biostratigraphy report by Robertson Research gives the age of the interval 1649 to 1890 metres as not older than Senonian. This, and the fact that definite

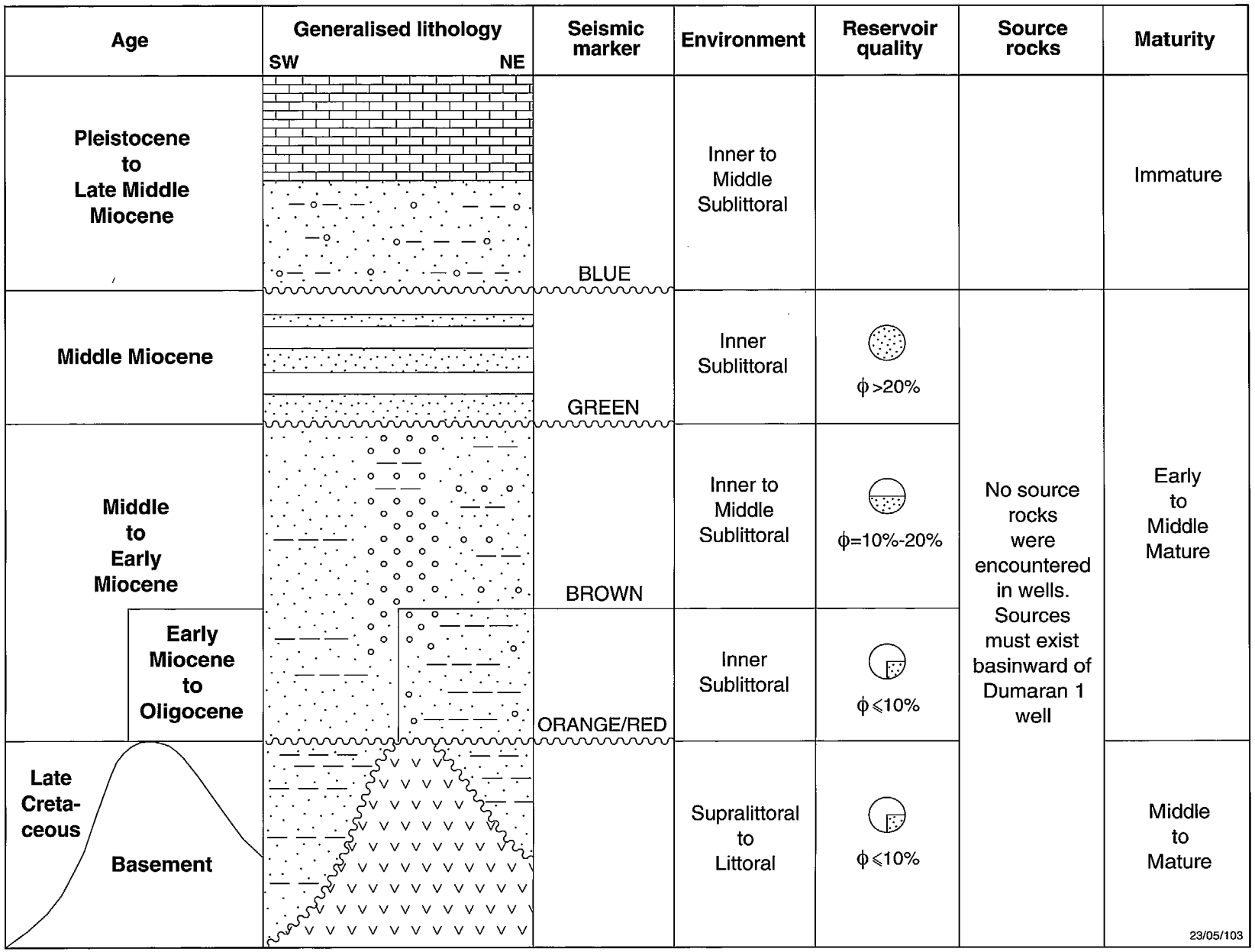

Figure 6 Generalised stratigraphic column.

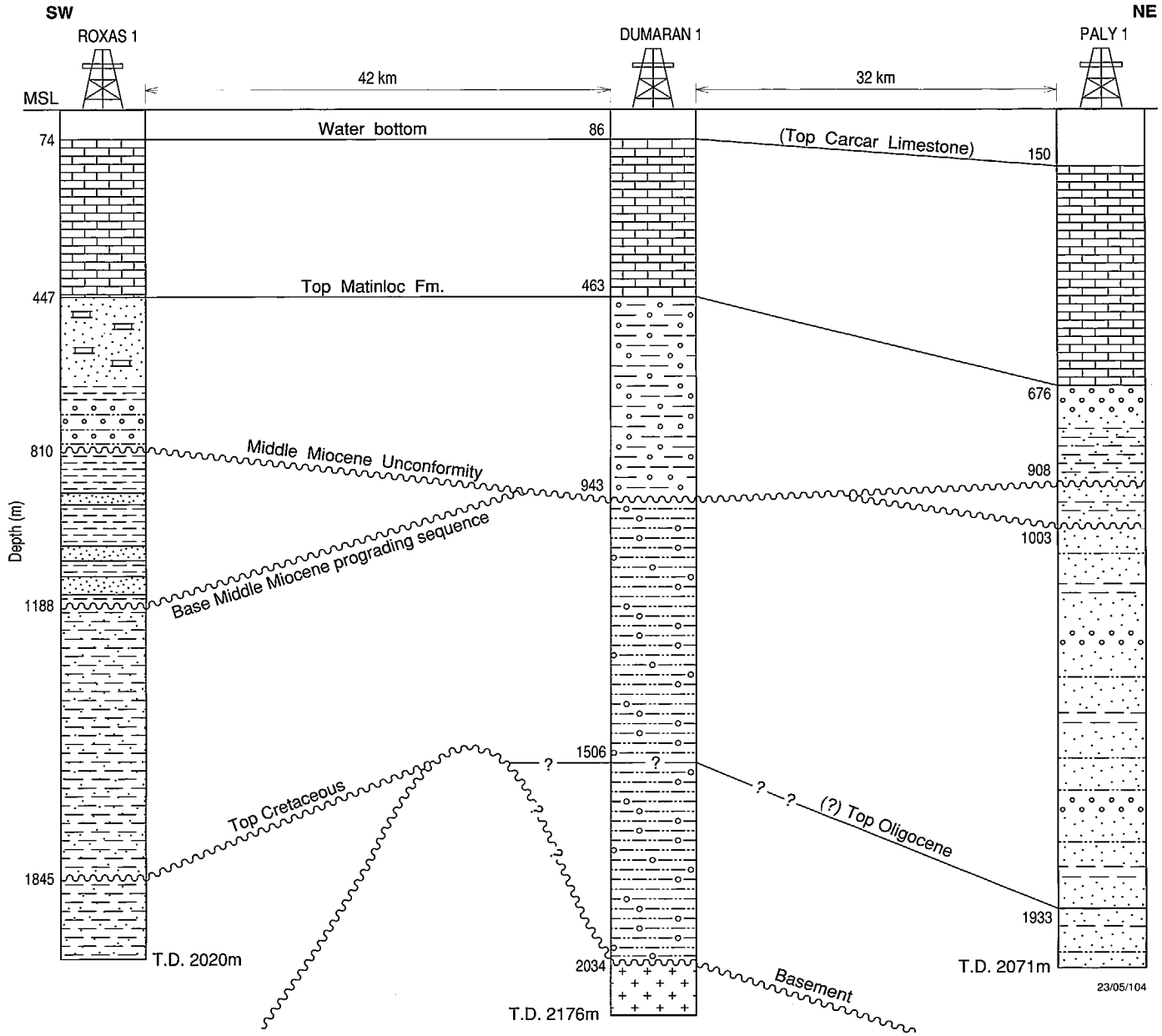

Figure 7 Well lithologies and seismic horizons.

Tertiary-restricted forms were not observed, are taken to suggest the possibility that the sediments are of Late Cretaceous age. However, such a dating must be treated with great caution in view of the lack of foraminifera and the paucity of identifiable palynomorphs in this interval.

Paly-1 was prognosed to test the hydrocarbon bearing potential of a series of supposedly Upper Cretaceous sandstones truncated by the Middle Miocene unconformity and overlain by fine to coarse clastics of Late Middle Miocene to Pliocene age which act as a seal (CITCO, 1982). The well was drilled in a more basinward position than Dumaran-1, and it was expected that the sandstones would in consequence be younger and of better reservoir quality.

The section above the Middle Miocene unconformity conformed with prognosis. Underlying the unconformity the section was much younger than prognosed. A clastic sequence of Oligocene to Miocene age, the result of apparent prograding and thickening in a basinward direction, was encountered. Sands were of poor reservoir quality, and no significant hydrocarbons were present. Log and sample analysis indicated no zones of interest to warrant drill stem testing. Gas readings remained very low throughout, and C_2 was only recorded over the interval 893 to 1000 metres, with a peak of 264 ppm at 981 metres. No C_3 was recorded.

CITCO regarded the poor shows in Paly-1, and the lack of improvement in source and reservoir quality as seriously downgrading the Northeast Palawan Service Contract Area. The company relinquished the acreage in November, 1981.

Depths and travel times to formation tops in wells are given in Table 1.

SEISMIC INTERPRETATION

Data Description

The principal data set used in the interpretation was the 1978 survey by CITCO. This was supplemented by 177 kilometres of data from the 1979 survey in the Dumaran area, and by the 580 kilometres of AGSO data in areas of sparse control including the Honda Bay area. Use was also made of deep water, SS-2XX-80 series lines shot in 1980 by Phillips Petroleum International Palawan Limited.

The 1978 data comprises 100 lines totalling 1899 kilometres, which form a regular grid of dip lines oriented NW-SE and strike lines oriented NE-SW. Seismic horizons were correlated over the entire grid but only horizons as picked on the dip lines were digitised and used for mapping. Data quality is fair to good, considering the vintage of the data, but low frequencies predominate and interpretation objectives requiring high resolution, such as delineating an uneven angular unconformity surface or revealing tilted fault blocks beneath a deeply buried erosion surface, are not achievable.

The 1979 data comprises 177 kilometres along 18 lines oriented mainly northwest at a spacing of 750 metres. Data quality is poor and interpretation problems were compounded by the fact that only unmigrated sections were available. To reduce these problems, stack sections for 11 lines were scanned and migrated by Petroconsultants Digimap of Sydney. Although interpretation was facilitated, data quality is considerably worse in the Dumaran area than in any other part of the Northeast Palawan Shelf.

The AGSO data consists of 580 kilometres along 13 lines (Lee and Ramsay, 1992). Problems were experienced in tying to the CITCO lines, due in part to differing phase and

Table 1. Depths and Travel Times to Horizons identified in wells

	ROXAS-1			DUMARAN-1			PALY-1		
HORIZON	Depth ft. RKB	Depth m. ss	Time sec. TWT	Depth ft. RKB	Depth m. ss	Time sec. TWT	Depth ft. RKB	Depth m. ss	Time sec. TWT
Water Bottom		74			86			150	
Top Matinloc	1500	447		1518	463	0.46	2306	676	0.679
Middle Miocene Unconformity	2690	810	0.705	3125	943	0.823	3068	908	0.874
Base Middle Miocene Prograding Sequence	3930	1188	0.983				3380 (?)	1003	0.96
Top Oligocene (?)							6432	1933	1.598
Top Cretaceous	6085	1845	1.368						
Basement				6704	2034	1.387			
T.D.	6660	2020	1.45	7172	2176	1.44	6883	2071	1.682

frequency content of the two data sets. AGSO lines were used for mapping control in the Honda Bay area, and other areas of sparse seismic control.

Seismic Horizons

Six horizons corresponding to major sequence boundaries were picked on seismic sections, of which five were mapped. From youngest to oldest the mapped horizons are Water Bottom (Maps P-1, P-6, and P-12), Middle Miocene Unconformity (Maps P-2, P-7, and P-8; Plates P-1 and P-2), Base Middle Miocene Prograding Sequence (Maps P-3, and P-9), (?)Top Oligocene (Map P-4), Top Cretaceous (Maps P-10, P-11, P-13, and P-14; Plates P-3 and P-4)) and Base Tertiary (Map P-5). A generalised stratigraphic column and well lithologic columns are shown in Figures 6 and 7 respectively. To remove the distorting effects on time structure maps of varying water depths, a water replacement velocity, V = 6250 + 0.433 D (where D is water depth in feet and V is in ft/sec), was assumed for certain key horizons in the Roxas and Honda Bay areas. This velocity was derived from an average velocity function for Roxas-1 well, regarded as having a fairly typical lithologic column over the area affected by rapidly varying water depths.

Water Bottom was mapped by converting echo-sounder depths to reflection times, plotting on seismic sections and digitising. This procedure was regarded as more accurate than attempting to pick the water bottom reflection directly (often missing in shallow water areas due to pre- stack muting) though less accurate than the more painstaking method of keying in several thousand echo-sounder depths. Comparison with bathymetric charts indicates that the accuracy of water bottom contours is better than 20 metres in areas of low to moderate gradient.

The Middle Miocene Unconformity (blue horizon) is a surface of erosion separating truncated, seaward dipping sediments below, from sediments parallel to the unconformity above. It was correlated and mapped over the entire Northeast Palawan Shelf, except in the Honda Bay area. The seismic pick at Roxas-1 on both CITCO and AGSO lines is about 100 milliseconds higher than the well time derived from the calibrated velocity log. One possible reason for the mistie is that the unconformity surface is locally uneven in the vicinity of Roxas-1 with the horizontal resolution of the seismic data being inadequate for correct imaging of surface irregularities due, for instance, to channel incision.

The Base Middle Miocene Prograding Sequence (green horizon) corresponds to the base of a prograding sequence, the upper part of which has been removed by erosion except in the outer shelf and slope where erosion was less marked (see AGSO line 109/02; Figure 8).

The (?) Top Oligocene (brown horizon) is correlated with the top of an interval dated as Middle/Early Miocene to Oligocene in Paly-1. The event is clearly evident as a moderate to high amplitude reflection in the Paly region. Correlation into the Dumaran region is less certain, but the horizon is interpreted to extend to the Dumaran-1 location. Hence, the seismic interpretation does not support the questionable dating of sediments below the Middle Miocene Unconformity as being Late Cretaceous.

The Top Cretaceous (orange horizon) corresponds to an unconformity at the top of a sequence dated as Late Cretaceous in Roxas-1. The horizon is easily recognisable as a high amplitude seismic event over the Roxas and Honda Bay areas. To the northeast, the event appears to merge with a basement reflection as the Cretaceous section pinches out against a basement high. A strong event at the base of reflections in the Paly area is

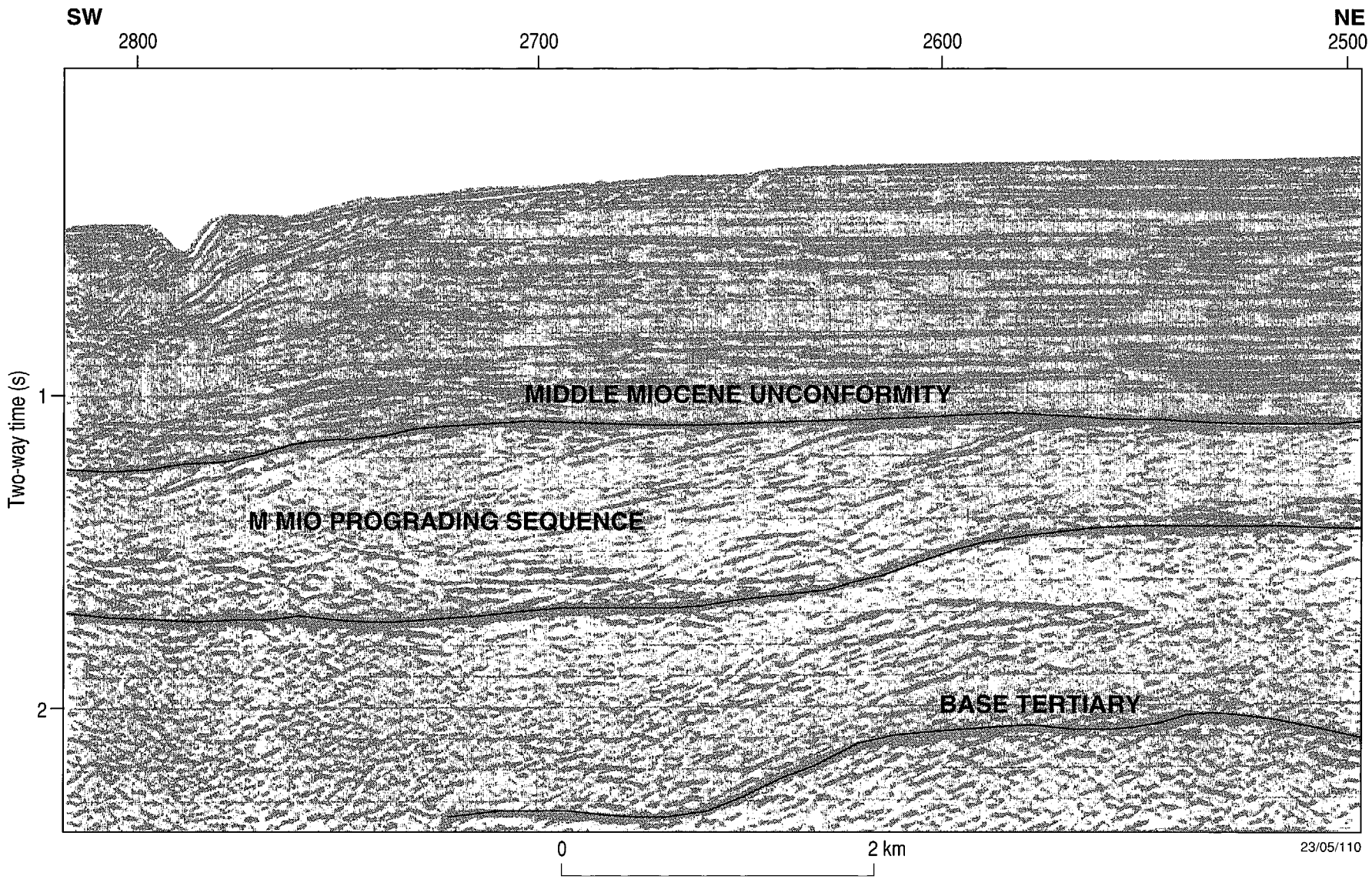

Figure 8 Seismic line 109/02 showing Middle Miocene prograding sequence.

termed Base Tertiary as it could represent either metamorphic basement or the top of highly consolidated Cretaceous or older sediments.

Basement (red horizon) can be correlated and mapped in the Dumaran area. It is buried beneath several kilometres of Cretaceous sediments in the Roxas area, and only becomes visible as it shallows towards the eastern edge of the area (see line 109/02; Fig. 9). The only well to encounter basement was Dumaran-1 which penetrated 140 m of serpentinized peridotite. These rocks are not typical of the Jurassic and older basement complex cropping out over much of northern Palawan, but may have affinities to the Cretaceous/Paleogene peridotites of central Palawan which are generally upthrusted or faulted into Tertiary and older formations (Bureau of Mines, 1963).

Seismic Sequences

Five seismic sequences have been identified from the seismic data tied to three exploration wells (Table 2; Fig. 10). From youngest to oldest these are described below.

The Pleistocene to Late Middle Miocene seismic sequence (Fig. 10) extends from the seabed to the Middle Miocene unconformity and is characterised by parallel reflections of moderate continuity, disrupted by channelling in a few areas. It correlates with limestones of the Carcar Formation conformably overlying conglomerates, shales and sandstones of the Matinloc Formation, deposited in a middle to inner sublittoral environment. The transition from clastic to carbonate deposition probably reflects diminishing clastic supply as streams returned to equilibrium after the Middle Miocene period of uplift and erosion.

The Middle Miocene Prograding Sequence (Fig. 10) is characterised by seaward dipping reflections of moderate to high amplitude and poor to moderate continuity, abruptly truncated up dip by the Middle Miocene unconformity. The sequence is most clearly seen to be prograding in deep water where erosion was less marked (Fig. 8). It consists of conglomerates, shales and siltstones with well developed, clean sandstone intervals where intersected in Roxas-1. It was probably deposited in the regressive phase marking the onset of Middle Miocene uplift. Sediments are likely to consist of reworked shelf deposits which may help to explain the clean, reservoir quality of the sandstones.

The Middle to Early Miocene seismic sequence (Fig. 10) consists of parallel to sub-parallel reflections of low to moderate amplitude, truncated above by the Middle Miocene unconformity, and onlapping the Late Cretaceous sequence in the Roxas area. In the wells it corresponds to an interval of argillaceous sandstones, siltstones, red clays and volcaniclastics deposited in an inner to middle sublittoral environment. The sequence is believed to be a mainly transgressive wedge built up on the margin of the Kalayaan-Calamian microplate as it drifted southwards. The Early Miocene to Oligocene seismic sequence consists of reflections of low to moderate continuity. The sequence in Paly-1 well comprises sandstones and conglomerates with minor clays, siltstones and volcaniclastics deposited in an inner sublittoral environment. Sediments were probably laid down in high energy conditions at the onset or in the early stages of drifting of the Kalayaan-Calamian microplate. Due to the difficulty in identifying the (?)Top Oligocene horizon outside the Paly region, and the general paucity of biostratigraphic markers in the pre-Middle Miocene Tertiary section, the umbrella term Oligo-Miocene sequence is applied to the undifferentiated interval between Base Middle Miocene prograding sequence (green horizon), and Top Cretaceous (orange) or Basement (red horizon).

Seismic penetration is insufficient to assess the seismic character of the Cretaceous sequence (Fig. 10). Sediments have been faulted, tilted and severely eroded. At Roxas-1

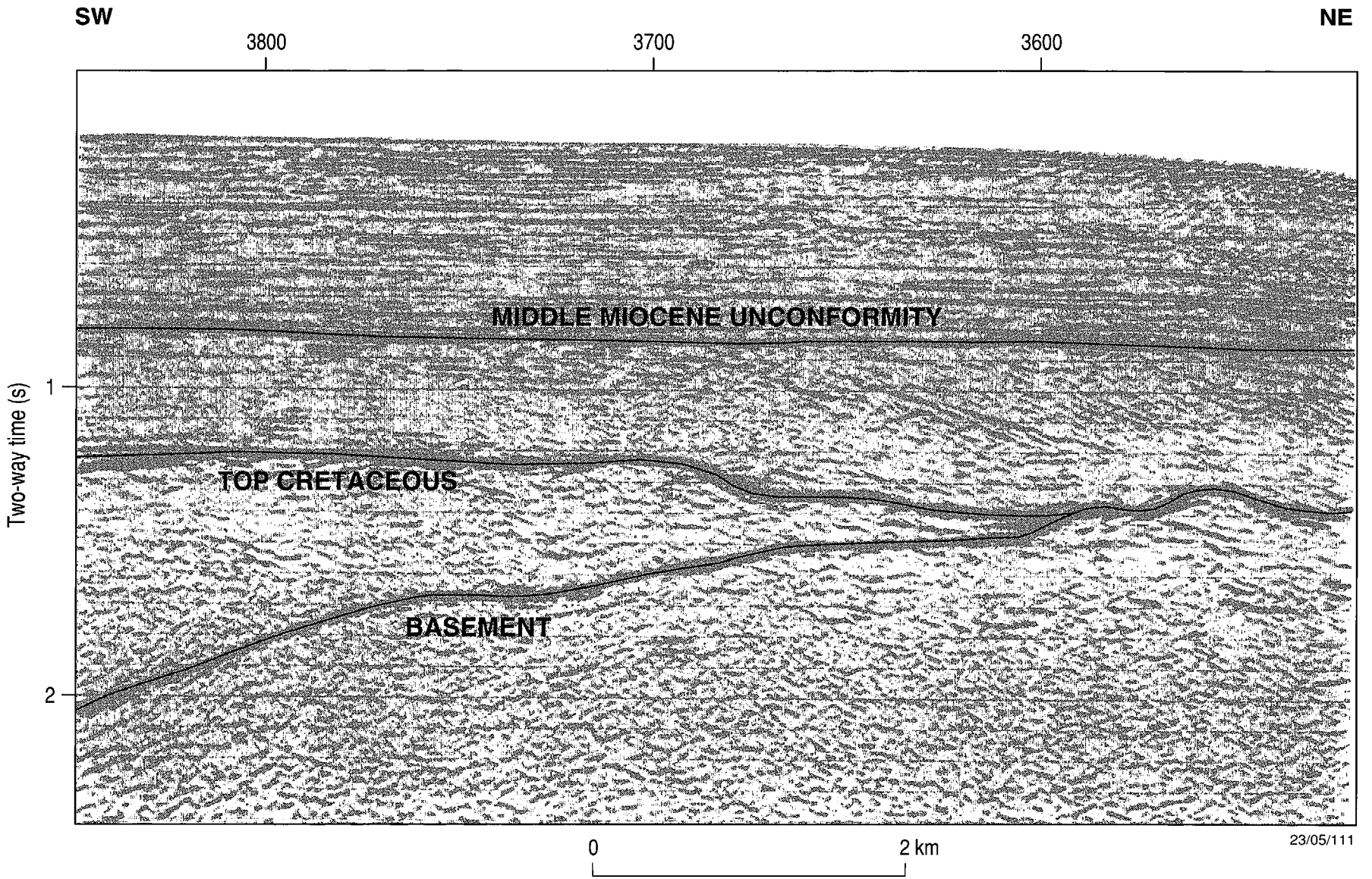

Figure 9 Seismic line 109/02 showing basement high.

Table 2. Seismic Horizons and Sequences

Seismic Horizon (colour code)	Areas Identified	Sequence Name/Age	Reflector termination (upper)	Reflector termination (lower)	Internal Configuration	Generalised Lithology	Environment
Water Bottom	All areas	Late Middle Miocene to Pleistocene (includes Carcar Limestone and Matinloc Formation)	Parallel	Onlap	Paralle, moderately continuous, occasionally channelised	Limestones overlying conglomerate/shale/ sandstone sequence	Inner-Middle Sublittoral
Middle Miocene Unconformity (blue)	All areas except Honda Bay	Middle Miocene prograding sequence	Truncation	Onlap/Downlap	Oblique to Sigmoid Prograding	Conglomerates, siltstones, shales with well developed sandstone intervals	Inner sublittoral
Base Middle Miocene Prograding Sequence (green)	All areas except Honda Bay	Middle - Early Miocene	Truncation	Onlap	Parallel, divergent in places	Argillaceous sandstone with red clays, siltstones, conglomerates and volcaniclastics	Inner to Middle sublittoral
Top Oligocene (?) (brown)	Paly - Dumaran	Early Miocene - Oligocene	Parallel	Onlap	Parallel, divergent in places	Sandstones & conglomerates with minor clay, siltstone, and volcaniclastics	Inner sublittoral
Top Cretaceous (orange)	Roxas, Honda Bay	Cretaceous	Truncation	Onlap	Tilted fault blocks	Sandstones, shales and siltstone	Supralittoral to littoral
Basement (red)	N and NW Roxas, Dumaran	(?) Mesozoic Basement				Serpentinized peridotite in Dumaran-1, metamorphic complex onshore	

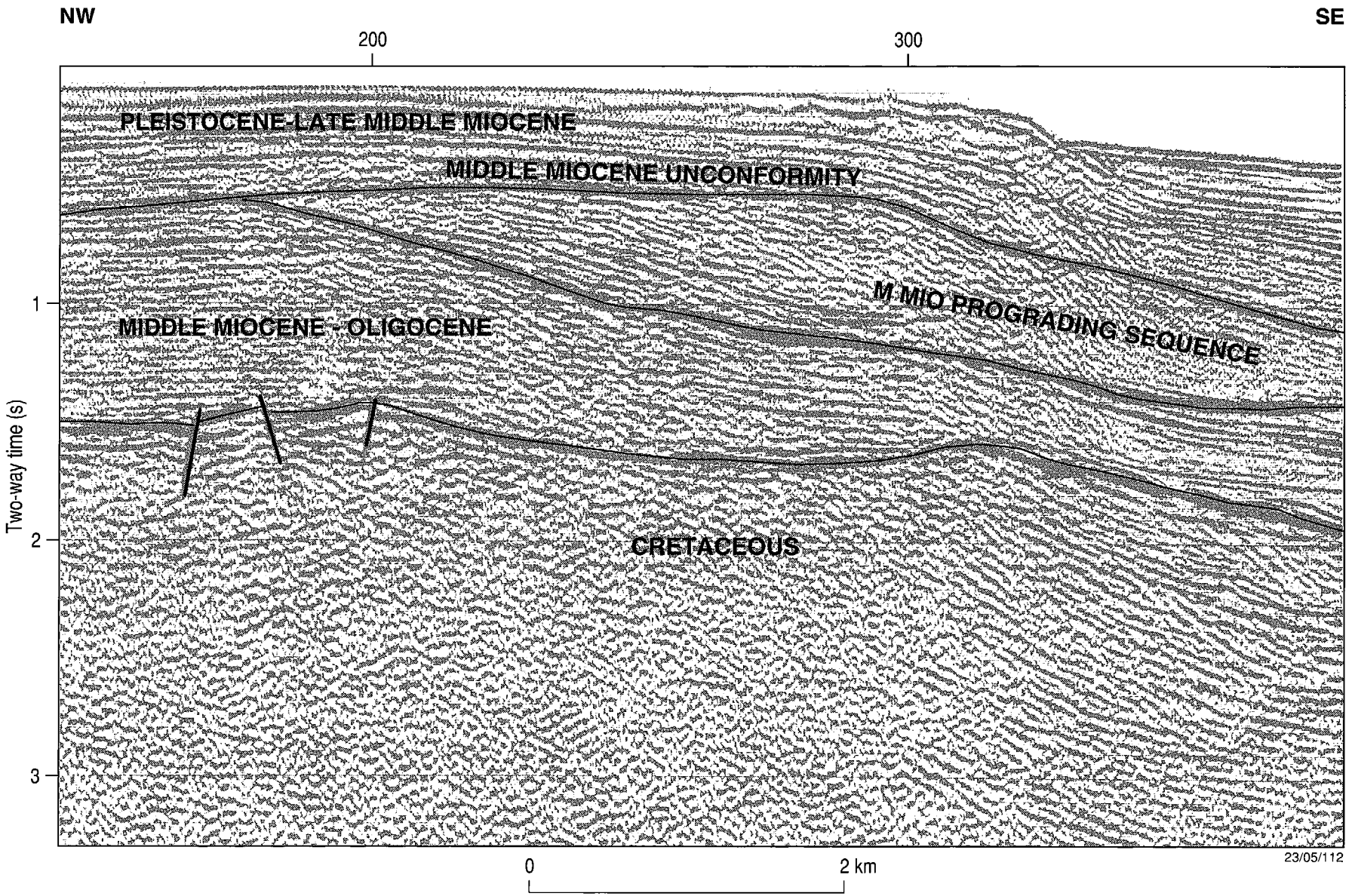

Figure 10 Seismic line 78-52 showing seismic sequences.

they consist of sandstones, shales and siltstones deposited in a supralittoral to littoral environment in a rift basin on the southern margin of China, before separation and southward drift of the Kalayaan-Calamian microplate.

Structural Divisions

The Northeast Palawan Shelf may be divided into three regions of differing structural style. These are the Roxas-Honda Bay region, the Dumaran region and the Paly region.

The Roxas-Honda Bay region is characterised by a largely unfaulted seaward thickening wedge of Cainozoic sediments overlying a block faulted, deeply eroded Cretaceous section. Seismic penetration was not adequate for mapping reflections beneath the Top Cretaceous unconformity. Small fault displacements (generally less than 100 milliseconds) mapped on the unconformity, thus reflect the degree of erosion which took place during Paleogene times, rather than indicating that the phase of rifting preceding the opening of the South China Sea was unusually subdued. Fault displacements and general relief of the Top Cretaceous surface are greatest (200 to 300 milliseconds) in the Pasig Reef area (southwestern part of Roxas sheet). This area may have been subjected to less erosion than elsewhere, perhaps as a result of earlier submergence and/or later structuring.

There is little evidence for rejuvenation of Cretaceous or Paleogene 'rift stage' faulting in Neogene times. Possible exceptions are faults apparently controlling the development of bathymetric salients in the Pasig Reef area, and near the intersection of line 109/06 with lines 109/01P2 and 109/11 in the Honda Bay area (Map P-15). Northwest trending faults west of Roxas-1 well are related to Neogene wrenching as they form, in the overburden, distinctive flower structures which displace the Middle Miocene unconformity. A slight rise of the Middle Miocene unconformity towards the shelf edge indicates mild basin inversion, probably a flexural response of the crust to earlier sediment loading at the base of the slope. The inversion provides important counter-regional dip for the development of potential hydrocarbon structural traps along the shelf edge.

The Dumaran region is separated from the Roxas region by a broad basement high with a crest near shotpoint 3550 on line 109/02 (Fig. 9). The structural and stratigraphic character of the region is quite anomalous compared to neighbouring parts of the shelf. These anomalous characteristics are:

1. The continental slope and the underlying Middle Miocene Unconformity are unusually steep and have the overall form of an embayment or re-entrant opposite the Dumaran region.
2. Unlike in other regions, the pre-Middle Miocene basin is fault-bounded on its landward side. The boundary is formed by a series of northeast trending en echelon faults, offset (presumably) by northwest trending faults. Faults are reverse and of large displacement (e.g. line 78-78; Fig. 11).
3. In the area between the basin and Dumaran Island, the Middle Miocene unconformity surface rises to form a broad, 500 millisecond, structural high. The high is onlapped by post-unconformity sediments indicating that it is not a recently formed feature.
4. The monotonous quartzite conglomeratic sequence of high thermal maturity encountered below the Middle Miocene Unconformity in Dumaran-1 well, contrasts with the sand/clay dominated pre-unconformity sequence of moderate maturity encountered in Roxas-1 and Paly-1 wells.

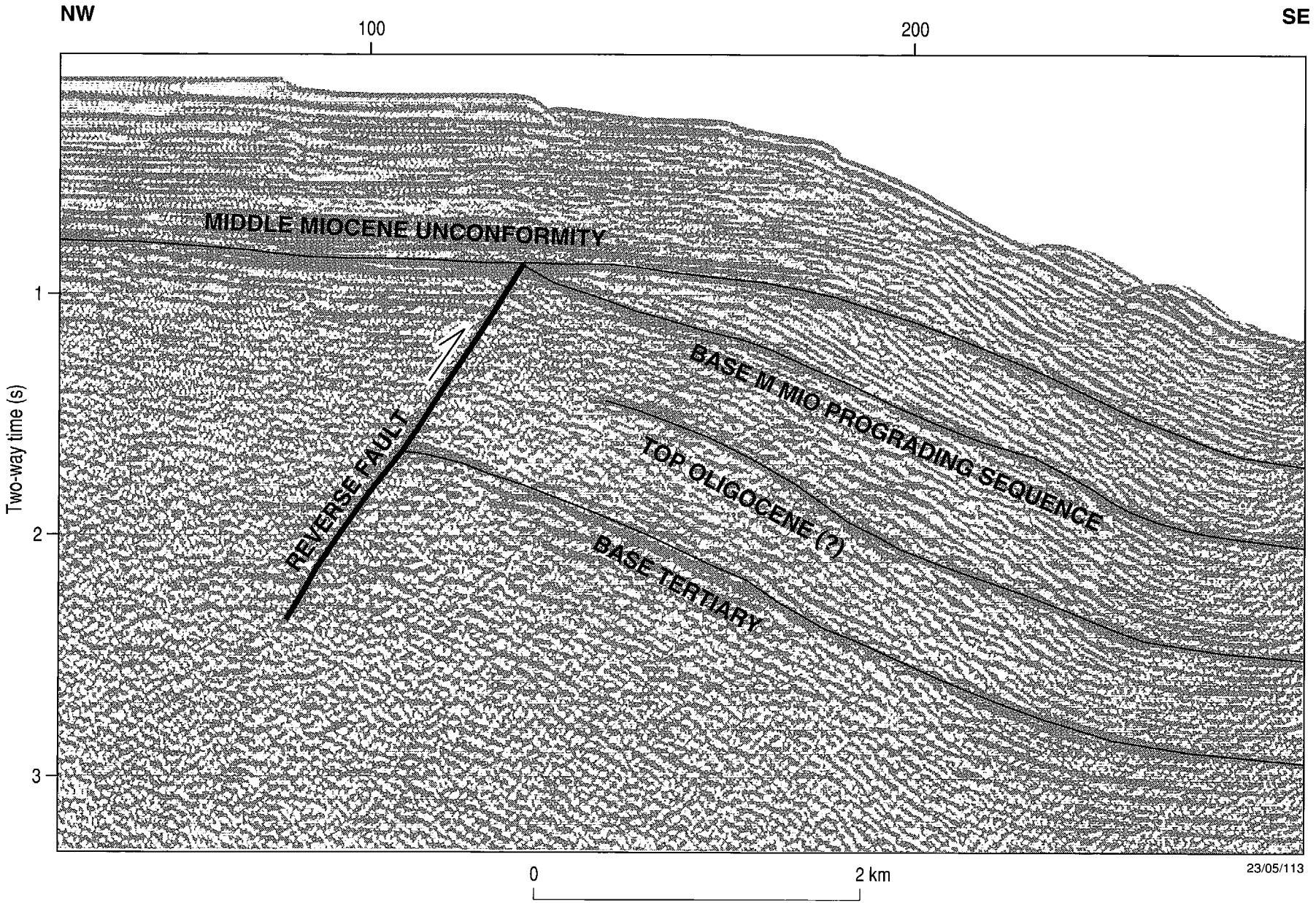

Figure 11 Seismic line 78-78 showing reverse fault in Dumaran area.

5. Dumaran-1 encountered plutonic igneous basement rocks with similar lithology (serpentinized peridotite) to bodies in southern and central Palawan believed to have been thrust upwards into Tertiary and older formations.

The Paly region is separated from the Dumaran region by a down-to-the-southwest normal fault between lines 79-15 and 78-80. The Base Tertiary reflector dips steeply and uniformly beneath a seaward thickening wedge of Tertiary sediments. Several normal faults of significant throw occur close to the eroded landward edge of the basin in the northwest. The basin is bounded in the northeast by normal faults of large throw.

Synthesis

Sedimentation began in Cretaceous times with rifting along the southern margin of China and the deposition, under terrestrial to marginal marine conditions, of several kilometres of clastics derived from the China craton. Rotated fault blocks were severely eroded, resulting in peneplanation to a surface of low relief by early Paleogene times. Erosion was less marked in the Pasig Reef area, probably as a consequence of early submergence beneath waters of the proto-South China Sea.

Continued extension through the Paleogene led eventually to mid-Oligocene continental breakup some distance north of the ancestral Palawan area. A rifted microcontinent drifted southwards as the South China Sea opened to the north, while subduction of the proto-South China Sea commenced at the site of the Cagayan Ridge to the south.

Transgressive and highstand sequences of mainly clastic sediments were built up on the margin of the Palawan microcontinent during Late Oligocene and Early Miocene times. A major regression in the Middle Miocene resulted in the deposition of lowstand units, notably a prograding sequence, beyond the shelf edge. Regression probably marked the onset of a compressive tectonic phase as the Palawan microcontinent collided with the Cagayan Ridge subduction complex. This was followed by a brief period of subduction at the Palawan Trench, as oceanic crust to the north of Palawan was consumed. Collision of a second continental fragment (which included the Reed Bank area) with the Palawan microcontinent brought about a cessation of spreading in the South China Sea.

The Palawan area and neighbouring parts of the Philippine island arc were subjected to compression and uplift as a result of the collisional events. Compressive deformation was particularly severe in the Dumaran Island area where basement blocks on the margin of the shelf were uplifted along major, south verging, reverse faults, and peridotites of the deep crust were upfaulted to shallow crustal levels.

Compression caused exposure and seaward tilting of shelf sediments along the northeast Palawan margin. The sediments were rapidly eroded in the wet tropical climate and re-deposited, together with erosion products from the hinterland, as basin floor fans along the outer margin. The rapid and sustained nature of erosion is evidenced by the almost planar erosion surface truncating seaward dipping shelf sediments—the Middle Miocene unconformity.

Subsidence in Late Middle Miocene times led to a resumption of clastic deposition on the shelf. Mild basin inversion, causing slight arching near the shelf edge in the Roxas area, was probably a flexural response of the crust to earlier loading of the slope. As streams equilibrated on Palawan in the Late Miocene, clastic input to the shelf area declined, giving way to widespread carbonate deposition which has continued to the present.

PETROLEUM GEOLOGY

Reservoirs

Evaluation of reservoirs is based on porosity values derived from sonic, density and neutron logs in three exploration wells (method of calculation described in Appendix 1), together with analyses of cores and cuttings, and litho-stratigraphic descriptions. From well evidence, reservoirs are best developed within and immediately below the Middle Miocene prograding sequence. In terms of sequence stratigraphy (Vail, 1988), this zone is believed to correspond to a lowstand systems tract comprising basin floor fan, slope fan complex and prograding complex. These elements were laid down in the regressive phase which marked the onset of collision-induced uplift. Reservoirs are likely to be deltaic and shoreface sands in the upper part, channel and overbank sands lower down, and shingled turbidites and basin floor fans in distal areas. Several sand bodies with thicknesses ranging from 20 to 50 metres were encountered in Roxas-1. Porosity values of 18% to 27% were calculated for these sandstones from sonic, density and neutron logs (Fig. 12).

The Middle Miocene to Oligocene sequence encountered in Roxas-1 and Paly-1 wells is a truncated, transgressive/highstand, clastic wedge built up on the margin of the Kalayaan-Calamian microplate as it drifted southwards. Reservoirs beneath the shelf area are likely to be of fluvio-deltaic origin with best characteristics found in beach/shoreface sands of the transgressive systems tract. The interval is sandstone dominated but porosities are generally lower than in the overlying sequence. Calculated porosities of sandstones are mainly in the range 14% to 22% (Figs. 12 and 13).

The quartzite conglomeratic sequence encountered beneath the Middle Miocene unconformity in Dumaran-1 well was deposited under high energy, supralittoral conditions, probably as an alluvial fan. The conglomerate is gas bearing but not of reservoir quality. Porosities determined from logs and from core analysis range from 10% to 15% (Fig. 14), but the results of four drill stem tests in a sidetrack well indicate permeabilities to be only in the range 0.001 to 0.01 millidarcies.

The Cretaceous section in Roxas-1 comprises mainly coarse clastics deposited in a rift basin under terrestrial to marginal marine conditions. Reservoirs are likely to be of fluvial or lacustrine origin. The interval from 1920 to 1935 metres has been described as a fine-grained, moderately well-sorted, feldspathic lithic sandstone, largely calcite cemented, with a probable metamorphic terrain as the provenance (Robertson Research, 1985b). Calculated sandstone porosities are in the range 4% to 15%.

Traps and Seals

Five different types of trap are recognised in the Northeast Palawan Shelf. Unconformity traps are formed by updip truncation of reservoirs by the Middle Miocene unconformity and seal by the post-unconformity sediments. The Dumaran trap is of this type, with top seal provided by shales in the post-unconformity section, and lateral seal by juxtaposed basement rocks at the basin boundary fault. Tilted fault blocks at base Tertiary level may have independent structural closure as in the southwest of the Roxas area, or be dependent on sealing faults for closure as in the Paly area. Anticlinal traps formed by mild basin inversion occur in a zone near the edge of the Middle Miocene paleo-shelf in the Roxas area. Possible reef build-ups are seen on several seismic lines along the edge of the paleo-shelf (e.g. line 78-67; Fig.15). Basin floor mounds at Middle Miocene levels are observed in deep water areas though seismic coverage is insufficient to establish closure.

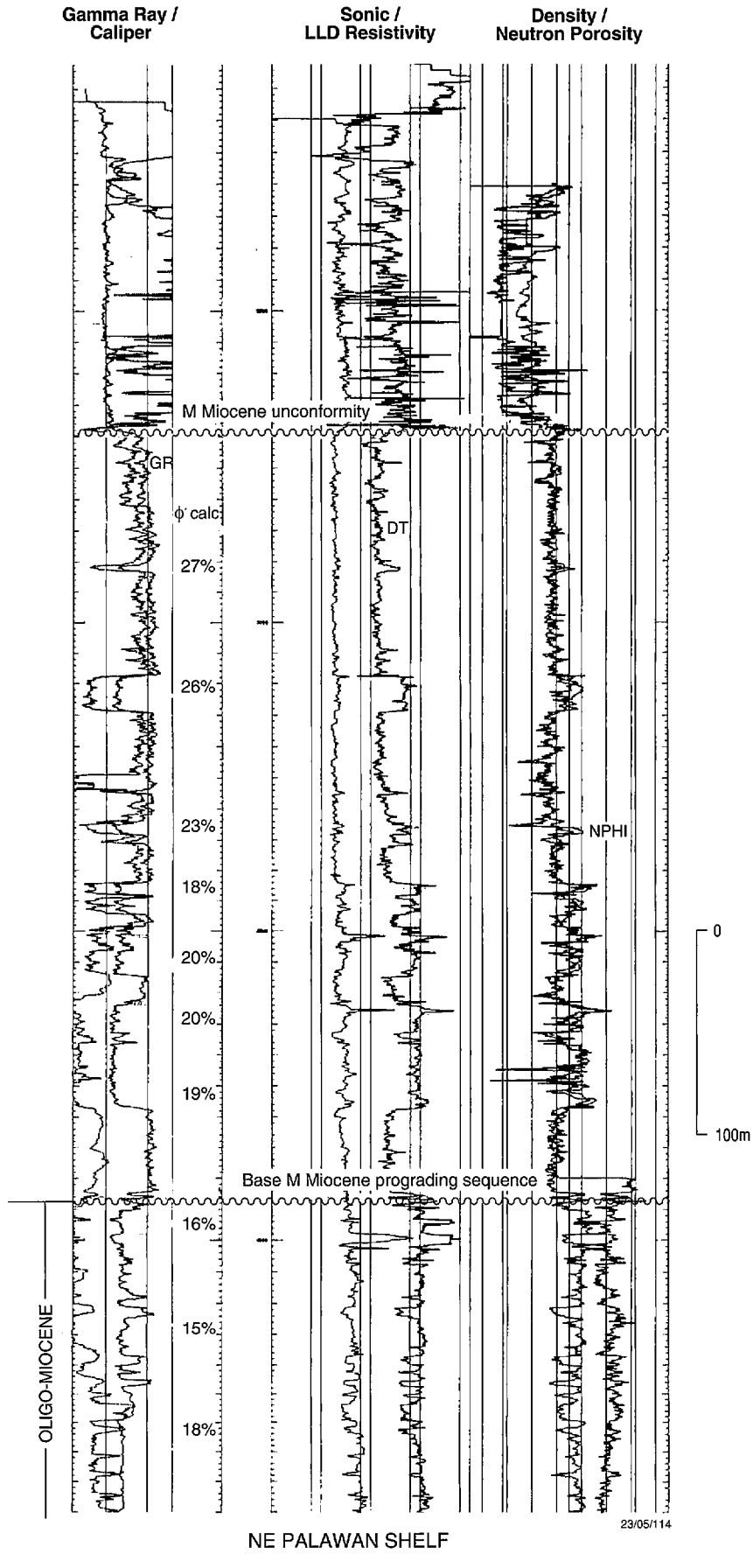

Figure 12 Roxas-1 well logs and calculated porosities.

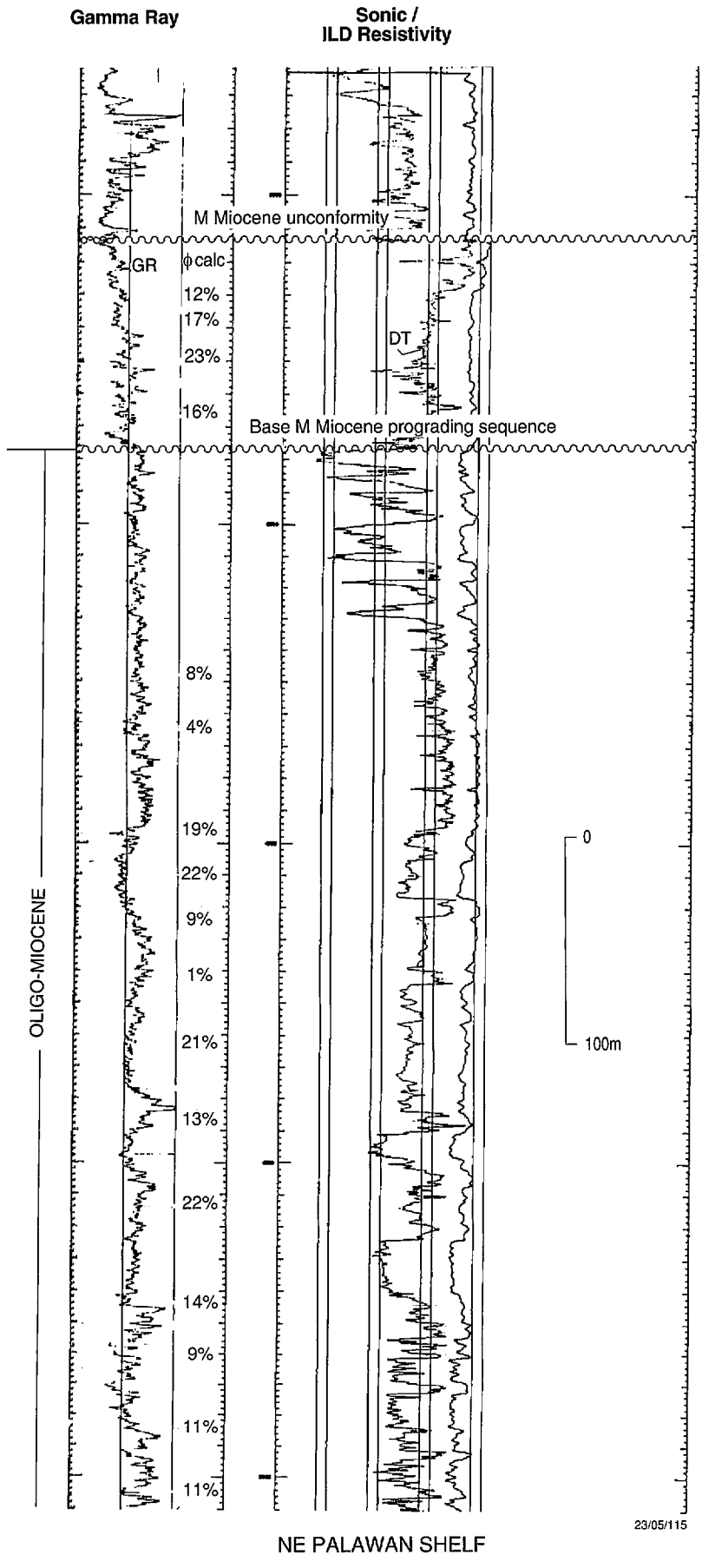

Figure 13 Paly-1 well logs and calculated porosities.

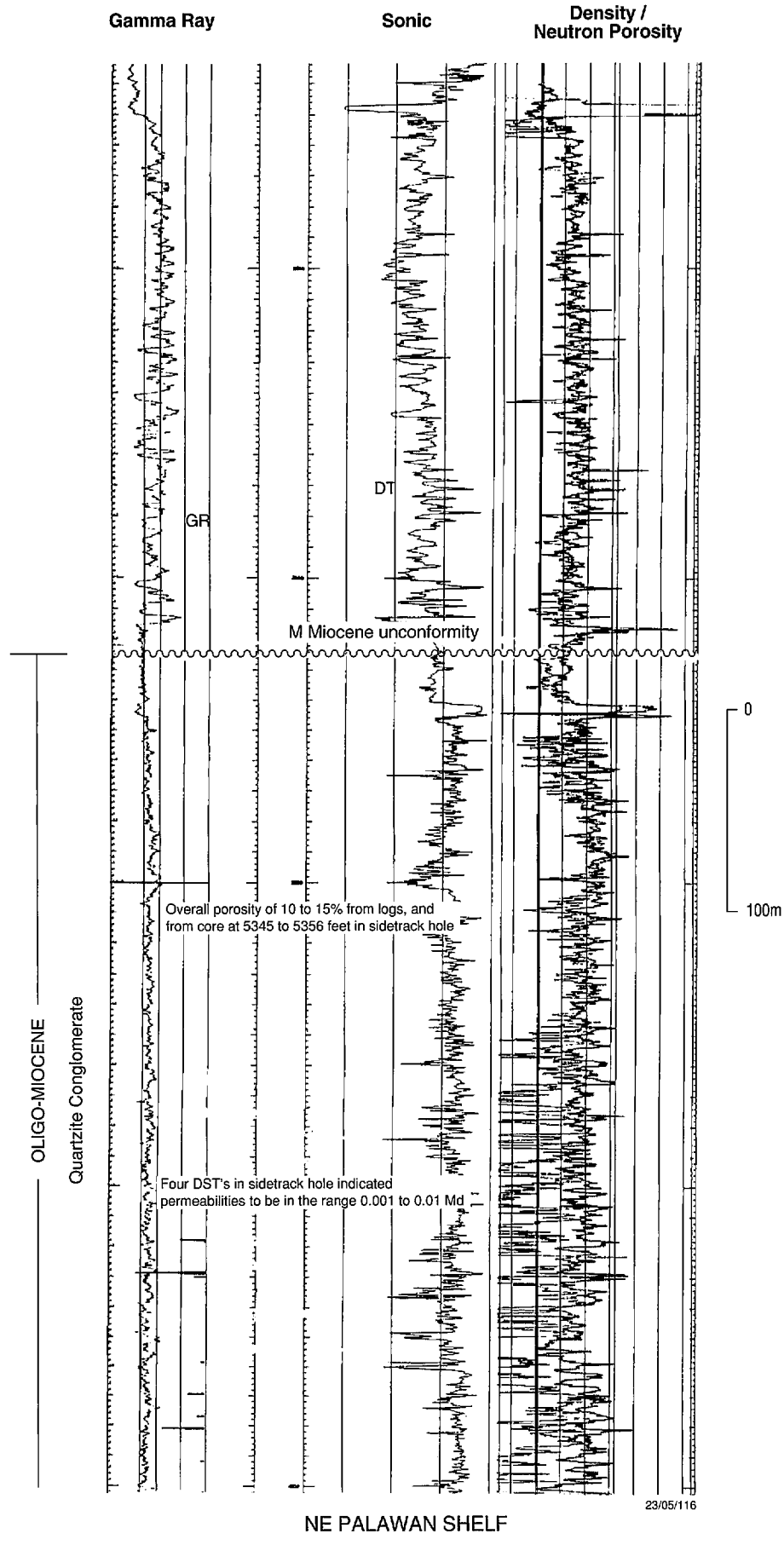

Figure 14 Dumaran-1 well logs and calculated porosities.

The effectiveness of seals in the post-Middle Miocene unconformity section is an important factor for hydrocarbon accumulation in Middle Miocene unconformity traps, anticlinal traps, and reefs. The sealing shales are certainly effective in the Dumaran area, but log evidence suggests that the post-unconformity sections at Paly-1 and Roxas-1 are not shale-prone. It is of interest to note however, firstly that shales several hundred feet above the unconformity may provide effective seals for anticlinal traps, and secondly that the post-unconformity section at Roxas-1 may be only locally sandy due to the presence of a channel (see line 109/02).

Geochemical Sampling

Concurrently with seismic acquisition, AGSO carried out a geochemical direct hydrocarbon detection (DHD) sampling survey. The survey utilised a submerged towfish to detect light hydrocarbons dissolved in bottom waters through continuous water sampling. DHD anomalies may indicate the presence of mature source rocks in an area, and the existence of migration pathways extending from source beds into reservoirs en route to the surface.

DHD results were prepared in map form at the same scale as the seismic maps. Maps of total hydrocarbon content (THC) were found to be the most useful (Figures 16 to 18) though maps of methane (C_1), propane and ethane (C_2+C_3); and ethane/ethylene and propane/propylene ratios were also prepared. The following general observations can be made:

1. The strongest THC anomalies in the Northeast Palawan Shelf are about double the background, but are an order of magnitude weaker than anomalies detected in a similar survey of the Ragay Gulf off southern Luzon (Lee et al, 1993).
2. Due to movement of dissolved hydrocarbons with tides and currents, such weak anomaly measurements are non-repeatable. In the Roxas area for instance, misties of line 12 with lines 1 and 2 (surveyed 3 or 4 days earlier) are large compared to the mistie with lines 11 and 13 (surveyed consecutively).
3. The THC and C_1 anomaly that coincides with the Dumaran-1 location is probably indicative of gas leakage from the abandoned well, in which gas shows had been encountered (Fig. 16).
4. Weak THC and C_1 anomalies coincide with the Roxas Lead, a broad, low relief anticline at Middle Miocene unconformity level (Fig. 17).
5. Weak C_2+C_3 and propane/propylene anomalies were found about 10 km west-northwest of Paly-1 well in an area characterised by normal faulting at Base Tertiary level.
6 A weak C_2+C_3 anomaly was identified about 4 km south of the Honda Bay Lead, a closed structural high at Top Cretaceous level.

Source Rocks and Maturation

No hydrocarbon source rocks of significance were encountered in the wells. The sediments have poor to average organic carbon contents which are dominated by inertinitic kerogens. The existence of source rocks in the area however, is proven by the presence of dead oil traces and gas in the Dumaran-1 well. Presumably, an initial oil accumulation was displaced by a later gas charge. No Cretaceous sediments were mapped in the Dumaran area, implying that source rocks for this accumulation are of Oligocene to Middle Miocene age.

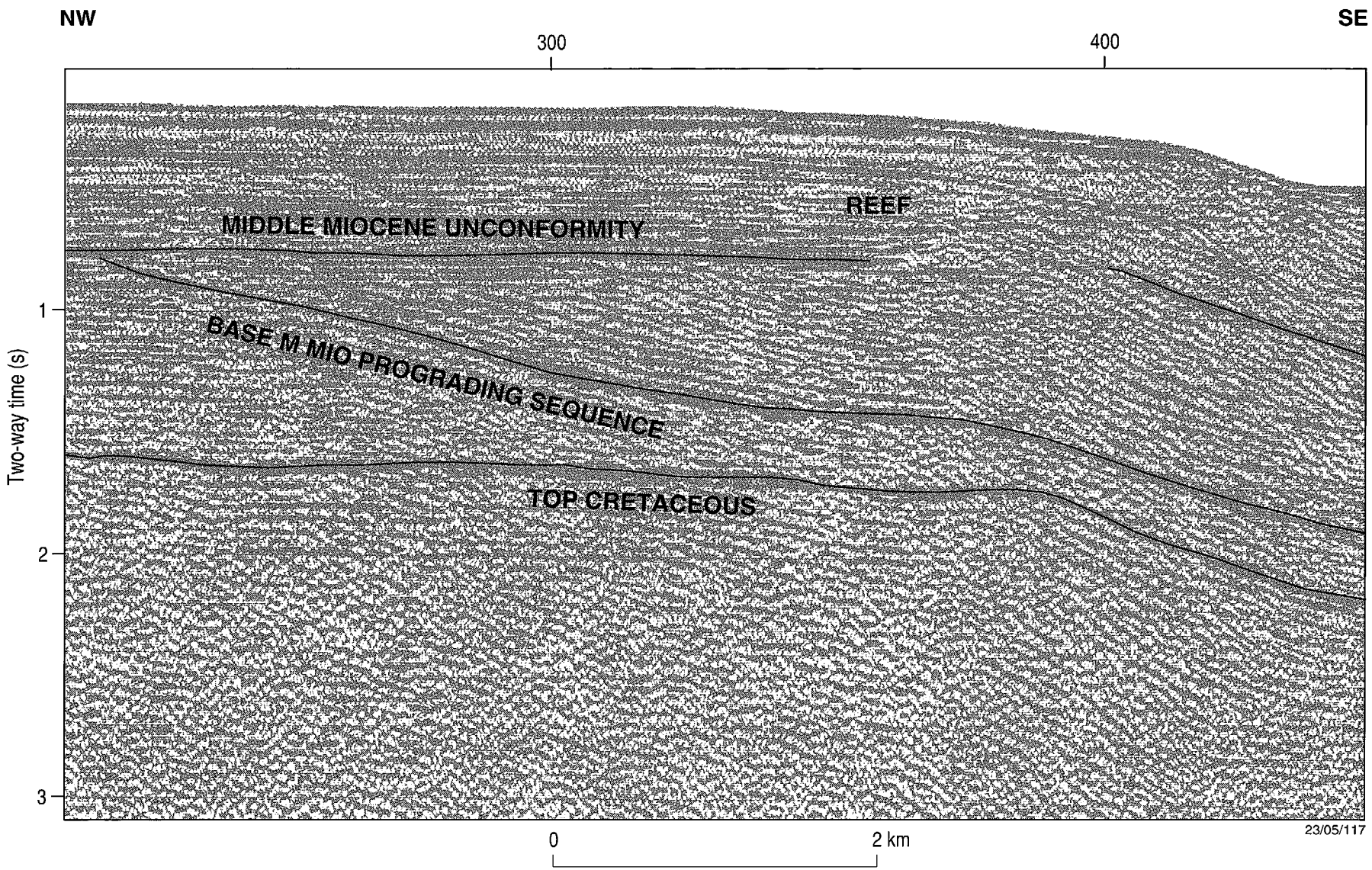

Figure 15 Seismic line 78-67 showing possible Middle Miocene reef.

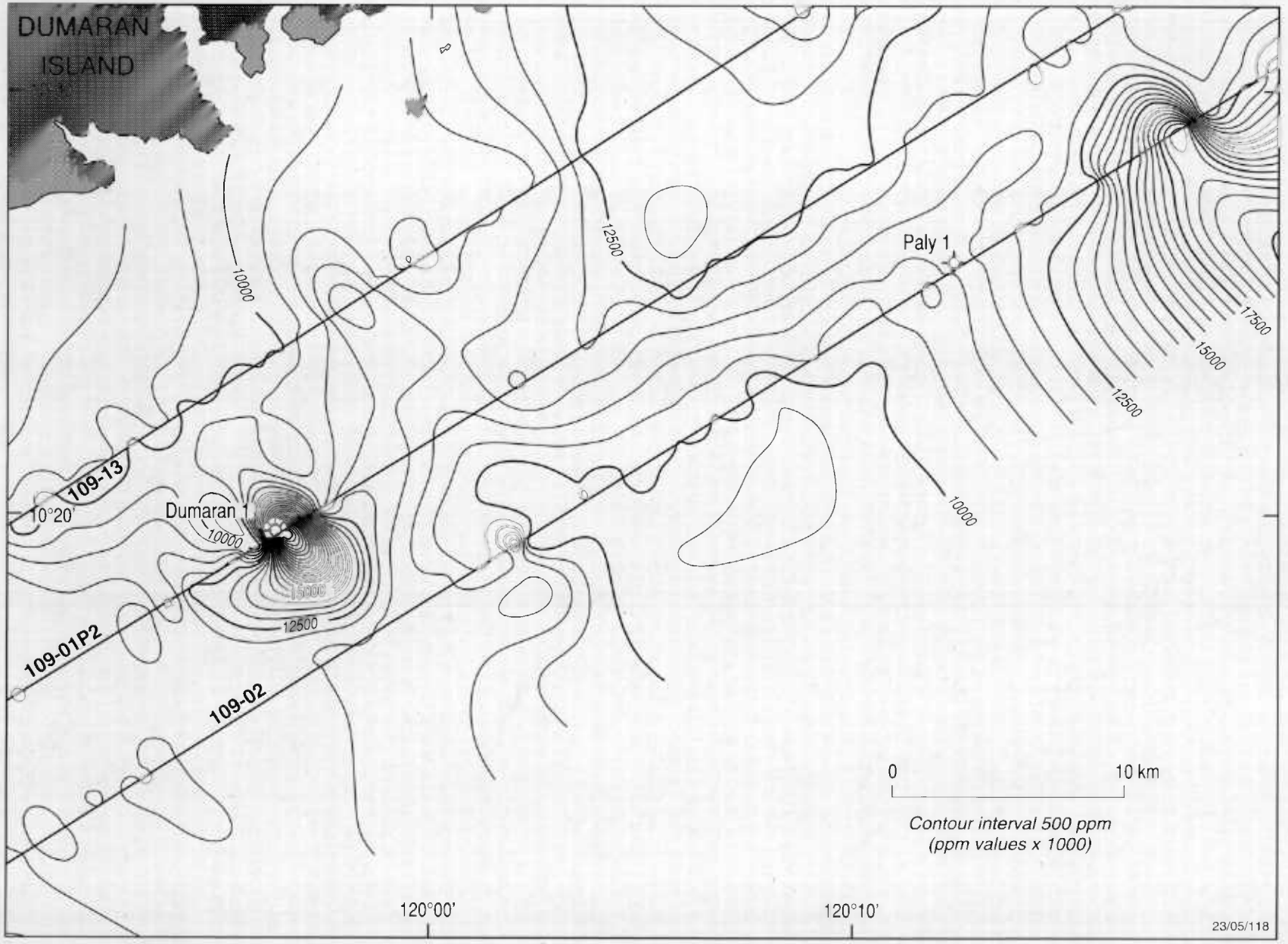

Figure 16 Paly-Dumaran area total hydrocarbon content.

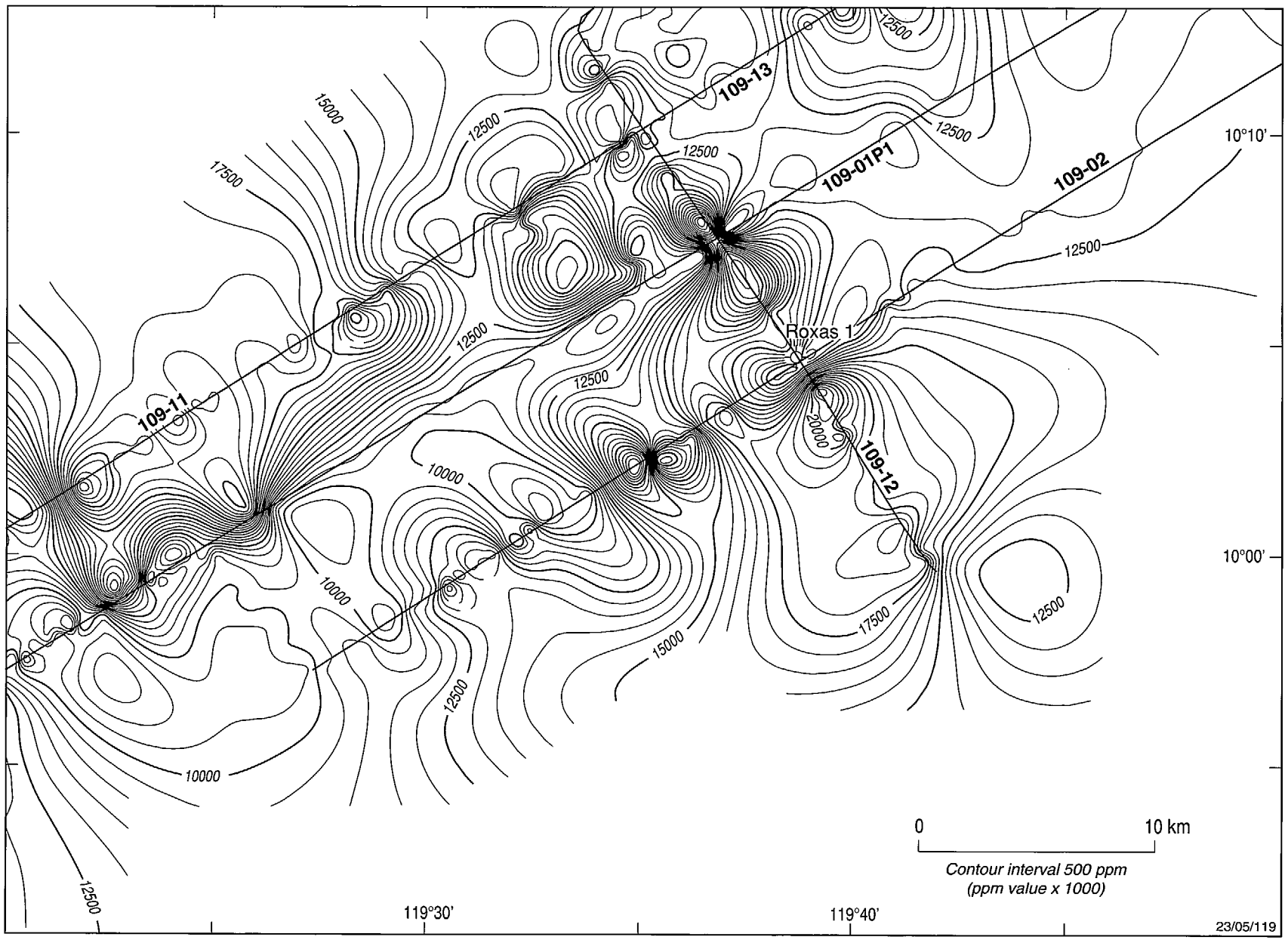

Figure 17 Roxas area total hydrocarbon content.

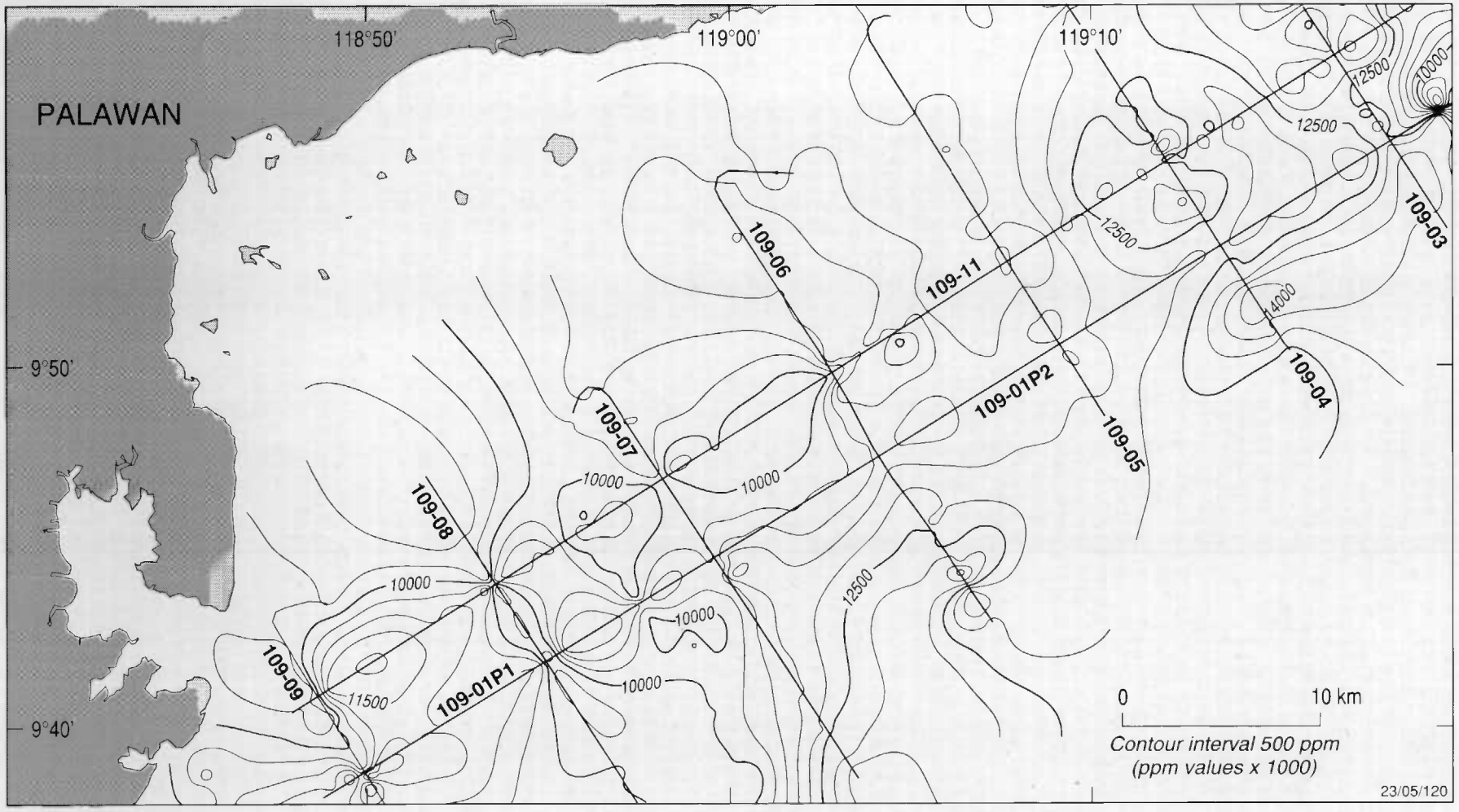

Figure 18 Honda Bay area total hydrocarbon content.

Vitrinite reflectance analysis of samples from Roxas-1 suggested the section to be immature to a depth of about 610 metres, early mature from 610 metres to 1905 metres, and middle mature below 1905 metres (Robertson Research, 1979, 1985a). From the established thermal maturity gradient it was estimated that some 1500 metres of section was missing as a result of uplift and erosion. Vitrinite reflectances are thus indicative of paleo-maturity rather than present day generative potential. Rock-eval pyrolysis and vitrinite reflectance analyses of samples from Paly-1 indicated the section to 1650 metres to be immature; it was predicted that the base of the well lay within the upper part of the zone of oil generation. Spore coloration analysis from the same well suggested most of the section to be mature for oil.

Geohistory modelling (Appendix 3) indicates that observed maturity levels in these wells were attained in the Middle Miocene, just prior to the period of collision-induced uplift. Oil generation would have taken place at well locations then if suitable kerogen was available. Middle Miocene uplift and erosion were followed by gradual subsidence as the Matinloc and Carcar Formations were deposited. Subsidence however was insufficient for pre-collision maturity levels to be attained, so no further generation took place near the wells.

Present-day generation is probably occurring in source rock kitchen areas 15 to 30 km down dip from the wells, where the effects of Middle Miocene uplift were much reduced. Geohistory plots for the Dumaran and Roxas sub-basins (Plates P-5 and P-6) suggest that the Oligo-Miocene section is more deeply buried than now than during the previous maximum burial period, just before the Middle Miocene collision. Modelled maturity levels in the Dumaran sub-basin are consistent with continuous oil and gas generation since the Middle Miocene.

Migration and Timing

The Dumaran gas accumulation is testimony to the existence of migration pathways from source rocks in distal areas into traps beneath the continental shelf, and to trap timing. The Dumaran trap requires post-Middle Miocene unconformity shales for top seal indicating that hydrocarbon migration post-dates late Middle Miocene times. Geohistory modelling indicates that generation has probably continued since the Middle Miocene until the present within a 3 to 4 second TWT thick wedge of Oligo-Miocene sediments about 15 kilometres down dip from the Dumaran area (line SS-205-80, Plate P-5). Similar thick Oligo-Miocene wedges are seen less than 10 kilometres south of Paly-1 (line 78-95, Fig. 19) and about 30 kilometres south of Roxas-1 (line SS-207-80, Plate P-6). All traps pre-date the late Middle Miocene, so if migration paths exist between these wedges and traps on the shelf, then migration and timing does not pose a major geologic risk for hydrocarbon accumulation.

Traps defined at Top Cretaceous level were formed by Oligocene to Early Miocene times. Charge of these traps by hydrocarbons derived from either Cretaceous or Oligo-Miocene sources is therefore a possibility. Oligo-Miocene sources close to the traps would have attained maturity prior to Middle Miocene uplift (Appendix 3).

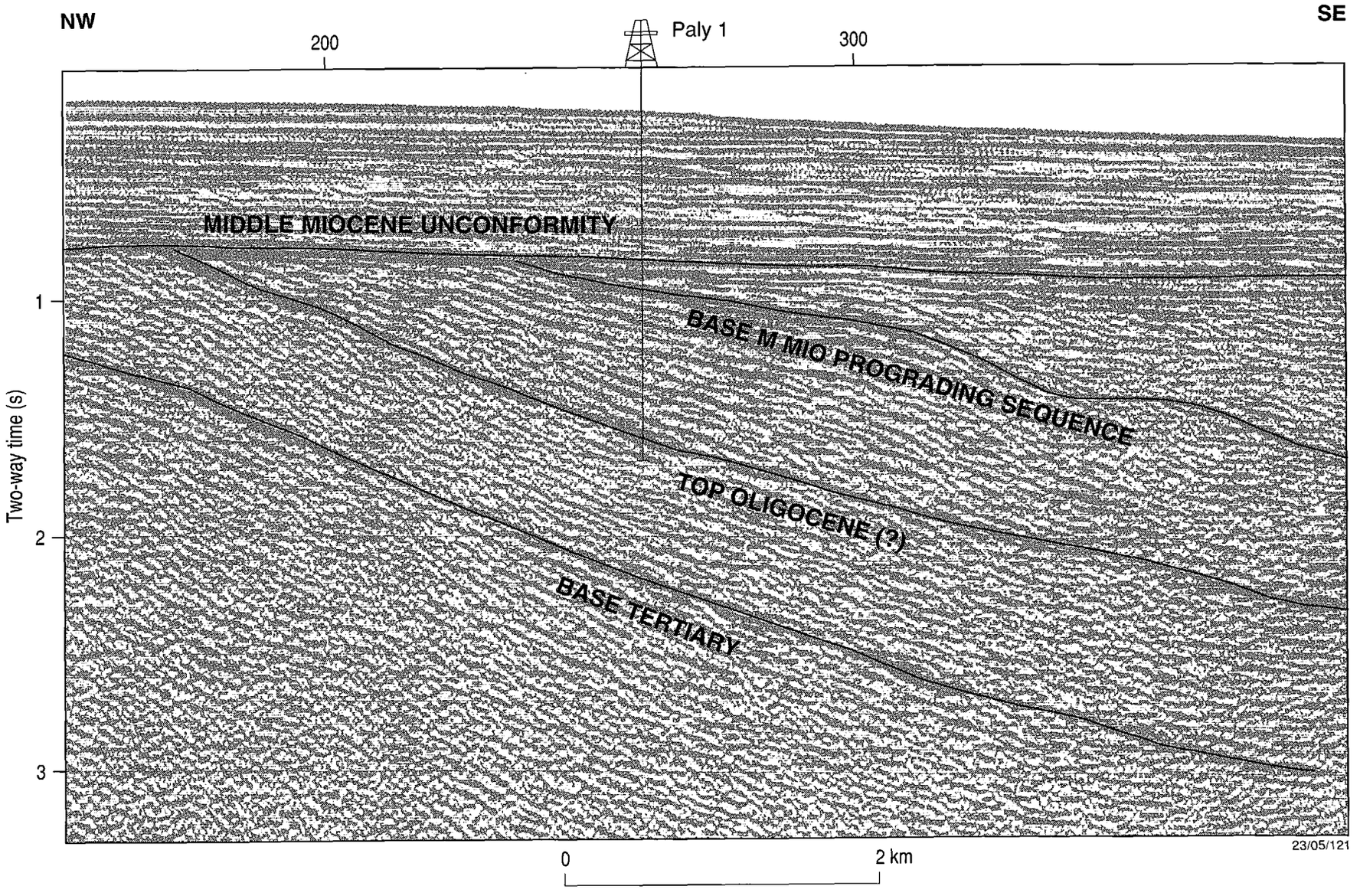

Figure 19 Seismic line 78-95 thro ıgh Paly-1 well.

Drilling Analysis

Seismic mapping indicates that Roxas-1 was drilled outside structural closure at both Middle Miocene unconformity and Top Cretaceous levels (Maps P-8 and P-11). This is regarded as the most likely reason for the absence of hydrocarbon shows in the well.

Dumaran-1 encountered gas shows over the entire sedimentary section below the Middle Miocene unconformity (0.82 to 1.40 sec. TWT). The section consists of non-reservoir, quartzite conglomerate, with small gas flows being recorded in three drill stem tests conducted in a sidetrack hole. No shows of significance were recorded in Paly-1 although much of the pre-unconformity section in the well is above 1.40 seconds (Middle Miocene unconformity at 0.87 sec.), and there are no obvious barriers to migration between Dumaran-1 and Paly-1. The Dumaran accumulation must therefore be bounded to the northeast by a truncational or intra-formational permeability barrier and may be of significant size if it encompasses part of the Middle Miocene prograding sequence, in which good reservoirs were encountered in Roxas-1. This sequence is interposed between Dumaran-1 and the proposed kitchen area to the southeast.

Evaluation of Leads

Four structural highs with potential for hydrocarbon entrapment, together with the Dumaran gas accumulation, were evaluated. These 'leads' are named the Dumaran, Roxas, Pasig (two levels) and Honda Bay Leads and are described in Plates P-5 to P-8 and summarised in Tables 3 to 6. Reserves for each lead were calculated using both conservative assumptions (Case 1) and optimistic assumptions (Case 2).

All leads have independent structural closure with the exception of Dumaran which is open to the northwest and northeast. Closure in these directions must exist in the form of intra-formational or truncational permeability barriers. For evaluation purposes, the boundaries of the Dumaran accumulation are taken to be the 1.4 second time structure contour (corresponding to the 'gas down-to' level in Dumaran-1) to the south and southeast; the mapped landward limit of the Middle Miocene Prograding Sequence (which contains reservoir quality sandstones where intersected in Roxas-1) to the northwest; and a hypothetical sandstone pinchout line to the northeast, defined just north of a zone of strongly reflecting clinoforms in the Middle Miocene Prograding Sequence as seen on line 109-02, SP 2540 (Case 1), or at around SP 2180 on the same line where there is a reversal of apparent prograding direction (Case 2).

CONCLUSIONS

(1) The Northeast Palawan shelf is underlain by an extensional, margin fracture/margin sag basin of Cretaceous to Pleistocene age, modified by compressional events associated with Middle Miocene collisions of the Palawan microcontinent, firstly with a subduction complex—the Cagayan Ridge, and secondly with a rifted continental fragment to the northwest of Palawan.

(2) Major sequences recognised are:

- A Cretaceous rift sequence of clastic sediments deposited in terrestrial to marginal marine environments when the area was attached to the China craton;
- An Oligocene to Middle Miocene, mainly transgressive sequence of clastics deposited in inner to middle sublittoral environments while the Palawan microcontinent drifted southwards as a result of opening of the South China Sea;

Table 3. Parameters for Dumaran Lead

PLAY DESCRIPTION

HORIZON	**: Middle Miocene Unconformity**
RESERVOIR	**: Sandstones of the Middle Miocene prograding sequence**
SOURCE ROCKS	**: Oligo-Miocene shales 10 to 15 km down dip**
TRAP AND SEAL	**: Unconformity trap of Late Middle Miocene age with top seal provided by shales of the post-unconformity section**

RESERVE ESTIMATE

LOCATION	**: Line SS 205-80, SP 800**
WATER DEPTH	**: 247 m**
CREST/BASE	**: 920/1400 milliseconds subsea**
WATER SATURATION	**: 30%**
RECOVERY FACTOR (GAS)	**: 80%**
FORM. VOL. FACTOR	**: 0.007**

	Case 1	Case 2
Closure Area(Ha)	**8628**	**15863**
Net Res. Thickness(m)	**20**	**30**
Net Res. Volume(Ha m)	**172560**	**475890**
Porosity	**20%**	**20%**
Gas Reserves(TCF)	**1.0**	**2.7**

Table 4. Parameters for Roxas Lead

PLAY DESCRIPTION

HORIZON	**: Middle Miocene Unconformity**
RESERVOIRS	**: Southeast dipping sandstones of the Middle Miocene prograding sequence in the east (Area A); flat lying sandstones of the Early to Middle Miocene sequence in the west (Area B)**
SOURCE ROCKS	**: (i)Oligo-Miocene shales in a thick wedge beneath the slope 20 to 30km to the southeast (ii)Cretaceous shales beneath the lead area**
TRAP AND SEAL	**: Anticline at Middle Miocene unconformity level sealed by shales in the post-unconformity section**

RESERVE ESTIMATE

LOCATION	**: Line 78-52, SP 230**
WATER DEPTH	**: 71m**
CREST/BASE	**: 440/520 milliseconds (water-compensated time)**
WATER SATURATION	**: 30%**
RECOVERY FACTOR	**: 30%**
FORM. VOL. FACTOR	**: 1.4**

Area A	**Case 1**	**Case2**
Closure area(Ha)	**3846**	**3846**
Gross Volume(Ha.m)	**137474**	**137474**
Net Res. Thickness(m)	**50**	
Net/Gross		**0.25**
Net Res. Volume(Ha.m)	**10300**	**34369**
Porosity	**20%**	**20%**
Reserves(MMBO)	**19**	**65**
Area B	**Case 1**	**Case 2**
Closure Area(Ha)	**6920**	**6920**
Net Res. Thickness(m)	**10**	**20**
Net Res. Volume(Ha.m)	**69203**	**138406**
Porosity	**10%**	**15%**
Reserves(MMBO)	**65**	**196**
==========	==========	==========
Total Reserves(A+B)	**84 MMBO**	**261 MMBO**

Table 5. Parameters for Pasig Leads

PLAY DESCRIPTION

HORIZONS	: Middle Miocene Unconformity, Top Cretaceous
RESERVOIRS	: Oligo-Miocene and Cretaceous sandstones
SOURCE ROCKS	: (i)Oligo-Miocene shales in a thick wedge beneath the slope 20 to 30km to the southeast (ii)Cretaceous shales beneath the lead area
TRAP AND SEAL	: (i)Structural high formed in Paleogene times sealed intraformationally or by Oligo-Miocene shales (ii)Anticline at Middle Miocene unconformity level sealed by post-unconformity shales

RESERVE ESTIMATE

LOCATION	: Line 78-37, SP 240
WATER DEPTH	: 22 m
WATER SATURATION	: 30%
RECOVERY FACTOR	: 30%
FORM. VOL. FACTOR	: 1.4

HORIZON	M.Mio.Unc.		Top Cret.	
Crest/Base (ms)	440/520		800/1400	
Closure area(Ha)	2492		4833	
Gross Vol. (Ha.m)	100097		1508803	
	Case 1	Case 2	Case 1	Case 2
Net Res. Thckns(m)	10	20	10	20
Net Res. Vol. (Ha.m)	24920	49840	48330	96660
Porosity	10	20	10	12
Reserves(MMBO)	24	71	46	109

Table 6. Parameters for Honda Bay Lead

PLAY DESCRIPTION

HORIZON	**: Top Cretaceous**
RESERVOIRS	**: Cretaceous sandstones**
SOURCE ROCKS	**: (i)Oligo-Miocene shales in a thick wedge beneath the slope 20 to 30km to the southeast** **(ii)Cretaceous shales beneath the lead area**
TRAP AND SEAL	**: Anticline at Top Cretaceous level sealed by interbedded shales and Oligo-Miocene shales**

RESERVE ESTIMATE

LOCATION	**: Line 109-01P2, SP 3250**
WATER DEPTH	**: 109 m**
CREST/BASE	**: 1520/1840 milliseconds (water-compensated time)**
WATER SATURATION	**: 30%**
RECOVERY FACTOR	**: 30%**
FORM. VOL. FACTOR	**: 1.4**

	Case 1	Case2
Closure Area(Ha)	**6863**	**6863**
Gross Volume(Ha.m)	**987067**	**987067**
Net Res. Thickness(m)	**10**	**20**
Net Res. Volume(Ha.m)	**68630**	**137260**
Porosity	**10%**	**12%**
Reserves(MMBO)	**65**	**155**

- A Middle Miocene prograding sequence deposited during a regressive phase which probably marked the onset of collision tectonics; and
- A Late Middle Miocene to Pleistocene sequence of clastics and limestones deposited on the shelf and slope after the collision-induced Middle Miocene phase of uplift and erosion.

(3) The best potential reservoirs encountered in exploration wells are well developed intervals of clean sandstone within the Middle Miocene prograding sequence. This sequence subcrops the Middle Miocene unconformity under the outer shelf and slope along most of the northeast Palawan margin. Possible reef buildups on the edge of the Middle Miocene paleo-shelf may also have good potential as reservoirs. The potential of the Oligocene to Middle Miocene and Cretaceous sequences is rated as moderate.

(4) No source rocks were penetrated in wells, but their existence in the basin is confirmed by the presence of a gas accumulation and dead oil traces in a 1000 metre thick section of non-reservoir conglomerates in the Dumaran-1 well. Measurements of vitrinite reflectance and spore coloration indicate maturity levels ranging from early to middle mature in the pre-unconformity section. These levels were attained prior to Middle Miocene uplift however, and are not indicative of present-day generative capacity at the well locations.

(5) Traps were seismically defined at the Middle Miocene unconformity and Top Cretaceous levels. Middle Miocene anticlinal and (?)reef traps may be sealed by shales in the post-unconformity section, and charged by hydrocarbons generated from Cretaceous sources beneath the traps, or from sources in a thick wedge of Oligo-Miocene sediments under the continental slope 15 to 30 kilometres away. Traps defined at Top Cretaceous level may be sealed intra-formationally or by shales in the overlying Oligo-Miocene section. The traps had formed by the Oligocene and could have been charged by hydrocarbons generated from Cretaceous sources or from Oligo-Miocene shales prior to Middle Miocene uplift. Early charging of traps could have helped preserve porosity by inhibiting calcite cementation.

(6) Three lead areas and the Dumaran gas accumulation were evaluated for potential hydrocarbon reserves. The leads are closed structural highs at Middle Miocene unconformity and Top Cretaceous levels. The Dumaran gas accumulation is not structurally closed and must be limited to the northwest and northeast by intra-formational permeability barriers. The accumulation may be of a significant size if it encompasses good reservoir sandstones of the Middle Miocene prograding sequence three kilometres to the southeast of the well. This sequence is interposed between the well and a probable source 'kitchen' area to the southeast. The accumulation may include oil as well as gas if dead oil traces, observed over a 300 metre interval in the well, are remnants of an oil column displaced down dip by gas.

REFERENCES

BERNARD, F. and MULLER, C.,1986. Synthetic Geological Map obtained by Remote Sensing; an application to Palawan Island. *Symposium on Remote Sensing for Resources and Environmental Management*- August, 1986 (Commission VII-ISPRS), Report.

BUREAU OF ENERGY DEVELOPMENT,1986. Sedimentary Basins of the Philippines - their Geology and Hydrocarbon Potential. World Bank financed petroleum exploration project prepared by the Bureau of Energy Development, under the supervision of Robertson Research (Australia) Pty Limited and Flower Doery and Buchan Pty. Ltd.,Report.

BUREAU OF MINES, 1963. Philippines Geological 1:1,000,000 Map for Palawan

CITCO PHILIPPINES PETROLEUM CORPORATION, 1978. Marine Seismic and Magnetic Survey, Northeast Palawan. Report by Offshore-Onshore Exploration Consultants (unpublished)

CITCO PHILIPPINES PETROLEUM CORPORATION, 1979a. East Palawan seismic, gravity and magnetic survey. Report by Offshore-Onshore Exploration Consultants (unpublished)

CITCO PHILIPPINES PETROLEUM CORPORATION ET AL, 1979b. Roxas No. 1. Final Well Report (unpublished).

CITCO PHILIPPINES PETROLEUM CORPORATION ET AL, 1980. Dumaran No. 1. Final Well Report (unpublished).

CITCO PHILIPPINES PETROLEUM CORPORATION ET AL, 1982. Paly No. 1. Final Well Report (unpublished).

HOLLOWAY, N.H.,1982. The stratigraphy and tectonic relationship of Reed Bank, North Palawan and Mindoro to the Asian mainland and its significance in the evolution of the South China Sea. *American Association of Petroleum Geologists Bulletin*, 66, 1357-1383.

LEE, C.S. and RAMSAY, D.,1992. Philippines Marine Seismic Survey Project Cruise Report. *Bureau of Mineral Resources, Australia Record*, 1992/49.

LEE, C.S., GALLOWAY, M.C., MOORE, A., WEST, P., APOSTOL, R., TRINIDAD, N., ABANDO, R., PANGANIBAN, D. and GUAZON, E.,1993. Structure, stratigraphy and petroleum potential of Ragay Gulf, southeast Luzon, Philippines. *Philippine Marine Seismic Survey Project Interim Report*, Chapter 1.

RANGIN ,C. JOLIVET, L. PUBELLIER, M. and the Tethys working group, 1990. A simple model for the tectonic evolution of southeast Asia and Indonesia region for the past 43 m.y. *Bull. Soc Geol France* 1990 (8) t. VI No. 6, 889-905

RANGIN, C. 1991. The Philippine Mobile Belt: a complex plate boundary. *Journal of Southeast Asian Earth Sciences*, 6(3/4), 209-220.

ROBERTSON RESEARCH, 1979. Vitrinite reflectance analysis of one sample from the Roxas-1 and two samples from the Dumaran-1 well, Philippines. Memorandum No. S/582 (unpublished).

ROBERTSON RESEARCH (SINGAPORE) PRIVATE LIMITED, 1985a. Vitrinite reflectance determinations on samples from the Roxas-1 Well. BED/World Bank study: Hydrocarbon potential of the Philippines. Preliminary Report No. 28 (unpublished).

ROBERTSON RESEARCH (SINGAPORE) PRIVATE LIMITED, 1985b. Results of petrographic and X-ray diffraction analyses of ditch cutting samples from the interval 3980'-6600' of the Roxas-1 well, Philippines. Memorandum No. S/1298 (unpublished).

ROBERTSON RESEARCH (SINGAPORE) PRIVATE, 1985c. Results of petrographic examination of six core chips from the Dumaran-1 well, Philippines. Memorandum No. S/1301 (unpublished).

VAIL, P.R., 1988. Sequence stratigraphy workbook. Fundamentals of sequence stratigraphy. *American Association of Petroleum Geologists.* 1988 Annual Convention Short Course Notes.

PART 4

GEOLOGY AND PETROLEUM POTENTIAL OF CUYO PLATFORM

by

E. F. Pablico[1] and C. S. Lee[2]

1 Department of Energy, Makati, Metro Manila, Philippines
2 Australian Geological Survey Organisation, Canberra, ACT, Australia

ABSTRACT

In March 1992, the Australian Geological Survey Organisation and the Philippine Department of Energy conducted a cooperative marine seismic, gravity, magnetic, bathymetry and geochemical survey, under funding from the Australian International Assistance Bureau, in four offshore Philippine basins. The project resulted in the acquisition of 730 line kilometres of new seismic data over the Cuyo Platform. The interpreted seismic data show deeper horizons which were not mapped from previous seismic surveys. The new interpretation was used to infer the possible existence of source and reservoir rocks deeper than the Middle Miocene unconformity. With a relatively wide seismic line spacing, only one lead was delineated sufficiently for hydrocarbon evaluation. It is an anticlinal structure bounded by normal faults.

As no well has yet been drilled in the survey area, information from wells drilled in the northeast Palawan shelf, southern Mindoro and offshore Panay were used as a basis for stratigraphic evaluation. Potential reservoir rocks may be present in the form of sandstones in the Jurassic interval, and calcarenites in the Oligocene to Early Miocene interval. Offshore geochemical sampling data, and reports of onshore hydrocarbon seepages were also used to evaluate the source potential of the area. Possible source rocks are believed to exist in carbonaceous clastic sequences both in the Jurassic and Oligocene-Early Miocene intervals. Weak geochemical anomalies are coincident with mapped structural highs.

CONTENTS

INTRODUCTION 7

TECTONIC SETTING 7

EXPLORATION HISTORY 11
- Licence History
- Seismic Surveys
- Exploration Wells

STRATIGRAPHY 12
- Triassic Chert
- Mansalay Formation
- Batangan Formation
- Ananawin Formation
- Punso Conglomerate
- Carcar Limestone

SEISMIC INTERPRETATION 15
- Data Description
- Seismic Horizons
- Seismic Sequences
- Structural Interpretation
- Geologic History

PETROLEUM GEOLOGY 17
- Reservoirs
- Traps and Seals
- Geochemical Studies
- Source rocks and Maturation
- Migration and Timing
- Lead Evaluation

CONCLUSIONS 20

REFERENCES 22

TABLES

Table 1 Summary of wells from Northeast Palawan, Mindoro and Panay Islands.
Table 2 Parameters for Manamoc Lead.

FIGURES

Figure 1 Survey areas of the Philippine-Australia Marine Seismic Survey Project.
Figure 2 Cuyo Platform showing location of AGSO/DOE/AIDAB survey and previous seismic lines.
Figure 3 Stratigraphy of Cuyo Platform.
Figure 4 Schematic geologic diagram of Cuyo Platform.
Figure 5 Total hydrocarbon content map of Cuyo Platform.

ENCLOSURES

Maps (see Volume 3)

Map C-1 Bathymetry map of Cuyo Platform from seismic survey data. Scale 1:150,000.
Map C-2 Time structure map at top of Mesozoic Masnalay Formation (Purple Horizon). Scale 1:150,000.
Map C-3 Time structure map at top of Early Eocene - Early Miocene Ananawin/ Batangan Formation (Red Horizon). Scale 1:150,000.
Map C-4 Tectonic elements of Northeast Palawan-Cuyo Platform-Mindoro areas. Scale 1:500,000.

Plates (see Volume 4)

Plate C-1 Time structure map at top of Mesozoic Mansalay Formation (Purple Horizon). Scale 1:250,000.
Plate C-2 Time structure map of Early Eocene to Early Miocene Ananawin/ Batangan Formation (Red Horizon). Scale 1:250,000.
Plate C-3 Montage for Manamoc Lead.

INTRODUCTION

The Cuyo Platform (Fig. 1) lies east of the prolific petroliferous province of the northwest Palawan shelf. It forms part of a remnant continental block that separated from the China craton during Late Oligocene to Middle Miocene times (Hamilton, 1979; BED, 1986) Most of the platform area is now underwater except for a number of small islands with typical areas of 10 to 25 square kilometres. The main one is Cuyo Island (Fig. 2) after which the platform was named. The islands in the southeast are dominantly covered by basalts and andesites of Pliocene age, whereas those in the northwest are made up of radiolarian cherts of Mesozoic age (Alcala, 1987). The present Cuyo Platform lies in water depths ranging from 20 to 140 m. Bathymetric contours derived from the seismic data are accurate to ±20m. They show that the deepest portion is situated between Dumaran Island and Quiniluban Island (Map C-1). Most of the area is less than 100 m deep and is underlain by reefs and other shallow water carbonate build-ups.

The seismic interpretation is based on 730 line kilometres of data (Fig. 2) acquired by the Australian Geological Survey Organisation (AGSO) in conjunction with the Philippine Department of Energy (DOE), under funding from the Australian International Development Assistance Bureau (AIDAB). Reprocessed lines from surveys by Philippine Oil and Geothermal Inc.(POGEI) and Petro-Canada were also used in the interpretation. Three horizons were picked on seismic sections: a Middle Miocene unconformity (blue horizon); an Eocene-Early Miocene marker (red horizon); and a Mesozoic marker (purple horizon). Only the two deep horizons are presented in this report (Map C-2 and C-3).

No wells have been drilled on the platform. The tentative ages assigned to the three mapped horizons were derived from comparison with the stratigraphic succession encountered in wells drilled in onshore southeast Mindoro (Central-1, Mindoro-1, Semirara-1, and Progreso-1X), offshore Panay (Maniguin-A-1X), and the northeast Palawan shelf (Roxas-1, Dumaran-1, and Paly-1). A summary of results of these wells is given in Table 1.

Several anticlinal structures bounded by normal faults were mapped. Most of these were defined from single seismic lines only. Seismic coverage was adequate to confirm only one petroleum lead which was intersected by AGSO, Petro-Canada and POGEI lines. Geochemical, direct hydrocarbon detection (DHD) readings were taken along the AGSO seismic lines. There appears to be some degree of correlation between geochemical anomalies and structural highs.

TECTONIC SETTING

Information on the surface geology of islands within the study area was taken from Voce (1981) and Alcala (1987) as well as from a remote sensing report by Bernard and Muller (1986). Information on the tectonic setting of Cuyo Platform in relation to the Philippine arc system was derived from studies by Hamilton (1979), Taylor and Hayes (1980), Mitchell et al (1986), BED (1986), Rangin (1990) and Rangin et al (1991).

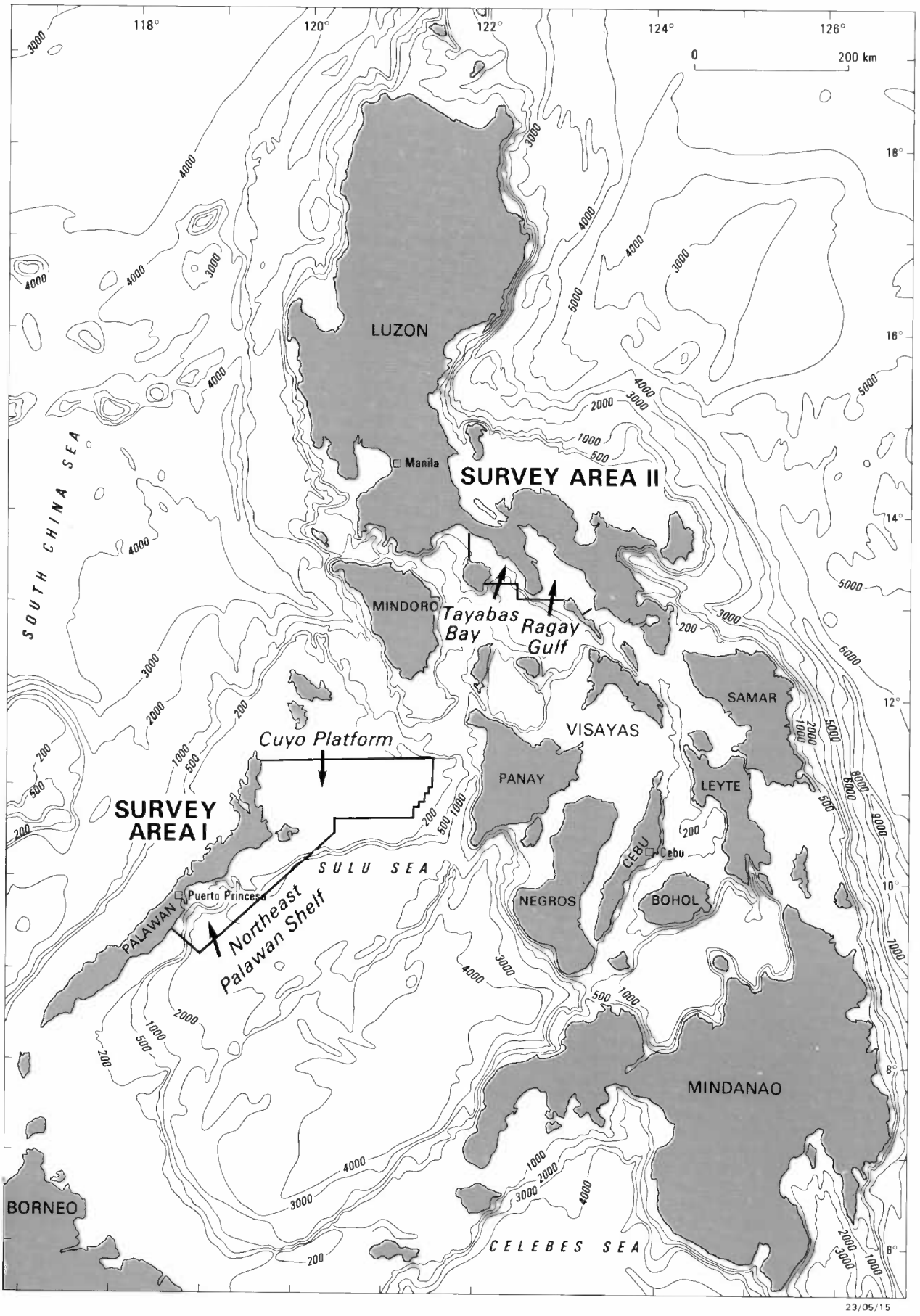

Figure 1 Survey areas of the Philippine - Australia Marine Seismic Survey Project.

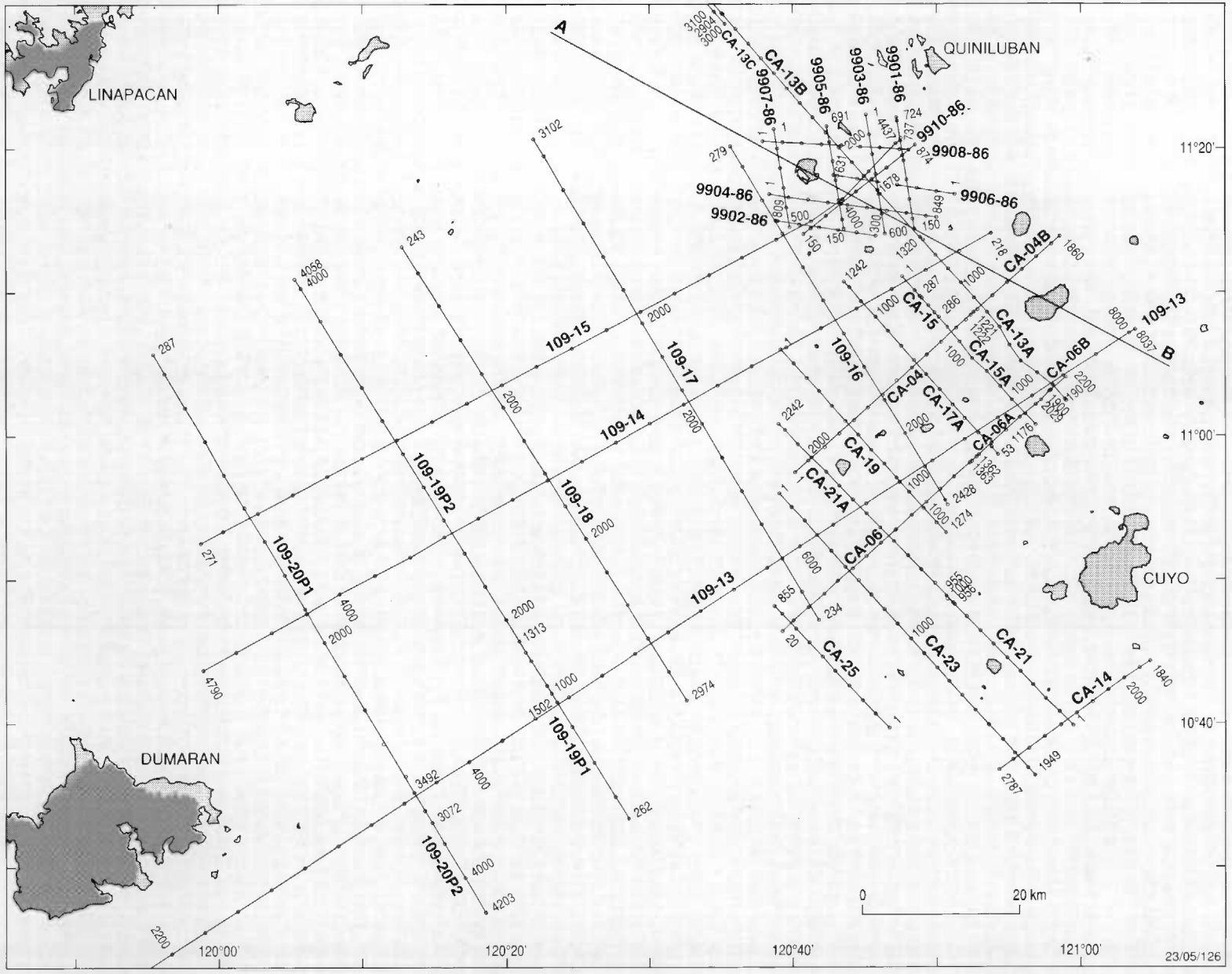

Figure 2 Cuyo Platform showing location of AGSO/DOE/AIDAB survey and previous seismic lines.

Table 1. Summary of previous drilling in NE Palawan-Cuyo Platform-Mindoro area

WELL NAME	DRILLING COMPLETION DATE	TOTAL DEPTH (M and ft) (water depth, m)	PLAY TYPE	DEFINED BY	TARGET	AGE OF ROCK AT T.D.	RESULTS	REMARKS (Validity of Test)
ROXAS-1 (CITCO)*	1979	2030.7 (6663') (73.7 m)	Buildup or erosional high on carbonate platform	Seismic	E. Miocene reef	L. Cretaceous clastics	Dry. No shows	No reef or carbonate present. Not valid test.
DUMARAN-1 (CITCO)	1979	2186 (7172') (86.8 m)	Buildup or sediments draped over basement high	Seismic	Miocene reef or sandstones draped over high	Igneous basement	**gas shows**	No reef and drape over basement doubtful. Not valid test.
PALY-1 (CITCO)	1981	2097.8 (6883') (149.6 m)	Truncation trap below M. Miocene unconformity	Seismic	Late Cretaceous sandstones	(?)Oligocene – E. Miocene clastics	Dry	No L. Cretaceous found. Lateral closure uncertain. Not valid test.
CENTRAL-1 (REDECO)	1962	1915.9 (6286') (onshore)	Anticline	Seismic/ Gravity	Eocene quartz sand	Unknown	Dry	Valid test
MINDORO-1 (BP/INTERPORT)	1979	1523.9 (5000') (onshore)	Anticline	Outcrop mapping	Eplog Anticline, Omega Structure	Eocene(?) Jurassic(?)	Dry	Objective section mission. Not valid test.
SEMIRARA-1 (BRITISH PETROLEUM)	1980	2994.8 (9826') (onshore)	Anticline	Seismic & onshore geology	Eocene Crocker Formation	E. Miocene	Dry	Target not reached. Not valid test.
PROGRESO-1X (SEDCO)	1982	1594 (5230') (onshore)	Anticline	Seismic	Miocene clastic	L. Eocene	Dry	Valid test
MANIGUIN A-1X (PHILLIPS)	1982	1658.6 (5442') (121.9 m)	Large wrench-faulted anticlinal high	Seismic	Miocene sandstone	Eocene	Dry	Valid test

The Cuyo Platform is considered to be part of a continental block called the Kalayaan-Calamian microplate that was rifted from the main China continental margin in the Late Oligocene, and after a period of drifting, became incorporated into an arc-trench system in the Middle Miocene (Bureau of Energy Development, BED, 1986). To the east, the platform is bounded by a subduction complex between the Mindoro and Panay islands (Map C-4), which is composed of a Paleogene-Neogene melange and Cretaceous ophiolites. This complex appears to mark the collision zone between the Kalayaan-Calamian microplate and the central Philippine arc system.

The main phases of tectonic evolution of the study area are summarised as follows:

Oligocene-Early Miocene - Rifting and separation of the Kalayaan-Calamian microplate from the China continental margin leading to the opening of the South China Sea.

Middle Miocene - Collision of the Kalayaan-Calamian microplate with the Philippine arc caused major uplift and erosion. During this period, Cuyo Platform is believed to have collided with the main island arc system near the present Panay Island, resulting in sub-aerial exposure and compression-induced structuring.

Late Miocene to Pleistocene - A period of clastic sedimentation corresponding to erosion of the exposed landmass, until Pleistocene time when a reduction in clastic supply caused carbonate deposition to become more predominant. During Plio-Pleistocene time, igneous bodies were intruded under the southern part of the Cuyo Island group.

EXPLORATION HISTORY

Licence History And Geophysical Surveys

Prior to this project, a total of 5600 line kilometres of marine seismic data had been acquired in the Cuyo Platform by various Philippine and foreign companies. The first seismic survey of the area was carried out by Philippine Overseas Drilling Company and consisted of about 474 kilometres of regional seismic lines. In the early 1980's, Seafront and Philippine Oil and Geothermal Energy Inc. (POGEI) conducted an extensive seismic survey of the area to fulfil commitments under Geophysical Survey and Exploration Contract (GSEC) No. 28, covering portion of the northeast Sulu Sea. PetroCanada acquired about 721 kilometers of seismic lines for a World Bank-assisted Project. This survey led to the delineation of two leads situated in the northeastern quadrant of the study area. However, full scale versions of the seismic data were not available for incorporation into this study. In 1989, Kirkland Resources annexed the southeastern part of the study area and used the available seismic data for a regional correlation of the GSEC No. 52 block. The work was mainly a study of southern Mindoro - both onshore and offshore.

Previous seismic surveys in the Cuyo area are tabulated below:

Acquired By	Year	Line	Kilometres
PODCO/United	1970	R-*	474
Brascan/Western	1974	P*	800
Oceanic/Western	1974	Line*	210
Multi-Natural/Dresser	1976	Multi*	1503
Seafront/GSI	1980	S*	1032
POGEI/GSI	1980	CA-**	715
Seafront/GSI	1982	-	145
Petro-Canada/Sonix	1986	99**-86	721.

Most of these data are scattered in a series of irregular grids along the eastern and southern margins of the platform, and lie beyond the boundary of the project area (Voce, 1981; Seafront, 1981 and Maceda, 1982). The surveys were generally undertaken for regional investigations and companies did not proceed to more intensive exploration. Unfortunately, much of the survey data and reports could not be located and only the POGEI and Petro-Canada data were available for this study.

POGEI's CA-** lines were recorded by GSI onboard the MV Dunlap in December 1980. A 96 group, 25 m group interval, 2400 m length streamer was utilized during the survey, and the shot interval was 25 m. This geometry gave 48-fold coverage. The energy source was a 2000 cubic inch airgun and data were recorded by a DFS-V system. Only 715 out of the planned 1100 line km were acquired because of inclement weather conditions. Petro-Canada lines were recorded on board Sonix's MV Bernier in February 1986 as part of a World-Bank-assisted petroleum exploration project. A 96 channel, 25 m group interval, 2375 m cable was used, together with a Bolt Par airgun as source. Shot interval was 25 m. The survey delineated two leads which are described in the project report (BED, 1986)

In March 1992, the Australian AGSO in co-operation with the Philippine DOE acquired 730 km of new seismic data at 10 to 20 km spacing over the Cuyo Platform using the Australian research vessel, *Rig Seismic* (Lee and Ramsay, 1992; Figures 1 and 2). This was part of a project funded by AIDAB. AGSO reprocessed a further 110 line km of POGEI and Petro-Canada seismic data to improve coverage in areas of interest.

Exploration Wells

None of the eight wells used for stratigraphic correlation purposes were drilled within the project area.

STRATIGRAPHY

Stratigraphic information on the Cuyo Platform is derived mainly from wells drilled 100 to 150 km away in the southern Mindoro, northeast Palawan shelf, and offshore Panay areas. Interpretation of seismic horizons and sequences in terms of age, lithology and environment of deposition is thus highly tentative (Figure 3 and Table 1). A schematic geologic diagram of the Cuyo Platform is shown in Figure 4.

Triassic Chert

The oldest surface outcrops are cherts observed in the northernmost islands of the Cuyo Group (Alcala, 1987). The chert was found to be of Middle Triassic age based on conodont and radiolarian fossils (Hashimoto and Sato, 1973; Fontaine, 1979 and 1983).

Mansalay Formation

A Jurassic sequence consisting of ammonite bearing sandstone and shale, grading into quartzose sandstone and conglomerate is probably equivalent to the Mansalay Formation, of southeastern Mindoro (BED, 1986). The non-marine to shallow marine sediments were tentatively dated as Middle to Upper Jurassic in age.

Batangan Formation

Unconformably overlying the Mansalay sequence is the Batangan Formation. This is mainly composed of black shales, shale and sandstone deposited in transitional to shallow

Age	Formation Name	Lithology	Environment of Deposition	Tectonic event	Maximum Thickness (m.)	Mindoro-1	Progreso-1	Semirara-1	Maniguin-1
Pleistocene-Pliocene	Carcar Limestone	limestone which is typically porous,crystalline massive and poorly bedded; rich in mollusk, coral stem, algae and foraminifera	shallow water carbonate deposits associated with reefs and build-ups	Platform stage; Widespread carbonate deposition	1000	-	700	80	450
			BLUE HORIZON						
Pliocene-Middle Miocene	Punso Conglomerate	massive sequence of pebbles of gneiss, quartzite chert, slate,schist,and limestone set in siliceous and limy matrix occasional interbed of mudstone, shales, coal and limestone in the conglomeratic sequence	non-marine to inner neritic	Regional uplift and erosion; Collision of microplate with island arc system	1500	25	450	1500	500
			RED HORIZON						
Early Miocene-Late Oligocene	Ananawin Formation	calcarenitic-calcisiltic grading into limestone Pandayan gas seep, 81%C1 8.5%C2	shallow marine to non-marine	Drifting and sea-floor spreading	700	-	-	700	300
Early Oligocene-Early Eocene	Batangan Formation	shale and siltstone sequence; occasionally calcarenitic Sibiawan oil seep 20°API	shallow marine to deep marine	Rifting of microplate from China plate	4260	-	250	350	150
			PURPLE HORIZON						
Late Jurassic-Late Middle Jurassic	Mansalay Formation	ammonite bearing sandstone and siltstone, generally carbonaceous with carbonates and conglomerate	inner neritic to lagoonal	Pre-Rifting of original continental margin sediment	3000	1500	-	-	-
Triassic-Late Paleozoic	no name	chert, crystalline rocks schist, slates, and marbles	?		indeterminate	-	-	-	-

Figure 3 Stratigraphy of Cuyo Platform.

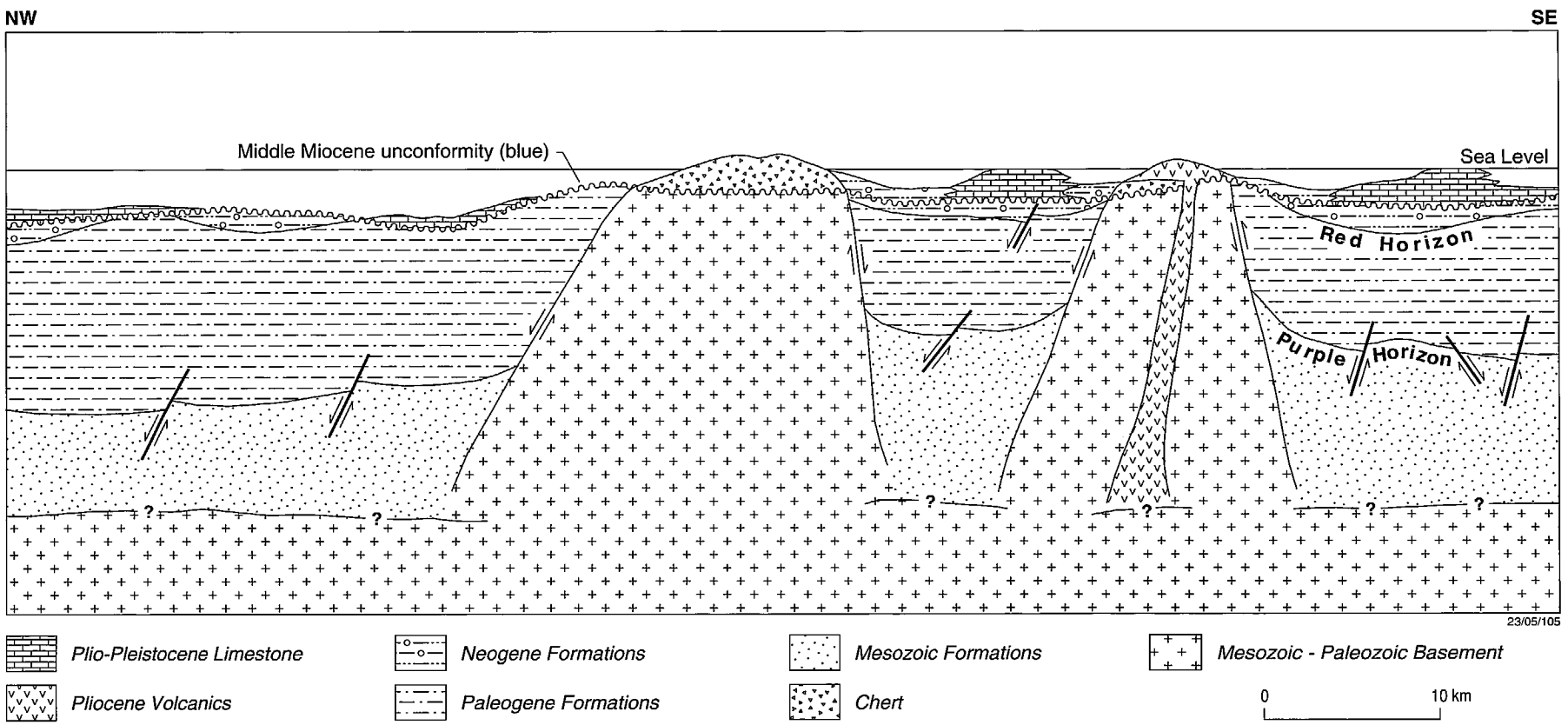

Figure 4 **Schematic geologic diagram of Cuyo Platform.**

marine environments. The presence of *Nummulites sp.* and *Operculina sp.* suggests a Middle Eocene to Early Oligocene age for this formation (BED, 1986).

Ananawin Formation

Lying unconformably above the Batangan Formation is the bedded carbonate and shale/ sandstone sequence of Ananawin Formation. The upper part is dominantly a carbonate sequence while the lower part is a cross-bedded sandstone grading into argillaceous, fine- to coarse-grained sandstone and claystone interbeds (BED, 1986). A Late Oligocene to Middle Miocene age has been assigned to this formation, deposited in a transgressive marine environment with non-marine sedimentary influx.

Punso Conglomerate

The Middle to Late Miocene Punso Conglomerates pervade the whole southern Mindoro area and were also intersected in Maniguin-A-1X and Semirara -1 wells. It is believed that this sequence may extend southward beneath the Cuyo Platform. The sequence was probably deposited in transitional to very shallow marine environments as there are occurrences of coal and occasional shale/sandstone interbeds. The conglomeratic clasts were derived from older rocks underlying the formation.

Carcar Limestone

This Plio-Pleistocene carbonate deposit is probably the most widely distributed in the survey area. The shallow water limestone deposits consists of reefs and carbonate build-ups.

SEISMIC INTERPRETATION

Data Description

The seismic interpretation is based on the AGSO data consisting of 730 kilometres along 20 lines (Lee and Ramsay, 1992). The data was recorded in 48-fold configuration and SEGY format. In the Cuyo area seismic processing and interpretation were hampered by the presence of multiple reflections associated with shallow carbonate build-ups, volcanic extrusives and radiolarian cherts. Additional seismic data from the POGEI and Petro-Canada lines were reprocessed to improve the data quality and provide further control for mapping.

Seismic Horizons

Three seismic horizons were correlated over the entire grid and digitized. Maps were prepared for two horizons. Only tentative stratigraphic identification could be made of seismic reflections due to the absence of well control in the area. For this reason, seismically defined horizons and sequences are referred to by a colour code rather than a stratigraphic term.

The Purple Horizon (Map C-2) is the deepest reflector mapped in the area, forming the top of the inferred Jurassic Mansalay Formation (Figure 3). It has a low amplitude character but can be traced on all lines. The Red Horizon (Map C-3) is of higher amplitude than the purple horizon; it marks the top of the inferred Eocene to Early Miocene Batangan/Ananawin Formation. The reflector is truncated by the Middle Miocene unconformity. The Blue Horizon is interpreted to be the Middle Miocene unconformity. It is a rugged to undulating erosional surface, with its deepest portion near Dumaran Island and becoming shallower toward the northeastern part of the Cuyo

Platform. At its shallowest point it lies close to the seabed. Following the horizon in some shallow water areas is difficult due to the presence of multiples and muting of seismic traces.

Seismic Sequences

The Pre-purple Interval below the purple horizon is considered to correspond to the Mesozoic sequence including the Mansalay Formation. Its lithology in Mindoro and offshore Panay wells is generally coaly with carbonates and conglomerates deposited in inner neritic to lagoonal environments (Maceda, 1982). Vitrinite reflectances indicate that the section is mature.

The Purple-Red Interval is the thickest one in the area. Towards the flanks of the study area, it attains a thickness of about 1.5 to 2.0 seconds two-way time (TWT) and forms minor basins beneath the Cuyo Platform. In the central portion of the area, it underlies a very shallow platform at about 0.5 seconds TWT. The lithology is believed to be shales and siltstones with some calcarenite deposited in shallow marine to deep marine environments. The onshore oil and gas seeps of Pandayan and Sibiawan may be sourced from this interval.

The Red-Blue Interval occupies a 15 to 45 km wide, sinuous, erosion channel which probably formed prior to the Middle Miocene uplift. The base of the interval is equivalent to the top of the early Eocene Batangan Formation which is host to numerous coal measures in the southern Mindoro Islands and offshore western Panay Island. The interval exhibits two different types of internal reflection configuration. The first, consisting of medium amplitude reflections onlapping a scoured surface, is indicative of channel fill. In the second, internal reflections are concordant with the red horizon below. These patterns of onlap and concordance suggest that both erosion and fill processes occurred in the area during the Early Middle Miocene. Lithologic data from wells indicate that the interval may consist of a conglomerate comprising pebbles of gneiss, quartzite, chert, slate, schist and limestone, occasionally interbedded with mudstones, shales, coals and limestones. It was deposited in a marginal marine environment.

The Post-Blue Interval is exposed on minor islands in the Cuyo Group. Its lower part is the Carcar Limestone which has a high acoustic impedance and limits seismic penetration of the underlying section. Mounded structures within the interval, particularly in the northwest, could be of either volcanic or reefal origin.

Structural Interpretation

The Cuyo Platform is dominated by N-S and NE-SW trending normal faults forming a series of horsts and grabens (Map C-4). These structures may have been caused by rifting during Cretaceous and Paleocene times. Grabens appear to contain at least 2 to 3 km of sedimentary section. Downthrown blocks have created step faults with increasing depth and displacement towards the northeast portion of the study area (Map C-2), resulting in the formation of a basin-like depression near Manamoc Island. Strike-slip and deep-seated thrust faults are also in evidence. Due to a lack of detailed seismic control, many faults with similar trends and throws could not be correlated with any confidence. Faults in the northern half of the area appear to have similar orientations to major faults northwest of Palawan in the South China Sea (Map C-4).

Geologic History

Cherts were deposited in Triassic times on a basement which had been subjected to slight metamorphism, as evident from Mindoro-1 well cuttings. Deposition of the Mansalay Formation commenced in the Jurassic and continued until the Cretaceous. Sediments were probably sourced from the China craton as the Cuyo Platform formed part of the original Chinese continental margin at this time. A brief period of deposition in Cretaceous times was followed by a long period of non-deposition and erosion resulting in the removal of most Cretaceous and Early Tertiary rocks. The Cuyo Platform existed as a landmass at this time. A marine transgression in Eocene to Late Oligocene times had less effect on the Cuyo Platform than neighbouring areas, and sediments were laid down in a marginal marine environment. Late in the Oligocene deposition ceased.

Significant tectonic movement in Early to Middle Miocene times raised the Cuyo Platform causing a relative fall in sea level. Coals and carbonaceous clastics found in southern Mindoro wells indicate that sediments were deposited in terrestrial to near-shore environments. Abrupt changes in eustatic sea level caused major breaks in deposition. After a non-depositional/erosional event in the Middle Miocene, clastic sedimentation resumed in the Late Miocene, resulting in the deposition of sand and conglomeratic sequences (Fig. 3). Gradual shallowing of seas in Plio-Pleistocene times brought widespread deposition of carbonates, in particular the Carcar Limestone. Volcanics were extruded episodically on various islands of the Cuyo Group.

PETROLEUM GEOLOGY

Reservoirs

A thick Mesozoic sandstone interval was intersected in the Mindoro-1 well. For this reason, the best potential reservoirs in the Cuyo Platform area are believed to be sandstones of the pre-purple interval, equivalent to the Jurassic Mansalay Formation. The purple-red interval, equivalent to the Batangan Formation, may also contain reservoirs, although porosities would have to be greater than those measured in onshore wells (3 to 10%, BED, 1986). These reservoirs are probably truncated by the Middle Miocene unconformity and may be sealed by post-unconformity shales.

Traps and Seals

The mapped horizons show several structural and stratigraphic features which are potential hydrocarbon traps. The purple horizon, believed to correspond to the top of the Mesozoic Mansalay Formation, exhibits a series of rolling highs and lows from southeast to northwest which gradually shallow towards the central part of the area (Map C-2). In the area enclosed by lines 109-13, 15, 17, and 20, the purple horizon is near the surface, and prominent anticlinal structures are not considered to be prospective due to their shallow depth and consequent lack of sedimentary overburden that could act as a seal.

Stratigraphic pinchouts may occur within the purple-red interval, considered to be equivalent to the Eocene-Early Miocene Batangan/Ananawin Formations (Map C-3). In addition, unconformity traps could have formed as a result of erosional truncation of Batangan sandstones in the Middle Miocene uplift phase, followed by the deposition of sealing shales.

Geochemical Studies

Several oil and gas seepages are known in southern Mindoro Island (BED, 1986; Maceda, 1982). Oil from the Sibiawan seepage was reported to be 94.6% alkane and is considered to be paraffinic and heavily biodegraded. Pandayan gas seep samples contained about 85% methane and 8.5% ethane. The characteristics of hydrocarbon samples extracted from the Middle Miocene section of Semirara -1 well are similar to those of the Sibiawan seeps. Seepages were also reported at Lumintao and Mianao (Maceda, 1982).

A geochemical, direct hydrocarbon detection (DHD) survey was conducted simultaneously with the marine seismic survey of the Cuyo Platform. More than 730 km of DHD data were collected to investigate possible light hydrocarbon anomalies in bottom waters (Evans et al, 1992). The results show that the total hydrocarbon content ranges from 5 to 20 parts per million (ppm). Although the DHD results in the Cuyo Platform show no major hydrocarbon anomalies, comparable with those detected in the Ragay Gulf, it is interesting to note that anomalies of moderate size (2 to 5 times the background value) were observed to be coincident with mapped structural highs. The largest anomaly of 16.0 ppm to 16.5 ppm was found to be associated with a structural lead southwest of Manamoc Island (Figure 5, Plate C-3).

Source Rocks and Maturation

The best potential source rocks in the Cuyo Platform are believed to be Eocene-Early Miocene shales of the Batangan/Ananawin Formation. According to the World Bank report (BED, 1986), 'coals and coaly shales of Eocene age in Mindoro are organically very rich, containing significant quantities of sapropelic kerogen with fair to good hydrocarbon (gas) source potential.' Black shales and coals of Early Miocene age investigated in Semirara-1 on Mindoro contain average to above average amounts of mainly vitrinitic organic matter, with significant quantities of sapropel. This facies could be an important oil source rock if it thickens and deepens basinward of the well location. The carbonaceous clastic sequence of the Jurassic Mansalay Formation may have source potential, although coaly seams found in Mindoro-1 and other wells contain mainly inertinitic kerogen (BED, 1986).

The thermal and tectonic history of the Cuyo Platform and the Northeast Palawan Shelf was deduced from well data using WINBURY software (Appendix 3). Vitrinite reflectance values measured in wells indicate that depths of burial exceeded two kilometres prior to Middle Miocene uplift. Burial and heat flow were then sufficient to initiate hydrocarbon generation from sources present in pre-Middle Miocene rocks. The north Palawan - Mindoro area was subjected to strong uplift during the Middle Miocene, followed by erosion and removal of at least one kilometre of sediments. The generation of hydrocarbons ceased and has not resumed since then in most areas. Only the deepest parts of the Cuyo kitchen area have subsided below pre-unconformity levels, and in these areas hydrocarbon generation may have resumed in the Late Pliocene.The analysis shows that oil can be generated at a depth in excess of 1900 m based on the calculated geothermal gradient.

Migration And Timing

Most hydrocarbon generation occurred prior to Middle Miocene uplift, so preservation is dependent on the existence of traps which have remained structurally high continuously since early Middle Miocene times, or alternatively on re-migration from pre-unconformity traps into post-unconformity traps. Because of the risk associated with re-migration,

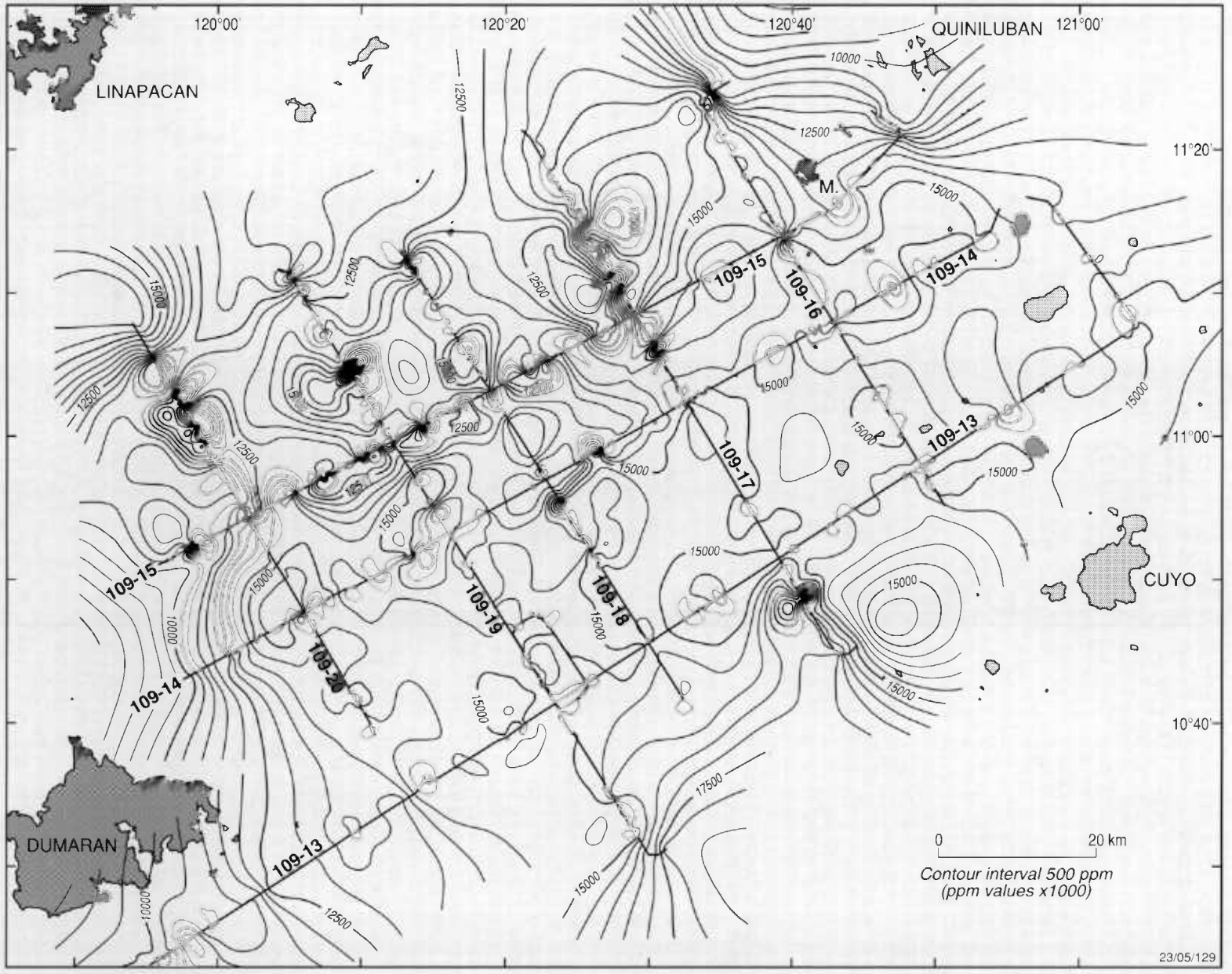

Figure 5 Total hydrocarbon content map of Cuyo Platform.

traps into post-unconformity traps. Because of the risk associated with re-migration, post-unconformity traps are considered to be less prospective, although they may have captured small amounts of hydrocarbons generated in recent times in the deeper parts of the Cuyo Platform, particularly in the northeast of the study area. Exploration risks are considered to be high due to the apparent lack of a present-day source "kitchen" area for hydrocarbon generation, and possible breach of trap seals by recent faulting

Lead Evaluation

The most significant lead in the Cuyo Platform area is situated southwest of Manamoc Island and is called the Manamoc Lead. It is mapped as an anticlinal structural closure, bounded by normal faults, at the Top Jurassic (purple) horizon. The lead was defined from six seismic lines - AGSO lines 109-14, 15 and 16 (SP 850-1030), Petro-Canada lines 9905-86 and 9907-86, and POGEI line CA-17. Potential oil and gas reserves were calculated assuming the parameters listed in Table 2. The lead is depicted in Plate C-3.

CONCLUSIONS

Interpretation of about 730 line km of seismic and geochemical DHD data acquired by AGSO/DOE, under funding from AIDAB, shows deeper horizons which were not previously mapped. The new interpretation was used to infer the possible existence of source and reservoir rocks deeper than the Middle Miocene unconformity. The seismic line spacing is relatively wide, and only one lead was delineated sufficiently for hydrocarbon evaluation. The main conclusions are:

- Seismic data are of poor quality due to the difficulty in penetrating beneath shallow carbonates, volcanics and cherts.
- The best potential source rocks in the Cuyo Platform are believed to be Eocene-Early Miocene shales of the Batangan/Ananawin Formation.
- Most hydrocarbon generation occurred prior to Middle Miocene uplift, but a depocentre mapped in the northeastern part of the platform is a possible site of present-day generation.
- Wells drilled near the survey area encountered potential reservoirs in the form of sandstones in the Jurassic interval and calcarenites in the Early Eocene-Oligocene interval.
- Possible traps are anticlinal structures bounded by normal faults, such as the Manamoc lead.
- Sealing of traps may be provided by massive claystone and mudstone sequences of Oligocene to Miocene age.
- Weak geochemical anomalies are observed to coincide with several closed structural highs.

Table 2. Parameters for Manamoc Lead

PLAY DESCRIPTION

HORIZON	**: (?) Top Mansalay Formation (purple horizon)**
RESERVOIRS	**: Sandstones within the Mansalay formation**
SOURCE ROCKS	**: Mansalay, Ananawin and Batangan Formations**
TRAP AND SEAL	**: Anticline with sandtone reservoir sealed by interbedded siltstones or claystones of the Mansalay Formation, or by claystones and mudstones of the overlying Batangan Formation**
MIGRATION	**: Migration via faults from the underlying section, or updip from the carbonaceous clastic sequence in the Mansalay Formation**

RESERVE ESTIMATE

LOCATION	**: Line 109-16, SP 950**
WATER DEPTH	**: 82 m**
CREST/BASE	**: 1050/1250 milliseconds TWT**
WATER SATURATION	**: 30%**
RECOVERY FACTOR	**: 30% (oil) 80% (gas)**
FORM. VOL. FACTOR	**: 1.4 (oil) 0.007 (gas)**

	Maximum	Median	Minimum
Area of Closure (Ha)	**9969**	**9969**	**9969**
Potential Res. Interval (m)	**30**	**30**	**30**
Gross/Potential	**0.4**	**0.3**	**0.1**
Net/Gross	**0.3**	**0.3**	**0.3**
Net Res. Thickness (m)	**3.6**	**2.7**	**0.9**
Porosity	**10%**	**10%**	**10%**
Reserves-oil (MMBO)	**34**	**25**	**8**
Reserves-gas (BCF)	**101**	**76**	**25**

REFERENCES

ALCALA, M., 1987. Notes on the Geology of Cuyo and Calauit Islands, Palawan. Bureau of Energy Development. Manila, Philippine. (unpublished).

BERNARD, F. and MULLER C., 1986. Synthetic Geological Map Obtained By Remote Sensing; An Application to Palawan Island , *Symposium on Remote Sensing for Resources and Environmental Management*, Enschede Commission VII-ISPRS.

BED, 1986. Sedimentary Basins of the Philippine - their Geology and Hydrocarbon Potential. World Bank Financed Petroleum Exploration Promotion Project, prepared by the Bureau of Energy Development Office of the President , under the Supervision of Robertson Research (Australia) and Flower Doery and Buchan Pty. Ltd. 1986.

BUREAU OF MINES AND GEO-SCIENCES, 1981. Geology and Mineral Resources of the Philippine. Volume 1. Manila. 406 p.

EVANS, D., HEGGIE, D.T., BISHOP, J.H., REYES, E. N., & LEE, C.S., 1992. Light Hydrocarbon Geochemistry in Bottom Waters of the Philippine Continental Shelf Part B; Northeast Palawan Shelf and Cuyo Platform Rig Seismic Survey 109. *Australian Geological Survey Organization Record* 1992/92, 164 p.

FONTAINE, H, 1979. Note on the Geology of the Calamian Islands: *CCOP Newsletter*, 6/2, 40-45.

FONTAINE, H.,1983. A Note on the Northwest Panay - Tablas Area. *CCOP Newsletter* 10, 8-13.

HAMILTON, W., 1979. Tectonics of the Indonesian Region. *US Geological Survey Professional Paper* 1078, 345 p.

HASHIMOTO, W. and SATO, T., 1973. Geological Structure on the North Palawan and Its Bearing on the Geological History of the Philippine. *Journal of Geology and Paleontology of Southeast Asia* 13, 145-146

LEE, C.S. and RAMSAY, D., 1992. Philippine Marine Seismic Survey Project Cruise Report. *Bureau of Mineral Resources, Australia, Record* 1992/49, 69p.

MACEDA, R.,1982. Seismic Interpretation Report-POGEI/Lepanto 1982 Seismic Survey - Cuyo Shelf, NE Palawan. (unpublished).

RANGIN, C., 1991. The Philippine Mobile Belt: A Complex Plate Boundary. *Journal of Southeast Asian Earth Sciences* 6:3-4 pp. 209-220.

RANGIN, C., JOLIVET, L. PUBELLIER, M., 1990. A Simple Model for the Tectonic Evolution of Southeast Asia and Indonesia Region for the Past 43 m.y. *Bulletin of Soc. Geol. France* 8:6, 889-905.

SEAFRONT, 1981. Seismic Interpretation Report 1980 Seismic Survey in the Cuyo Shelf., (unpublished).

TAYLOR, B. & HAYES, D. E., 1980. The Tectonic Evolution of South China Sea Basin, *American Geophysical Union Monograph* 23, 89-104.

VOCE, B., 1981. Seismic Survey in the Cuyo Shelf. Seismic Interpretation Report, 1980. (unpublished).

PHILIPPINES-AUSTRALIA MARINE SEISMIC SURVEY PROJECT

GEOLOGY AND PETROLEUM POTENTIAL OF RAGAY GULF, TAYABAS BAY, NORTHEAST PALAWAN SHELF AND CUYO PLATFORM, PHILIPPINES

VOLUME 2: APPENDICES

AGSO RECORD 1994/41

PREPARED BY:
AUSTRALIAN GEOLOGICAL SURVEY ORGANISATION
PHILIPPINE DEPARTMENT OF ENERGY

FUNDED BY:
AUSTRALIAN INTERNATIONAL DEVELOPMENT ASSISTANCE BUREAU

1994

CONTENTS

Appendix 1: Evaluation of Reservoirs, Bondoc Peninsula

Appendix 2: Geohistory Modelling of Ragay Gulf and Tayabas Bay

Appendix 3: Geohistory Modelling of Northeast Palawan Shelf and Cuyo Platform

Appendix 4: New Hydrocarbon Geochemistry of Oil and Gas Seeps from Bondoc and Bicol Peninsulas, Southeast Luzon

Appendix 5: Direct Hydrocarbon Detection in Bottom Waters with Application to Offshore Petroleum Exploration in the Philippines

Appendix 6: Palynological Analysis of San Francisco-1 and Katumbo Creek-1 Wells, Southeast Luzon

ISSN 1039-0073
ISBN 0 642 21253 8

APPENDIX 1

EVALUATION OF RESERVOIRS, BONDOC PENINSULA

by

A. R. Fraser[1]

1 Australian Geological Survey Organisation, Canberra, ACT, Australia

INTRODUCTION

This brief evaluation of Bondoc Peninsula reservoirs is based on porosity values derived from sonic, density and neutron logs in three exploration wells, together with analyses of cores and cuttings, litho-stratigraphic descriptions, and results of drill stem tests where available. Four main areas are considered: San Francisco-Aurora, Katumbo, Bondoc wells and Mayantok.

Density and neutron porosities were read directly from log displays. Sonic porosity was computed from the Wyllie equation:

$t_{log} = t_{ma}(1-\phi-v_{sh}) + t_{fl}\phi + t_{sh}v_{sh}$, giving

$\phi = (t_{log} - t_{ma} + v_{sh}t_{ma} - v_{sh}t_{sh})/(t_{fl} - t_{ma})$

where t_{log} is transit time in reservoir

t_{ma} is matrix transit time (55.5 µs/ft for sandstone)

t_{fl} is transit time for fluid (189 µs/ft for water)

t_{sh} is transit time for shale

v_{sh}, the volume of shale, is given by $v_{sh} = 0.083(2^{3.7v} -1)$

where $v = (gr - gr_{cs})/(gr_{sh} - gr_{cs})$

where gr is gamma log value at level of interest

gr_{cs} is gamma value for clean sandstone

gr_{sh} is gamma value for shale.

A compaction-corrected sonic porosity was calculated from ϕ above by multiplication by $100/t_{sh}$ if t_{sh} is greater than 100.

AURORA-SAN FRANCISCO AREA

Aurora-1 drilled in 1971 near the crest of an anticline encountered thick sandstones (combined thickness of 216m) at 1280m in the Middle Miocene Vigo Formation. Analyses of sidewall cores indicated sandstone porosities ranging from 24% to more than 30%, and permeabilities from 15 to 400 md. Aurora-2 on the flank of the same anticline also encountered sandstones of reservoir quality at 1000m. Circulation was lost at 1100m where a strong flow of gas was recorded. The well was eventually plugged and abandoned due to inability to control the pressure.

Wells San Francisco-1 and -2 were drilled in 1977 on the Aurora structure to the northwest of the Aurora wells. San Francisco-1 encountered sandstones in both the Lower Canguinsa and Vigo Formations. These have a very coarse texture, comprising poorly to moderately sorted volcanic and feldspathic rock fragments, but permeabilities are low due to argillaceous matrix filling voids. It was thought that a permeability increase may be associated with a 100m wide shear zone in the Vigo Formation. Drill stem testing of two intervals in the Vigo Formation and one in the Lower Canguinsa all produced weak gas flows. Porosities were calculated from sonic, density and neutron logs to be in the range 14% to 27% (Table 1). Sandstones appear to be best developed in the upper portion of the Vigo Formation (905 to 1450m) where they attain thicknesses of 30m or more.

San Francisco-2 was drilled to test the potential of the sheared zone within the Vigo Formation. The zone was found to be thicker and 300m higher than in San Francisco-1, but permeability was still regarded as negligible due to chloritic clay matrix and no tests were conducted.

Table 1. Porosity Calculations, San Francisco-1 Well

Sonic Log

$gr_{cs} = 10$ $gr_{sh} = 50$

$t_{ma} = 55.5$ µs/ft $t_{fl} = 189$ $t_{sh} = 125$

No.	Depth(ft)	t_{log}	gr	v_{sh}	ϕ_s	ϕ_n	ϕ_d	ϕ_{sd}	ϕ_{snd}
1	2840	107	25	0.13	25	34	23	24	27
2	3100	96	15	0.03	23	29	15	19	22
3	3135	97	15	0.03	24	31	18	21	24
4	3315	100	21	0.09	23	31	20	22	25
5	3400	88	14	0.02	19	27	15	17	20
6	3455	90	13	0.02	20	27	15	18	21
7	3610	93	13	0.02	22	29	16	19	22
8	3690	88	16	0.04	18	29	14	16	20
9	3835	84	16	0.04	15	28	12	14	18
10	3850	90	18	0.06	18	29	14	16	20
11	4030	89	14	0.02	19	26	18	19	21
12	4045	89	14	0.02	19	28	16	18	21
13	4075	70	21	0.09	5	26	12	9	14
14	4260	95	15	0.03	22	33	18	20	24
15	4585	86	14	0.02	17	29	19	18	22
16	5810	90	27	0.16	14	32	16	15	21
17	6060	100	21	0.09	23	30	16	20	23
18	6130	100	23	0.11	22	34	16	19	24

KATUMBO CREEK AREA

Katumbo Creek-1 well was drilled in 1980 to test a possible reef facies developed within the Panaon Limestone, secondary objectives being sandstones and limestones in the overlying Vigo Formation. The well encountered volcanic wackes and shales with minor limestones, of Early Miocene to Pliocene age, before bottoming in metamorphic basement. The main mapped horizon proved to correspond to the top of a thick accumulation of quartz and volcanic sands and conglomerates, poorly sorted with abundant interstitial clays, representing a fan build-up at the base of a major fault. There was no good development of reservoirs, the sandstones being mainly feldspathic with little or no porosity.

Porosities derived from well logs (Table 2) largely confirm the above picture. Sonic and density porosities higher than 20% occur in the top 700m of section, but deeper than this values do not exceed 13% and are commonly less than 10%. High neutron porosity values (greater than 30%) are attributable to water-bearing interstitial shales.

BONDOC WELLS AREA

Of seven wells drilled since 1948, only Bondoc-3 (1691m) and Bondoc-7 (1300m) were drilled deeper than 1000m. Only Bondoc-7 well reached the Vigo Formation; the other wells bottomed in the Canguinsa Formation. Bondoc-2 tested up to 50000 cubic feet of gas and 230 bbls/day from limestone lenses within the Upper Canguinsa Formation.

Formations penetrated in the area were the Upper Canguinsa Formation composed of calcareous sandstones and calcarenite grading to calcareous, silty or sandy shales; the Lower Canguinsa Formation, consisting of an upper member of calcareous sandstones grading into calcarenite with occasional conglomerate lenses, and a lower member of monotonous calcareous shales; and the Vigo Formation comprising basinal shale with rare thin lenses of limy sandstone. Of these formations, the upper member of the Lower Canguinsa Formation is considered to have the best reservoir potential. Well correlations and paleo-environment studies suggest that sand percentage of the Lower Canguinsa decreases from west to east implying that better reservoirs may exist west of the Bondoc well area. The Vigo Formation appears to have low potential owing to the rarity of sand development in Bondoc 7 well.

MAYANTOK AREA

Mayantok-1 was drilled in 1989 to test sandstone and/or conglomerate intervals within the Upper Member of the Lower Canguinsa Formation at depths between 30 and 300m. A secondary objective was sandstones possibly developed within the Lower Member of the Lower Canguinsa Formation at expected depths of 300 to 800m. The well penetrated only 220m of the Canguinsa Formation, followed by Upper and Lower parts of the Vigo Formation to TD. A repeated section of Upper Vigo occurred near the bottom of the well, below a major reverse fault with an estimated throw of 500m.

Table 2. Porosity Calculations, Katumbo Creek-1 Well

Sonic Log

gr_{cs} = 10 gr_{sh} = 45 (1000-5862 ft) gr_{sh} = 90 (5862 ft -TD)

t_{ma} = 55.5 μs/ft t_{sh} = 140 (1000-5862 ft) t_{sh} = 70 (5862 ft -TD)

t_{fl} = 189 μs/ft

No.	Depth(ft)	t_{log}	gr	v_{sh}	ϕ_s	ϕ_n	ϕ_d	ϕ_{sd}
1	1465	123	10	0	36	47	25	31
2	2090	106	15	0.04	25	38	16	21
3	3280	83	23	0.13	9	37	13	11
4	3650	82	15	0.04	12	36	13	13
5	3910	84	18	0.07	12	37	13	13
6	4360	75	23	0.13	5	36	11	8
7	4530	85	26	0.18	8	35	10	9
8	4680	93	20	0.09	16	39	10	13
9	5056	84	25	0.17	8	37	10	9
10	5490	80	26	0.18	5	32	14	10
11	5620	73	27	0.20	0	31	13	7
12	5877	66	33	0.09	5	32	11	8
13	5913	70	29	0.07	10	36	10	10
14	5975	82	20	0.03	14	19	10	12
15	6005	58	15	0.01	1	21	10	6
16	6125	66	16	0.02	5	32	10	8

The Canguinsa Formation was found to consist of sandstone, siltstone, claystone , limestone and occasional thin coal stringers. The sandstones are very fine to fine-grained, poor to moderately sorted, with calcareous cement and argillaceous matrix. The Vigo Formation comprises predominantly siltstone and sandstone with several interbeds of limestone and claystone. The sandstones are fine-grained, moderately sorted with calcareous cement and argillaceous matrix.

No good reservoir build-ups could be identified on logs and it was not possible to derive realistic porosity values. Analyses of sidewall cores indicated very poor reservoir characteristics. Because of lack of reservoir, no tests were carried out despite the presence of gas-saturated zones and oil shows .

APPENDIX 2

GEOHISTORY MODELLING OF RAGAY GULF AND TAYABAS BAY

by

A. M. G. Moore[1]

1 Australian Geological Survey Organisation, Canberra, ACT, Australia

ABSTRACT

Stratigraphic and petroleum-related data for seven wells drilled on the Bondoc Peninsula in the Republic of the Philippines were compiled and entered into the BURY basin and well analysis program. Model stratigraphic data were also analysed, at two onshore well sites below TD, at four offshore 'kitchen' areas near depocentres, and at an offshore lead. The results of the well and model geohistory analyses are presented here, and some of the implications for hydrocarbon exploration are discussed.

The study of well data finds that the Ragay Gulf and Tayabas Bay areas have very moderate heatflow averaging about 50 mW/m^2 (1.2 HFU), with temperature gradients generally less than 35°C/km. The Pliocene - Late Miocene Canguinsa Formation and the upper part of the Middle Miocene Vigo Formation are immature for hydrocarbon generation at most of the onshore well sites and at the particular offshore leads studied. The lowermost Vigo Formation is now entering the zone of maturity in the deeper wells. The Late Oligocene - Early Miocene Panaon Limestone and the undrilled succession between it and the Eocene - Early Oligocene Unisan Formation are in the oil generation zone.

The model data shows that in the oil generating areas of the Bondoc Sub-basin (the Tayabas and Bondoc East 'kitchens') a major part of the Vigo Formation, the regional seal and likely source of Bondoc Peninsula seeps, is mature for hydrocarbons. In the Ragay Sub-basin, the Lower Canguinsa is also early-mature near the base, and the Vigo and Panaon Formations are at the optimum depth of burial for hydrocarbon generation. Because the Southeast Luzon Basin is not 'hot', the hydrocarbon window has a potential vertical extent of three kilometres, and this increases the chances of good source rocks occurring within it in the thick 'kitchen' areas.

CONTENTS

INTRODUCTION **7**

METHOD **7**
The BURY Software
The Input Data

RESULTS **9**

DISCUSSION **9**

CONCLUSIONS **10**

REFERENCES **11**

WELL DATA
Aurora 1
Bondoc 3
Bondoc 7
Katumbo Creek 1
Mayantok 1
San Francisco 1
San Francisco 2

MODELS
Anima Sola Lead
Bondoc Sub-Basin
Burias Sub-Basin
Mayantok-A (Ext =Well Model Extended Below TD)
Ragay Sub-Basin
San Francisco-A (Ext) And San Francisco-A (Hot)
Tayabas Bay

INTRODUCTION

Many petroleum exploration wells have been drilled on the Bondoc Peninsula in the Republic of the Philippines. In this study, stratigraphic and petroleum-related data for seven wells were compiled and entered into the BURY basin and well analysis program. Bottom-Hole Temperatures (BHTs) were used to estimate the present heatflow (HF). Plots of burial history were made. These and and related parameters such as maturity versus depth, and calculated versus observed values of downhole temperature and vitrinite reflectance, are presented in this report, and some of their implications are discussed. Hypothetical stratigraphic data also was analysed, below TD in two onshore wells, in four 'kitchen' areas near depocentres offshore, and at an offshore lead. The predicted maturation profiles are presented.

The seven studied wells are listed alphabetically below. They are -
Aurora 1
Bondoc 3
Bondoc 7
Katumbo Creek 1
Mayantok 1
San Francisco 1 (cool model) and San Francisco 1 (hot model) and
San Francisco 2.

The model data were as follows -
Anima Sola Lead (the predicted stratigraphic succession on the Anima Sola Lead offshore)
Bondoc Sub-Basin
Burias Sub-Basin
Mayantok-A (extended; the succession at Mayantok 1 well with data below TD)
San Francisco-A (extended; the succession at San Francisco 1(cool) plus data below TD)
San Francisco-A (hot)
Ragay Sub-Basin and
Tayabas Bay.

METHOD

The BURY Software

BURY is a commercial software program developed in Australia since 1978 for the modelling and analysis of burial and thermal histories of well sequences and basins in petroleum exploration (Paltech, 1993). It uses industry standard 1-D models for sediment compaction and decompaction, thermal maturity, and kinetic generation of hydrocarbons from source rock, with default values that can, in many cases, be varied. A useful summary of the features of BURY and comparisons with other similar packages such as MATOIL and BASINMOD can be found in Radlinski (1991), although the software has continued to evolve since then. The Windows versions 1.1 and 1.3 (WINBURY 1.1 and 1.3) were used in this study.

The Input Data

Data from wells for input to the BURY software came from the well completion reports (WCRs) submitted to the Department of Energy of the Philippines, and related reports which are listed in the references. WCRs are referenced under company name and year. There was no WCR for Bondoc 3 well, and the report on Aurora 1 lacked maturity data, hence the data input for those two wells was limited, and the resulting model is very basic.

Model data were derived from seismic interpretation of horizon depths below TD at two onshore well locations, and at five locations offshore.

Well Header data includes well name, operator and year drilled, latitude and longitude, kelly bushing (KB), ground elevation above sea level or water depth, termination depth (TD), and bottom hole temperature (BHT). Estimated basement depth, and an estimated present-day value of heat flow (HF) are also entered. All depths are related to KB. The present-day surface temperature and past seabed temperatures are given as 28^{o}C.

Unit age and depth. The age of the top of the first unit in each well is 0 million years (0 My) and the depth to the top is the KB depth of the ground surface - usually just a few metres onshore, more offshore. Depth to top of units is taken from WCRs. The absolute ages of geological stages are those currently used in-house by the Australian Geological Survey Organisation. They are broadly compatible with those of Harland et al (1982).

Modelled water depths of deposition of the formations lie within the range 0m to 50m, and an actual value of 20m was used in the models.The exception is the present surface unconformity in land wells, which in some cases is more than 200m negative (above sea level).

Heatflow modelling. BHTs and downhole temperatures measured on logs, together with the thermal conductivities of the formations, were used to calculate the present-day heatflow and geothermal gradient. This provided a reference curve for checking such observations as temperature and vitrinite reflectivity (Ro) versus depth. It is the basis for calculation of the Ro indices on the geohistory plots (e.g. 0.5, 0.7 etc on the plot of Aurora 1), except where otherwise annotated. This initial reference heatflow was modified where it was found incompatible with observed data, e.g. in San Francisco 1 (see below in the relevant section dealing with that well). Variation of heatflow with time was not used in this study.

Lithology for the purpose of geohistory modelling is used mainly for calculating the thermal conductivity, density, initial porosity and depth of deposition, and compaction factors of units. In this study it is kept very simple, consisting of three matrix materials, namely sand, clay and limestone.

Unconformities. The constraint generally used in basin history studies to quantify section eroded at unconformities is either the maturity profile, based on measured vitrinite reflectance (Ro) and its equivalents, or/and seismic. Many of the wells did not have Ro measurements. The measured profiles of Ro that were available, e.g. at Katumbo Creek 1 (Sedco, 1980) and San Francisco 1 (Yap, 1977), did not show clearly the kind of sudden increase in maturity often seen at unconformities. The seismic was often ambiguous regarding the amount of erosion at unconformities. Hence there was very little attempt to 'restore' eroded section.

Other observed data. Kerogen data were available very sparsely , e.g. at Aurora 1 and Katumbo Creek 1, and consisted of TOCs determined at a few levels, together with organic matter type. Very little porosity data was available.

Hydrocarbon maturity is expressed in terms of the reflectance of vitrinite (Ro). Other measures, such as spore coloration, are translated onto a scale of Ro in the plots generated by this study.

RESULTS

The results of the analysis are presented in the following pages. They consist of plots of measured and expected hydrocarbon maturity, temperature and other parameters, plotted against geological time, or depth in the wells, or both. The results are presented for each well in alphanumeric order of well name, followed by the modelled locations offshore, also in alphabetical order. There are several plots for each well, beginning with a header containing basic well data such as location and TD, a first-pass burial history plot, and a table of the basic stratigraphic data used by the BURY program. For one well, San Francisco 1, two alternative models or versions using different values of heatflow are presented, each accompanied by a separate header record and data entry table. For this well it is difficult to choose between the 'cool' and the 'hot' models, because of contradictions in the data on temperature and maturity. Comments on features of significance are added to the plots themselves, rather than being collected in the textual portion of this report. The deepest well stratigraphically is Katumbo Creek 1, and there is measured maturity data available also, so it is considered an important well for the understanding of the history of the area.

Model geohistories are presented for the successions below TD at Mayantok 1 and near San Francisco 1, for four depocentres and for the Anima Sola lead.

DISCUSSION

The temperatures measured during formation tests at Aurora 1 and San Francisco 1 and quoted by Rutherford and Qureshi (1981) are much higher than the temperature measurements made during logging runs and noted on the logs. They indicate a warmer regime than that observed in the other wells, with heatflow between 65 mW/m^2 (1.5 Heatflow Units) at San Francisco 1, and 88 mW/m^2 (2.1 HFU) at Aurora 1. At the latter well, this formation test data is the only measured temperature available, and the maturation model shows higher levels than in other wells. This study had no means of checking this figure against other measures of maturity, or of viewing the measurement documentation. At San Francisco 1 other measures were available, and they indicate lower levels of maturity than that suggested by the formation test temperature. Those other measures themselves are not definitive of maturity. Log temperatures are reduced by cool drilling mud, and the correction for this (the Horner correction) might not be adequate. Vitrinite reflectance, too, can be depressed in oil-prone sediments. For San Francisco 1, therefore, two models have been presented in this report, a 'cool' and a 'hot' model.The majority of the data supports the 'cool' model of the province, and cannot be ignored, despite doubts. At prognosed locations offshore, therefore, an intermediate level of heatflow (64 mW/m2, 1.5 HFU) has been used to model and predict the maturity of the succession.

CONCLUSIONS

Most of the available data indicate that the present-day heatflow and the temperature gradient are not high in the Southeast Luzon Basin. Where log temperature data are available, they show heatflow of between 50 and 64 mW/m^2, (1.2 - 1.5 HFU), e.g. at Katumbo Creek 1 and Bondoc 7. Temperature gradients of around 30 to 35^{o}C/km would be representative of this regime. Vitrinite reflectance (Ro) measurements appear to confirm this argument, e.g. at Katumbo Creek 1 and at San Francisco 1. However, the temperatures of formation fluids recovered by Drill Stem Tests (DSTs) in two wells, Aurora 1 and San Francisco 1, are at variance with other wells and with the e-log temperature from the latter well itself. They indicate a higher heatflow in those two wells (65 - 88 mW/m^2, 1.5 - 2.1 HFU). In San Francisco 1 well, the maturity calculated from Ro measurements is lower than that from DST temperature measurements. This contradiction in maturity data could be due to depression of Ro. Vitrinite reflectance can be suppressed, e.g. in the presence of formation oil, or if a significant part of the organic matter is very oil-prone (Jeffrey et al, 1991, Snowdon & Powell, 1982) and this may be the cause of disagreement between measures of heatflow and of maturity. Resolution of this disagreement was achieved by using values intermediate between the two, in areas modelled for this report. The succession drilled by exploration wells on the Bondoc Peninsula appears to be immature to marginally mature. Full maturity for hydrocarbons will occur in the largely undrilled lowermost parts of the Vigo Formation and below, in the Panaon Limestone or a hypothesised underlying succession similar in age and lithology to the Taog equivalent in Leyte.

At the offshore sites, the Bondoc, Burias, Ragay and Tayabas Bay 'kitchen' areas and on the Anima Sola lead, a model using an intermediate heatflow figure (64 mW/m^2, 1.5 HFU) was used to predict maturity. The lowermost part of the Pliocene - Late Miocene Canguinsa Formation is early mature in the Ragay Sub-basin only, not elsewhere. The Middle Miocene Vigo Formation and the underlying Early Miocene Panaon Formation are mature for hydrocarbons. In the deepest part of the Bondoc Sub-basin the Panaon Formation and the base of the Vigo Formation may be post-mature. The undrilled unit lying between the Panaon and Unisan Formations occupies the prime zone for generation of hydrocarbons on offshore leads, e.g. Anima Sola. It is hoped that there may be a stratigraphic equivalent of the oil-productive Taog Formation within this unexplored portion of the geological succession in the Ragay Gulf and in Tayabas Bay.

REFERENCES

FAR EAST RESOURCES PLC/RAN RICKS OF THE PHILIPPINES, INC., 1990. Final Well Report, Mayantok No.1.

HARLAND, W.B., Cox, A.V., Llewellyn, P.G., Pickton, C., Smith, A. & Walters, R., 1982. A Geologic Time Scale. Cambridge University Press.

JEFFREY, A.W.A., Alimi, H.M., & Jenden, P.D., 1991 Geochemistry of Los Angeles Basin Oil and Gas Systems. In BIDDLE, K.T., Active Margin Basins; AAPG Memoir 52.

PALTECH, 1993: BURY for WINDOWS (WINBURY) User Manual. Paltech Pty Ltd., Sydney, Australia.

PODCO, 1960. Well Completion Report, Bondoc No7, Bondoc Peninsula, Quezon Province. By Albert A. Carrey for Philippine Oil Development Co., Inc., 11p.

PODCO, 1977a. Well Completion Report, San Francisco No1 Well. By Philippine Oil Development Co., Inc. 100p.

PODCO, 1977b. Well Completion Report, San Francisco No2 Well. By Philippine Oil Development Co., Inc. 52p.

Radlinski, A. 1991. An Analysis of Methodology Used in Commercial Geohistory and Geochemistry Programs: Bury 5.41, Basinmod 2.55 and Matoil 1.4. BMR Record 1991/110. 46p.

Rutherford, K. J. & Qureshi, M. K., 1981 Geothermal Gradient Map of South East Asia, 2nd Edition. Joint Publication of the Southeast Asia Petroleum Exploration Society and the Indonesian Petroleum Association. 51p.

SEDCO, 1980. Katumbo Creek No 1 Final Geological Report. Sedco Exploration Company of the Philippines, 6p, 5 Appendices.

SNOWDON, L.R., and Powell, T.G. 1982. Immature oil and condensates-modification of hydrocarbon generation model for terrestrial organic matter; AAPG Bulletin,v.66, pp.775-588.

WHITE EAGLE, 1971. Aurora No 1 Final Well Report. By White Eagle Overseas Oil Co., Inc. 29p.

Yap, A.L., 1977. Geological Evaluation of the Service Contract No 20 Area, Bondoc Peninsula, Quezon Province, Philippines. For Philippines Oil Development Co Inc, 7p.

AURORA 1

WHITE EAGLE 1971

Latitude: 13° 23' 48" N
KB: ?120m asl
Surface Temperature: 28°C
BHT: 132°C (Rutherford & Qureshi, 1981)

Longitude: 122° 31' 01" E
TD: 2089mKB
Surface Elevation:117m asl
BHT Depth: 2089m

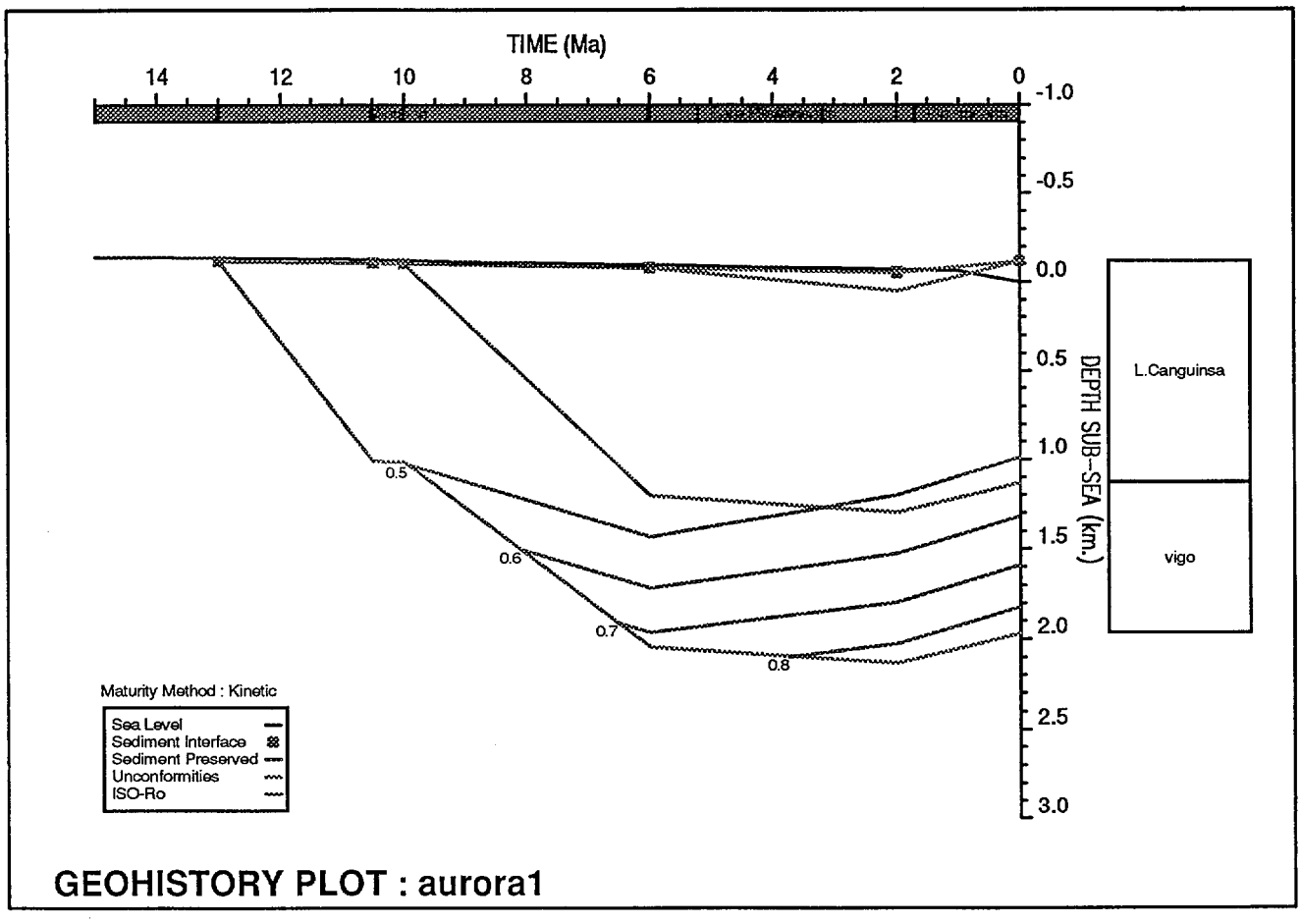

GEOHISTORY PLOT : aurora1

The geohistory diagram for Aurora 1 well shows the late uplift that has raised the sediment surface on this part of the Bondoc Peninsula to its present elevation, 117m above sea level. The well spudded into the Lower Canguinsa Formation at the surface. In this model, the Upper Canguinsa is assumed to have been deposited in shallow water to a thickness of 100m, then eroded during the succeeding uplift (see Horizon Data table over page)

	Stratigraph. Unit/Event	E V	Depth to Top of Unit	Age (Ma)	Minimum WtrDpth	Maximum WtrDpth	Modelled WtrDpth	Sea Bed Temp.	Heatflow	Lithology Data	Kerogen Data	Variable Beds
1	Surface unconf.	E	3.00	0.00	-117.00	-117.00	-117.00	28.00	86.00	*	*	
2	Deposit TCu	E	(100.00)	2.00	0.00	50.00	20.00	28.00	86.00	*	*	
3	L.Canguinsa	N	3.00	6.00	0.00	50.00	20.00	28.00	86.00	*	*	
4	Top Vigo uncnf - Red	H	1250.00	10.00	0.00	50.00	20.00	25.00	86.00	*	*	
5	vigo	N	1250.00	10.50	0.00	50.00	20.00	25.00	86.00	*	*	
6	TD	N	2089.00	13.00	0.00	50.00	20.00	25.00	86.00	*	*	

HORIZON DATA : AURORA1

	Stratigraph. Unit/Event	SHALE	SAND	CHALK	LST	COAL	HALIT	VOLCS	CONV	GY/ANH	Initial Porosity	Por/Depth Factor	Conductivity	Density
1	Surface unconf.	25	60		15						0.470	1.030	10.920	2.700
2	Deposit TCu	50	10		40						0.550	1.740	7.110	2.760
3	L.Canguinsa	40	45		15						0.520	1.330	9.060	2.720
4	Top Vigo uncnf - Red		20								0.640	2.020	5.900	2.770
5	vigo	80	20								0.640	2.020	5.900	2.770
6	TD	80	20								0.640	2.020	5.900	2.770

HORIZON DATA : AURORA1 - MATRIX LITHOLOGY

The input data for the geohistory model of Aurora 1 shows the parameters used for each layer. Layer 1 is the surface, where erosion is now active. Layer 4 is a seismic unconformity (the Red horizon) at the base of the Canguinsa Formation.

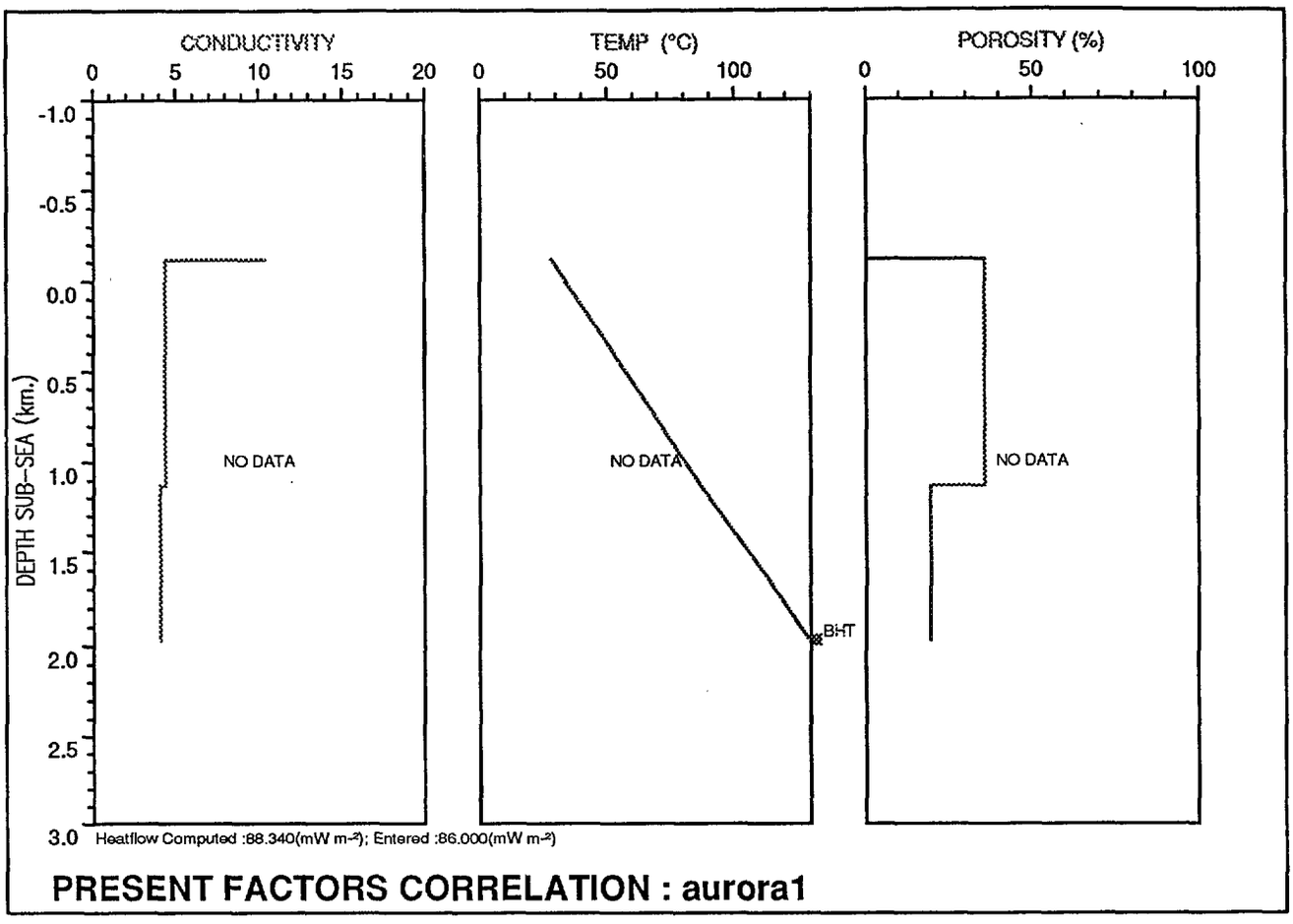

The Bottom Hole Temperature (BHT) quoted by Rutherford & Qureshi (1981) is the only temperature/maturity information available for this simple model of the history of Aurora 1. It indicates that the heatflow is high in this area. The plotted lines in this diagram indicate the expected variation of conductivity, temperature and porosity resulting from the parameters entered into the model (see Horizon Data: Aurora 1).

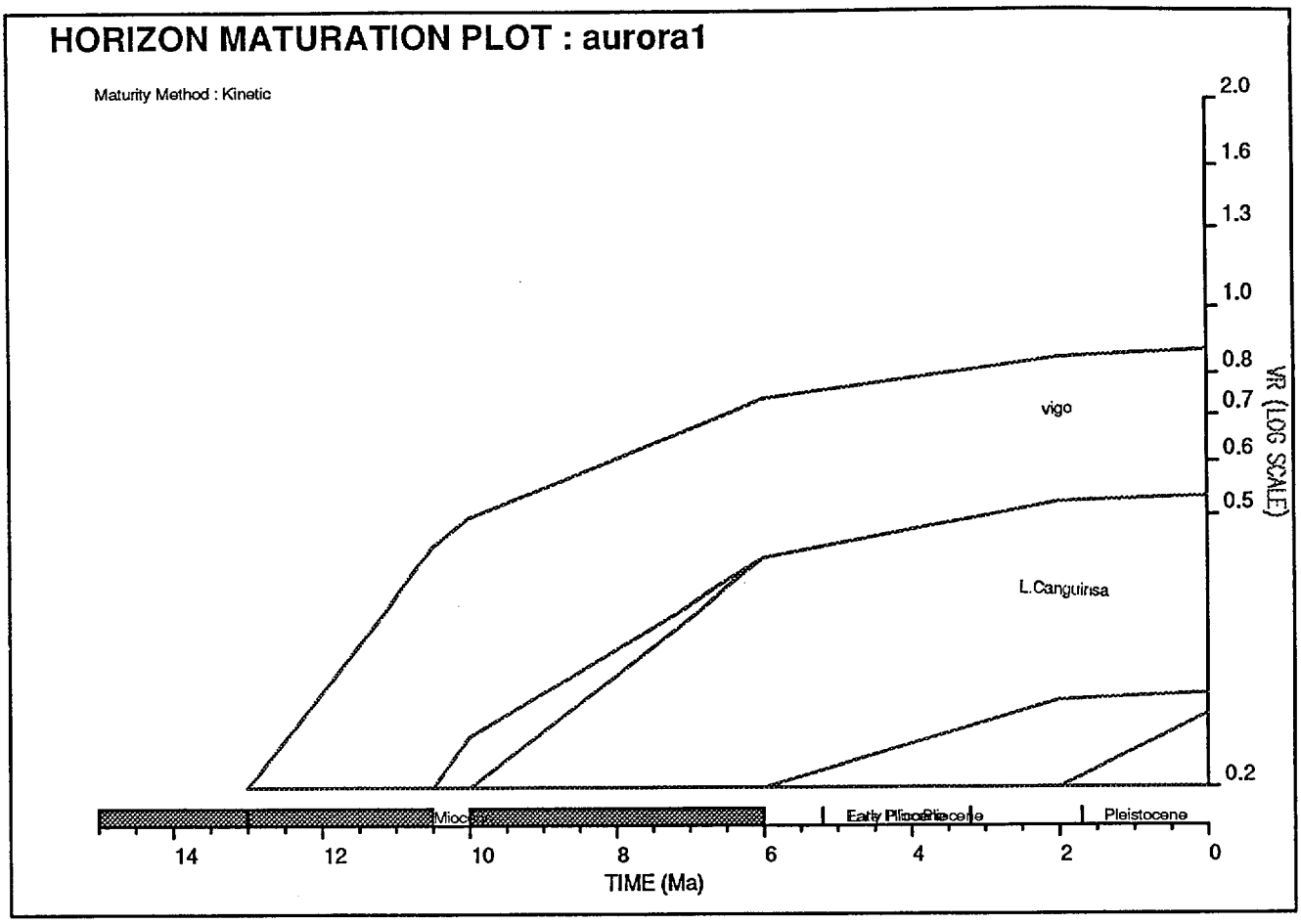

The horizon maturation plot for Aurora 1 shows that the Vigo Formation at TD reached a vitrinite reflectance level of 0.6 at 8.5Ma BP, and that the whole of that formation is now early-mature for hydrocarbons. The two gaps in the plot, at 10 to 10.5Ma and from 6 to 2, represent hiatuses or unconformies.

BONDOC 3

PODCO 1949

Latitude: 13° 20' 24.5" N
KB: 269m asl
Surface Temperature: 28°C
BHT: 86°C (estimated)

Longitude: 122° 38' 15.4" E
TD: 1691mKB
Surface Elevation:263m asl
BHT Depth: 1691m

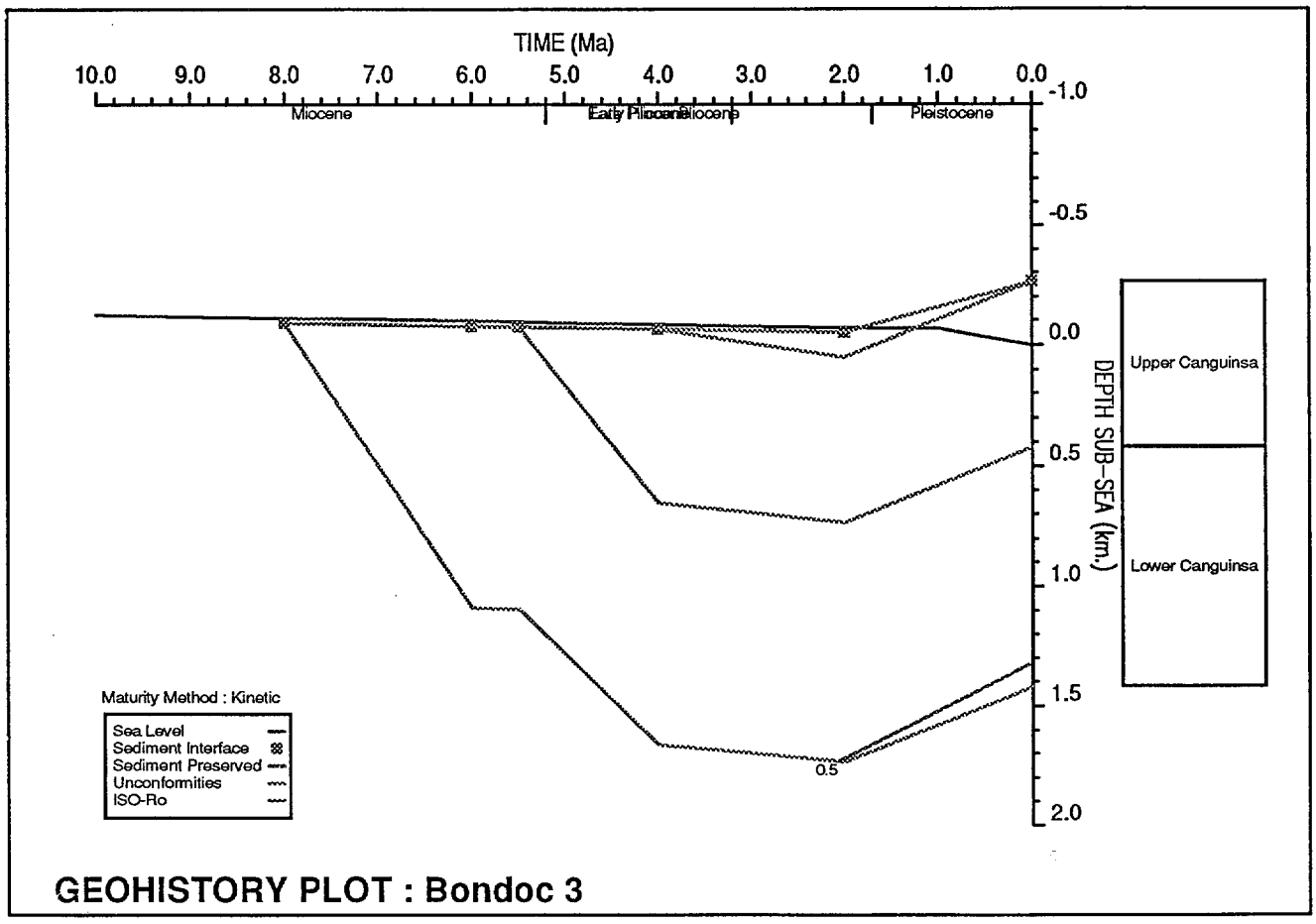

GEOHISTORY PLOT : Bondoc 3

The geohistory plot for Bondoc 3 shows the succession intersected by the well, aged from 4 Ma, now at surface, to 8Ma, now at TD. A Hiatus occurs between the Upper and Lower Canguinsa at 5.5 to 6Ma (the seismic Yellow horizon). It is proposed that Upper Canguinsa deposition continued from 4Ma until 2Ma (Deposit A on the Horizon Data table over page), and that uplift from near sea level to the present elevation was accompanied by erosion of the 100m of sediment deposited.

	Stratigraph. Unit/Event	E V	Depth to Top of Unit	Age (Ma)	Minimum WtrDpth	Maximum WtrDpth	Modelled WtrDpth	Sea Bed Temp.	Heatflow	Lithology Data	Kerogen Data	Variable Beds
1	Surface	E	6.00	0.00	-263.00	-263.00	-263.00	28.00	62.00	*		
2	Deposit A	E	(100.00)	2.00	0.00	50.00	20.00	28.00	62.00	*		
3	Upper Canguinsa	N	6.00	4.00	0.00	50.00	20.00	28.00	62.00	*		
4	Hiatus	H	690.00	5.50	0.00	50.00	20.00	28.00	62.00	*		
5	Lower Canguinsa	N	690.00	6.00	0.00	50.00	20.00	28.00	62.00	*		
6	TD	N	1691.00	8.00	0.00	50.00	20.00	28.00	62.00	*		

HORIZON DATA : BONDOC3

	Stratigraph. Unit/Event	SHALE	SAND	CHALK	LST	COAL	HALIT	VOLCS	CONV	GY/ANH	Initial Porosity	Por/Depth Factor	Conductivity	Density
1	Surface	80	20								0.640	2.020	5.900	2.770
2	Deposit A	50	10		40						0.550	1.740	7.110	2.760
3	Upper Canguinsa	50	10		40						0.550	1.740	7.110	2.760
4	Hiatus	40	45		15						0.520	1.330	9.060	2.720
5	Lower Canguinsa	40	45		15						0.520	1.330	9.060	2.720
6	TD	40	45		15						0.520	1.330	9.060	2.720

HORIZON DATA : BONDOC3 - MATRIX LITHOLOGY

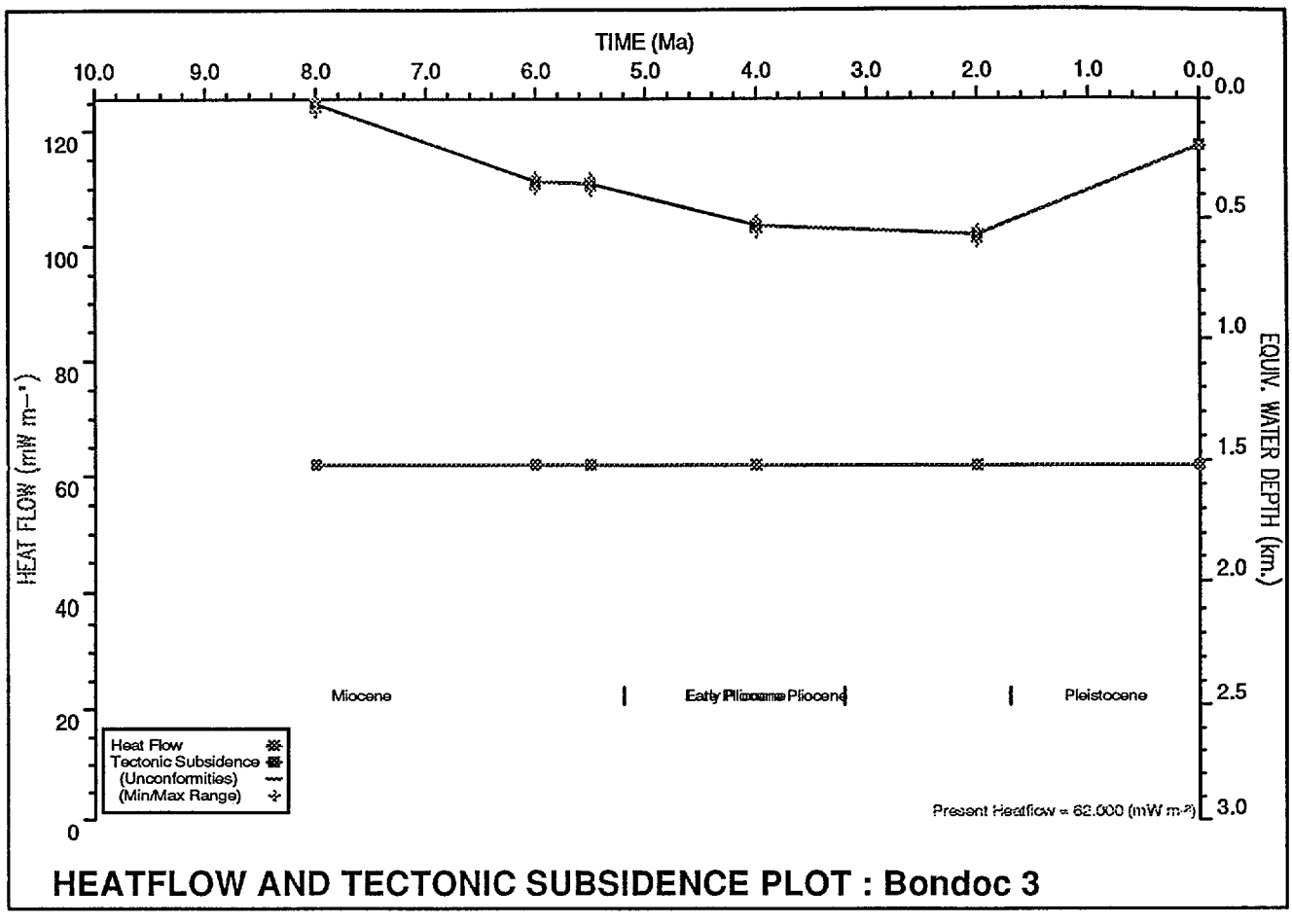

HEATFLOW AND TECTONIC SUBSIDENCE PLOT : Bondoc 3

BONDOC 7

PODCO 1960

Latitude: 13° 19' 52.82" N
KB: 291m asl
Surface Temperature: 28°C
BHT: 70°C (estimated)

Longitude: 122° 38' 32.3" E
TD: 1299mKB
Surface Elevation:289m asl
BHT Depth: 1299m

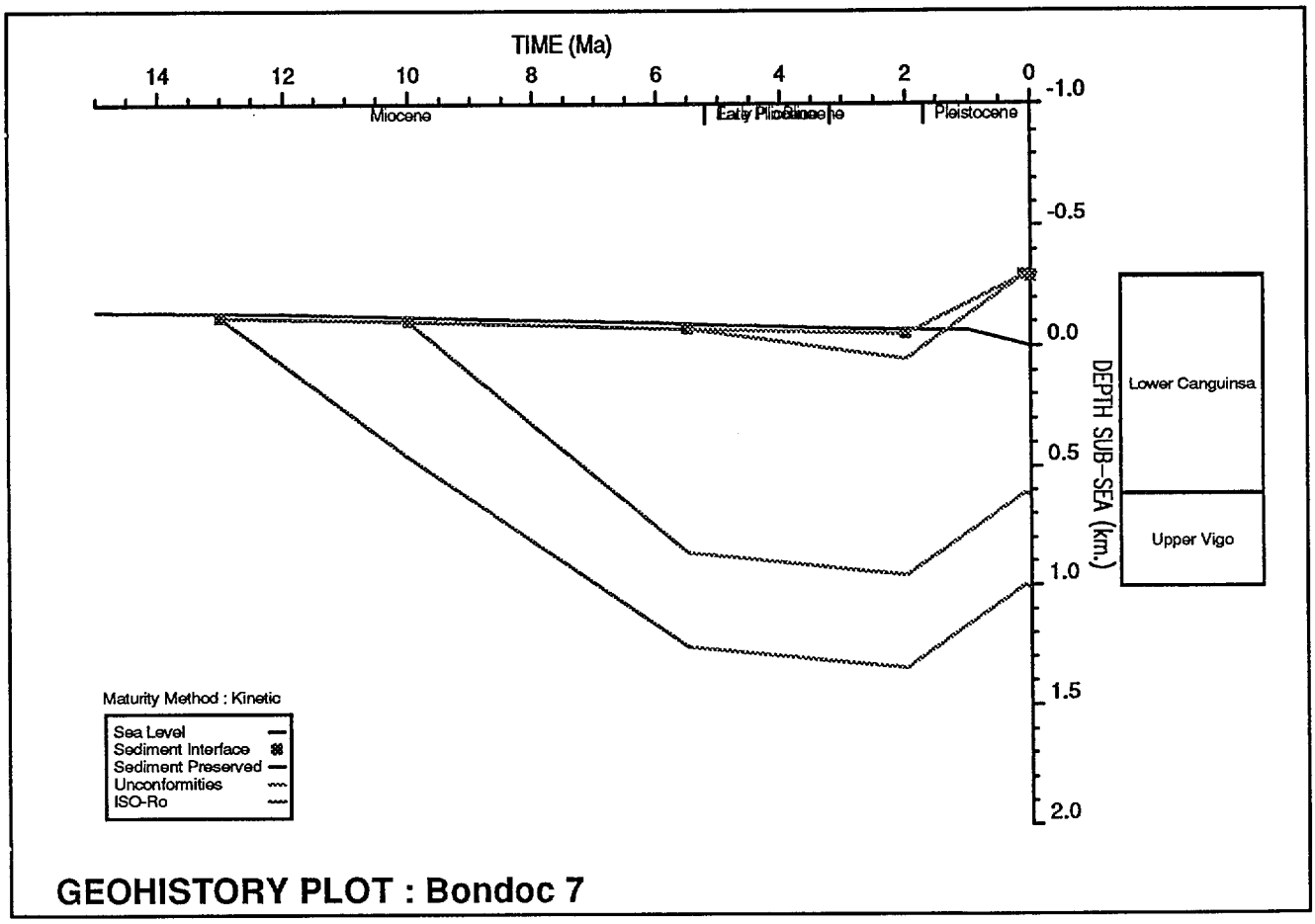

GEOHISTORY PLOT : Bondoc 7

	Stratigraph. Unit/Event	E V	Depth to Top of Unit	Age (Ma)	Minimum WtrDpth	Maximum WtrDpth	Modelled WtrDpth	Sea Bed Temp.	Heatflow	Lithology Data	Kerogen Data	Variable Beds
1	Surface	N	0.00	0.00	-289.00	-289.00	-289.00	28.00	55.00	*		
2	Surface unconf	E	3.00	0.10	-289.00	-289.00	-289.00	28.00	55.00	*		
3	Deposit A	E	(100.00)	2.00	0.00	50.00	20.00	28.00	55.00	*		
4	Lower Canguinsa	N	3.00	5.50	0.00	50.00	20.00	28.00	55.00	*		
5	Upper Vigo	N	910.00	10.00	0.00	50.00	20.00	28.00	55.00	*		
6	TD	N	1299.00	13.00	0.00	50.00	20.00	28.00	55.00	*		

HORIZON DATA : BONDOC7

	Sample Depth	T P	Observed Temp.	Circulation Time	Estimated Temp.	F L
1	160.00	0	39.00	1.00	43.00	0
2	411.00	0	42.22	1.50	46.00	0
3	514.00	0	43.33	2.50	47.00	0
4	617.23	0	45.00	1.50	49.00	0

TEMPERATURE DATA : BONDOC7

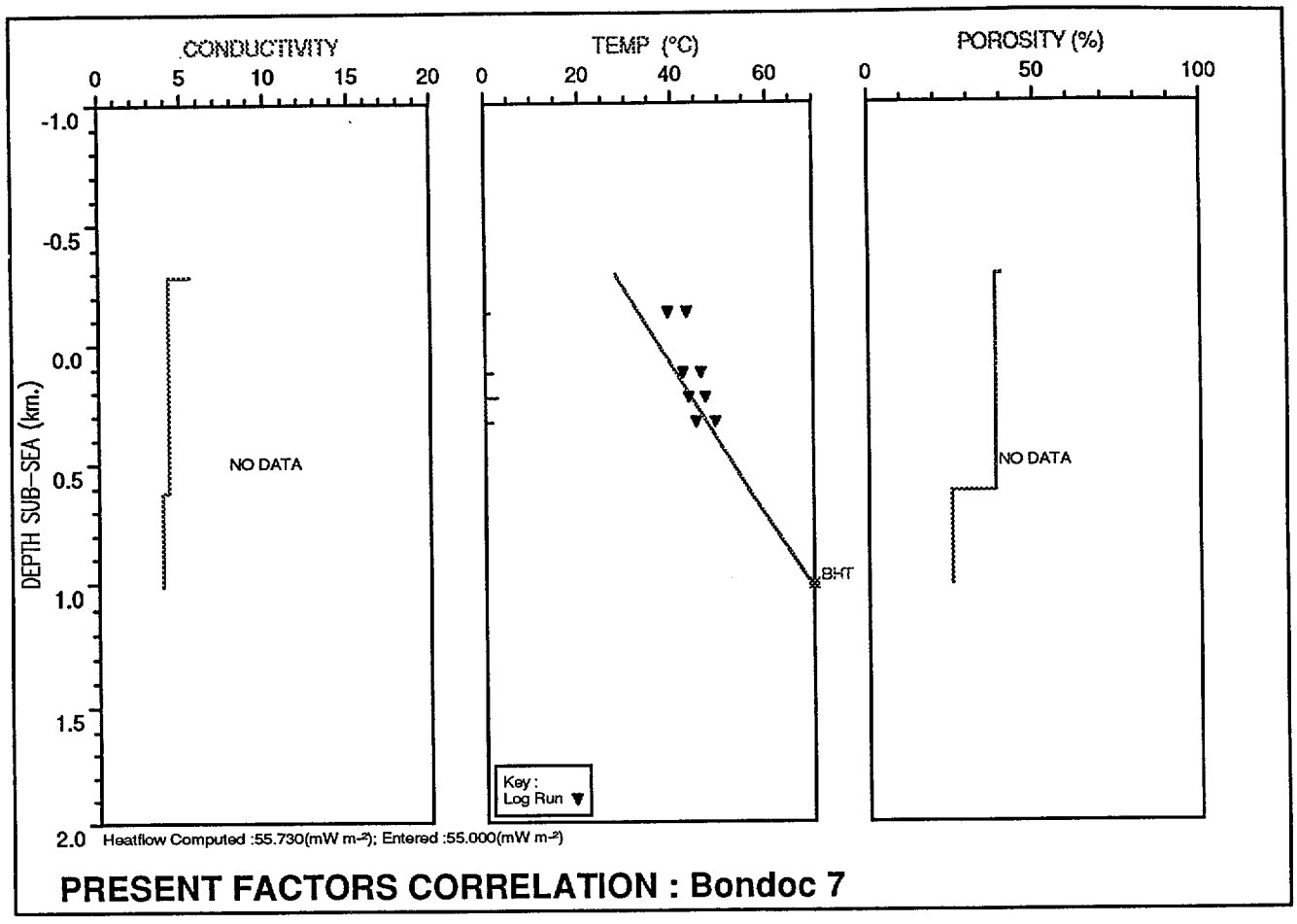

PRESENT FACTORS CORRELATION : Bondoc 7

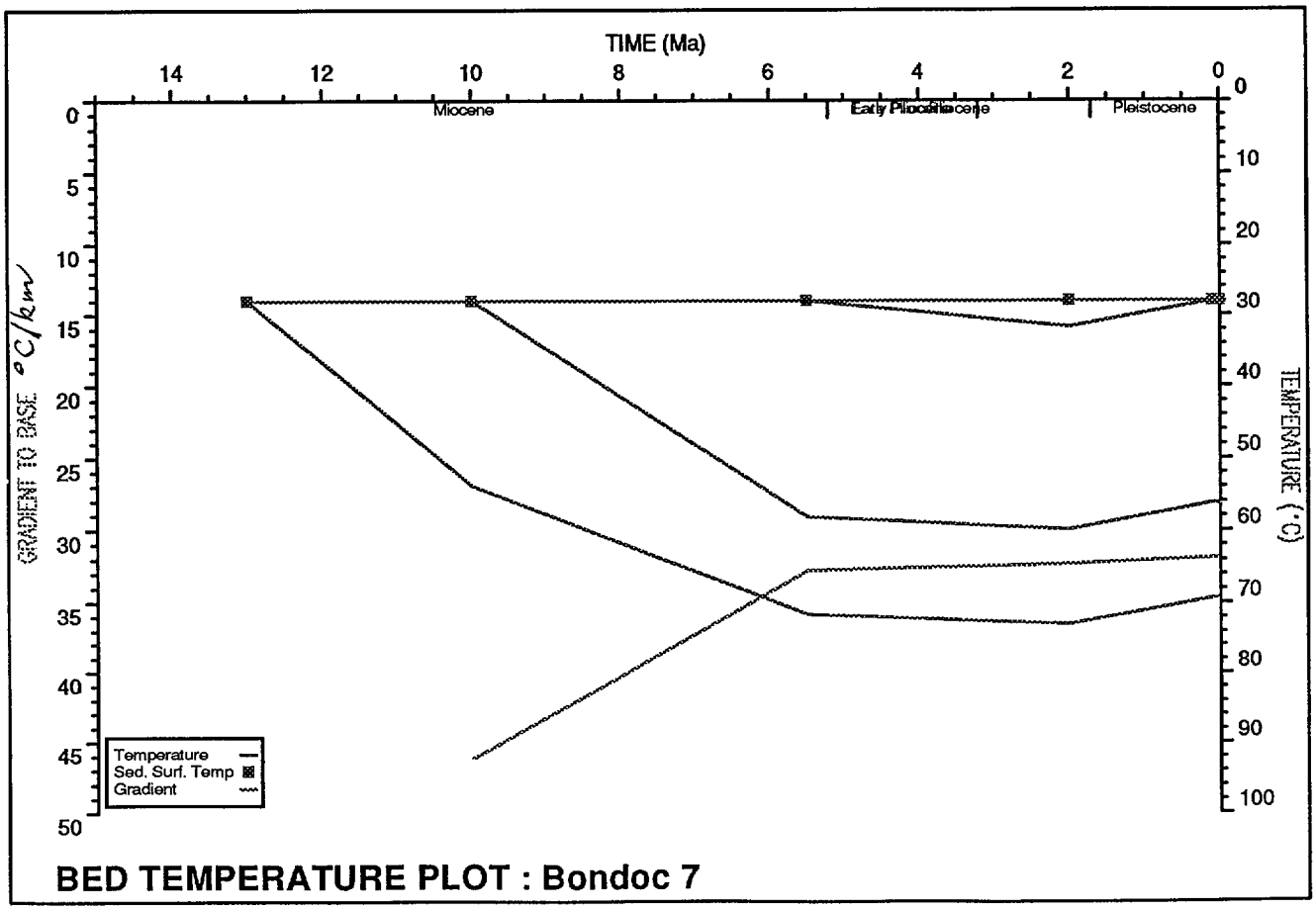

BED TEMPERATURE PLOT : Bondoc 7

HORIZON MATURATION PLOT : Bondoc 7

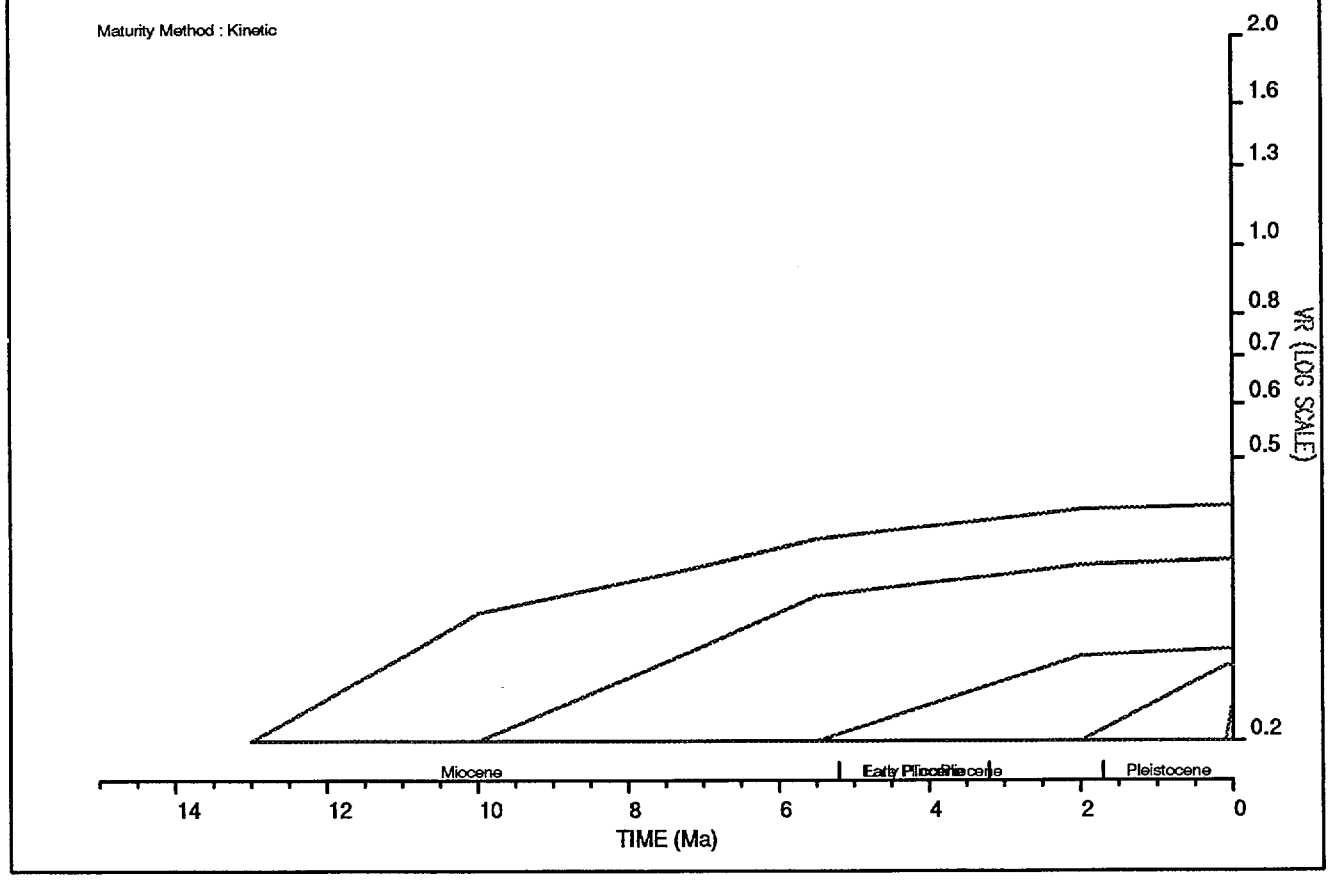

KATUMBO CREEK 1

SEDCO 1980

Latitude: 13° 40' 42.4" N
KB: 92m asl
Surface Temperature: 28°C
BHT: 77°C (e-log)

Longitude: 122° 10' 18.3" E
TD: 1951mKB
Surface Elevation:87m asl
BHT Depth: 1951m

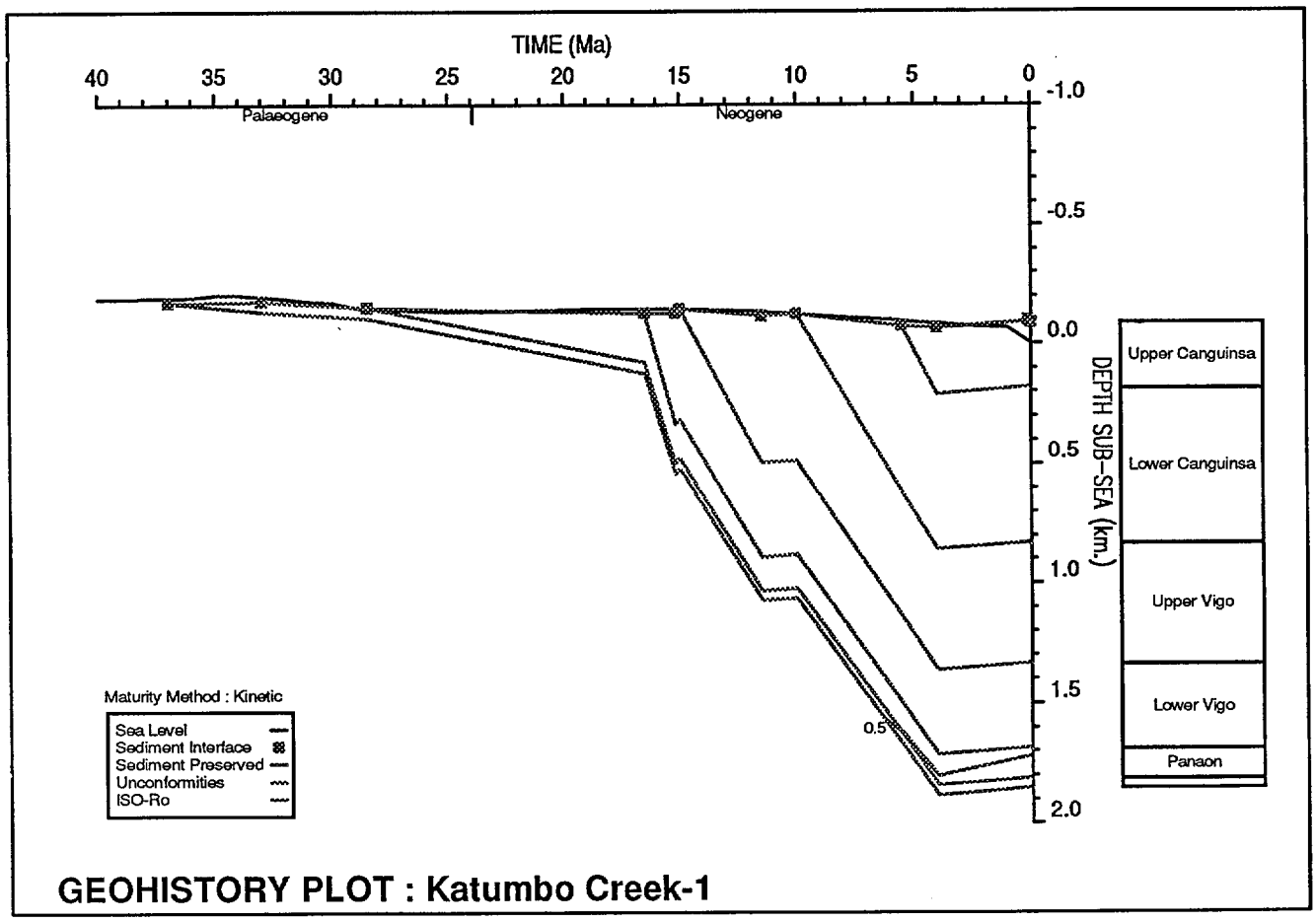

GEOHISTORY PLOT : Katumbo Creek-1

The geohistory plot for Katumbo Creek assumes a constant heatflow of 50 mW/m^2 throughout the nearly 40Ma history of the succession. The base of the succession in the well is barely mature for hydrocarbons.

	Stratigraph. Unit/Event	E V	Depth to Top of Unit	Age (Ma)	Minimum WtrDpth	Maximum WtrDpth	Modelled WtrDpth	Sea Bed Temp.	Heatflow	Lithology Data	Kerogen Data	Variable Beds
1	Surface	E	5.00	0.00	-87.00	-87.00	-87.00	28.00	50.00	*		
2	Deposit A	E	(100.00)	2.00	0.00	50.00	20.00	28.00	50.00	*		
3	Upper Canguinsa	N	5.00	4.00	0.00	50.00	20.00	27.78	50.00	*		
4	Lower Canguinsa	N	280.42	5.50	0.00	50.00	20.00	27.78	50.00	*		
5	Pre-Canguinsa Unc.	H	927.00	10.00	0.00	0.00	0.00	27.78	50.00	*		
6	Upper Vigo	N	927.00	11.50	0.00	50.00	20.00	27.78	50.00	*		
7	Mid-Miocene Unc.	H	1433.00	15.00	0.00	0.00	0.00	27.78	50.00	*		
8	Lower Vigo	N	1433.00	15.20	0.00	50.00	20.00	27.78	50.00	*		
9	Panaon	N	1785.00	16.50	0.00	50.00	20.00	27.78	50.00	*		
10	Base Panaon unc.	H	1910.00	28.50	0.00	0.00	0.00	27.78	50.00	*		
11	Volcanoclastics	N	1910.00	33.00	0.00	50.00	20.00	27.78	50.00	*		
12	TD	N	1951.05	37.00	0.00	50.00	20.00	33.50	50.00	*		

HORIZON DATA : KATCREEK

	Stratigraph. Unit/Event	SHALE	SAND	CHALK	LST	COAL	HALIT	VOLCS	CONV	GY/ANH	Initial Porosity	Por/Depth Factor	Conductivity	Density
1	Surface	100									0.700	2.430	4.600	2.800
2	Deposit A	50	10		40						0.550	1.740	7.110	2.760
3	Upper Canguinsa	50	10		40						0.550	1.740	7.110	2.760
4	Lower Canguinsa	40	45		15						0.520	1.330	9.060	2.720
5	Pre-Canguinsa Unc.	40	45		15						0.520	1.330	9.060	2.720
6	Upper Vigo	80	20								0.640	2.020	5.900	2.770
7	Mid-Miocene Unc.	80	20								0.640	2.020	5.900	2.770
8	Lower Vigo	75	20		5						0.630	1.960	6.140	2.770
9	Panaon		25		75						0.400	1.000	11.250	2.730
10	Base Panaon unc.										0.000	1.000	1.000	1.000
11	Volcanoclastics	35	35					30			0.400	1.140	7.070	2.740
12	TD	10	40					50			0.260	0.650	7.490	2.720

HORIZON DATA : KATCREEK - MATRIX LITHOLOGY

	Sample Depth	T P	Average Maturity	Minimum Maturity	Maximum Maturity	F L
1	355.00	3	2.25	2.00	2.50	1
2	355.00	0	0.26	0.25	0.27	0
3	795.00	0	0.33	0.32	0.34	0
4	795.00	3	2.50	2.25	2.75	1
5	1143.00	3	3.00	2.75	3.25	1
6	1143.00	0	0.37	0.36	0.38	0
7	1606.00	0	0.49	0.48	0.47	0
8	1606.00	3	4.25	4.00	4.50	1
9	1885.00	3	4.75	4.25	4.50	1
10	1885.00	0	0.52	0.51	0.53	0

MATURITY DATA : KATCREEK

	Sample Depth	T P	Observed Temp.	Circulation Time	Estimated Temp.	F L
1	1053.71	0	58.33	5.00	60.00	0
2	1630.39	0	68.89	8.00	76.67	0
3	1946.17	0	86.67	32.50	87.78	0

TEMPERATURE DATA : KATCREEK

Samples from Katumbo Creek 1 were measured for thermal maturity (Sedco, 1980, upper table) using Spore Coloration Indices (type 3, flag 1) and vitrinite reflectance (type 0, flag 0). Temperatures downhole (lower table) were observed during logging runs.
These data were used to determine the heatflow used in the geohistory model.

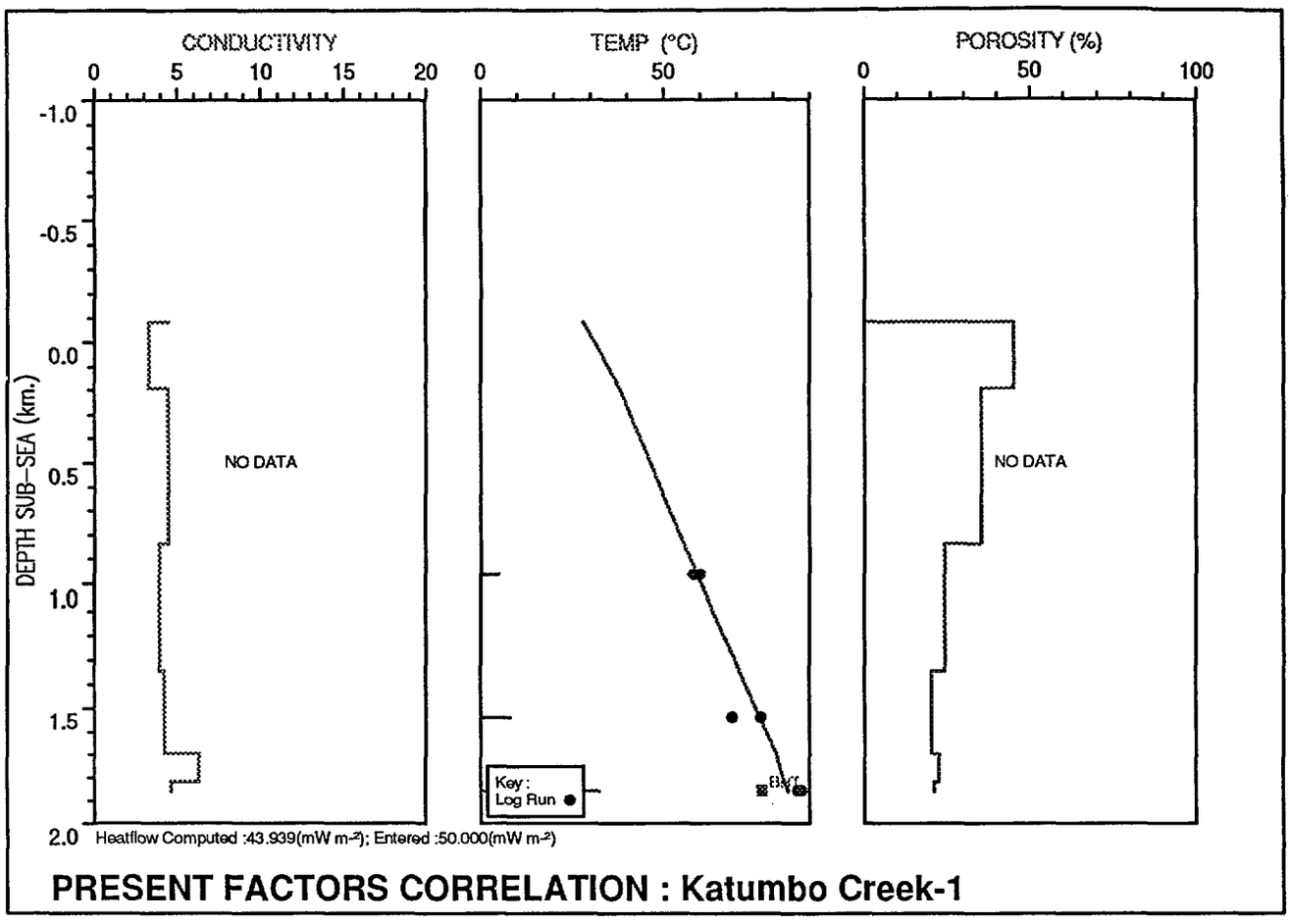

The calculated temperatures (plotted line) down-hole at Katumbo Creek 1, based on heatflow of 50mW/m^2, are in fair agreement with temperatures observed on well logs.

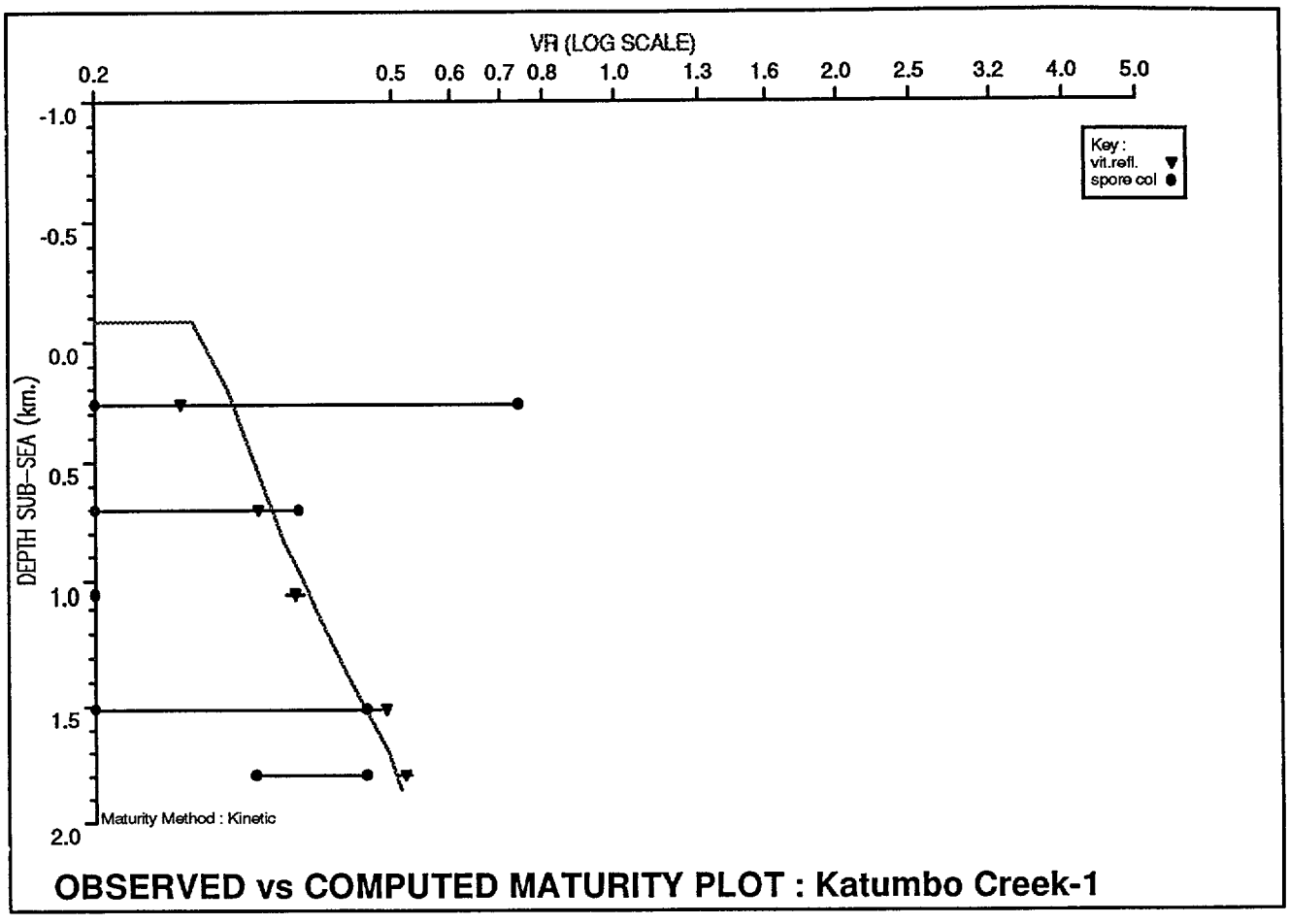

The computed maturity (curved line) of the succession at Katumbo Creek 1, based on heatflow of 50mW/m^2, is in good agreement with the maturity observed in samples measured for vitrinite reflectance (triangles).

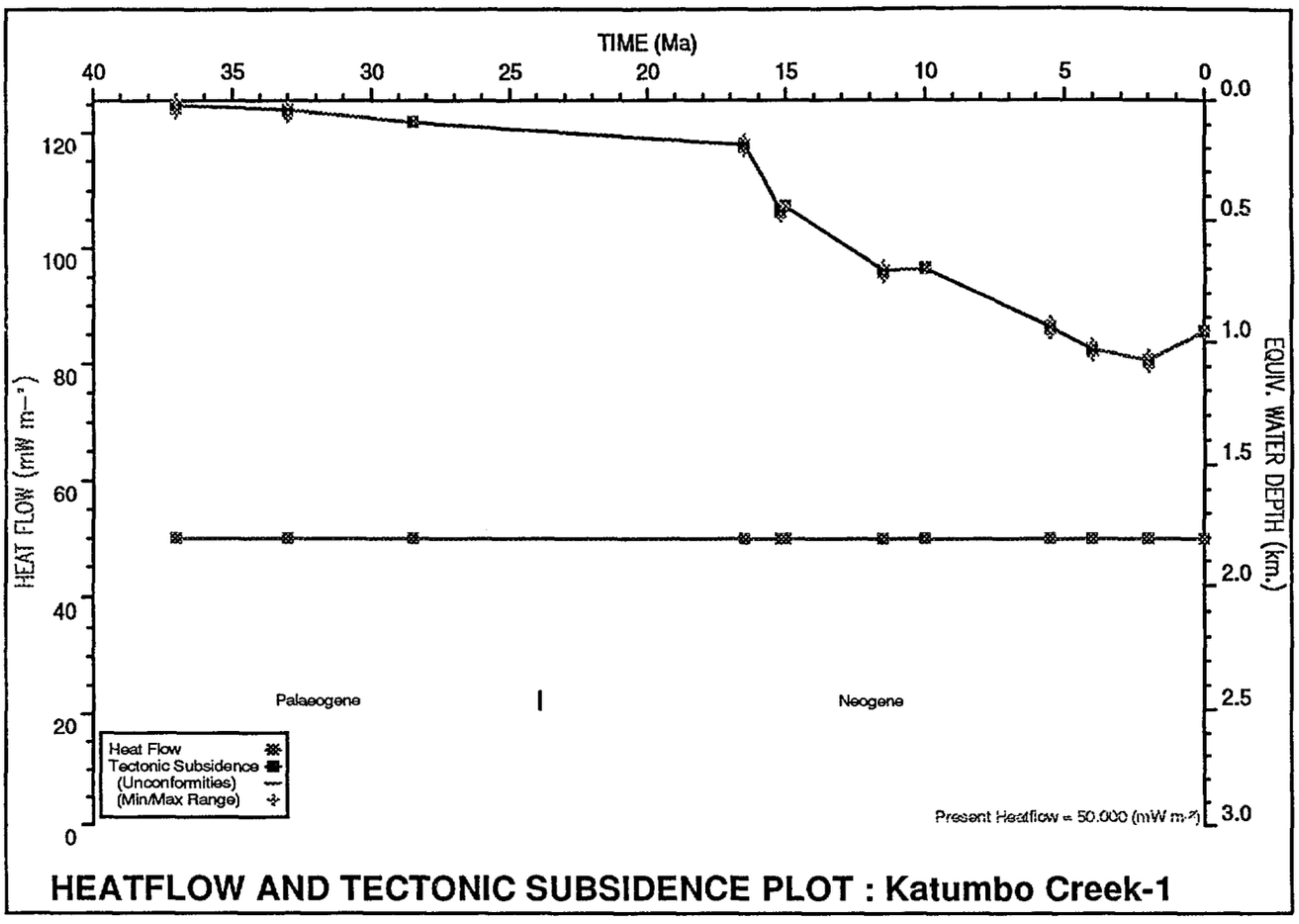

HEATFLOW AND TECTONIC SUBSIDENCE PLOT : Katumbo Creek-1

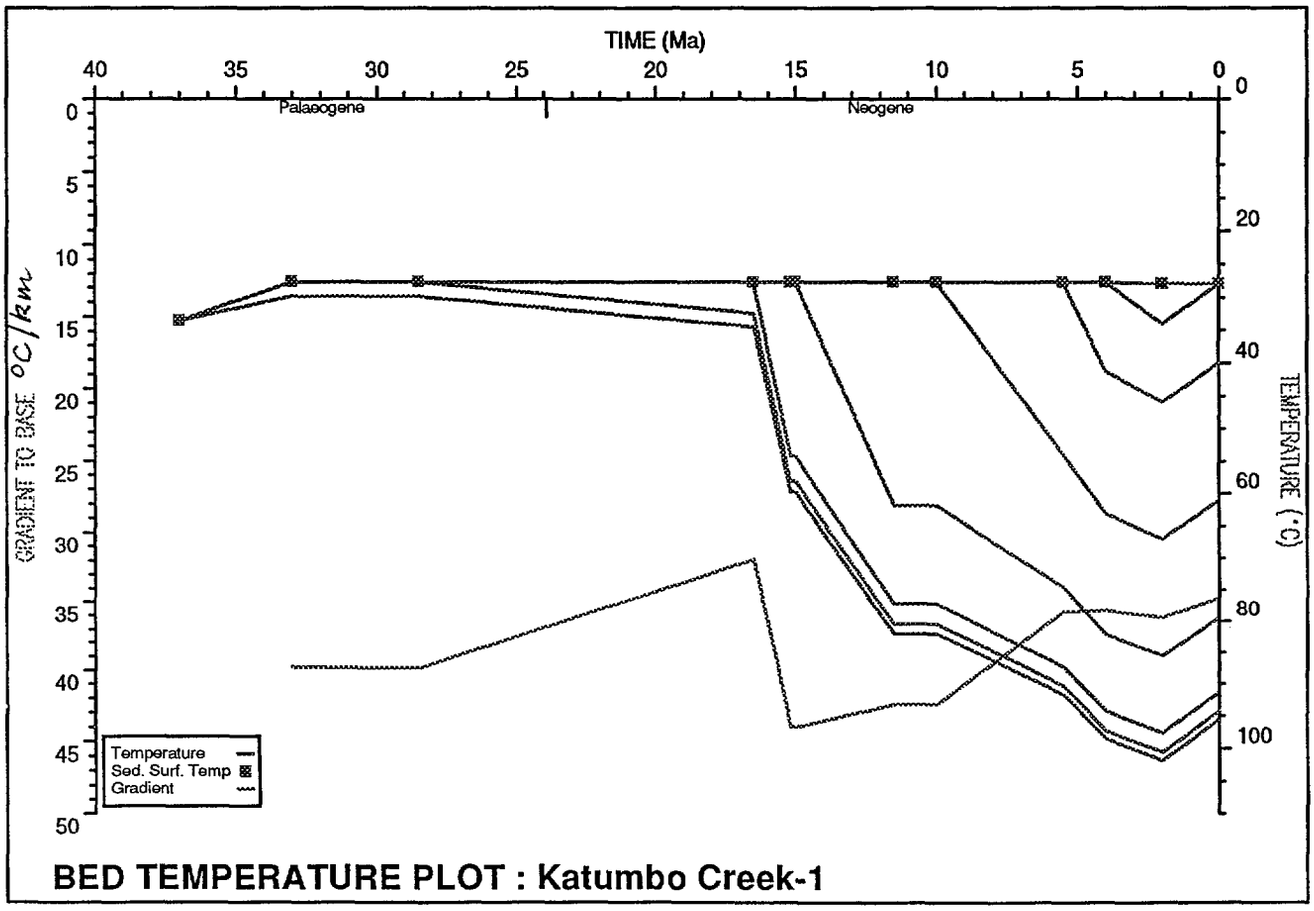

BED TEMPERATURE PLOT : Katumbo Creek-1

MAYANTOK 1

FAR EAST RESOURCES PLC /RAN RICKS1989

Latitude: 13° 13' 26.8" N
KB: 22.5m asl
Surface Temperature: 28°C
BHT: 53°C (e-logs)

Longitude: 122° 40' 12.3" E
TD: 773mKB
Surface Elevation:16m asl
BHT Depth: 773m

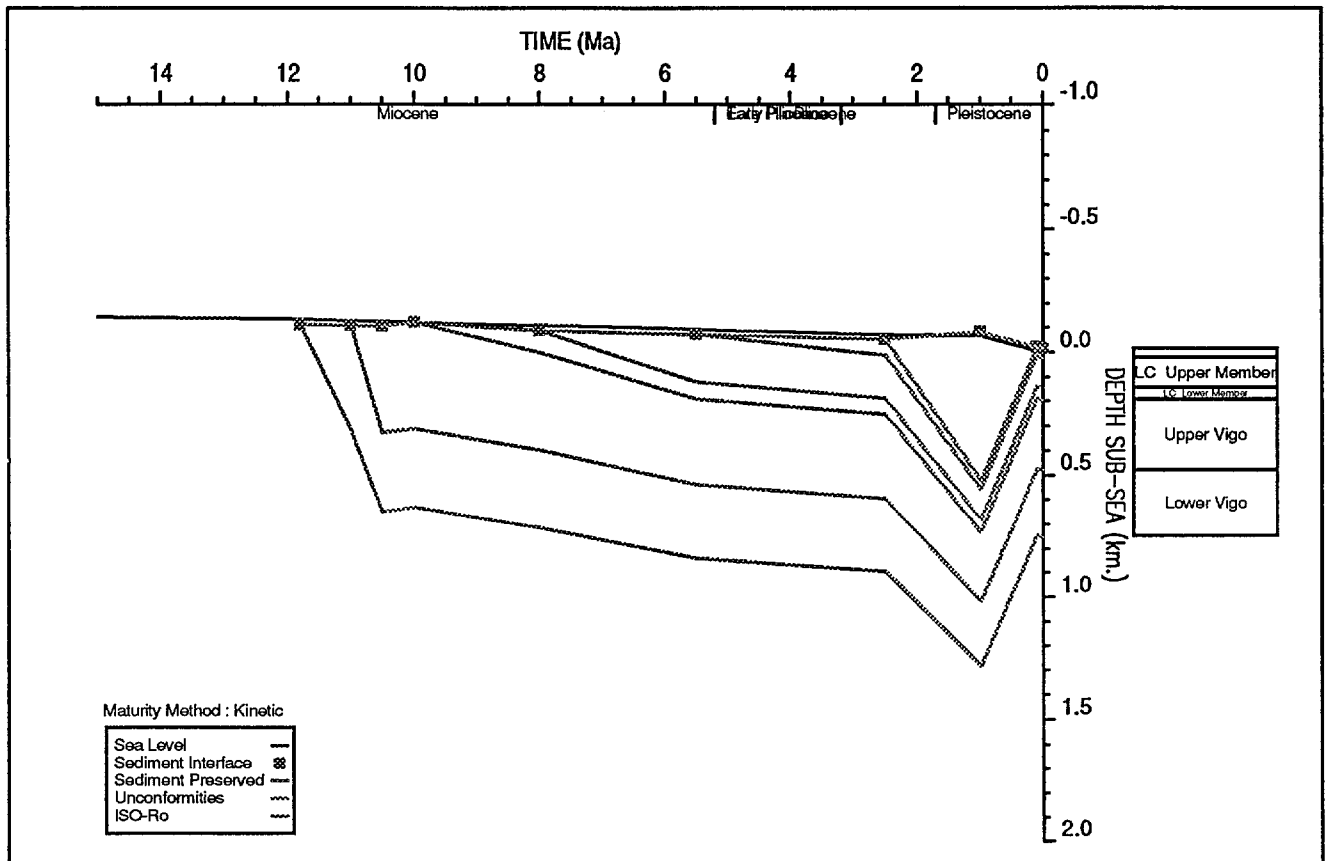

GEOHISTORY PLOT : Mayantok-1

The geohistory plot of Mayantok 1 well shows rapid deposition in the early Pleistocene, followed by uplift and erosion to the present day. Despite this, none of the succession shows maturity for hydrocarbons.

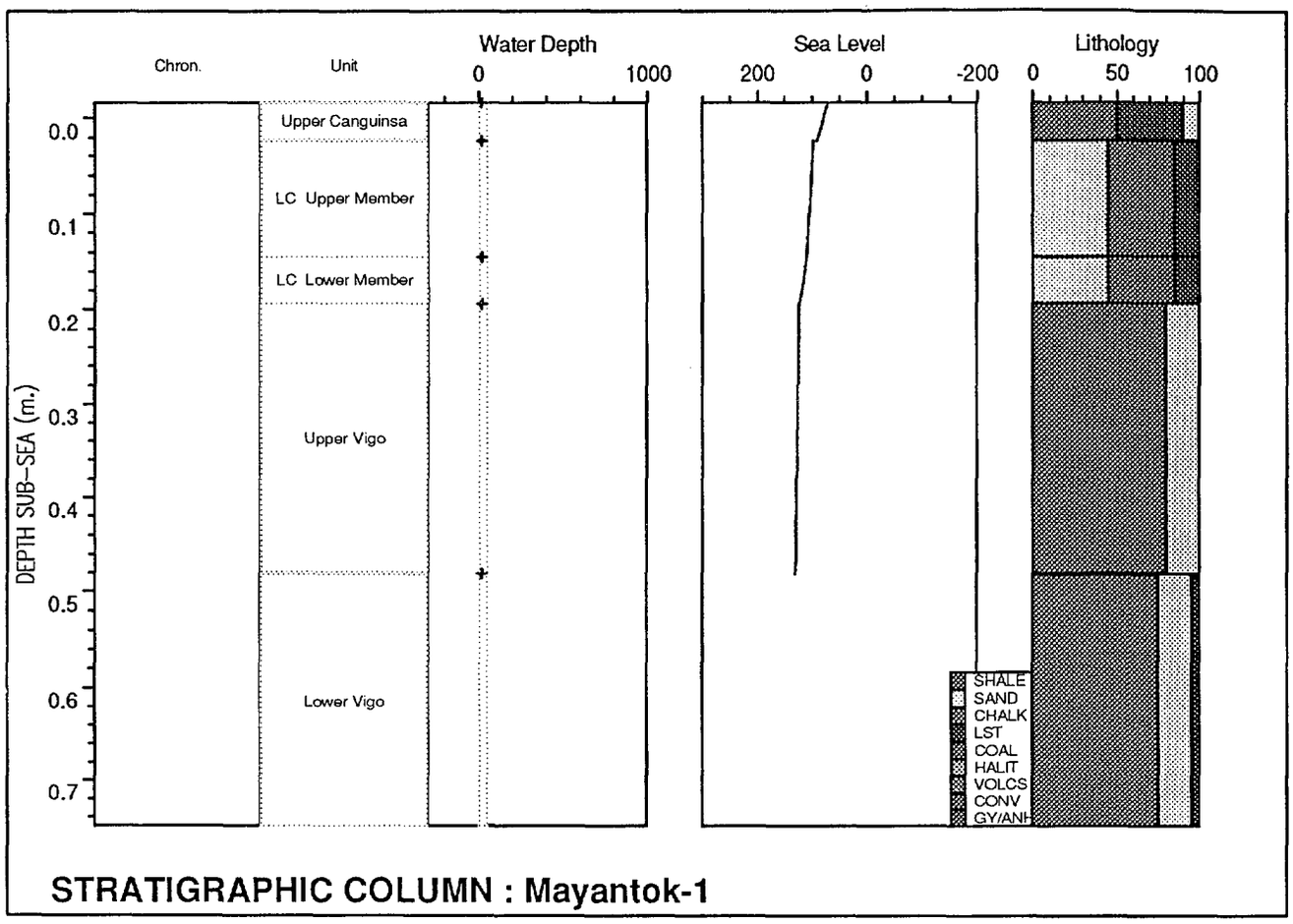

STRATIGRAPHIC COLUMN : Mayantok-1

The stratigraphy of the succession at Mayantok 1 well is shown here in graphical form. The depth of deposition of the sediments is shown as a range (dotted lines at 0m and 50m), together with the water depth used in the well history model (crosses at 20m). The sea level from 2.5 to 12Ma, relative to present, is shown as a black line. It is higher throughout than the present day level.

For the calculation of initial porosity, the porosity/depth factor, thermal conductivity and density, three rock matrices are recognised. They are, sand (light shade), clay (intermediate shade) and limestone (dark shade), and they occur in different proportions in the various formations.

	Stratigraph. Unit/Event	E V	Depth to Top of Unit	Age (Ma)	Minimum WtrDpth	Maximum WtrDpth	Modelled WtrDpth	Sea Bed Temp.	Heatflow	Lithology Data	Kerogen Data	Variable Beds
1	Surface	H	6.45	0.00	-16.00	-16.00	-16.00	28.00	51.00	*		
2	Surface unconf.	E	6.50	0.10	-16.00	-16.00	-16.00	28.00	51.00	*		
3	Deposit A	E	(600.00)	1.00	-16.00	-16.00	-16.00	28.00	51.00	*		
4	Upper Canguinsa	N	6.50	2.50	0.00	50.00	20.00	27.78	51.00	*		
5	LC Upper Member	N	45.72	5.50	0.00	50.00	20.00	27.78	51.00	*		
6	LC Lower Member	N	167.64	8.00	0.00	50.00	20.00	27.78	51.00	*		
7	Pre-Canguinsa unc.	H	217.00	10.00	0.00	0.00	0.00	27.78	51.00	*		
8	Upper Vigo	N	217.00	10.50	0.00	50.00	20.00	27.78	51.00	*		
9	Lower Vigo	N	502.93	11.00	0.00	50.00	20.00	27.78	51.00	*		
10	TD	N	773.00	11.80	0.00	50.00	20.00	27.78	51.00	*		

HORIZON DATA : MAYANTOK

	Stratigraph. Unit/Event	SHALE	SAND	CHALK	LST	COAL	HALIT	VOLCS	CONV	GY/ANH	Initial Porosity	Por/Depth Factor	Conductivity	Density
1	Surface										0.000	1.000	1.000	1.000
2	Surface unconf.	80			20						0.640	2.180	5.370	2.790
3	Deposit A	80			20						0.640	2.180	5.370	2.790
4	Upper Canguinsa	50	10		40						0.550	1.740	7.110	2.760
5	LC Upper Member	40	45		15						0.520	1.330	9.060	2.720
6	LC Lower Member	40	45		15						0.520	1.330	9.060	2.720
7	Pre-Canguinsa unc.	80	5		15						0.640	2.140	5.500	2.780
8	Upper Vigo	80	20								0.640	2.020	5.900	2.770
9	Lower Vigo	75	20		5						0.630	1.960	6.140	2.770
10	TD	75	20		5						0.630	1.960	6.140	2.770

HORIZON DATA : MAYANTOK - MATRIX LITHOLOGY

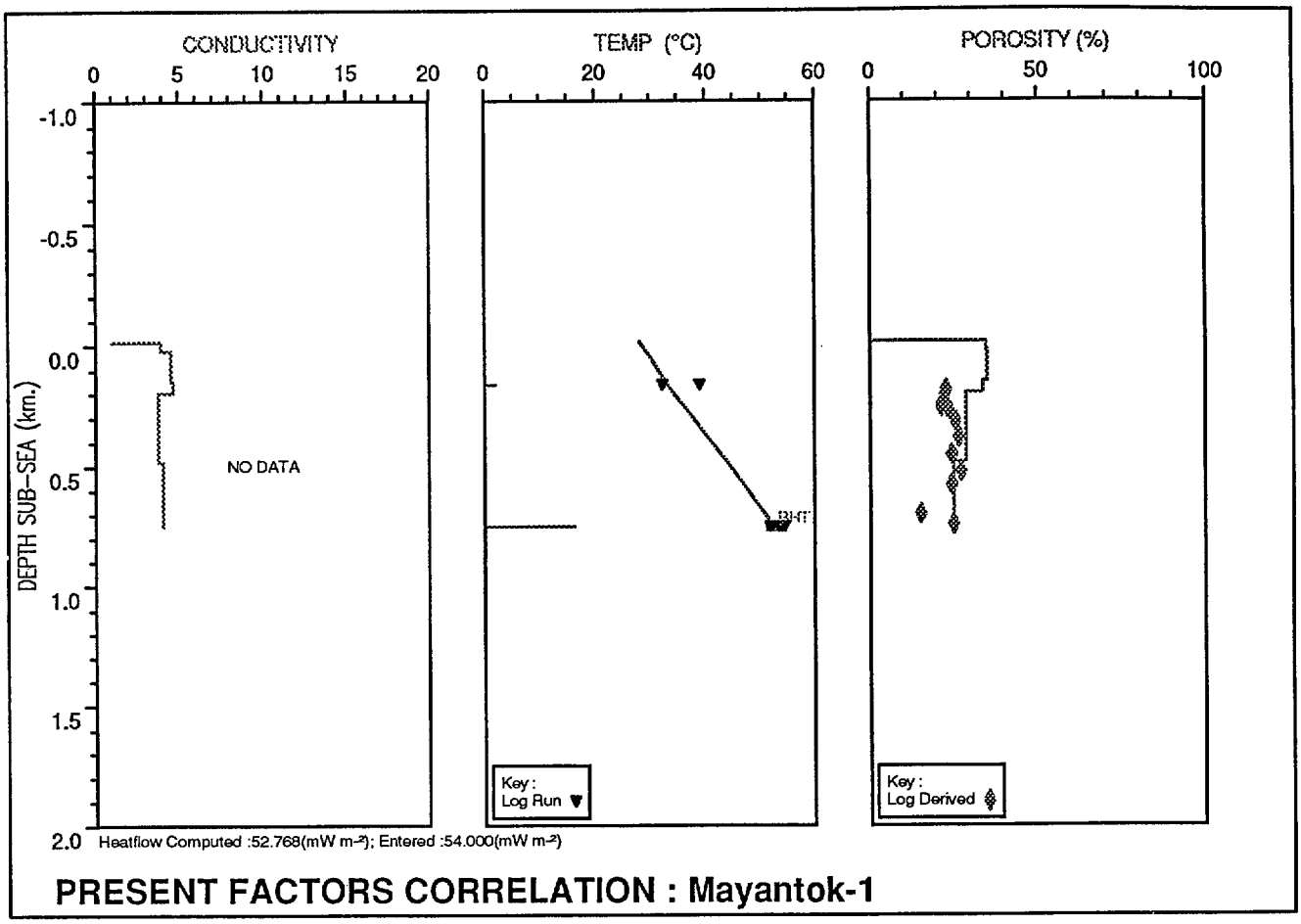

The observed temperatures in Mayantok 1 (black triangles) and the observed porosities (grey diamonds) were used to constrain the heatflow and the rock matrices used in the model. The agreement between computed and observed parameters is good, as shown here. Use of a different set of rock matrices (different sand-shale ratios) yields results that are at variance with observed values (next plot, overleaf).

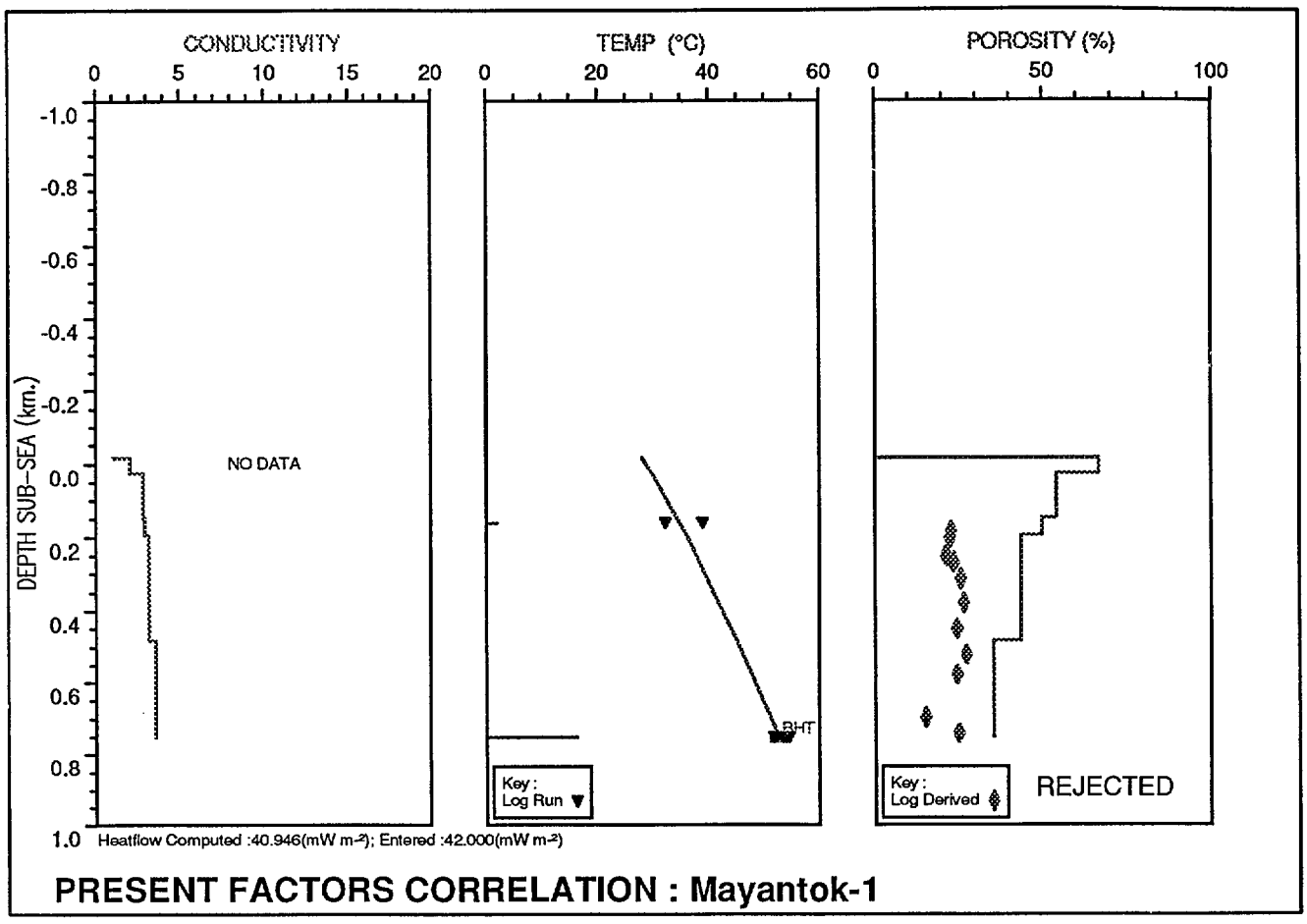

	Stratigraph. Unit/Event	SHALE	SAND	CHALK	LST	COAL	HALIT	VOLCS	CONV	GY/ANH	Initial Porosity	Por/Depth Factor	Conductivity	Density
1	Surface										0.000	1.000	1.000	1.000
2	Upper Canguinsa	25	35		40						0.480	1.230	9.710	2.730
3	LC Upper Member	25	60		15						0.470	1.030	10.920	2.700
4	LC Lower Member	25	60		15						0.470	1.030	10.920	2.700
5	Pre-Canguinsa unc.	25	60		15						0.470	1.030	10.920	2.700
6	Upper Vigo	37	63								0.510	1.150	10.090	2.710
7	Lower Vigo	58	37		5						0.570	1.620	7.580	2.740
8	TD	23	77								0.470	0.870	12.010	2.680

HORIZON DATA : MAYANTOK - MATRIX LITHOLOGY - ALTERNATIVE - REJECTED

Measured porosity (diamonds) in Mayantok-1 was used to test an alternative lithology containing less shale. The result (the stepped line) was gross disagreement of calculated with measured porosity.

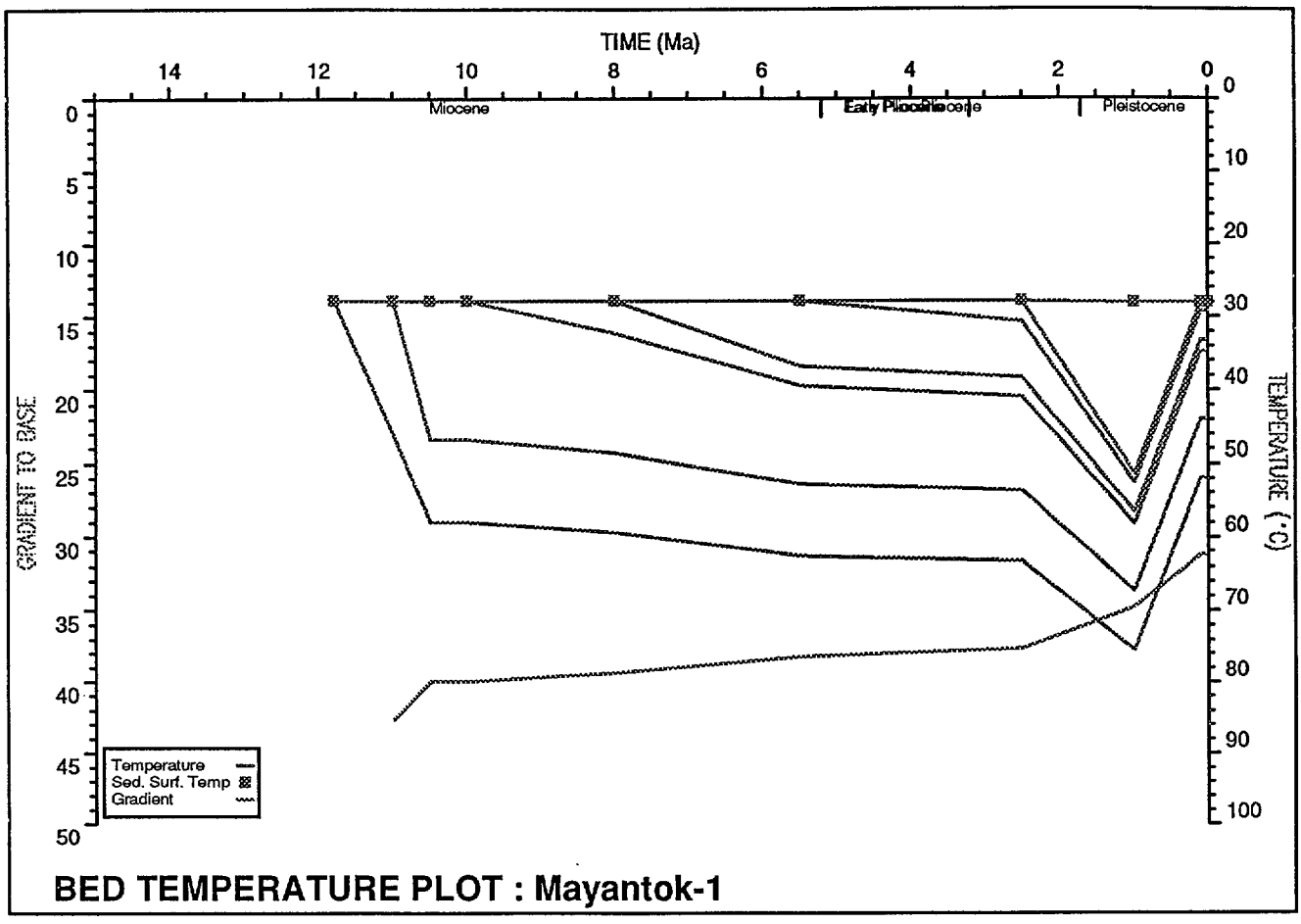

BED TEMPERATURE PLOT : Mayantok-1

SAN FRANCISCO 1

PODCO 1977

Latitude: 13° 23' 56" N
KB: 48m asl
Surface Temperature: 28°C
BHT: 84°C (e-log)

Longitude: 122° 30' 13" E
TD: 2100mKB
Surface Elevation:46m asl
BHT Depth: 2100m

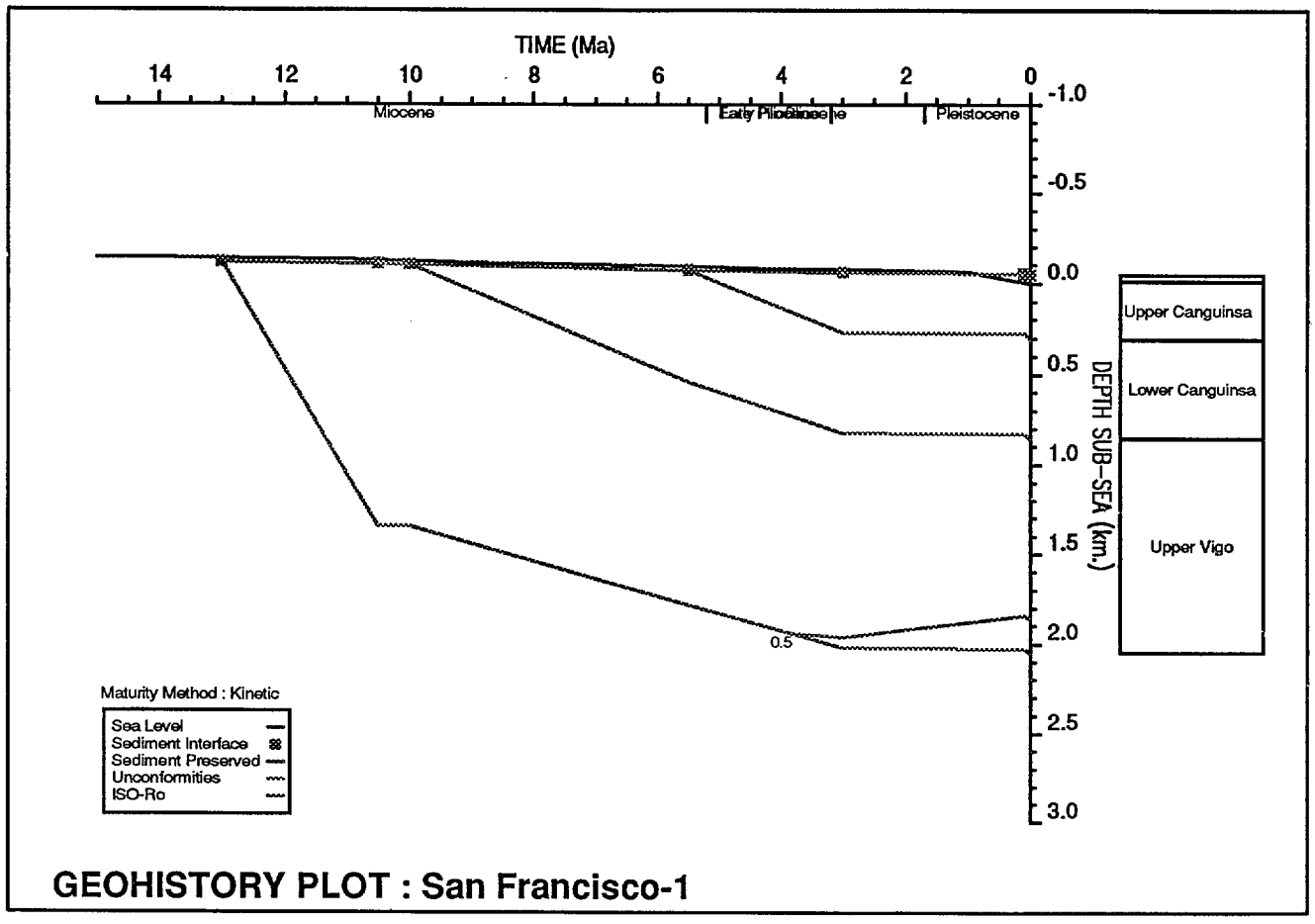

GEOHISTORY PLOT : San Francisco-1

Version 1. Heatflow (HF) = 50mW/m^2.
The succession at San Francisco 1 well is almost entirely immature in this model of the geohistory. The model used well temperatures observed during logging runs, which are lower than the BHT quoted by Rutherford and Qureshi, (1981).

	Stratigraph. Unit/Event	E V	Depth to Top of Unit	Age (Ma)	Minimum WtrDpth	Maximum WtrDpth	Modelled WtrDpth	Sea Bed Temp.	Heatflow	Lithology Data	Kerogen Data	Variable Beds
1	Malumbang	N	2.00	0.00	-46.00	-46.00	-46.00	28.00	50.00	*		
2	Base Malumbang	H	38.00	0.10	-46.00	-46.00	-46.00	28.00	50.00	*		
3	Upper Canguinsa	N	38.00	3.00	0.00	50.00	20.00	28.00	50.00	*		
4	Lower Canguinsa	N	357.00	5.50	0.00	50.00	20.00	28.00	50.00	*		
5	Pre-Canguinsa Unc.	H	905.00	10.00	0.00	50.00	20.00	28.00	50.00	*		
6	Upper Vigo	N	905.00	10.50	0.00	50.00	20.00	28.00	50.00	*		
7	TD	N	2099.00	13.00	0.00	50.00	20.00	28.00	50.00	*		

HORIZON DATA : SANFRAN1

	Stratigraph. Unit/Event	SHALE	SAND	CHALK	LST	COAL	HALIT	VOLCS	CONV	GY/ANH	Initial Porosity	Por/Depth Factor	Conductivity	Density
1	Malumbang	30	10		60						0.490	1.490	8.300	2.750
2	Base Malumbang	30	10		60						0.490	1.490	8.300	2.750
3	Upper Canguinsa	50	10		40						0.550	1.740	7.110	2.760
4	Lower Canguinsa	40	45		15						0.520	1.330	9.060	2.720
5	Pre-Canguinsa Unc.	40	45		15						0.520	1.330	9.060	2.720
6	Upper Vigo	80	20								0.640	2.020	5.900	2.770
7	TD	80	20								0.640	2.020	5.900	2.770

HORIZON DATA : SANFRAN1 - MATRIX LITHOLOGY

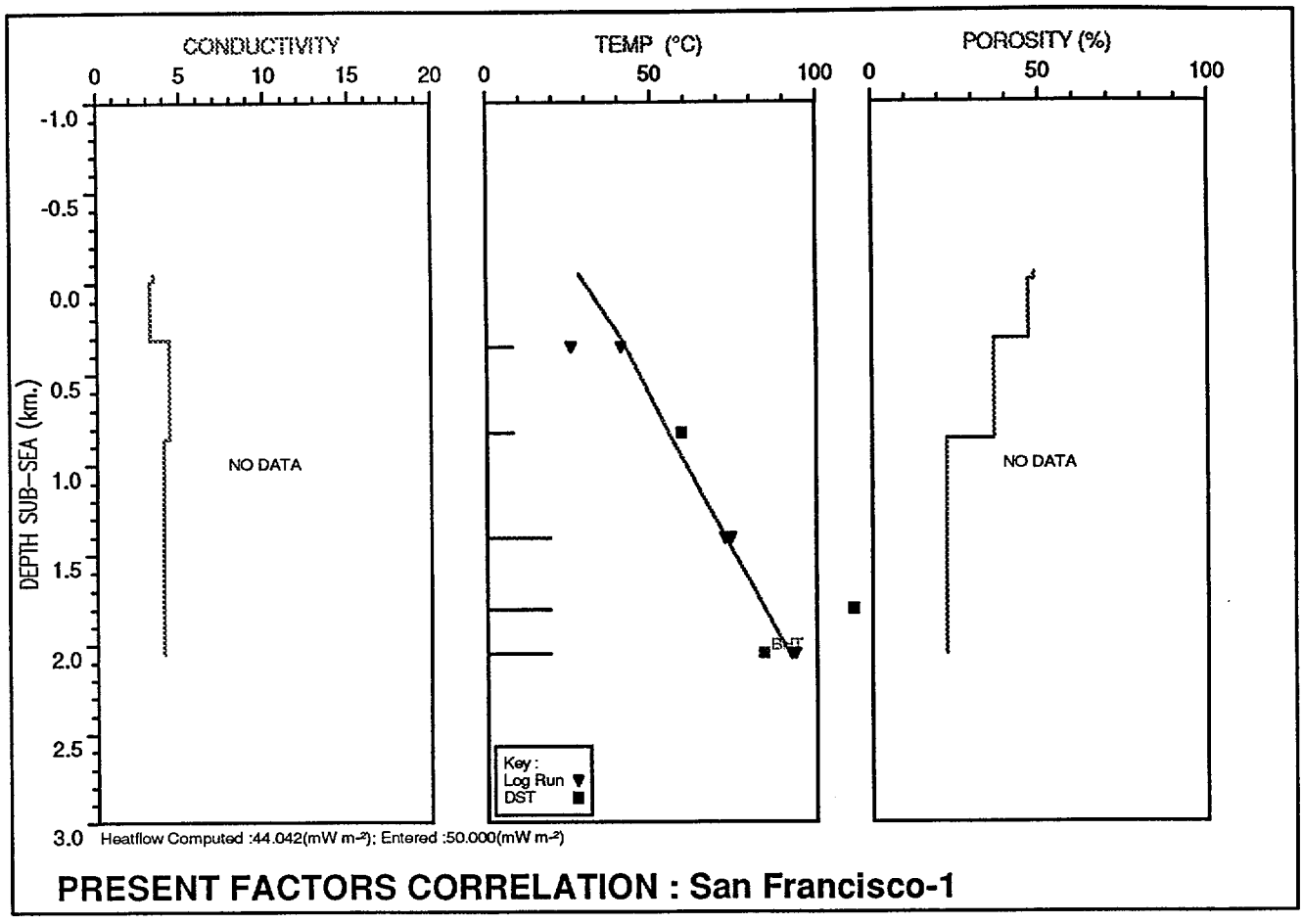

	Sample Depth	T P	Observed Temp.	Circulation Time	Estimated Temp.	F L
1	396.25	0	25.56	8.00	40.56	0
2	869.00	1	59.00	8.00	59.00	1
3	1453.91	0	72.22	19.00	73.89	0
4	1848.00	1	111.00	19.00	111.00	1
5	2099.79	0	92.22	19.00	93.33	0

TEMPERATURE DATA : SANFRAN1

Version 1. HF = 50mW/M^2

The calculated temperature downhole in San Francisco 1 well (plotted line) agrees with temperatures observed on e-logs (triangles).

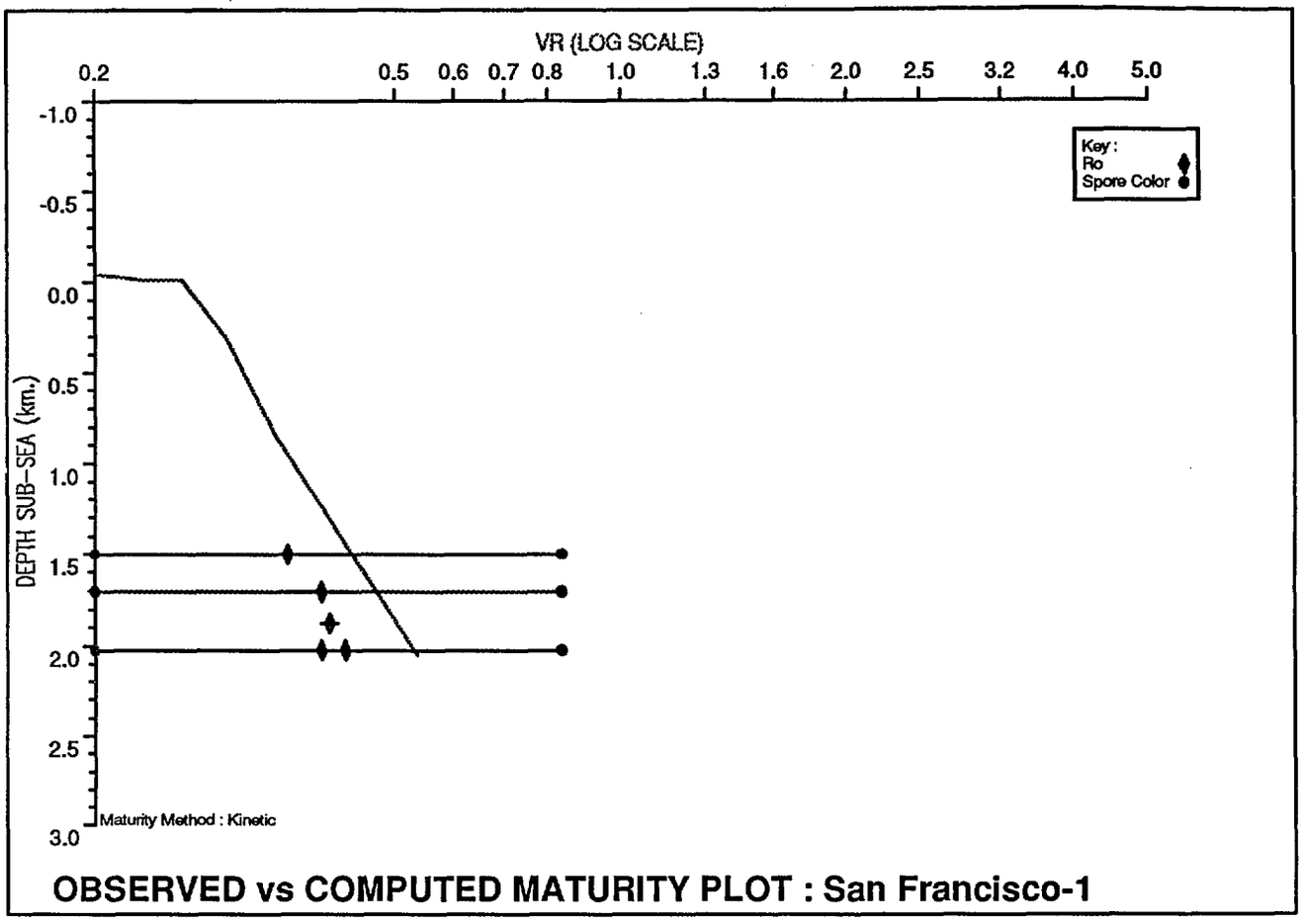

Version 1. HF = 50mW/m^2

The calculated maturity (plotted line) in San Francisco 1 well does not disagree too badly with observed vitrinite reflectance Ro (diamonds), although it still lies above the Ro values. Ro is known to be depressed in the presence of oil, so the departure of the calculated from the observed values is expected.

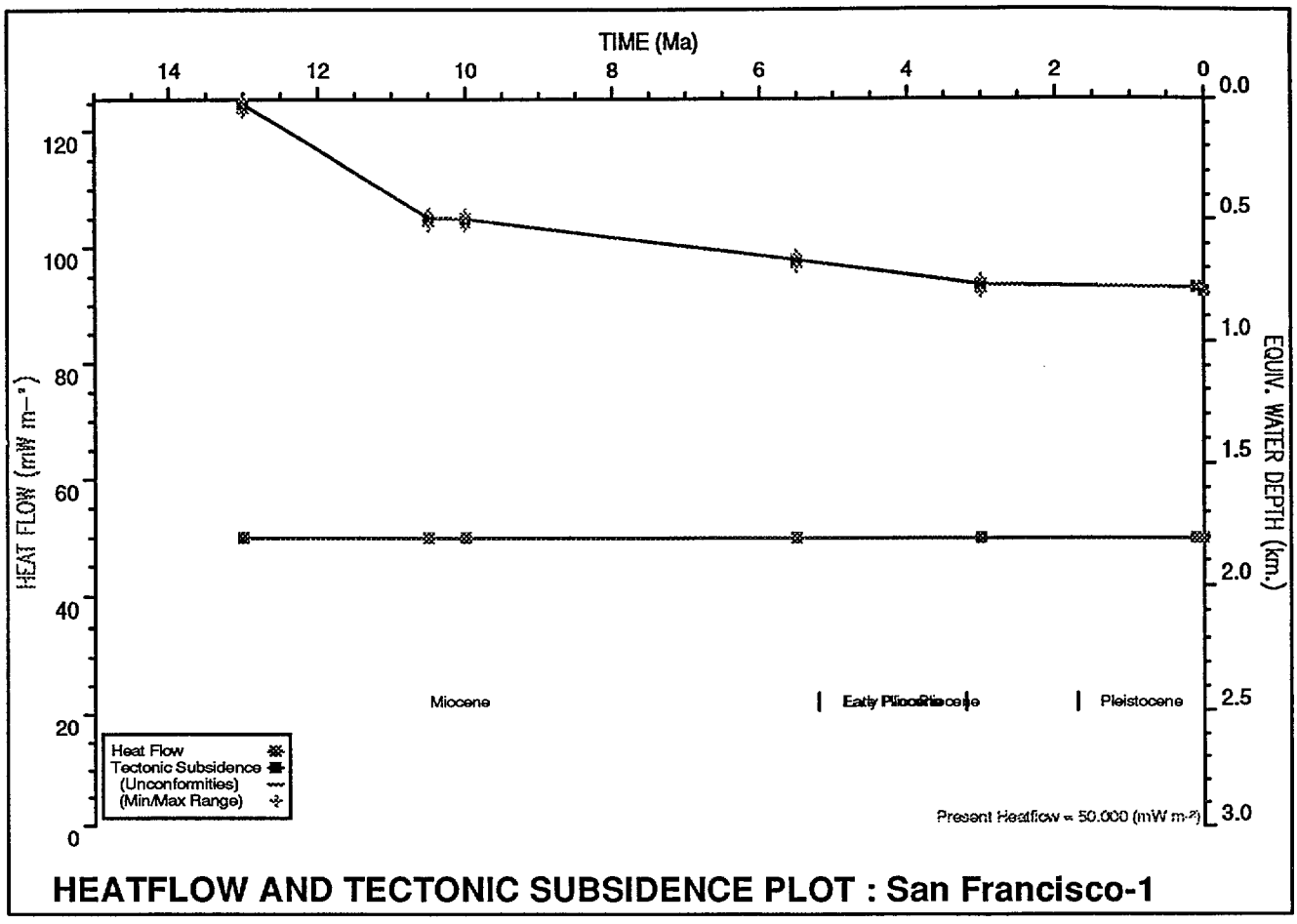

HEATFLOW AND TECTONIC SUBSIDENCE PLOT : San Francisco-1

SAN FRANCISCO 1

PODCO 1977

Latitude: 13° 23' 56" N
KB: 48m asl
Surface Temperature: 28°C
BHT:111°C (Rutherford & Qureshi, 1981)

Longitude: 122° 30' 13" E
TD: 2100mKB
Surface Elevation:46m asl
BHT Depth: 2100m

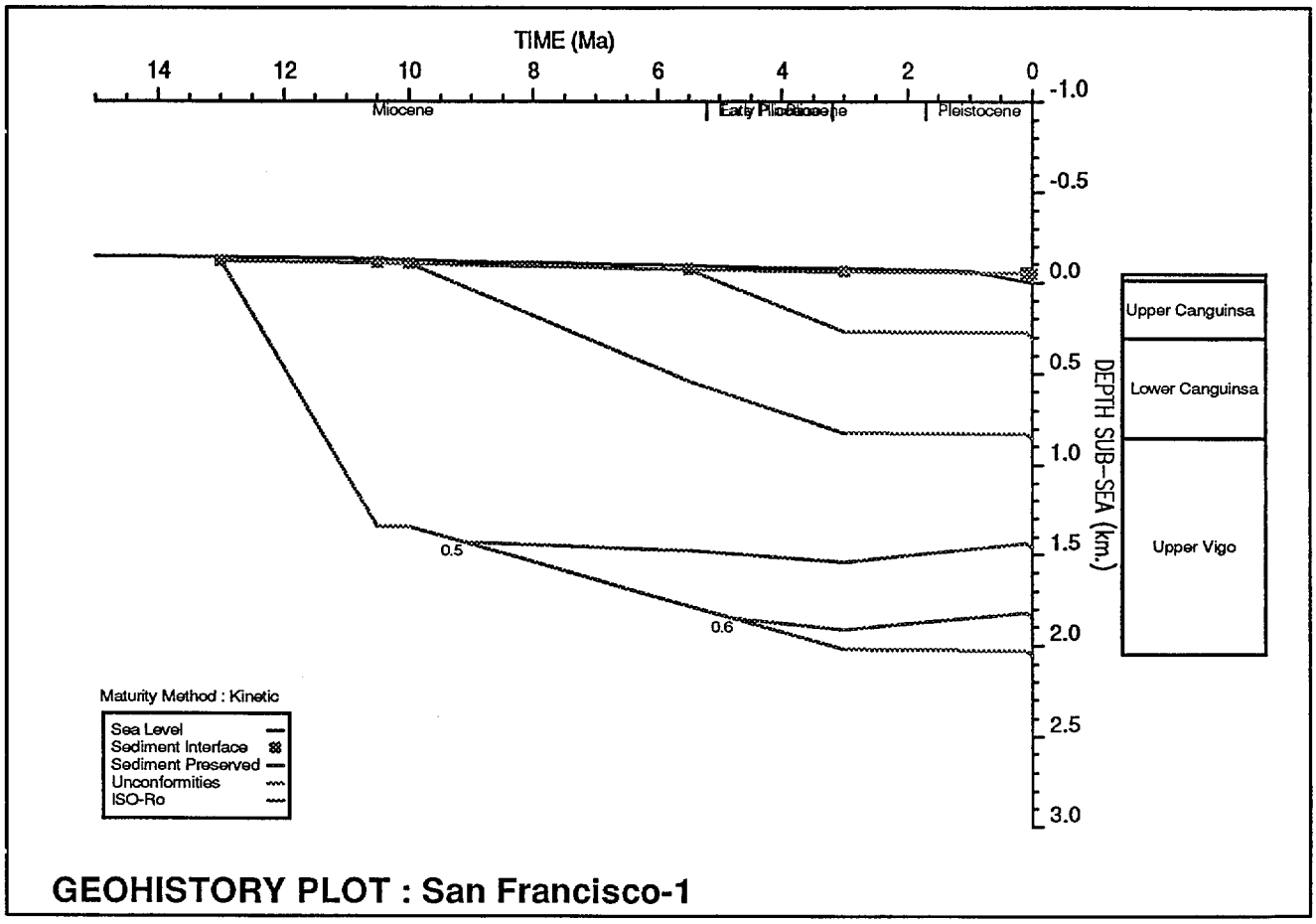

Version 2

This model of the geohistory of San Francisco 1 well uses the BHT quoted by Rutherford and Qureshi (1981). As a result, the heatflow is higher (64 mW/m^2, as against 50 mW/m^2 if temperatures measured on logs are used) and the succession is more mature at TD.

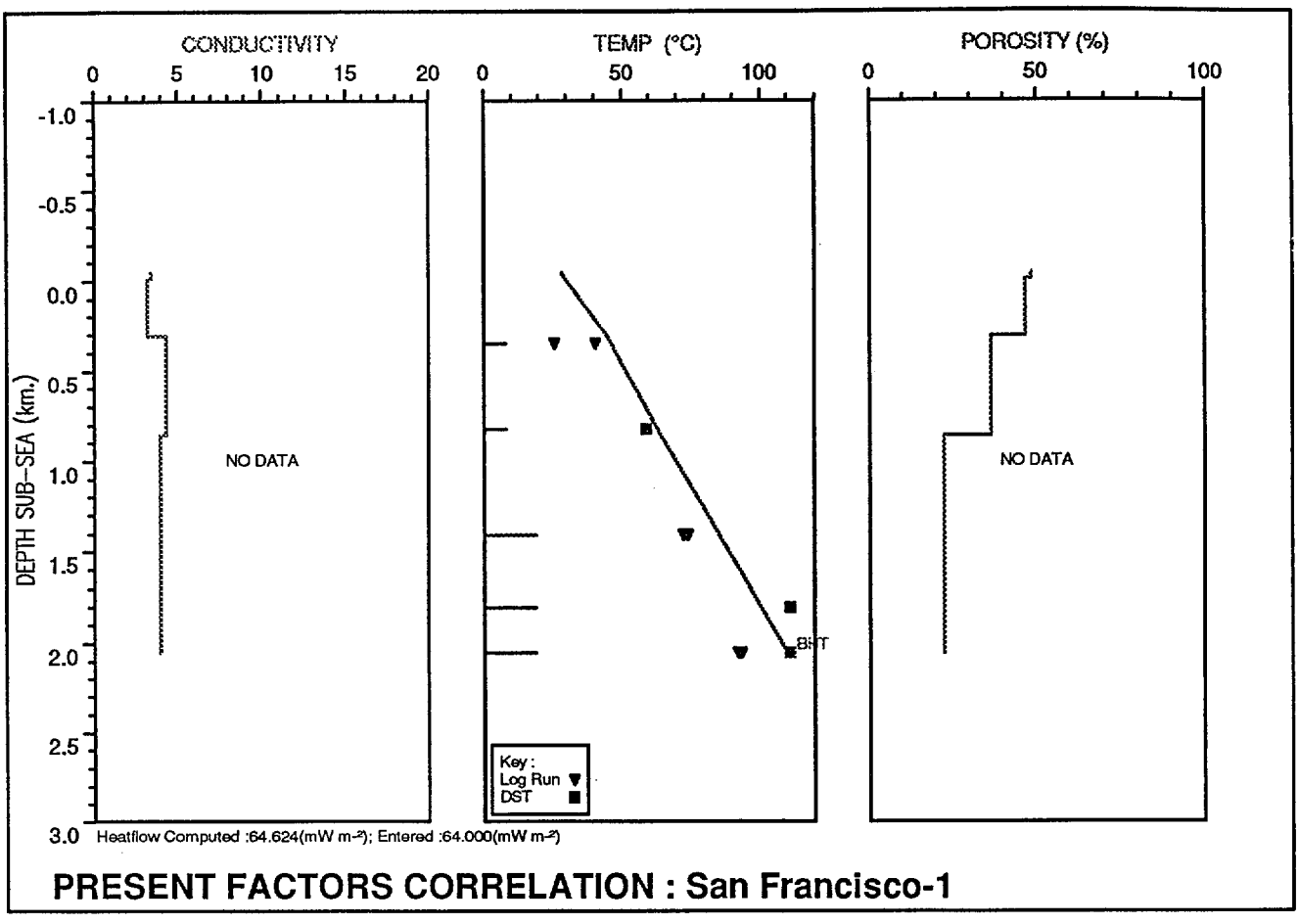

Version 2. HF = 64mW/m^2.

The calculated temperature in the San Francisco 1 well (plotted line) differs widely from the values recorded on Schlumberger logs (triangles). The temperatures. measured during formation testing, quoted by Rutherford and Qureshi (Q&R), (1981) shown as squares on this plot, lie off the line made by observed temperatures on the e-logs. It is difficult to decide which is more realistic. E-log temperatures do tend to be low, and they may not have been completely corrected for circulation time, but the divergence is clear.

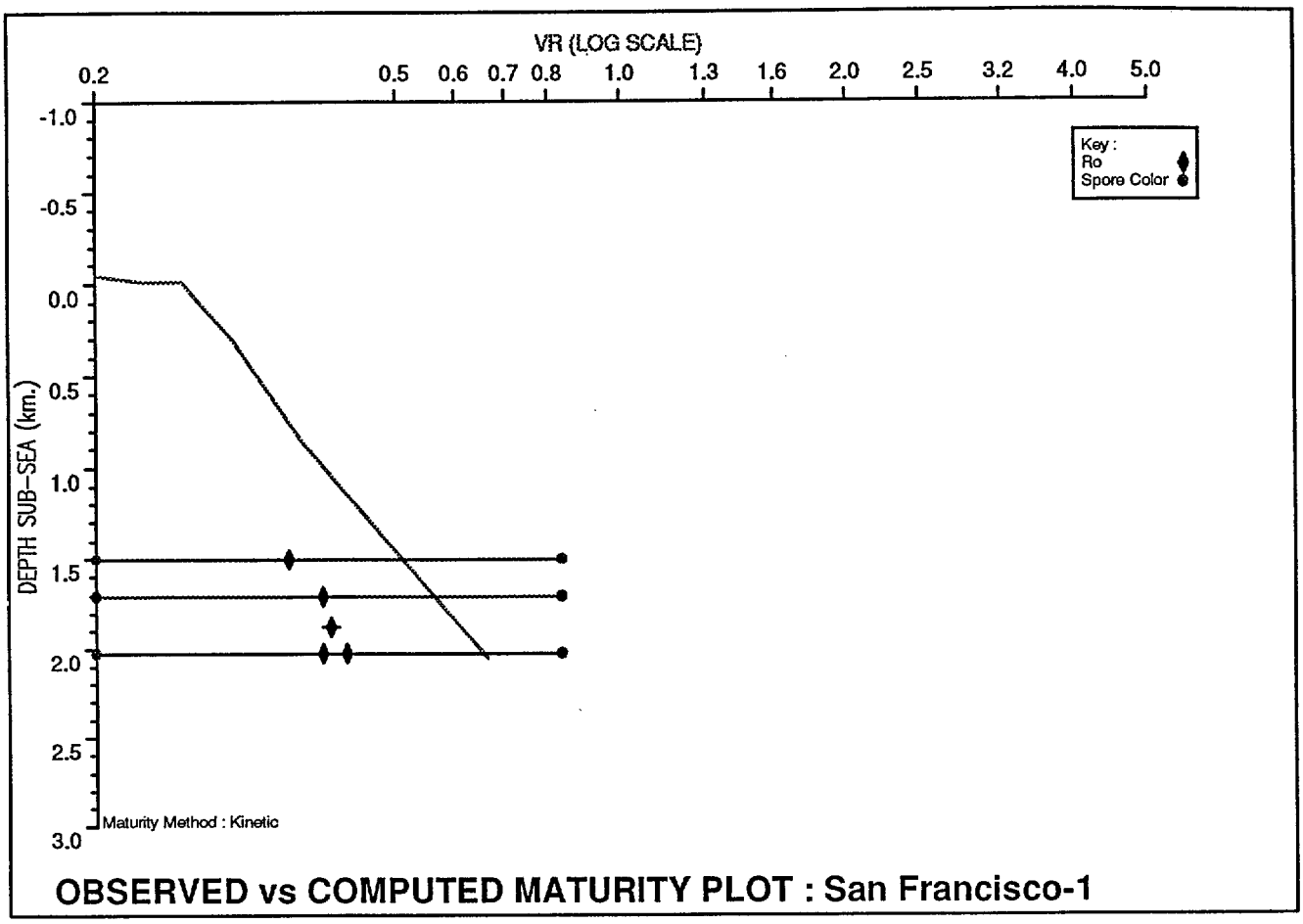

Version 2. HF = 64mW/m^2.
The expected maturity (sloping black line) in San Francisco 1 is widely at variance with the vitrinite reflectance (Ro) measurements (diamonds) quoted by Yap (1977). This leads one to prefer the lower heatflow of version 1, and to query the BHT quoted in (Q&R, 1981).

SAN FRANCISCO 2

PODCO 1977

Latitude: 13° 24' 14" N
KB: 38.6m asl
Surface Temperature: 28°C
BHT: 85°C (e-log)

Longitude: 122° 29' 58" E
TD: 1635mKB
Surface Elevation:35.5m asl
BHT Depth: 1635m

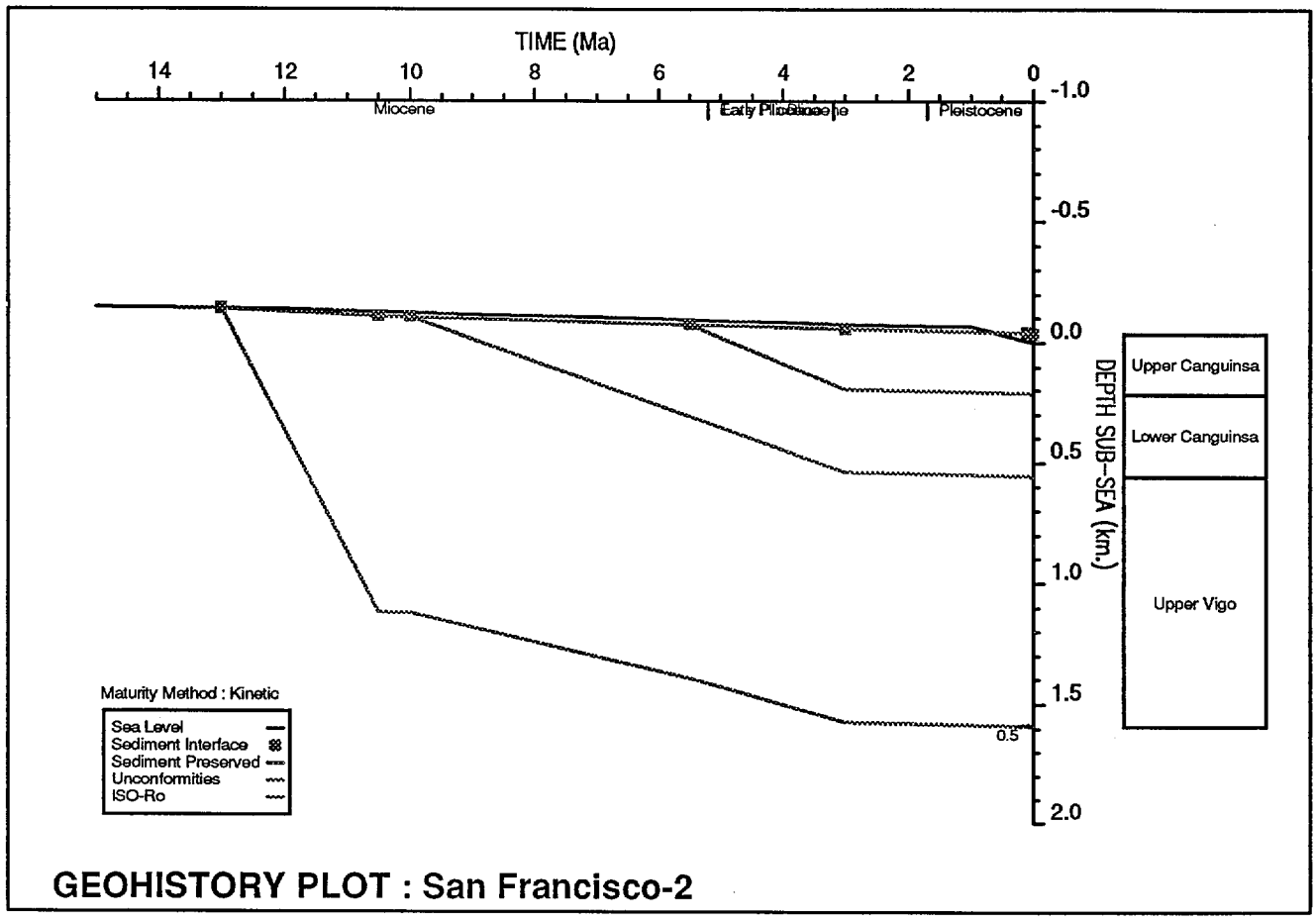

GEOHISTORY PLOT : San Francisco-2

The Vigo Formation at TD is barely mature in this simple model of the geohistory of San Francisco 2 well. Rutherford & Qureshi (1981) quote log temperatures only, for this well, hence the heatflow is moderate and is compatible with that from San Francisco 1 version 1.

	Stratigraph. Unit/Event	E V	Depth to Top of Unit	Age (Ma)	Minimum WtrDpth	Maximum WtrDpth	Modelled WtrDpth	Sea Bed Temp.	Heatflow	Lithology Data	Kerogen Data	Variable Beds
1	Malumbang	N	3.10	0.00	-35.50	-35.50	-35.50	28.00	54.00	*		
2	Base Malumbang	H	5.00	0.10	-35.50	-35.50	-35.50	28.00	54.00	*		
3	Upper Canguinsa	N	5.00	3.00	0.00	50.00	20.00	28.00	54.00	*		
4	Lower Canguinsa	N	256.00	5.50	0.00	50.00	20.00	28.00	54.00	*		
5	Pre-Canguinsa Unc.	H	600.00	10.00	0.00	50.00	20.00	28.00	54.00	*		
6	Upper Vigo	N	600.00	10.50	0.00	50.00	20.00	28.00	54.00	*		
7	TD	N	1635.00	13.00	0.00	0.00	0.00	28.00	54.00	*		

HORIZON DATA : SANFRAN2

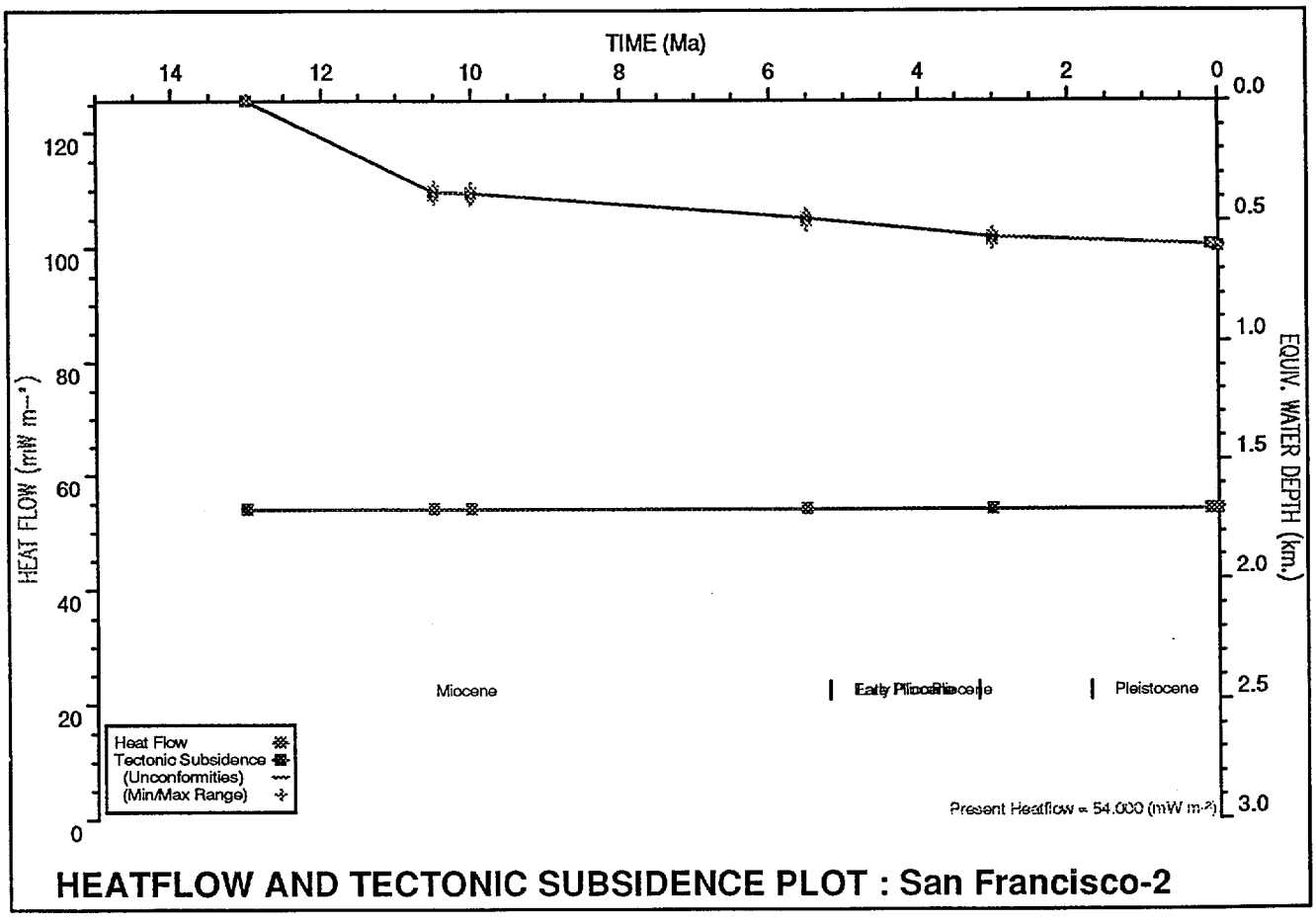

HEATFLOW AND TECTONIC SUBSIDENCE PLOT : San Francisco-2

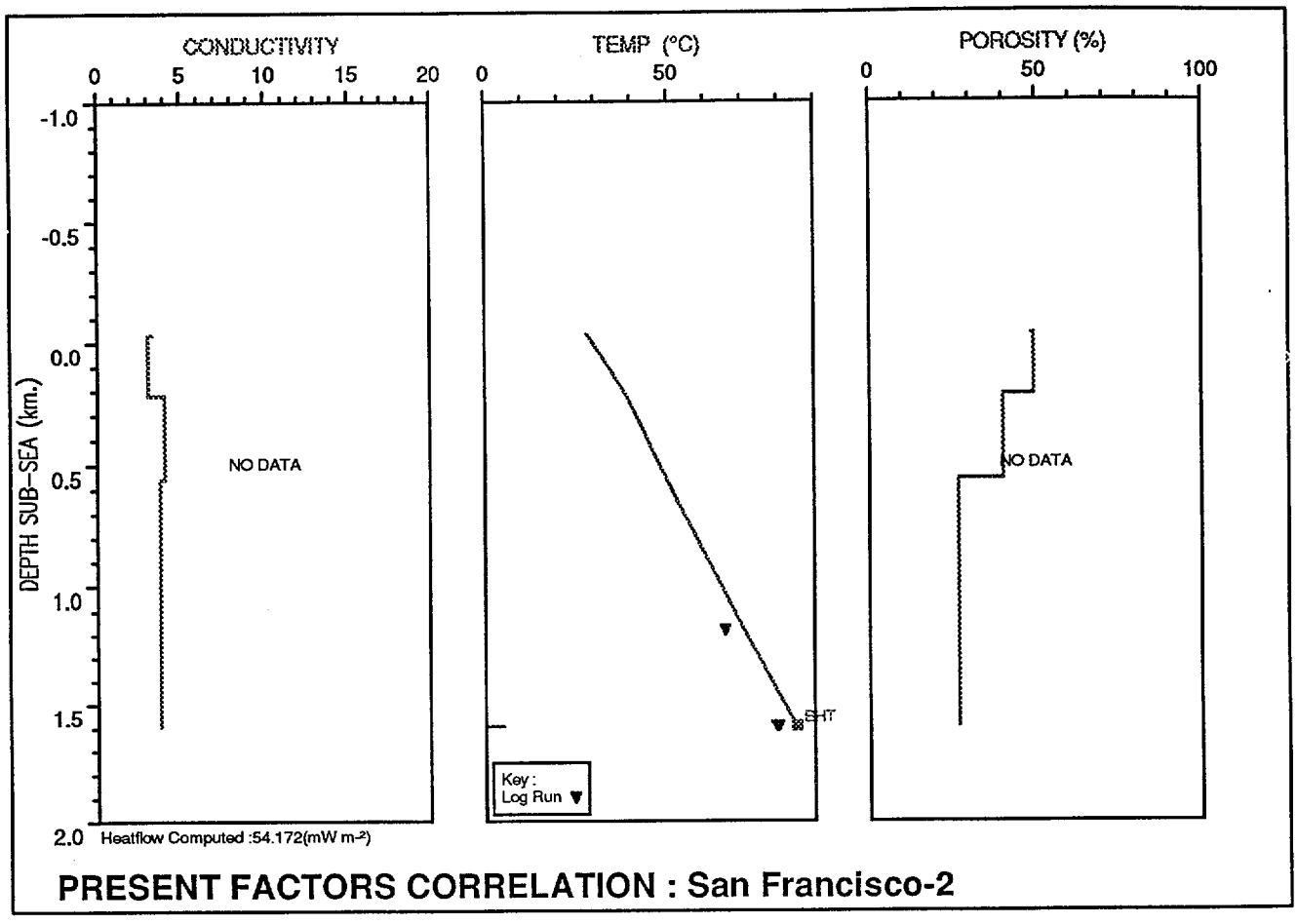

PRESENT FACTORS CORRELATION : San Francisco-2

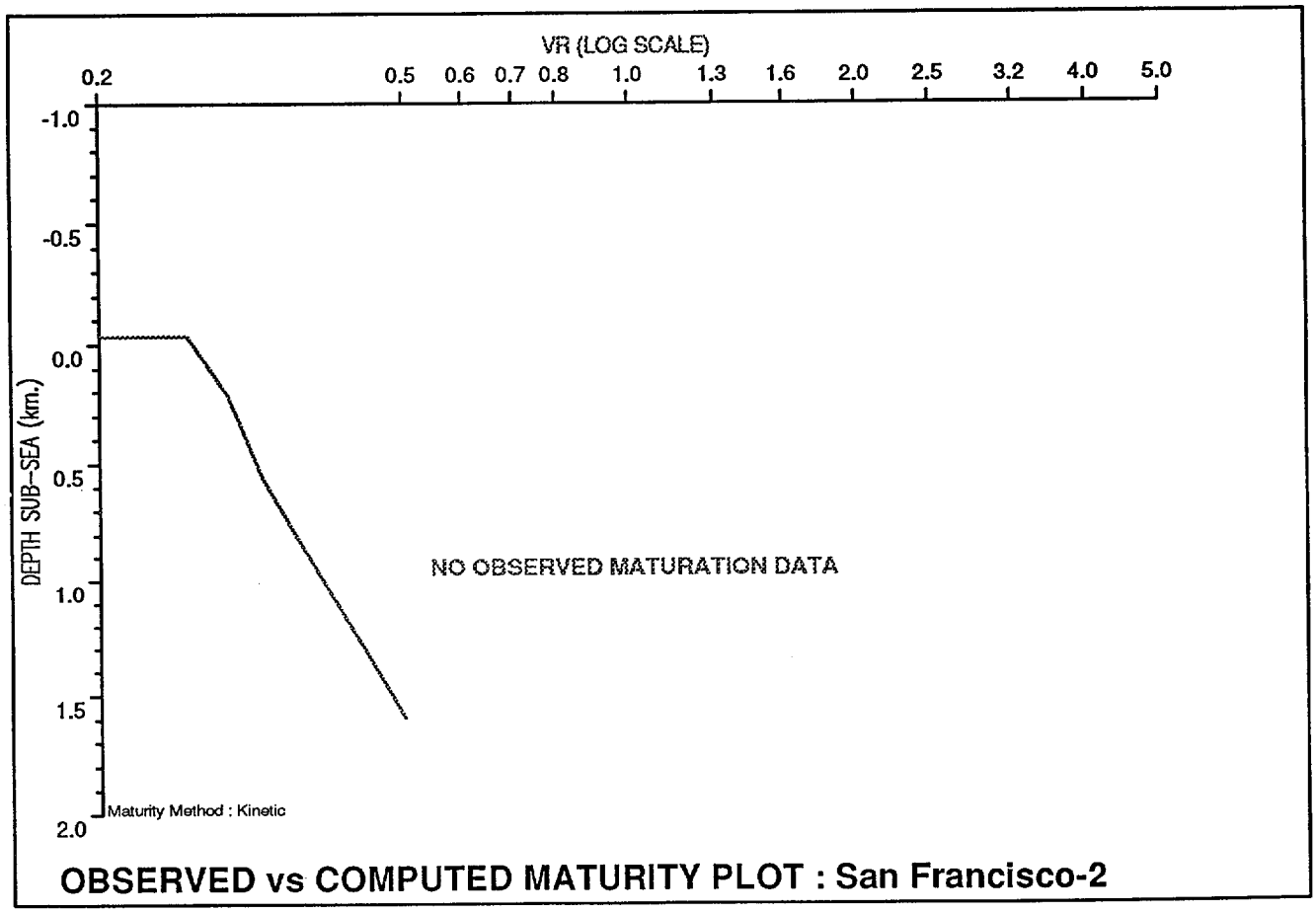

OBSERVED vs COMPUTED MATURITY PLOT : San Francisco-2

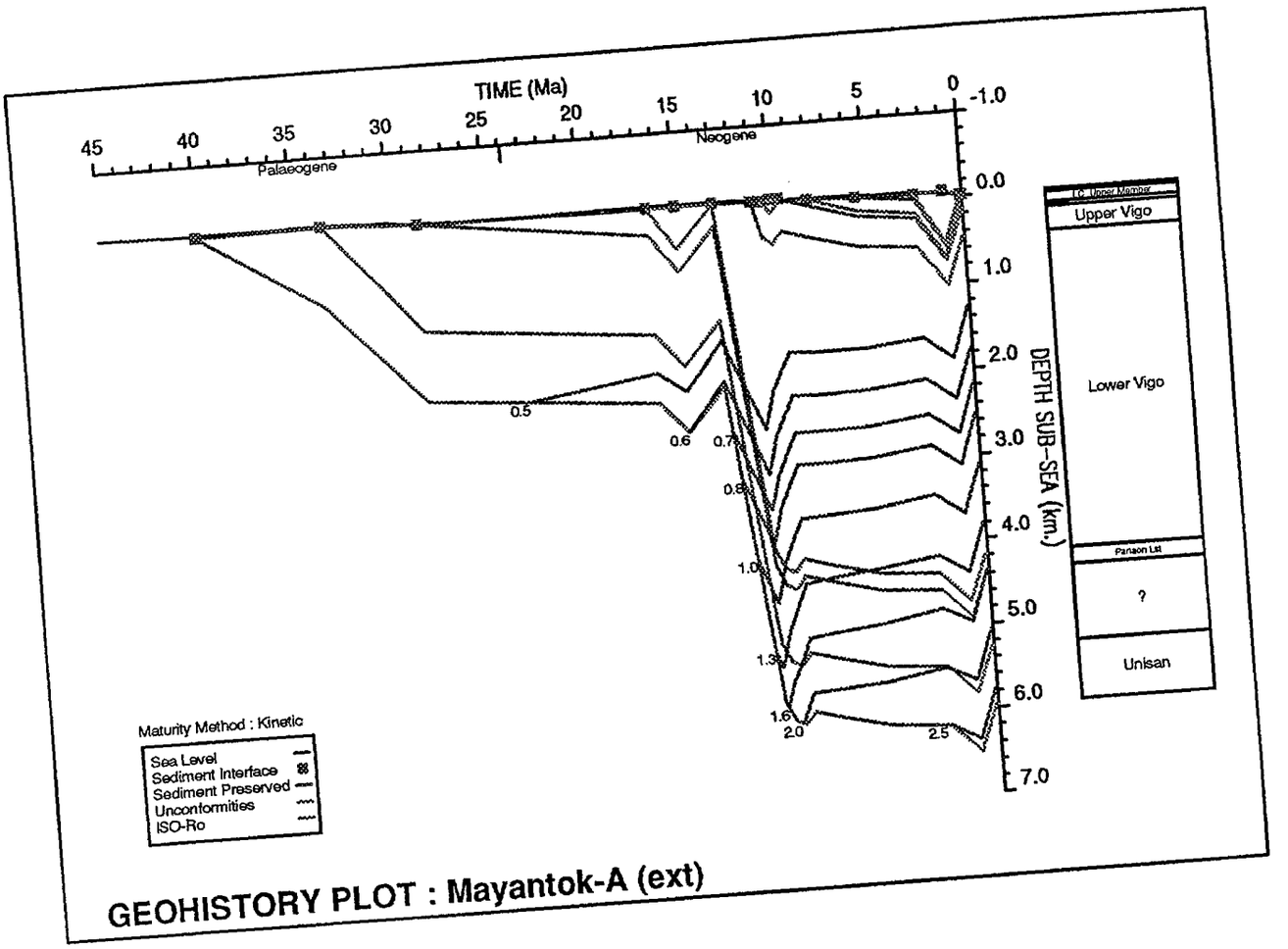

The geohistory plot for Mayantok-A (extended) shows formation tops below TD of the Mayantok 1 well, as determined by seismic interpretation. The plot shows the very thick Lower Vigo Formation, and the underlying formations down to 8 km.

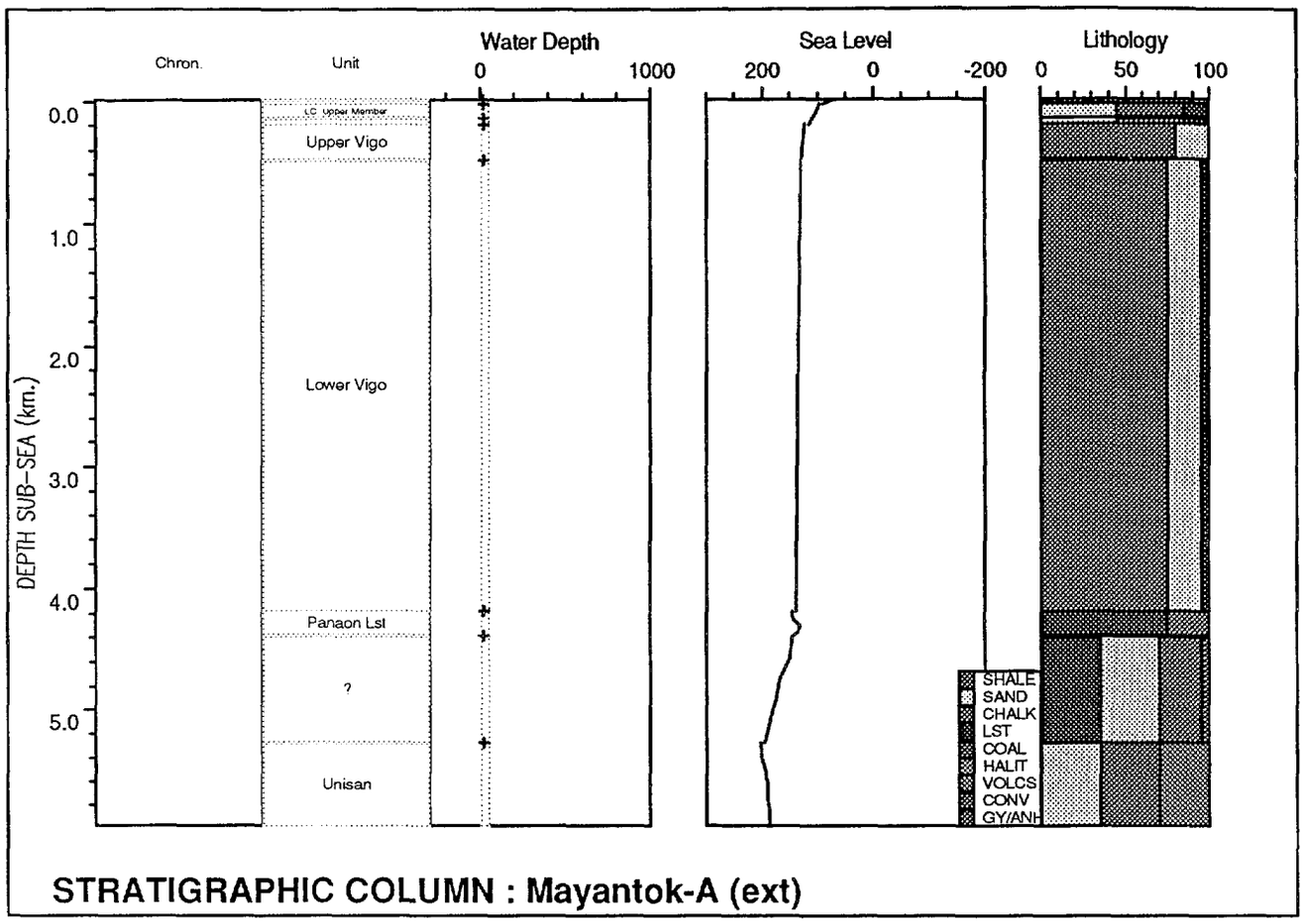

STRATIGRAPHIC COLUMN : Mayantok-A (ext)

	Stratigraph. Unit/Event	E V	Depth to Top of Unit	Age (Ma)	Minimum WtrDpth	Maximum WtrDpth	Modelled WtrDpth	Sea Bed Temp.	Heatflow	Lithology Data	Kerogen Data	Variable Beds
1	Surface	H	6.45	0.00	-16.00	-16.00	-16.00	28.00	54.00	*		
2	Surface unconf.	E	6.50	0.10	-16.00	-16.00	-16.00	28.00	54.00	*		
3	Deposit A	E	(600.00)	1.00	-16.00	-16.00	-16.00	28.00	54.00	*		
4	Upper Canguinsa	N	6.50	2.50	0.00	50.00	20.00	27.78	54.00	*		
5	LC Upper Member	N	45.72	5.50	0.00	50.00	20.00	27.78	54.00	*		
6	LC Lower Member	N	167.64	8.00	0.00	50.00	20.00	27.78	54.00	*		
7	Pre-Canguinsa unc.	E	217.00	9.50	0.00	0.00	0.00	27.78	54.00	*		
8	Deposit B	E	(150.00)	10.00	0.00	0.00	0.00	27.78	54.00	*		
9	Upper Vigo	N	217.00	10.50	0.00	50.00	20.00	27.78	54.00	*		
10	Lower Vigo	N	502.93	11.00	0.00	50.00	20.00	27.78	54.00	*		
11	Base Vigo unc.	E	4200.00	13.00	0.00	50.00	20.00	27.78	54.00	*		
12	Deposit C	E	(500.00)	15.00	0.00	50.00	20.00	27.78	54.00	*		
13	Panaon Lst	N	4200.00	16.50	0.00	50.00	20.00	27.78	54.00	*		
14	?	N	4400.00	28.50	0.00	50.00	20.00	27.78	54.00	*		
15	Unisan	N	5300.00	33.50	0.00	50.00	20.00	28.00	50.00	*		
16	Base Unisan	N	6000.00	40.00	0.00	50.00	20.00	27.78	54.00	*		

HORIZON DATA : MAYNTOKA

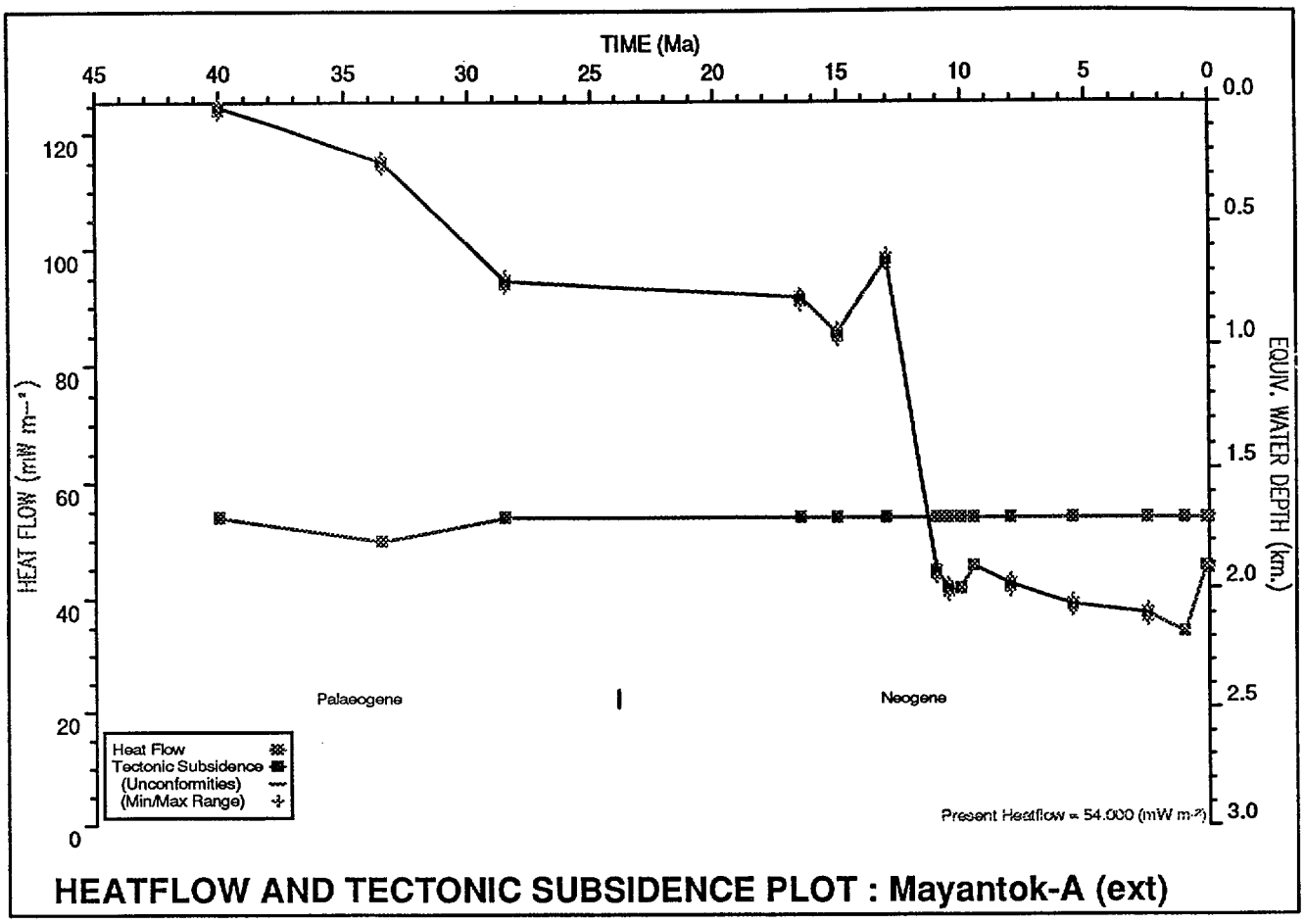

The subsidence plot for Mayantok-A shows the very rapid deposition of the lowermost Vigo Formation between 13 and 11 Ma. at the Mayantok 1 wellsite. Heatflow must have varied, but the variation is not quantifiable, and HF has been held constant at a moderate 54 mW/m^2.

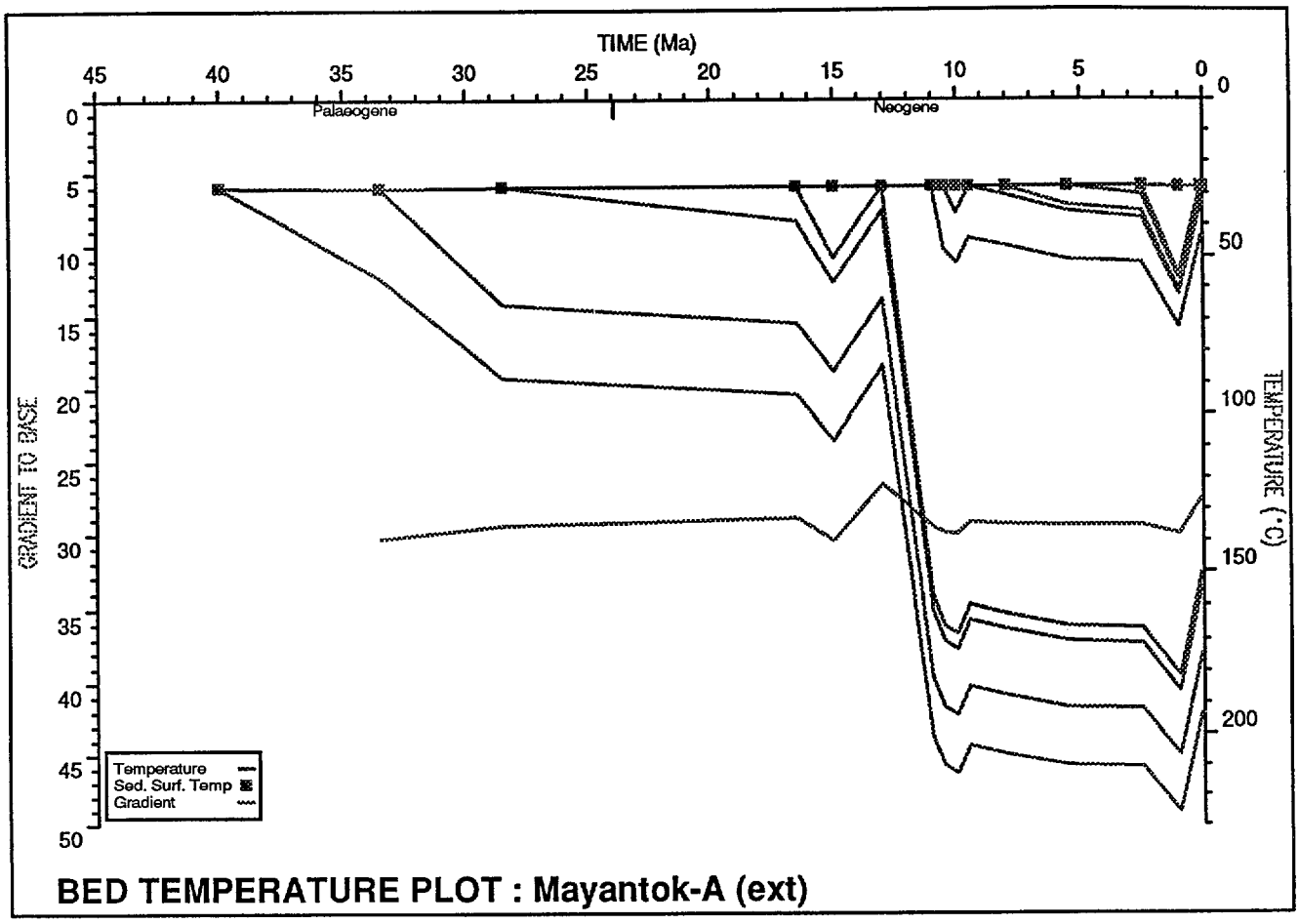

The bed temperature plot at the Mayantok 1 wellsite shows that most of the Lower Vigo Formation was heated to greater than 100°C by 11Ma before present.

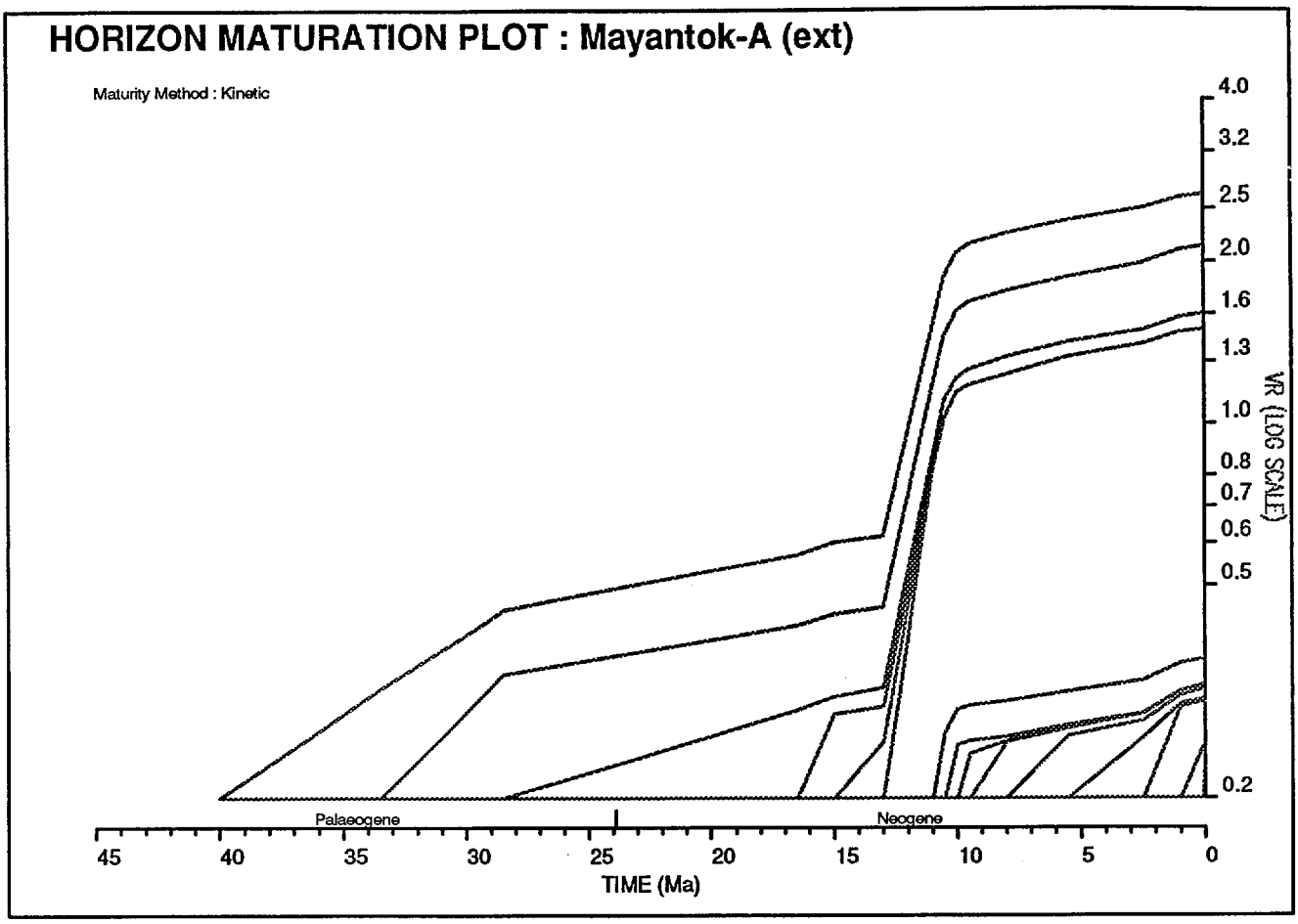

The horizon maturation plot shows that most of the Lower Vigo Formation became mature for hydrocarbons at 11Ma. The Panaon is overmature.

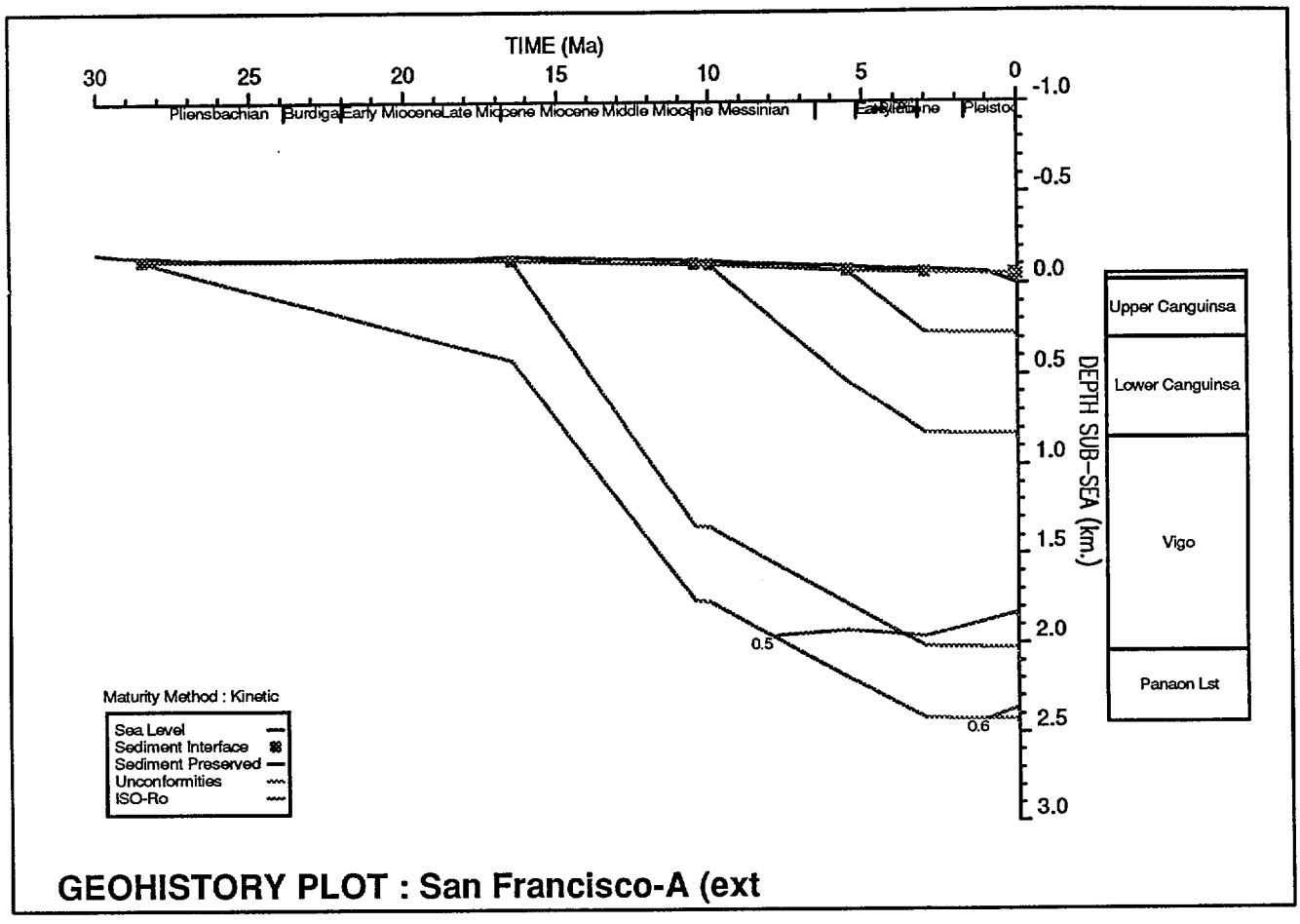

The geohistory plot of San Francisco-A (extended) shows the formations below TD of the San Francisco 1 well. This is the 'cool' model, similar to version 1 above. The lowermost Vigo Formation is just reaching maturity now, and thePanaon Limestone is in an early-maturity stage.

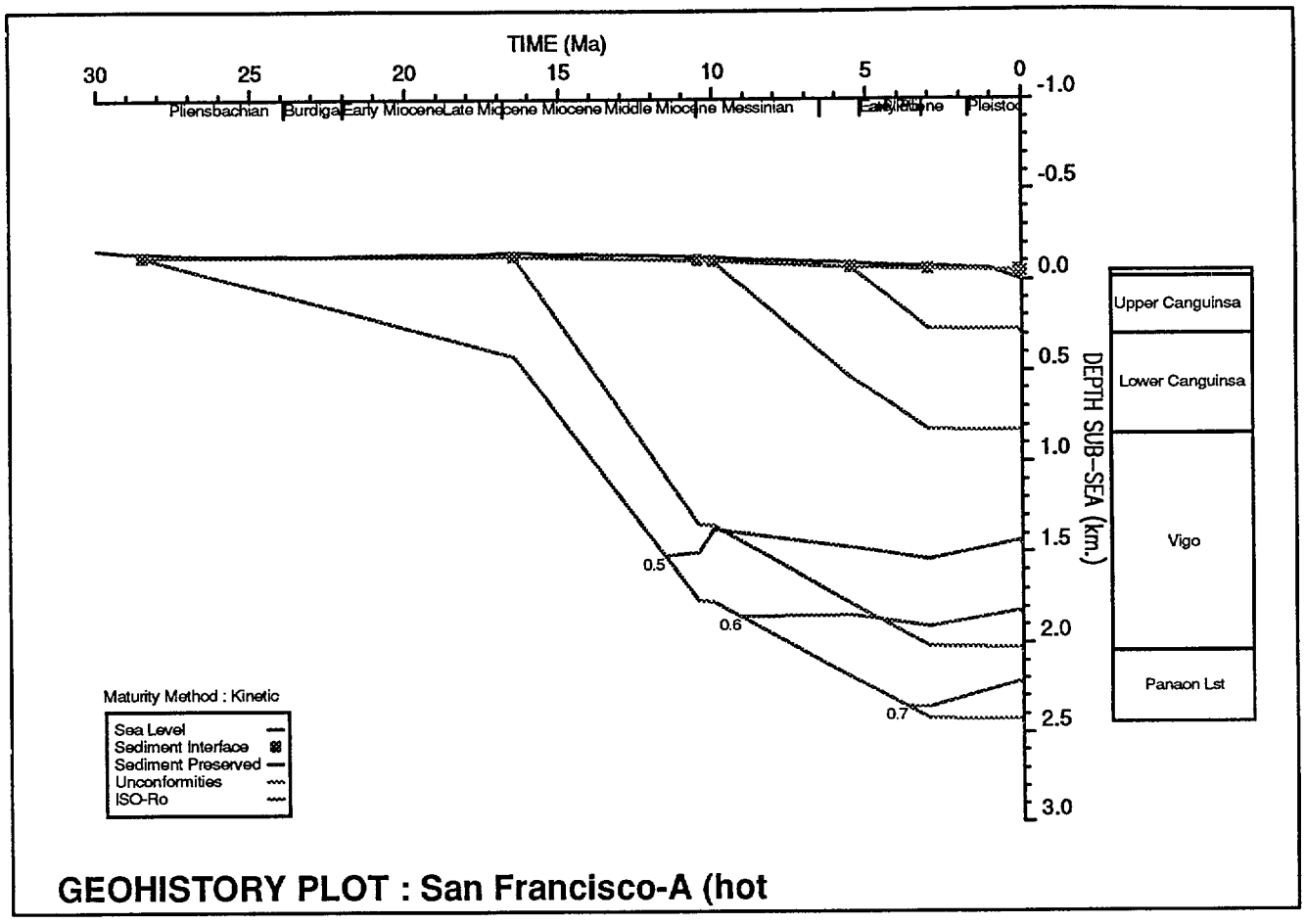

This geohistory plot of the San Francisco location near SF1 uses the higher temperatures of the warmer version 2. In this model, the Lower Vigo Formation is mature for hydrocarbons, and the Panaon Limestone is approaching the zone of peak generation of hydrocarbons.

ANIMA SOLA LEAD

AGSO 1993

Latitude: 13° 21' N
KB: 10m asl
Surface Temperature: 28°C
BHT: 100°C (hypothetical)
Seismic location: Line RG-83-805 sp 832

Longitude: 123° 02' E
TD: 4000mKB
Surface Elevation:50m bsl
BHT Depth: 2000m

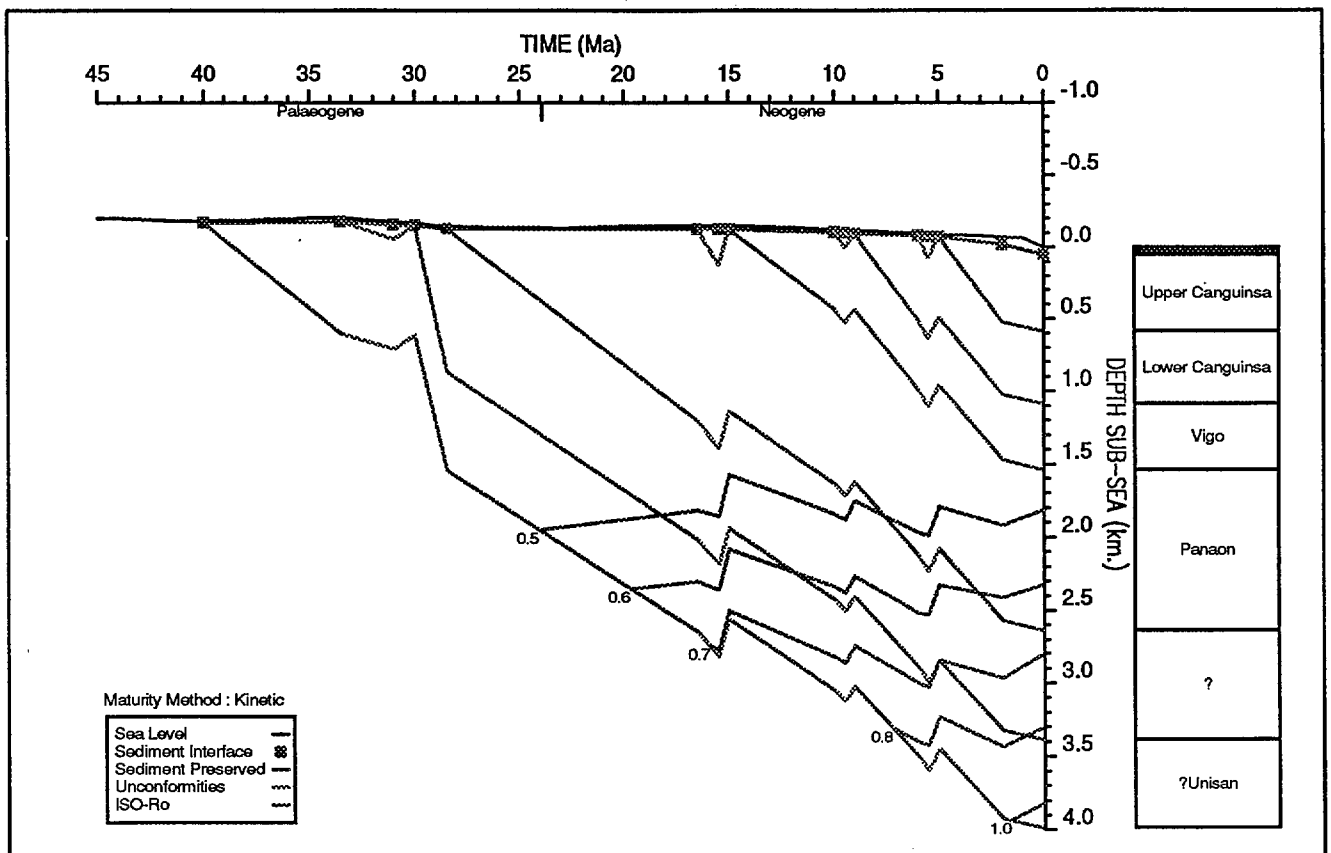

GEOHISTORY PLOT : Anima Sola Lead

The geohistory plot of the Anima Sola Lead in the Ragay Gulf shows that the Canguinsa and Vigo formations are immature for hydrocarbons, but that the Panaon Formation is early mature. The succession beneath (the age-equivalent of the Taog) is now reaching the peak of the hydrocarbon generation zone. The small steps in the burial and the maturity curves are the expression of minor unconformities at the seismic horizons.

	Stratigraph. Unit/Event	E V	Depth to Top of Unit	Age (Ma)	Minimum WtrDpth	Maximum WtrDpth	Modelled WtrDpth	Sea Bed Temp.	Heatflow	Lithology Data	Kerogen Data	Variable Beds
1	Sea Bed	N	60.00	0.00	50.00	50.00	50.00	28.00	64.00	*		
2	Upper Canguinsa	N	63.00	2.00	50.00	50.00	50.00	28.00	64.00	*		
3	Yellow Horizon	E	600.00	5.00	0.00	50.00	20.00	28.00	64.00	*		
4	Deposit A	E	(150.00)	5.50	0.00	50.00	20.00	28.00	64.00	*		
5	Lower Canguinsa	N	600.00	6.00	0.00	50.00	20.00	28.00	64.00	*		
6	Red Horizon	E	1100.00	9.00	0.00	50.00	20.00	28.00	64.00	*		
7	Deposit B	E	(100.00)	9.50	0.00	50.00	20.00	28.00	64.00	*		
8	Vigo	N	1100.00	10.00	0.00	50.00	20.00	28.00	64.00	*		
9	Green Horizon	E	1550.00	15.00	0.00	50.00	20.00	28.00	64.00	*		
10	Deposit C	E	(250.00)	15.50	0.00	50.00	20.00	28.00	64.00	*		
11	Panaon	N	1550.00	16.50	0.00	50.00	20.00	28.00	64.00	*		
12	?	N	2650.00	28.50	0.00	50.00	20.00	28.00	64.00	*		
13	Blue Horizon	E	3400.00	30.00	0.00	50.00	20.00	28.00	64.00	*		
14	Deposit D	E	(100.00)	31.00	0.00	50.00	20.00	28.00	64.00	*		
15	?Unisan	N	3400.00	33.50	0.00	50.00	20.00	28.00	64.00	*		
16	TD	N	4000.00	40.00	0.00	50.00	20.00	28.00	64.00	*		

HORIZON DATA : ANISOLA

The horizon data table for the Anima Sola Lead is controlled largely by seismic interpretation of line RG-83-805 at shotpoint 832. This location is on the north-eastern flank of the lead. Deposits A to D are small amounts of deposition, later eroded, at seismic horizon unconformities.

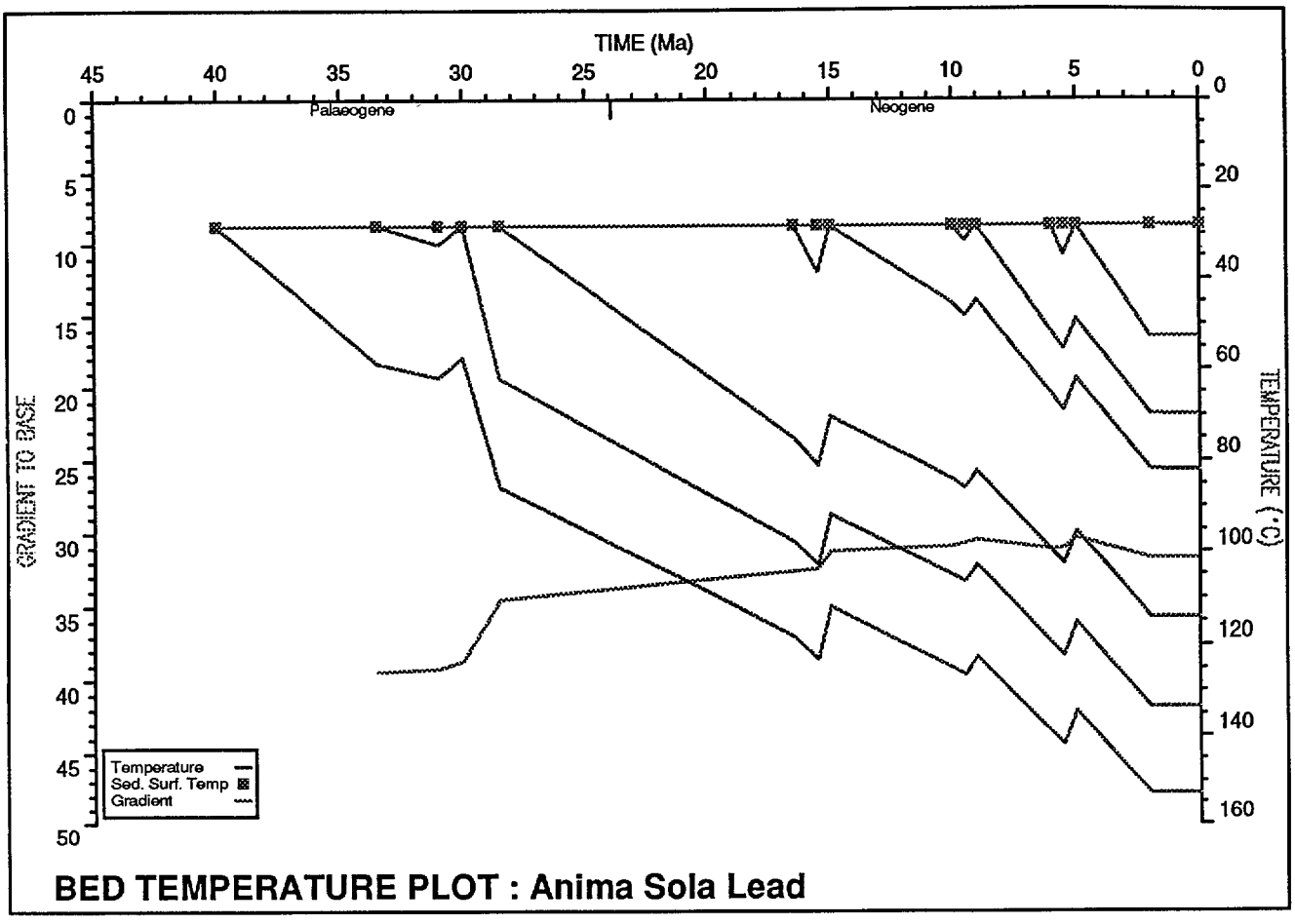

The bed temperature plot of the Anima Sola lead shows a present-day 134°C at the top of the Unisan Volcanics. This implies that the base of the prospective succession is in the zone of peak generation of hydrocarbons. The thermal gradient lies between 40 and 30°C throughout the history of the lead.

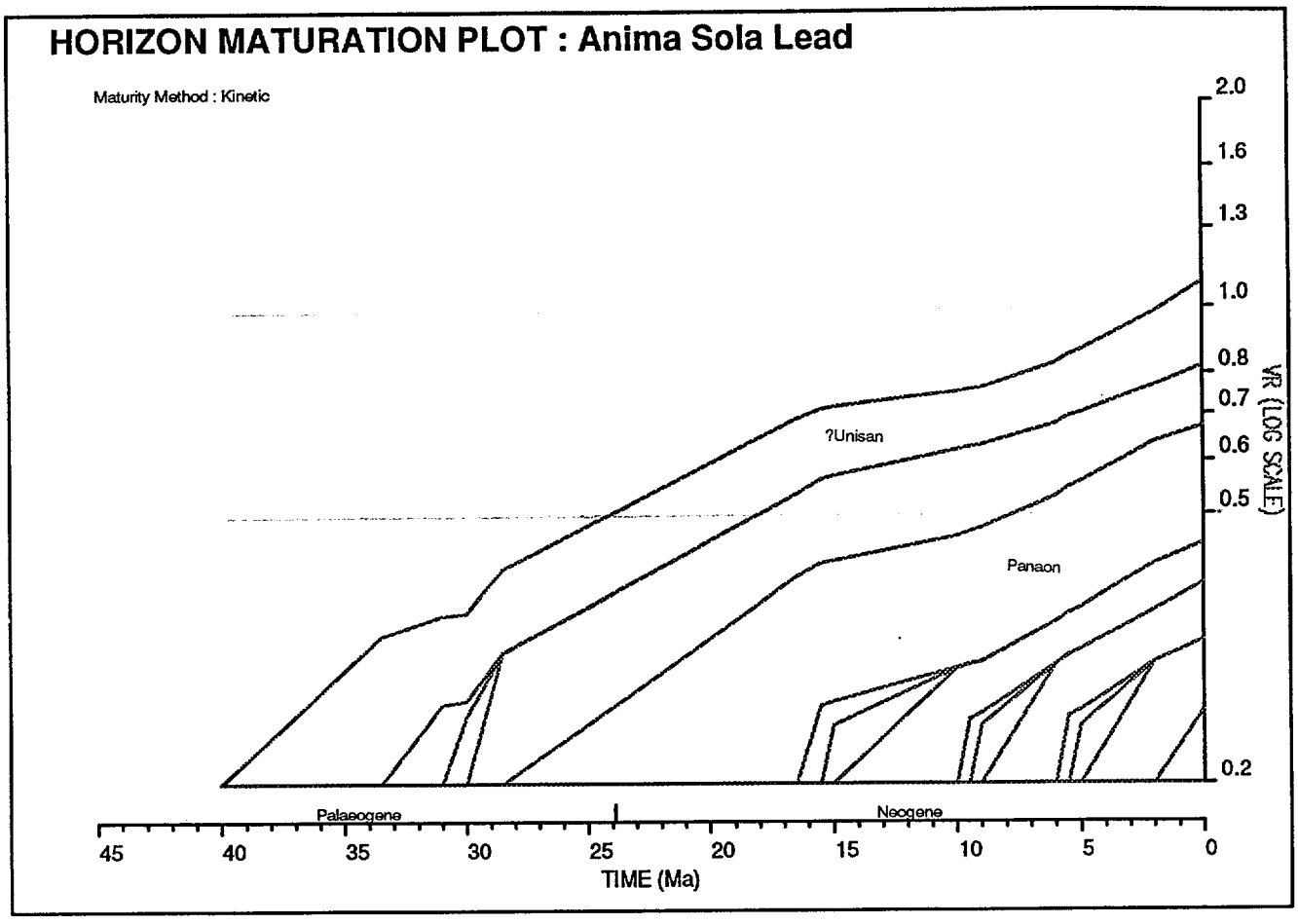

The horizon maturation plot for the Anima Sola Lead shows the base of the Panaon Limestone entering the zone of maturity for hydrocarbons (Ro = 0.5) at 8 million years BP. The base of the underlying formation (an age-equivalent of the Taog?) entered the zone of maturity at 18 million years BP, and is now approaching the zone of peak generation. These figures are based on a very moderate heatflow of 64 mW/m^2

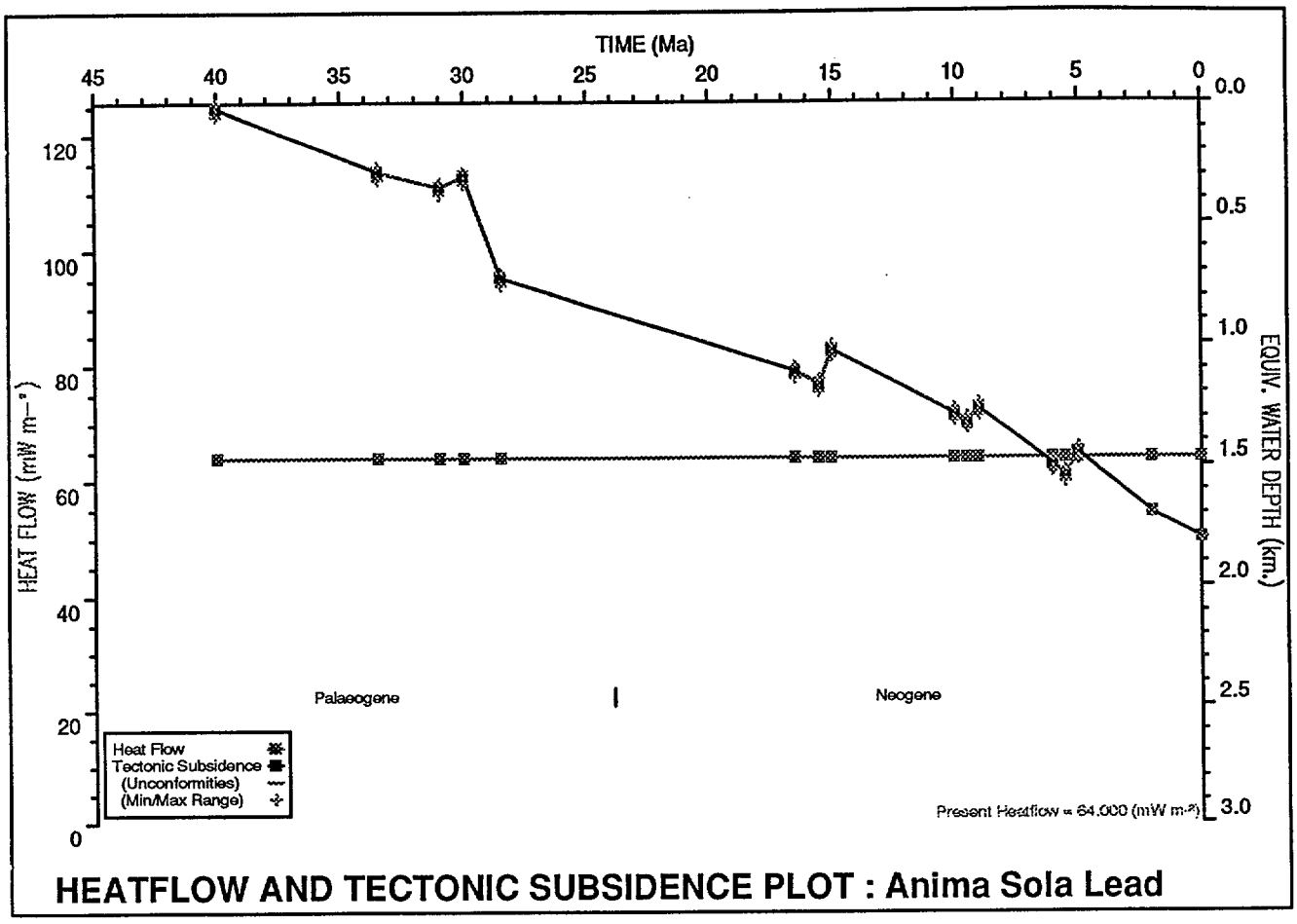

HEATFLOW AND TECTONIC SUBSIDENCE PLOT : Anima Sola Lead

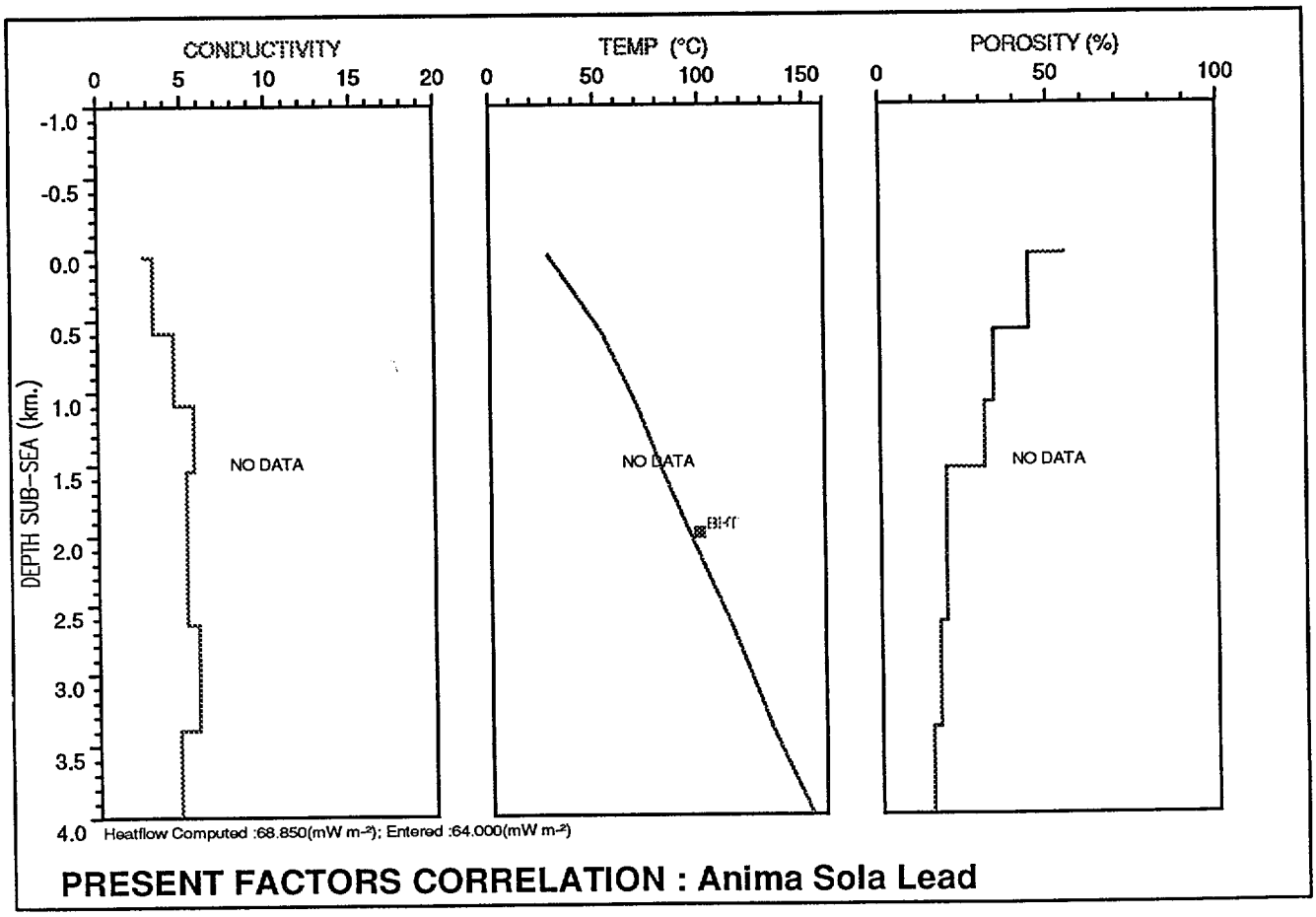

PRESENT FACTORS CORRELATION : Anima Sola Lead

BONDOC SUB-BASIN

AGSO 1994

Latitude: 13° 17' 27.6" N
KB: 0m asl
Surface Temperature: 28°C
BHT: 100°C (estimate)
Seismic location: Line RG-83-803A sp 1620

Longitude: 122° 43' 53.4" E
TD: 5000mKB
Surface Elevation: 103m bsl
BHT Depth: 2000m

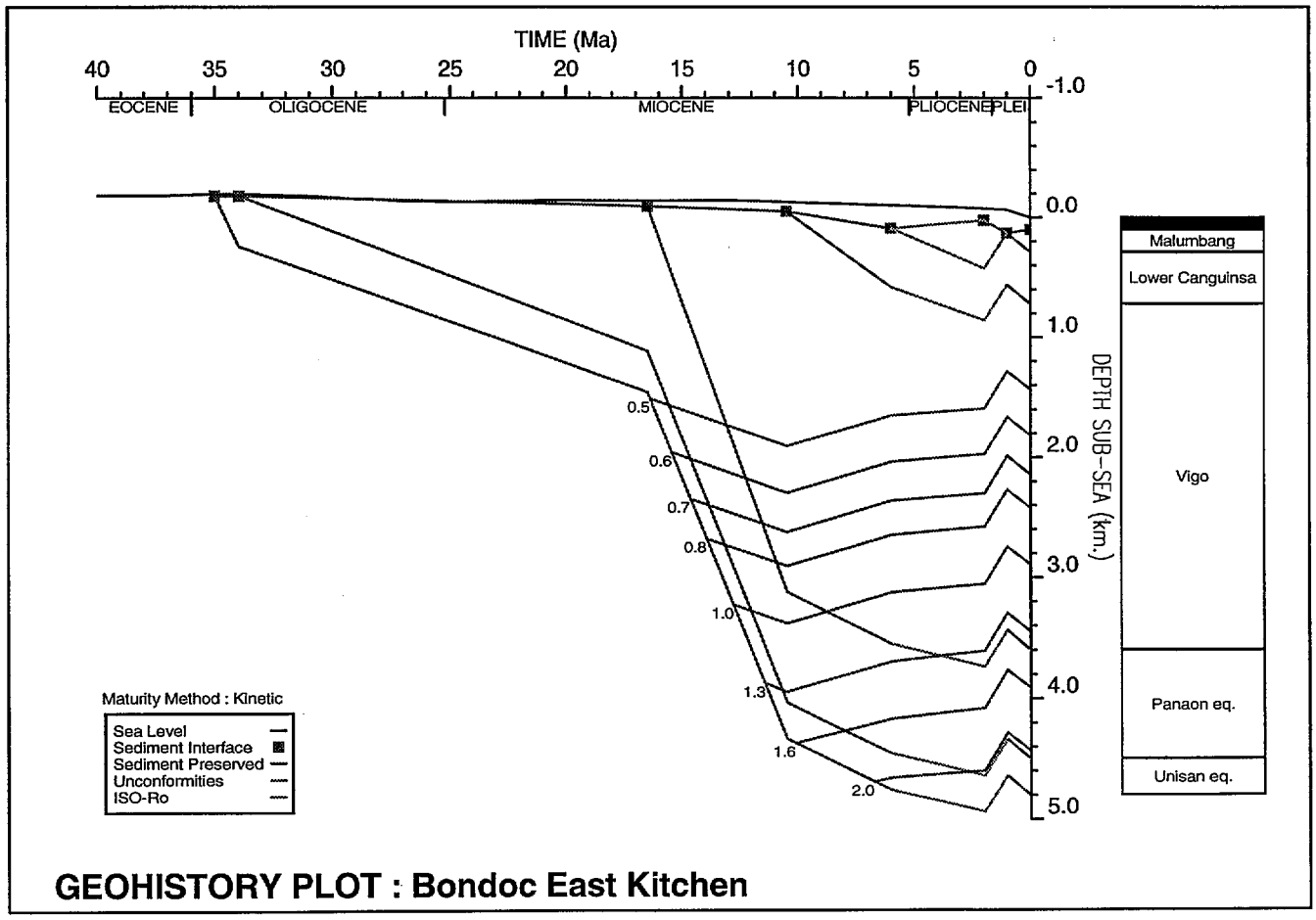

GEOHISTORY PLOT : Bondoc East Kitchen

The burial history of the Bondoc Sub-basin shows it developing mainly during mid-Miocene time, burying Oligocene to Early Middle Miocene carbonate-bearing sediments under a mass of clastics.About 3 kilometres of sediments with a significant organic content lie within the 'oil and gas window', making the Bondoc Sub-basin a likely prolific source of hydrocarbons.

	Stratigraph. Unit/Event	E V	Depth to Top of Unit	Age (Ma)	Minimum WtrDpth	Maximum WtrDpth	Modelled WtrDpth	Sea Bed Temp.	Heatflow	Lithology Data	Kerogen Data	Variable Beds
1	Malumbang	N	103.00	0.00	103.00	103.00	103.00	28.00	70.00	*		
2	Unconformity	E	290.00	1.00	50.00	200.00	195.00	28.00	70.00	*		
3	Pliocene Deposit	E	(400.00)	2.00	50.00	200.00	100.00	28.00	70.00	*		
4	Lower Canguinsa	N	290.00	6.00	50.00	200.00	190.00	28.00	70.00	*		
5	Vigo	N	720.00	10.50	50.00	300.00	80.00	28.00	70.00	*		
6	Panaon eq.	N	3600.00	16.50	0.00	100.00	50.00	28.00	70.00	*		
7	Unisan eq.	N	4500.00	34.00	0.00	50.00	20.00	28.00	70.00	*		
8	TD	N	4800.00	35.00	0.00	50.00	20.00	28.00	70.00	*		

HORIZON DATA : BONEKCN

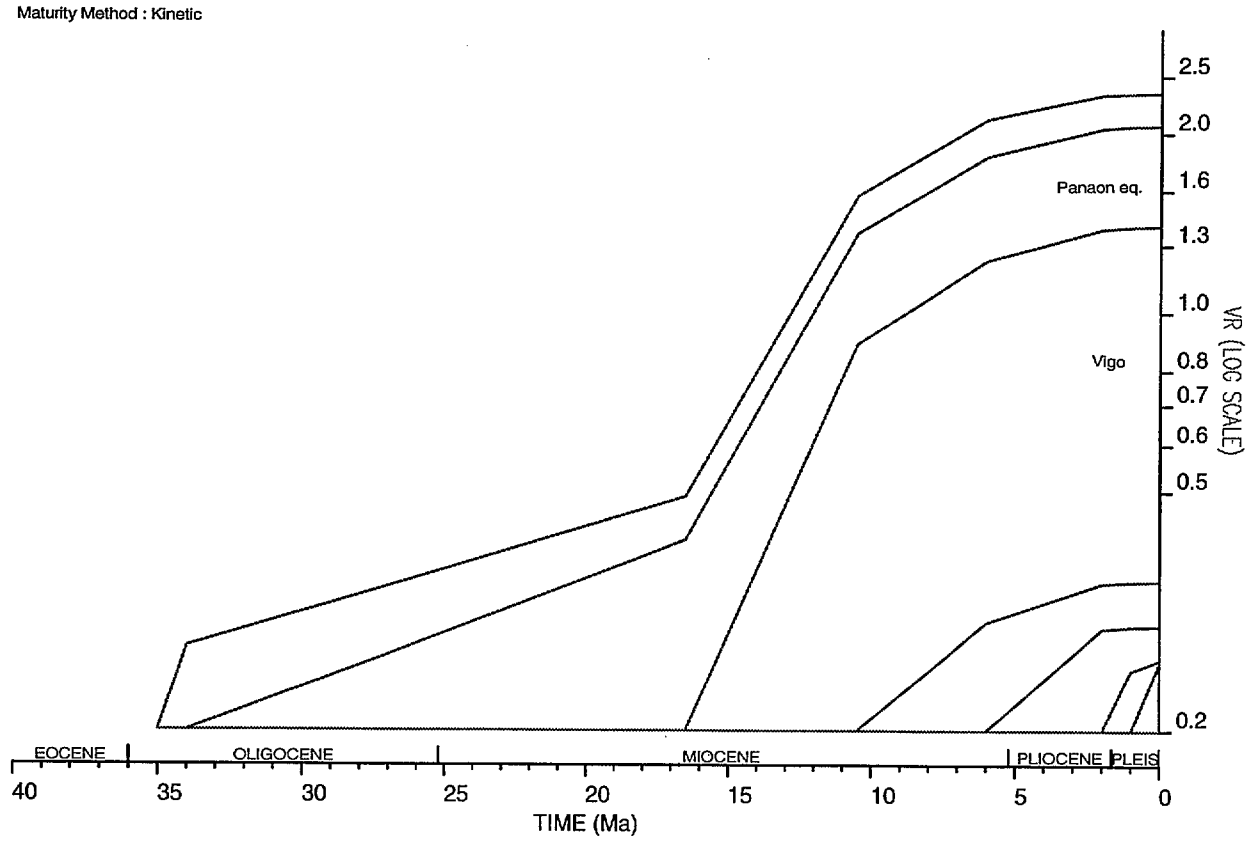

The plot of maturity versus time for the Bondoc Sub-basin kitchen area shows the Panaon formation equivalent (Oligocene to Lower Miocene) beginning to achieve maturity for hydrocarbons between 16 and13 Ma (during the Middle Miocene). The Vigo formation has been subsiding into the zone of early maturity from 13 Ma till the present, and the base of the formation is now past the zone of oil generation at this site deep within the sub-basin.

	Stratigraph. Unit/Event	SHALE	SAND	CHALK	LST	COAL	HALIT	VOLCS	CONV	GY/ANH	Initial Porosity	Por/Depth Factor	Conductivity	Density
1	Malumbang	30	10		60						0.490	1.490	8.300	2.750
2	Unconformity	40	45		15						0.520	1.330	9.060	2.720
3	Pliocene Deposit	40	45		15						0.520	1.330	9.060	2.720
4	Lower Canguinsa	40	45		15						0.520	1.330	9.060	2.720
5	Vigo	65	25		10						0.600	1.800	6.790	2.760
6	Panaon eq.	25			75						0.480	1.510	8.240	2.760
7	Unisan eq.	35	35					30			0.400	1.140	7.070	2.740
8	TD	35	35					30			0.400	1.140	7.070	2.740

HORIZON DATA : BONEKCN - MATRIX LITHOLOGY

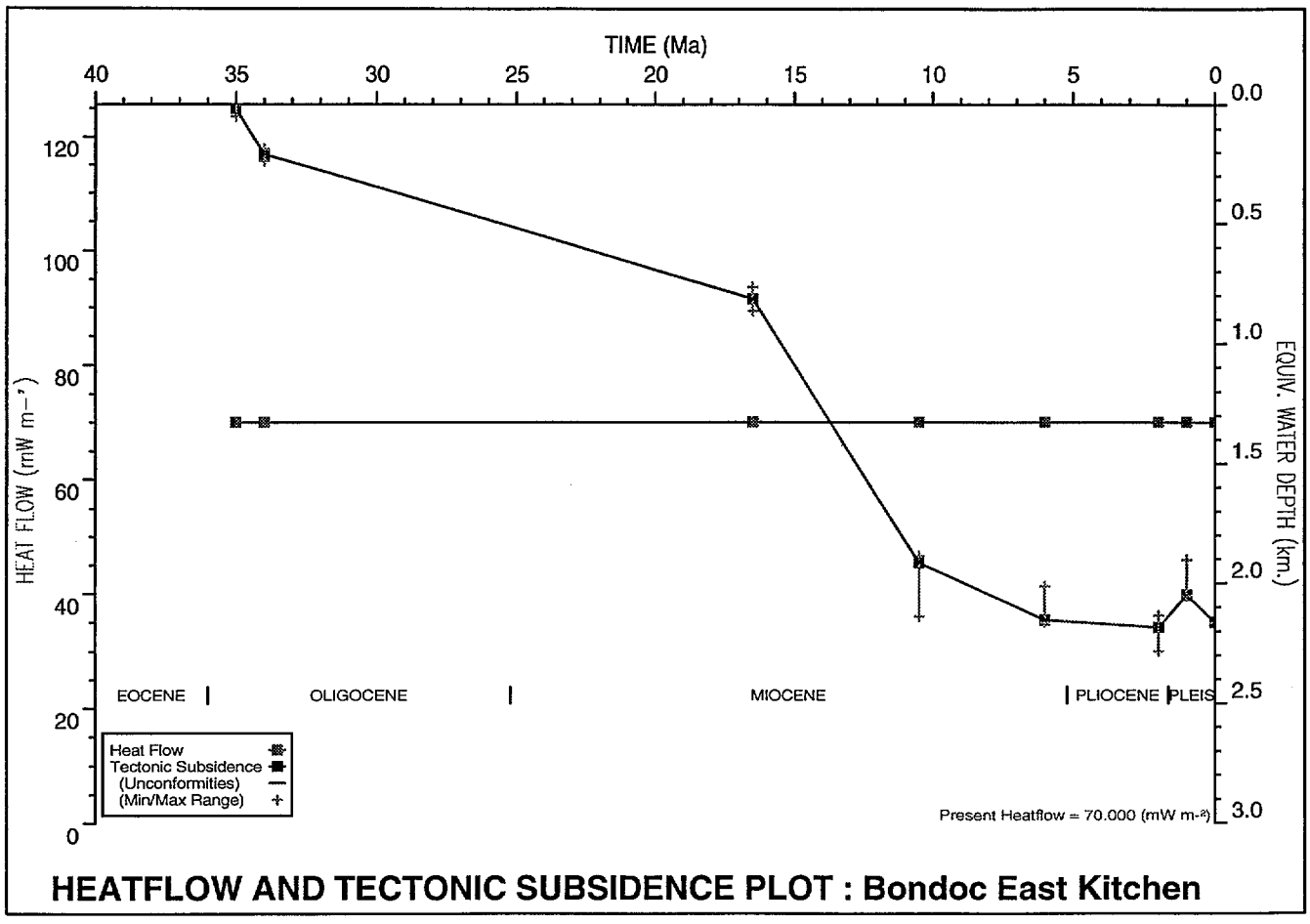

HEATFLOW AND TECTONIC SUBSIDENCE PLOT : Bondoc East Kitchen

The matrix lithology table for the Bondoc Sub-basin kitchen area shows the physical parameters associated with each major unit. The Vigo Formation with its low conductivity acts as a thermal 'blanket' for the whole area, as well as containing regional seals and probable good source rocks.

The subsidence plot shows the rapid development of the sub-basin between 16 and 10 Ma, during which the Vigo Formation was deposited, and the uplift beginning about 2 Ma that resulted in the absence today of the Pliocene Upper Canguinsa Formation. Heatflow must have varied, but its variation is not quantifiable, so it has been held constant at 70 mW/m^2.

BURIAS SUB-BASIN

AGSO 1994

Latitude: 13° 01' 06" N
KB: 0m asl
Surface Temperature: 28°C
BHT: 100°C (hypothetical)
Seismic location: Line 109-55 sp 320

Longitude: 123° 11' 48" E
TD: 3000mKB
Surface Elevation: 139m bsl
BHT Depth: 1700m

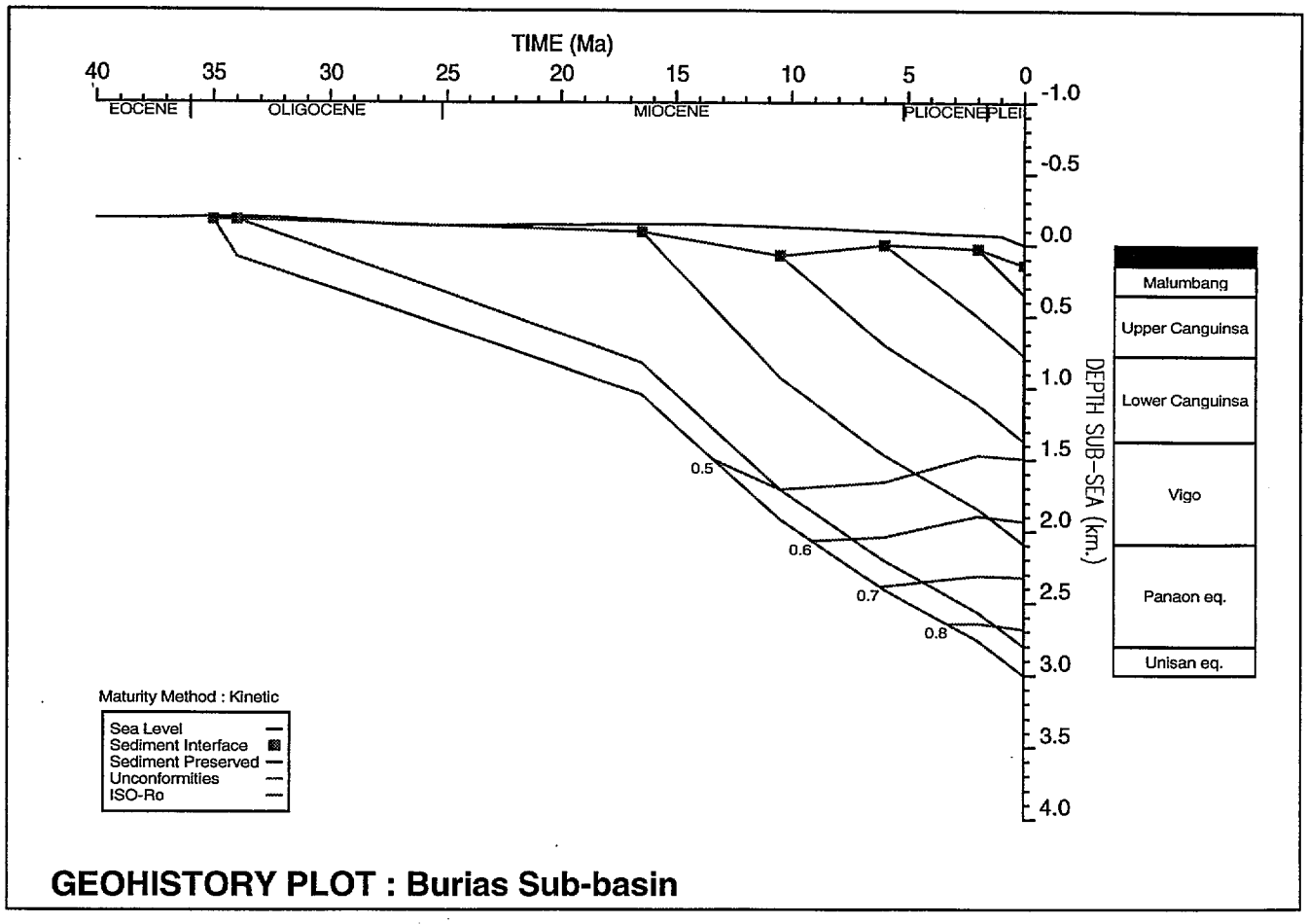

GEOHISTORY PLOT : Burias Sub-basin

The burial history plot of the Burias Sub-basin kitchen (oil generating) area shows that the Vigo Formation is early mature, and that the Panaon equivalent (the Upper Oligocene and Early Miocene) is in the zone of maximum generation of oil.

	Stratigraph. Unit/Event	E V	Depth to Top of Unit	Age (Ma)	Minimum WtrDpth	Maximum WtrDpth	Modelled WtrDpth	Sea Bed Temp.	Heatflow	Lithology Data	Kerogen Data	Variable Beds
1	Malumbang	N	139.00	0.00	139.00	139.00	139.00	28.00	80.00	*		
2	Upper Canguinsa	N	350.00	2.00	50.00	200.00	100.00	28.00	80.00	*		
3	Lower Canguinsa	N	775.00	6.00	50.00	200.00	100.00	28.00	80.00	*		
4	Vigo	N	1370.00	10.50	50.00	300.00	200.00	28.00	80.00	*		
5	Panaon eq.	N	2090.00	16.50	0.00	100.00	50.00	28.00	80.00	*		
6	Unisan eq.	N	2800.00	34.00	0.00	50.00	20.00	28.00	80.00	*		
7	TD	N	3000.00	35.00	0.00	50.00	20.00	28.00	80.00	*		

HORIZON DATA : BURIASKN

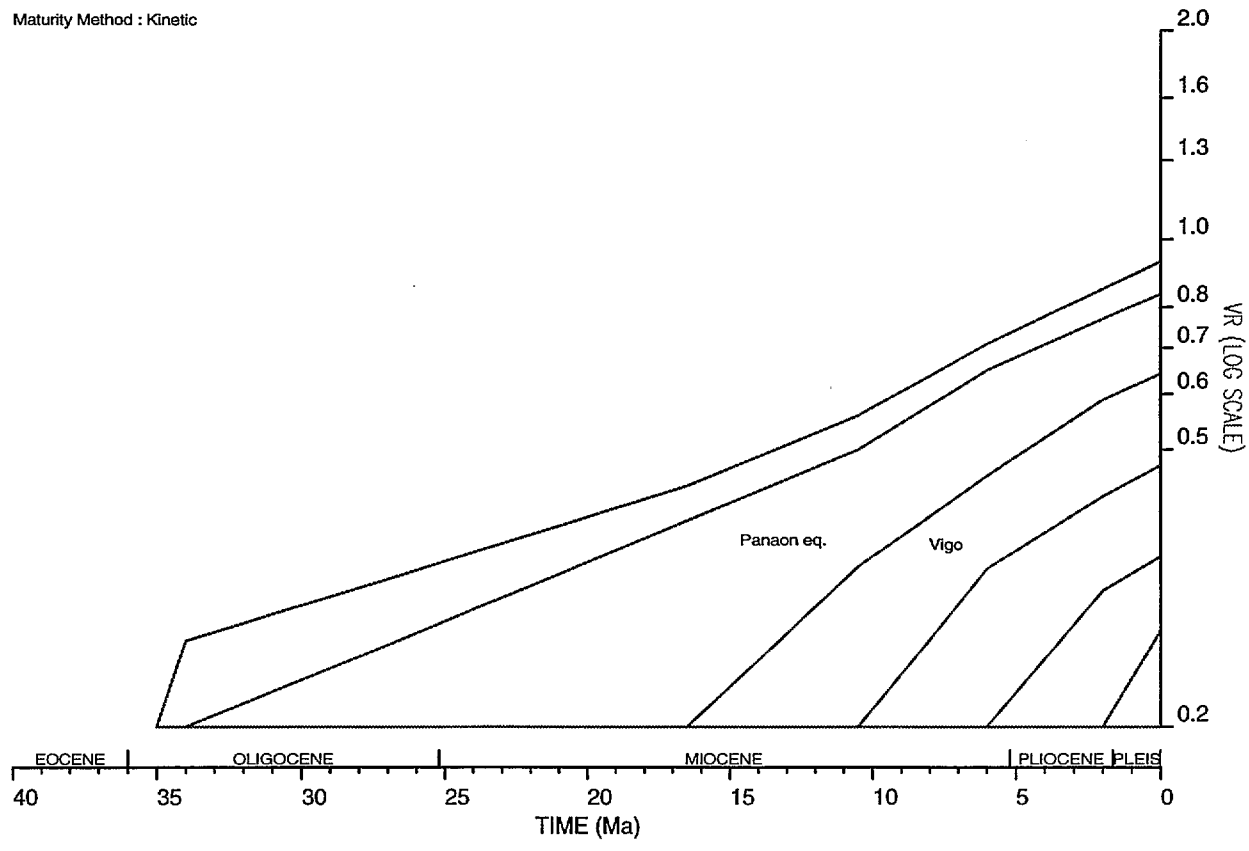

The horizon maturation plot of the Burias Sub-basin shows that the Panaon Formation became early-mature for hydrocarbons at 10Ma and is now at the peak of oil generation. The Vigo Formation is early mature. The overlying Canguinsa Formation is not yet mature for hydrocarbons.

RAGAY SUB-BASIN

AGSO 1994

Latitude: 13° 22'13.2" N
KB: 0m asl
Surface Temperature: 28°C
BHT: 100°C (estimated)
Seismic location: Line 109-45 sp 1750

Longitude: 123° 07'01.8" E
TD: 4500mKB
Surface Elevation:540m bsl
BHT Depth: 2000m

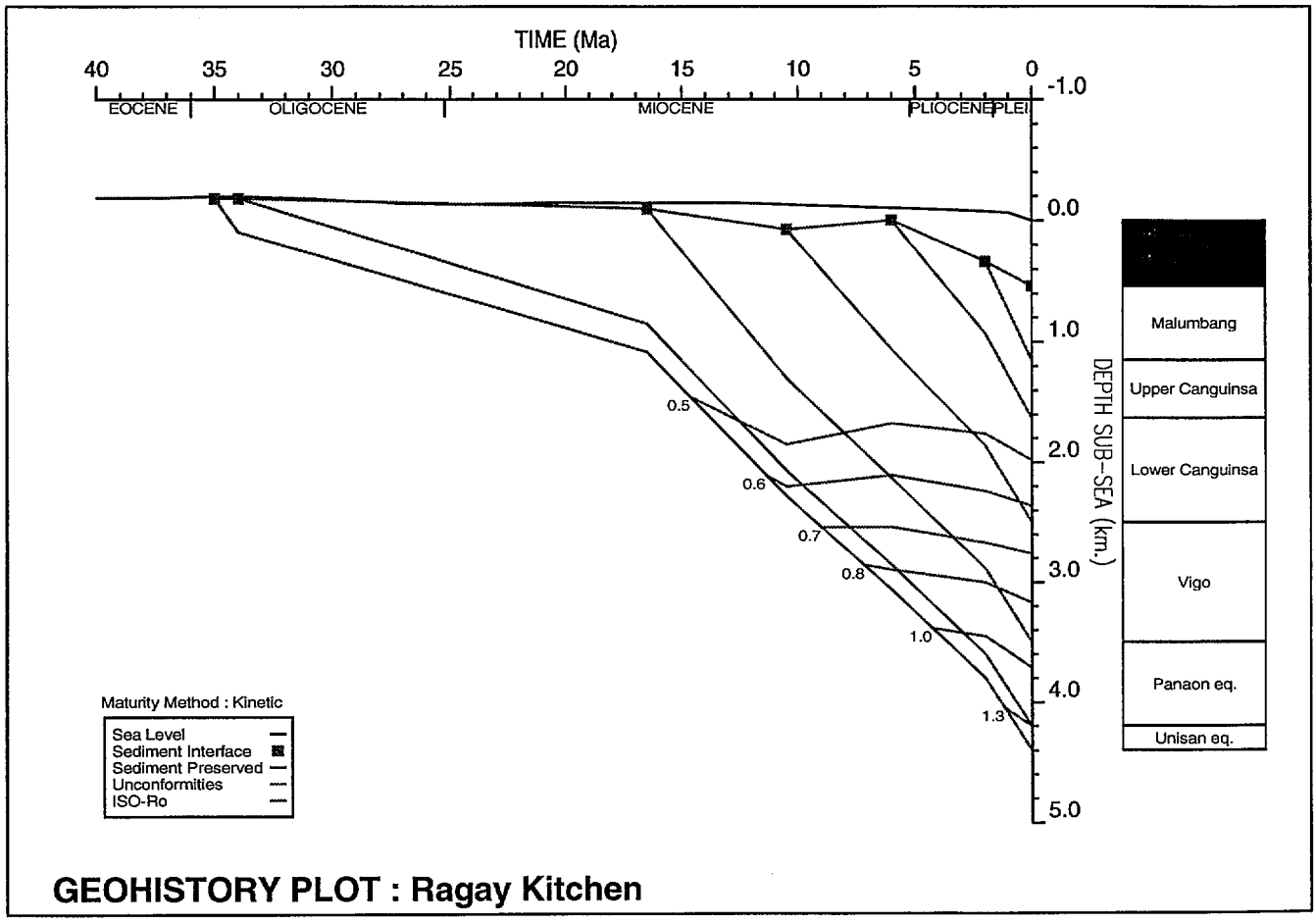

GEOHISTORY PLOT : Ragay Kitchen

The geohistory plot of the Ragay Sub-basin kitchen (oil generating) area shows subsidence beginning in the Early Oligocene and accelerating from the Middle Miocene onward to the present. Unconformities are not evident in this area near the depocenter. Oil generation begins at around 2000m. The Lower Canguinsa formation of Late Miocene age is early-mature for hydrocarbons and the Middle Miocene Vigo formation, containing regional seals and probably major source rocks as well, is near the peak of oil generation. The underlying Panaon equivalent (Lower Miocene and Upper Oligocene) passed through the peak of oil generation during the Pliocene.

	Stratigraph. Unit/Event	E V	Depth to Top of Unit	Age (Ma)	Minimum WtrDpth	Maximum WtrDpth	Modelled WtrDpth	Sea Bed Temp.	Heatflow	Lithology Data	Kerogen Data	Variable Beds
1	Sea Bed	N	540.00	0.00	540.00	540.00	540.00	28.00	80.00	*		
2	Upper Canguinsa	N	1150.00	2.00	300.00	500.00	410.00	28.00	80.00	*		
3	Lower Canguinsa	N	1630.00	6.00	50.00	200.00	100.00	28.00	80.00	*		
4	Vigo	N	2500.00	10.50	50.00	300.00	200.00	28.00	80.00	*		
5	Panaon eq.	N	3500.00	16.50	0.00	100.00	50.00	28.00	80.00	*		
6	Unisan eq.	N	4200.00	34.00	0.00	50.00	20.00	28.00	80.00	*		
7	TD	N	4400.00	35.00	0.00	50.00	20.00	28.00	80.00	*		

HORIZON DATA : RAKICHN2

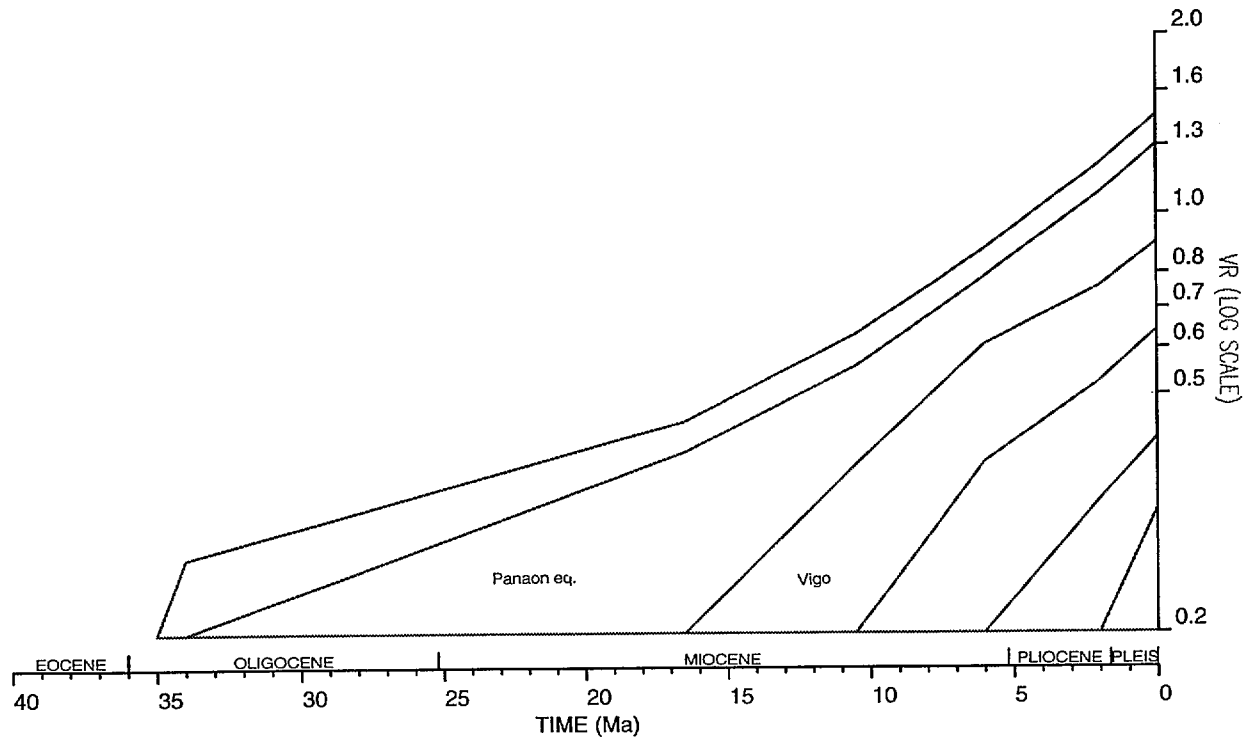

The maturation versus time plot of the Ragay Sub-basin kitchen area shows the base of the Panaon (Upper Oligocene - Lower Miocene) entering the zone of maturity for hydrocarbons at 13 Ma BP, in the Middle Miocene. The base of the Lower Canguinsa formation (Upper Miocene) reaches the threshold of maturity at 2.5 Ma BP. The Upper Canguinsa formation (Pliocene) does not achieve maturity in this model.

TAYABAS BAY

AGSO 1994

Latitude: 13° 27' 01.6" N
KB: 0m asl
Surface Temperature: 28°C
BHT: 100°C (hypothetical)
Seismic location: Line 109-64 sp 800

Longitude: 122° 22' 07.6" E
TD: 5500mKB
Surface Elevation:256m bsl
BHT Depth: 2000m

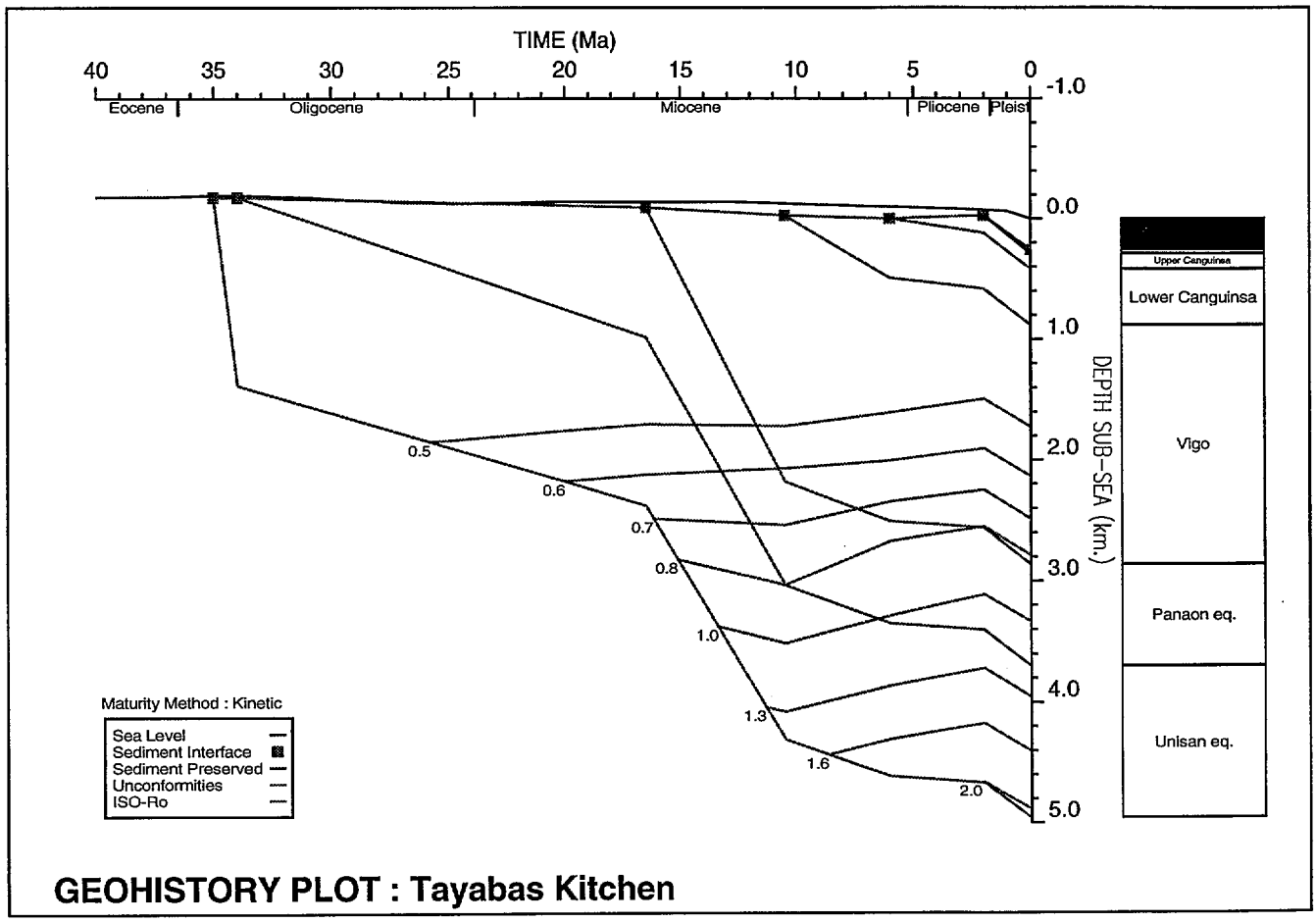

GEOHISTORY PLOT : Tayabas Kitchen

The western part of the Bondoc Sub-basin is the kitchen area for Tayabas Bay. The Lower Vigo and Panaon Formations are at optimum maturity for hydrocarbons, and oil and gas seeps are very abundant on the Bondoc Peninsula. This site lies between the Mulanay and Yuni leads on the northeastern side of the Tayabas Bay Fault.

	Stratigraph. Unit/Event	E V	Depth to Top of Unit	Age (Ma)	Minimum WtrDpth	Maximum WtrDpth	Modelled WtrDpth	Sea Bed Temp.	Heatflow	Lithology Data	Kerogen Data	Variable
1	Malumbang	N	256.00	0.00	256.00	256.00	256.00	28.00	65.00	*		
2	Upper Canguinsa	N	285.00	2.00	0.00	100.00	50.00	28.00	65.00	*		
3	Lower Canguinsa	N	420.00	6.00	50.00	200.00	100.00	28.00	65.00	*		
4	Vigo	N	880.00	10.50	50.00	300.00	100.00	28.00	65.00	*		
5	Panaon eq.	N	2860.00	16.50	0.00	100.00	50.00	28.00	65.00	*		
6	Unisan eq.	N	3700.00	34.00	0.00	50.00	20.00	28.00	65.00	*		
7	TD	N	4960.00	35.00	0.00	50.00	20.00	28.00	65.00	*		

HORIZON DATA : BONWKCN

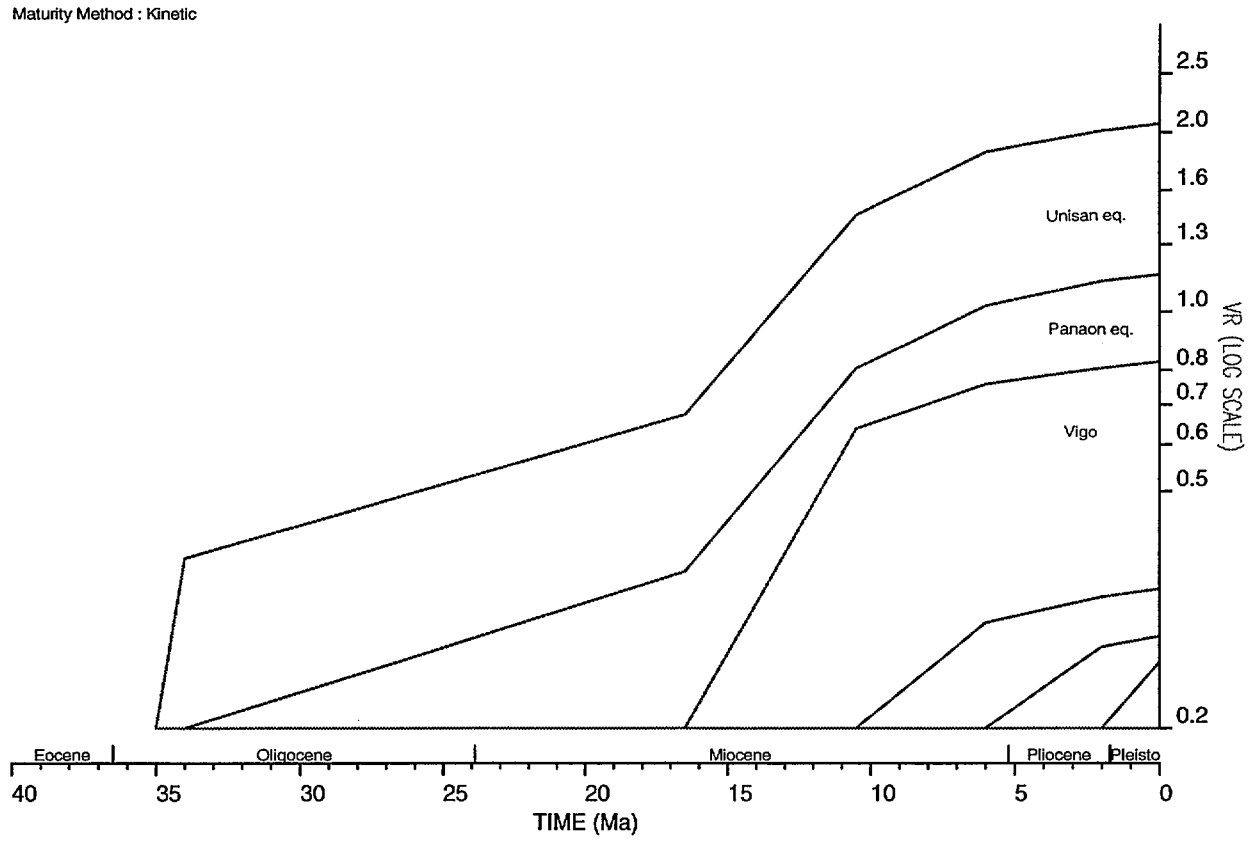

The Maturity versus Time plot for the Tayabas Bay kitchen area shows the Panaon equivalent reaching early maturity for hydrocarbons at 14 Ma BP, and the base of the Vigo Formation likewise at 12 Ma. The base Vigo\top Panaon is now in the optimum maturity zone. The source rock for the widespread shows on the Bondoc Peninsula should lie within either the lower Vigo or the Panaon equivalent formations and is generating oil and gas today.

APPENDIX 3

GEOHISTORY MODELLING OF NORTHEAST PALAWAN SHELF AND CUYO PLATFORM

by

A. M. G. Moore[1]

1 Australian Geological Survey Organisation, Canberra, ACT, Australia

ABSTRACT

Stratigraphic and petroleum-related data for seven wells drilled offshore in northeast Palawan, and on the Cuyo Platform and in southernmost Mindoro and adjacent islands, were compiled and entered into the BURY basin and well analysis program. Model stratigraphic data were also analysed, at three 'kitchen' areas near depocentres. The results of the well and basin history analyses are presented here, and some of the implications for hydrocarbon exploration are discussed.

The study finds that the area has a long history of deposition dating from the Cretaceous, and that the pre Miocene succession was early mature for hydrocarbons as early as theMiddle Miocene. Significant uplift at that time, and the resulting erosion and cooling, halted the evolution of maturity. Subsidence since then has not been sufficient to return the pre-Miocene sediments to their previous depth of burial in high shelf and platform areas. In depocentres, however, e.g. in the Dumaran and Roxas areas downdip from the wells, the succession is now at maximum depth of burial and should be generating hydrocarbons from any source rocks present.

CONTENTS

INTRODUCTION 7

METHOD 7
The BURY Software
The Input Data

RESULTS 9

DISCUSSION 9

CONCLUSIONS 9

REFERENCES 11

WELL DATA
Dumaran 1
Maniguin 1
Mindoro 1
Paly 1
Progreso 1
Roxas 1
Semirara 1

MODEL DATA
Cuyo Kitchen
Dumaran Sub-Basin
Roxas Area

INTRODUCTION

The tectonic and thermal history of the area stretching from the Roxas-1 well offshore northeast Palawan, through the Cuyo Platform to the coasts of Panay and Mindoro, was investigated in this study. Stratigraphic and petroleum-related data for seven wells were compiled and entered into the BURY basin and well analysis program. Bottom-Hole Temperatures (BHTs) were used to estimate the present heatflow (HF). Plots of burial history were made. These and and related parameters such as maturity versus depth, and calculated versus observed values of downhole temperature and vitrinite reflectance, are presented in this report, and some of their implications are discussed. Hypothetical stratigraphic data also was analysed, near three basinal depocentres and at an offshore lead, and the predicted maturation profiles are presented.

The seven wells are listed alphabetically below. They are -

Dumaran 1
Maniguin 1
Mindoro 1
Paly 1
Progreso 1x
Roxas 1 and
Semirara 1.

The model data were as follows -

Cuyo Kitchen (the succession near the depocentre downdip from the Manamoc Lead)

Dumaran Sub Basin (the predicted stratigraphic succession near the depocentre)

Roxas Area (the predicted succession near the depocentre 30 km downdip from the lead).

METHOD

The BURY Software

BURY is a commercial software program developed in Australia since 1978 for the modelling and analysis of burial and thermal histories of well sequences and basins in petroleum exploration (Paltech, 1993). It uses industry standard 1-D models for sediment compaction and decompaction, thermal maturity, and kinetic generation of hydrocarbons from source rock, with default values that can, in many cases, be varied. A useful summary of the theoretical foundations and features of BURY, and comparisons with other similar packages such as MATOIL and BASINMOD, can be found in Radlinski (1991), although the software has continued to evolve since then. The Windows versions 1.2 and 1.3 (WINBURY 1.2 and 1.3) were used in this study.

The Input Data

Data from wells for input to the BURY software came from the well completion reports (WCRs) submitted to the Department of Energy of the Philippines, and related reports which are listed in the references. WCRs are referenced under company name and year.

Model data were derived from seismic interpretation of horizon depths at the specified locations.

Well Header data includes well name, operator and year drilled, latitude and longitude, kelly bushing (KB), ground elevation above sea level or water depth, termination depth (TD), and bottom hole temperature (BHT), estimated basement depth, and an estimated present-day value of heat flow (HF). All depths are related to KB. The present-day surface temperature and past seabed temperatures are given as 28°C.

Horizon Data: Unit age and depth. The age of the top of the first stratigraphic unit in each well is 0 million years (0 My) and the depth to the top is the KB depth of the ground surface - usually just a few metres for onshore wells, more for offshore. Depth to top of units is taken from WCRs. The absolute ages of geological stages are those used in-house by the Australian Geological Survey Organisation. They are broadly compatible with those of Harland et al (1982).

Modelled water depths of deposition of the formations lie normally within the range 0m to 100m, reflecting the inner neritic character of most of the sediments. Unusual conditions during the Middle Miocene have produced depths both above and below this range, being in places negative (subaerial).

Heatflow modelling. BHTs and downhole temperatures measured on logs, together with the thermal conductivities of the formations, were used to calculate the present-day heatflow and geothermal gradient. This provided a reference curve for checking such observations as temperature and vitrinite reflectivity (Ro) versus depth. It is the basis for calculation of the Ro indices on the geohistory plots (e.g. 0.5, 0.7 etc on the plot of Mindoro 1), except where otherwise annotated. Where temperature measurements were not available, e.g. at Maniguin 1, a present day geothermal gradient of 30°C per km depth was assumed, and the BHT and heatflow were estimated from that. The well header has been annotated with '?' to show that there is no measured value. Variation of heatflow with time was used sparingly in this study, because of lack of data, and heatflow is generally kept constant at today's value.

Lithology for the purpose of geohistory modelling is used mainly for calculating the thermal conductivity, density, initial porosity and depth of deposition, and compaction factors of units. In this study it is kept very simple, consisting of three matrix materials, namely sand, clay and limestone. Coal was used as a constituent in kerogen/hydrocarbon conversion estimates, e.g. at Semirara 1.

Unconformities. The constraint generally used in basin history studies to quantify section eroded at unconformities is either the maturity profile, based on measured vitrinite reflectance (Ro) and its equivalents, or/and seismic. Dumaran 1 and Mindoro 1 are examples of the use of vitrinite reflectance to calculate and 'restore' eroded sequences. Vitrinite is a crude measure, as the plot of Mindoro 1 shows.

Other observed data. Kerogen data were available at Mindoro 1 and Semirara 1, and consisted of TOCs determined at a few levels, together with sparse reference to organic matter type. Very little *porosity* data was available.

Hydrocarbon maturity is expressed in terms of the reflectance of vitrinite (Ro). Other measures, such as spore coloration, are translated onto a scale of Ro in the plots generated by this study.

RESULTS

The results of the analysis are presented in the following pages. They consist of plots of measured and expected hydrocarbon maturity (expressed as vitrinite reflectance Ro), temperature and other parameters, plotted against geological time, or depth in the wells, or both. The results are presented for each well in alphanumeric order of well name. There are several plots for each well, beginning with a header containing basic well data such as location and TD, a burial history plot, and a table (Horizon Data) of the basic stratigraphic data used by the BURY program. Comments on features of significance are added to the plots themselves, rather than being collected in the textual portion of this report.

The deepest well stratigraphically is Mindoro 1, which appears to have spudded into Jurassic rocks below the surface sediments in the weathered zone.

Data are presented separately for the successions at the so-called 'kitchen' areas near local depocentres.

DISCUSSION

Some areas have a long depositional history, extending back to the Cretaceous. Because of the major unconformity in the Middle Miocene, a lot of that history has been lost through erosion. This is reflected in the burial history (the geohistory plot) of Roxas 1, for example. The flat profile from 75 Ma to 26 Ma reflects not so much the tectonic history of the area, as our ignorance of it. A notable feature of the burial history curves at Dumaran, Paly and Roxas wells is an apparent reversal of the usual pattern of rifted continental margins whereby basin subsidence decreases with time. This is remarked on in the plot of Paly 1. The extra subsidence required to accommodate the Middle Miocene prograding sequence which is so prominent on seismic, and the uplift on the shelf which supplied a large amount of sediment quickly, indicate unusual conditions, perhaps depression of the margin by loading on the seaward side, and uparching of the adjacent land in a 'forebulge'. This increased early Middle Miocene subsidence is closely followed by marked uplift and erosion. The justification for this feature of the burial curves is the vitrinite reflectance, e.g. at Dumaran, which is much higher than it should be in the moderate heat environment at the site.

CONCLUSIONS

Analysis of the burial history of the area from northeast Palawan to Mindoro, based on stratigraphic data in wells, and vitrinite reflectance in well samples, shows that the thickness of the sedimentary succession prior to the mid Miocene unconformity was sufficient to allow the onset of maturity for hydrocarbons. Migration is thought to have begun as early as latest Oligocene time, and certainly during the early part of the Middle Miocene. The area was subjected to downwarping, and then strong uplift, during the Early and Middle Miocene, and a large amount of erosion, exceeding one kilometre, occurred. This could have been a consequence of collision of the rifted continental margin of the Kalayaan-Calamian microplate with the volcanic island arc. The uplift and erosion that accompanied the Middle Miocene unconformity would have caused disturbance and re-direction of migration. It is important that traps should be already in existence and charged with hydrocarbons before these events

Subsidence since the mid Miocene has not been enough in most of the area to return the sediments to the state of maturity they were in before the uplift and erosion. This means that generation of hydrocarbons stopped in the Middle Miocene and has not resumed, except in the deeper parts of the area, the Dumaran and Roxas 'kitchens' downdip from the wells. In the Cuyo area even the deepest parts (the Cuyo 'Kitchen') have only recently subsided below the level that obtained prior to the unconformity, and generation may have resumed in the Pleistocene.

Traps recently formed (post Middle Miocene) are less prospective than ones that predate the regional unconformity, but they may be in a position to receive the smaller amount of hydrocarbons that are now being generated in the deeper parts of the Cuyo, Dumaran and Roxas 'kitchens' near the present depocentres.

REFERENCES

CITCO PHILIPPINES PETROLEUM CORP., 1979. Final Well Report, Roxas#1 (unpublished).

CITCO PHILIPPINES PETROLEUM CORP., 1980. Final Well Report, Dumaran-1 (unpublished).

CITCO PHILIPPINES PETROLEUM CORP., 1982. Final Well Report, Paly No.1 (unpublished).

HARLAND, W.B., Cox, A.V., Llewellyn, P.G., Pickton, C., Smith, A. & Walters, R., 1982. A Geologic Time Scale. Cambridge University Press.

PALTECH, 1993: BURY for WINDOWS (WINBURY) User Manual. Paltech Pty Ltd., Sydney, Australia.

RADLINSKI, A. 1991. An Analysis of Methodology Used in Commercial Geohistory and Geochemistry Programs: Bury 5.41, Basinmod 2.55 and Matoil 1.4. BMR (now AGSO) Record 1991/110. 46p.

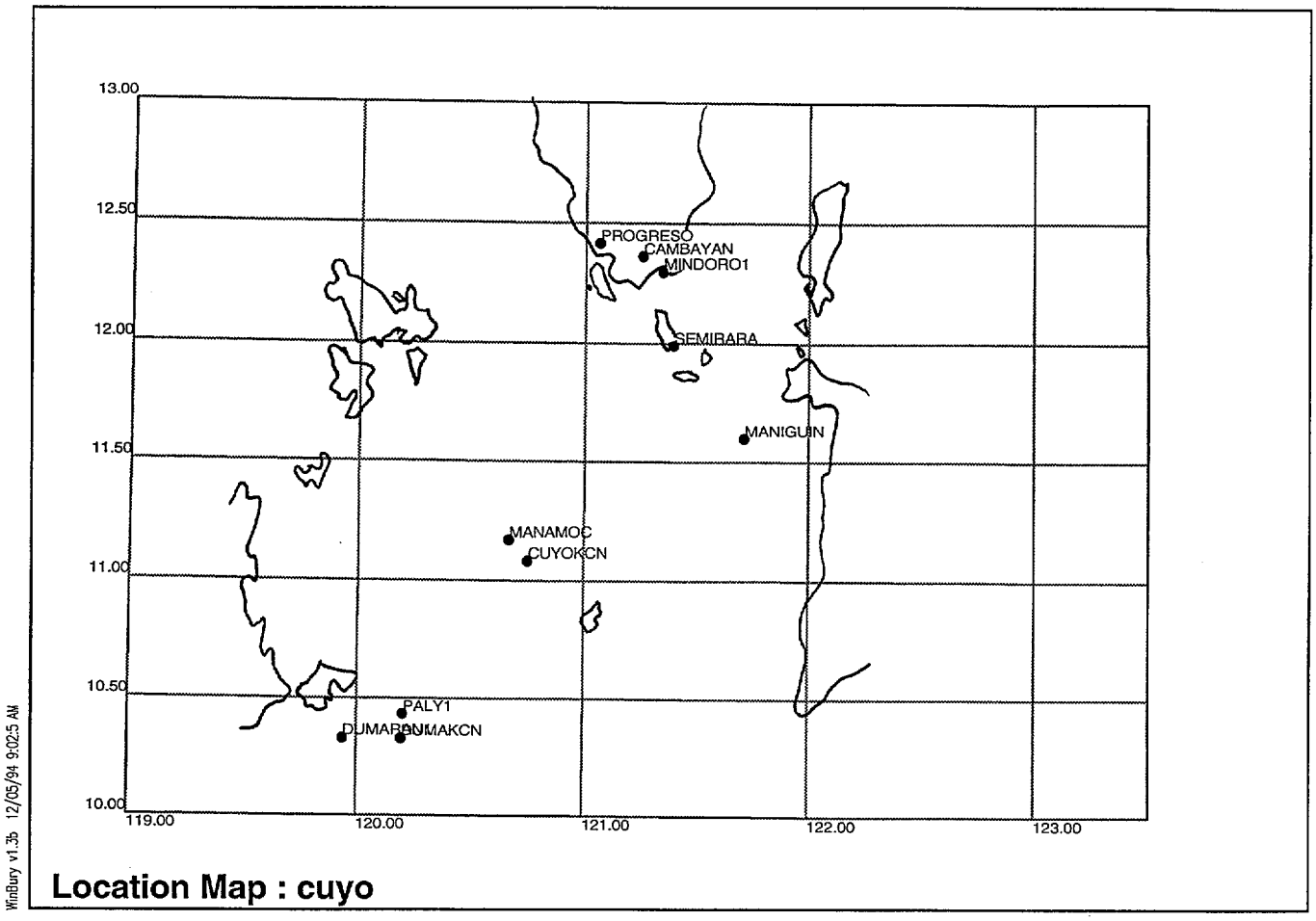

The relative locations of wells and basinal depocentres (hydrocarbon 'kitchen areas') in the northwest Palawan and Cuyo areas are shown on the location map. Part of the coastline of Palawan appears on the left, Panay on the right, Mindoro at the top.

The Manamoc Lead on the Cuyo Platform lies northwest of the local depocentre, the Cuyo 'kitchen area' (CUYOKCN) in the centre of the map. The Dumaran 'kitchen area' (DUMAKCN) lies south of Paly 1 well and east of Dumaran 1.

DUMARAN 1

CITCO 1979

Latitude: 10° 19' 36.58" N
KB: ?10m asl
Surface Temperature: 28°C
BHT: 86°C (extrapolated)

Longitude: 119° 56' 22" E
TD: 1882mKB
Water Depth: 87m
BHT Depth: 1879m

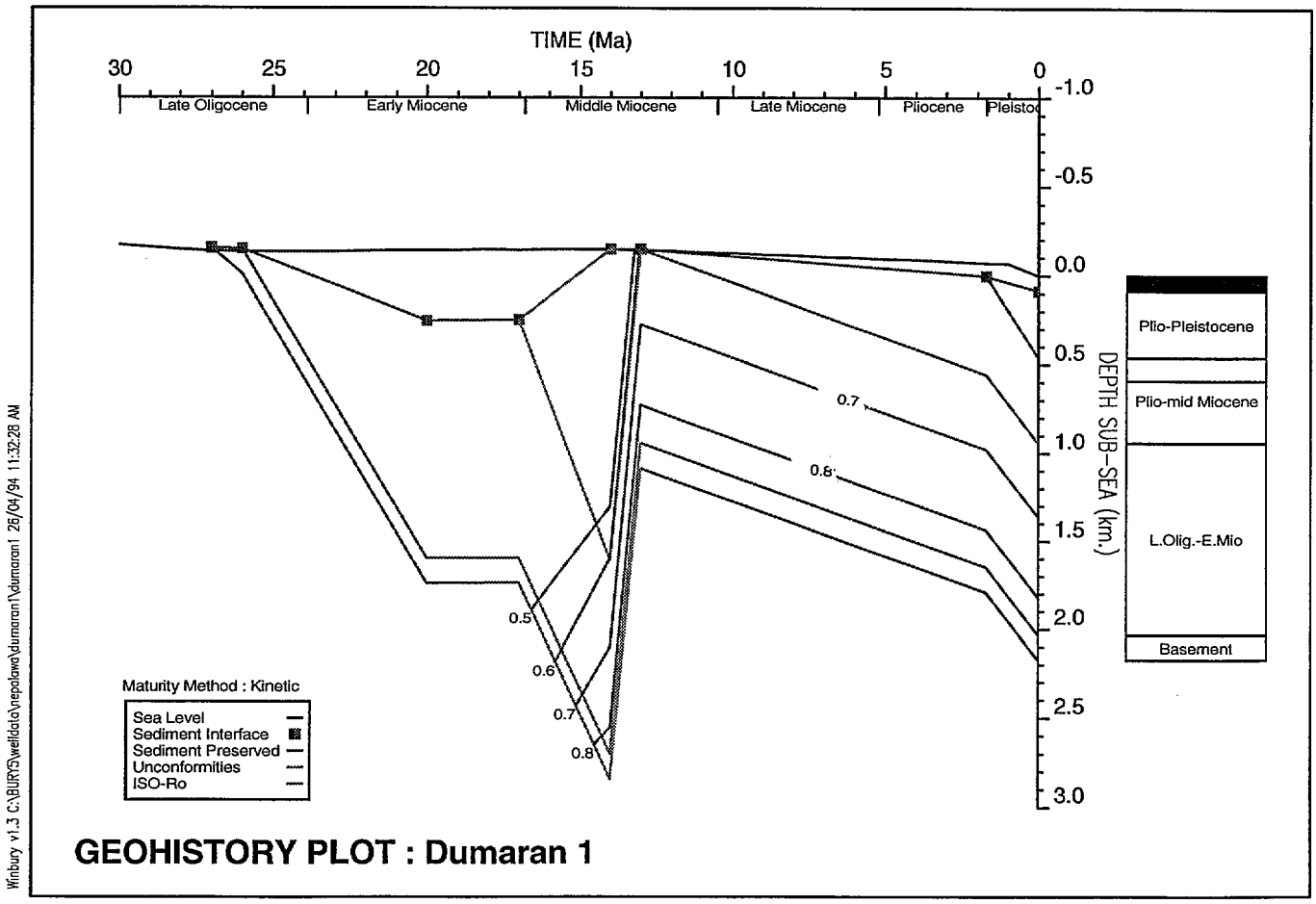

GEOHISTORY PLOT : Dumaran 1

The geohistory diagram for Dumaran 1 well shows the base of the sedimentary succession entering the zone of major generation of hydrocarbons. The well had significant gas shows throughout the sedimentary succession below the Middle Miocene unconformity. The target reservoir was absent, with basement in place of the hoped-for Miocene carbonate reef.

	Stratigraph. Unit/Event	E V	Depth to Top of Unit	Age (Ma)	Minimum WtrDpth	Maximum WtrDpth	Modelled WtrDpth	Sea Bed Temp.	Heatflow	Lithology Data	Kerogen Data	Variable Beds
1	Plio-Pleistocene	N	95.71	0.00	85.95	85.95	85.95	27.78	57.00			
2	Plio-mid Miocene	N	472.45	1.70	15.24	91.44	76.20	27.78	60.00			
3	Mid Miocene unconf	E	952.51	13.00	-15.24	0.00	-6.10	27.78	70.00			
4	Deposit A3	E	(800.00)	14.00	0.00	198.12	0.01	27.78	70.00			
5		N	600.00	17.00	-15.24	400.00	394.15	27.78	70.00			
6	L.Olig.-E.Mio	N	952.51	20.00	-15.24	400.00	394.15	27.78	70.00			
7	Basement	N	2043.40	26.00	-15.24	-15.24	-15.24	27.78	70.00			
8	TD	N	2186.05	27.00	-15.24	-15.24	-15.24	27.78	70.00			

HORIZON DATA : DUMARAN1

	Stratigraph. Unit/Event	SHALE	SAND	CHALK	LST	COAL	HALIT	VOLCS	CONV					
	Plio-Pleistocene		10		90						0.400	1.120	10.480	2.740
	Plio-mid Miocene	50	50								0.550	1.420	8.580	2.730
	Mid Miocene unconf	50	50								0.550	1.420	8.580	2.730
	Deposit A3	90	10								0.670	2.230	5.210	2.780
		30	70								0.490	1.010	11.010	2.690
	L.Olig.-E.Mio	30	70								0.490	1.010	11.010	2.690
	Basement							100			0.050	0.500	4.500	2.760
	TD							100			0.050	0.500	4.500	2.760

HORIZON DATA : DUMARAN1 - MATRIX LITHOLOGY

The input data for the geohistory model of Dumaran 1 shows the parameters used for each layer.There is an unconformity spanning the period from 20 to 13 Ma.
In this model, sedimentation is assumed to have continued during the period 17 to 14 Ma, to a thickness of 800m, then to have been eroded following uplift resulting from plate collision during the Middle Miocene, 14 to 13 Ma BP.This brings the model into agreement with measured vitrinite reflectance, shown on the observed vs computed maturity plot over page.

The Bed Temperature Plot shows the Late Oligocene - Early Miocene being heated by burial to well over 100°C during the early Middle Miocene, then cooled again by uplift accompanied by erosion during the mid Middle Miocene. It has never since reached that maximum depth of burial.
The Horizon Maturation Plot shows maturity being reached during the Middle Miocene, and remaining at the same level since then. Generation and migration of hydrocarbons occurred during the Middle Miocene. Generation has probably not occurred since.

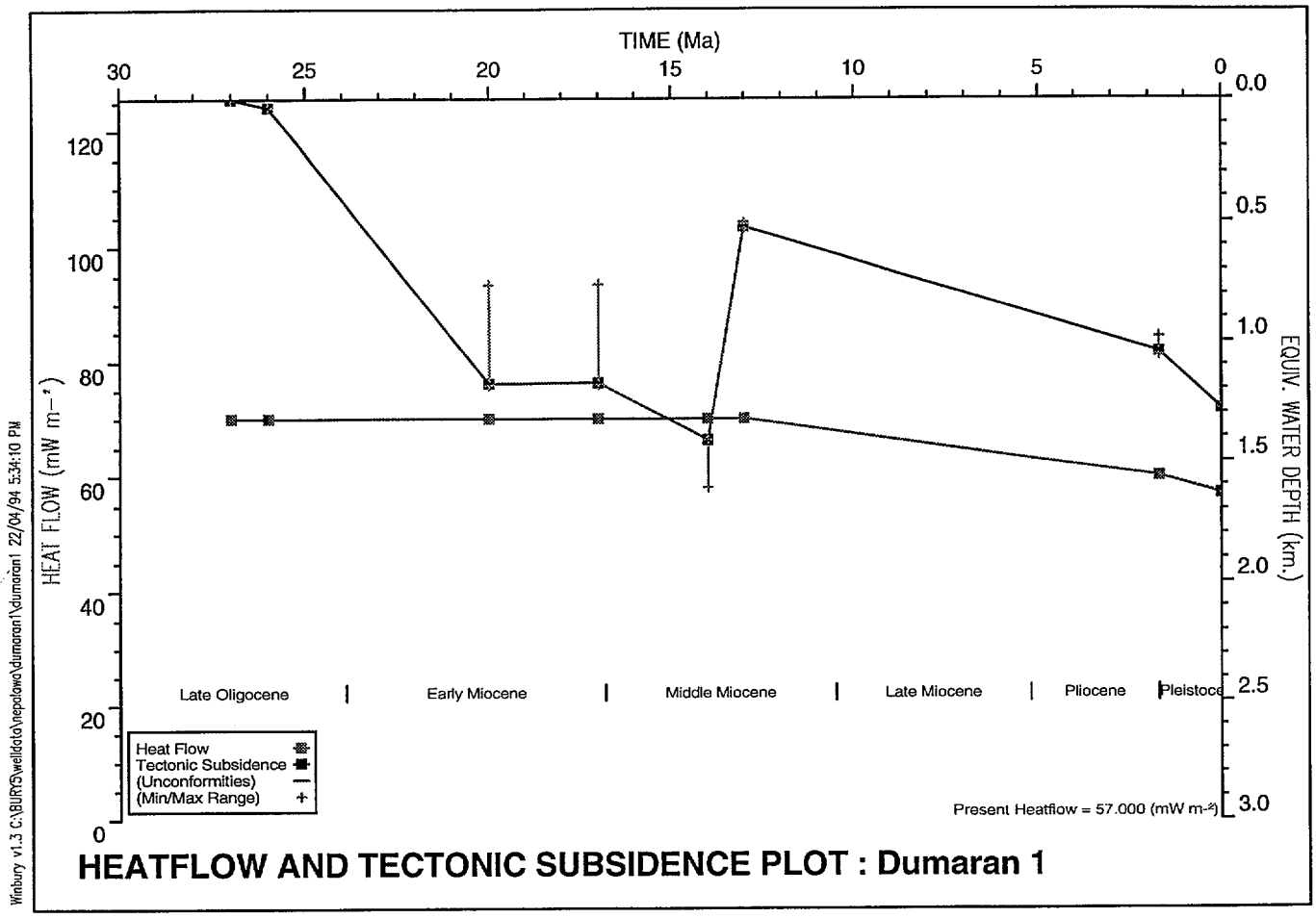

HEATFLOW AND TECTONIC SUBSIDENCE PLOT : Dumaran 1

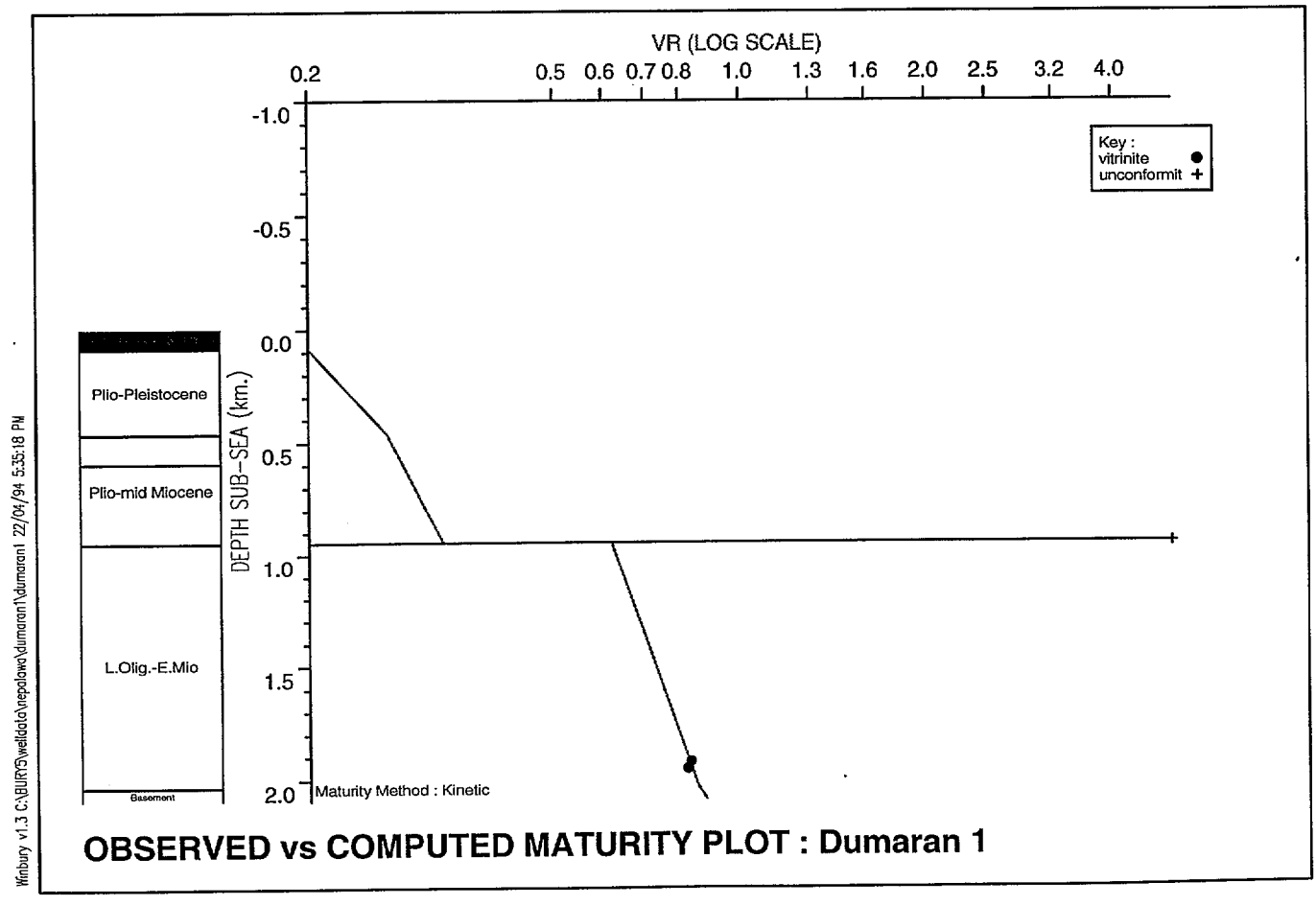

OBSERVED vs COMPUTED MATURITY PLOT : Dumaran 1

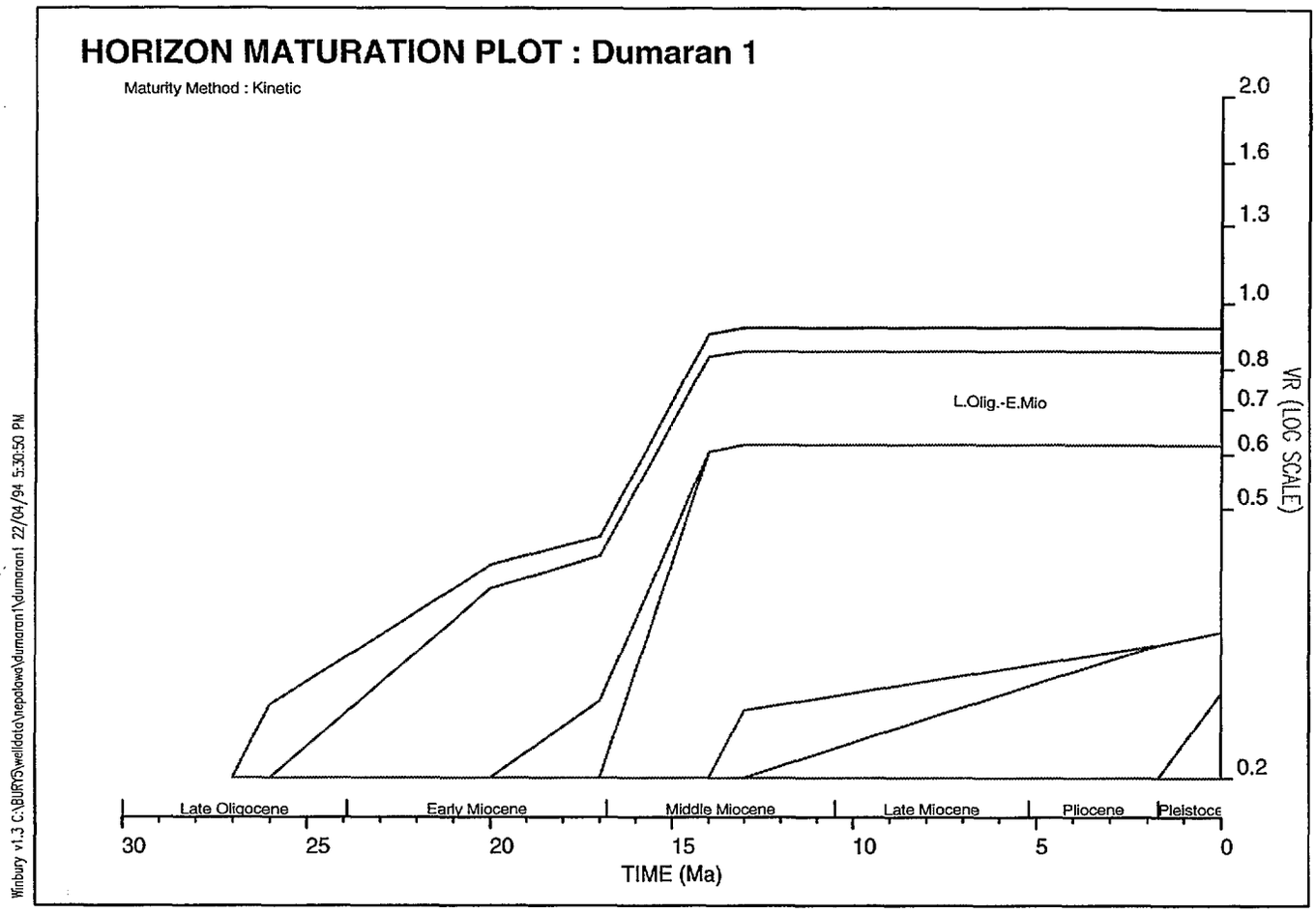
HORIZON MATURATION PLOT : Dumaran 1
Maturity Method : Kinetic
2.0
1.6
1.3
1.0
0.8
0.7
0.6
0.5
0.2
VR (LOG SCALE)
L.Olig.-E.Mio
Late Oligocene
Early Miocene
Middle Miocene
Late Miocene
Pliocene
Pleistoce
30
25
20
15
10
5
0
TIME (Ma)
Winbury v1.3 C:\BURYS\welldata\nepalowa\dumaran1\dumaran1 22/04/94 5:30:50 PM

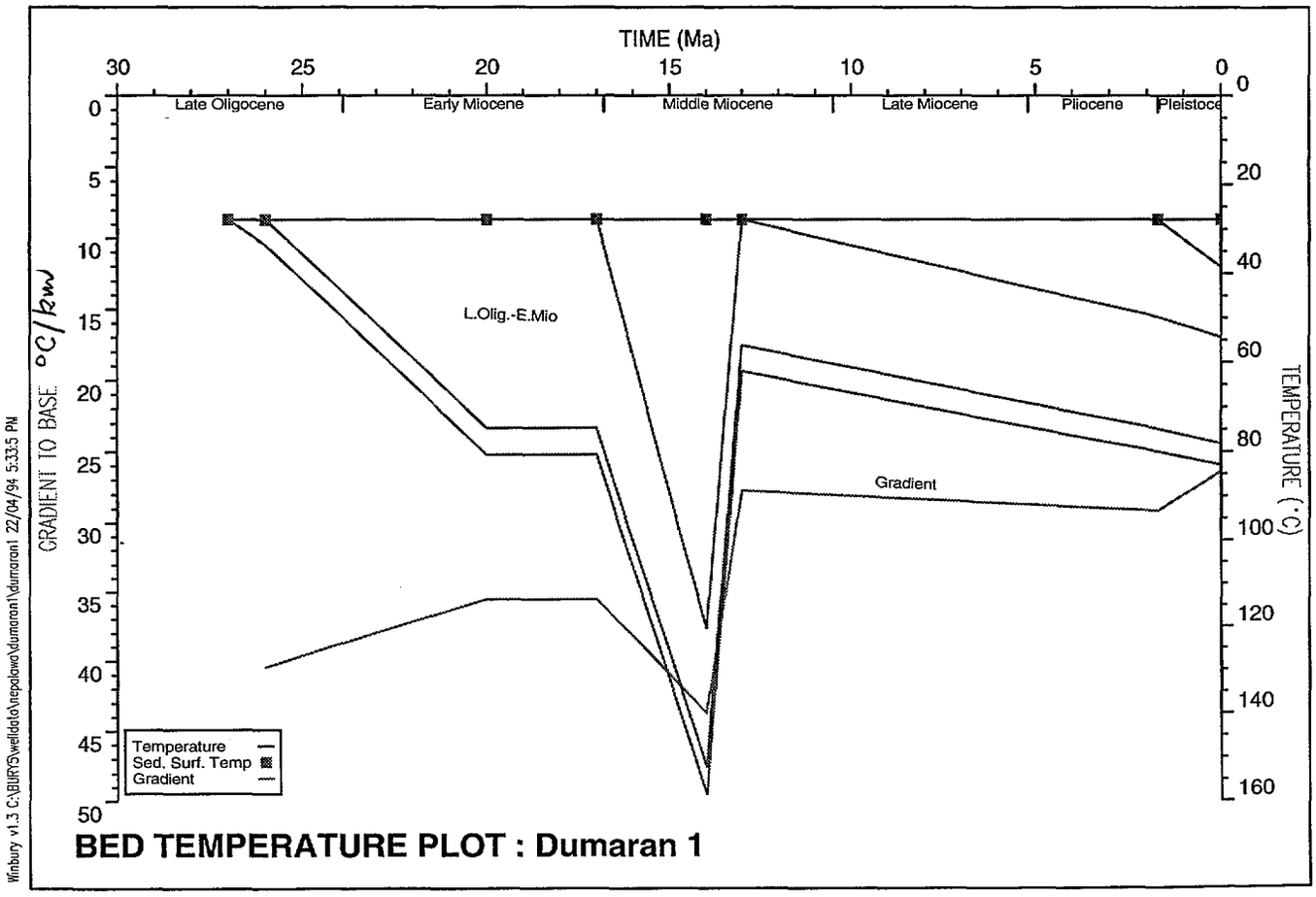
TIME (Ma)
30
25
20
15
10
5
0
Late Oligocene
Early Miocene
Middle Miocene
Late Miocene
Pliocene
Pleistoce
GRADIENT TO BASE °C/km
TEMPERATURE (°C)
L.Olig.-E.Mio
Gradient
Temperature
Sed. Surf. Temp
Gradient
BED TEMPERATURE PLOT : Dumaran 1
Winbury v1.3 C:\BURYS\welldata\nepalowa\dumaran1\dumaran1 22/04/94 5:33:5 PM

MANIGUIN 1

PHILLIPS 1982

Latitude: 11° 35' 51" N
KB: 31m asl
Surface Temperature: 28°C
BHT: ? (79°C)

Longitude: 121° 42' 49" E
TD: 1690mKB
Water depth: 122m
BHT Depth: 1690m

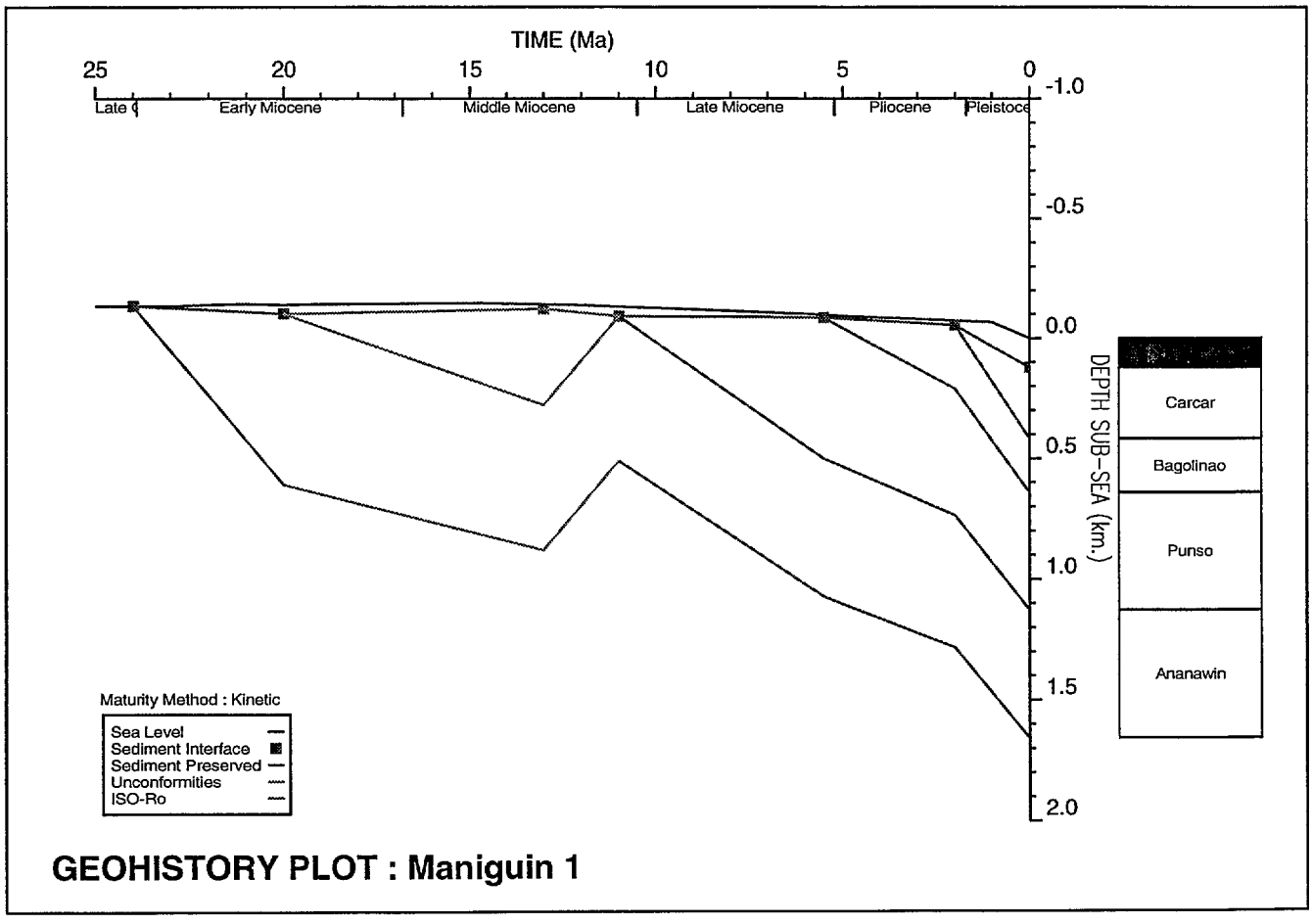

GEOHISTORY PLOT : Maniguin 1

The geohistory diagram for Maniguin 1 well shows a simple burial history beginning in the Early Miocene and interrupted by an unconformity spanning the period from 20 to 10 Ma. During this period (from early to middle Miocene), sediments are assumed to have been deposited in shallow water to a thickness of 400m, then eroded during the succeeding uplift at about the end of the Middle Miocene (see Horizon Data table over page). The absence of vitrinite reflectance contours on this plot indicates that the section is immature for hydrocarbons, nowhere exceeding a Ro of 0.5.

MINDORO 1

BP/INTERPORT 1979

Latitude: 12° 17' 52" N
KB: 5m asl
Surface Temperature: 28°C
BHT: 71°C

Longitude: 121° 20' 50" E
TD: 1524mKB
Surface Elevation:2m asl
BHT Depth: 1524m

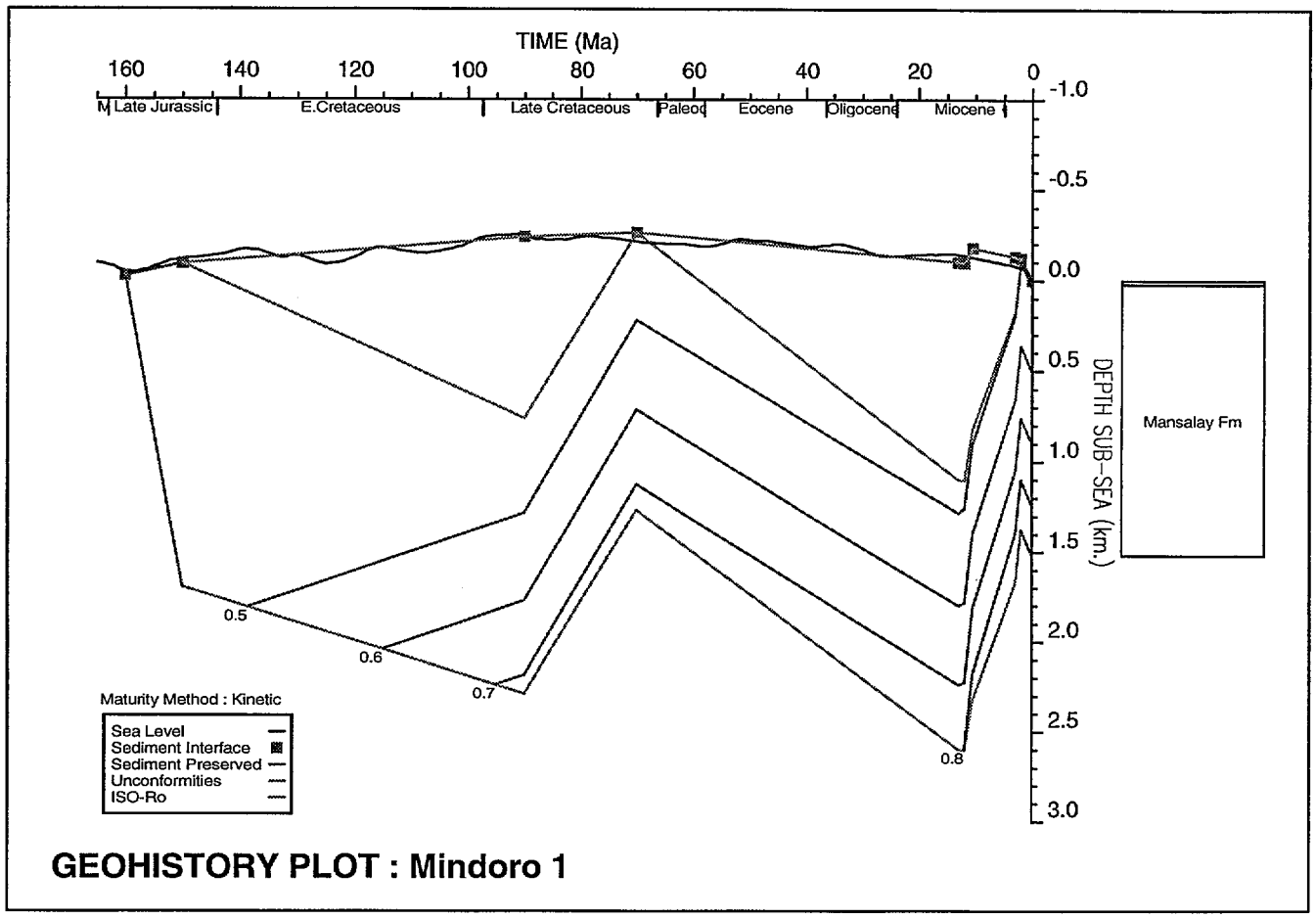

The geohistory plot for Mindoro 1 shows episodes of uplift in the Late Cretaceous, and in the Middle Miocene to Pleistocene This model brings calculated maturity into agreement with measured vitrinite reflectance.

	Stratigraph. Unit/Event	E V	Depth to Top of Unit	Age (Ma)	Minimum WtrDpth	Maximum WtrDpth	Modelled WtrDpth	Sea Bed Temp.	Heatflow	Lithology Data	Kerogen Data	Variable Beds
1	Quaternary	N	5.00	0.00	0.00	0.00	0.00	28.00	60.00	*		
2	Pleistocene uplift	E	25.00	2.00	-50.00	50.00	-50.00	28.00	60.00	*		
3	Deposit 1	E	(300.00)	3.00	-50.00	50.00	-50.00	28.00	60.00	*		
4	Mid Miocene uplift	E	(500.00)	10.50	-50.00	50.00	-50.00	28.00	70.00	*		
5	Deposit 2a	E	(1200.00)	12.00	-50.00	50.00	39.32	28.00	70.09	*		
6	Deposit 2	E	(1200.00)	13.00	-50.00	50.00	39.32	28.00	70.00	*		
7	Cretaceous uplift	E	25.00	70.00	0.00	50.00	25.00	28.00	70.00	*		
8	Deposit 3	E	(500.00)	90.00	0.00	50.00	25.00	28.00	60.03	*		
9	Mansalay Fm	N	25.00	150.00	0.00	50.00	25.00	28.00	59.68	*		
10	TD	N	1524.00	160.00	0.00	50.00	25.00	28.00	60.00	*		

HORIZON DATA : MINDORO1

	Stratigraph. Unit/Event	SHALE	SAND	CHALK	LST	COAL	HALIT	VOLCS	CONV		Initial Porosity	Por/Depth Factor	Conductivity	Density
	Quaternary		100								0.400	0.400	16.000	2.650
	Pleistocene uplift	75	25								0.630	1.920	6.280	2.760
	Deposit 1	75	25								0.630	1.920	6.280	2.760
	Mid Miocene uplift	75	25								0.630	1.920	6.280	2.760
	Deposit 2a	75	25								0.630	1.920	6.280	2.760
	Deposit 2	75	25								0.630	1.920	6.280	2.760
	Cretaceous uplift	55	43		2						0.560	1.530	7.990	2.730
	Deposit 3	55	43		2						0.560	1.530	7.990	2.730
	46m - 320m	55	43		2						0.560	1.530	7.990	2.730
	Mansalay Fm	55	43		2						0.560	1.530	7.990	2.730
	793m - 1098m	55	43		2						0.560	1.530	7.990	2.730
	1098m - 1524m	55	43		2						0.560	1.530	7.990	2.730
	TD	55	43		2						0.560	1.530	7.990	2.730

HORIZON DATA : MINDORO1 - MATRIX LITHOLOGY

Model 2

The figures in brackets show hypothetical deposits now eroded at unconformities.

A surprising amount of this 'stripping' was required in order to bring the calculated vitrinite reflectivity into agreement with observed values at Mindoro 1 The header sheet for the well shows the resulting plot of burial history.

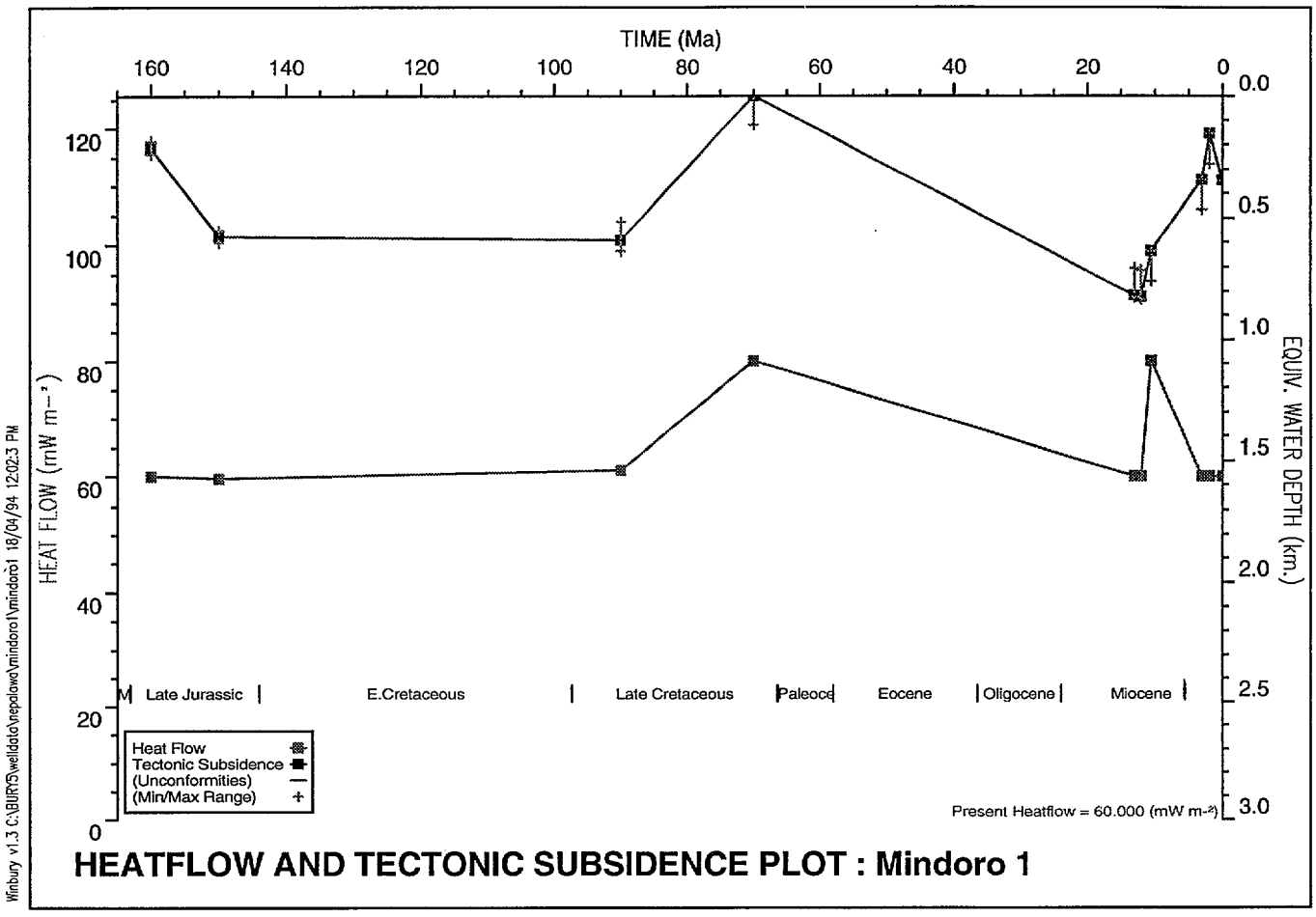

HEATFLOW AND TECTONIC SUBSIDENCE PLOT : Mindoro 1

Winbury v1.3 C:\BURYS\welldata\vepalawa\vmindoro1\vmindoro1 18/04/94 12:02:3 PM

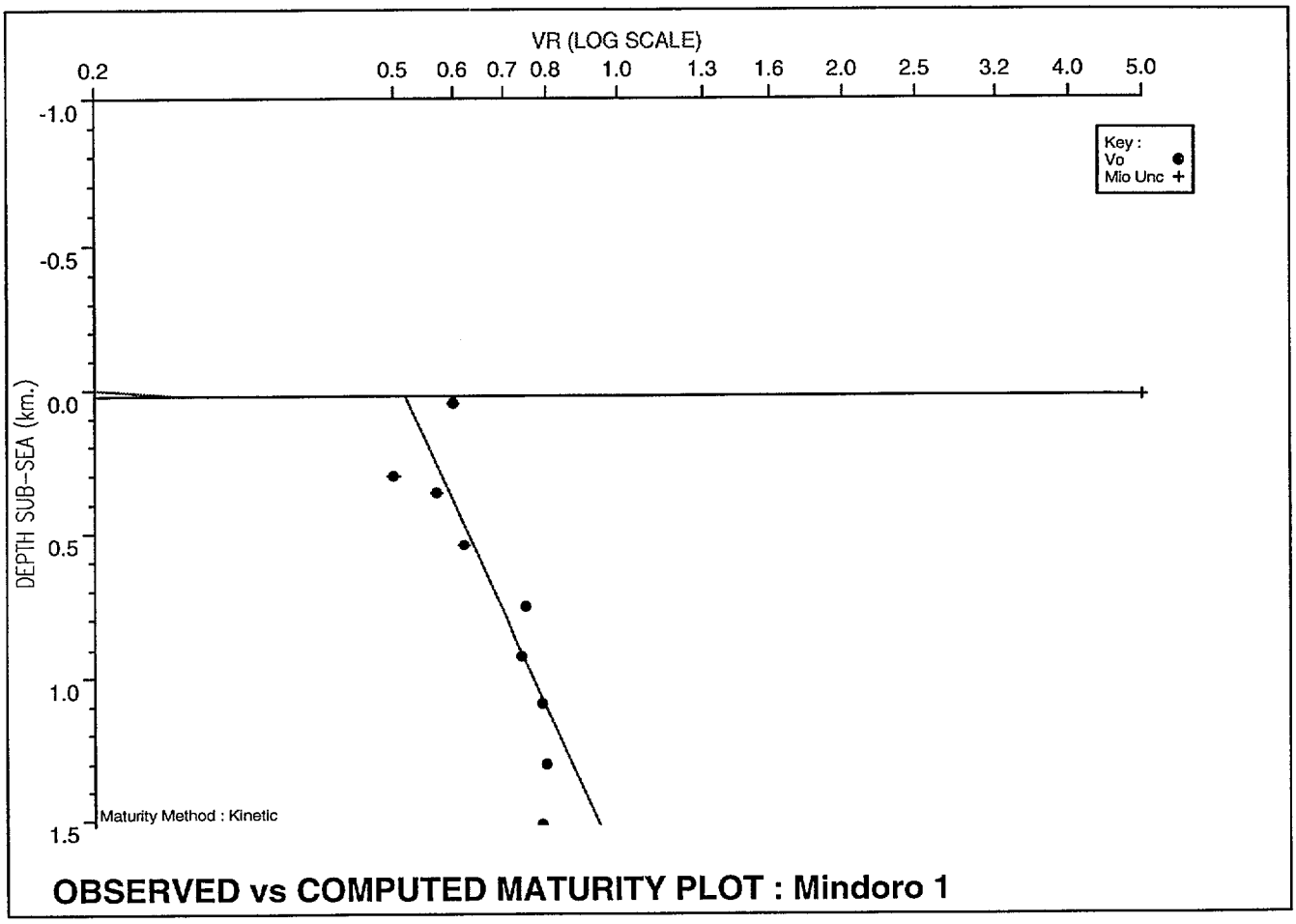

OBSERVED vs COMPUTED MATURITY PLOT : Mindoro 1

	Sample Depth	T P	Average Maturity	Minimum Maturity	Maximum Maturity	F L
1	51.00	0	0.60	0.59	0.61	0
2	306.00	0	0.50	0.49	0.51	0
3	366.00	0	0.57	0.56	0.58	0
4	549.00	0	0.62	0.61	0.63	0
5	764.00	0	0.75	0.74	0.76	0
6	928.00	0	0.74	0.73	0.75	0
7	1096.00	0	0.79	0.78	0.80	0
8	1310.00	0	0.80	0.79	0.81	0
9	1522.00	0	0.79	0.78	0.80	0

MATURITY DATA : MINDORO1

The computed maturity (sloping line) of the succession at Mindoro 1, based on the parameters displayed in Model 2 and on the header sheet, is in good agreement with the maturity observed in samples measured for vitrinite reflectance (dots).

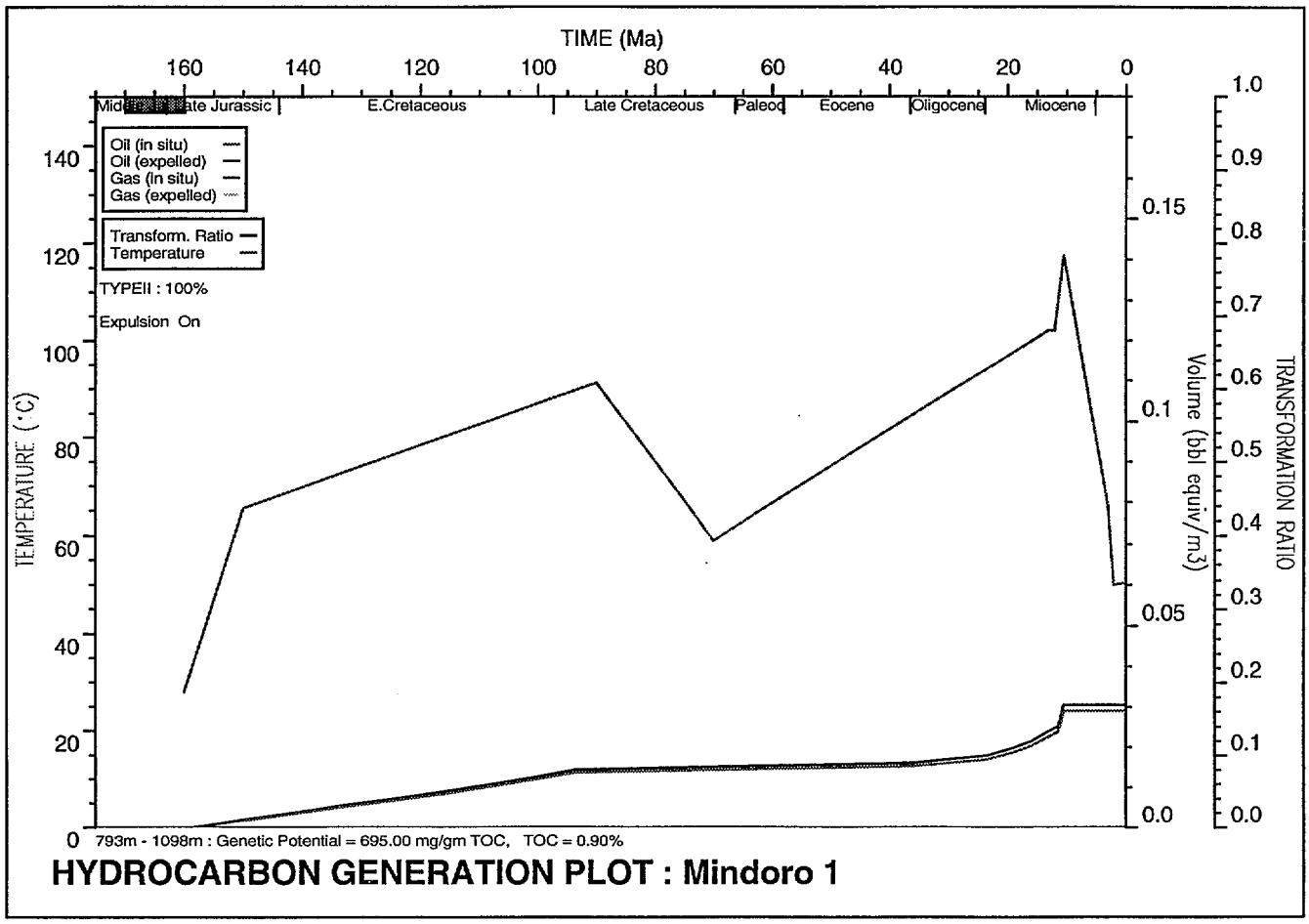

HYDROCARBON GENERATION PLOT : Mindoro 1

Winbury v1.3 C:\BURY5\welldata\nepalawa\mindoro1\mindoro1 18/04/94 11:47:5 AM

	Stratigraph. Unit/Event	TYPEIII	TYPEII	Expulsion	TOC
9	46m - 320m	100		On	1.080
11	793m - 1098m		100	On	0.930
12	1098m - 1524m		100	On	0.580

HORIZON DATA : MINDORO1 - KEROGEN COMPONENTS

PALY 1

CITCO 1981

Latitude: 10° 25' 57.8" N
KB: 27m asl
Surface Temperature: 28°C
BHT: 92°C (e-log, extrapolated)

Longitude: 120° 12' 22.6" E
TD: 2098mKB
Water Depth:150m
BHT Depth: 2096m

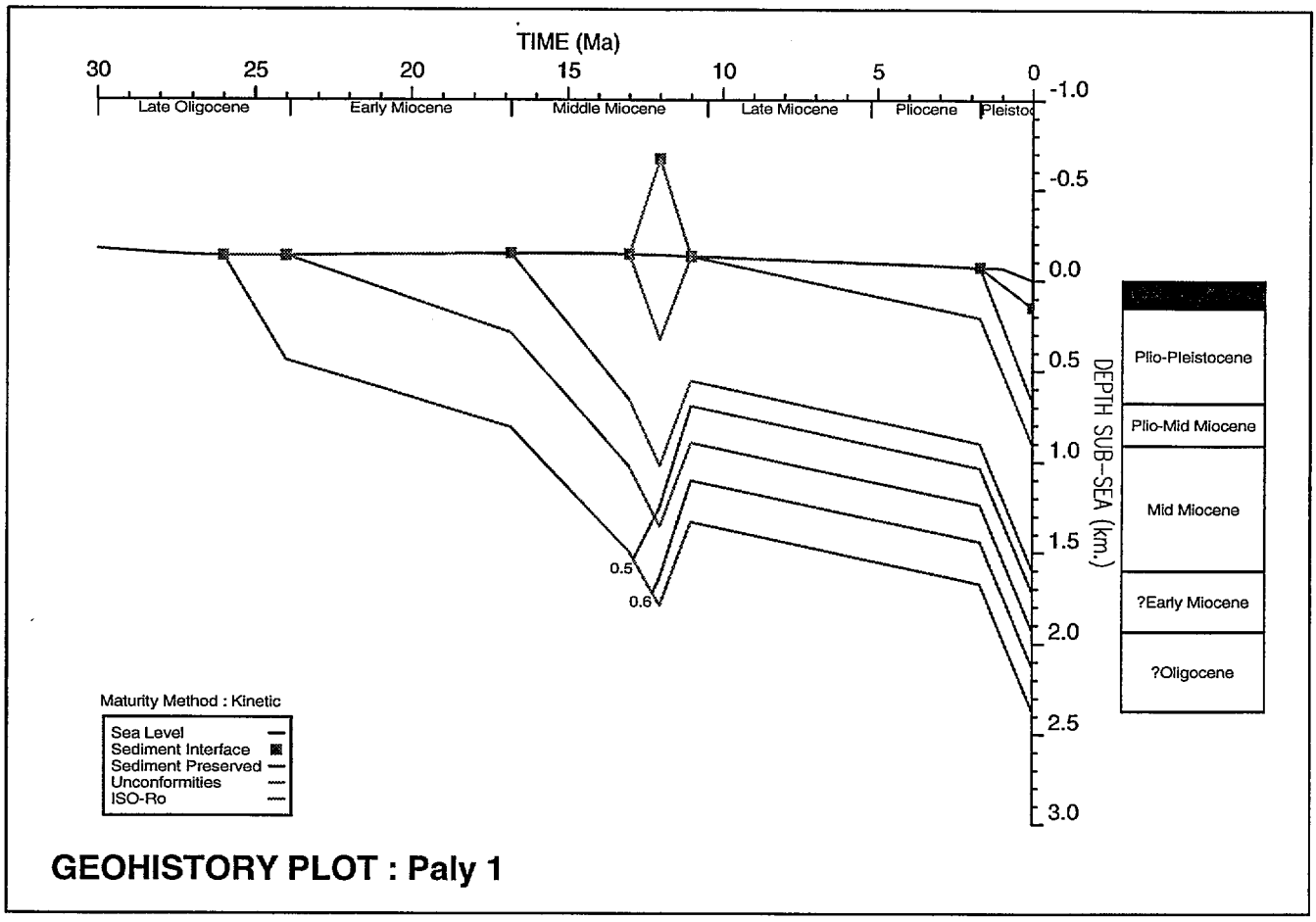

The geohistory plot of Paly 1 well shows accelerating subsidence from the end of the Oligocene to the Middle Miocene. This is not a normal rifted margin history, but indicates that the well site was approaching a plate boundary. The over-running of this boundary in the Middle Miocene was followed by uplift and erosion, then subsidence to the present day. The pre Middle Miocene unconformity succession may now again have barely reached the previous maximum depth of burial. Hydrocarbon maturity starts today in the Lower Miocene succession, and full maturity is not attained at TD. The post unconformity succession is immature.

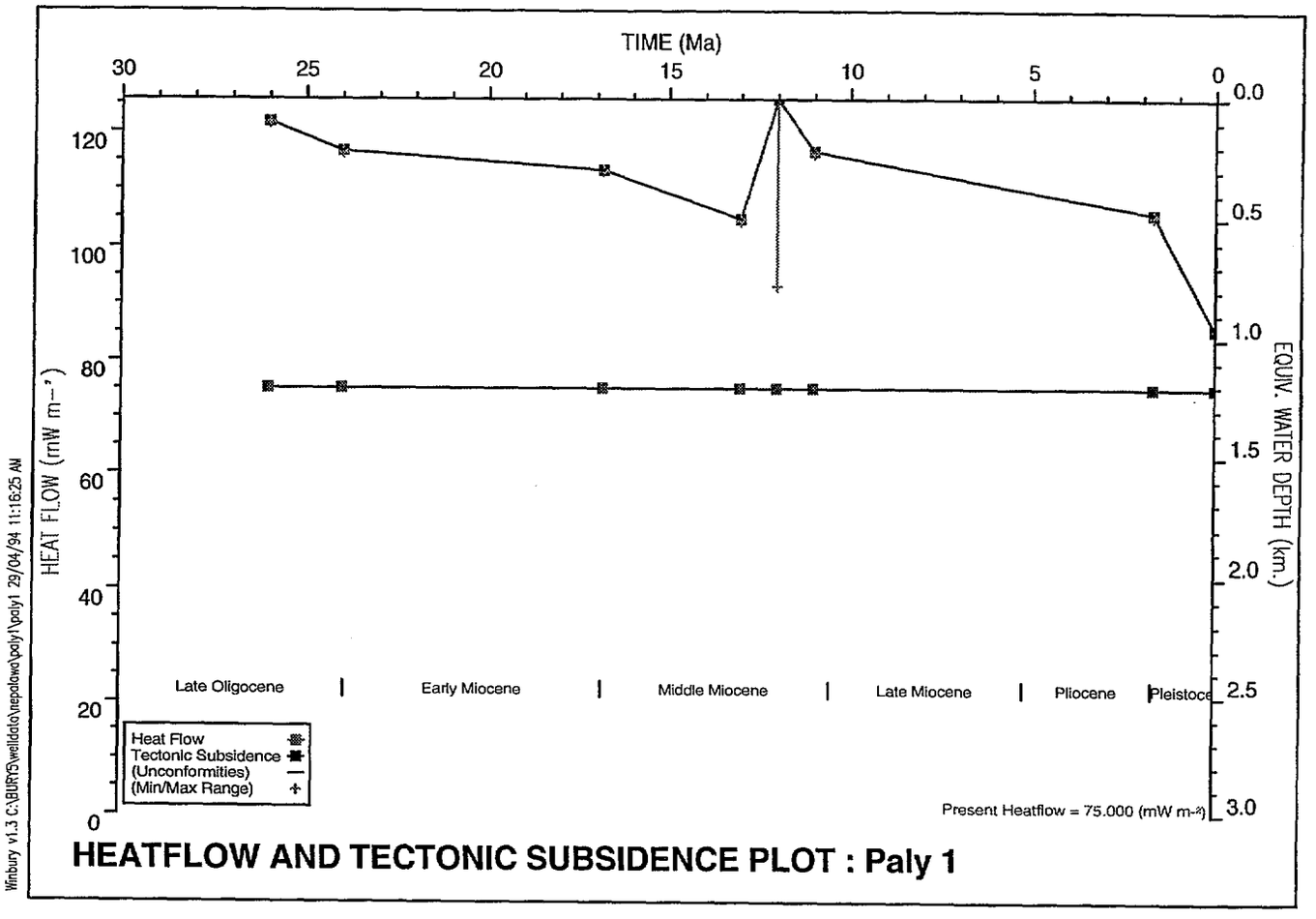

Winbury v1.3 C:\BURYS\welldata\nepalaw\paly1\paly1 29/04/94 11:16:25 AM

HEATFLOW AND TECTONIC SUBSIDENCE PLOT : Paly 1

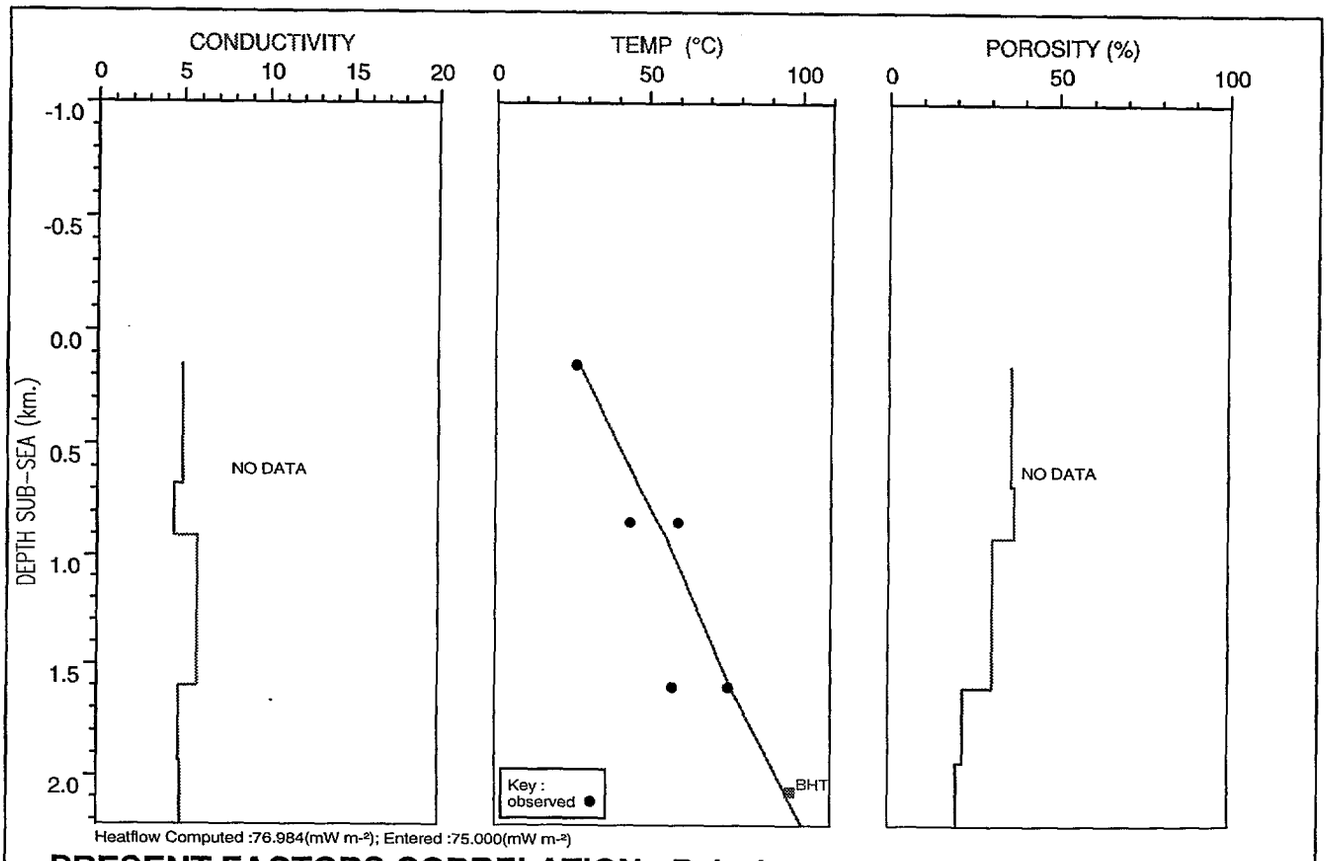

Winbury v1.3 C:\BURYS\welldata\nepalaw\paly1\paly1 29/04/94 11:56:18 AM

PRESENT FACTORS CORRELATION : Paly 1

	Stratigraph. Unit/Event	E V	Depth to Top of Unit	Age (Ma)	Minimum WtrDpth	Maximum WtrDpth	Modelled WtrDpth	Sea Bed Temp.	Heatflow	Lithology Data	Kerogen Data	Variable Beds
1	Plio-Pleistocene	N	176.79	0.00	149.66	149.66	149.66	27.78	75.00			
2	Plio-Mid Miocene	N	702.88	1.70	0.00	9.14	0.00	27.78	75.00			
3	Mid Miocene Unconf	E	935.14	11.00	0.00	9.14	0.00	27.78	75.00			
4	Deposit A	E	(1000.00)	12.00	-1000.00	9.14	-532.51	27.78	75.00			
5	Mid Miocene	N	935.14	13.00	0.00	9.14	0.00	27.78	75.00			
6	?Early Miocene	N	1625.21	16.80	0.00	9.14	0.00	27.78	75.00			
7	?Oligocene	N	1960.50	24.00	0.00	9.14	0.00	27.78	75.00			
8		N	2400.00	26.00	0.00	9.14	0.00	27.78	75.00			

HORIZON DATA : PALY1

	Stratigraph. Unit/Event	SHALE	SAND	CHALK	LST	COAL	HALIT	VOLCS	CONV	GY/ANH	Initial Porosity	Por/Depth Factor	Conductivity	Density
1	Plio-Pleistocene		20		80						0.400	1.040	10.990	2.730
2	Plio-Mid Miocene	40	60								0.520	1.210	9.720	2.710
3	Mid Miocene Unconf	40	60								0.520	1.210	9.720	2.710
4	Deposit A	60	40								0.580	1.620	7.570	2.740
5	Mid Miocene	20	80								0.460	0.810	12.470	2.680
6	?Early Miocene	40	40					20			0.450	1.230	7.540	2.730
7	?Oligocene	40	40					20			0.450	1.230	7.540	2.730
8		40	40					20			0.450	1.230	7.540	2.730

HORIZON DATA : PALY1 - MATRIX LITHOLOGY

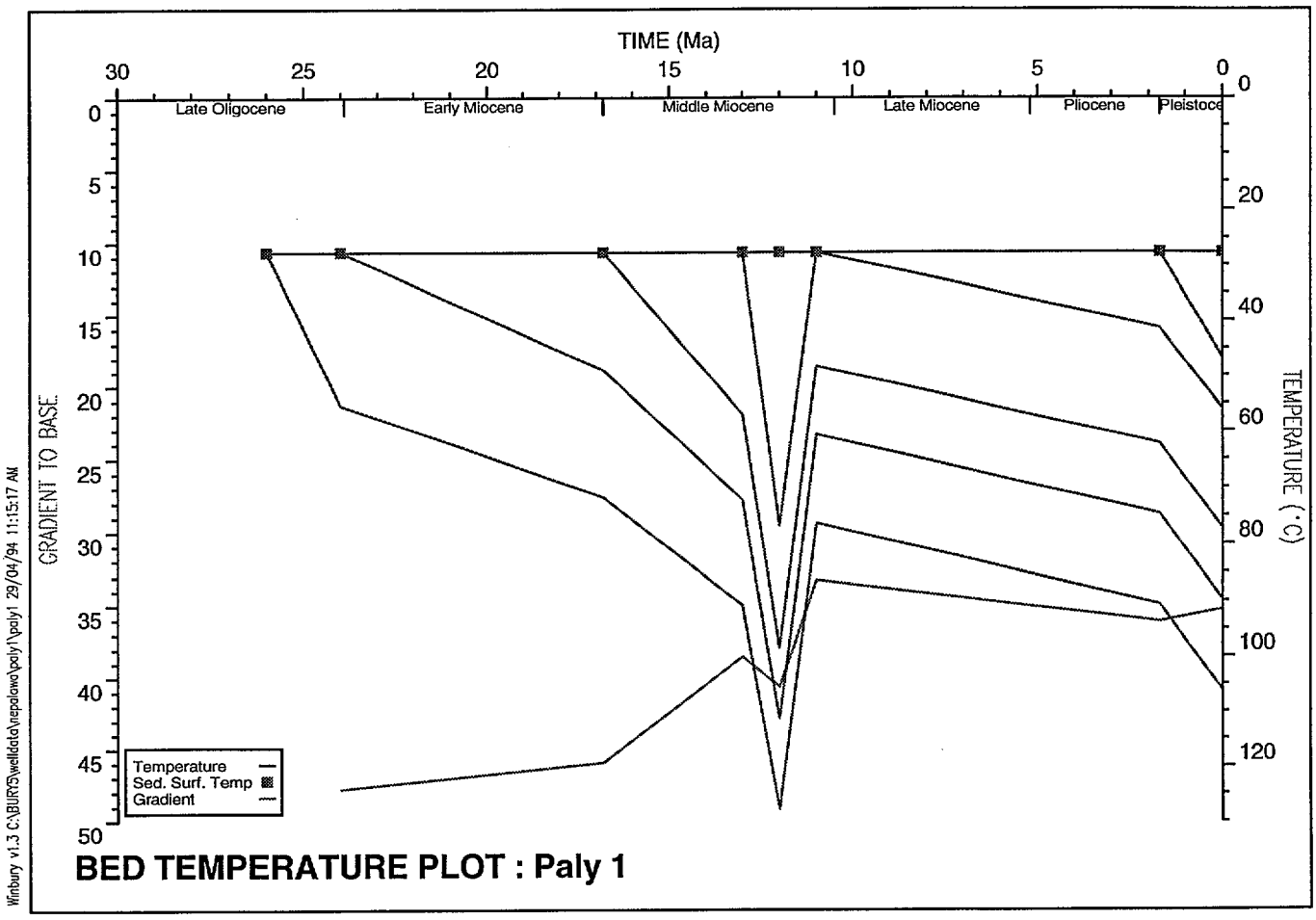
TIME (Ma)
30
25
20
15
10
5
0
Late Oligocene
Early Miocene
Middle Miocene
Late Miocene
Pliocene
Pleistoce
GRADIENT TO BASE
TEMPERATURE (°C)
0
5
10
15
20
25
30
35
40
45
50
0
20
40
60
80
100
120
Temperature
Sed. Surf. Temp
Gradient
BED TEMPERATURE PLOT : Paly 1
Winbury v1.3 C:\BURYS\welldata\nepalowe\paly1\paly1 29/04/94 11:15:17 AM

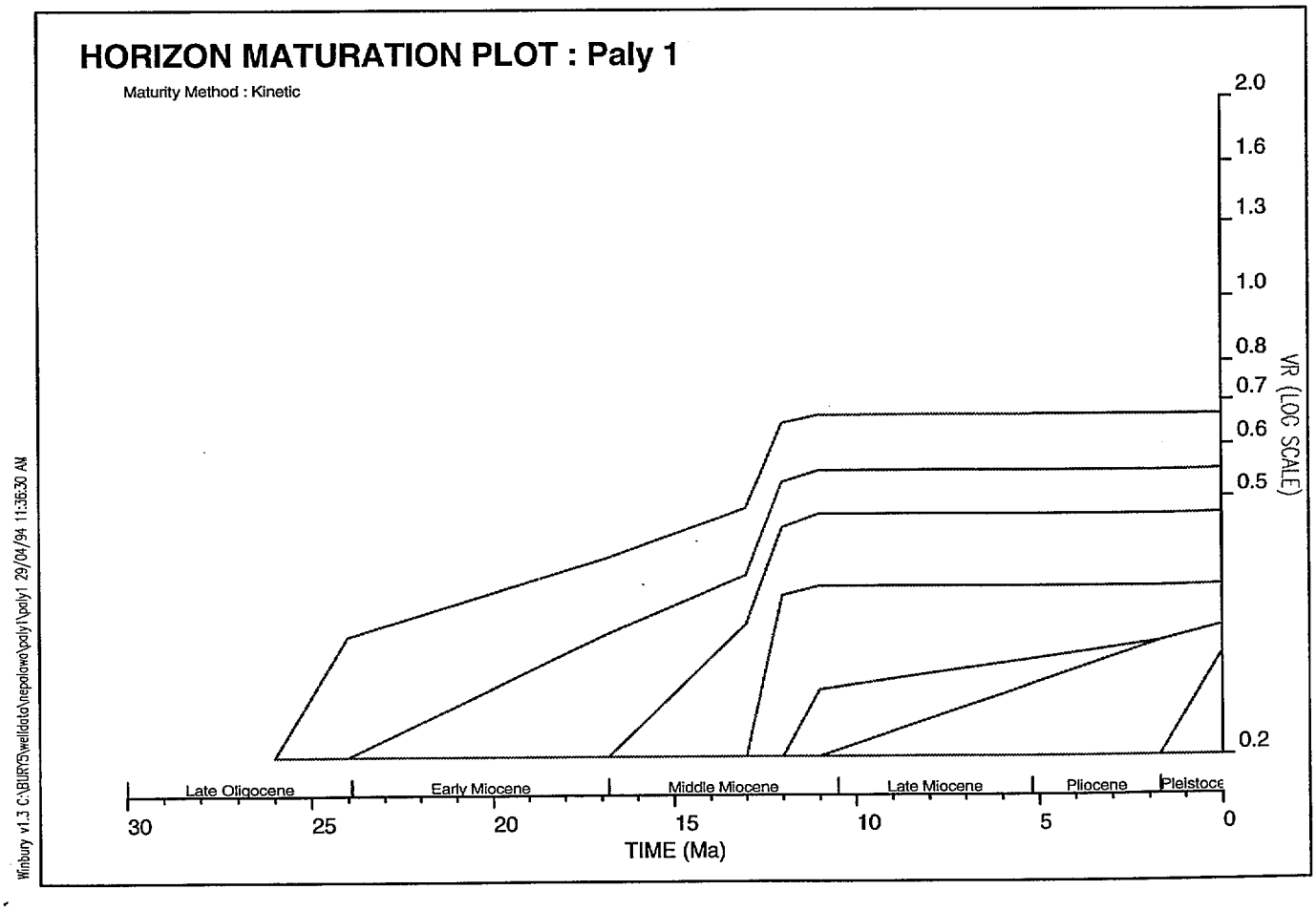
HORIZON MATURATION PLOT : Paly 1
Maturity Method : Kinetic
2.0
1.6
1.3
1.0
0.8
0.7
0.6
0.5
0.2
VR (LOG SCALE)
Late Oligocene
Early Miocene
Middle Miocene
Late Miocene
Pliocene
Pleistoce
30
25
20
15
10
5
0
TIME (Ma)
Winbury v1.3 C:\BURYS\welldata\nepalowe\paly1\paly1 29/04/94 11:36:30 AM

PROGRESO 1X

SEDCO 1982

Latitude: 12° 24' 56" N
KB: 17m asl
Surface Temperature: 28°C
BHT: 74°C

Longitude: 121° 03' 45" E
TD: 1602mKB
Surface Elevation: 11m asl
BHT Depth:1602m

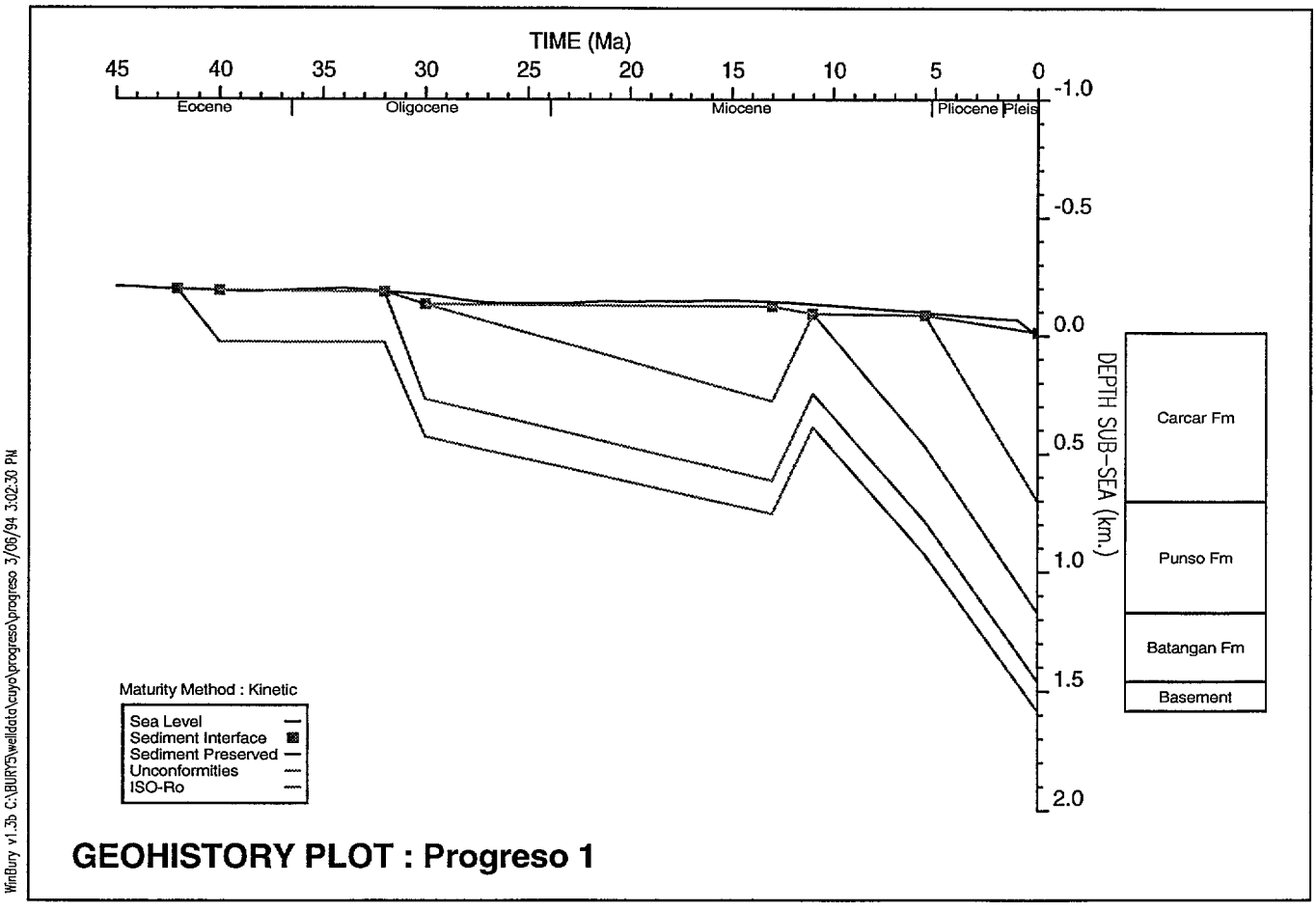

GEOHISTORY PLOT : Progreso 1

The geohistory plot of Progreso 1x well shows deposition from the Late Eocene, interrupted by two unconformities, one, in the Late Eocene - Early Oligocene, a hiatus only, the other, in the Middle Miocene, showing a minor amount of uplift and erosion. None of the succession shows maturity for hydrocarbons.

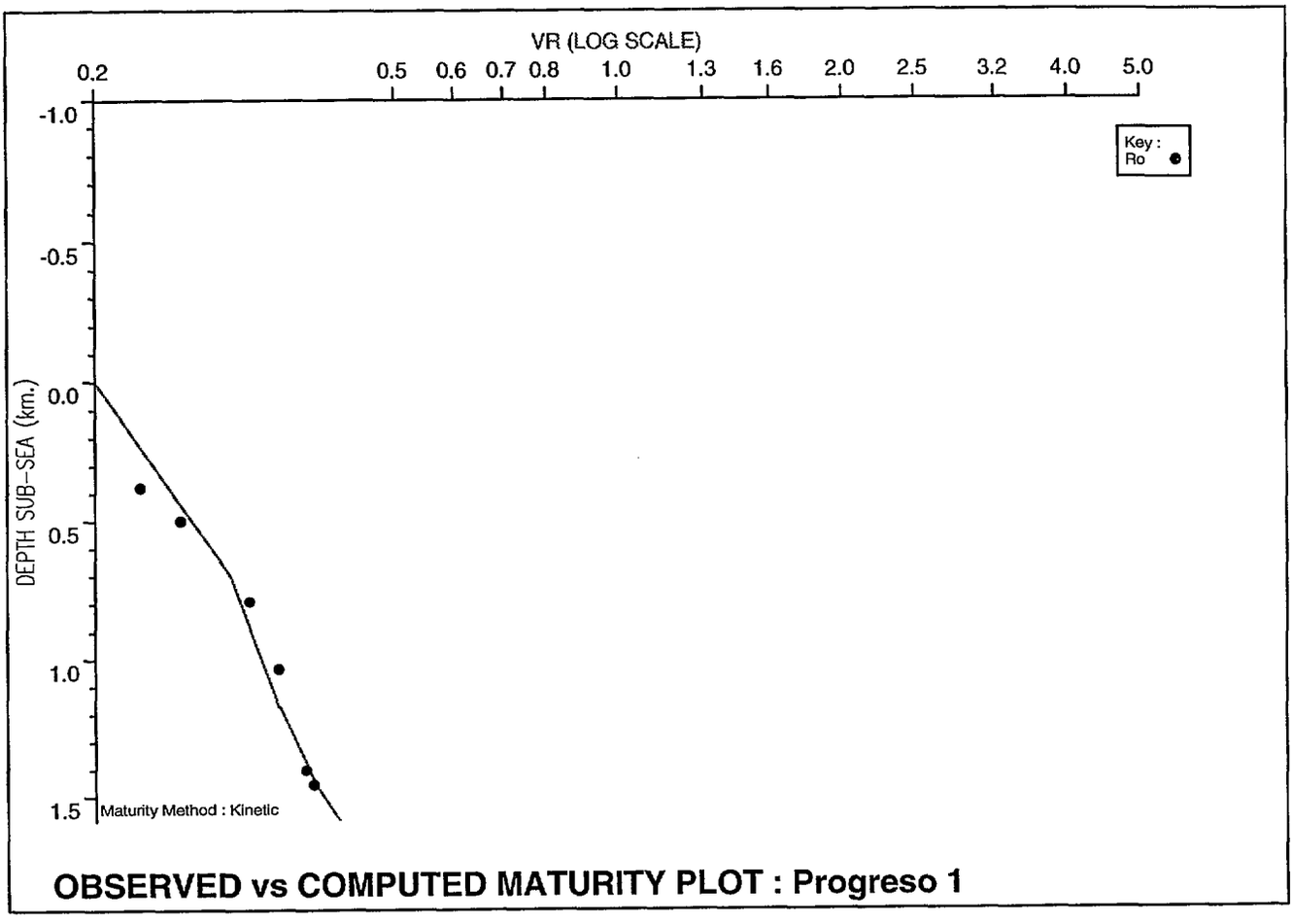

OBSERVED vs COMPUTED MATURITY PLOT : Progreso 1

	Stratigraph. Unit/Event	E V	Depth to Top of Unit	Age (Ma)	Minimum WtrDpth	Maximum WtrDpth	Modelled WtrDpth	Sea Bed Temp.	Heatflow	Lithology Data	Kerogen Data	Variable Beds
1	Carcar Fm	N	6.00	0.00	-11.00	-11.00	-11.00	28.00	58.00			
2	Punso Fm	N	720.00	5.50	0.00	10.00	10.00	28.00	58.00			
3	Miocene Unc	E	1190.00	11.00	20.00	40.00	40.00	28.00	58.00			
4	Deposit A	E	(400.00)	13.00	20.00	40.00	20.01	28.00	58.00			
5	Batangan Fm	N	1190.00	30.00	20.00	40.00	40.00	28.00	58.00			
6	Olig. Unconf	H	1475.00	32.00	0.00	20.00	0.00	28.00	58.00			
7	Basement	N	1475.00	40.00	0.00	20.00	0.00	28.00	58.00			
8	TD	N	1602.00	42.00	0.00	20.00	0.00	28.00	58.00			

HORIZON DATA : PROGRESO

ROXAS 1

CITCO 1979

Latitude: 10° 04' 42.5" N
KB: 10m asl
Surface Temperature: 28°C
BHT: 78°C (e-log, extrapolated)

Longitude: 119° 38' 40.7" E
TD: 2031mKB
Water Depth: 74m
BHT Depth: 2025m

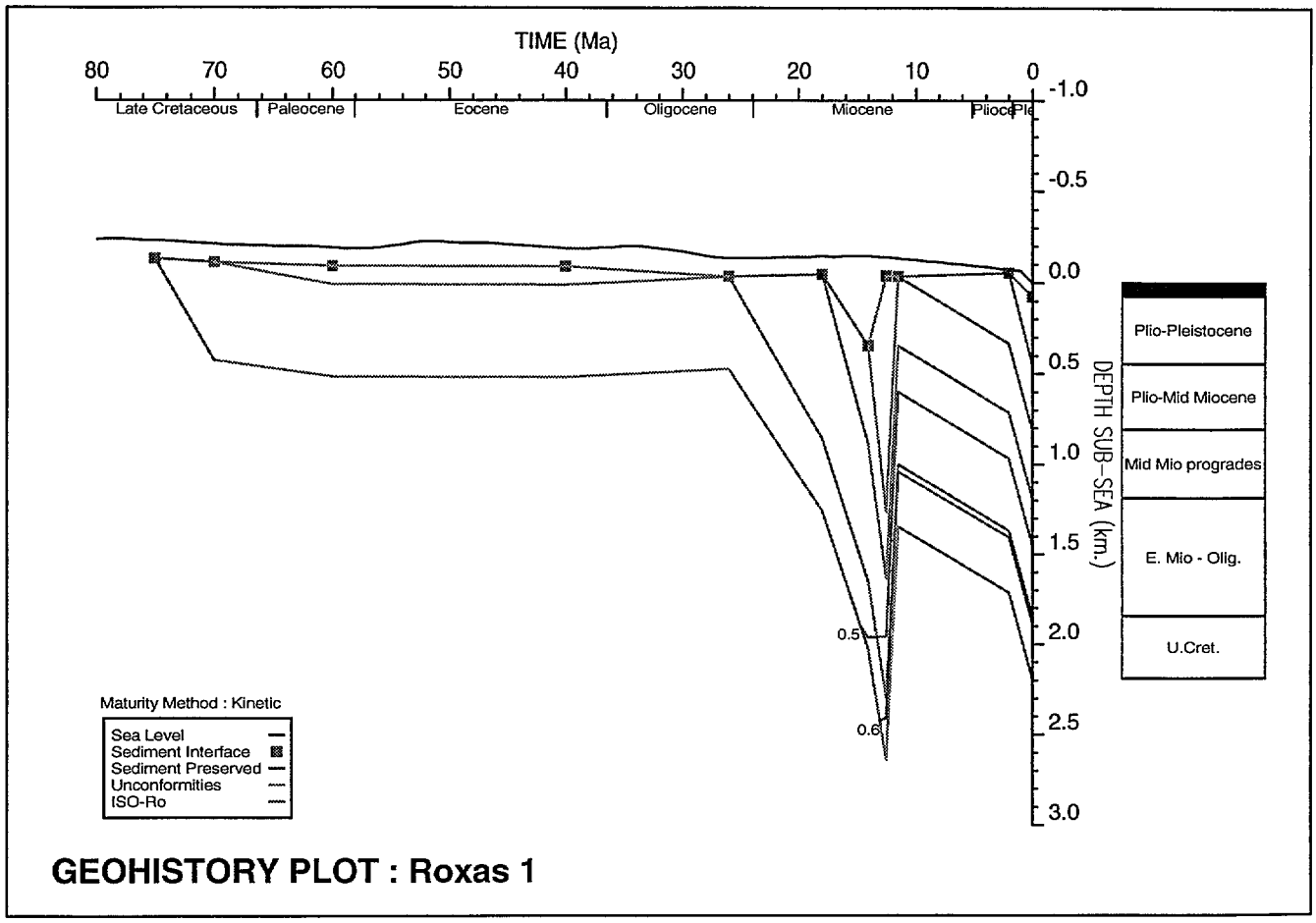

GEOHISTORY PLOT : Roxas 1

Little is known of the early Tertiary history of Roxas-1. On the geohistory plot the time interval from end Cretaceous to Late Oligocene is shown as featureless, without marked subsidence or erosion. This reflects the lack of data for the period of the 'base Tertiary' unconformity at 1855 m in the well. Northeast Palawan subsided increasingly rapidly from the Late Oligocene through the Early Miocene and the base of the succession reached the early stages of maturity for hydrocarbons. Marked uplift during the Middle Miocene brought the generation of hydrocarbons at this location to an end. Subsidence since then has not been sufficient to restart generation at the wellsite, although in the depocentre of the Roxas area to the SSE (see ROXAS AREA geohistory plot) the situation is quite different. There, the Middle Miocene uplift was less, and maturation was hardly interrupted.

	Stratigraph. Unit/Event	E V	Depth to Top of Unit	Age (Ma)	Minimum WtrDpth	Maximum WtrDpth	Modelled WtrDpth	Sea Bed Temp.	Heatflow	Lithology Data	Kerogen Data	Variable Beds
1	Plio-Pleistocene	N	84.00	0.00	74.00	74.00	74.00	28.00	55.00			
2	Plio-Mid Miocene	N	457.00	2.00	0.00	20.00	20.00	28.00	55.00			
3	Mid Mio unconf	E	820.00	11.50	0.00	100.00	100.00	28.00	55.00			
4	Deposit a	E	(1300.00)	12.50	0.00	100.00	100.00	28.00	65.00			
5	Mid Mio prograde	N	820.00	14.00	0.00	500.00	489.45	28.00	65.00			
6	E. Mio - Olig.	N	1198.00	18.00	0.00	100.00	100.00	28.00	65.00			
7	Base Tertiary unconf	E	1855.00	26.00	0.00	100.00	100.00	28.00	65.00			
8	deposit b	E	(100.00)	40.00	0.00	100.00	100.00	28.00	65.00			
9	deposit c	E	(100.00)	60.00	0.00	100.00	100.00	28.00	65.00			
10	U.Cret.	N	1855.00	70.00	0.00	100.00	100.00	28.00	65.00			
11	dummy	N	2200.00	75.00	0.00	100.00	100.00	28.00	65.00			

HORIZON DATA : ROXAS1

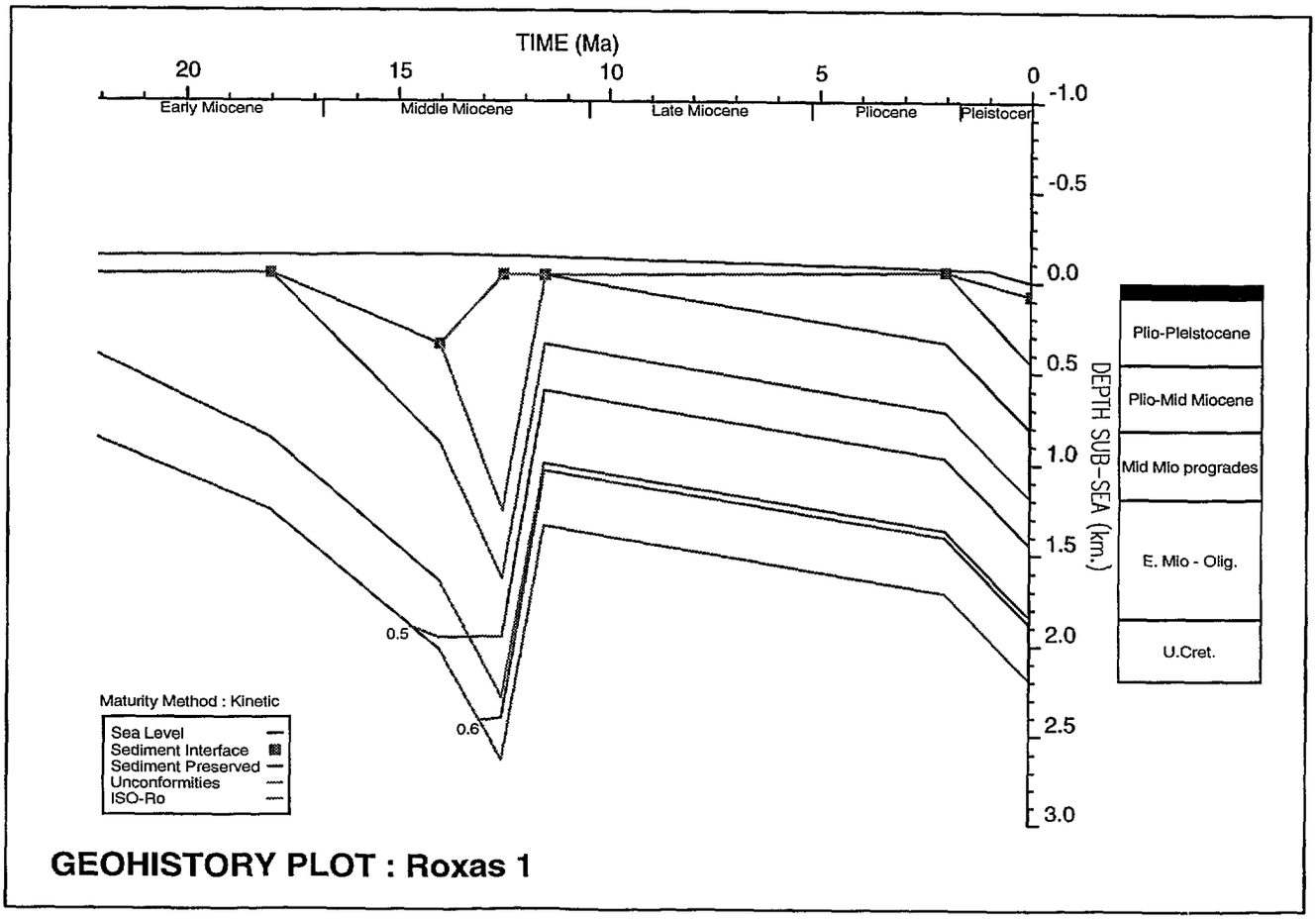

The zoomed view of the Neogene portion of the geohistory plot for Roxas-1 shows detail of the process of early maturation and the uplift during the Middle Miocene that brought the process to an end.

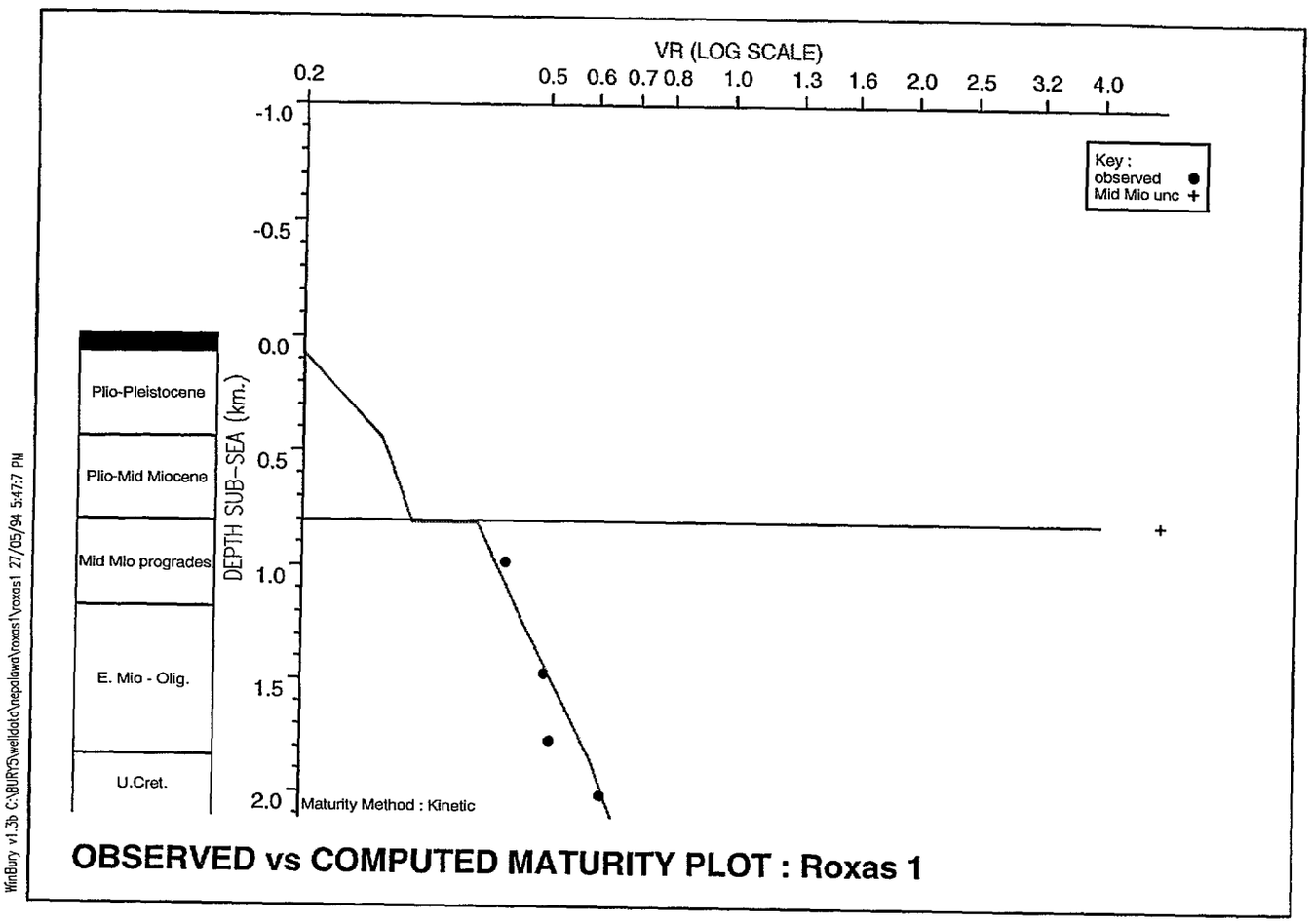

OBSERVED vs COMPUTED MATURITY PLOT : Roxas 1

	Sample Depth	T P	Average Maturity	Minimum Maturity	Maximum Maturity	F L
1	810.00	0	5.00	0.20	4.00	7
2	992.00	0	0.43	0.43	0.43	0
3	1483.00	0	0.50	0.50	0.50	0
4	1781.00	0	0.51	0.51	0.51	0
5	2025.00	0	0.62	0.62	0.62	0

MATURITY DATA : ROXAS1

The maturity data for Roxas-1 based on vitrinite reflectance shows the effects of the Middle Miocene unconformity. There are no observed maturity data (dots) above the unconformity, and the calculated maturity (bent black line) is based on modern heatflow calculated from the bottom-hole temperature.

SEMIRARA 1

BP 1980

Latitude: 11° 59' 20" N
KB: 5m agl
Surface Temperature: 28°C
BHT: 120°C

Longitude: 121° 23' 50" E
TD: 2995mKB
Surface Elevation: 2m asl
BHT Depth: 2995m

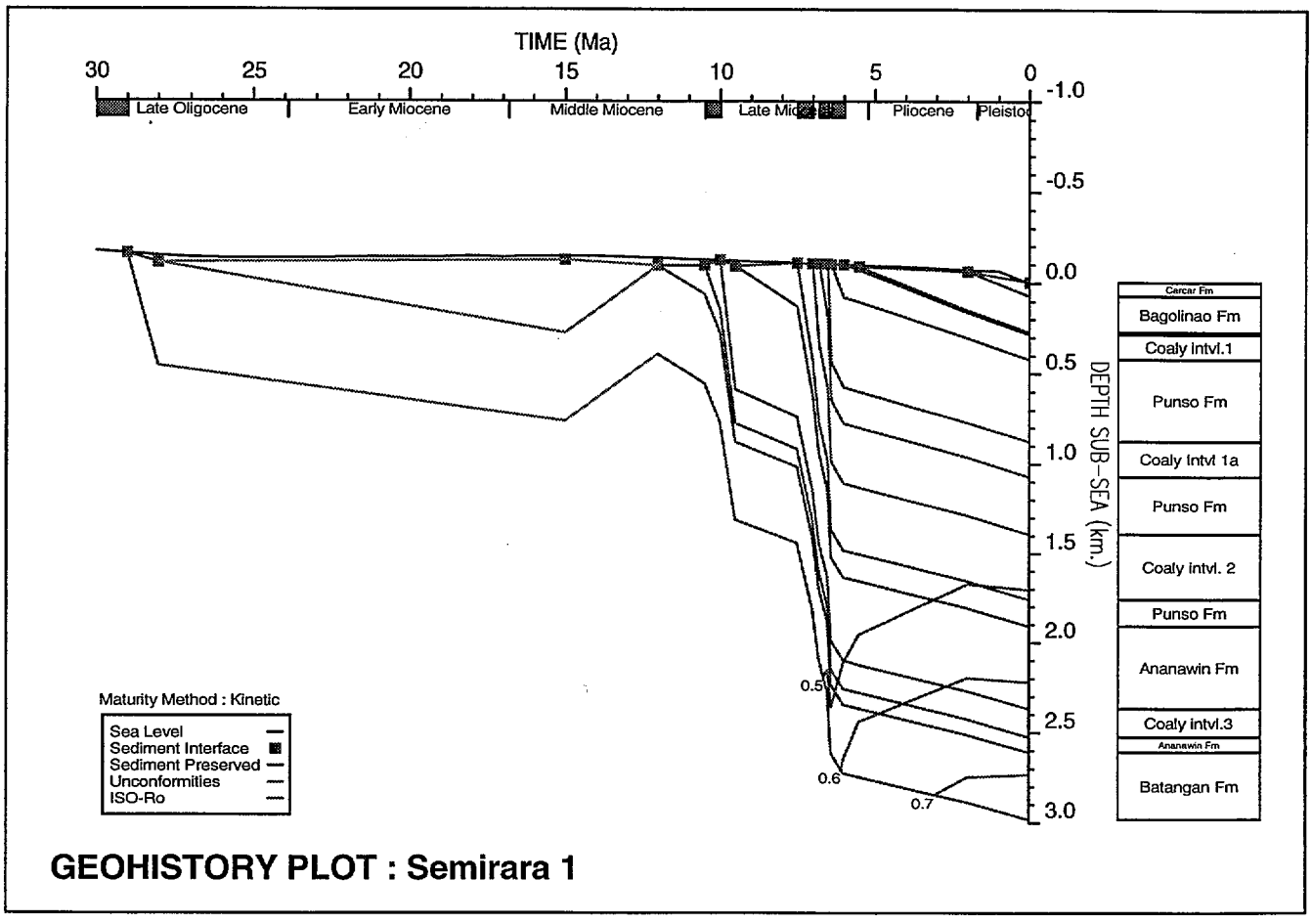

The burial history plot of Semirara 1 shows only one significant unconformity (theMiddle Miocene).
Three significant coal-bearing intervals have been highlighted within the Punso Formation, and one (coaly interval 3) within the Ananawin. They show faster accumulation (hence faster subsidence) than the adjacent marginal marine intervals.

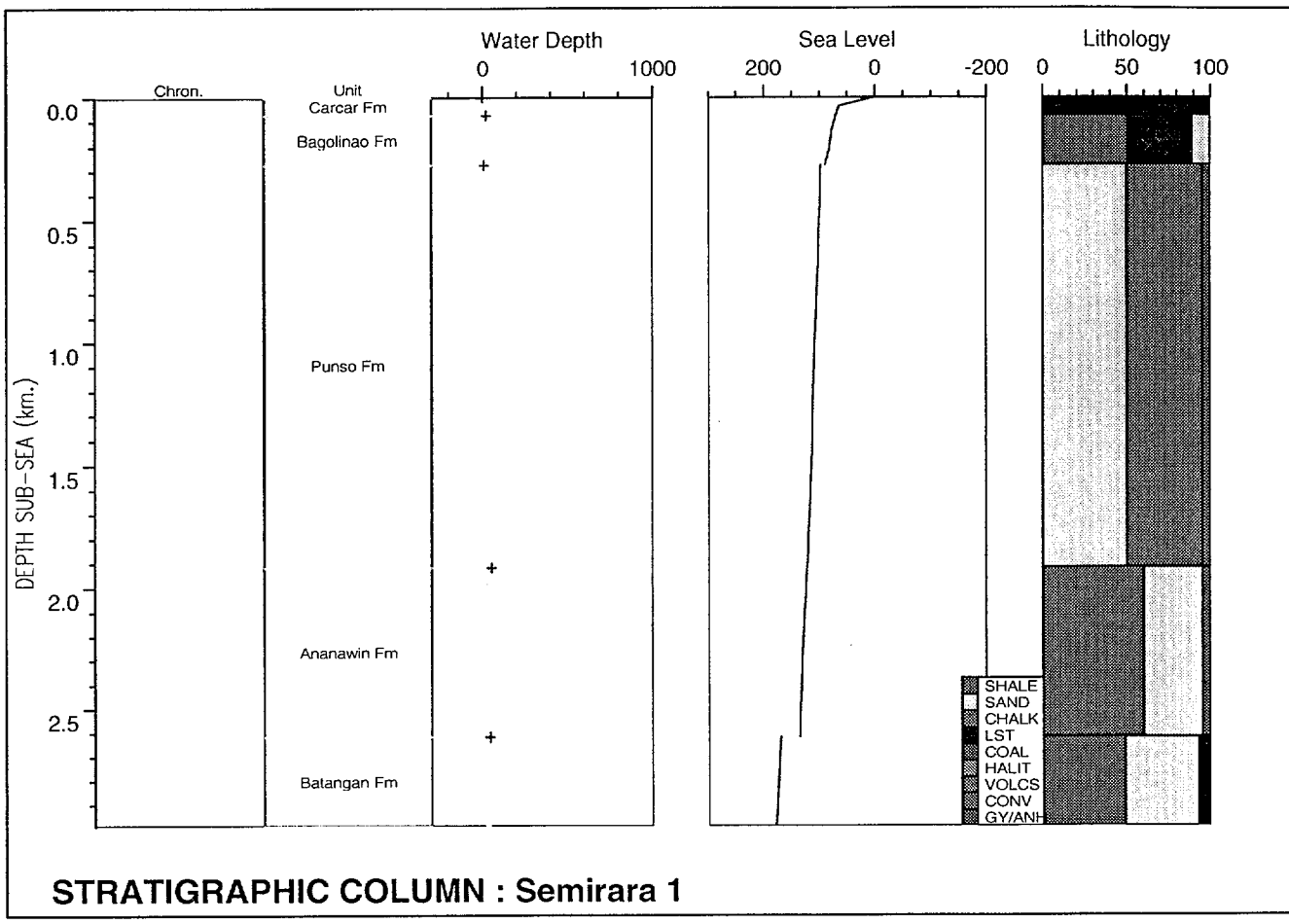

STRATIGRAPHIC COLUMN : Semirara 1

	Stratigraph. Unit/Event	SHALE	SAND	CHALK	LST	COAL	HALIT	VOLCS	CONV	GY/ANH	Initial Porosity	Por/Depth Factor	Conductivity	Density
1	Carcar Fm				100						0.400	1.200	10.000	2.750
2	Bagolinao Fm	51	11		38						0.550	1.740	7.090	2.760
3	Punso Fm	45	50			5					0.550	1.540	7.950	2.660
4	Ananawin Fm	60	35			5					0.600	1.850	6.590	2.690
5	Miocene Unc	49	44		7						0.550	1.450	8.410	2.730
6	Deposit A	49	44		7						0.550	1.450	8.410	2.730
7	Batangan Fm	49	44		7						0.550	1.450	8.410	2.730
8	TD	49	44		7						0.550	1.450	8.410	2.730

HORIZON DATA : SEMIRARA - MATRIX LITHOLOGY

	Stratigraph. Unit/Event	E V	Depth to Top of Unit	Age (Ma)	Minimum WtrDpth	Maximum WtrDpth	Modelled WtrDpth	Sea Bed Temp.	Heatflow	Lithology Data	Kerogen Data	Variable Beds
1	Carcar Fm	N	5.00	0.00	-5.00	-5.00	-5.00	28.00	52.00			
2	Bagolinao Fm	N	80.00	2.00	0.00	10.00	10.00	28.00	52.00			
3	Punso Fm	N	280.00	5.50	0.00	10.00	10.00	28.00	52.00			
4	Coaly intvl.1	N	293.00	6.00	0.00	10.00	0.00	28.00	52.00			
5	Punso Fm	N	430.00	6.40	0.00	10.00	0.00	28.00	52.00			
6	Coaly Intvl 1a	N	887.00	6.50	0.00	10.00	0.00	28.00	52.00			
7	Punso Fm	N	1079.00	6.80	0.00	10.00	0.00	28.00	52.00			
8	Coaly intvl. 2	N	1402.00	7.00	0.00	10.00	0.00	28.00	52.00			
9	Punso Fm	N	1768.00	7.50	0.00	10.00	0.00	28.00	52.00			
10	Ananawin Fm	N	1920.00	9.50	10.00	30.00	30.00	28.00	52.00			
11	Coaly intvl.3	N	2378.00	10.00	0.00	20.00	0.00	28.00	52.00			
12	Ananawin Fm	N	2534.00	10.50	10.00	30.00	30.00	28.00	52.00			
13	Miocene Unc	E	2620.00	12.00	20.00	40.00	40.00	28.00	52.00			
14	Deposit A	E	(400.00)	15.00	20.00	40.00	20.01	28.00	52.00			
15	Batangan Fm	N	2620.00	28.00	20.00	40.00	40.00	28.00	52.00			
16	TD	N	2995.00	29.00	0.00	20.00	0.00	28.00	52.00		TYPEI TYPEII COAL	

HORIZON DATA : SEMIRARA

	Stratigraph. Unit/Event	COAL	Expulsion	TOC
4	Coal intvl.1	100	On	33.000
6	Coaly Intvl 1a	100	On	42.000
8	Coaly intvl. 2	100	On	40.000
11	Coaly intvl.3	100	On	30.000

HORIZON DATA : SEMIRARA - KEROGEN COMPONENT

HORIZON MATURATION PLOT : Semirara 1

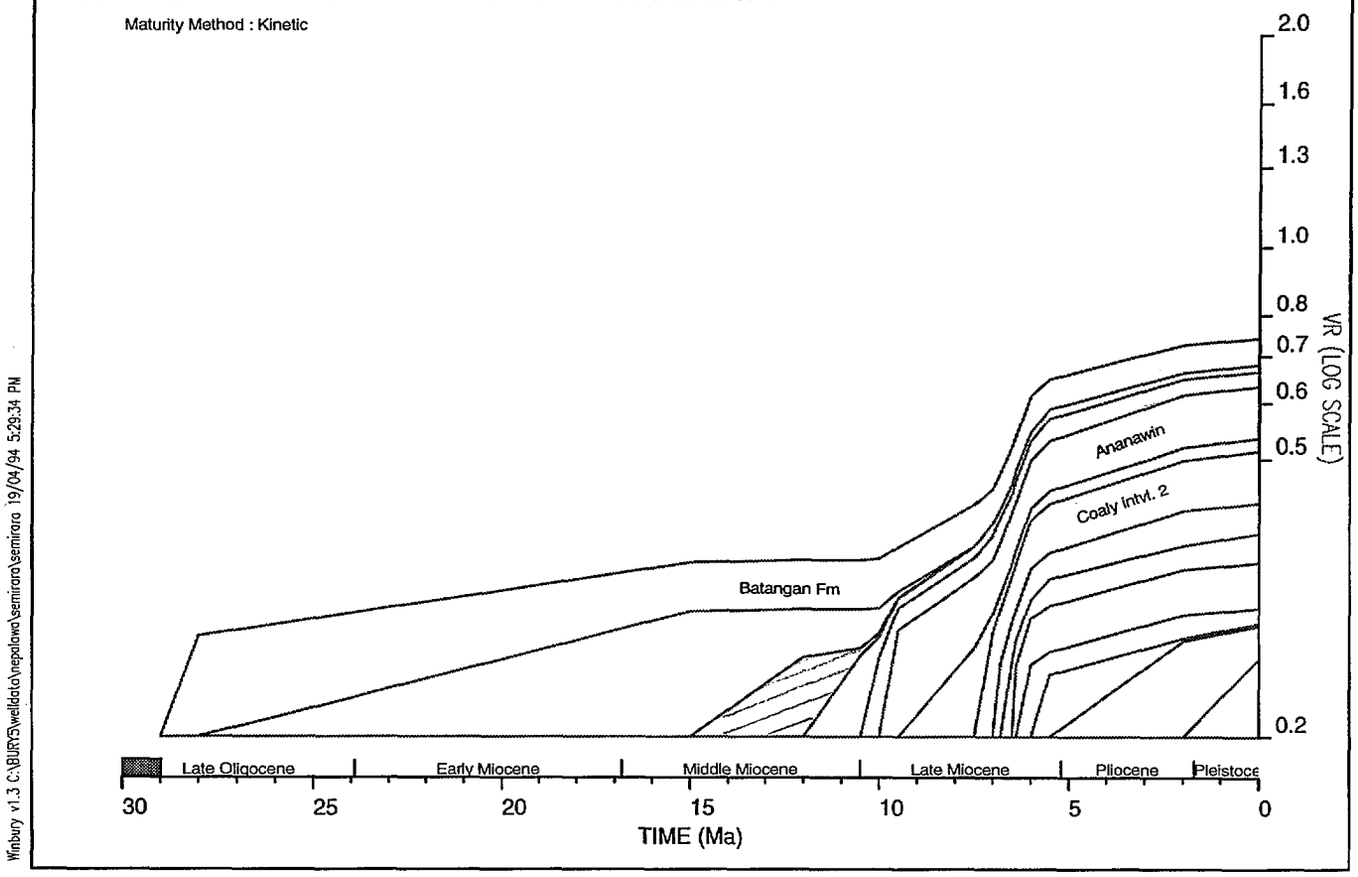

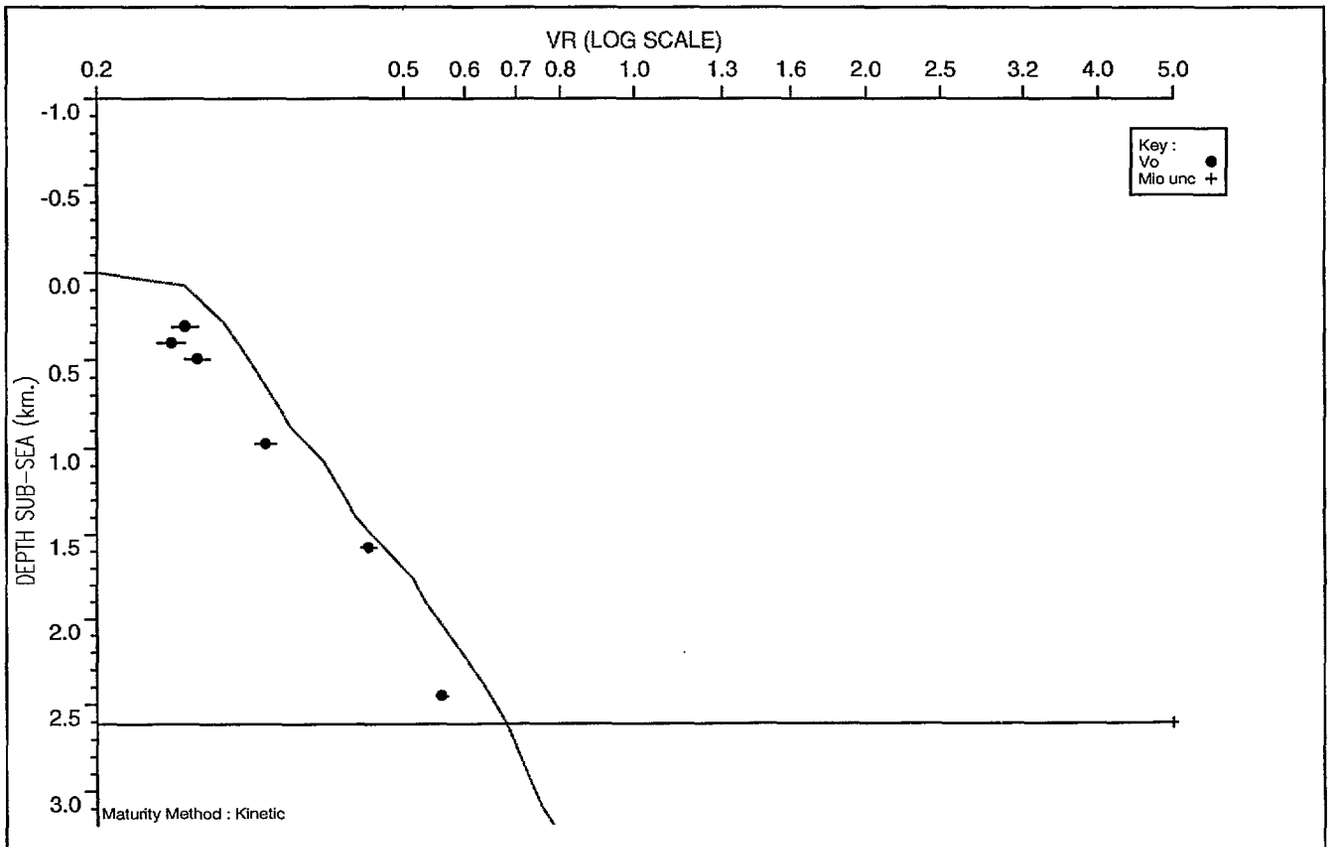

OBSERVED vs COMPUTED MATURITY PLOT : Semirara 1

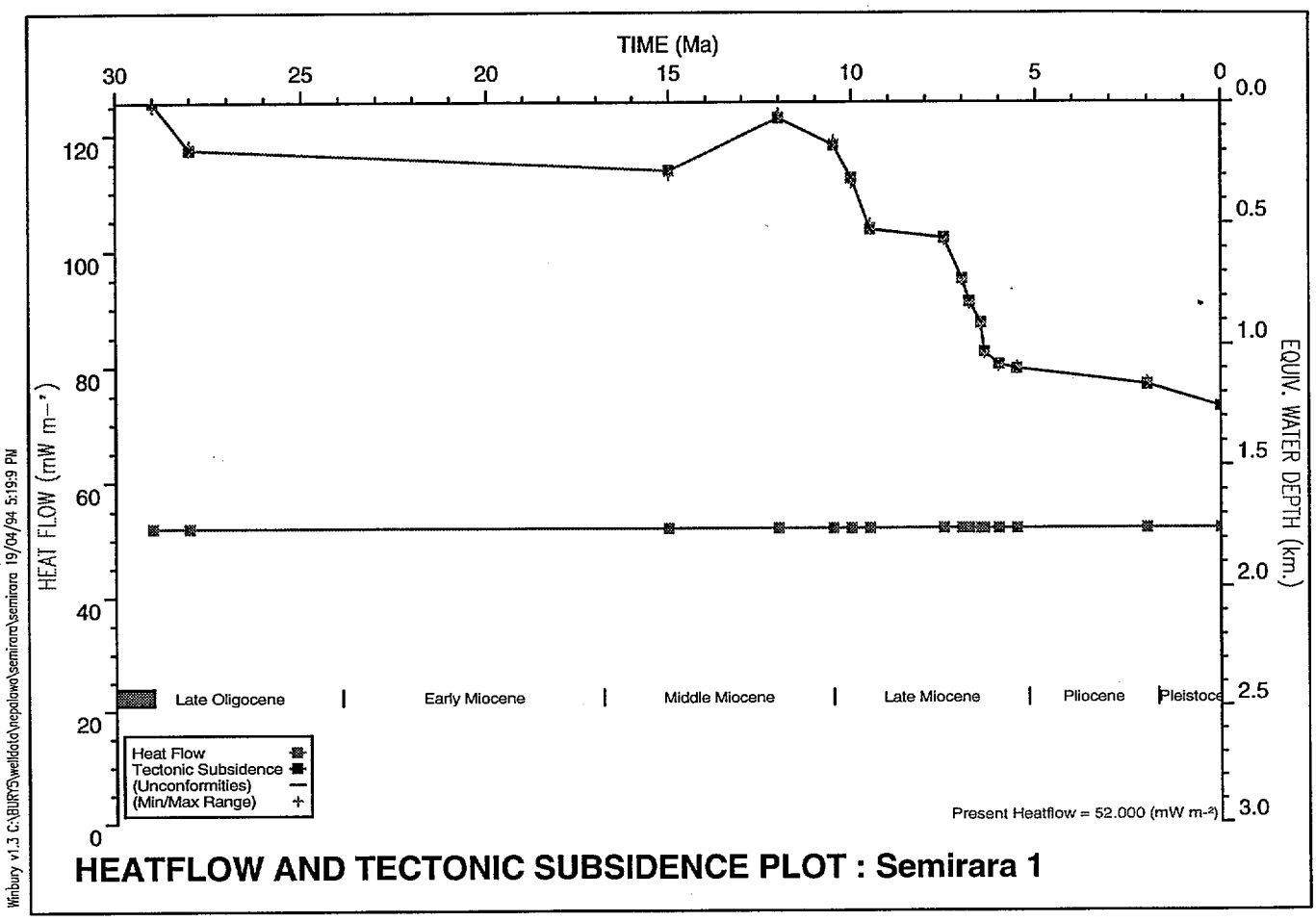

Winbury v1.3 C:\BURY5\welldata\nepalowo\semirara\semirara 19/04/94 5:19:9 PM

HEATFLOW AND TECTONIC SUBSIDENCE PLOT : Semirara 1

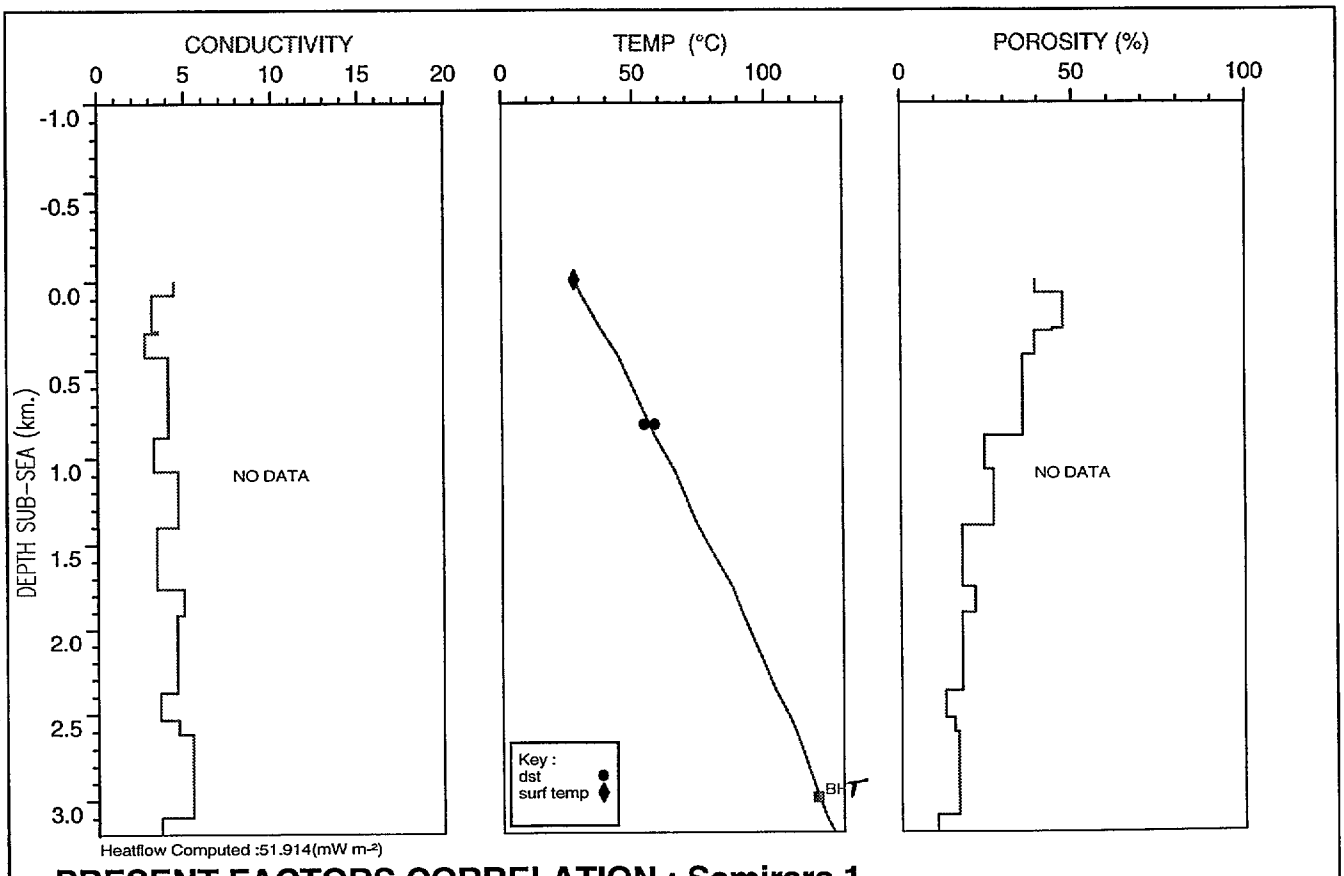

Winbury v1.3 C:\BURY5\welldata\nepalowo\semirara\semirara 14/04/94 10:43:35 AM

PRESENT FACTORS CORRELATION : Semirara 1

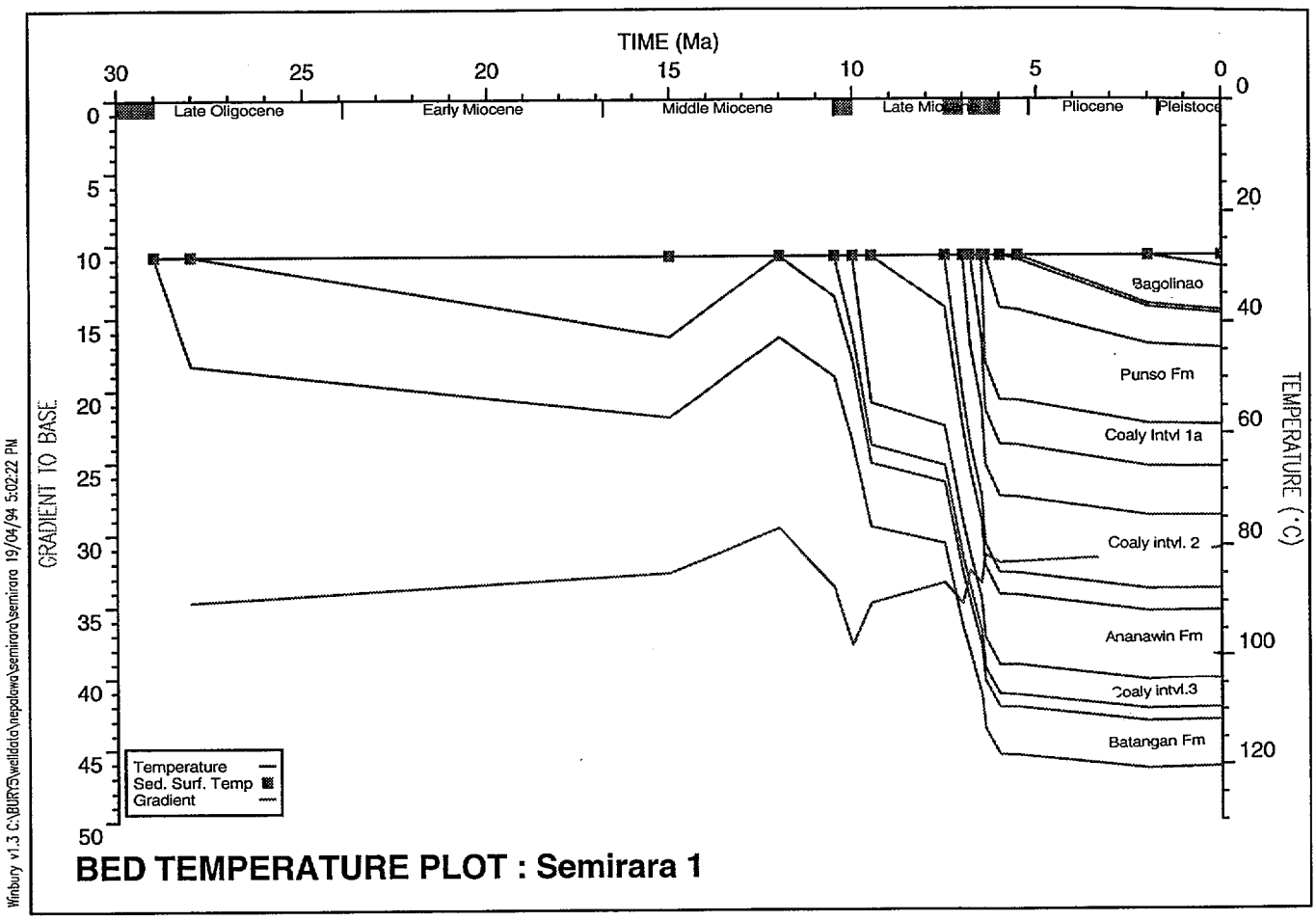

BED TEMPERATURE PLOT : Semirara 1

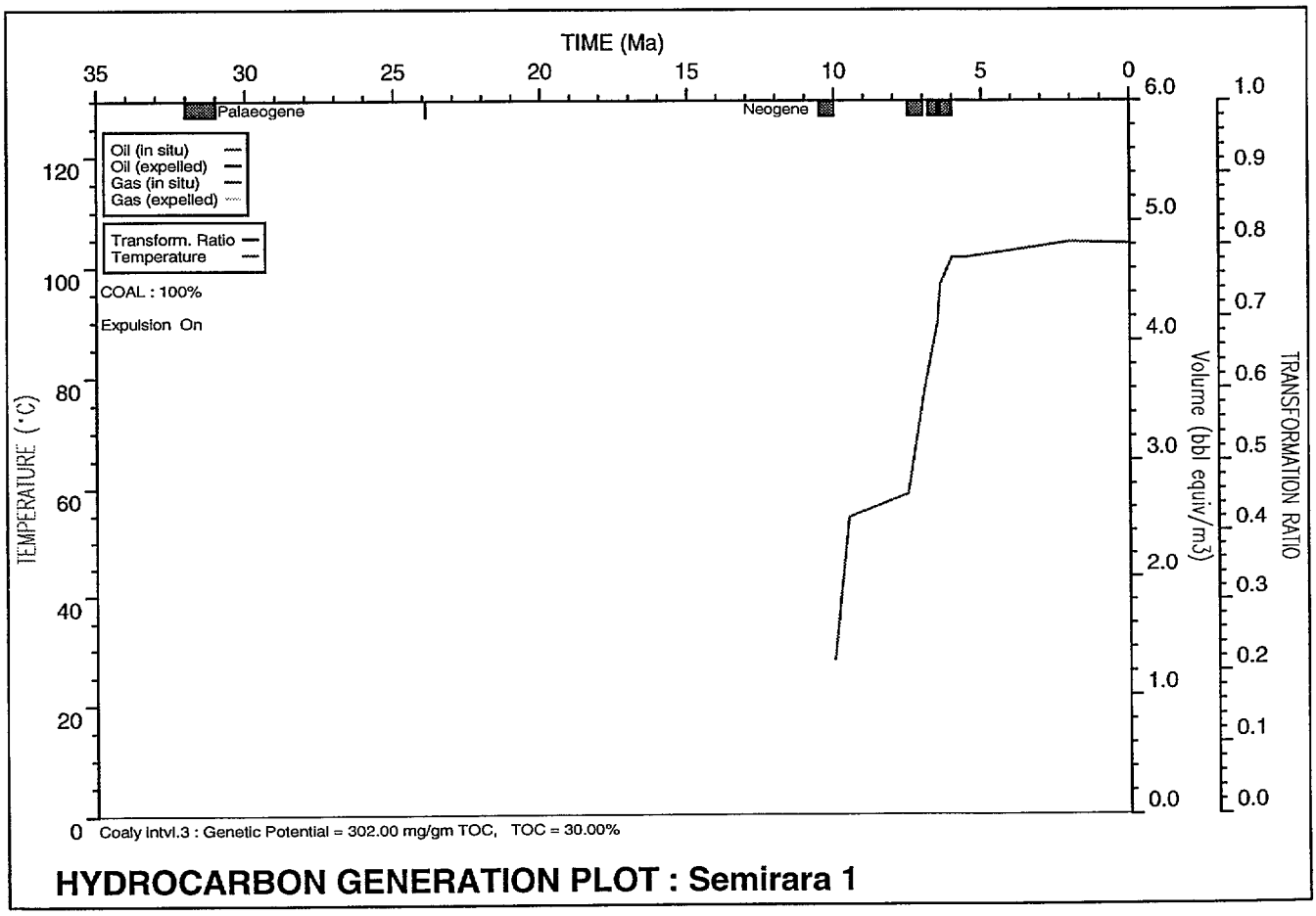

HYDROCARBON GENERATION PLOT : Semirara 1

	Stratigraph. Unit/Event	E V	Depth to Top of Unit	Age (Ma)	Minimum WtrDpth	Maximum WtrDpth	Modelled WtrDpth	Sea Bed Temp.	Heatflow	Lithology Data	Kerogen Data	Variable Beds
1	Carcar	N	88.00	0.00	88.00	88.00	88.00	28.00	57.00			
2	Blue Hor.	E	738.00	8.00	88.00	88.00	88.00	28.00	57.00			
3	Late Miocene dep.	E	(280.18)	10.00	88.00	88.00	88.00	28.00	57.00			
4	Punso	N	738.00	14.00	-50.00	400.00	200.00	28.00	57.00			
5	Batangan	N	868.00	33.00	0.00	200.00	6.38	28.00	57.00			
6	Base Te	E	4375.00	53.00	0.00	10.00	0.00	28.00	57.00			
7	Deposit A	E	(1100.00)	65.00	0.00	10.00	0.00	28.00	75.00			
8	Deposit B	E	(1000.00)	80.00	0.00	100.00	84.49	28.00	57.00			
9	Deposit C	E	(700.00)	110.00	0.00	100.00	50.00	28.00	57.00			
10	Mansalay	N	4375.00	150.00	0.00	10.00	10.00	28.00	57.00			
11	dummy	N	4700.00	155.00	0.00	10.00	10.00	28.00	57.00			

HORIZON DATA : CUYOKCN

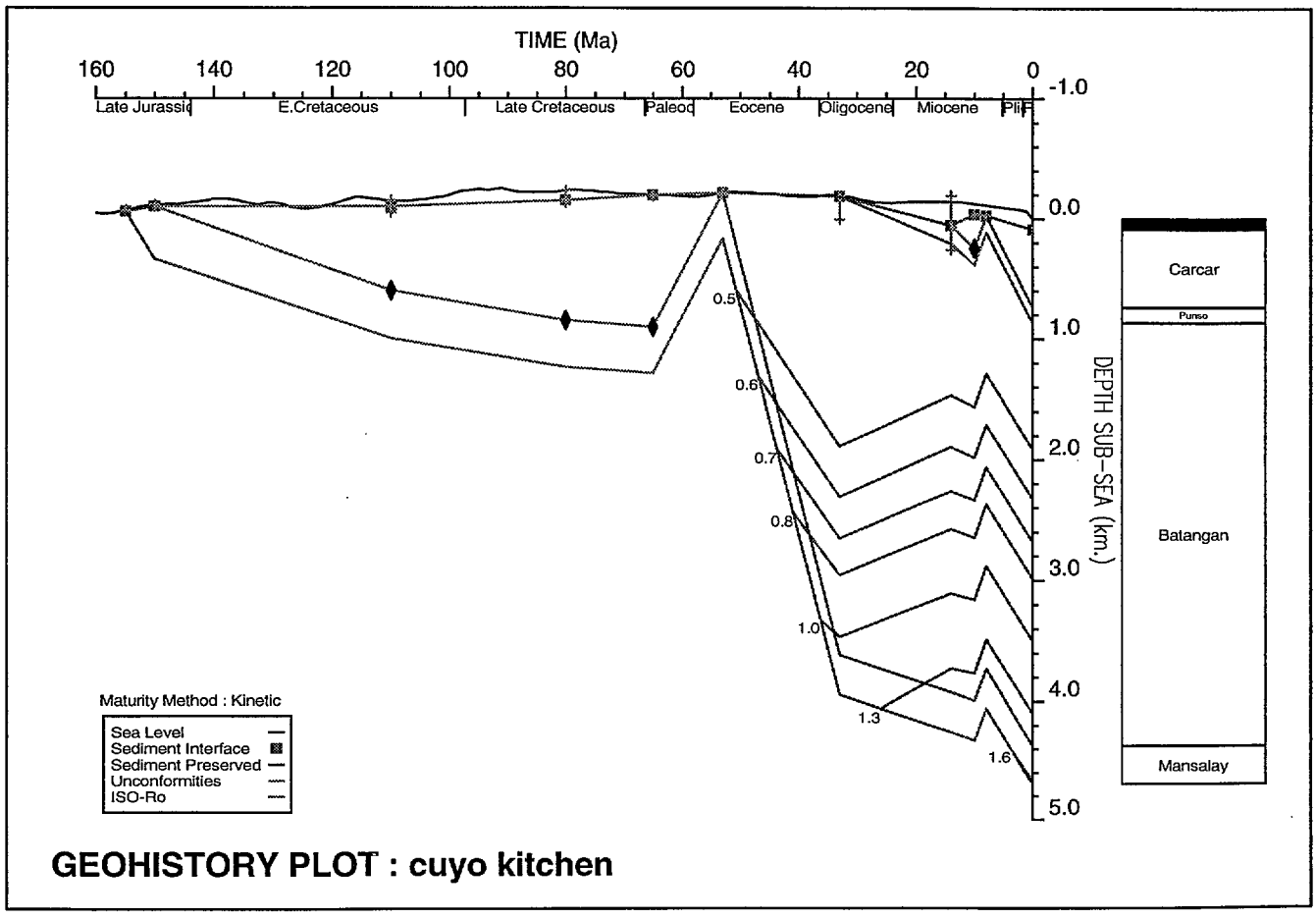

WinBury v1.3b C:\BURY\welldata\cuyo\cuyokcn\cuyokcn 3/06/94 10:06:28 AM

HORIZON MATURATION PLOT : cuyo kitchen

Maturity Method : Kinetic

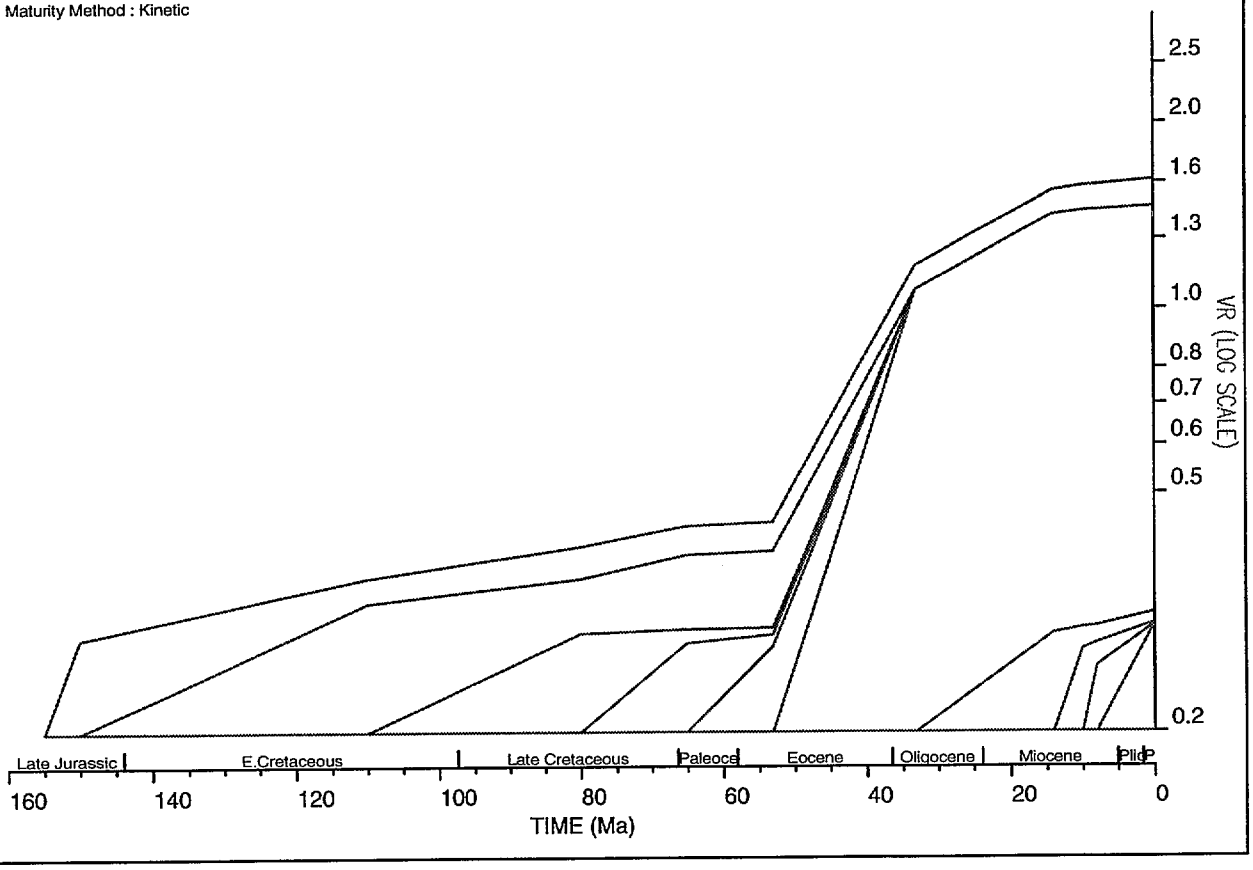

WinBury v1.3b C:\BURY5\welldata\cuyo\cuyokcn\cuyokcn 3/06/94 12:10:9 PM

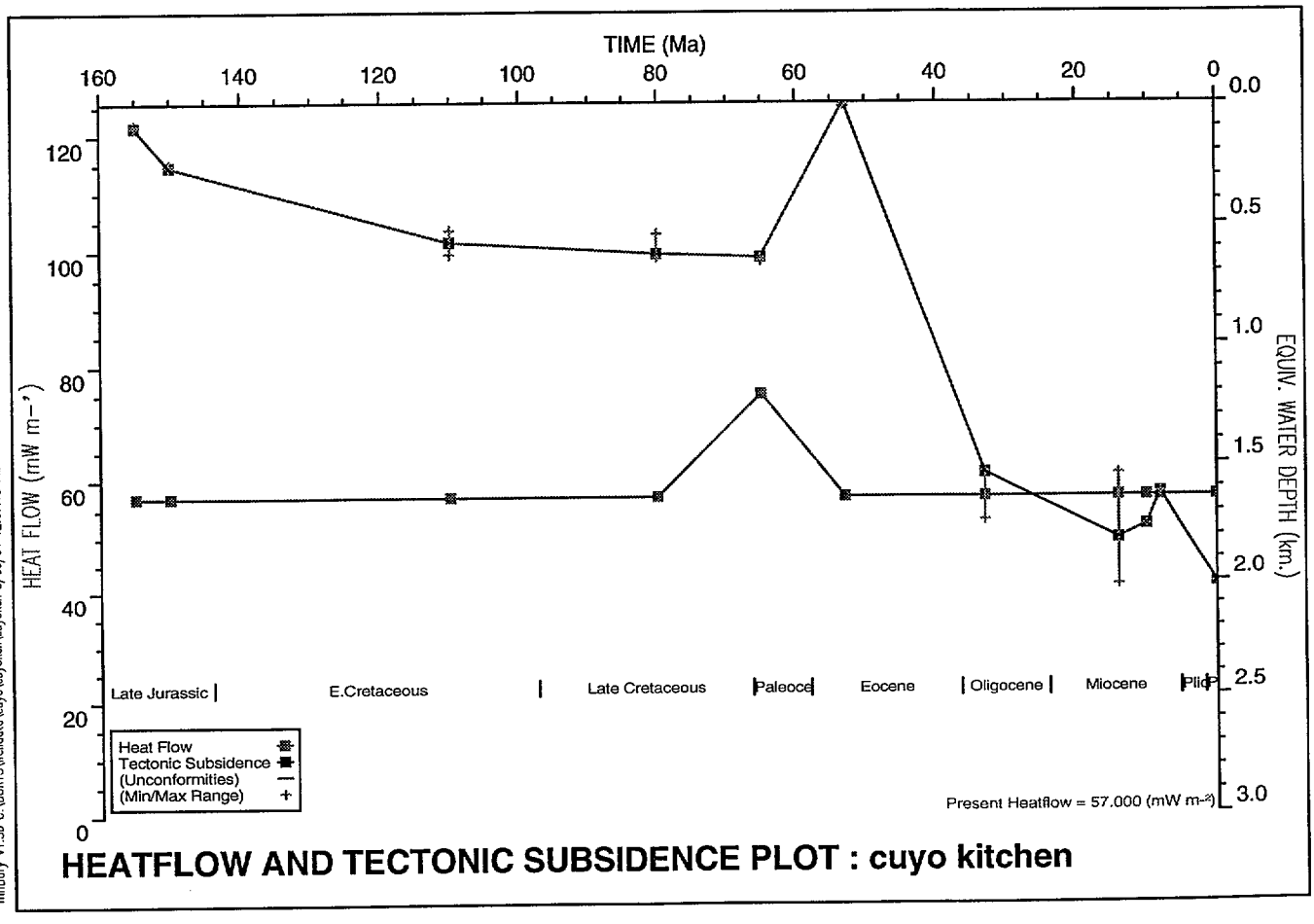

WinBury v1.3b C:\BURY5\welldata\cuyo\cuyokcn\cuyokcn 3/06/94 12:07:13 PM

HEATFLOW AND TECTONIC SUBSIDENCE PLOT : cuyo kitchen

DUMARAN SUB-BASIN

AGSO 1994

Latitude: 10° 05' 12" N
KB: 0m asl
Surface Temperature: 28°C
BHT: 90°C (estimate)
Seismic location: Line SS-205-80 sp 80

Longitude: 120° 00' 48" E
TD: 7000mKB
Surface Elevation: 1464m bsl
BHT Depth: 3000m

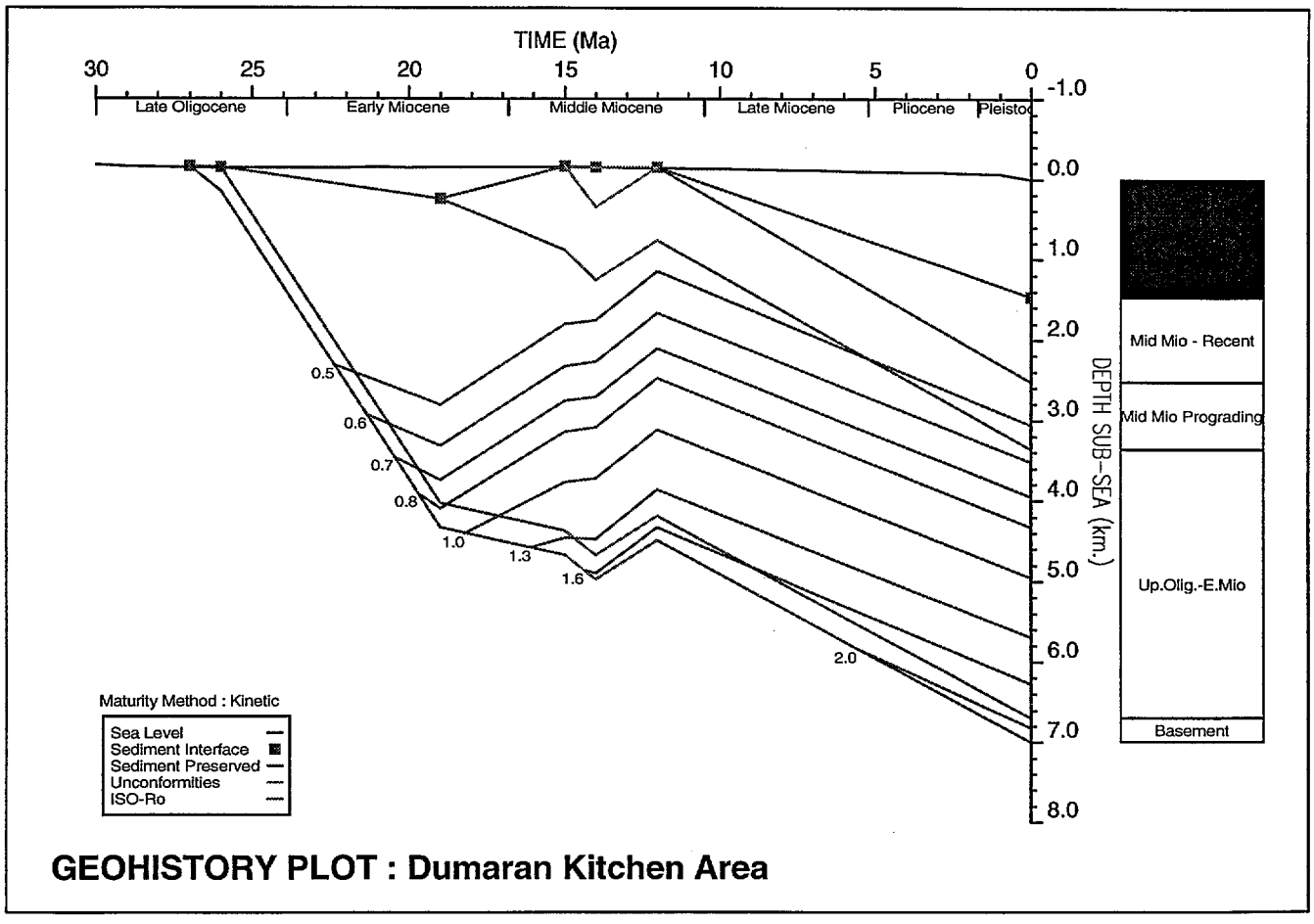

GEOHISTORY PLOT : Dumaran Kitchen Area

WinBury v1.3b C:\BURY5\welldata\nepdlawo\dumaken\dumaken 6/05/94 1:44:42 PM

The burial history plot of the kitchen (HC-generating area) downdip from the Dumaran prospect shows the prograding Middle Miocene sequence marginally mature for hydrocarbons. The underlying Late Oligocene to Early Miocene succession occupies the rest of the liquid hydrocarbon window, and contains more than three kilometres of sediments.

	Stratigraph. Unit/Event	E V	Depth to Top of Unit	Age (Ma)	Minimum WtrDpth	Maximum WtrDpth	Modelled WtrDpth	Sea Bed Temp.	Heatflow	Lithology Data	Kerogen Data	Variable Beds
1	Mid Mio - Recent	N	1464.00	0.00	1464.00	1464.00	1464.00	28.00	70.00			
2	Mid Mio unconf	E	2526.00	12.00	-15.24	0.00	-6.10	27.78	70.00			
3	Mid Mio eroded	E	(500.00)	14.00	-15.24	0.00	-6.10	27.78	70.00			
4	Mid Mio Prograding	N	2526.00	15.00	-15.24	0.00	-6.10	27.78	70.00			
5	Up.Olig.-E.Mio	N	3355.00	19.00	-15.24	400.00	394.15	27.78	70.00			
6	Basement	N	6700.00	26.00	-15.24	-15.24	-15.24	27.78	70.00			
7	TD	N	7000.00	27.00	-15.24	-15.24	-15.24	27.78	70.00			

HORIZON DATA : DUMAKCN

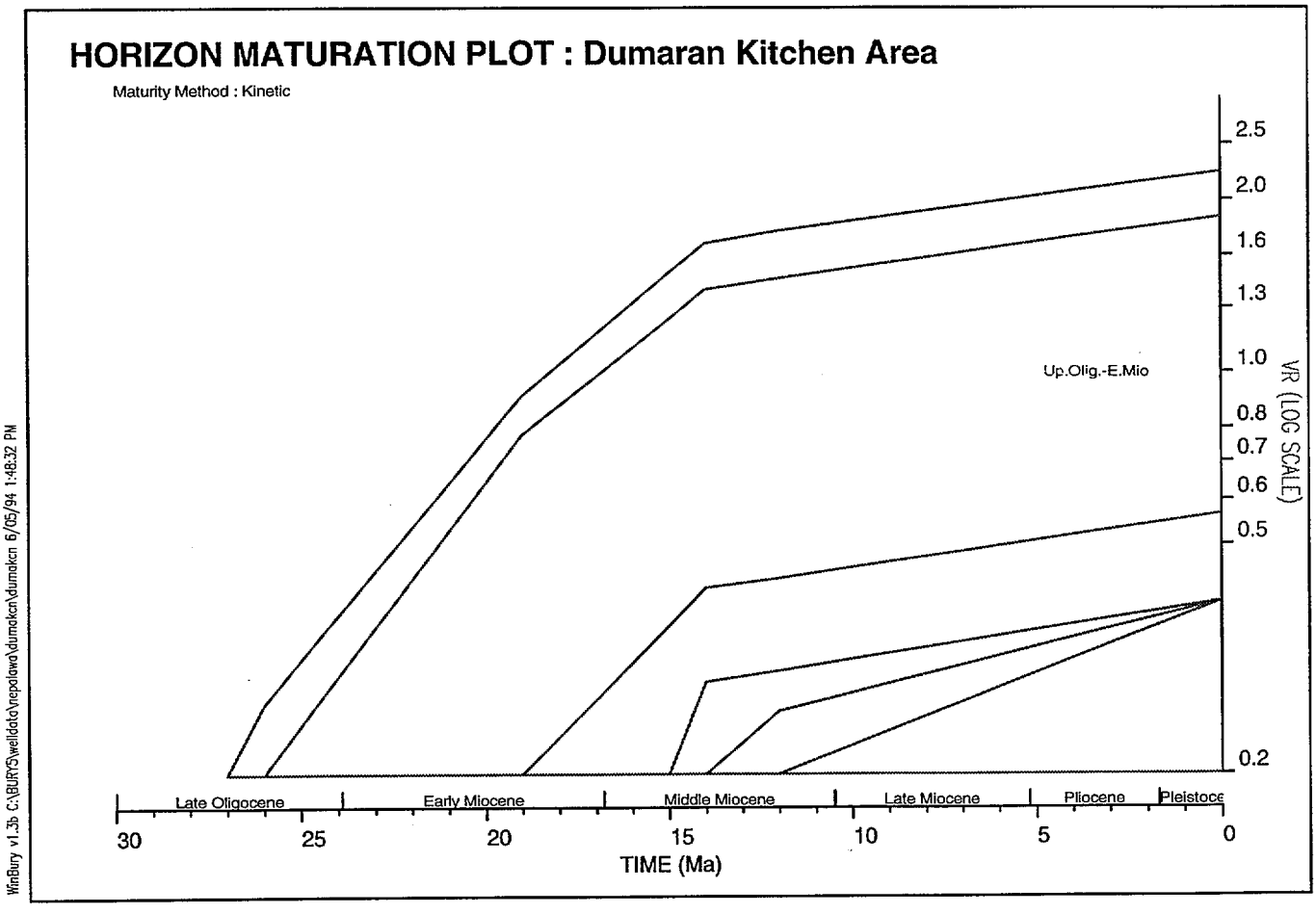

The time versus maturity plot of the Dumaran generating area, 23 km downdip from the proposed well location.

ROXAS AREA

AGSO 1994

Latitude: 9° 49' 36" N
KB: 0m asl
Surface Temperature: 28°C
BHT: 100°C (hypothetical)
Seismic location: Line SS-207-80 sp 1

Longitude: 119° 44'18" E
TD: 4500mKB
Surface Elevation: 1058m bsl
BHT Depth: 3000m

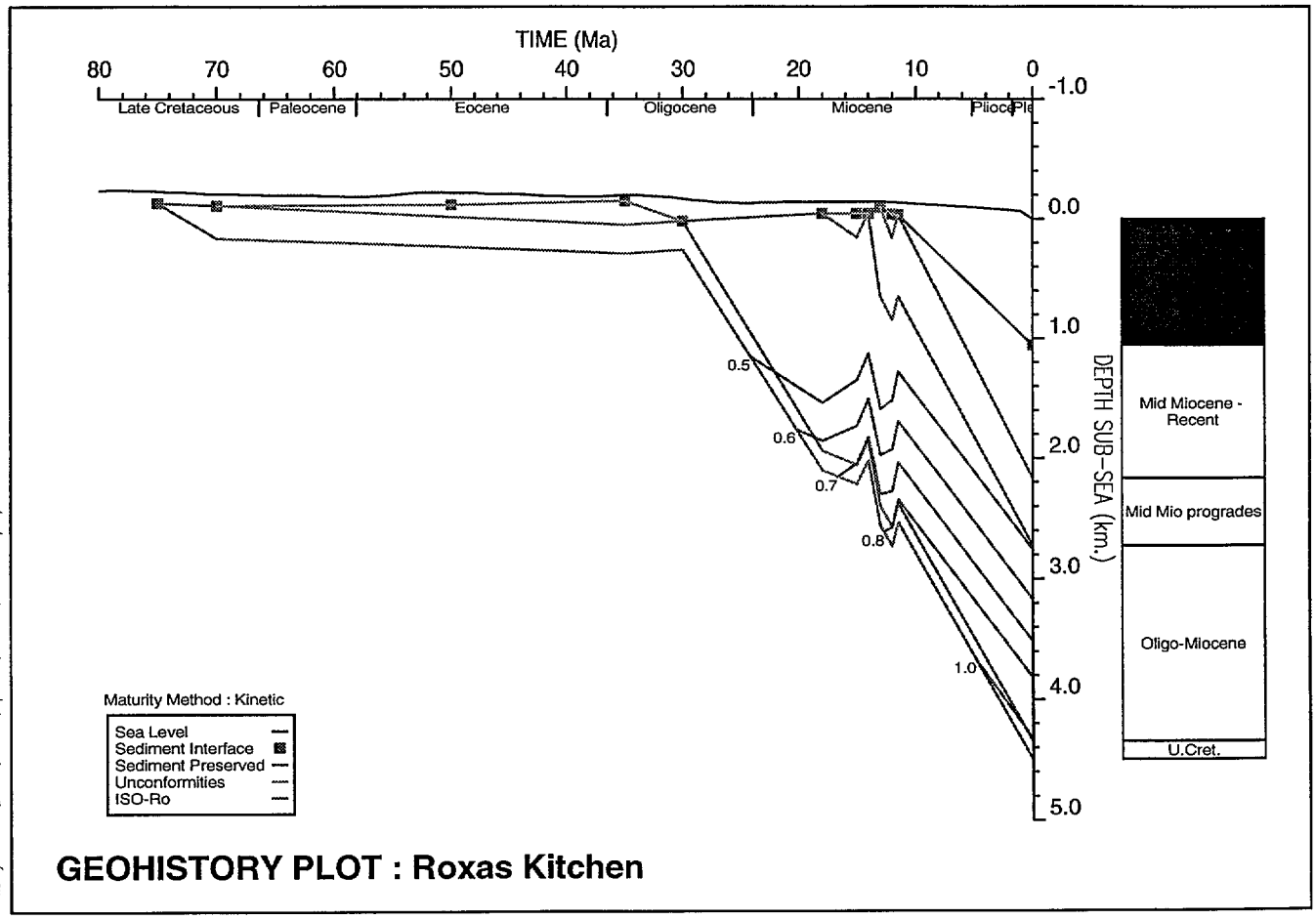

GEOHISTORY PLOT : Roxas Kitchen

The geohistory plot of the Roxas kitchen area, 30 km downdip from the Roxas M prospect. The succession from the Late Cretaceous to the Oligocene has not been drilled and is not known, but the plot shows some uplift and erosion attributed to the early Oligocene, possibly at rift onset. The area, which is near a depocentre, shows rapid subsidence since the later Oligocene, with a brief interruption in the Middle Miocene. This is a minor version of the substantial Middle Miocene uplift and erosion that has occurred on the platform areas of Palawan and Cuyo to the northwest. The subsidence has continued to the present day, and the succession below the Middle Miocene prograding sequence is mature for hydrocarbons.

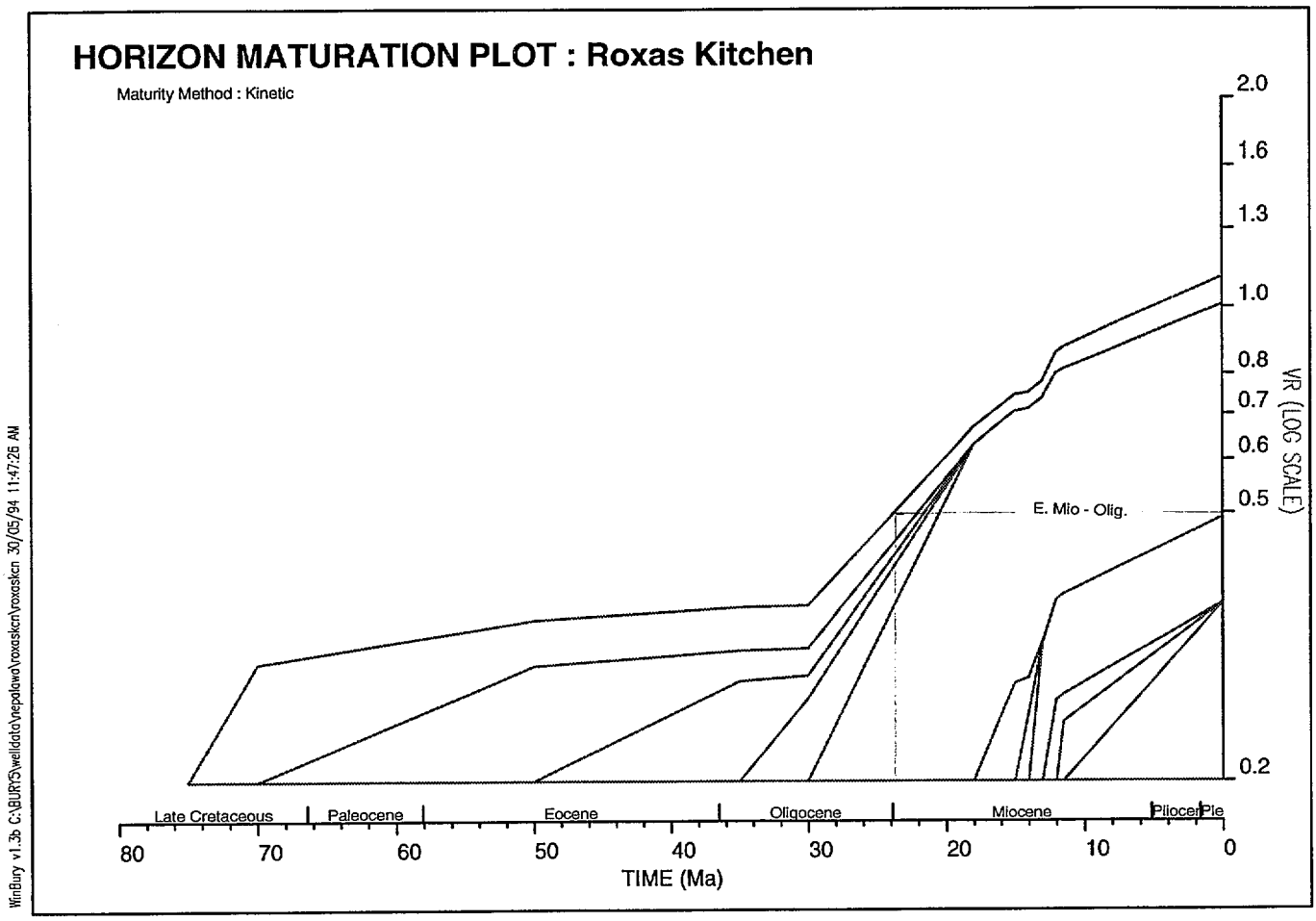

The horizon maturation versus time plot of the Roxas kitchen area shows that Cretaceous sediments began to achieve maturity at about 25 Ma BP, and the succession above the 'base Tertiary' unconformity at 20 Ma. The sloping lines indicate steadily increasing maturity to the present day, with a minor halt in the Middle Miocene. The base of the Middle Miocene prograding sequence has just reached the threshold of maturity at a Vitrinite reflectance of 0.5.

	Stratigraph. Unit/Event	E V	Depth to Top of Unit	Age (Ma)	Minimum WtrDpth	Maximum WtrDpth	Modelled WtrDpth	Sea Bed Temp.	Heatflow	Lithology Data	Kerogen Data	Variable Beds
1	Mid Miocene - Recent	N	1058.00	0.00	1058.00	1058.00	1058.00	28.00	75.00			
2	Mid Mio unconf	E	2170.00	11.50	0.00	100.00	100.00	28.00	75.00			
3	deposit m1	E	(200.00)	12.00	0.00	100.00	100.00	28.00	75.00			
4	Mid Mio progrades	N	2170.00	13.00	0.00	50.00	50.00	28.00	75.00			
5	Base Mid Mio prog	E	2727.00	14.00	0.00	100.00	100.00	28.00	75.00			
6	deposit m3	E	(200.00)	15.00	0.00	100.00	100.00	28.00	75.00			
7	Oligo-Miocene	N	2727.00	18.00	0.00	100.00	100.00	28.00	75.00			
8	Base Te	E	4347.00	30.00	0.00	200.00	190.33	28.00	75.00			
9	Deposit O	E	(200.00)	35.00	0.00	200.00	50.00	28.00	95.00			
10	deposit Pg1	E	(100.00)	50.00	0.00	100.00	100.00	28.00	75.00			
11	U.Cret.	N	4347.00	70.00	0.00	100.00	100.00	28.00	85.00			
12	TD	N	4500.00	75.00	0.00	100.00	100.00	28.00	95.00			

HORIZON DATA : ROXASKCN

APPENDIX 4

NEW HYDROCARBON GEOCHEMISTRY OF OIL AND GAS SEEPS FROM BONDOC AND BICOL, SE LUZON BASIN

by

E. Cortez[1] and A. P. Murray[2]

1 Department of Energy, Makati, Metro Manila, Philippines
2 Australian Geological Survey Organisation, Canberra, ACT, Australia

ABSTRACT

This report deals with the hydrocarbon composition of oils and gases from the Bondoc and Bicol areas of the SE Luzon Basin, the Philippines. The oils were analysed by gas chromatography, gas chromatography/mass spectrometry, stable carbon isotope mass spectrometry and UV/Visible spectrophotometry (porphyrins). The stable carbon isotope composition of three gas samples was also determined. The aim of the oil analyses was to characterise the source rocks in terms of the type of organic matter present, depositional environment, probable age and maturity at generation. The gases were analysed to determine if they were of biogenic or thermogenic origin and whether they were isotopically similar to bottom water samples taken in the Ragay Gulf by the AGSO vessel *Rig Seismic*.

The results indicate that the source rocks for all five oils were rich in resinuous terrestrial organic matter and were deposited in oxic to sub-oxic conditions, probably in a lower delta plain, lacustrine plain, or inner neritic setting. In broad terms, the depositional environment can be classified as "Fluvio-Deltaic" by analogy with similar systems in Indonesia and New Zealand and the source rocks are probably hydrogen rich coals or carbonaceous shales.

The age of the source rocks is Cainozoic and probably Oligocene, Miocene or younger.

The Bondoc oils were generated from early mature source rocks. Alhough comparisons of maturity among SE Asian oils must be treated with caution, it appears that the Bicol oil was generated at higher maturity than those from Bondoc.

The isotopic composition of a gas from a well on the Bondoc Peninsula is consistent with it being of thermogenic origin and associated with the oils from this area. It is also similar to the isotopic composition of bottom water gas samples from the Ragay Gulf. Two gases sampled in the Bicol area have a different and probably biogenic origin.

CONTENTS

INTRODUCTION 7

ANALYSIS 7

RESULTS 10

DISCUSSION 10

Biodegradation
Organic Matter Type, Depositional Environment and Source Rock Lithology
Source Rock Age
Source Rock Maturity
Stable Isotope Composition of the Gas Samples
Isotopic Composition of Oil Fractions

REFERENCES 19

EXPLANATION OF THE SOURCE AND MATURITY PARAMETERS USED IN TABLE 1

APPENDIX 1A GAS CHROMATOGRAMS

APPENDIX 1B METASTABLE REACTION MONITORING GCMSMS CHROMATOGRAMS

INTRODUCTION

This report presents the results of analyses of five oil and four gas samples from the Bondoc and Bicol Peninsulas of the SE Luzon Basin, the Philippines. The samples were as follows (see Fig. 1 for locations):

Area	Name	Type	AGSO No.
Bondoc Peninsula	BP-OS-01	Oil seep	791
	BP-OS-02	Oil	792
	Bondoc-2	Oil in mud	793
	Maalat-Canilbo	Oil seep in mud	794
	BP-GS-01	Gas	
Bicol Peninsula	C-17	Oil trapped in Basalt rock vesicles	795
	Libon-1	Gas	
	Libon	Gas	
	Sto. Nino	Gas	

The samples were collected during May 1993 by Neil Trinidad, Ed Guazon and Lito Aniceto of the Department of Energy under the direction of the Philippines Marine Seismic Survey Group. The aim of the oil analyses was to characterise, as far as possible, the source rocks in terms of the type of organic matter, age, maturity and depositional environment. The stable isotope analyses of the gases were carried out to determine whether they were of biogenic or of thermogenic, oil associated origin and to provide a comparison with the light hydrocarbon geochemistry conducted by the AGSO vessel *Rig Seismic* in the bottom waters of the Ragay Gulf and the Tayabas Bay (Evans *et al.*, 1992). Only three of the gas samples were analysed, as the sample from Sto. Nino did not survive transport from the Philippines to Australia.

Earlier geochemical studies, done under a Department of Energy - World Bank Project on the SE Luzon basin, reported that the oils seeps in the area were sourced from resinuous kerogen (Bureau of Energy Development, 1986).

ANALYSIS

The whole oils were separated into saturate, aromatic and polar fractions by column chromatography on activated silica gel and weight percentages of non-volatile saturate, aromatic and polar fractions were determined by gravimetry. The saturate fractions were analysed by gas chromatography (GC) on a 25m x 0.2mm HP ultra 1 column

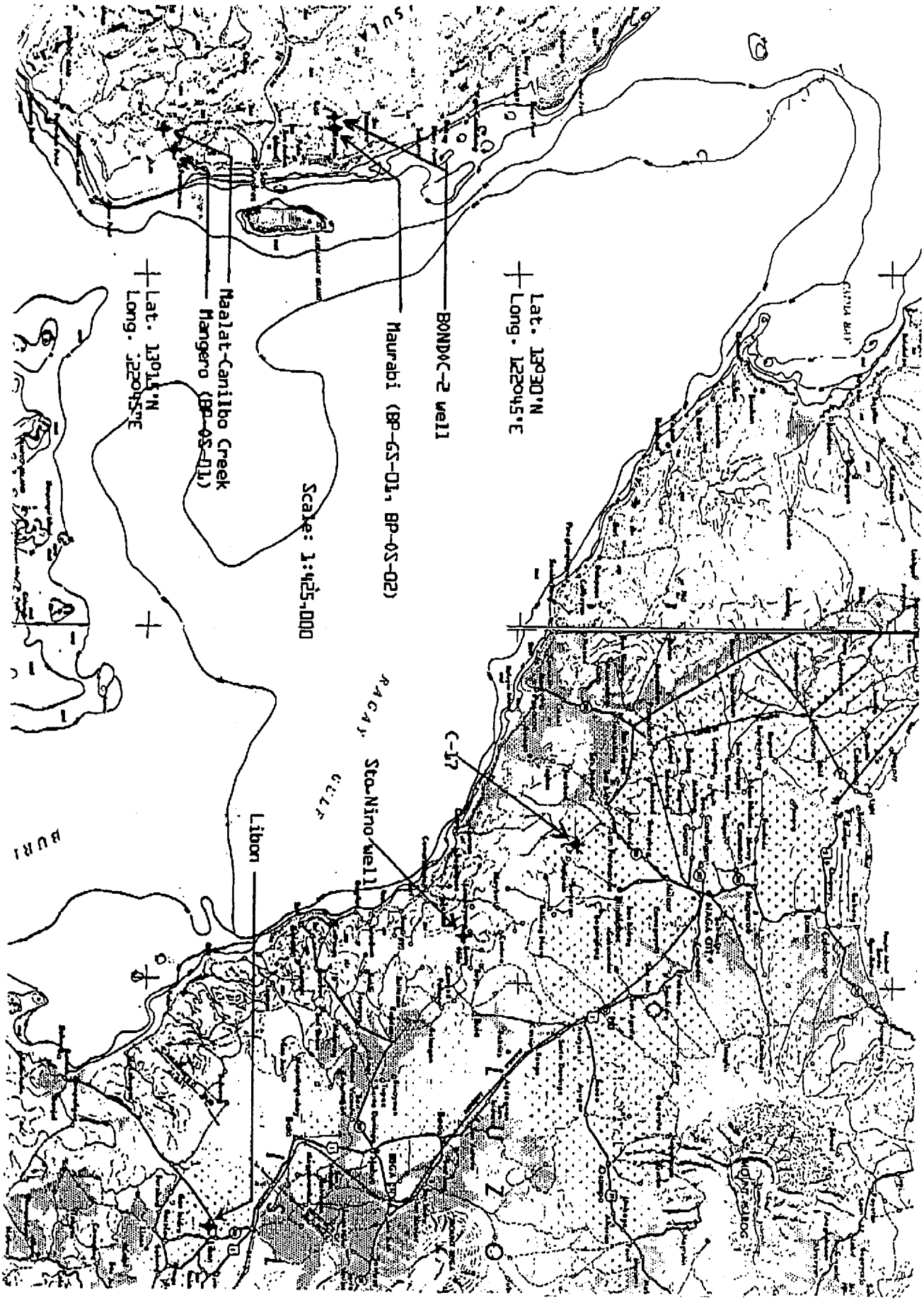

Fig. 1 ***Location map of the oil and gas samples taken from the Bondoc and Bicol Peninsulas of the SE Luzon Basin, Philippines.***

(methylsilicone) using on-column injection and a temperature program from 50 to 300 °C at 4 °C min^{-1}. The carrier gas used was H_2 with flow rate of 30 cm sec^{-1}. An internal standard (3-methylheneicosane) was added prior to analysis.

The saturate fractions were also analysed by metastable reaction monitoring gas chromatography-mass spectrometry (MRM-GCMS) on a VG70E double focussing mass spectrometer connected to a HP5790 gas chromatograph fitted with a 50m x 0.2mm HP Ultra-1 (methylsilicone) column. The GC was programmed from 50 to 180 °C at at 10 °C min^{-1} and then to 300 °C at 3 °C min^{-1}. The MS was operated in the metastable reaction monitoring (MRM) mode observing 26 parent-daughter ion pairs representing various biomarker compounds. One of these pairs (m/z 389 - 234) is generated by the trideuterated methylcholestane added as an internal standard (100 ng) prior to analysis. The aromatic fractions were analysed by GCMS in the selected ion monitoring mode (SIM-GCMS) observing ions characteristic of phenanthrene (m/e 178), methyl phenanthrenes (m/e 192), dimethyl phenanthrenes (m/e 206) and retene (m/e 219). To allow comparison to previous and subsequent work which may not employ MRM-GCMS methods, the saturate fractions were also analysed by SIM GCMS. This generated the more conventional (albeit less useful) series of m/e 191, 217, 412 etc mass chromatograms. These chromatograms are not reproduced here but were provided to the Philippines Department of Energy for use in methods development and quality control.

UV-VIS spectrophotometry was done on the aromatic and polar fractions in order to determine the two most common organometallo species in petroleum, i.e., the nickel (Ni^{2+}) and vanadyl (VO^{2+}) porphyrins. The fractions were dissolved in 1 ml of chloroform which had been modified by addition of 50 µl/litre cyclohexane and trimethylamine. The diluted sample were pipetted into 0.1 cm path length cells and scanned from 650 to 500 λ on a Hitachi 220 spectrophotometer. The concentration of the porphyrin species was then calculated from the absorbances at 550 nm and 570 nm using molar absorptivities of 30,000 l mol^{-1} cm^{-1} and 31,600 l mol^{-1} cm^{-1} for nickel and vanadyl species respectively.

For stable carbon isotope analysis of gases, about 3.0 ml of the sample was drawn out by means of a gas-tight syringe and injected, together with an equal volume of oxygen, into a Cu_2O furnace at 830 °C in a vacuum preparation line. Combustion was allowed to proceed for 90 minutes, after which the resulting water and carbon dioxide were cryogenically separated by successive immersion of the tube in an alcohol-solid CO_2 mixture and liquid nitrogen respectively. The purified CO_2 was analyzed for its $\delta^{13}C$ value on a VG SIRA 12 mass spectrometer.

Determination of the $^{13}C/^{12}C$ ratio of the saturate and aromatic fractions of the oils was carried out on a Finnigan Mat 252 isotope ratio mass analyzer. Approx. 2 mg of each fraction were sealed in a quartz tube and oxidized over cuprous oxide at 950 °C. The $^{13}C/^{12}C$ of the resultant CO_2 was measured and compared to a PDB belemnite standard to obtain values for $\delta^{13}C_{PDB}$.

The interpretation of biomarker data in this report follows guidelines set out in The Biomarker Guide (Peters and Moldowan,1993), as well as other recent literature and AGSO's own research.

RESULTS

Chromatograms obtained from GC and GCMS analyses are compiled in Appendix 1. Table 1 summarises the source, maturity and biodegradation parameters derived from the GC and GCMS chromatograms and compares them with similar data for fluvio-deltaic oils from the Ardjuna and Taranaki Basins (Java and New Zealand) and for an outcrop sediment from Leyte, the Philippines. The table is an excerpt from an excel spreadsheet/database which gives precedence to biomarker source parameters which are resistant to alteration by biodegradation. The raw data from which these parameters were calculated is available on request from AGSO or the Philippines Department of Energy. Table 2 gives the guidelines used at AGSO to rank the level of biodegradation of oils. Figure 2 plots the stable isotope values for the gas samples as compared with those of methane in bottom-water gases from the Ragay Gulf and Tabayas Bay and Figure 3 gives a speculative classification of Bondoc and Bicol oil samples based on carbon isotopes in the saturate and aromatic fractions. Figure 4 shows how the isotope ratio for an oil-associated gas is expected to differ from that of the oil at various maturity levels.

DISCUSSION

Biodegradation

All samples show either depletion or complete loss of n-alkanes due to biodegradation. The extent of biodegradation varies from light to moderate (1 to 5 on the scale given in Table 2). The loss of n-alkanes is due to the fact that these are the most susceptible of the compounds found in oils to biodegradation and none of the samples show evidence for attack on the more resistant cyclic biomarkers such as hopanes and steranes. However, substituted aromatic compounds including the methyl phenanthrenes were removed or depleted for all samples except BP-OS-01, meaning that the methyl phenanthrene maturity indicator is reliable for this sample only. Similarly, the isoprenoids pristane and phytane were partially or completely removed from samples BP-OS-02, Bondoc-2, Maalat Canilbo and C-17 and so the pristane/phytane ratio is strictly valid only for sample BP-OS-01. However, since biodegradation can reduce the pristane/phytane ratio, originally high values are also likely for samples BP-OS-02, Bondoc-2 and Maalat Canilbo (Table 1).

Organic Matter Type, Depositional Environment and Source Rock Lithology

In addtion to the ubiquitous hopanes of bacterial origin, the oils all contain abundant oleananes, bicadinanes and a series of oleanane-related compounds (tentatively identified as ring A-contracted triterpanes). These compounds are derived from precursors found in angiosperm land plants and together with the high pristane/phytane and pristane/nC_{17} ratios indicate a strong contribution from terrestrial plants to the source matter. However, there are several clues that algae also contributed to this source matter: Firstly, the ratios of C_{27}/C_{29} and $C28/C_{29}$ steranes are higher than is usually seen for oils sourced solely or primarily from land plant material. This can be seen from the comparison in Table 1 between these indices for the present samples and otherwise similar oils from NW Java and Borneo. Secondly, the samples contain 4-methyl-24-ethyl steranes. These compounds arise from precursor sterols present in some dinoflagellate, prymnesiophyte and macrophytic algae and are found in greatest concentration in oils sourced from lacustrine sediments. However, the concurrent presence of other C_{30} steranes, namely dinosteranes and traces of 24-n-propylcholestanes (unequivocal marine markers), suggests that marine algal matter is at least partly responsible for the abundance of C_{27} steranes and 4-methyl

Table 1. Bulk composition, stable isotope and biomarker source and maturity parameters for Bondoc/Bicol oils.

	AGSO No.	791	792	793	794	795	372	772	6013	Primary indication of each parameter listed with secondary indication where applicable. For parameters expected to have been affected by biodegradation "<" or ">" indicates the probable range of the original value, before degradation. A "~ "symbol indicates that the parameter has been affected in an unknown way by biodegradation. "bd" indicates that the value cannot be calculated due to complete loss of one or more component. "na" = not available. "nd"= not detected
	Name	**BP-OS-01**	**BP-OS-02**	**Bondoc-2(?)**	**Maalat C.**	**C-17**	**NW Java**	**Borneo**	**Sed**	
	Well No./Seep	Seep	Seep	Well	Seep	Seep	MMC	Oil	O'crop	
	Basin	SE Luzon	SE Luzon	SE Luzon	SE Luzon	SE Luzon	Ardjuna	Tarakan	Visayan	
	Region	Bondoc	Bondoc	Bondoc	Bondoc	Bicol	Java	K'mantan	Leyte	
	Country	Philippines	Philippines	Philippines	Philippines	Philippines	Indon.	Indon.	P'Pines	
	GCMS Run No. (Sats)	3JU5C-1	3JU15C-2	3JU15C-3	3JU15C-4	3JU15C-5	2DE24A-5	3MY14A-5	2AP30A-5	
	GCMS Run No. (Aroms.)	3JU6A-1	3JU16A-2	3JU16A-3	3JU16A-4	3JU6A-5	3JL2A-9	3MY15A-3	na	
	GC Run No.	791S	792S	793S	794S	795S	372REP1	772S	6013S	
1	Level of biodegradation	1	3	4	2	5	1	1	1	1= Intact, 5 = Moderate, 10 = Severe
2	% Saturates	57.8	>71.3	>38.9	>82.8	>50.8	52.3	45.8	13.6	As percentage of whole oil.
3	% Aromatics	6.5	<15.4	<35.2	<10.7	<23.8	23.6	31.1	18.2	As percentage of whole oil.
4	% Polars	2.1	<24.0	<16.3	<4.2	<10.5	27.5	5.3	26.9	As percentage of whole oil.
5	δ^{13}C Sats	-26.6	-26.4	-26.2	-26.5	-32.3	na	na	na	Relative to PD Belemnite
6	δ^{13}C Arom	-26.4	-29.3	-26.4	-27.5	-30.1	na	na	na	Relative to PD Belemnite
7	Most abundant n-alkane	C14	bd	bd	bd	bd	C25	C14	C29	Range C9 to C34
8	Pristane/nC17	3.0	bd	bd	11.8	bd	1.4	2.0	5.7	Source, Biodegradation
9	Phytane/nC18	0.54	bd	bd	2.1	bd	0.21	0.35	0.73	Source, Biodegradation, Maturity
10	Pristane/Phytane	7.0	2.5	3.6	7.5	bd	6.8	6.3	6.8	Source (> 3= Oxic, < 1= Anoxic or Hypersaline)
11	Carbon Preference Index (CPI)	1.17	bd	bd	bd	bd	1.09	1.12	1.23	Maturity, Source
Biomarker Source Parameters Resistant to Biodegradation below level 8:										
12	C27/C29 Diasteranes	0.41	0.42	0.37	0.43	0.56	0.18	0.11	0.16	Source (High for Algal vs. Terrestrial)
13	C28/C29 Diasteranes	0.69	0.58	0.73	0.62	0.60	0.38	0.21	0.31	Source (High for Algal vs.Terrestrial)
14	Oleanane/C29 Diasteranes	2.24	0.96	1.28	1.75	0.77	0.71	0.40	3.50	Source (High for Angiosperm vs. Eukaryote)
15	C30 Hopane/C29 Diasteranes	2.02	1.18	0.97	1.46	1.61	2.13	0.52	2.87	Source (High for Prokaryote vs Eukaryote)
16	Sum of Bicads/C30 Hopane	7.05	16.13	13.7	11.1	22.0	20.0	29.8	1.7	Source (High for A'sperm Resinite vs Prokaryote)
17	Oleanane/C30 Hopane	1.11	0.81	1.32	1.20	0.48	0.33	0.76	1.22	Source (High for Angiosperm vs. Prokarytote)
18	A Cont Triter/C30H	0.87	0.92	1.45	1.20	0.45	1.41	1.81	4.30	Source (High for Angiosperm vs. Prokarytote)
19	A Cont Triter/Olean	0.79	1.12	1.10	0.99	0.94	4.21	2.37	3.52	Correlation
20	Gammacerane/C30H	0.00	0.00	0.00	0.00	0.41	0.00	0.00	0.00	Often high for elevated salinity in dep. env.
21	C29/C30 Hopane	0.57	0.70	0.63	0.74	1.73	0.41	0.65	0.31	Source (Usually > 1 for anoxic, carbonate SR))
22	C31/C30 Hopane	0.29	0.26	0.34	0.28	0.27	0.39	0.43	0.20	Source (High for anoxic deposition)
23	C29 Neo/Regular Hopane	0.44	0.32	0.31	0.40	0.95	0.69	0.32	0.10	Source, Maturity (High for oxic, clastic SR)
24	Sum C31MeHop/C30 Hop	0.12	0.14	0.14	0.11	0.20	0.12	0.10	0.02	Correlation
25	2αMe/3βMe C31H/C30H	4.25	5.46	3.15	4.18	3.40	6.29	3.16	2.47	Correlation
26	Bicadinane T/MeT	0.72	0.64	0.54	0.57	0.76	0.53	1.42	1.16	Correlation
27	Bicadinane W/T	0.13	0.17	0.24	0.15	0.12	0.47	0.16	0.19	Correlation

Table 1. (cont.)

	AGSO No.	791	792	793	794	795	372	772	6013	Primary indication of each parameter listed with secondary indication where applicable. For parameters expected to have been affected by biodegradation "<" or ">" indicates the probable range of the original value, before degradation. A "~ "symbol indicates that the parameter has been affected in an unknown way by biodegradation. "bd" indicates that the value cannot be calculated due to complete loss of one or more component. "na" = not available. "nd"= not detected
	Name	**BP-OS-01**	**BP-OS-02**	**Bondoc-2(?)**	**Maalat C.**	**C-17**	**NW Java**	**Borneo**	**Sed**	
	Well No./Seep	Seep	Seep	Well	Seep	Seep	MMC	Oil	O'crop	
	Basin	SE Luzon	SE Luzon	SE Luzon	SE Luzon	SE Luzon	Ardjuna	Tarakan	Visayan	
	Region	Bondoc	Bondoc	Bondoc	Bondoc	Bicol	Java	K'mantan	Leyte	
	Country	Philippines	Philippines	Philippines	Philippines	Philippines	Indon.	Indon.	P'Pines	
	GCMS Run No. (Sats)	3JU5C-1	3JU15C-2	3JU15C-3	3JU15C-4	3JU15C-5	2DE24A-5	3MY14A-5	2AP30A-5	
	GCMS Run No. (Aroms.)	3JU6A-1	3JU16A-2	3JU16A-3	3JU16A-4	3JU6A-5	3JL2A-9	3MY15A-3	na	
	GC Run No.	791S	792S	793S	794S	795S	372REP1	772S	6013S	
Biomarker Source Parameters Resistant to Biodegradation below level 6:										
28	C27/C29 Total Steranes	0.39	0.40	0.61	0.40	0.44	0.17	0.09	0.10	Source (High for Algal vs. Terrestrial)
29	C29 Diast/Total C29 Steranes	0.26	0.36	0.40	0.30	0.24	0.51	0.50	0.33	Source, Maturity (High for clastic SR)
30	4Me-C30 Ster (R)/C29 Ster (R)	0.14	0.15	0.27	0.15	1.03	0.13	0.04	0.05	Source (High for most lacustrine SR)
31	Total Hopanes/Steranes	0.68	0.62	0.46	0.60	2.18	2.20	0.69	1.39	Source (High for Prokaryote vs. Eukaryote)
Biomarker Maturity Parameters:										
32	C29Steranes 20S/(20S+20R)	0.37	0.40	0.43	0.33	0.67	0.52	0.46	0.57	Maturity (0.5 - 0.6 maximum mid oil window))
33	C31Hopanes 22S/(22S+22R)	0.59	0.59	0.59	0.57	0.50	0.51	0.48	0.57	Maturity (Max. 0.5-0.6 pre oil window)
34	C29 Steranes αββ/(ααα+αββ)	0.39	0.37	0.39	0.37	0.43	0.53	0.58	0.47	Maturity (~0.7 at peak generation)
35	Ts/Tm	0.73	1.02	0.98	0.95	0.91	0.71	0.41	0.26	Maturity, Source, SR lithology
36	C30Moretane/Hopane	0.14	0.10	0.15	0.13	0.09	0.10	0.12	0.14	Maturity (Decreases with maturity, pre-oil window)
37	Methyl Phenanthrene Index	0.80	nd	0.48	0.50	0.90	0.99	0.93	na	Maturity (Caution with Mz oils)
38	Rc (Radke & Welte, 1983)	0.88	nd	0.69	0.70	0.94	0.99	0.96	na	Calculated Vr = 0.6MPI+0.4
39	%C27S/%C29S	1.26	1.13	1.07	1.42	0.97	0.57	0.97	0.93	Mixing indicated if < 0.5 or >1.5

Table 2. Ranking the Extent of Biodegradation

Extent	Ranking	Alteration
Light	1	Lower n-alkanes depleted
Light	2	General depletion of n-alkanes
Light	3	Only traces of n-alkanes remain
Moderate	4	No n-alkanes, Isoprenoids intact
Moderate	5	Acyclic isoprenoids absent
Heavy	6	Steranes partly degraded
Heavy	7	Steranes degraded, Diasteranes intact
Very Heavy	8	Hopanes partly degraded
Very Heavy	9	Hopanes absent, Diasteranes attacked
Severe	10	Diasteranes, Aromatic steroids lost

Note 1: *In cases where 25-norhopanes are formed, degradation of hopanes may occur earlier, in conjuction with loss of the steranes. See text for within-class susceptibility of biomarker compounds.*

Note 2: *The exact stage at which loss of phenanthrene and its homologs occurs is unknown but it is before loss of steranes begins and approximately contiguous with loss of acyclic isoprenoids (i.e., 4 - 5).*

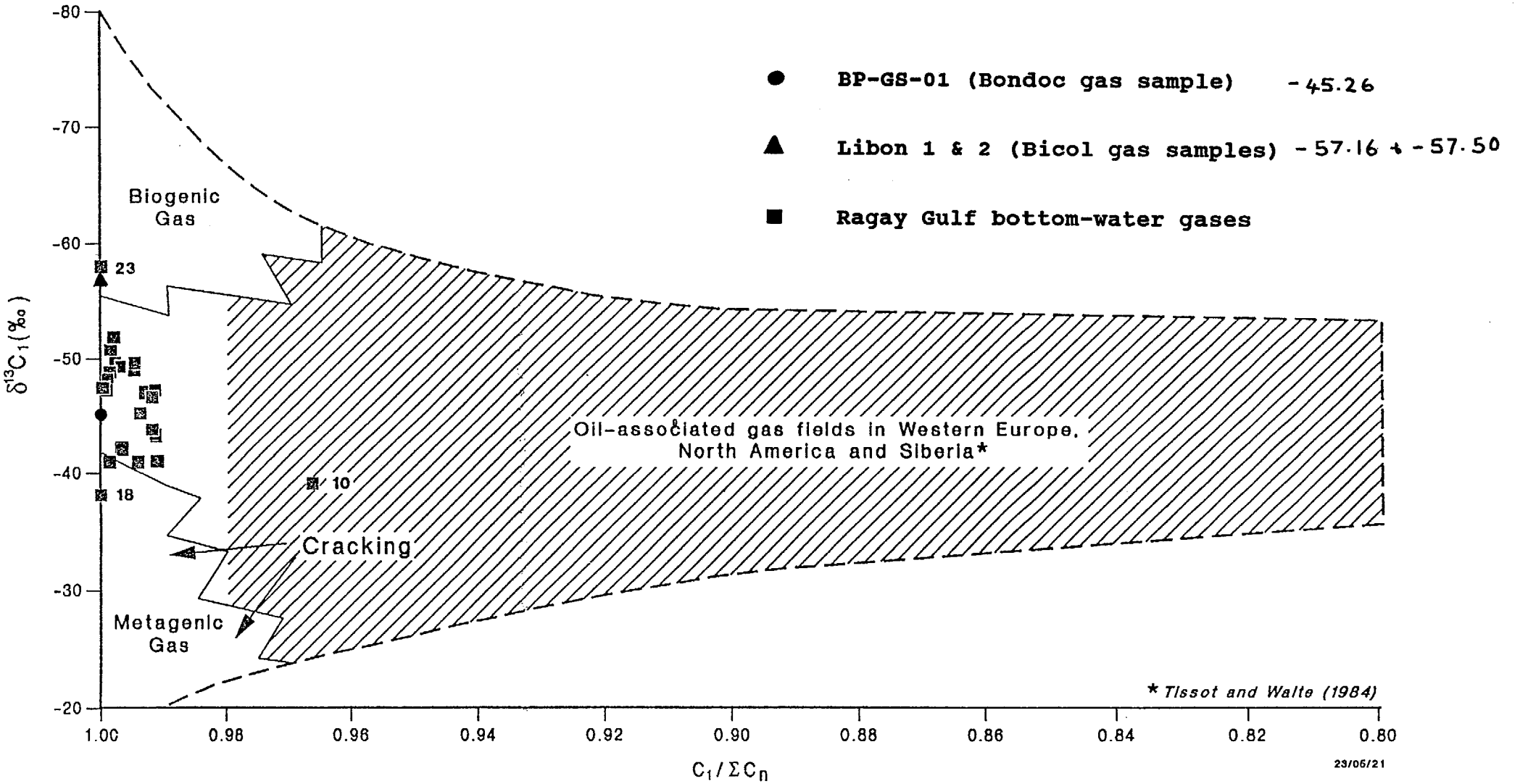

Fig. 2 ***Relative abundance and isotopic composition of methane in Bondoc and Bicol gas samples and in bottom-water gases from the Ragay Gulf.*** ***(after Even et al., 1992)***

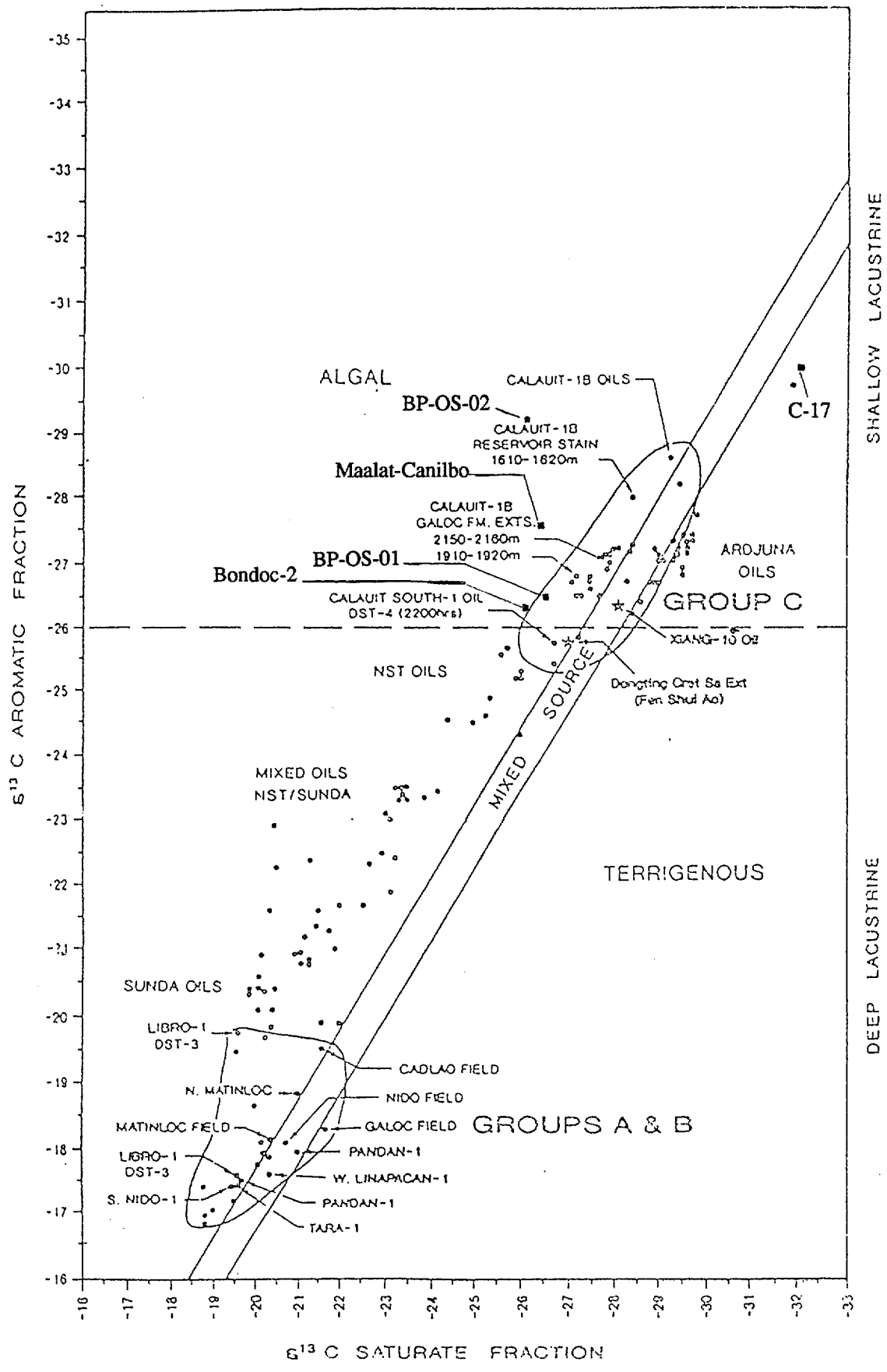

Fig. 3 Plot of Carbon Isotope Data (after Williams et al., 1992)

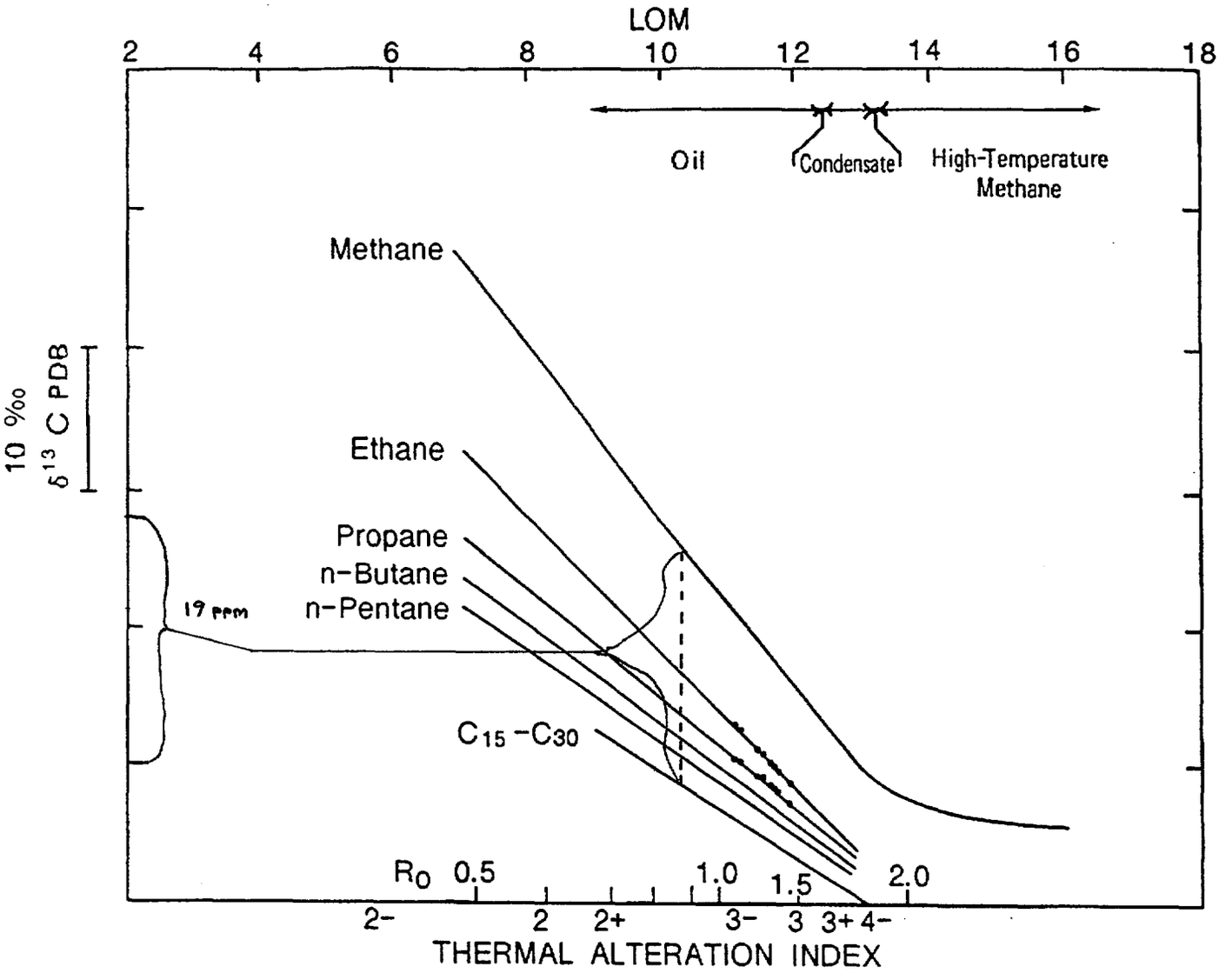

Fig. 4 ***Relation between isotopic composition of different hydrocarbon species as a function of maturity (after James, 1990)***

steranes. Since the high pristane/phytane ratios indicate oxic depositional conditions, this marine algal contribution could arise from periodic marine innundation of a peat swamp environment or alternatively, could indicate the contribution of a secondary marine source facies to the oils. Organofacies variation within a single source unit is known to occur in several instances and indeed might be expected in most deltaic and some lacustrine settings.

All samples show reasonably high diasterane/sterane ratios (Table 1). This is normally taken to indicate a clastic, clay rich source rock whereas low values (0.1 or below) are associated with anoxic, carbonate source rocks. While the diasterane/sterane ratio is not as high for the present samples as it is for some other fluvio-deltaic oils, it still is indicative of a clastic source rock. However, the biomarker composition of sample C-17 also shows a feature often associated with a carbonate source rock, that is, the presence of the 30-norhopane series along with the regular series of hopanes. This shows up most clearly in the greater abundance of the C_{29} as opposed to C_{30} hopane in sample C-17 but is also evident in the higher proportion of the C_{28} member (29,30 bisnorhopane) as compared with the other samples and in a small shoulder on the C_{30} hopane peak (due to the 30-nor compound). There are several possible explanations for the occurrence of 30-norhopanes in sample C-17 including: (a) migration of the oil through a mature carbonate sequence (b) co-sourcing of the oil from a carbonate-rich facies (c) more wide occurrence of these compounds than is currently recognised in the geochemical literature. At this stage we cannot determine which, if any, of these explanations is the correct one. However, it is interesting to note that many of the NW Palawan Basin oils also contain 30-norhopanes and yet have high diasterane/sterane ratios. These latter oils may have migrated long distances through early mature carbonates (Williams *et al.*, 1992; H. Williams, personal communication).

In addition to its 30-norhopane content the Bicol oil (C-17) differs from the Bondoc oils in several other respects, i.e., it has (a) a higher proportion of the 4-methyl steranes (b) a higher proportion of the C_{29} neohopane (c) a higher total hopane/sterane ratio and (d) a lower oleanane/hopane ratio and (e) a significant content of gammacerane (also called "g-Cerane"). The greater neohopane abundance is probably a maturity effect (see below) but the overall indication is that the source rocks for the oil from Bicol are not the same as those which sourced the Bondoc oils. The presence of gammacerane may indicate an evaporitic or carbonate facies in the source rock as this compound is often associated with hypersaline depositional conditions. However, it has also been reported to occur in some oils sourced from marine rocks. Given the abundance of terrestrial markers in the the Bicol oil, we may assume that, like the 30-norhopanes, it is a migration contaminant or is indicative of co-sourcing. Since we do not know the original pristane/phytane ratio for this oil, it is also possible that the biomarker suite represents anoxic deposition in a restricted circulation, lagoonal setting.

Trace amounts of Ni^{2+} porphyrins were observed in two of the Bondoc oils (BP-OS-01 and Bondoc-2) but these compounds were not detected in the remaining samples.These results are consistent with an origin for the oils from terrestrial/lacustrine organic matter and they effectively exclude the possibility of a major marine source component (Barwise,1990).

Source Rock Age

The main constraints on the age of the oils are the presence of abundant oleananes, oleanane-related ring A-contracted triterpenoids and bicadinanes. Oleananes and their

derivatives arise from precursor triterpenoids found in the flowering plants (angiosperms). Since these plants became dominant (over gymnosperms) during the late Cretaceous, this precludes an origin from rocks older than this. Bicadinanes are thought to arise primarily from the thermal destruction of resins exuded by some tropical hardwoods (e.g., those of the family *Dipterocarpaceae*). Though traces of bicadinanes are present in some early Tertiary and possibly some late Cretaceous oils, high concentrations have so far only been seen in oils sourced from late Oligocene, Miocene or younger strata. This accords with the fact that Dipterocarps did not become widespread and dominant in SE Asia until the Oligocene-Miocene (see references in Murray, 1993) and suggests that the Bondoc/Bicol oils were sourced from late Oligocene, Miocene or perhaps younger sediments. Further evidence for a post-Mesozoic source rock age is the absence of retene. This compound is a marker for conifer (gymnosperm) source matter and is usually found in terrigenous Mesozoic oils.

In considering biomarker evidence for source rock age, there is always a possibility that age-dependent compounds could be picked up as the oil migrates through younger strata. However, migration contamination would normally be accompanied by mixed maturity and or/source indications and no such indications were observed for the present samples. While it is true that there is some evidence for a mixed carbonate source for sample C-17, this should not lead to an erroneous age assessment as carbonate sediments should not be rich in terrestrially-derived bicadinane and oleanane compounds.

Source Rock Maturity

The four Bondoc oils have epimeric sterane and hopane distributions consistent with generation early in the oil window. However, it must be stressed that sterane epimer ratios (C_{29} S/S+R, Table 1) are often low for SE Asian oils, as compared with those from other regions and periods, and that sterane maturity indicators are not reliable when used in isolation. One of the most useful maturity indications - the n-alkane profile - is not applicable here because of the effects of biodegradation. Similarly, the methyl phenanthrene index (MPI) can also be affected by biodegradation and probably has been so affected for all samples except BP-OS-01. The MPI value for this sample (0.80) concurrs with the sterane ratio in suggesting generation in the early to middle oil window. The sole oil from the Bicol area, sample C-17, has a more mature looking sterane distribution than the Bondoc oils and a higher ratio of neo- to regular C_{29} hopanes (Table 1). Although this latter parameter also has a strong source dependence, high values are typical of advanced maturity (~ above R_V = 1.0). As mentioned earlier, the presence of gammacerane in the Bicol oil may indicate deposition under highly saline conditions and such conditions can disturb the normal relationship between sterane epimer ratios and maturity. However, the usual effect is to make the oil (or bitumen) seem less mature than would be apparent from bulk parameters. Thus, the possibility of a hypersaline depositional environment for the source of the Bicol oil does not alter our conclusion that it is more mature than those from Bondoc.

Stable Isotope Composition of the Gas Samples

As Fig. 2 shows, the gas sample from Bondoc had a $d^{13}C$ value similar to those collected from the bottom waters of the Ragay Gulf. This value is consistent with an oil associated gas whereas the two samples from Libon (Bicol), were found to be more depleted in ^{13}C and are probably of biogenic (i.e.,non-thermogenic) origin. An oil associated gas will normally contain ethane and other heavier hydrocarbons as well as methane, i.e., it will be a "wet" gas. We do not have any information on the "wetness" or otherwise of the gas

sample from Bondoc (BP-GS-01) but the samples from Bicol (Libon A and B were analysed in the Philippines Department of Energy Laboratories prior to transport to Australia. These analyses showed that the Libon gases were completely dry, i.e., no C_2 - C_4 hydrocarbons were detected. The isotope values for all three gas samples are plotted in Fig. 2 as if they were 100% methane.

James (1990) has presented a theoretical description of the relation between the isotopic composition of methane and the C_{15}-C_{30} hydrocarbons of an associated oil. This relationship, reproduced in Fig. 4, can be used to estimate the $d^{13}C$ value of an oil associated with the gas from BP-GS-1. Given a maturity in the early oil window (as suggested by biomarker evidence) this oil should have a $d^{13}C$ value 19 ppm heavier than the gas, i.e., -45.26 + 19 = - 26.26 ppm. This is within the range observed for the Bondoc oil saturate fractions (- 26.2 -> - 26.6 ppm, Table 1).

Isotopic Composition of Oil Fractions

Stable carbon isotope ratio ($d^{13}C$) values for saturate and aromatic fractions of the oils appear in Table 1 and are plotted in Fig. 3, along with values for some other oils of SE Asia. Stable isotope ratios are unreliable as a source indicator when used in isolation, especially where biodegradation has altered the oils. We therefore consider the classifications given in Fig. 3 to be speculative. However, isotope ratios can be useful when viewed in conjunction with biomarker data. This is evident from Fig. 3 where the indication of an algal contribution to the least biodegraded oil (BP-OS-01) agrees with the biomarker evidence. Furthermore, the biomarker indications of a different source for oil C-17 are supported by it's variant isotopic composition.

REFERENCES

BUREAU OF ENERGY DEVELOPMENT, ROBERTSON RESEARCH (AUSTRALIA) PTY. LTD. AND FLOWER DOERY BUCHAN PTY. LTD. (1986). *Sedimentary Basins of the Philippines their Geology and Hydrocarbon Potentia*l. Volume V . pp. 303-410.

BARWISE, A. J. G. (1990) Role of Nickel and Vanadium in Petroleum Classification. *Energy and Fuels*, **4**, pp. 647-652.

EVANS, D., HEGGIE, D. T., REYES, E. N.AND LEE, C. S. (1992). *Light Hydrocarbon Geochemistry in Bottom-Waters of the Philippines Continental Shelf Part A: Ragay Gulf and Tayabas Bay*, Rig Seismic Survey 109. AGSO Record 1992/92

JAMES, A. T., (1990). Correlation of Reservoired Gases Using the Carbon Isotopic Compositions of Wet Gas Components. *AAPG Bull.* **74**, 1441-1458.

MURRAY, A. P., SUMMONS, R. E., BRADSHAW, J. AND PAWIH, B. (1993). Cainozoic Oil in Papua New Guinea- Evidence from Geochemical Analysis of two Newly Discovered Seeps. In: *Petroleum Exploration and Development in Papua New Guinea*: Proceedings of the Second PNG Petroleum Convention, Port Moresby, 31st May-2nd June 1993. Carman, G. J. and Z., (Eds). pp. 489-498.

PETERS, K. E. AND MOLDOWAN, J. M. (1992). *The Biomarker Guide - Interpreting molecular fossils in petroleum and ancient sediments*. Prentice-Hall, New Jersey.

RADKE, M. AND WELTE, D.H. (1983). The methyl phenanthrene index (MPI): a maturity parameter based on aromatic hydrocarbons. In: *Advances in Organic Geochemistry, 1981* (Ed. M. Bjoroy *et al.*), Wiley, Chichester, pp. 504-512

ROBINSON, K. M. (1987) An Overview of Source Rocks and Oils in Indonesia. *Proceedings Indonesian Petroleum Association, 16th Annual Convention*, October 1987. pp. 96-122.

WILLIAMS, H. H., REYES, E. N. AND EUBANK, R. T. (1992). Geochemistry of Palawan Oils, Philippines: Source Implications. *OSEA 9th Conference and Exhibition* , 1-4 December 1992. pp. 509-523.

Explanation of the Source and Maturity parameters used in Table 1.

Except where otherwise stated, hopanes are the17α(H),21β(H) isomers, moretanes the 17β(H), 21α(H) isomers. Diasteranes are the 5β(H),14β(H),17α(H) isomers.

1 Level of biodegradation

See Table 2

2 % Saturates	Percent of whole oil by weight
3 % Aromatics	Percent of Whole oil by weight
4 % Polars	Percent of Whole oil by weight (includes asphaltenes)

5 $\delta^{13}C$ Sats

Carbon isotope ratio with respect to the Pee Dee Belemnite expressed in ppm ^{13}C depletion, for the saturates fraction.

6 $\delta^{13}C$ Arom

Carbon isotope ratio with respect to the Pee Dee Belemnite expressed in ppm ^{13}C depletion, for the aromatics fraction.

7 Most abundant n-alkane

From GC profile (C9 to C34 range)

8 Pristane/nC17

Source, high for most terrestrial oils.

9 Phytane/nC18

Source, maturity, decreases with maturity

10 Pristane/Phytane

Source, depositional environment (> 3 = Oxic, < 1 = Anoxic and/or Hypersaline, 1 -3 = Indeterminate)

11 Carbon Preference Index (CPI)

In the range C25 - C31, > 1 for terrestrial OM, decreases with maturity.

12 C27/C29 Diasteranes

Source, > ~ 0.5 for algal contribution to SR.

13 C28/C29 Diasteranes

Source, often high for lacustrine SR.

14 Oleanane/C29 Diasteranes

Source, Angiosperm contribution to overall eukaryote derived OM.

15 C30 Hopane/C29 Diasteranes

Source, indicates degree of prokaryote (bacterial) vs. eukaryote (plants, algae, etc) organic matter existing in the SR after reworking.

16 Sum of Bicads/C30 Hopane

Source, sum of all bicadinanes and methyl bicadinanes recognised/C30 Hopane. Indicates the contribution of Angiosperm resin vs. bacterial lipids to the source matter.

17 Oleanane/C30 Hopane

Source, indicates the contribution of Angiosperm vs. bacterial lipids to the source matter.

18 A Cont Triter/C30H

Source, sum of six, ring-A contracted triterpanes (angiosperm markers) vs. bacterial lipids. These compounds are related to, usually co-occur with, and behave under biodegradation in the same manner as oleanane.

19 A Cont Triter/Olean

Source, depositional environment. This ratio usually varies little for oils from the same SR, but seems to be high for oxic depositional conditions.

20 Gammacerane/C30 Hopane

Gammacerane is often present in source rocks deposited under conditions of elevated salinity.

21 C29/C30 Hopane

Source, usually high (> 1) in carbonate SR due to presence of 30-norhopane series. Sometimes also > 1 for terrestrial oils, from clastic SR.

22 C31/C30 Hopane

Source, usually high (> ~ 0.5) for carbonate SR, anoxic deposition.

23 C29 Neohopane ($C29T_S$)/C29 Hopane

Source, maturity, often high for clastic SR deposited in oxic or sub-oxic conditions

24 Sum C31Methylhopanes (2α and 3β)/C30 Hopane

Correlation, sometimes high for carbonate SR.

25 2αMethyl/3β Ring A-Methyl C31Hopane

Correlation, significance presently unknown, but low for some rocks deposited under hypersaline, anoxic conditions.

26 Bicadinane T/MeT

Correlation, trans-trans-trans bicadinane/it's ring methylated analog. Significance presently unknown.

27 Bicadinane W/T

Correlation, cis-cis-trans isomer/trans-trans-trans isomer. Significance unknown, but appears to increase with maturity before oil window.

28 C27/C29 Total Steranes

Source, high (> ~ 0.5), for algal contribution to source matter.

29 C29 Diasteranes/Total C29 Steranes

Source, high for clastic SR deposited under oxic conditions, low (< ~ 0.2) for carbonate SR deposited under anoxic conditions. Also increases with maturity.

30 4Me-C30 Ster (R)/C29 Ster (R)

Source, ratio of R epimers of 4α-methyl-24 ethyl cholestanes/24-ethyl cholestanes. Dinoflagellate or macrophyte origin for 4-methyl steranes so high values indicates an algal (marine or freshwater) contribution.

31 Total Hopanes/Steranes

Source, sum of all desmethyl hopanes C27 - C35 (excluding dia- and neo-forms except Ts)/all desmethyl steranes C27 - C30. Indicator of the contribution of bacterial (prokaryote) vs plant (eukaryote) lipids to the source matter.

32 C29 Steranes 20S/(20S+20R)

Maturity, ratio of 20S epimer of ααα C29 steranes/ total of S and R ααα epimers. Normally reaches equilibrium value ~ 0.55 within oil window.

33 C31Hopanes 22S/(22S+22R)

Maturity, ratio of 22S epimer of αβ C31 Hopanes/total of S and R αβ C31 Hopanes. Normally reaches equilibrium value ~ 0.6 before oil window.

34 C29 Steranes αββ/(ααα+αββ)

Maturity, normally reaches equilibrium ~ 0.7 within oil window.

35 T_s/T_m

Maturity, source, C27 Trisnorneohopane/C27 Trisnorhopane, continues to increase through oil window but is highly source and SR lithology dependant.

36 C30 Moretane/Hopane

Maturity, decreases with increasing maturity, normally reaches values ~ 0.1 prior to the oil window.

37 Methyl Phenanthrene Index

Maturity, MPI = 1.5 x (3MP+2MP)/(P+9MP+1MP). Phenanthrene response corrected by multiplication by 0.69. The relative abundance of methyl phenanthrene isomers is source dependent in terrestrial oils including conifer remains in the source (e.g. some Mesozoic oils).

38 Rc (Radke & Welte, 1983)

Maturity. Calculated vitrinite reflectance of the SR using the calibration of Radke and Welte (1983) for Rc < 1.5. Vr= 0.6MPI + 0.4

39 %C27S/%C29S

Mixed maturity indicator, S/R epimeric ratio for C27 vs. C29 steranes. Values < 0.5 or > 1.5 may indicate a mixture of oils of differing maturity or degree of biodegradation or both.

Appendix 1A

Gas Chromatograms

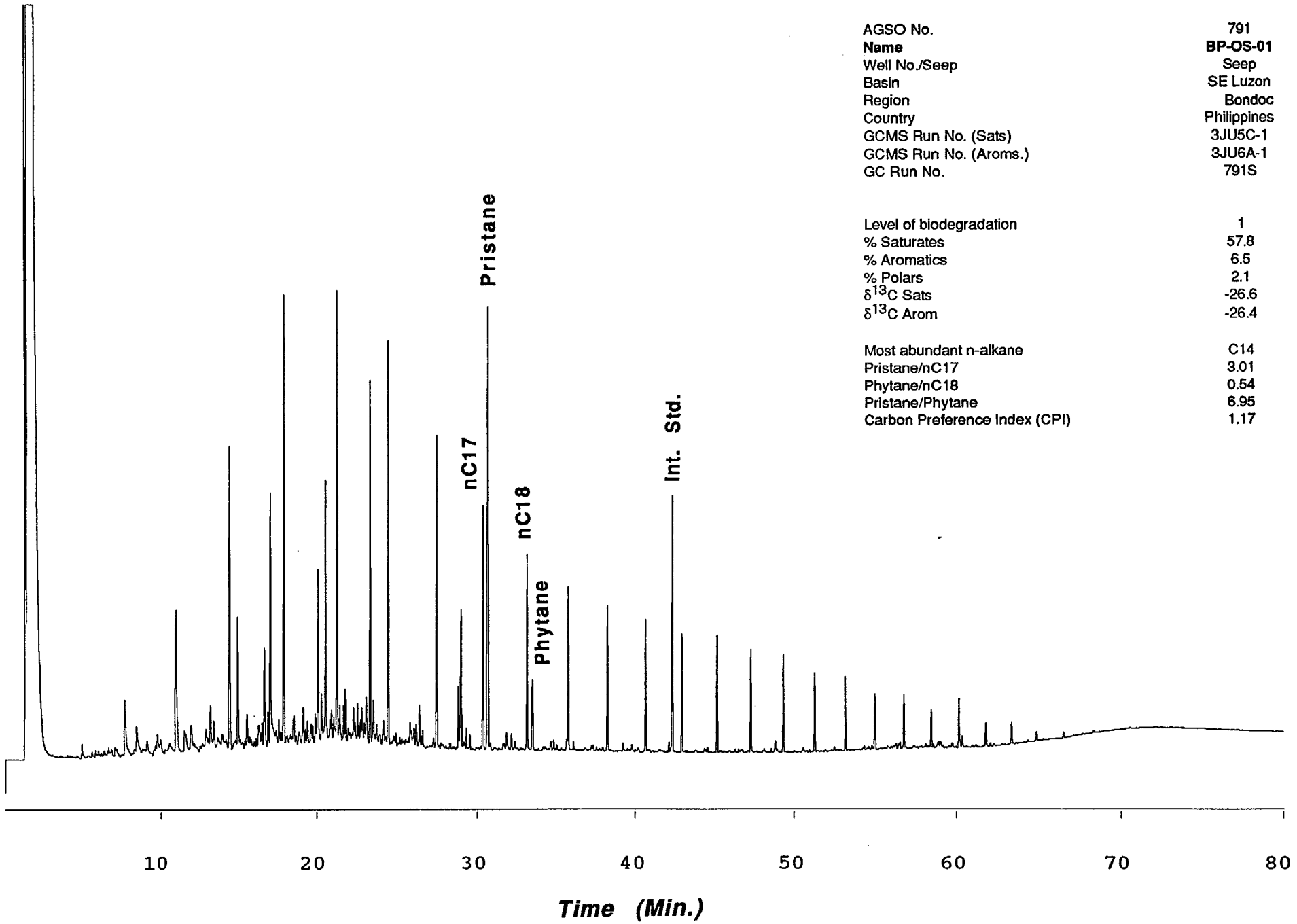

AGSO No.	791
Name	**BP-OS-01**
Well No./Seep	Seep
Basin	SE Luzon
Region	Bondoc
Country	Philippines
GCMS Run No. (Sats)	3JU5C-1
GCMS Run No. (Aroms.)	3JU6A-1
GC Run No.	791S
Level of biodegradation	1
% Saturates	57.8
% Aromatics	6.5
% Polars	2.1
$\delta^{13}C$ Sats	-26.6
$\delta^{13}C$ Arom	-26.4
Most abundant n-alkane	C14
Pristane/nC17	3.01
Phytane/nC18	0.54
Pristane/Phytane	6.95
Carbon Preference Index (CPI)	1.17

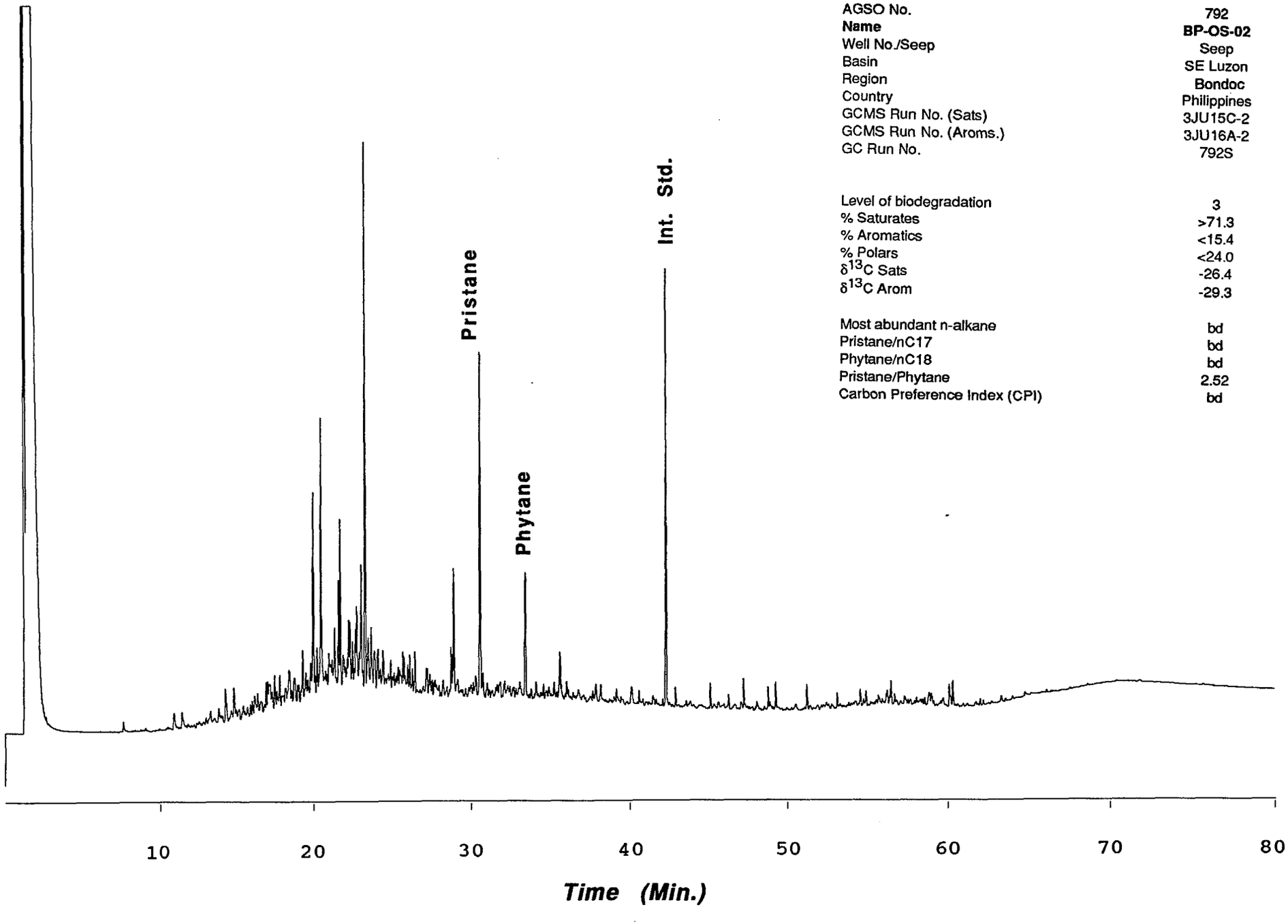

AGSO No.	792
Name	**BP-OS-02**
Well No./Seep	Seep
Basin	SE Luzon
Region	Bondoc
Country	Philippines
GCMS Run No. (Sats)	3JU15C-2
GCMS Run No. (Aroms.)	3JU16A-2
GC Run No.	792S
Level of biodegradation	3
% Saturates	>71.3
% Aromatics	<15.4
% Polars	<24.0
δ^{13}C Sats	-26.4
δ^{13}C Arom	-29.3
Most abundant n-alkane	bd
Pristane/nC17	bd
Phytane/nC18	bd
Pristane/Phytane	2.52
Carbon Preference Index (CPI)	bd

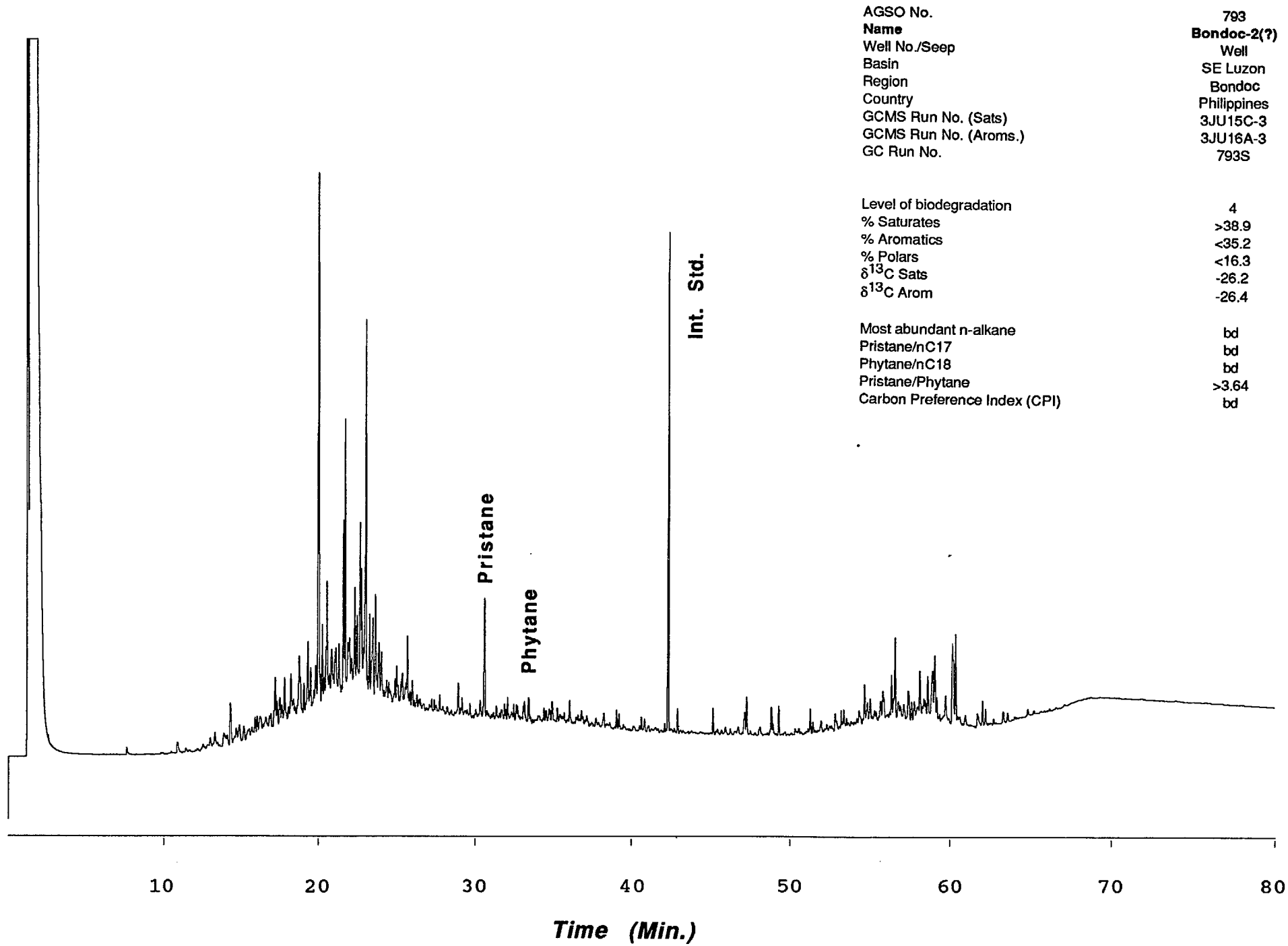

AGSO No.	793
Name	**Bondoc-2(?)**
Well No./Seep	Well
Basin	SE Luzon
Region	Bondoc
Country	Philippines
GCMS Run No. (Sats)	3JU15C-3
GCMS Run No. (Aroms.)	3JU16A-3
GC Run No.	793S
Level of biodegradation	4
% Saturates	>38.9
% Aromatics	<35.2
% Polars	<16.3
δ^{13}C Sats	-26.2
δ^{13}C Arom	-26.4
Most abundant n-alkane	bd
Pristane/nC17	bd
Phytane/nC18	bd
Pristane/Phytane	>3.64
Carbon Preference Index (CPI)	bd

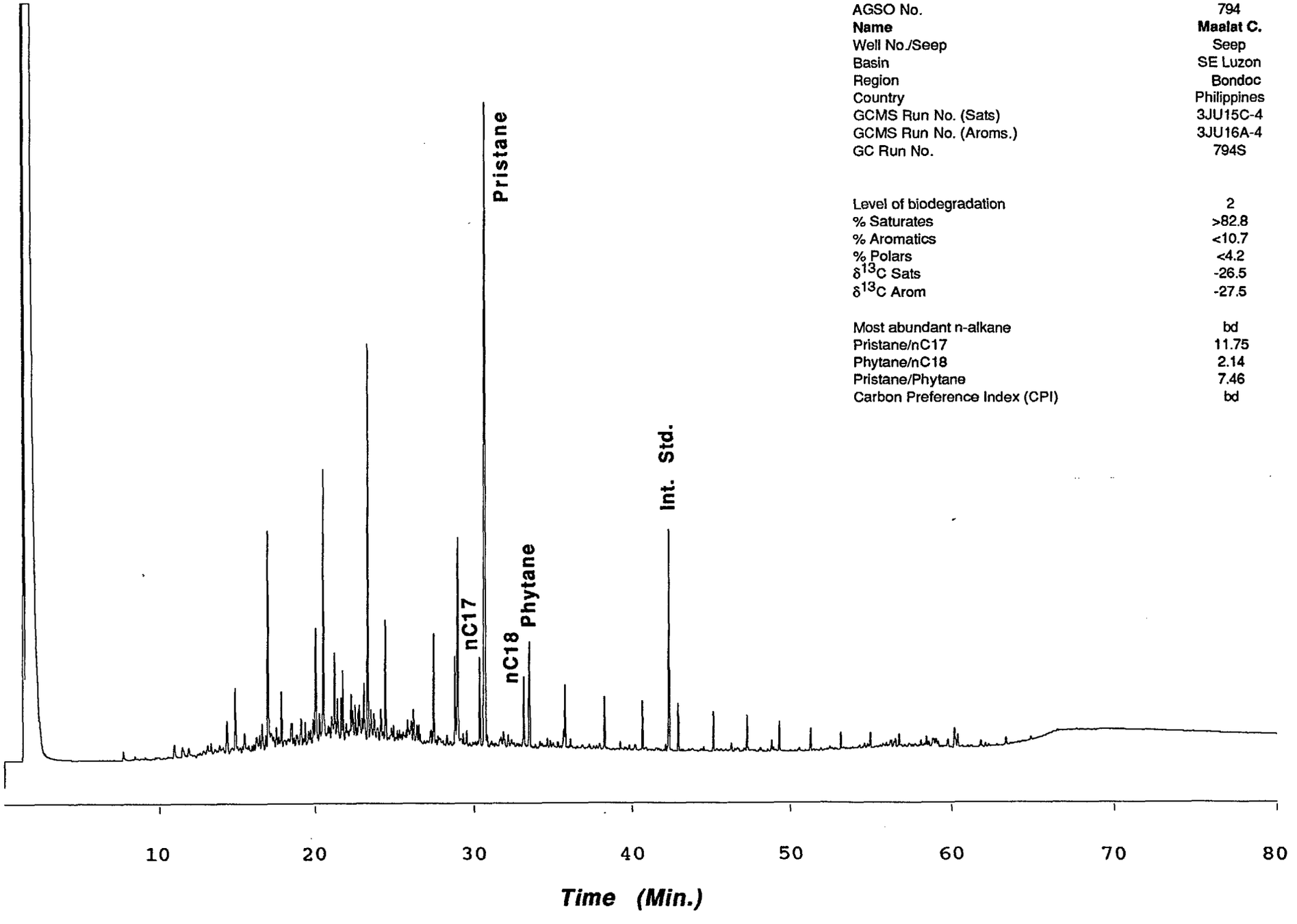

AGSO No.	794
Name	**Maalat C.**
Well No./Seep	Seep
Basin	SE Luzon
Region	Bondoc
Country	Philippines
GCMS Run No. (Sats)	3JU15C-4
GCMS Run No. (Aroms.)	3JU16A-4
GC Run No.	794S
Level of biodegradation	2
% Saturates	>82.8
% Aromatics	<10.7
% Polars	<4.2
$\delta^{13}C$ Sats	-26.5
$\delta^{13}C$ Arom	-27.5
Most abundant n-alkane	bd
Pristane/nC17	11.75
Phytane/nC18	2.14
Pristane/Phytane	7.46
Carbon Preference Index (CPI)	bd

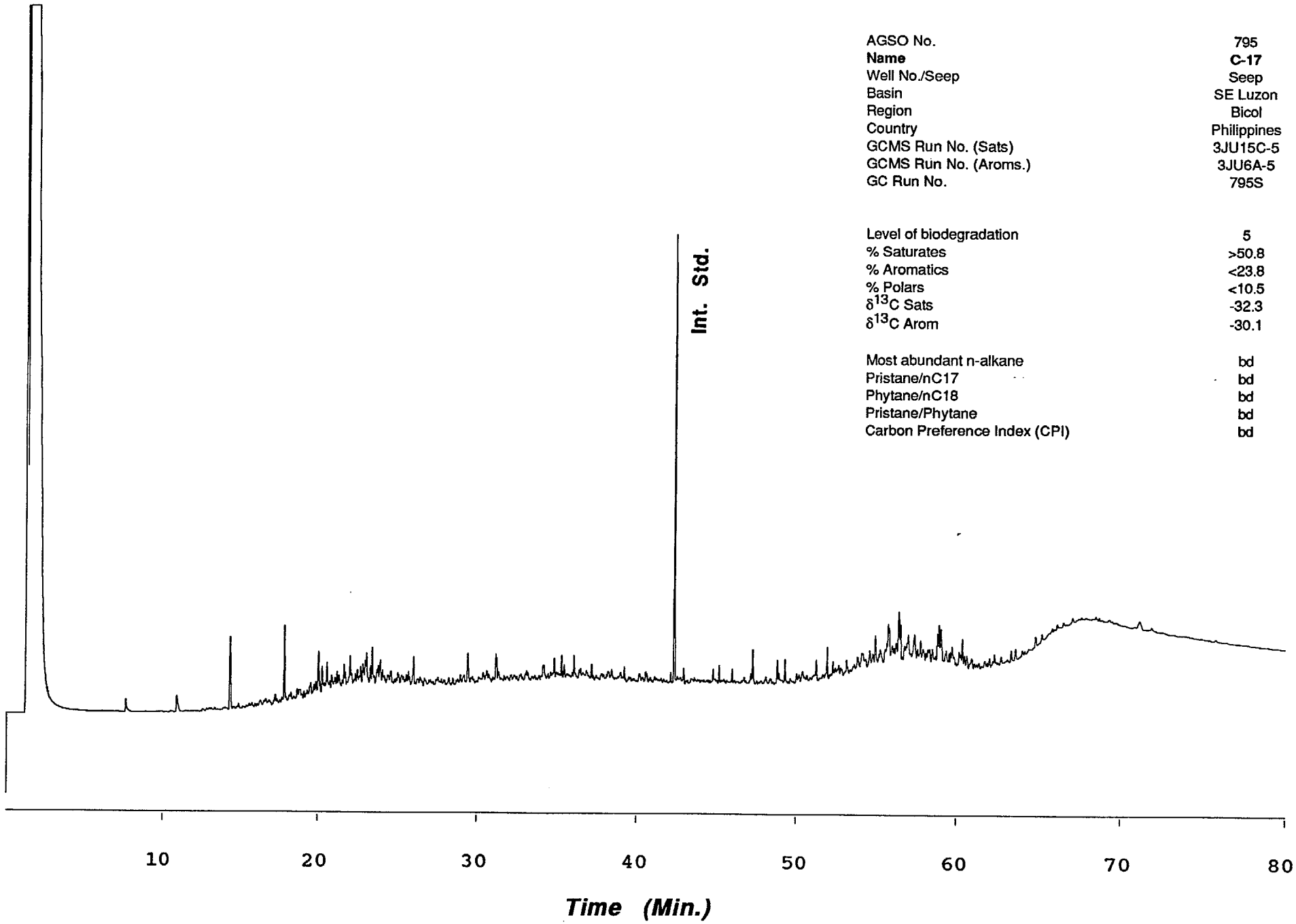

AGSO No.	795
Name	**C-17**
Well No./Seep	Seep
Basin	SE Luzon
Region	Bicol
Country	Philippines
GCMS Run No. (Sats)	3JU15C-5
GCMS Run No. (Aroms.)	3JU6A-5
GC Run No.	795S
Level of biodegradation	5
% Saturates	>50.8
% Aromatics	<23.8
% Polars	<10.5
δ^{13}C Sats	-32.3
δ^{13}C Arom	-30.1
Most abundant n-alkane	bd
Pristane/nC17	bd
Phytane/nC18	bd
Pristane/Phytane	bd
Carbon Preference Index (CPI)	bd

Appendix 1B

Metastable Reaction Monitoring GCMSMS Chromatograms

Annotation:

Norm:	Scale factor, the larger the number the more abundant the compounds shown in the particular trace, relative to others.
"αβ"and "βα"	Stereochemistry of Hopanes at the 17(H) and 21(H) positions.
S and R	For hopanes, epimeric configuration at C22, For Steranes, epimeric configuration at C20
"ααα" and "αββ"	For steranes, configuration at the 5(H), 14(H) and 17(H) positions.
"Dia"	Diasteranes, i.e, ββα configuration at 5,14 and 17 positions.
"CT"	Crosstalk - cross channel interference which results in compounds giving peaks in more than one trace. e.g. Bicadinanes cross talk from their main channel (412->369) into the sterane and some triterpane traces. Only a problem in MRM GCMS when one group of compounds is very abundant in the sample.
Tri	Tricyclics (Cheilanthanes)
Ol	Oleanane (18α+18β)
Ring A Cont Triterp	Ring A-contracted triterpanes (numbered 1 - 6). Compounds related to Oleanane.
Neo	e.g. neohopane - 18α(H) instead of 17α(H) stereochemistry (more stable).
29,30 BNH, 28,30 BNH	Bisnorhopanes
Ts	22,29,30 Trisnorneohopane
Tm	22,29,30 Trisnorhopane
2α, 3β	2α-methyl and 3β ring A methyl hopanes
I.S.	Internal Standard: trideuterated methyl cholestane
W, W1, W2, MeW	Cis-cis-trans bicadinanes and ring methylated analogs
V	bicadinane isomer (prob. cis-cis-trans)
T,T1, R, MeT, MeT1	Trans-trans-trans bicadinanes and ring methylated analogs.

3JU15C 15-JUN-93 Sir:Reaction 70-E Sys: ALLTERPC
Sample 1 Injection 1 Group 2 Mass 482.4020 482.4020->191.1790
Text:#791 BP-OS-01 SATS 0.2/100 = 1 MG + 100 NG STD

C35 Hopanes

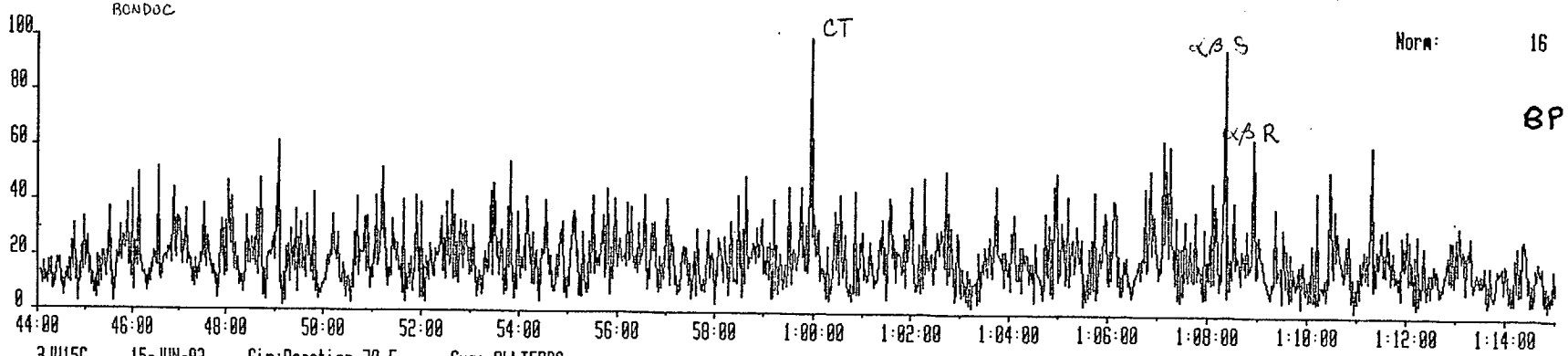

3JU15C 15-JUN-93 Sir:Reaction 70-E Sys: ALLTERPC
Sample 1 Injection 1 Group 2 Mass 468.4670 468.4670->191.1790
Text:#791 BP-OS-01 SATS 0.2/100 = 1 MG + 100 NG STD

C34 Hopanes

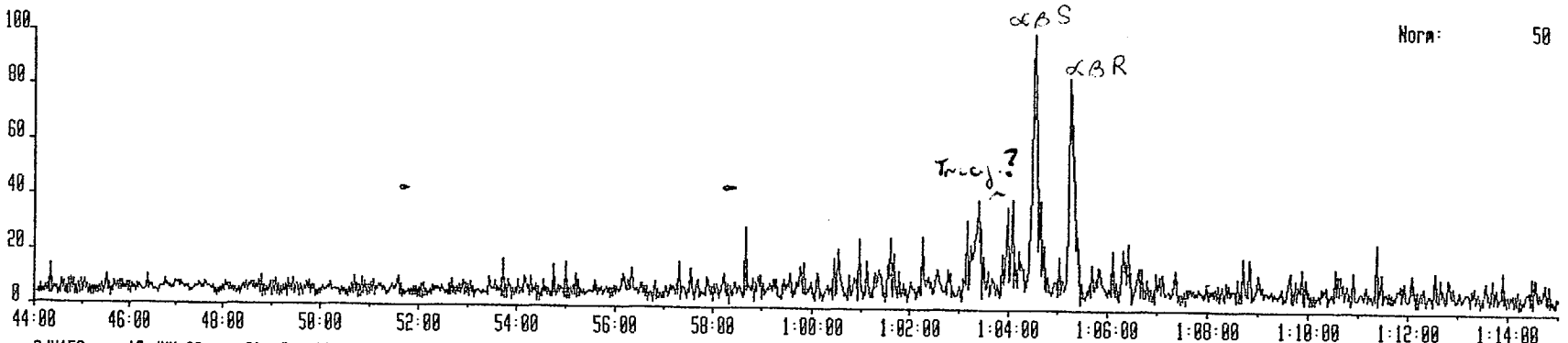

3JU15C 15-JUN-93 Sir:Reaction 70-E Sys: ALLTERPC
Sample 1 Injection 1 Group 2 Mass 454.4520 454.4520->191.1790
Text:#791 BP-OS-01 SATS 0.2/100 = 1 MG + 100 NG STD

C33 Hopanes

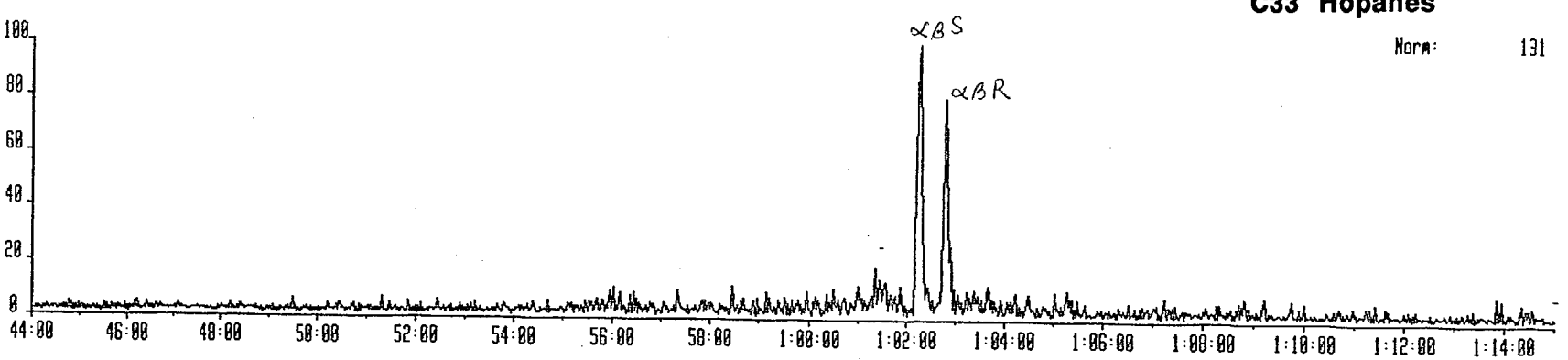

3JU15C 15-JUN-93 Sir:Reaction 70-E Sys: ALLTERPC
Sample 1 Injection 1 Group 2 Mass 440.4370 440.4370->191.1790
Text:#791 BP-OS-01 SATS 0.2/100 = 1 MG + 100 NG STD

BCNDOC

C32 Hopanes

Norm: 322

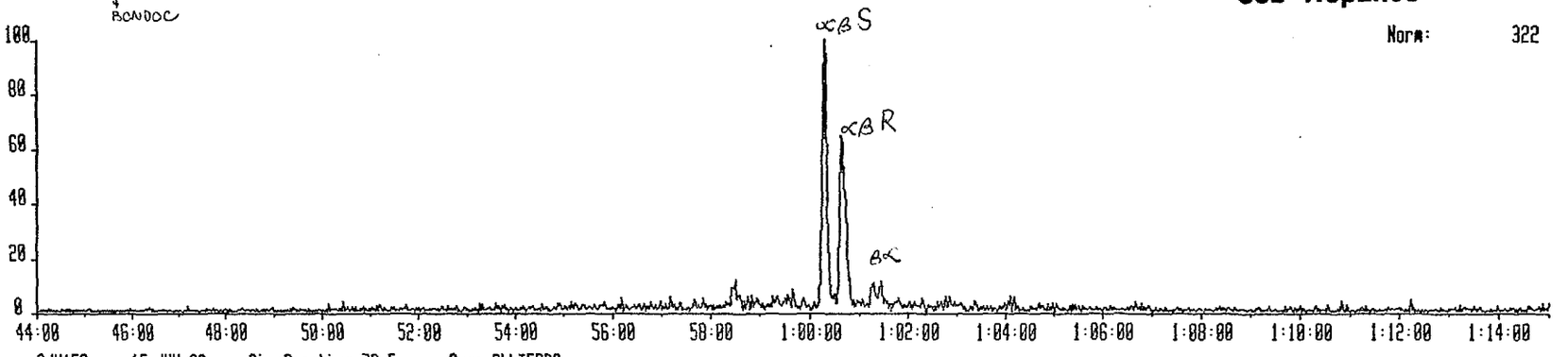

3JU15C 15-JUN-93 Sir:Reaction 70-E Sys: ALLTERPC
Sample 1 Injection 1 Group 2 Mass 426.4210 426.4210->191.1790
Text:#791 BP-OS-01 SATS 0.2/100 = 1 MG + 100 NG STD

C31 Hopanes

Norm: 1123

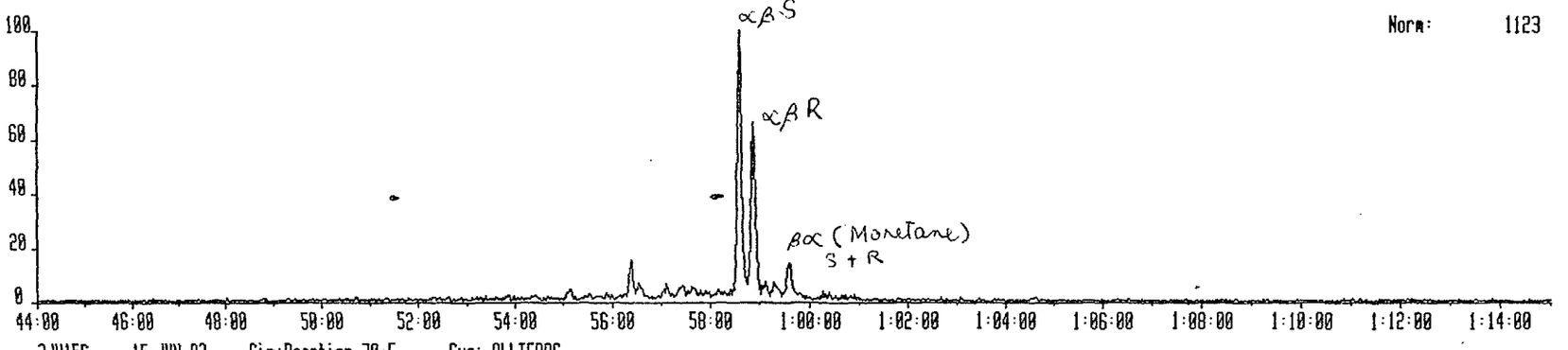

3JU15C 15-JUN-93 Sir:Reaction 70-E Sys: ALLTERPC
Sample 1 Injection 1 Group 2 Mass 416.4420 416.4420->191.1790
Text:#791 BP-OS-01 SATS 0.2/100 = 1 MG + 100 NG STD

C30 Tricyclics (Cheilanthanes)

Norm: 660

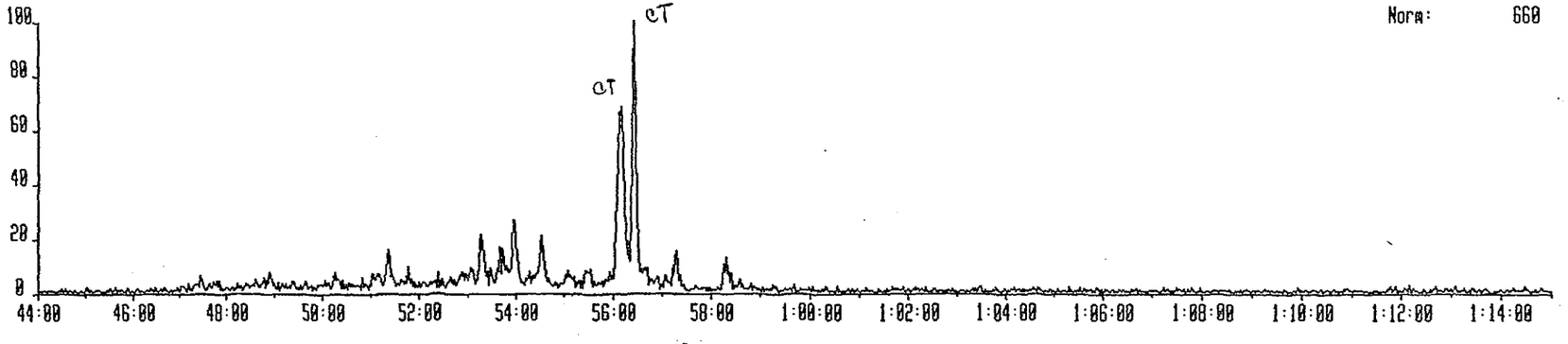

3JU15C 15-JUN-93 Sir:Reaction 70-E Sys: ALLTERPC
Sample 1 Injection 1 Group 2 Mass 412.4060 412.4060->191.1790
Text:#791 BP-OS-01 SATS 0.2/100 = 1 MG + 100 NG STD

C30 Hopanes

Norm: 6129

& other Triterpanes

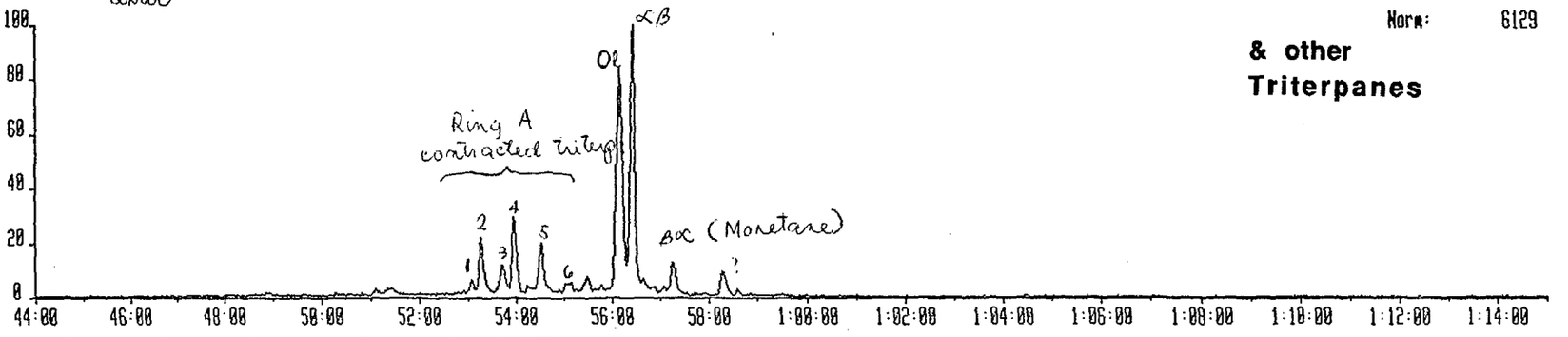

3JU15C 15-JUN-93 Sir:Reaction 70-E Sys: ALLTERPC
Sample 1 Injection 1 Group 2 Mass 398.3900 398.3900->191.1790
Text:#791 BP-OS-01 SATS 0.2/100 = 1 MG + 100 NG STD

C29 Hopanes

Norm: 3537

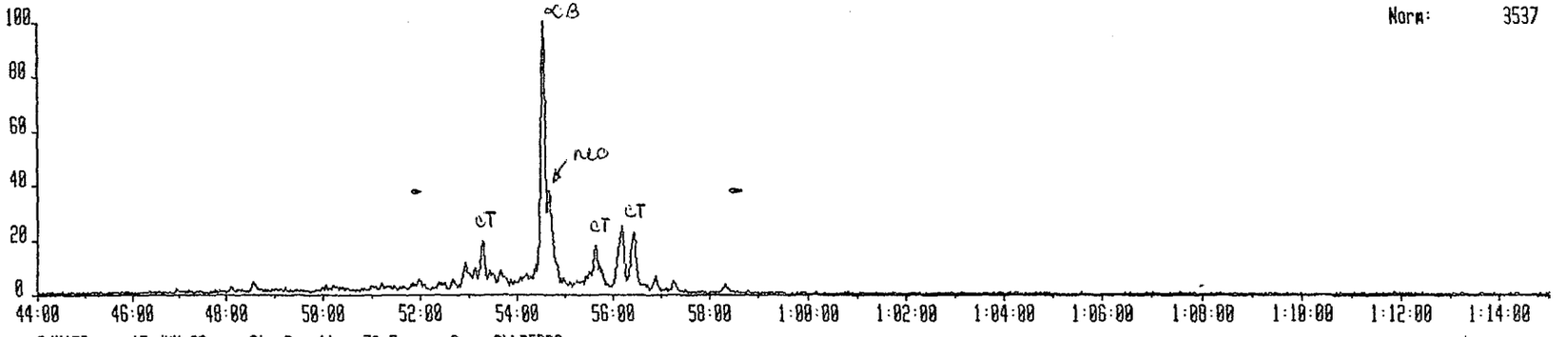

3JU15C 15-JUN-93 Sir:Reaction 70-E Sys: ALLTERPC
Sample 1 Injection 1 Group 2 Mass 384.3740 384.3740->191.1790
Text:#791 BP-OS-01 SATS 0.2/100 = 1 MG + 100 NG STD

C28 Hopanes

Norm: 395

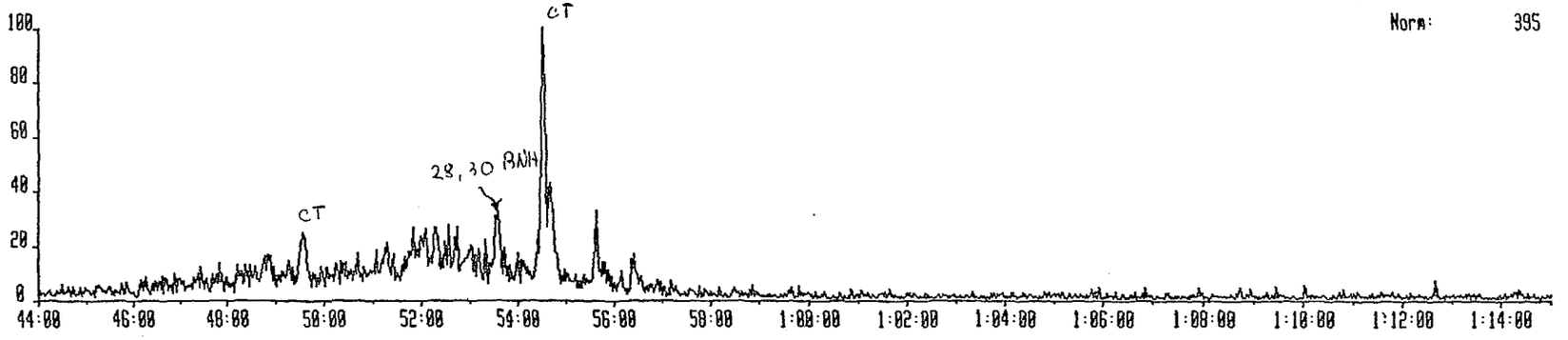

3JU15C 15-JUN-93 Sir:Reaction 70-E Sys: ALLTERPC
Sample 1 Injection 1 Group 2 Mass 370.3590 370.3590->191.1790
Text:#791 BP-OS-01 SATS 0.2/100 = 1 MG + 100 NG STD

C27 Hopanes

Norm: 1004

3JU15C 15-JUN-93 Sir:Reaction 70-E Sys: ALLTERPC
Sample 1 Injection 1 Group 2 Mass 426.4210 426.4210->205.1940
Text:#791 BP-OS-01 SATS 0.2/100 = 1 MG + 100 NG STD

C31 Ring A-Methyl Hopanes

Norm: 619

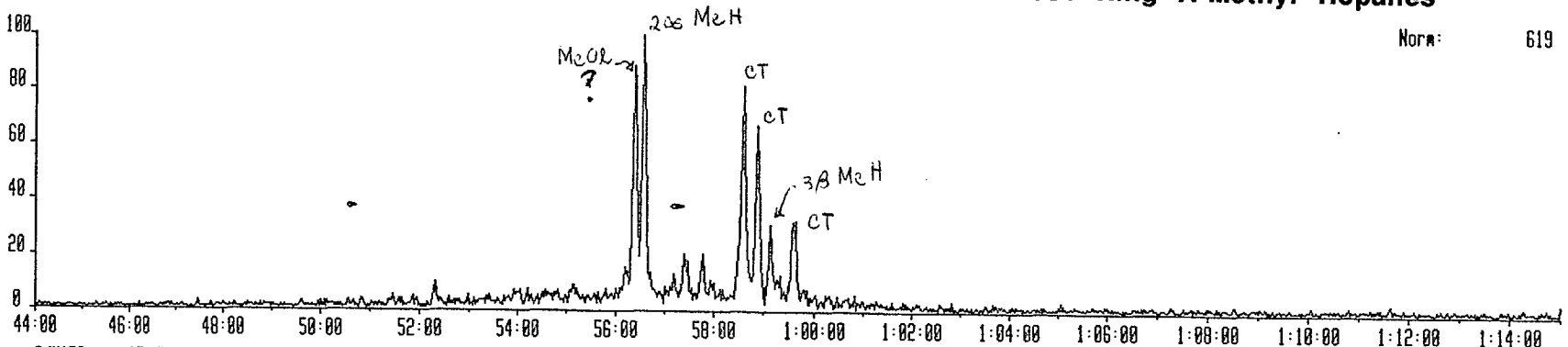

3JU15C 15-JUN-93 Sir:Reaction 70-E Sys: ALLTERPC
Sample 1 Injection 1 Group 2 Mass 414.4230 414.4230->217.1960
Text:#791 BP-OS-01 SATS 0.2/100 = 1 MG + 100 NG STD

C30 Desmethyl Steranes

Norm: 86

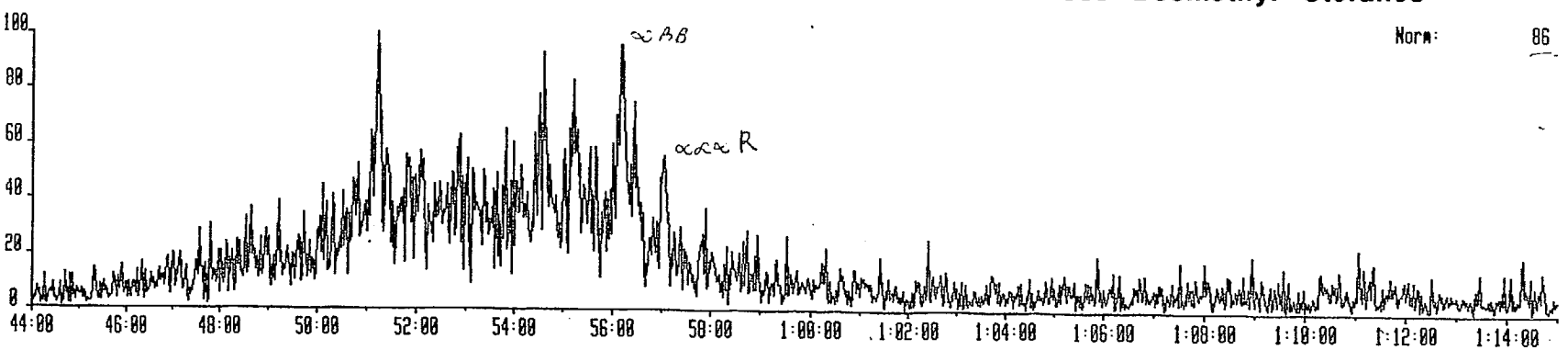

3JU15C 15-JUN-93 Sir:Reaction 70-E Sys: ALLTERPC
Sample 1 Injection 1 Group 2 Mass 400.4070 400.4070->217.1960
Text:#791 BP-OS-01 SATS 0.2/100 = 1 MG + 100 NG STD

C29 Steranes

Norm: 3184

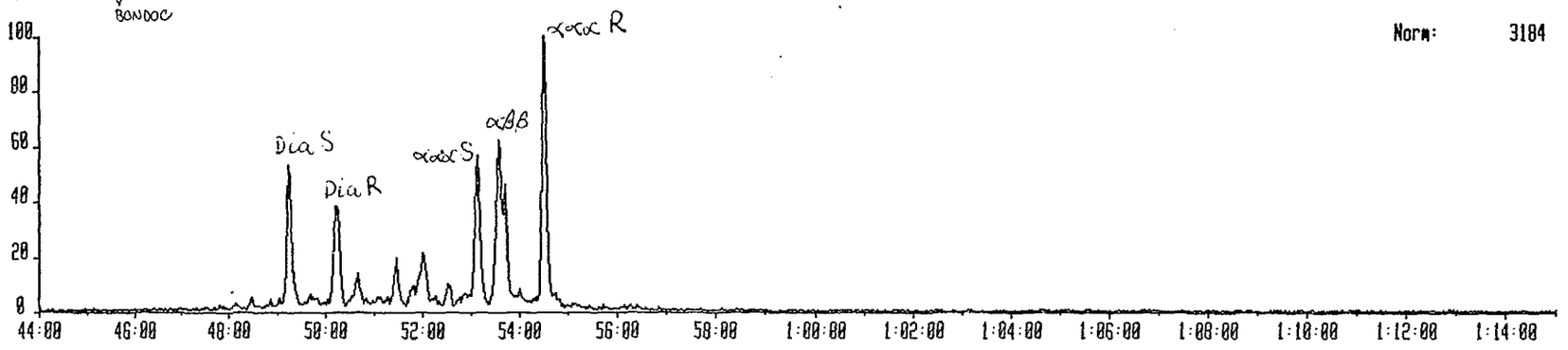

3JU15C 15-JUN-93 Sir:Reaction 70-E Sys: ALLTERPC
Sample 1 Injection 1 Group 2 Mass 386.3910 386.3910->217.1960
Text:#791 BP-OS-01 SATS 0.2/100 = 1 MG + 100 NG STD

C28 Steranes

Norm: 1822

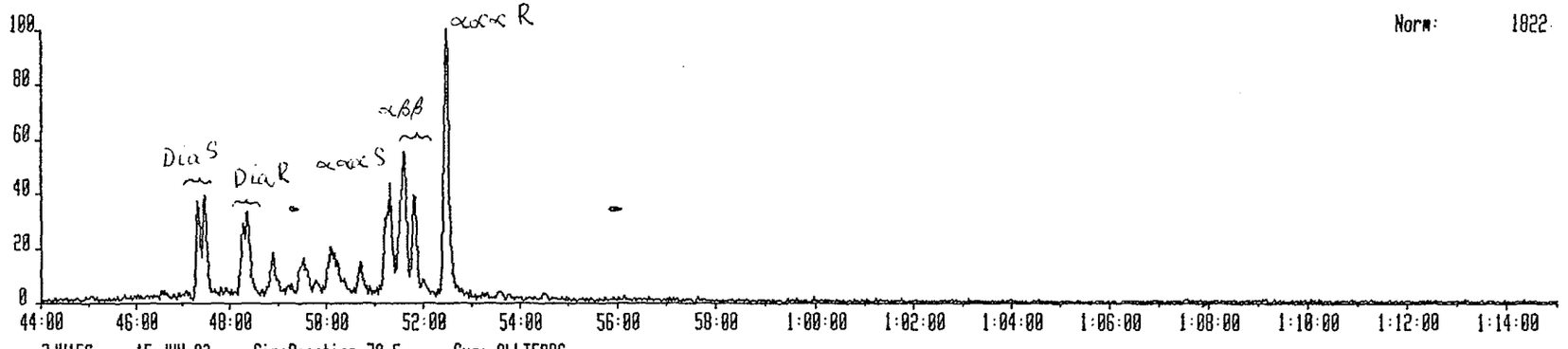

3JU15C 15-JUN-93 Sir:Reaction 70-E Sys: ALLTERPC
Sample 1 Injection 1 Group 2 Mass 372.3760 372.3760->217.1960
Text:#791 BP-OS-01 SATS 0.2/100 = 1 MG + 100 NG STD

C27 Steranes

Norm: 1397

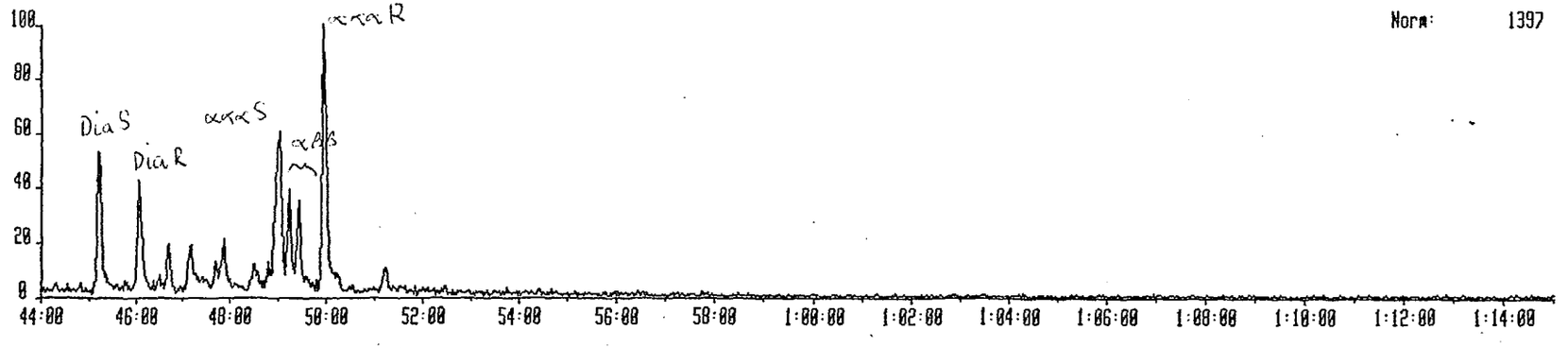

3JU15C 15-JUN-93 Sir:Reaction 70-E Sys: ALLTERPC
Sample 1 Injection 1 Group 2 Mass 414.4230 414.4230->231.2120
Text:#791 BP-OS-01 SATS 0.2/100 = 1 MG + 100 NG STD

C30 Ring A-Methyl Steranes

Norm: 469

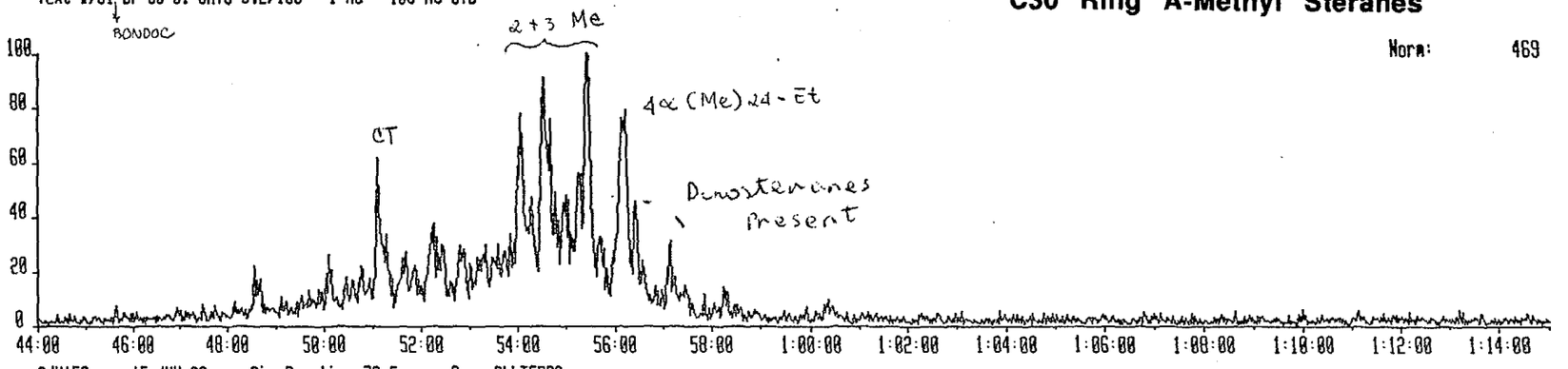

3JU15C 15-JUN-93 Sir:Reaction 70-E Sys: ALLTERPC
Sample 1 Injection 1 Group 2 Mass 389.4105 389.4105->234.2324
Text:#791 BP-OS-01 SATS 0.2/100 = 1 MG + 100 NG STD

Internal Standard

Norm: 1912

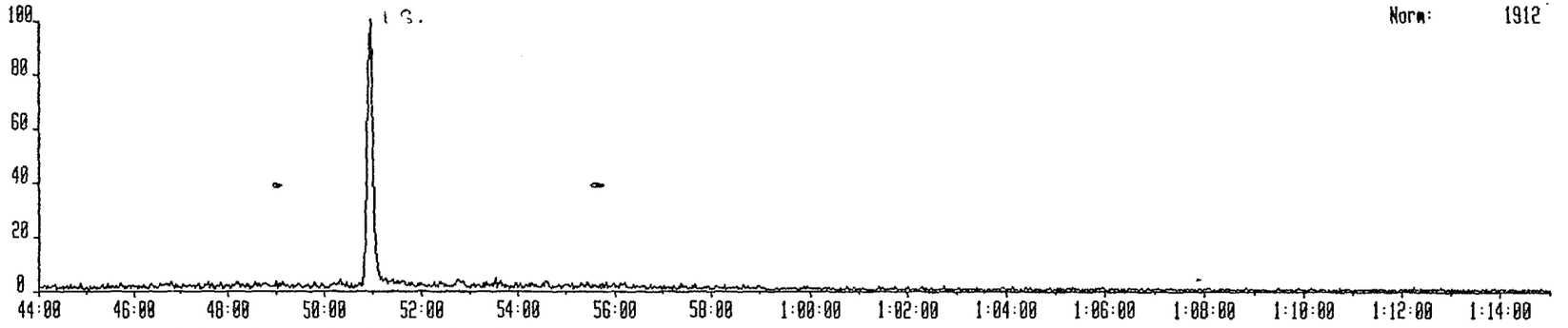

3JU15C 15-JUN-93 Sir:Reaction 70-E Sys: ALLTERPC
Sample 1 Injection 1 Group 2 Mass 412.4060 412.4060->369.3400
Text:#791 BP-OS-01 SATS 0.2/100 = 1 MG + 100 NG STD

C30 Bicadinanes

Norm: 12569

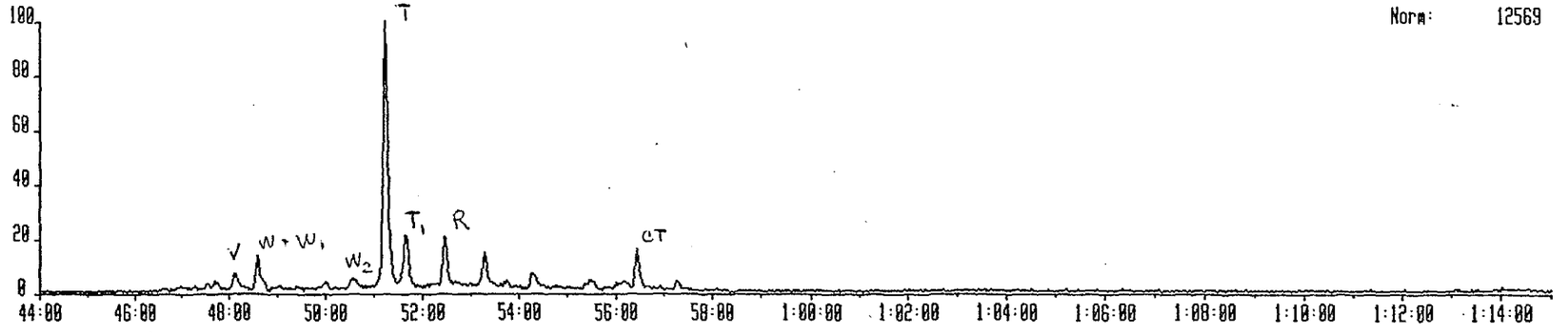

3JU15C 15-JUN-93 Sir:Reaction 70-E Sys: ALLTERPC
Sample 1 Injection 1 Group 2 Mass 426.4230 426.4230->383.3550
Text:#791 BP-DS-01 SATS 0.2/100 = 1 MG + 100 NG STD

C31 Methyl Bicadinanes

Norm: 19461

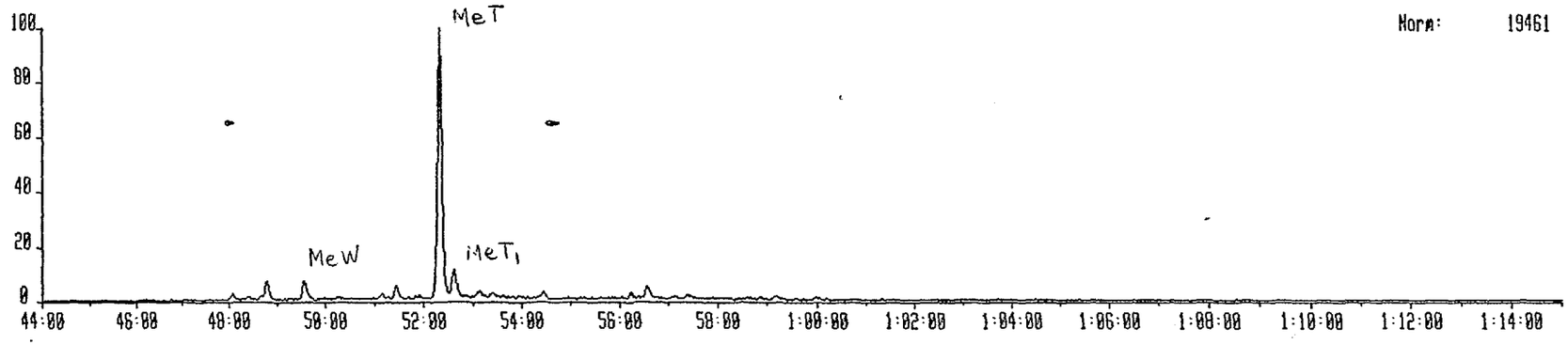

3JU16A 16-JUN-93 Sir:Magnetic 70-E Sys: MPI2
Sample 1 Injection 1 Group 2 Mass 178.0782
Text:#791 AROMS BONDOC SEEP BP-OS-01 1:200

Phenanthrene

Norm: 5698

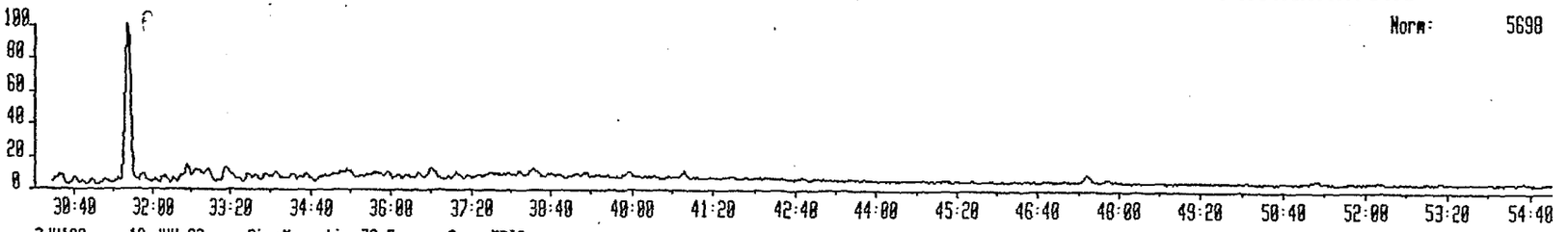

3JU16A 16-JUN-93 Sir:Magnetic 70-E Sys: MPI2
Sample 1 Injection 1 Group 2 Mass 192.0930
Text:#791 AROMS BONDOC SEEP BP-OS-01 1:200

Methyl Phenanthrenes

Norm: 2310

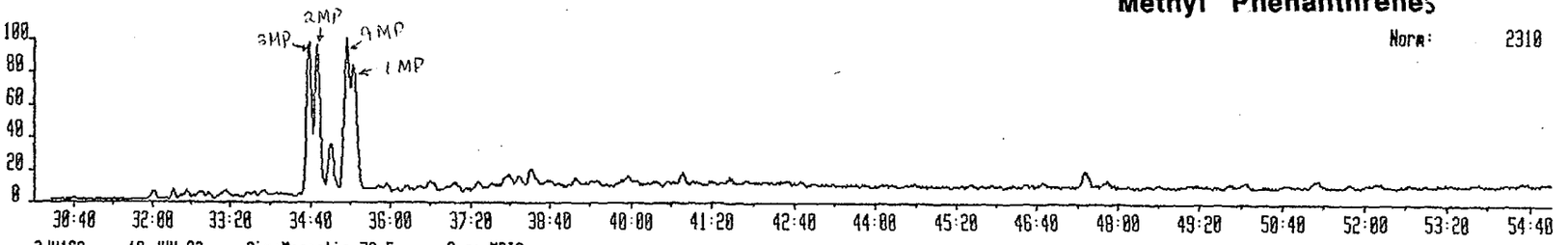

3JU16A 16-JUN-93 Sir:Magnetic 70-E Sys: MPI2
Sample 1 Injection 1 Group 2 Mass 206.1000
Text:#791 AROMS BONDOC SEEP BP-OS-01 1:200

Dimethyl Phenanthrenes

Norm: 1897

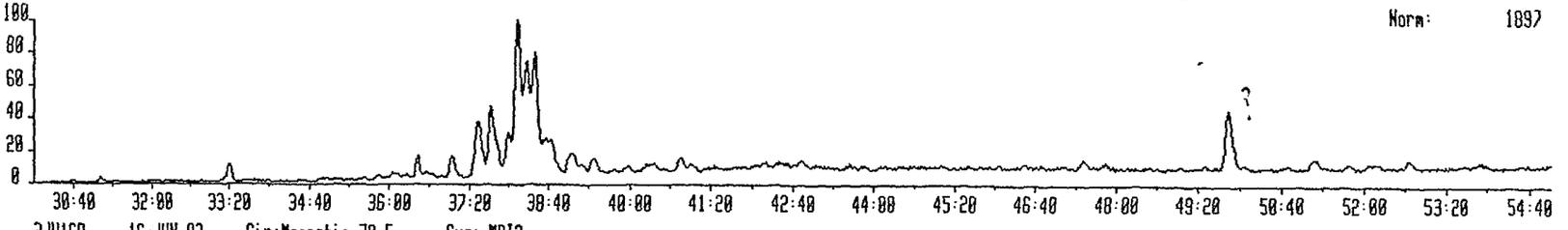

3JU16A 16-JUN-93 Sir:Magnetic 70-E Sys: MPI2
Sample 1 Injection 1 Group 2 Mass 219.1000
Text:#791 AROMS BONDOC SEEP BP-OS-01 1:200

Retene
(not detected)

Norm: 2635

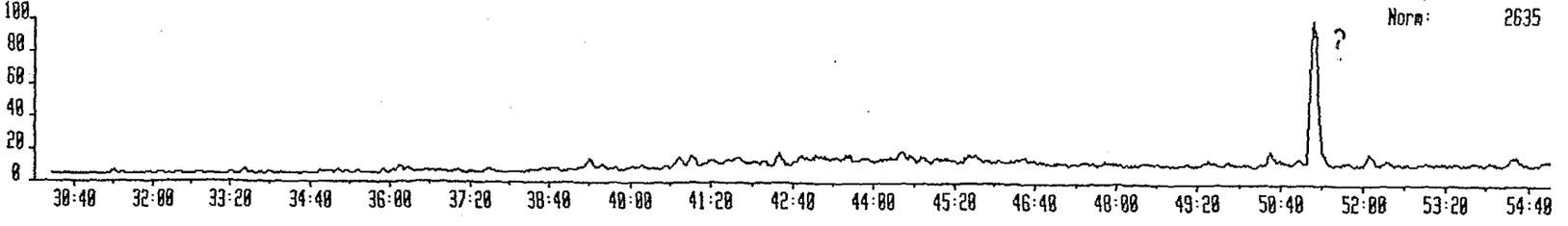

3JU15C 15-JUN-93 Sir:Reaction 70-E Sys: ALLTERPC
Sample 2 Injection 1 Group 2 Mass 482.4820 482.4820->191.1790
Text: #792 BP-OS-02 SATS 0.2/100 = 1 MG + 100NG STD
BONDOC

C35 Hopanes BP-OS-Ø2

Norm: 12

(no significant peaks)

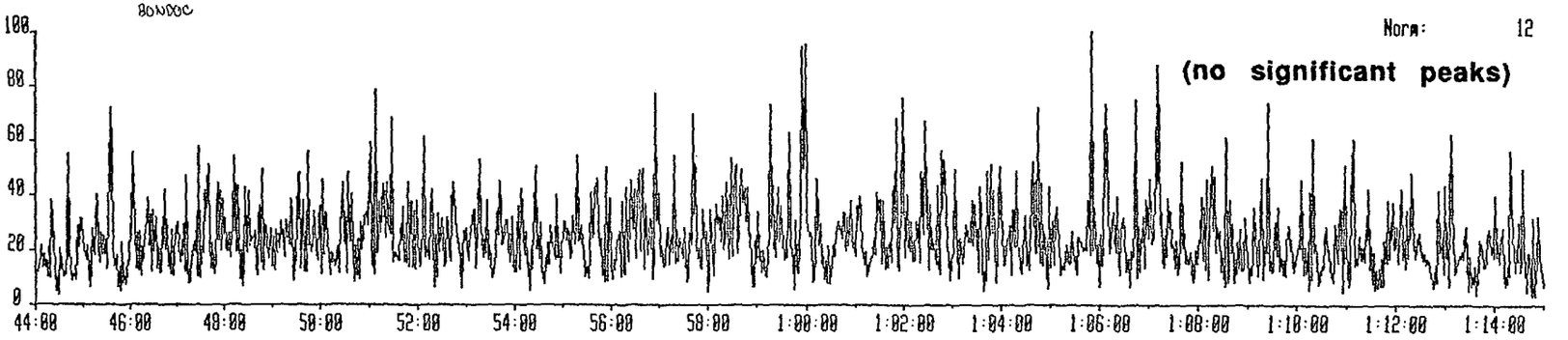

3JU15C 15-JUN-93 Sir:Reaction 70-E Sys: ALLTERPC
Sample 2 Injection 1 Group 2 Mass 468.4670 468.4670->191.1790
Text:

C34 Hopanes

Norm: 60

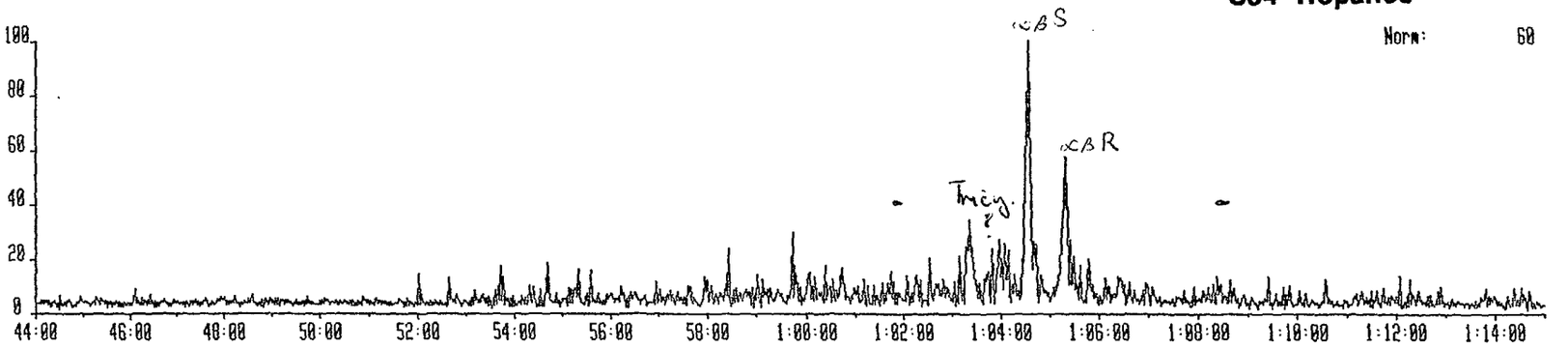

3JU15C 15-JUN-93 Sir:Reaction 70-E Sys: ALLTERPC
Sample 2 Injection 1 Group 2 Mass 454.4520 454.4520->191.1790
Text:

C33 Hopanes

Norm: 168

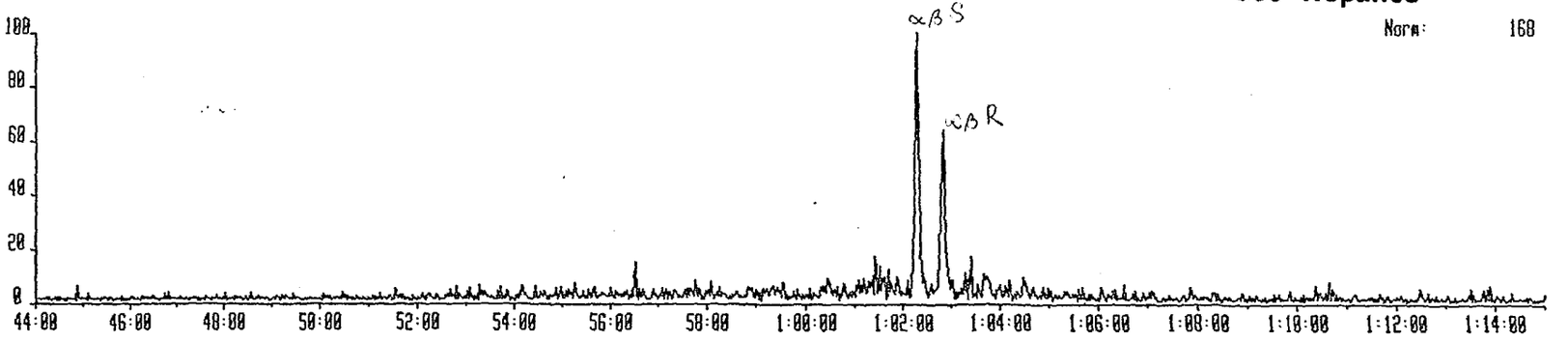

3JU15C 15-JUN-93 Sir:Reaction 70-E Sys: ALLTERPC
Sample 2 Injection 1 Group 2 Mass 440.4370 440.4370->191.1790
Text: #7924 BP-05-02 SATS 0.2/100 = 1 mg + 100 ng STD
BONDOC

C32 Hopanes

Norm: 334

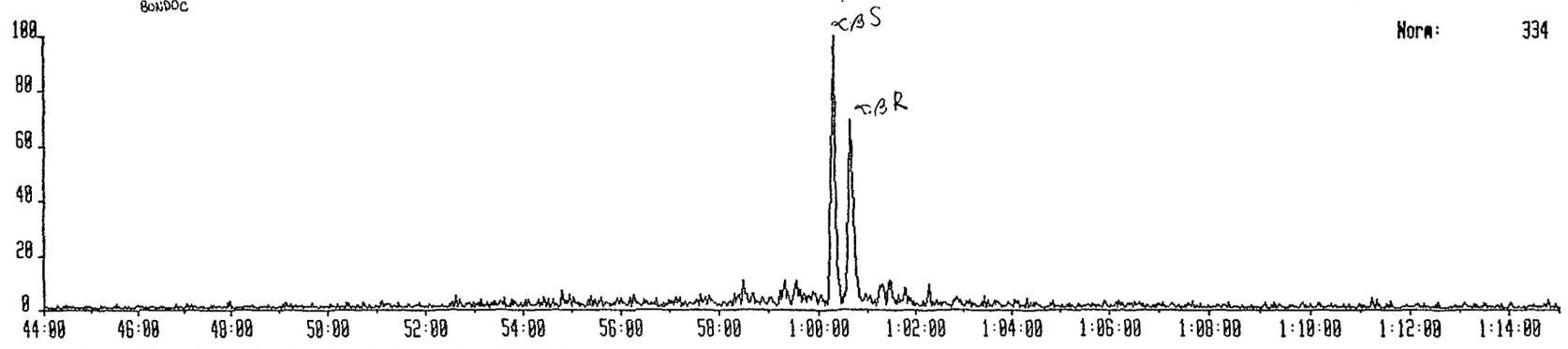

3JU15C 15-JUN-93 Sir:Reaction 70-E Sys: ALLTERPC
Sample 2 Injection 1 Group 2 Mass 426.4210 426.4210->191.1790
Text:

C31 Hopanes

Norm: 847

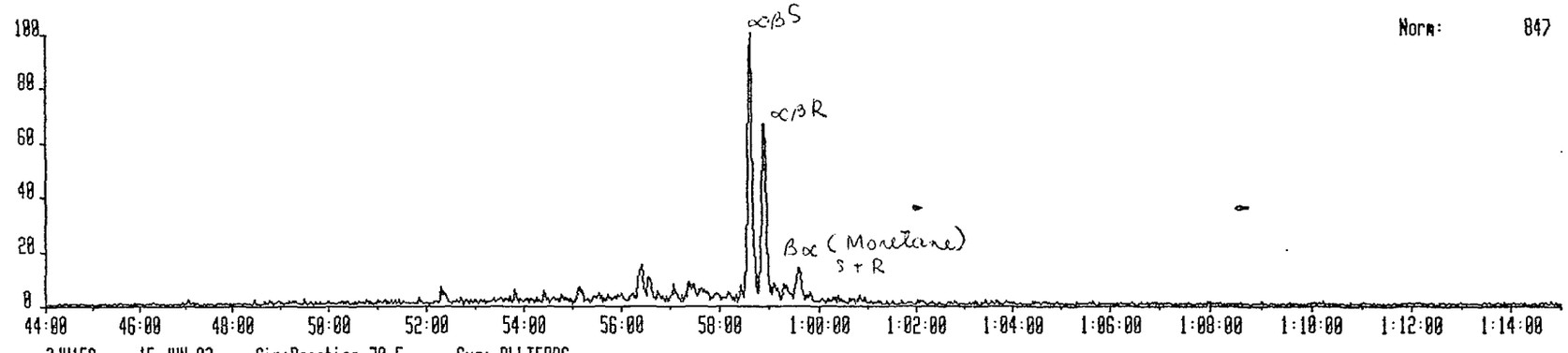

3JU15C 15-JUN-93 Sir:Reaction 70-E Sys: ALLTERPC
Sample 2 Injection 1 Group 2 Mass 416.4420 416.4420->191.1790
Text:

C30 Tricyclics (Cheilanthanes)

Norm: 549

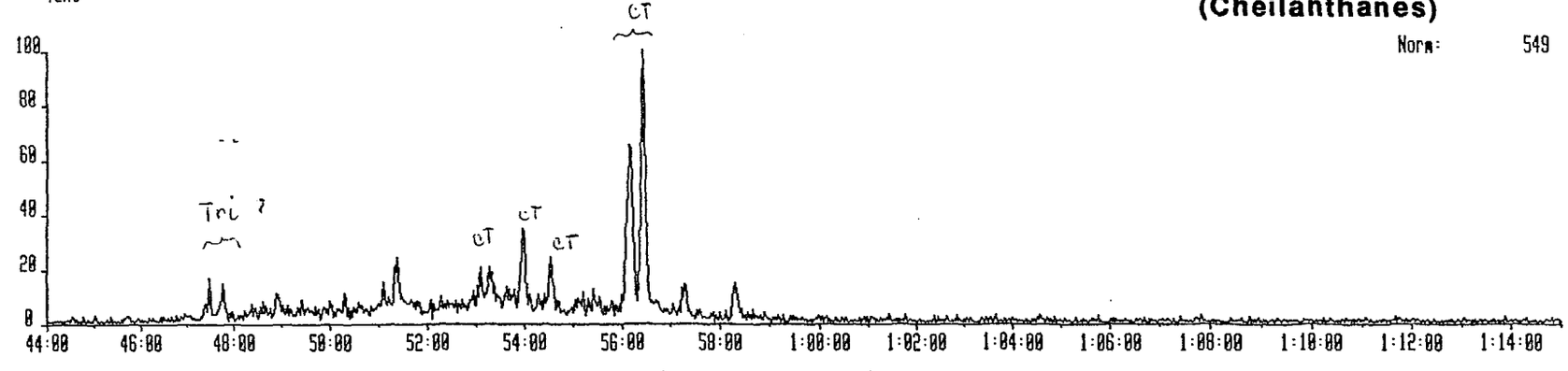

3JU15C 15-JUN-93 Sir:Reaction 70-E Sys: ALLTERPC
Sample 2 Injection 1 Group 2 Mass 412.4060 412.4060->191.1790
Text: #792 BowDoc BP-08-02 SATS 0.2/100 = 1 mg + 100 ng STD

C30 Hopanes & other Triterpanes

Norm: 5416

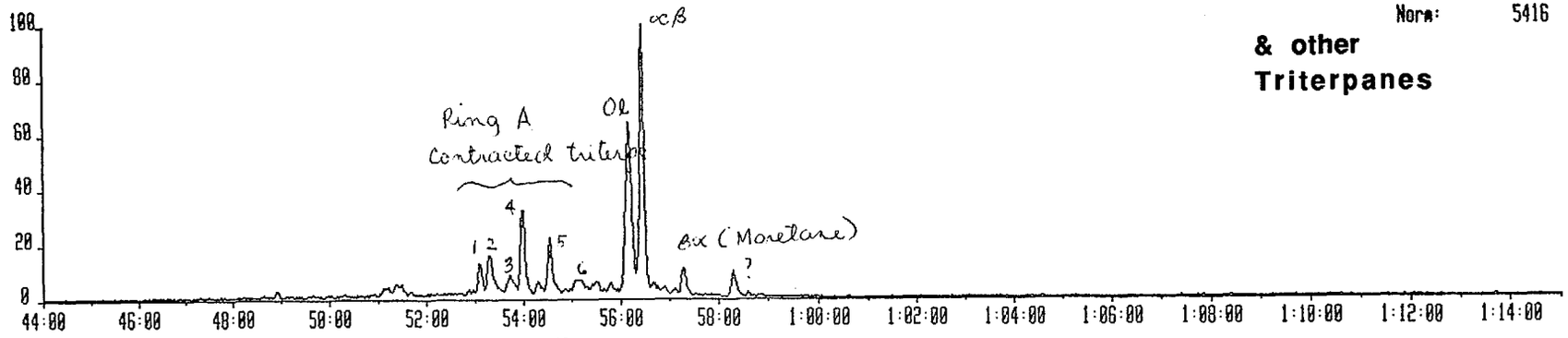

3JU15C 15-JUN-93 Sir:Reaction 70-E Sys: ALLTERPC
Sample 2 Injection 1 Group 2 Mass 398.3900 398.3900->191.1790
Text:

C29 Hopanes

Norm: 3357

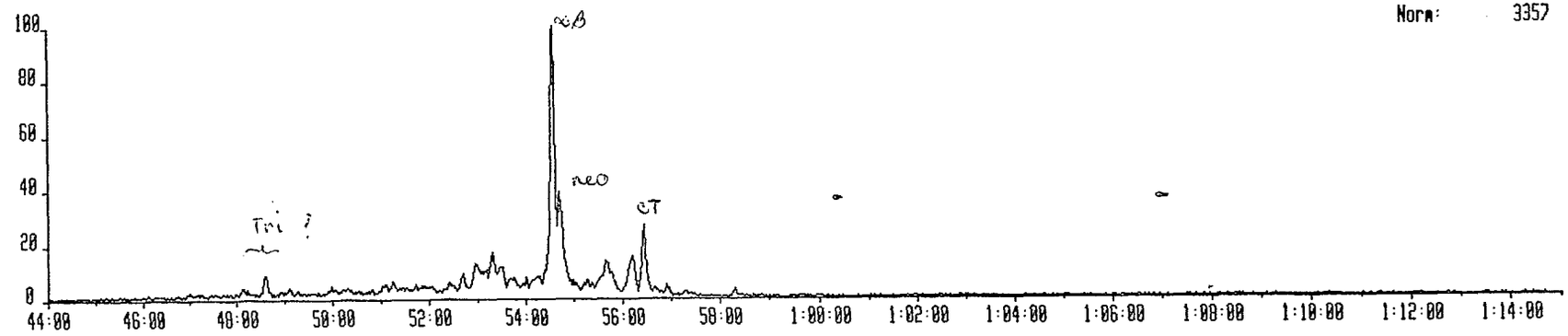

3JU15C 15-JUN-93 Sir:Reaction 70-E Sys: ALLTERPC
Sample 2 Injection 1 Group 2 Mass 384.3740 384.3740->191.1790
Text:

C28 Hopanes

Norm: 380

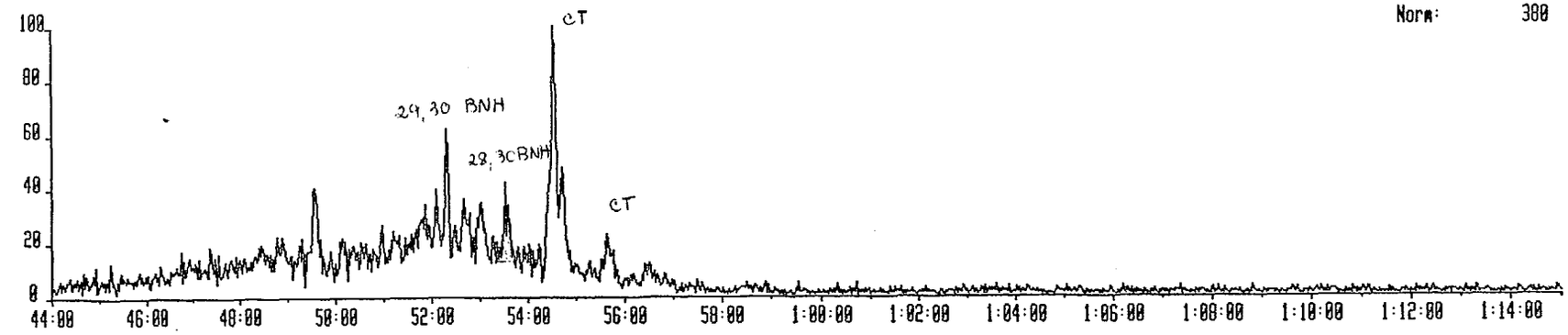

3JU15C 15-JUN-93 Sir:Reaction 70-E Sys: ALLTERPC
Sample 2 Injection 1 Group 2 Mass 370.3598 370.3598->191.1790
Text: #792 BONDOC BP-05-02 SATS 0.2/100 = 1 mg + 100 mg STD

C27 Hopanes

Norm: 2411

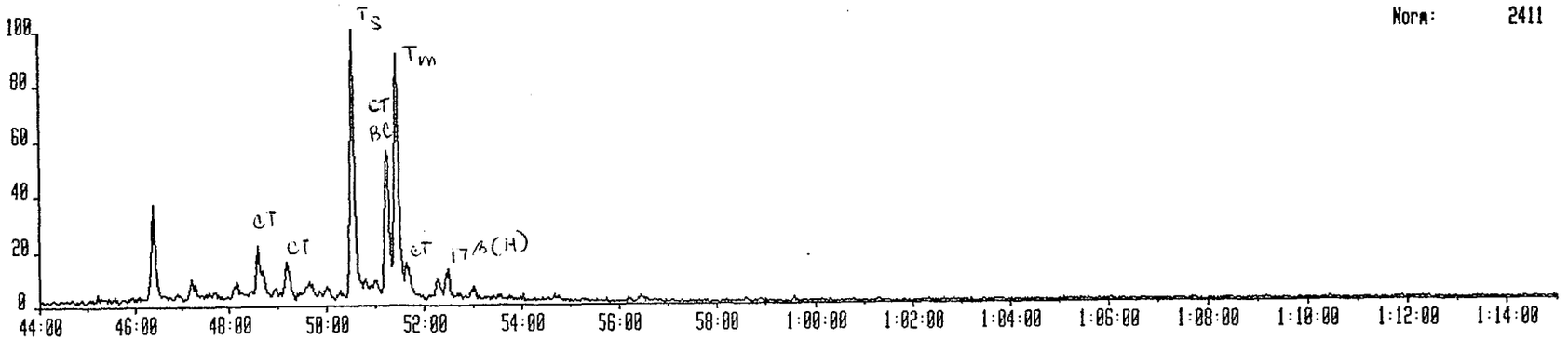

3JU15C 15-JUN-93 Sir:Reaction 70-E Sys: ALLTERPC
Sample 2 Injection 1 Group 2 Mass 426.4210 426.4210->205.1940
Text:

C31 Ring A-Methyl Hopanes

Norm: 696

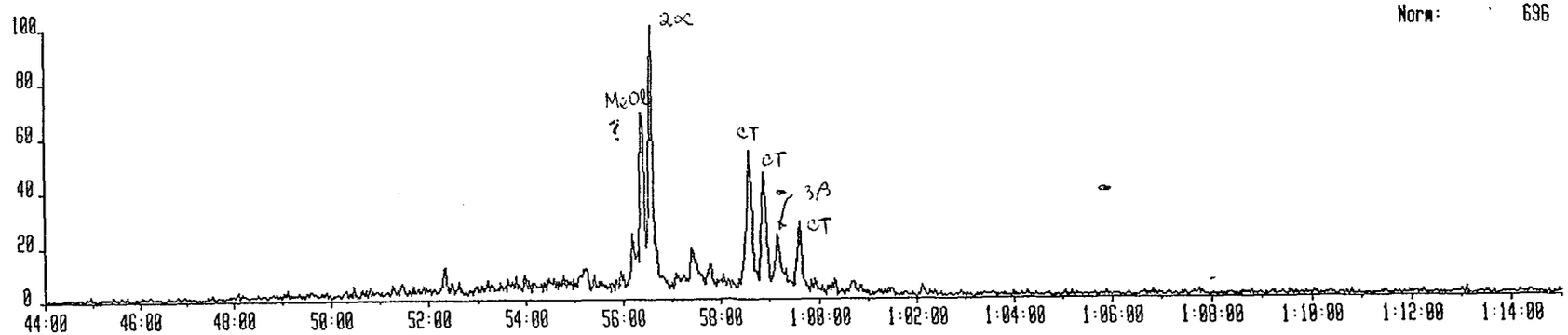

3JU15C 15-JUN-93 Sir:Reaction 70-E Sys: ALLTERPC
Sample 2 Injection 1 Group 2 Mass 414.4230 414.4230->217.1960
Text:

C30 Desmethyl Steranes

(absent)

Norm: 150

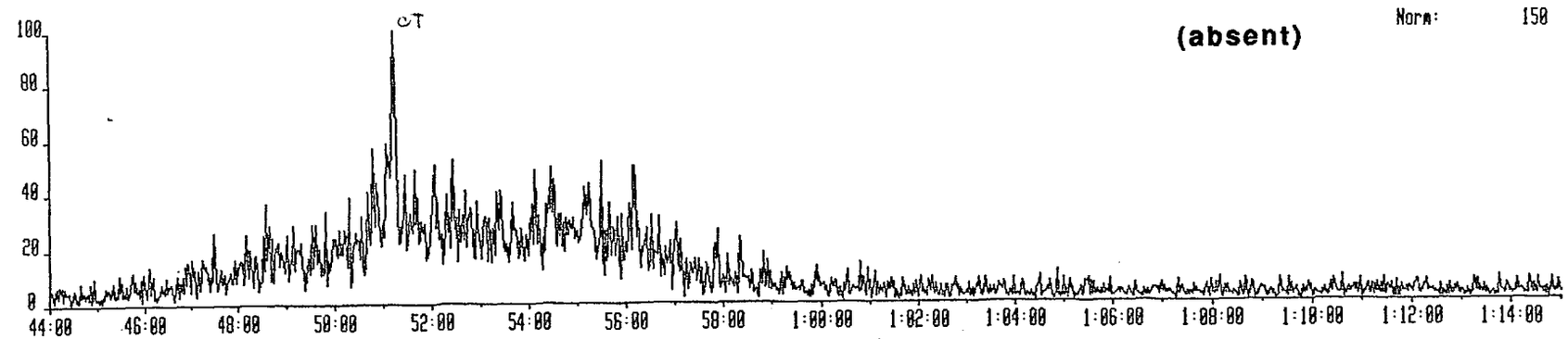

3JU15C 15-JUN-93 Sir:Reaction 70-E Sys: ALLTERPC
Sample 2 Injection 1 Group 2 Mass 400.4070 400.4070->217.1960
Text: #792 BONDOC BP-OS-02 SATS 0.2/100 = 1 mg + 100 ng STD

C29 Steranes

Norm: 2876

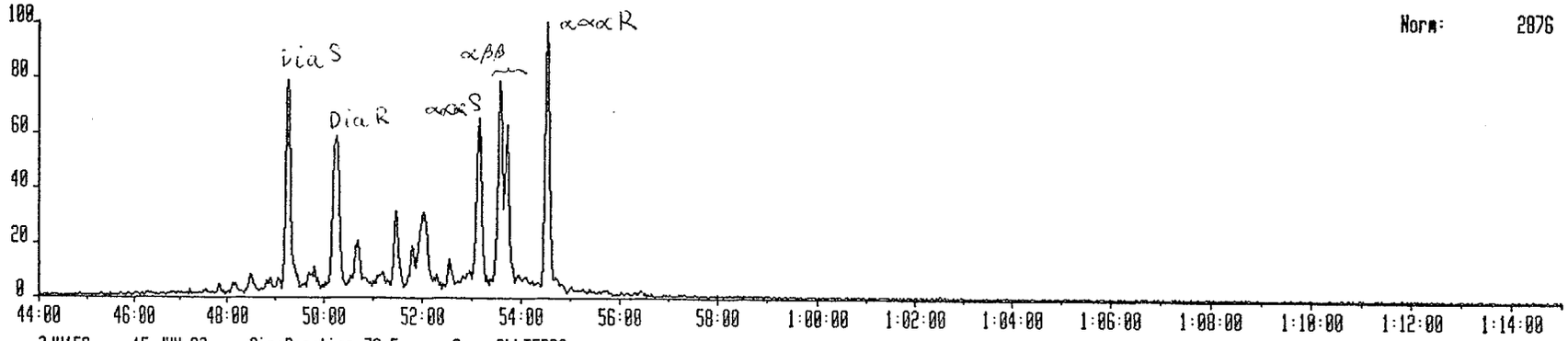

3JU15C 15-JUN-93 Sir:Reaction 70-E Sys: ALLTERPC
Sample 2 Injection 1 Group 2 Mass 386.3910 386.3910->217.1960
Text:

C28 Steranes

Norm: 1613

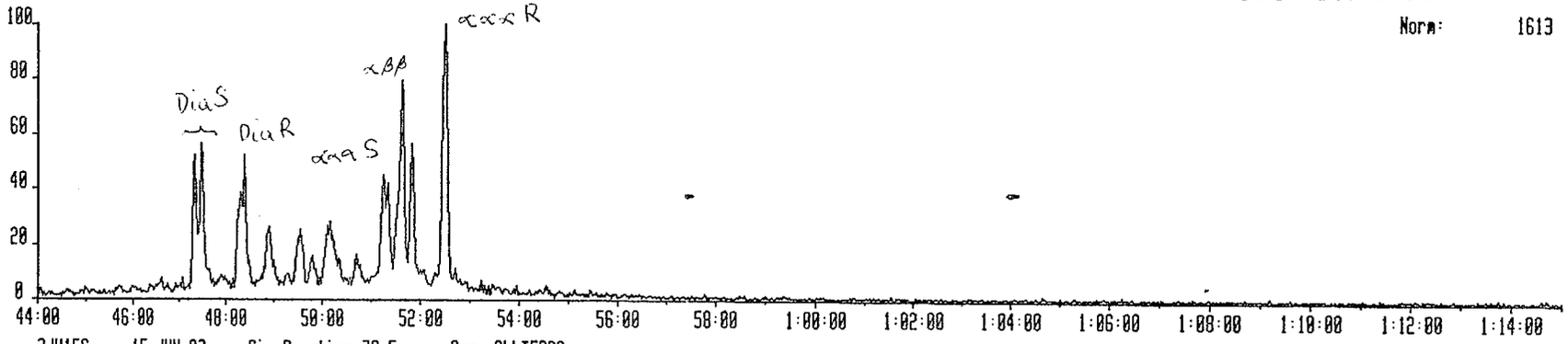

3JU15C 15-JUN-93 Sir:Reaction 70-E Sys: ALLTERPC
Sample 2 Injection 1 Group 2 Mass 372.3760 372.3760->217.1960
Text:

C27 Steranes

Norm: 1304

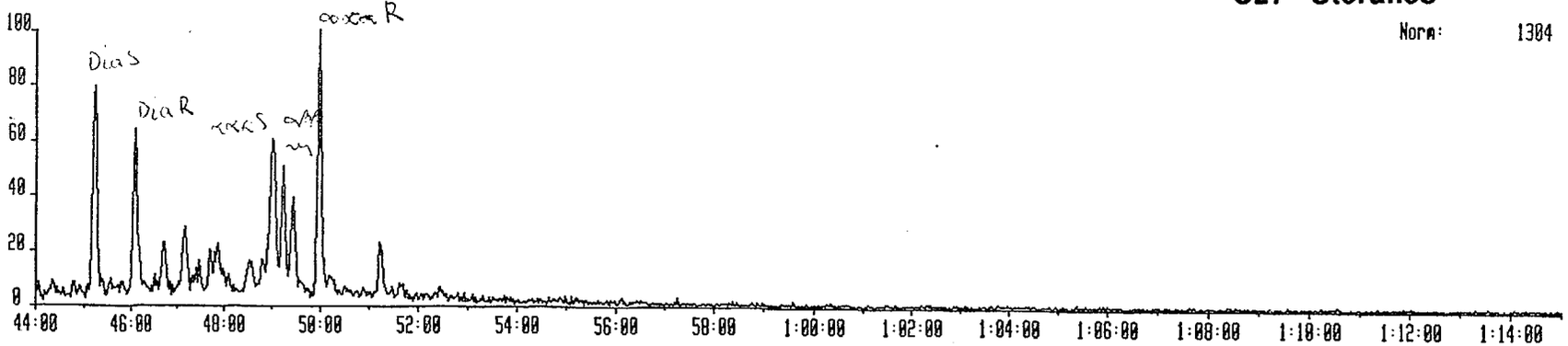

3JU15C 15-JUN-93 Sir:Reaction 70-E Sys: ALLTERPC
Sample 2 Injection 1 Group 2 Mass 414.4230 414.4230->231.2120
Text: #792 BONDOC BP-08-02 SATS 0.2/100 = 1 mg + 100 ng STD

C30 Ring A-Methyl Steranes

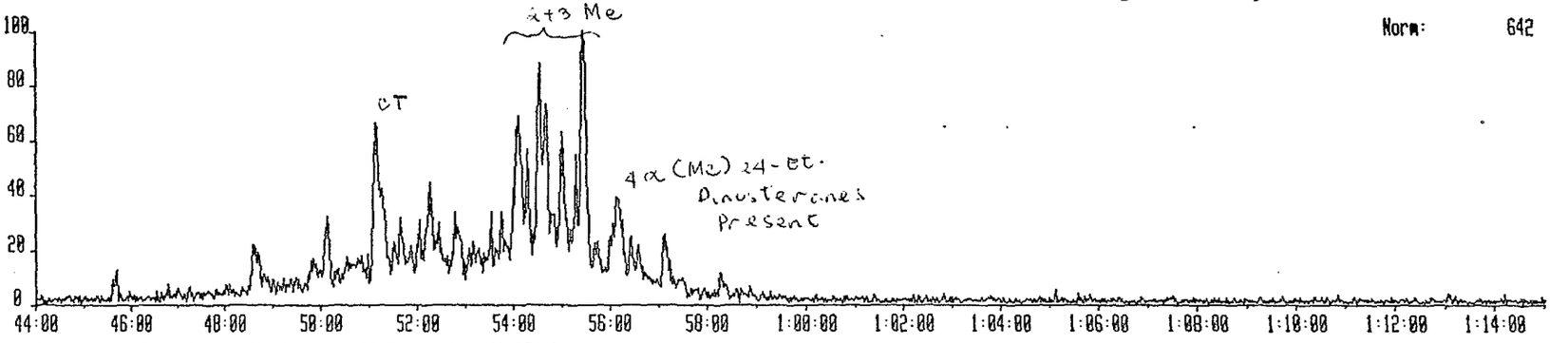

3JU15C 15-JUN-93 Sir:Reaction 70-E Sys: ALLTERPC
Sample 2 Injection 1 Group 2 Mass 389.4105 389.4105->234.2324
Text:

Internal Standard

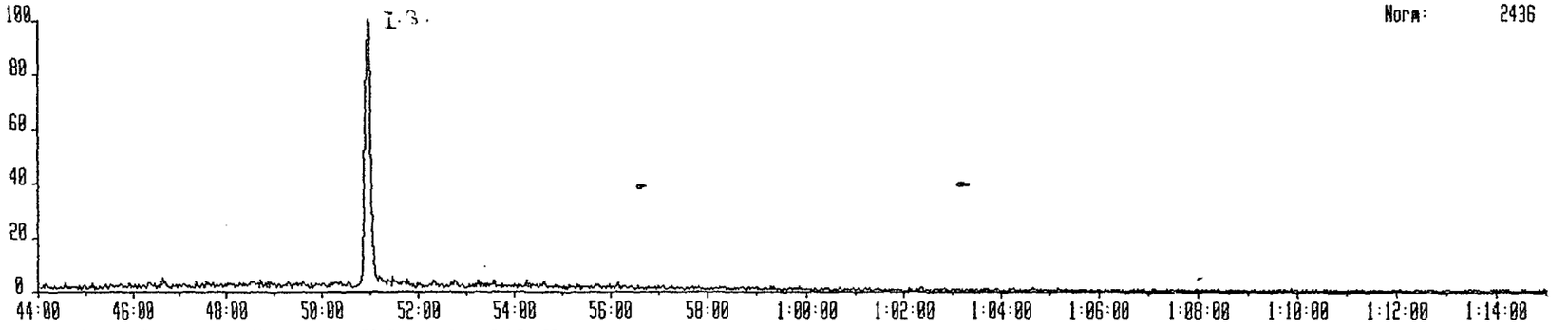

3JU15C 15-JUN-93 Sir:Reaction 70-E Sys: ALLTERPC
Sample 2 Injection 1 Group 2 Mass 412.4060 412.4060->369.3400
Text:

C30 Bicadinanes

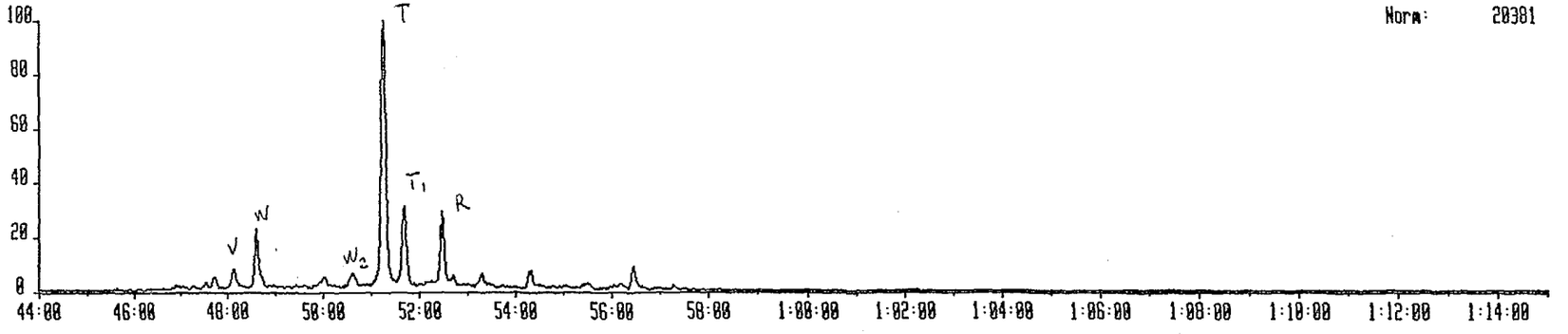

3JU15C 15-JUN-93 Sir:Reaction 70-E Sys: ALLTERPC
Sample 2 Injection 1 Group 2 Mass 426.4230 426.4230->383.3550
Text:#792 SATS BP-OS-01 BONDOC SEEP 0.2/100 1MG +100 NG STD

C31 Methyl Bicadinanes

Norm: 39829

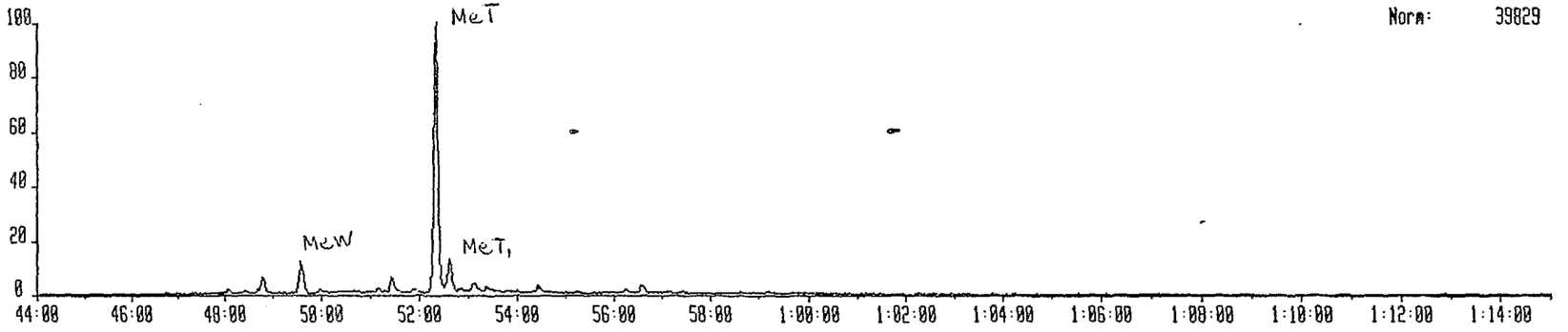

3JU16A 16-JUN-93 Sir:Magnetic 70-E Sys: MPI2
Sample 2 Injection 1 Group 2 Mass 178.0782
Text:#792 AROMS BONDOC SEEP BP-OS-02 1:200

Phenanthrene > derivatives
lost due to biodegradation

Phenanthrene

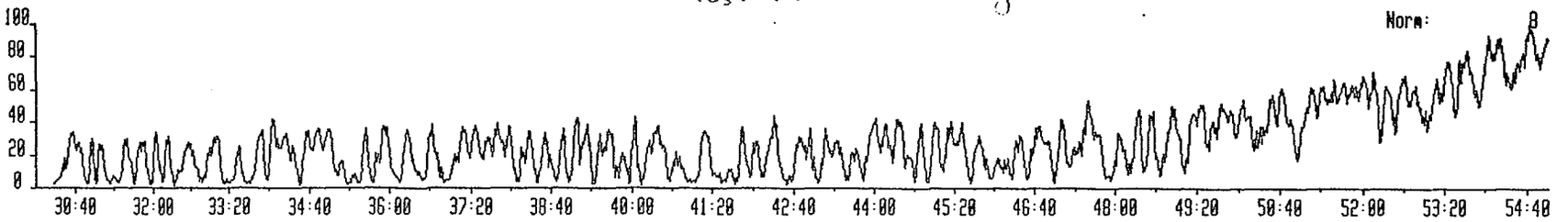

3JU16A 16-JUN-93 Sir:Magnetic 70-E Sys: MPI2
Sample 2 Injection 1 Group 2 Mass 192.0930
Text:#792 AROMS BONDOC SEEP BP-OS-02 1:200

Methyl Phenanthrene

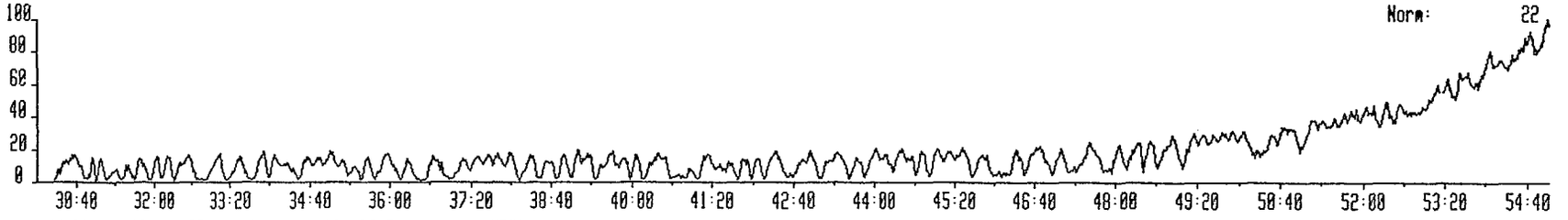

3JU16A 16-JUN-93 Sir:Magnetic 70-E Sys: MPI2
Sample 2 Injection 1 Group 2 Mass 206.1000
Text:#792 AROMS BONDOC SEEP BP-OS-02 1:200

Dimethyl Phenanthrene

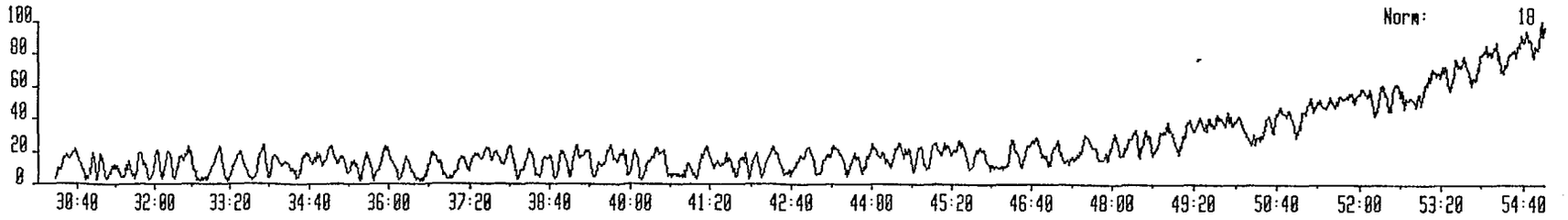

3JU16A 16-JUN-93 Sir:Magnetic 70-E Sys: MPI2
Sample 2 Injection 1 Group 2 Mass 219.1000
Text:#792 AROMS BONDOC SEEP BP-OS-02 1:200

Retene
(not detected)

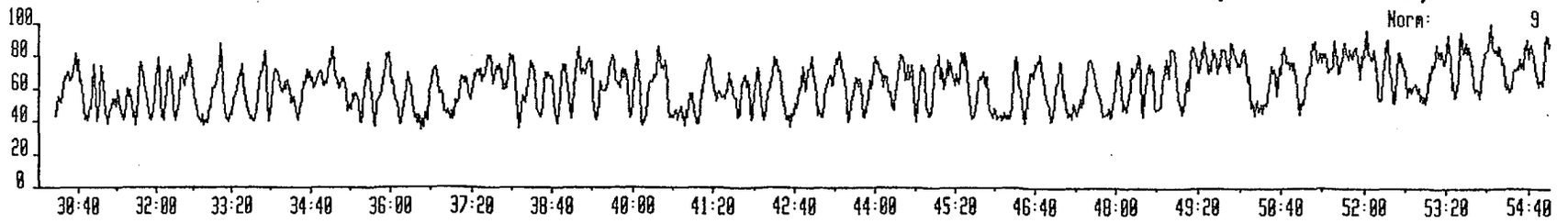

3JU15C 15-JUN-93 Sir:Reaction 70-E Sys: ALLTERPC
Sample 3 Injection 1 Group 2 Mass 482.4820 482.4820->191.1790
Text: #793 BONDOC-2 (?) WELL MUD EXTRACT SATS 0.2/100 = 1 mg + 100 ng STD

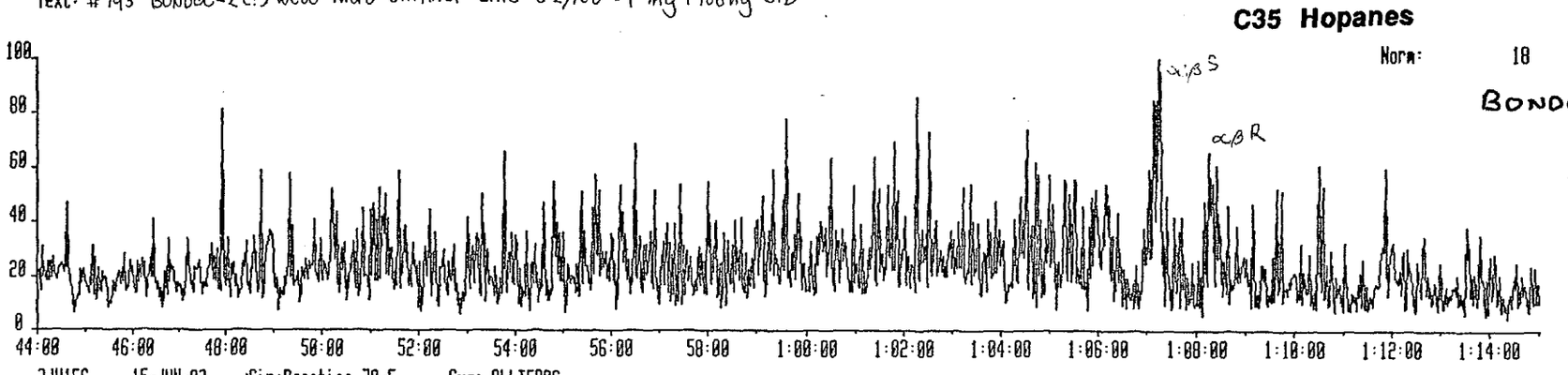

3JU15C 15-JUN-93 Sir:Reaction 70-E Sys: ALLTERPC
Sample 3 Injection 1 Group 2 Mass 468.4670 468.4670->191.1790
Text:

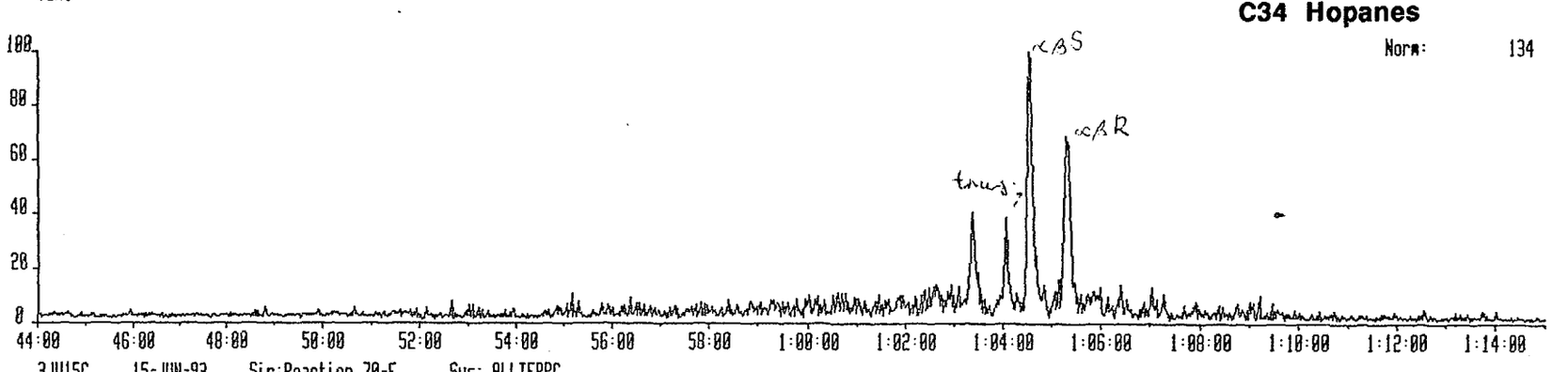

3JU15C 15-JUN-93 Sir:Reaction 70-E Sys: ALLTERPC
Sample 3 Injection 1 Group 2 Mass 454.4520 454.4520->191.1790
Text:

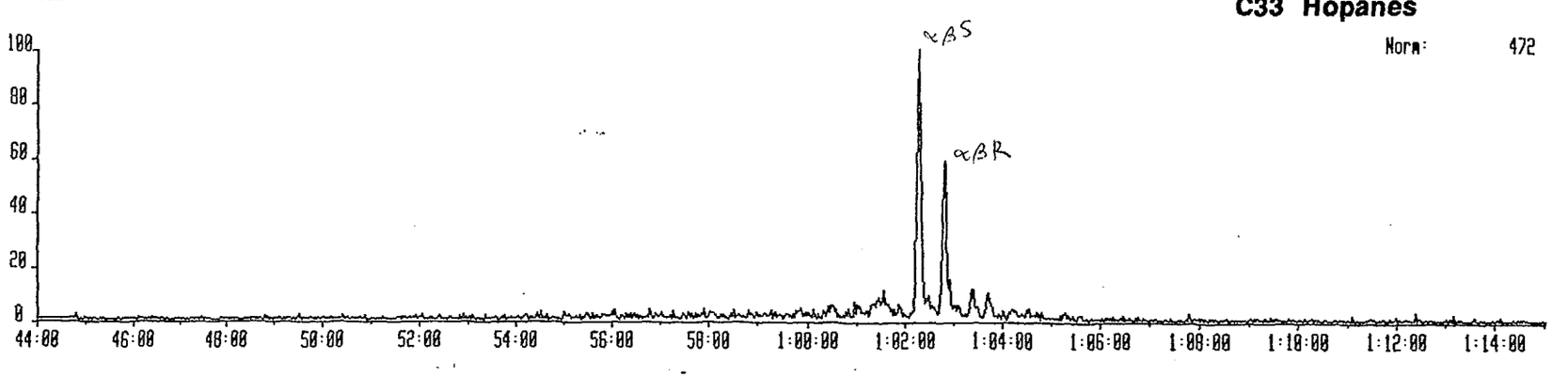

3JU15C 15-JUN-93 Sir:Reaction 70-E Sys: ALLTERPC
Sample 3 Injection 1 Group 2 Mass 440.4370 440.4370->191.1790
Text: #798 BONDOC-2 (?) WELL MUD EXTRACT SATS 0.2/100 = 1 mg + 100 ng STD

C32 Hopanes

Norm: 1021

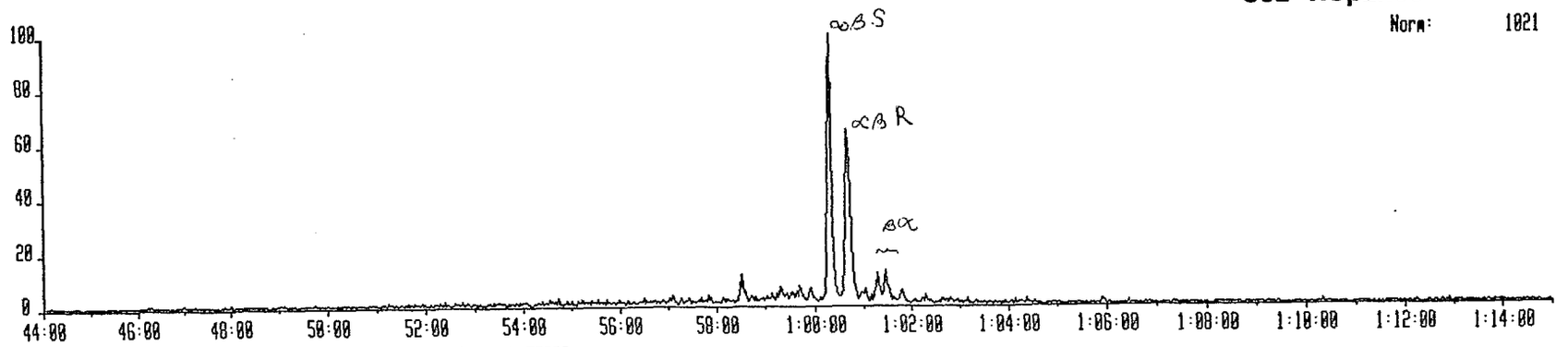

3JU15C 15-JUN-93 Sir:Reaction 70-E Sys: ALLTERPC
Sample 3 Injection 1 Group 2 Mass 426.4210 426.4210->191.1790
Text:

C31 Hopanes

Norm: 2727

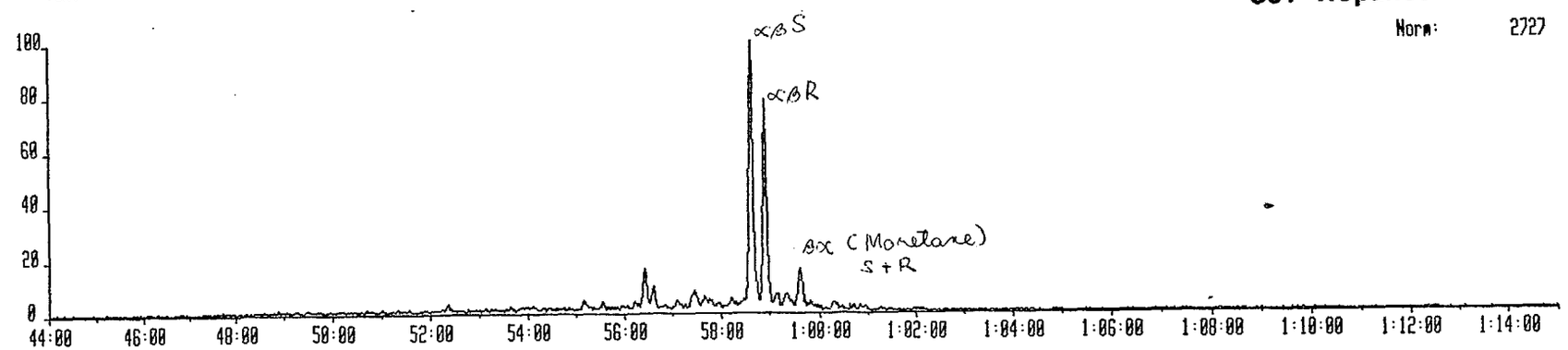

3JU15C 15-JUN-93 Sir:Reaction 70-E Sys: ALLTERPC
Sample 3 Injection 1 Group 2 Mass 416.4420 416.4420->191.1790
Text:

C30 Tricyclics (Cheilanthanes)

Norm: 2102

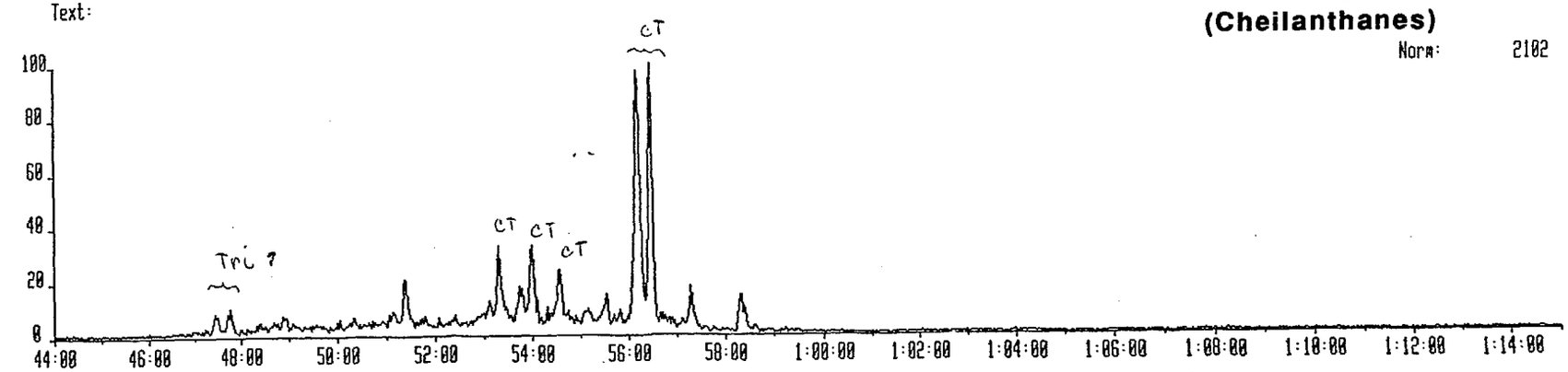

3JU15C 15-JUN-93 Sir:Reaction 70-E Sys: ALLTERPC
Sample 3 Injection 1 Group 2 Mass 412.4060 412.4060->191.1790
Text: #793 BONDOC-2(?) WELL MUD EXTRACT SATS 0.2/100 = 1 mg + 100 ng STD

C30 Hopanes & other Triterpanes

Norm: 12953

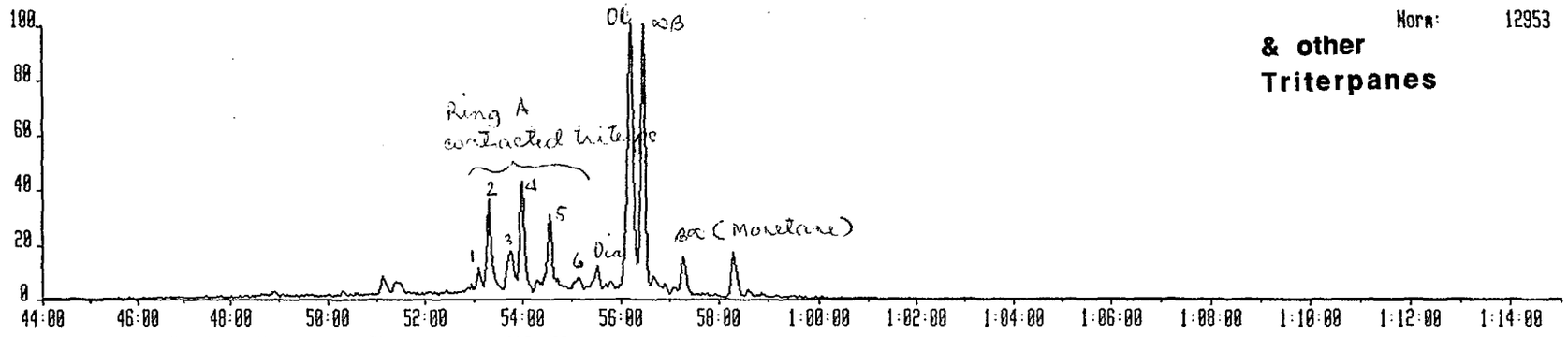

3JU15C 15-JUN-93 Sir:Reaction 70-E Sys: ALLTERPC
Sample 3 Injection 1 Group 2 Mass 398.3900 398.3900->191.1790
Text:

C29 Hopanes

Norm: 7180

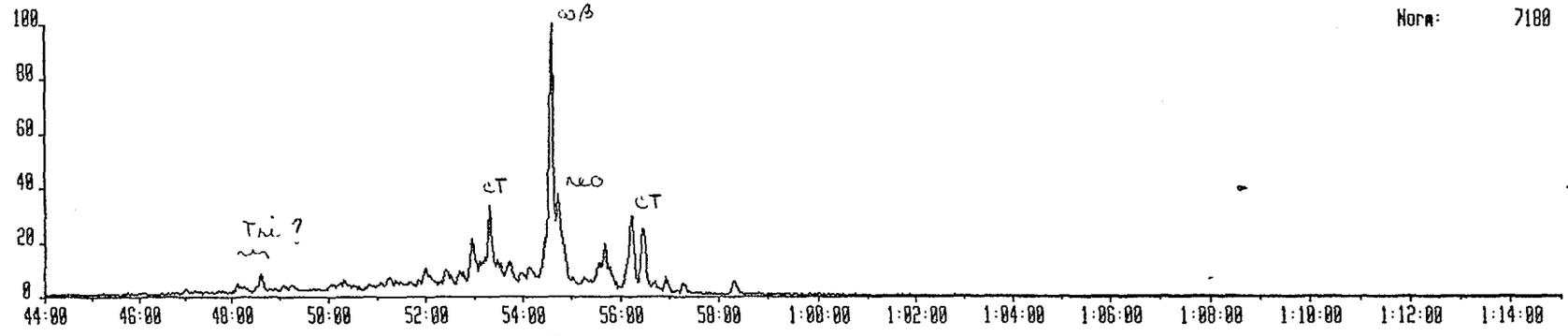

3JU15C 15-JUN-93 Sir:Reaction 70-E Sys: ALLTERPC
Sample 3 Injection 1 Group 2 Mass 384.3740 384.3740->191.1790
Text:

C28 Hopanes

Norm: 716

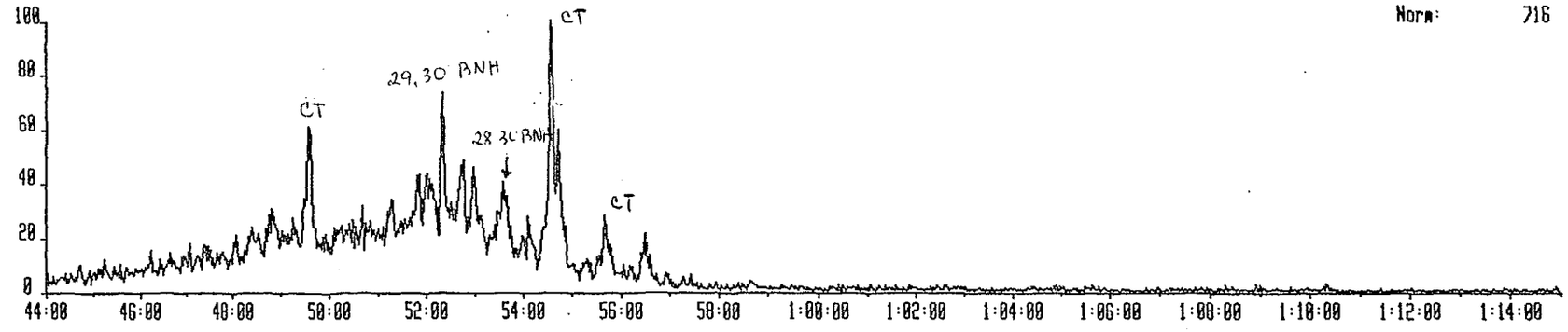

3JU15C 15-JUN-93 Sir:Reaction 70-E Sys: ALLTERPC
Sample 3 Injection 1 Group 2 Mass 370.3590 370.3590->191.1790
Text: #793 BONDOO-2(?) WELL MUD EXTRACT SATS 0.2/100 = 1 mg + 100 ng STD

C27 Hopanes

Norm: 4282

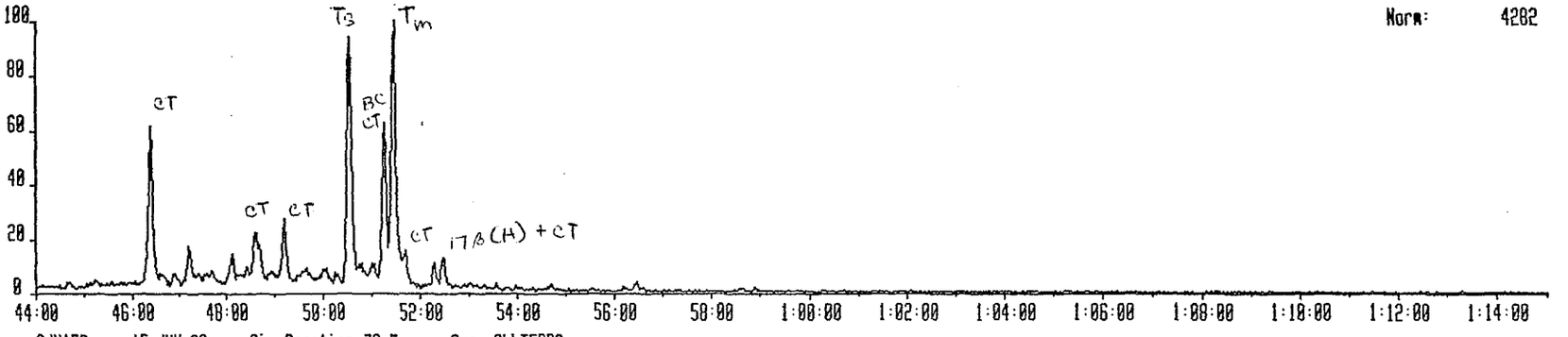

3JU15C 15-JUN-93 Sir:Reaction 70-E Sys: ALLTERPC
Sample 3 Injection 1 Group 2 Mass 426.4210 426.4210->205.1940
Text:

C31 Ring A-Methyl Hopanes

Norm: 1579

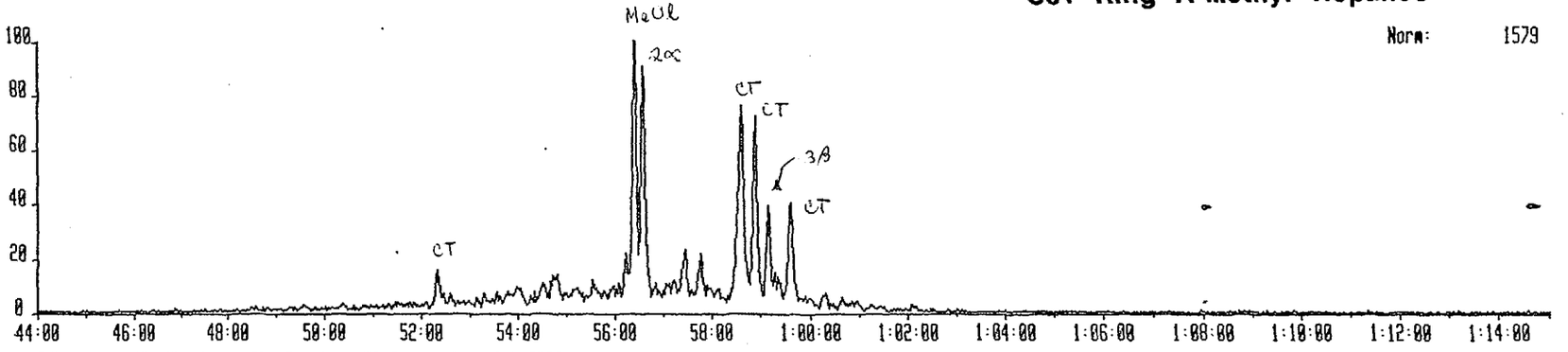

3JU15C 15-JUN-93 Sir:Reaction 70-E Sys: ALLTERPC
Sample 3 Injection 1 Group 2 Mass 414.4230 414.4230->217.1960
Text:

C30 Desmethyl Steranes

Norm: 253

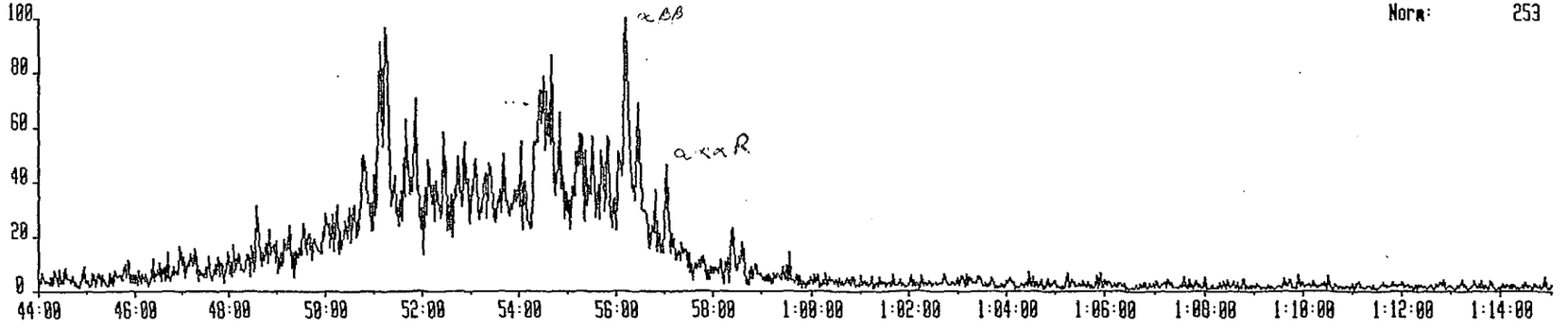

3JU15C 15-JUN-93 Sir:Reaction 70-E Sys: ALLTERPC
Sample 3 Injection 1 Group 2 Mass 400.4070 400.4070->217.1960
Text: #793 BONDOC-2 (?) WELL MUD EXTRACT SATS 0.2/100 = 1 mg + 100ng STD

C29 Steranes

Norm: 6761

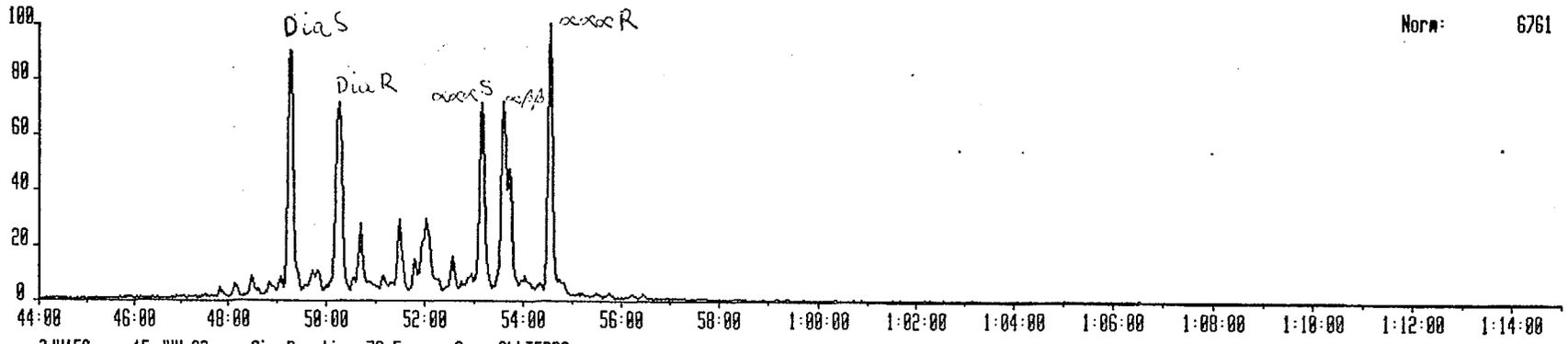

3JU15C 15-JUN-93 Sir:Reaction 70-E Sys: ALLTERPC
Sample 3 Injection 1 Group 2 Mass 386.3910 386.3910->217.1960
Text:

C28 Steranes

Norm: 4386

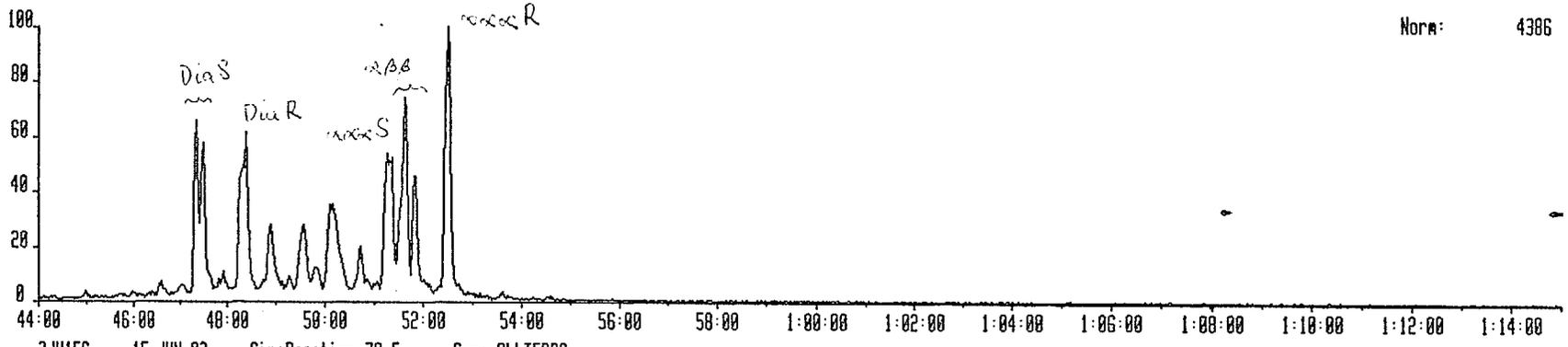

3JU15C 15-JUN-93 Sir:Reaction 70-E Sys: ALLTERPC
Sample 3 Injection 1 Group 2 Mass 372.3760 372.3760->217.1960
Text:

C27 Steranes

Norm: 3645

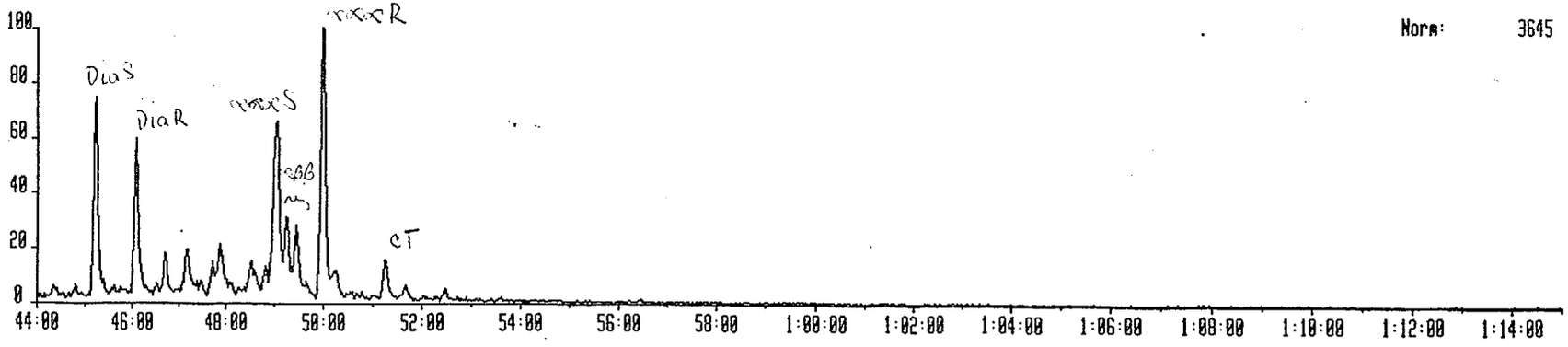

3JU15C 15-JUN-93 Sir:Reaction 70-E Sys: ALLTERPC
Sample 3 Injection 1 Group 2 Mass 414.4230 414.4230->231.2128
Text: #793 BONDOC-2 (?) WELL MUD EXTRACT SATS 0.2/100 = 1 mg + 100 ng STD

C30 Ring A-Methyl Steranes

Norm: 1524

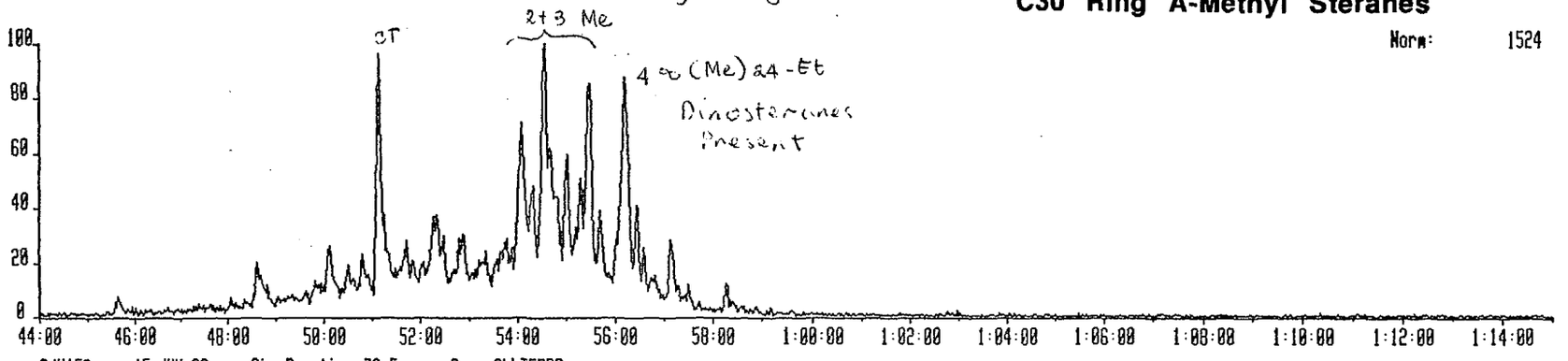

3JU15C 15-JUN-93 Sir:Reaction 70-E Sys: ALLTERPC
Sample 3 Injection 1 Group 2 Mass 389.4105 389.4105->234.2324
Text:

Internal Standard

Norm: 2155

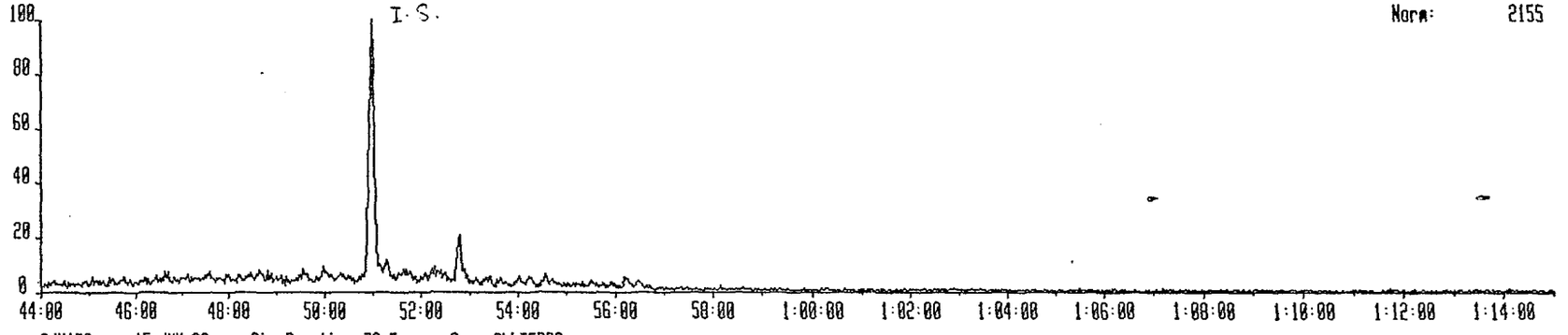

3JU15C 15-JUN-93 Sir:Reaction 70-E Sys: ALLTERPC
Sample 3 Injection 1 Group 2 Mass 412.4060 412.4060->369.3400
Text:

C30 Bicadinanes

Norm: 27148

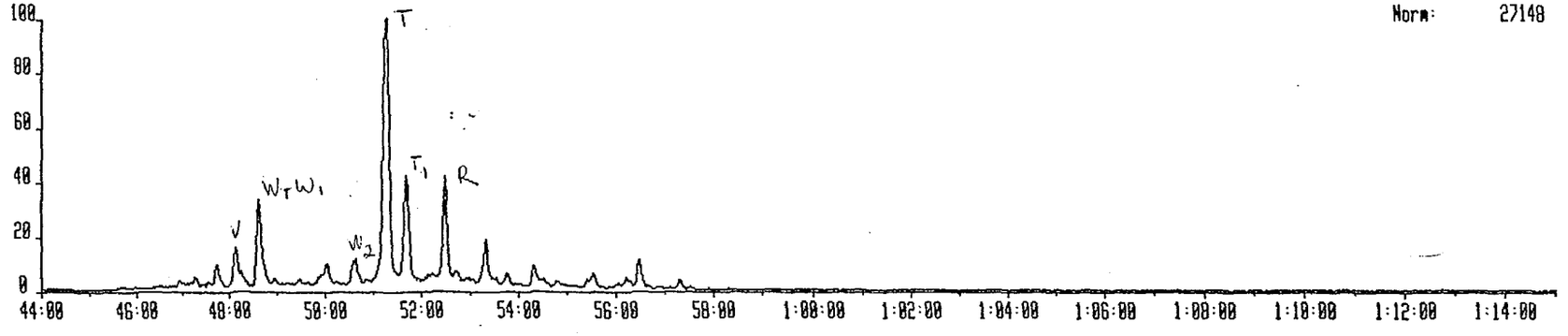

3JU15C 15-JUN-93 Sir:Reaction 70-E Sys: ALLTERPC
Sample 3 Injection 1 Group 2 Mass 426.4230 426.4230->383.3550
Text:#793 SATS BONDOC-2(?) WELL MUD EXTRACT 0.2/100 = 1 MG + 100 NG S

C31 Methyl Bicadinanes

Norm: 65229

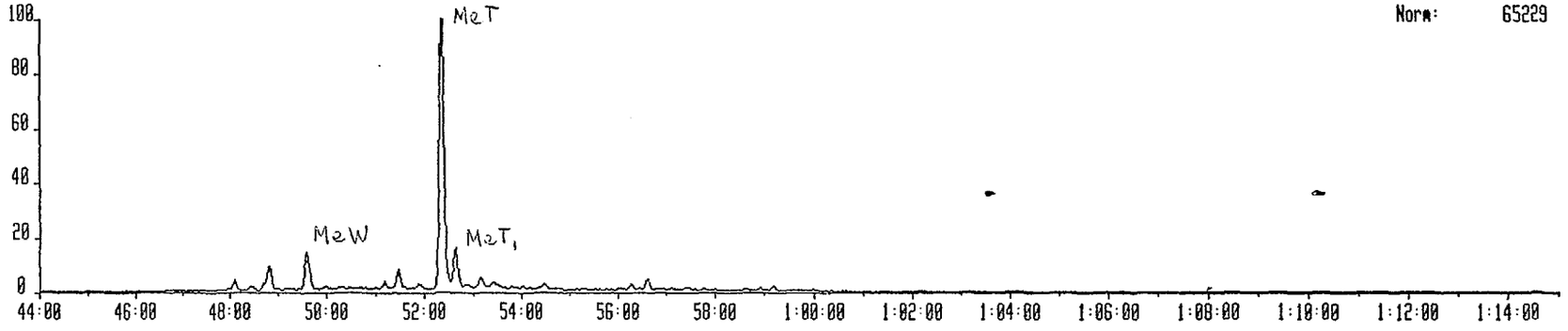

3JU16A 16-JUN-93 Sir:Magnetic 70-E Sys: MPI2
Sample 3 Injection 1 Group 2 Mass 178.0782
Text:#793 AROMS BONDOC-2 WELL MUD EXTRACT 1:200

Phenanthrene & homologs lost due to biodegradation

Phenanthrene

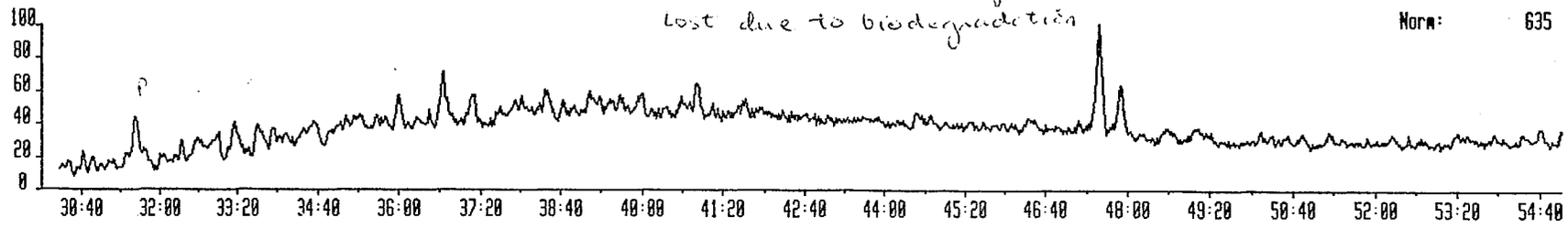

3JU16A 16-JUN-93 Sir:Magnetic 70-E Sys: MPI2
Sample 3 Injection 1 Group 2 Mass 192.0930
Text:#793 AROMS BONDOC-2 WELL MUD EXTRACT 1:200

Methyl Phenanthrene

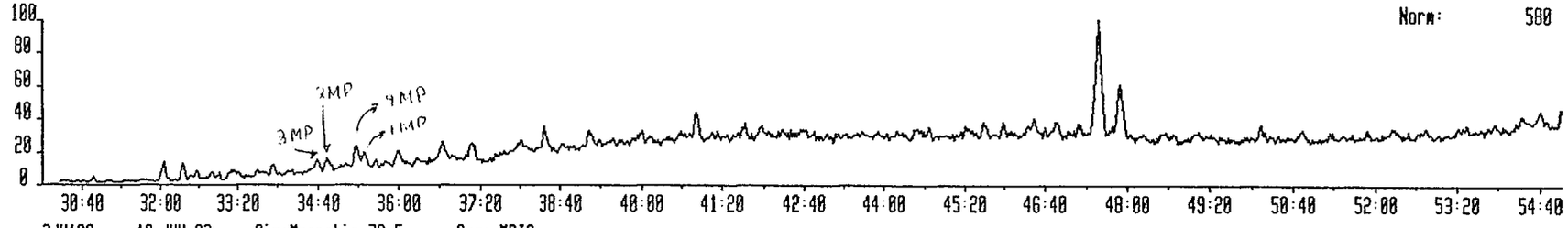

3JU16A 16-JUN-93 Sir:Magnetic 70-E Sys: MPI2
Sample 3 Injection 1 Group 2 Mass 206.1000
Text:#793 AROMS BONDOC-2 WELL MUD EXTRACT 1:200

Dimethyl Phenanthrene

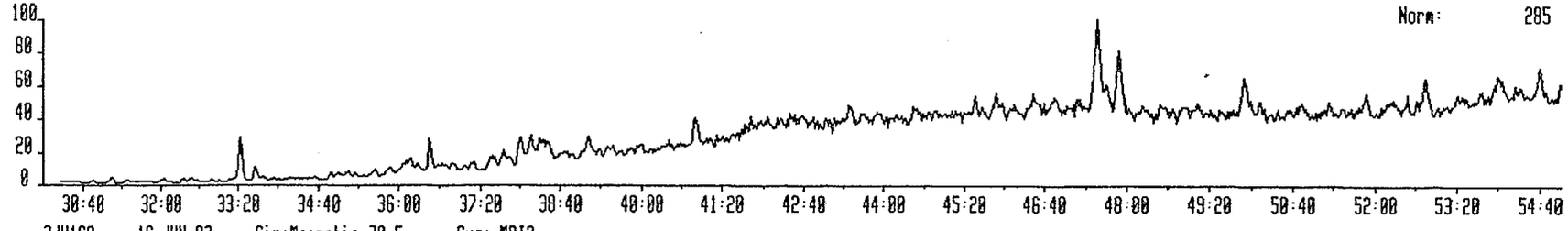

3JU16A 16-JUN-93 Sir:Magnetic 70-E Sys: MPI2
Sample 3 Injection 1 Group 2 Mass 219.1000
Text:#793 AROMS BONDOC-2 WELL MUD EXTRACT 1:200

Retene
(not detected)

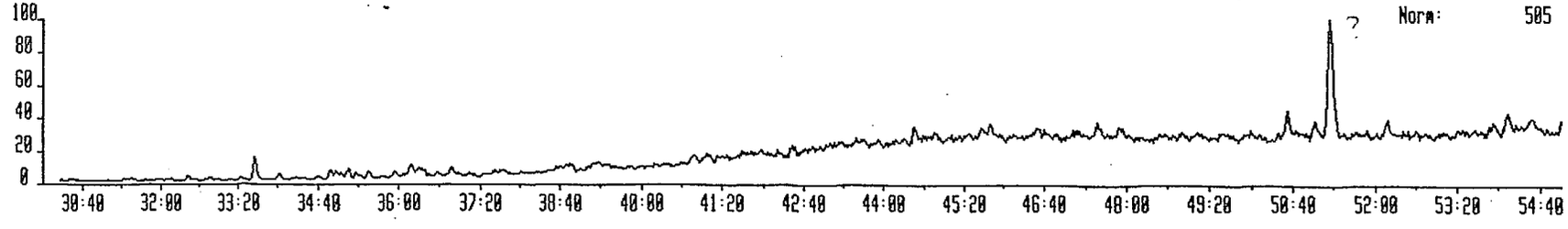

Maalat Canilbo

3JU15C 15-JUN-93 Sir:Reaction 70-E Sys: ALLTERPC
Sample 4 Injection 1 Group 2 Mass 482.4820 482.4820->191.1790
Text: #794 MAALAT-CANILBO MUD EXTRACT SATS 0.2/100 = 1 mg + 100 ng STD

C35 Hopanes

Norm: 16

(no significant peaks)

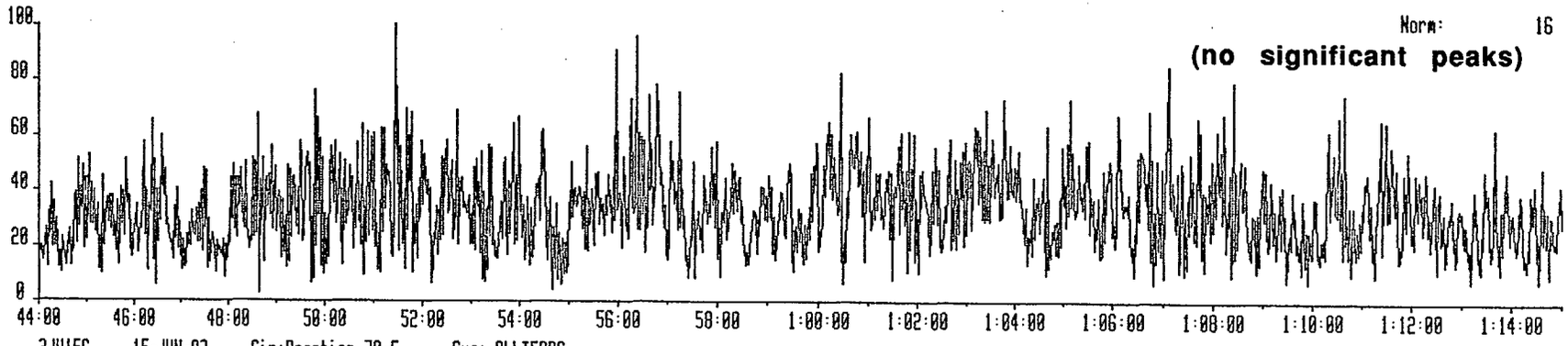

3JU15C 15-JUN-93 Sir:Reaction 70-E Sys: ALLTERPC
Sample 4 Injection 1 Group 2 Mass 468.4670 468.4670->191.1790
Text:

C34 Hopanes

Norm: 47

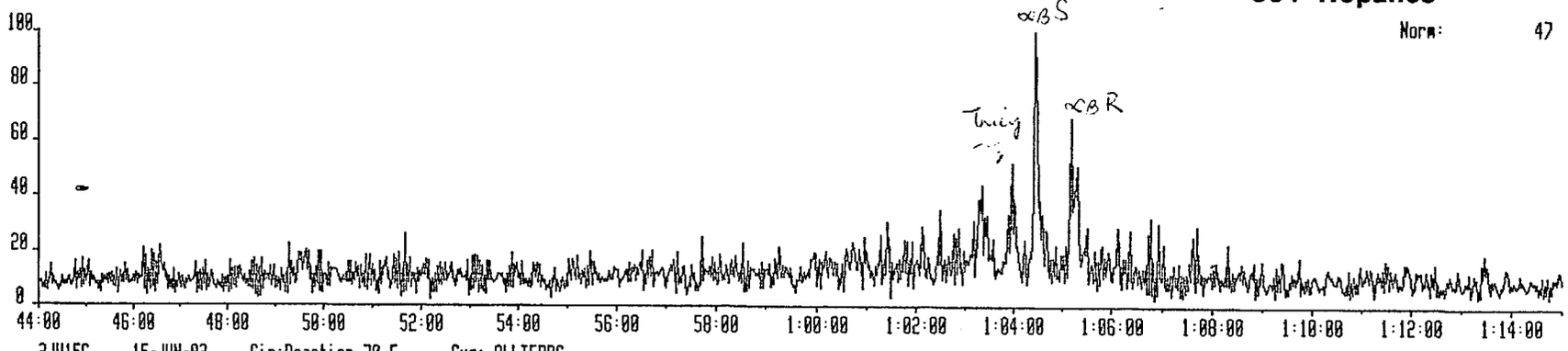

3JU15C 15-JUN-93 Sir:Reaction 70-E Sys: ALLTERPC
Sample 4 Injection 1 Group 2 Mass 454.4520 454.4520->191.1790
Text:

C33 Hopanes

Norm: 105

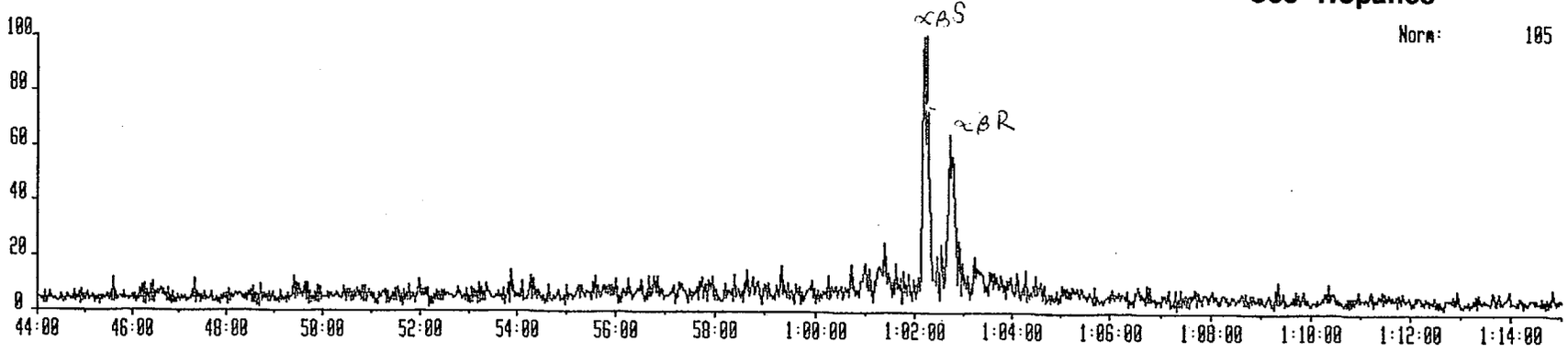

3JU15C 15-JUN-93 Sir:Reaction 70-E Sys: ALLTERPC
Sample 4 Injection 1 Group 2 Mass 440.4370 440.4370->191.1790
Text: #794 MAALAT- CANICBO MUD EXTRACT SATS 0.2/100 = 1 mg + 100 ng STD

C32 Hopanes

Norm: 225

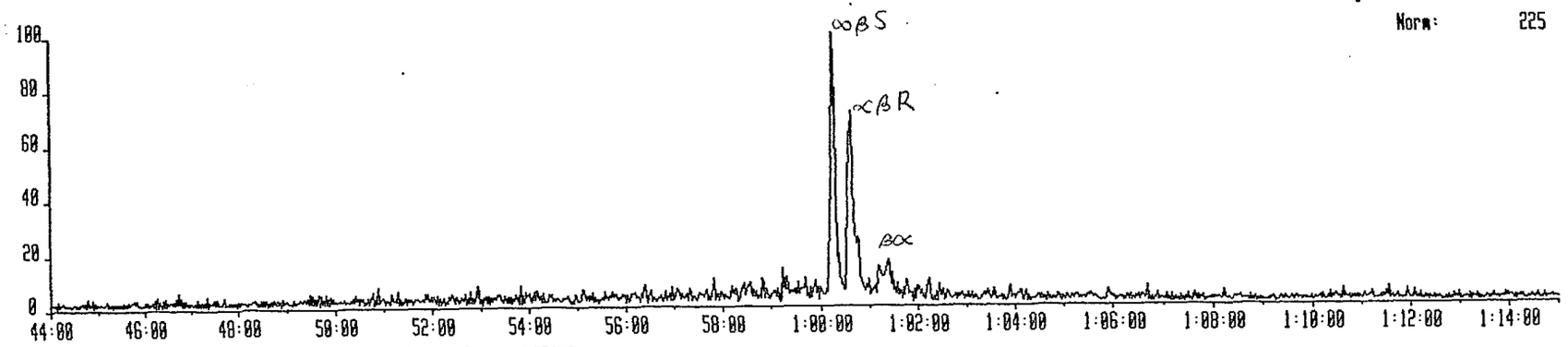

3JU15C 15-JUN-93 Sir:Reaction 70-E Sys: ALLTERPC
Sample 4 Injection 1 Group 2 Mass 426.4210 426.4210->191.1790
Text:

C31 Hopanes

Norm: 785

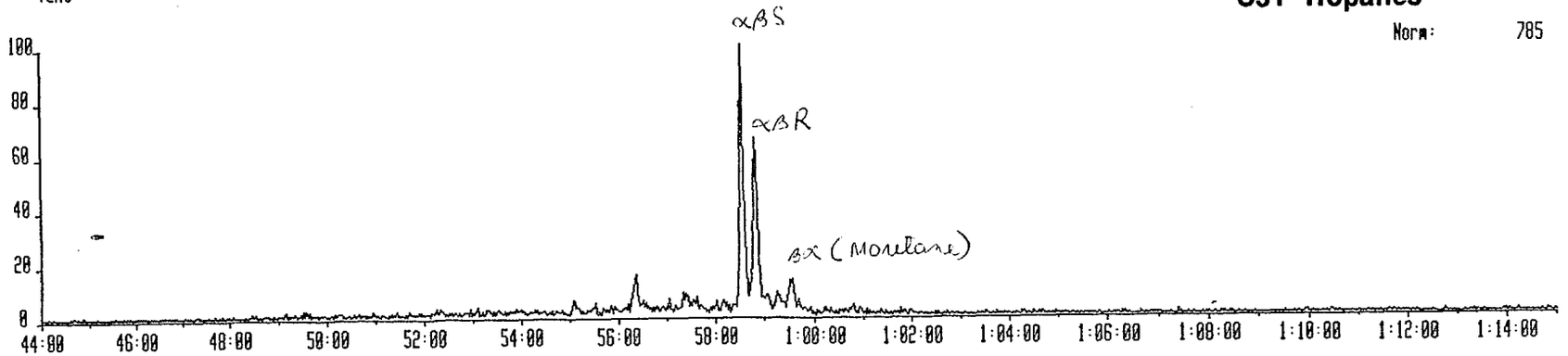

3JU15C 15-JUN-93 Sir:Reaction 70-E Sys: ALLTERPC
Sample 4 Injection 1 Group 2 Mass 416.4420 416.4420->191.1790
Text:

C30 Tricyclics (Cheilanthanes)

Norm: 608

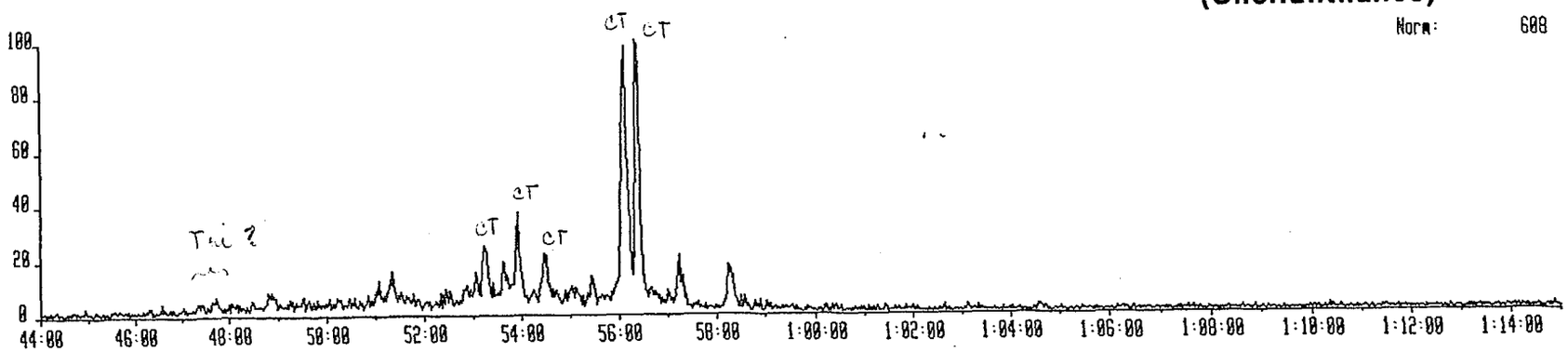

3JU15C 15-JUN-93 Sir:Reaction 70-E Sys: ALLTERPC
Sample 4 Injection 1 Group 2 Mass 412.4060 412.4060->191.1790
Text: #794 MAALAT-CANILBO MUD EXTRACT SATS 0.2/100 = 1 mg + 100 ng STD

C30 Hopanes

Norm: 4604

& other Triterpanes

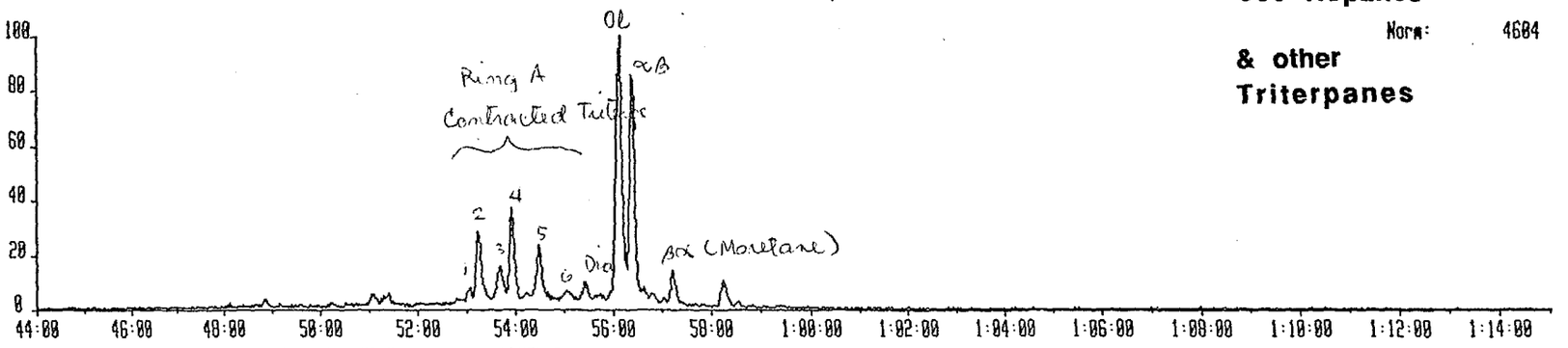

3JU15C 15-JUN-93 Sir:Reaction 70-E Sys: ALLTERPC
Sample 4 Injection 1 Group 2 Mass 398.3900 398.3900->191.1790
Text:

C29 Hopanes

Norm: 2792

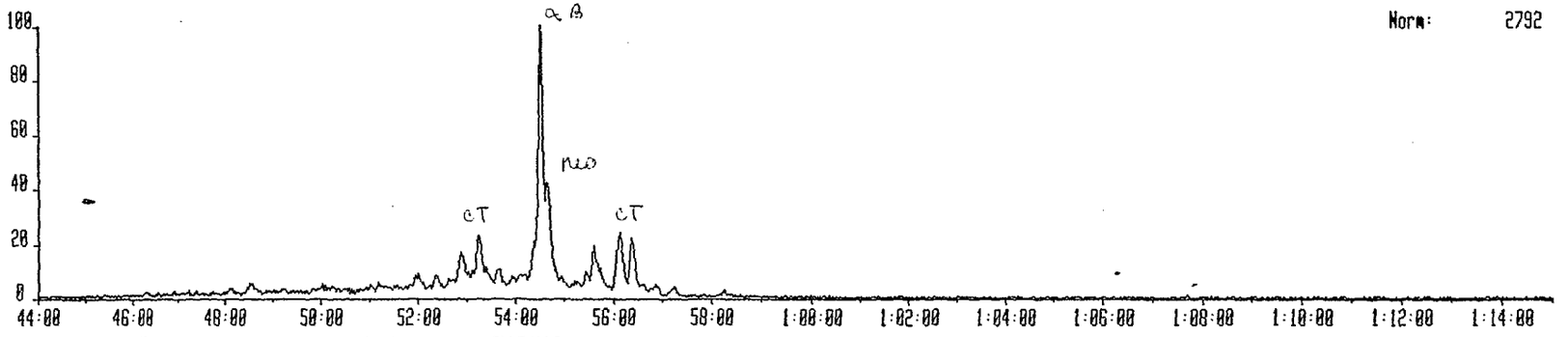

3JU15C 15-JUN-93 Sir:Reaction 70-E Sys: ALLTERPC
Sample 4 Injection 1 Group 2 Mass 384.3740 384.3740->191.1790
Text:

C28 Hopanes

Norm: 266

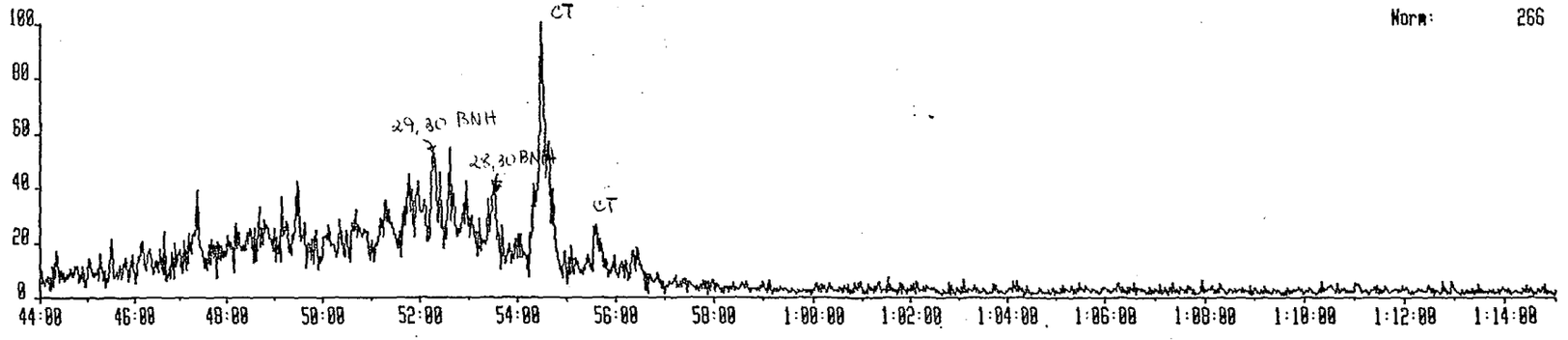

3JU15C 15-JUN-93 Sir:Reaction 70-E Sys: ALLTERPC
Sample 4 Injection 1 Group 2 Mass 370.3590 370.3590->191.1790
Text: #794 MAALAT-CANILBO MUD EXTRACT SATS 0.2/100 = 1 mg + 100 ng STD

C27 Hopanes

Norm: 1487

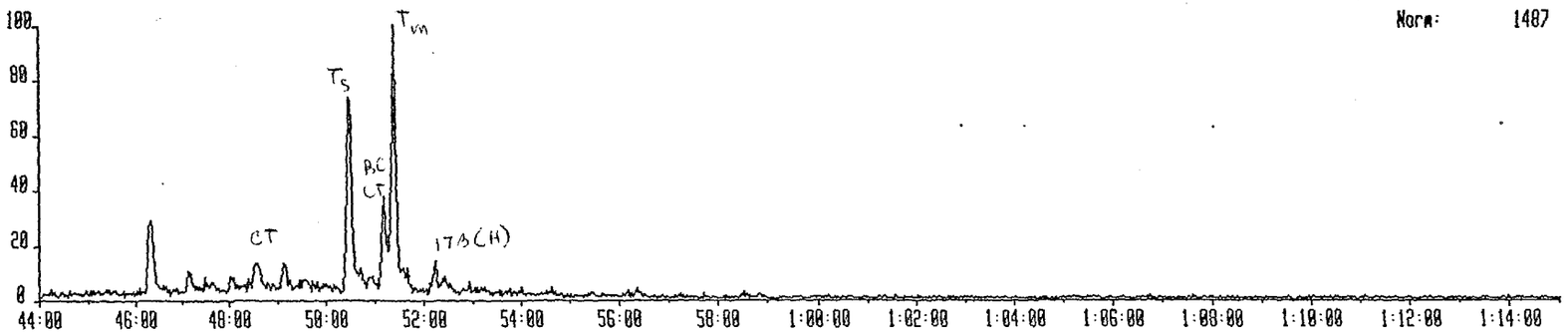

3JU15C 15-JUN-93 Sir:Reaction 70-E Sys: ALLTERPC
Sample 4 Injection 1 Group 2 Mass 426.4210 426.4210->205.1940
Text:

C31 Ring A-Methyl Hopanes

Norm: 432

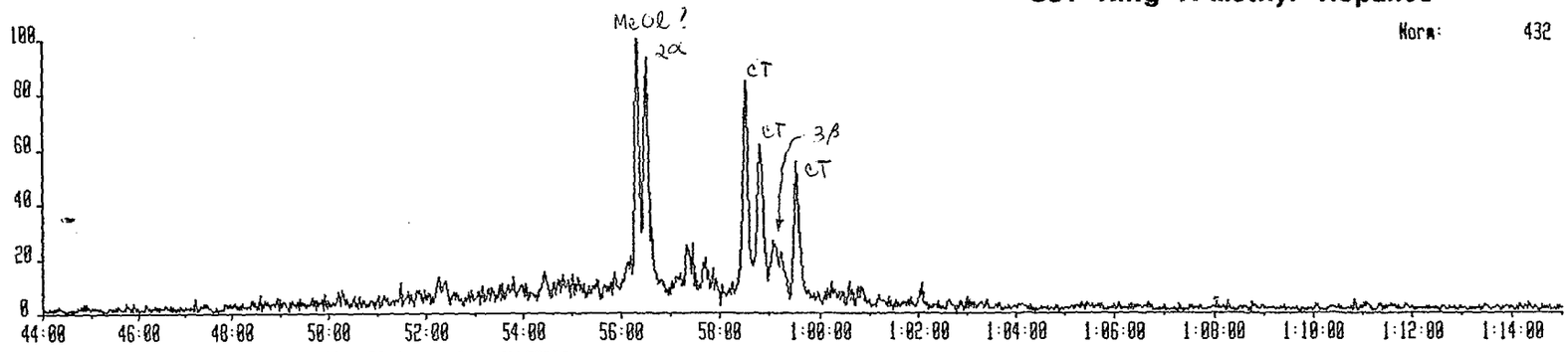

3JU15C 15-JUN-93 Sir:Reaction 70-E Sys: ALLTERPC
Sample 4 Injection 1 Group 2 Mass 414.4230 414.4230->217.1960
Text:

C30 Desmethyl Steranes

Norm: 107

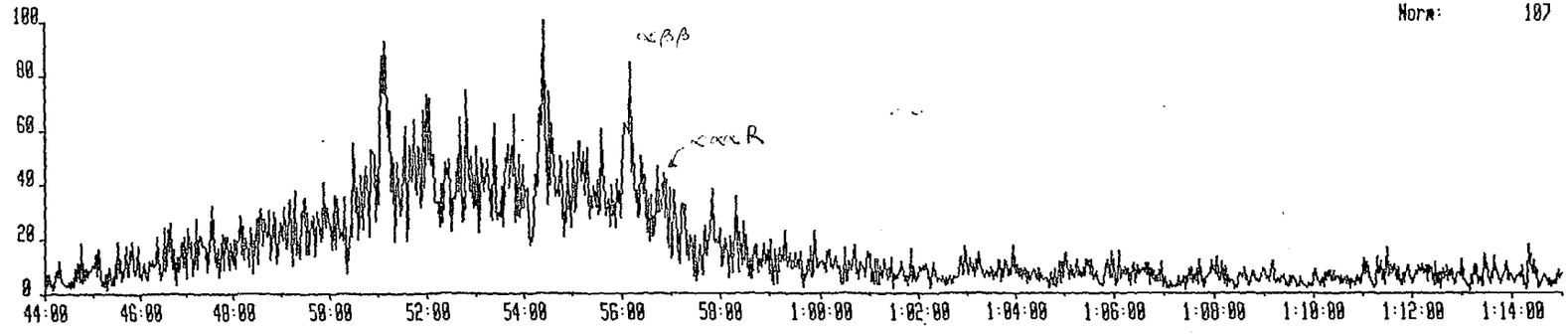

3JU15C 15-JUN-93 Sir:Reaction 70-E Sys: ALLTERPC
Sample 4 Injection 1 Group 2 Mass 400.4070 400.4070->217.1960
Text: #794 MAALAT- CANADO MUD EXTRACT SATS 0.2/100 = 1mg + 100 ng STD

C29 Steranes

Norm: 2475

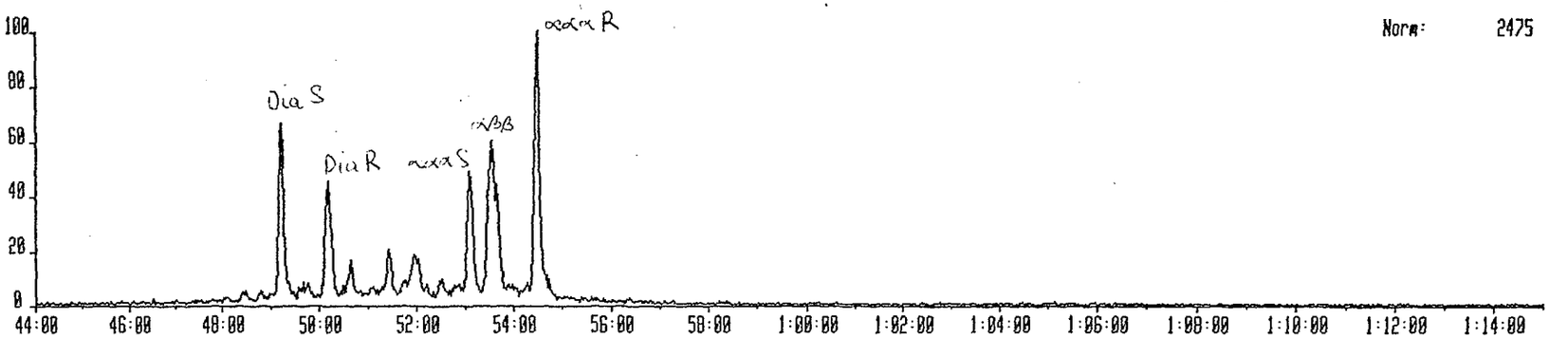

3JU15C 15-JUN-93 Sir:Reaction 70-E Sys: ALLTERPC
Sample 4 Injection 1 Group 2 Mass 386.3910 386.3910->217.1960
Text:

C28 Steranes

Norm: 1285

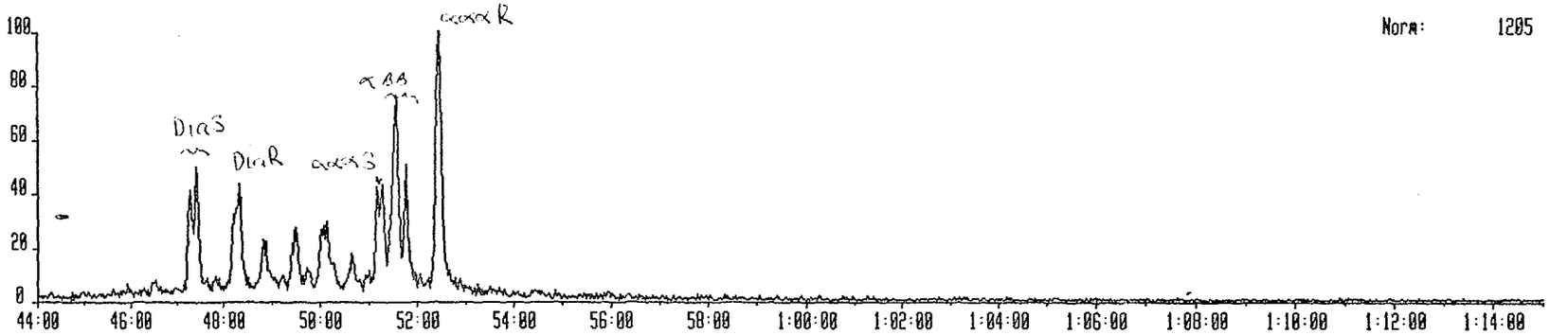

3JU15C 15-JUN-93 Sir:Reaction 70-E Sys: ALLTERPC
Sample 4 Injection 1 Group 2 Mass 372.3760 372.3760->217.1960
Text:

C27 Steranes

Norm: 1010

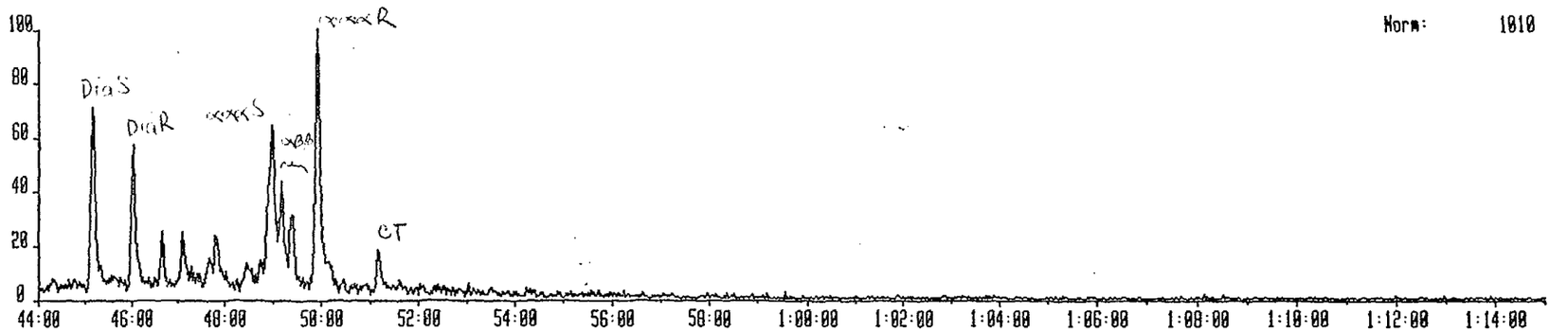

3JU15C 15-JUN-93 Sir:Reaction 70-E Sys: ALLTERPC
Sample 4 Injection 1 Group 2 Mass 414.4230 414.4230->231.2120
Text: #794 MAALAT-CANILBO MUD EXTRACT SATS 0.2/100 = 1 mg + 100 ng STD

C30 Ring A-Methyl Steranes

Norm: 388

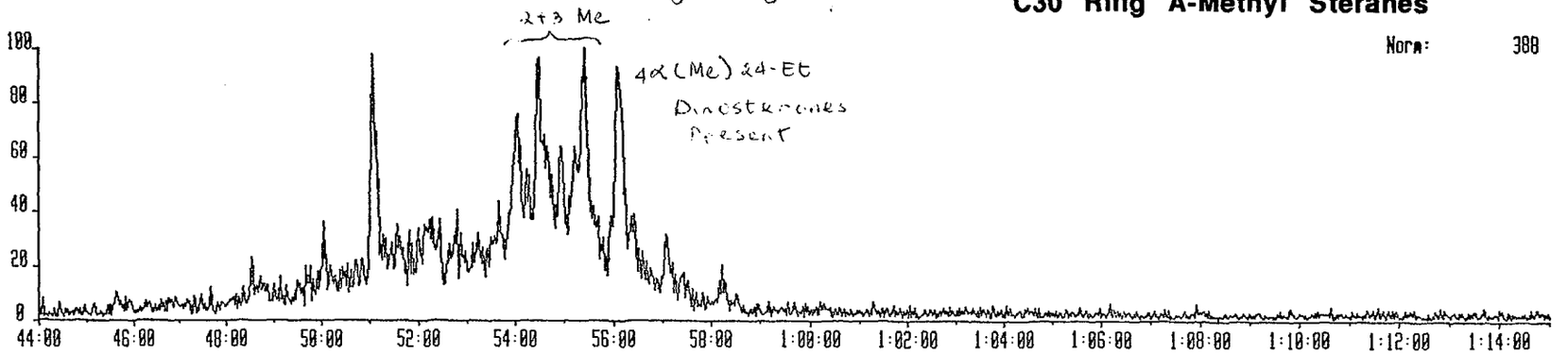

3JU15C 15-JUN-93 Sir:Reaction 70-E Sys: ALLTERPC
Sample 4 Injection 1 Group 2 Mass 389.4185 389.4185->234.2324
Text:

Internal Standard

Norm: 1739

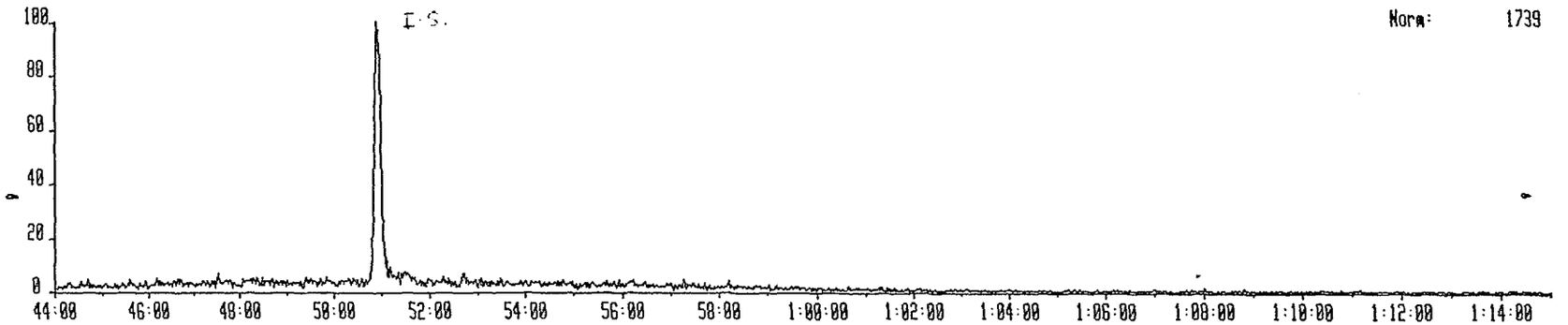

3JU15C 15-JUN-93 Sir:Reaction 70-E Sys: ALLTERPC
Sample 4 Injection 1 Group 2 Mass 412.4060 412.4060->369.3400
Text:

C30 Bicadinanes

Norm: 10530

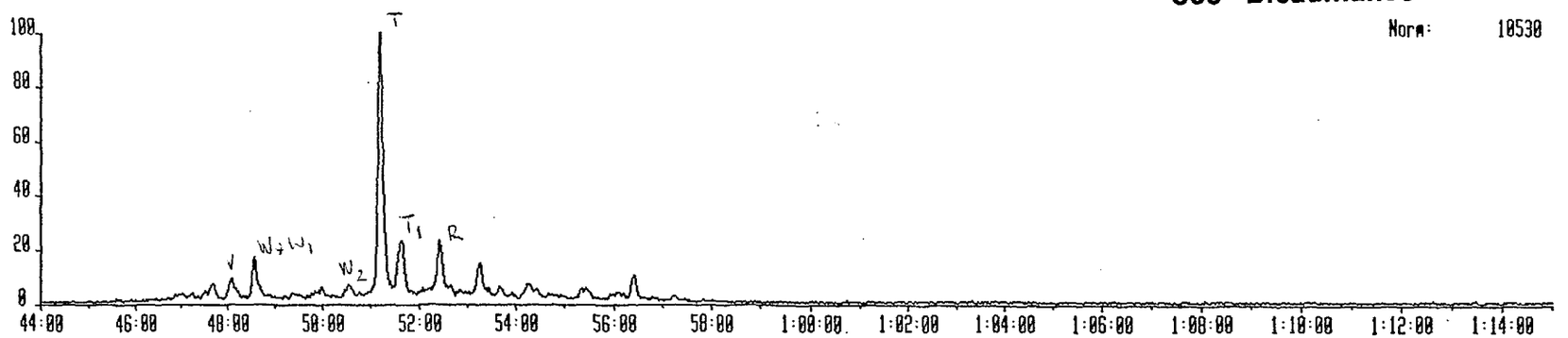

3JU15C 15-JUN-93 Sir:Reaction 70-E Sys: ALLTERPC
Sample 4 Injection 1 Group 2 Mass 426.4230 426.4230->383.3550
Text:#794 SATS MARLAT-CANILBO MUD EXTRACT 0.2/100 = 1 MG + 100 NG STD

C31 Methyl Bicadinanes

Norm: 18657

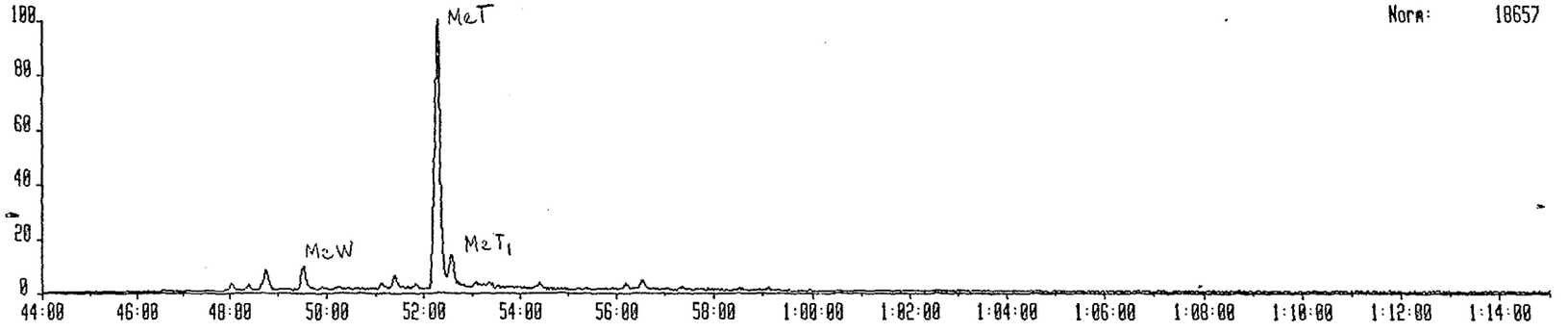

3JU16A 16-JUN-93 Sir:Magnetic 70-E Sys: MPI2
Sample 4 Injection 1 Group 2 Mass 178.0782
Text:#794 AROMS MAALAT-CANILBO MUD EXTRACT 1:200

Phenanthrene

Norm: 1321

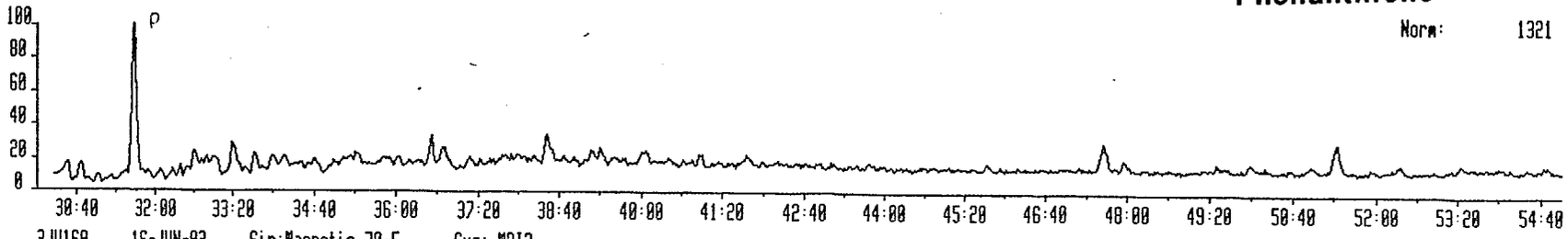

3JU16A 16-JUN-93 Sir:Magnetic 70-E Sys: MPI2
Sample 4 Injection 1 Group 2 Mass 192.0930
Text:#794 AROMS MAALAT-CANILBO MUD EXTRACT 1:200

Methyl Phenanthrene

Norm: 470

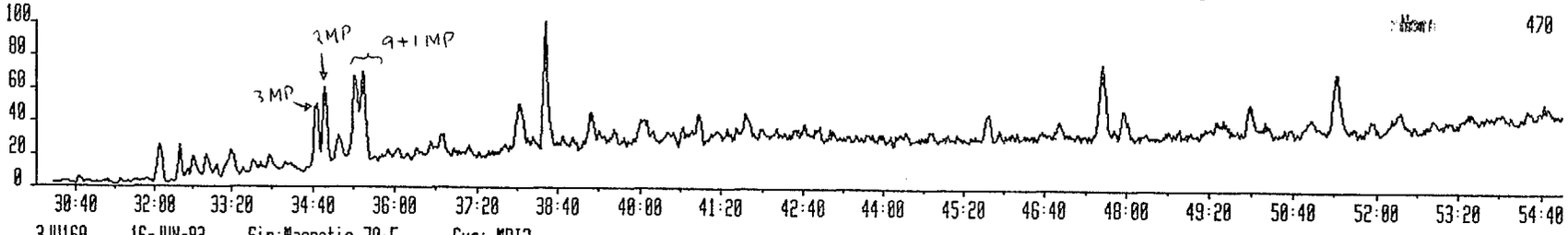

3JU16A 16-JUN-93 Sir:Magnetic 70-E Sys: MPI2
Sample 4 Injection 1 Group 2 Mass 206.1000
Text:#794 AROMS MAALAT-CANILBO MUD EXTRACT 1:200

Dimethyl Phenanthrene

Norm: 1331

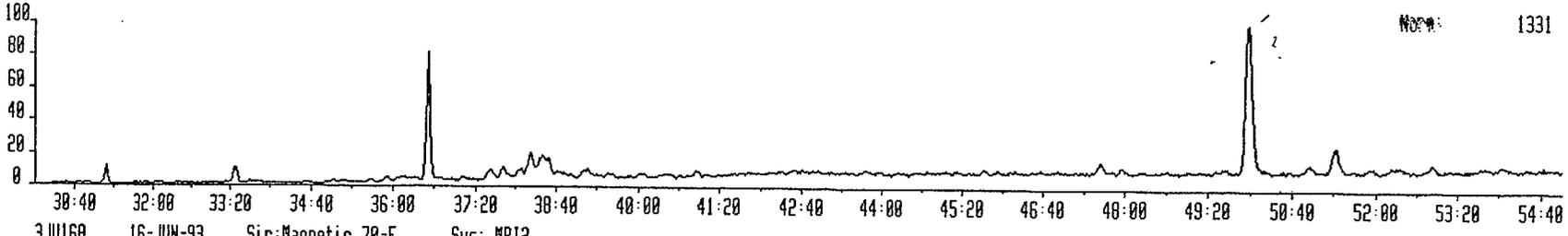

3JU16A 16-JUN-93 Sir:Magnetic 70-E Sys: MPI2
Sample 4 Injection 1 Group 2 Mass 219.1000
Text:#794 AROMS MAALAT-CANILBO MUD EXTRACT 1:200

Retene
(not detected)

Norm: 4557

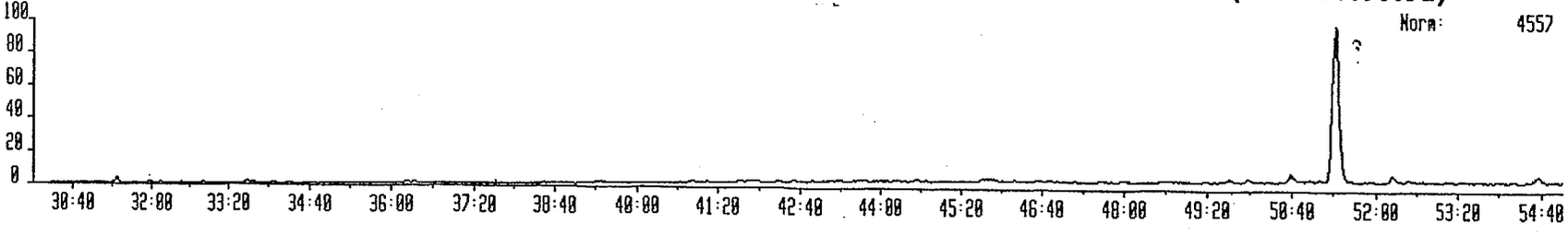

C-17

3JU15C 15-JUN-93 Sir:Reaction 70-E Sys: ALLTERPC
Sample 5 Injection 1 Group 2 Mass 482.4020 482.4020->191.1790
Text: #795 C-17 ROCK EXTRACT SAT. 0.2/100 = 1 mg + 100 ng STD

C35 Hopanes

Norm: 47

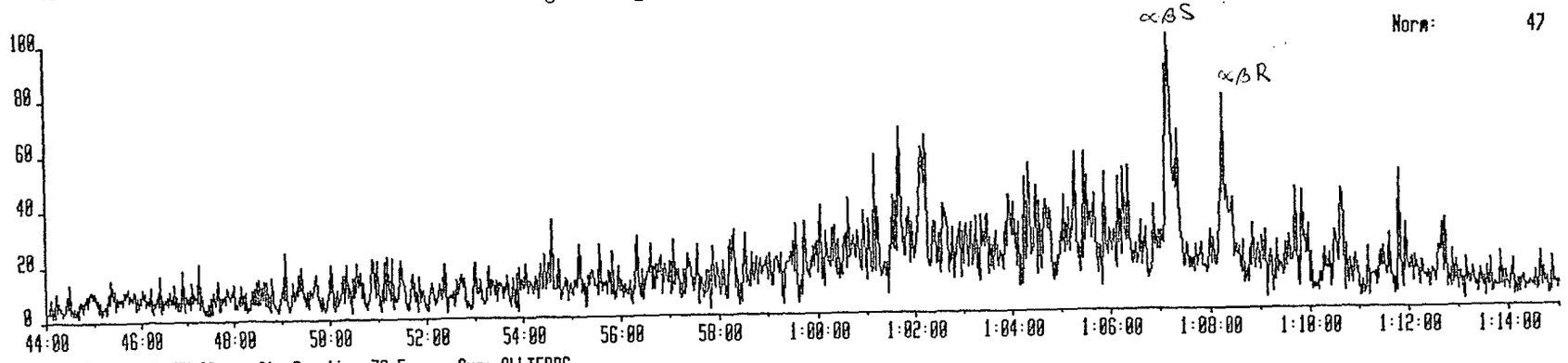

3JU15C 15-JUN-93 Sir:Reaction 70-E Sys: ALLTERPC
Sample 5 Injection 1 Group 2 Mass 468.4670 468.4670->191.1790
Text:

C34 Hopanes

Norm: 301

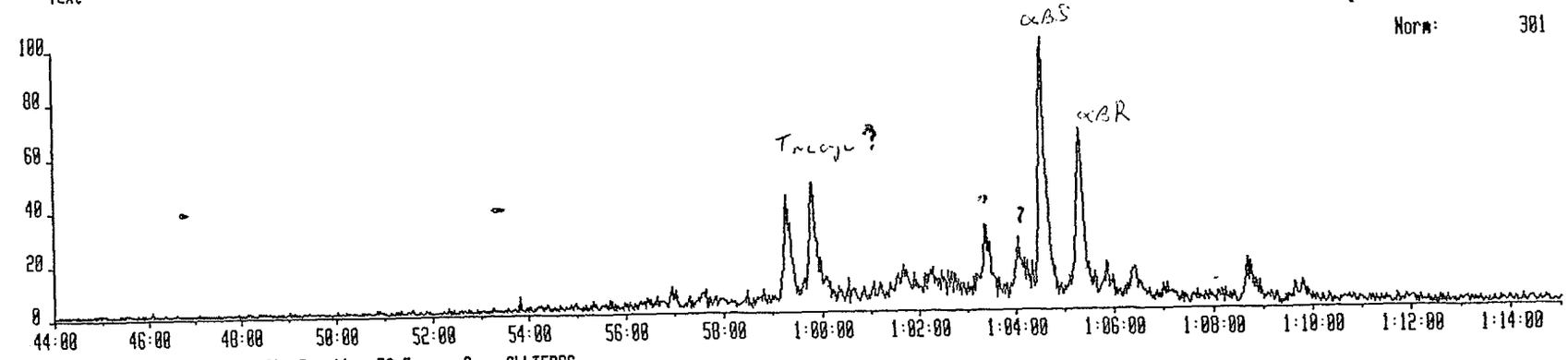

3JU15C 15-JUN-93 Sir:Reaction 70-E Sys: ALLTERPC
Sample 5 Injection 1 Group 2 Mass 454.4520 454.4520->191.1790
Text:

C33 Hopanes

Norm: 743

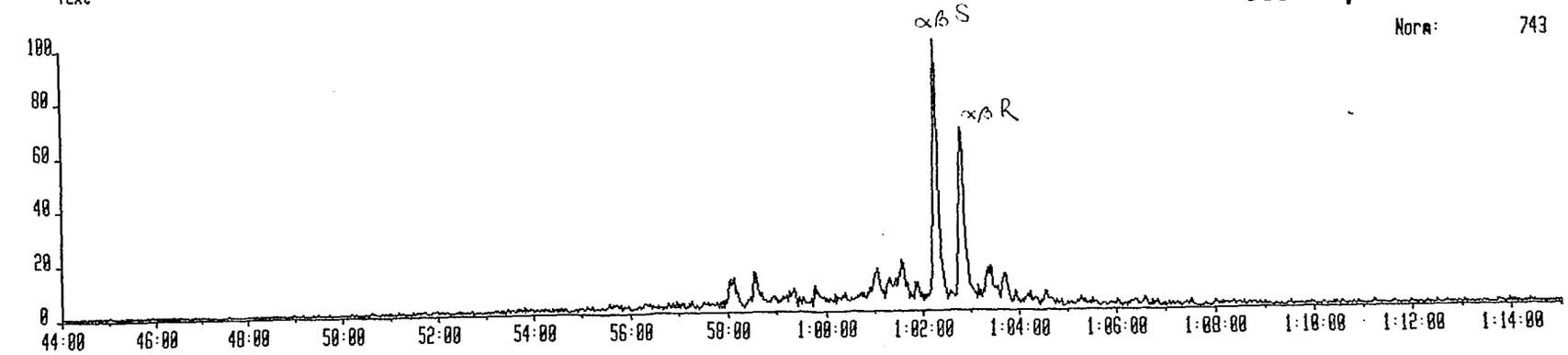

3JU15C 15-JUN-93 Sir:Reaction 70-E Sys: ALLTERPC
Sample 5 Injection 1 Group 2 Mass 448.4370 448.4370->191.1798
Text: #795 C-17 ROCK EXTRACT SATS 0.2/100 = 1 mg + 100 ng STD

C32 Hopanes

Norm: 806

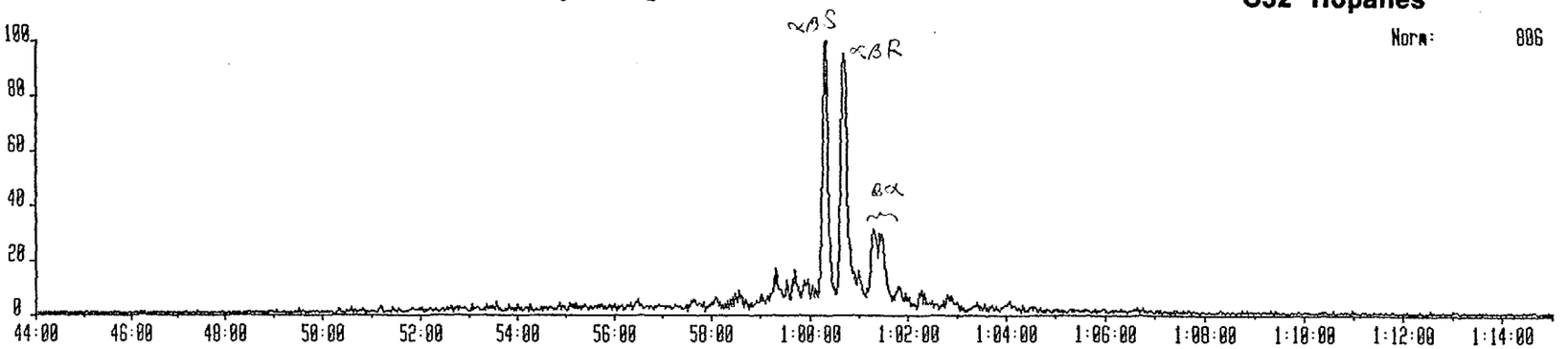

3JU15C 15-JUN-93 Sir:Reaction 70-E Sys: ALLTERPC
Sample 5 Injection 1 Group 2 Mass 426.4210 426.4210->191.1798
Text:

C31 Hopanes

Norm: 744

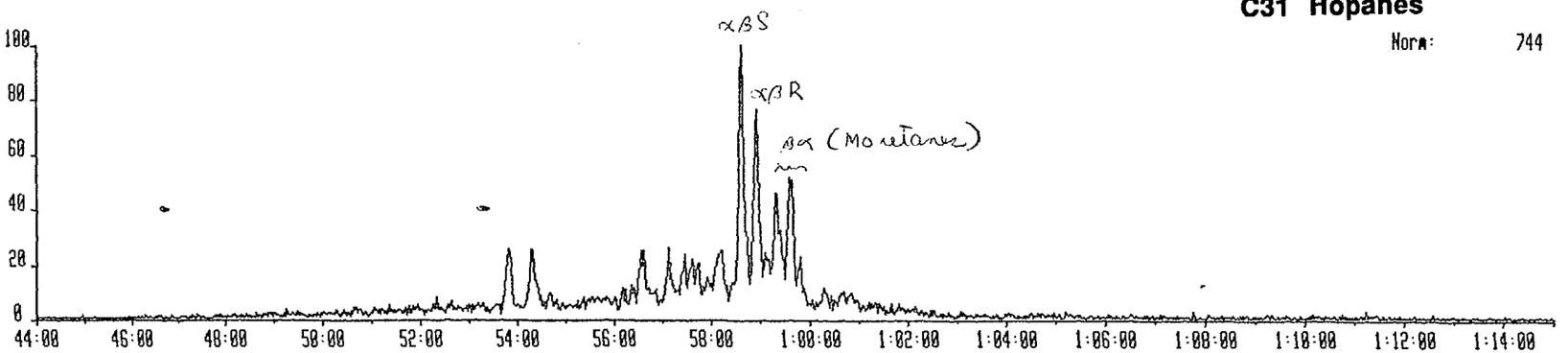

3JU15C 15-JUN-93 Sir:Reaction 70-E Sys: ALLTERPC
Sample 5 Injection 1 Group 2 Mass 416.4420 416.4420->191.1798
Text:

C30 Tricyclics (Cheilanthanes)

Norm: 644

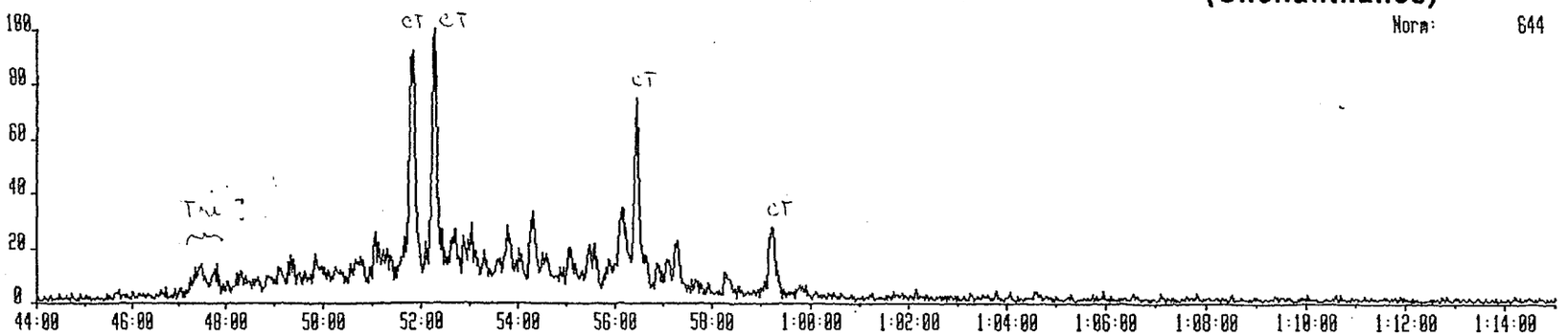

3JU15C 15-JUN-93 Sir:Reaction 70-E Sys: ALLTERPC
Sample 5 Injection 1 Group 2 Mass 412.4060 412.4060->191.1790
Text: #795 C-17 ROCK EXTRACT SATS 0.2/100 = 1 mg + 100 ng STD

C30 Hopanes & other Triterpanes

Norm: 3339

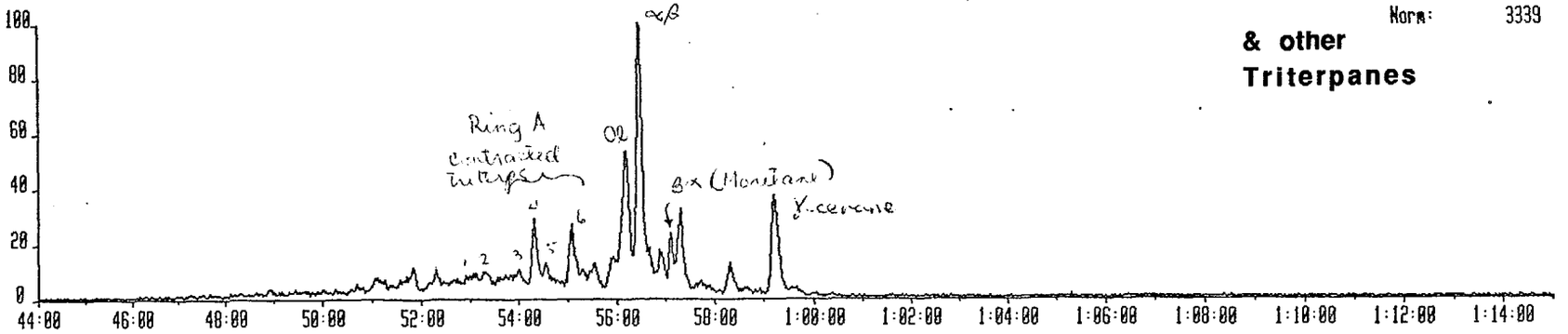

3JU15C 15-JUN-93 Sir:Reaction 70-E Sys: ALLTERPC
Sample 5 Injection 1 Group 2 Mass 398.3980 398.3980->191.1790
Text:

C29 Hopanes

Norm: 5837

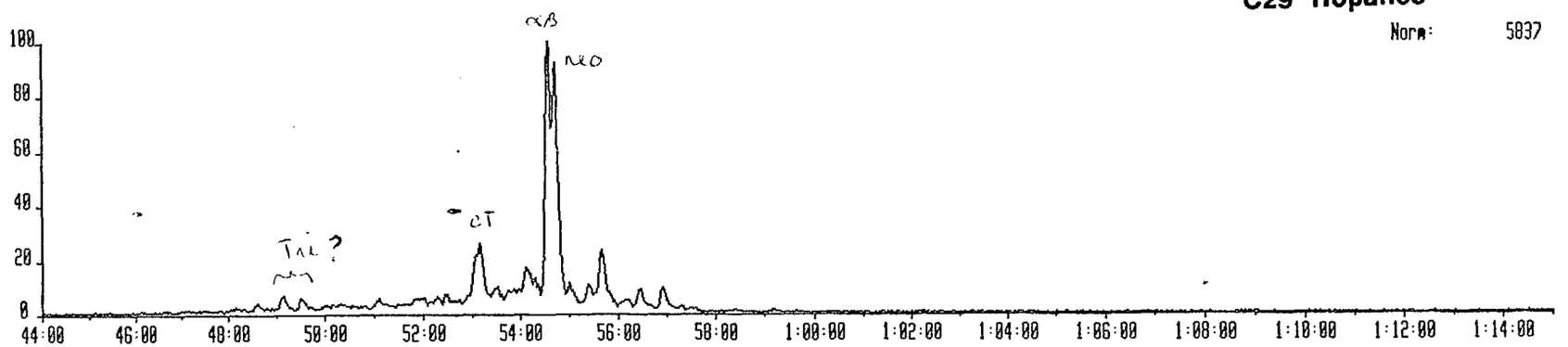

3JU15C 15-JUN-93 Sir:Reaction 70-E Sys: ALLTERPC
Sample 5 Injection 1 Group 2 Mass 384.3740 384.3740->191.1790
Text:

C28 Hopanes

Norm: 638

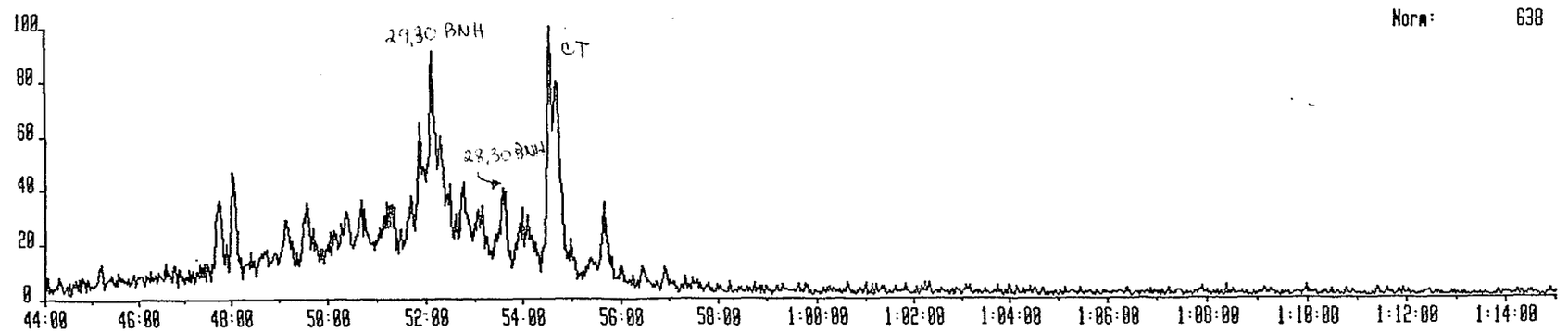

3JU15C 15-JUN-93 Sir:Reaction 70-E Sys: ALLTERPC
Sample 5 Injection 1 Group 2 Mass 370.3598 370.3598->191.1790
Text: #795 C-17 ROCK EXTRACT SATS 0.2/100 = 1 mg + 100 ng STD

C27 Hopanes

Norm: 9831

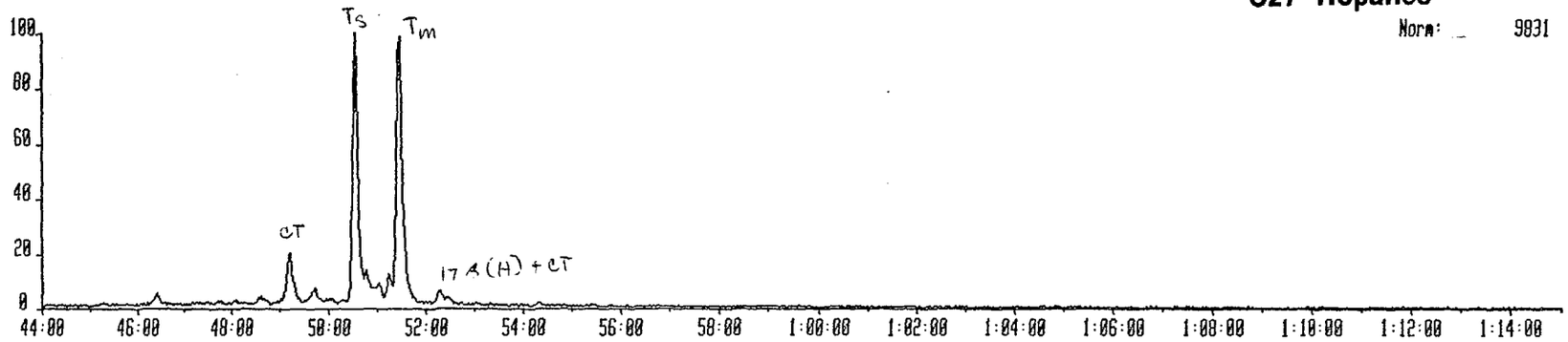

3JU15C 15-JUN-93 Sir:Reaction 70-E Sys: ALLTERPC
Sample 5 Injection 1 Group 2 Mass 426.4210 426.4210->205.1940
Text:

C31 Ring A-Methyl Hopanes

Norm: 1004

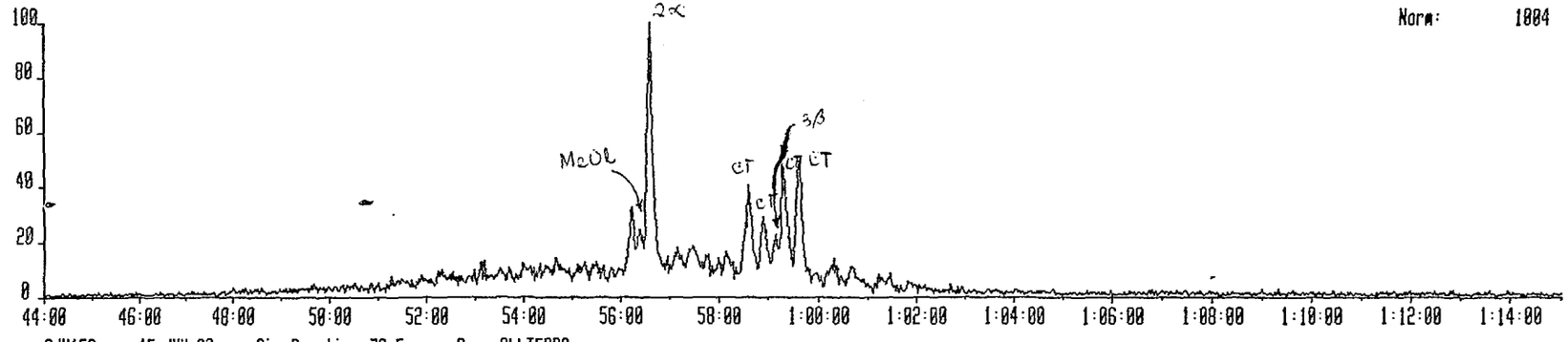

3JU15C 15-JUN-93 Sir:Reaction 70-E Sys: ALLTERPC
Sample 5 Injection 1 Group 2 Mass 414.4230 414.4230->217.1960
Text:

C30 Desmethyl Steranes

Norm: 161

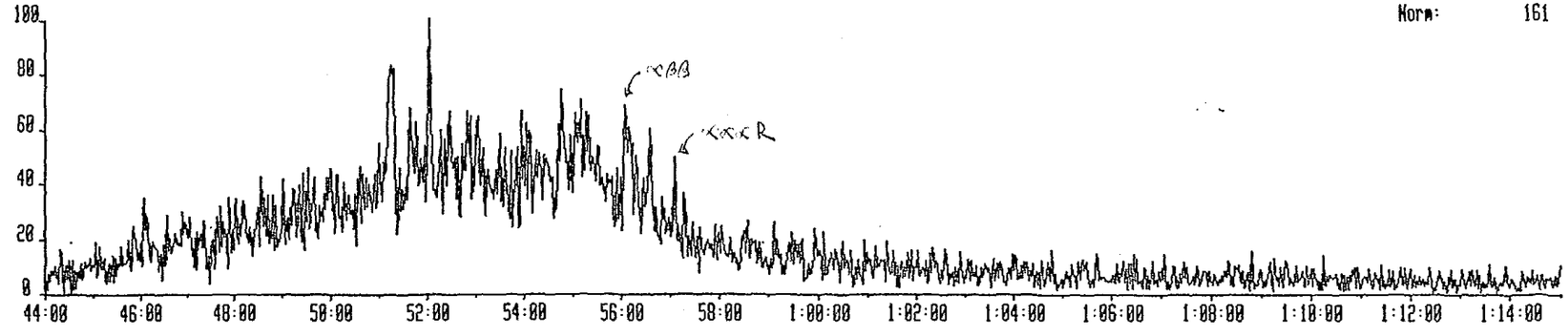

3JU15C 15-JUN-93 Sir:Reaction 70-E Sys: ALLTERPC
Sample 5 Injection 1 Group 2 Mass 400.4070 400.4070->217.1960
Text: #795 C-17 ROCK EXTRACT SATS 0.2/100 = 1 mg + 100 ng STD

C29 Steranes

Norm: 1906

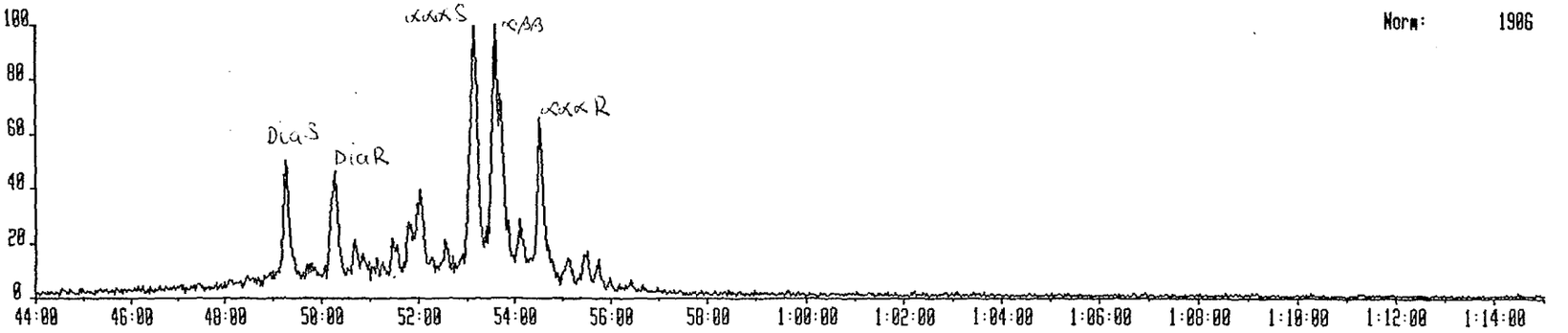

3JU15C 15-JUN-93 Sir:Reaction 70-E Sys: ALLTERPC
Sample 5 Injection 1 Group 2 Mass 386.3910 386.3910->217.1960
Text:

C28 Steranes

Norm: 989

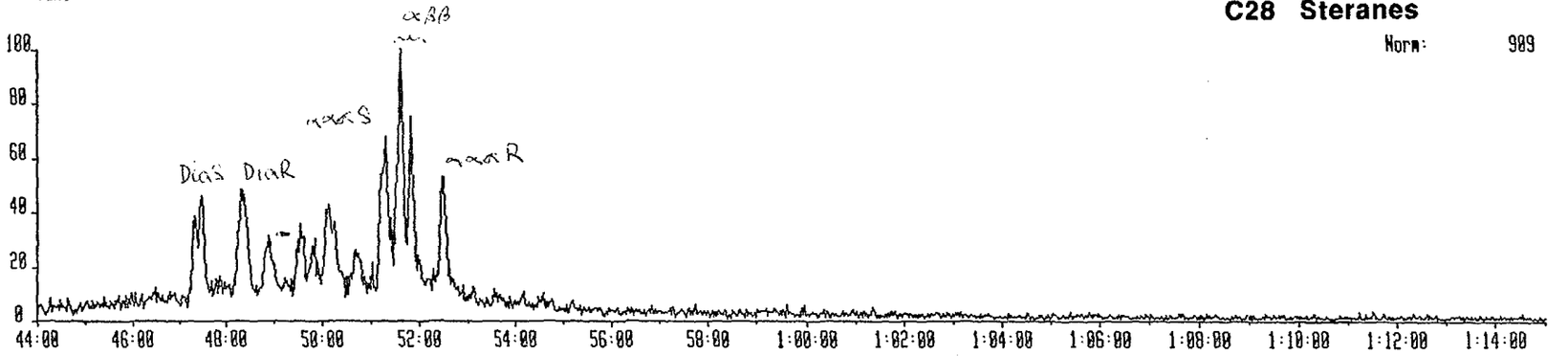

3JU15C 15-JUN-93 Sir:Reaction 70-E Sys: ALLTERPC
Sample 5 Injection 1 Group 2 Mass 372.3760 372.3760->217.1960
Text:

C27 Steranes

Norm: 758

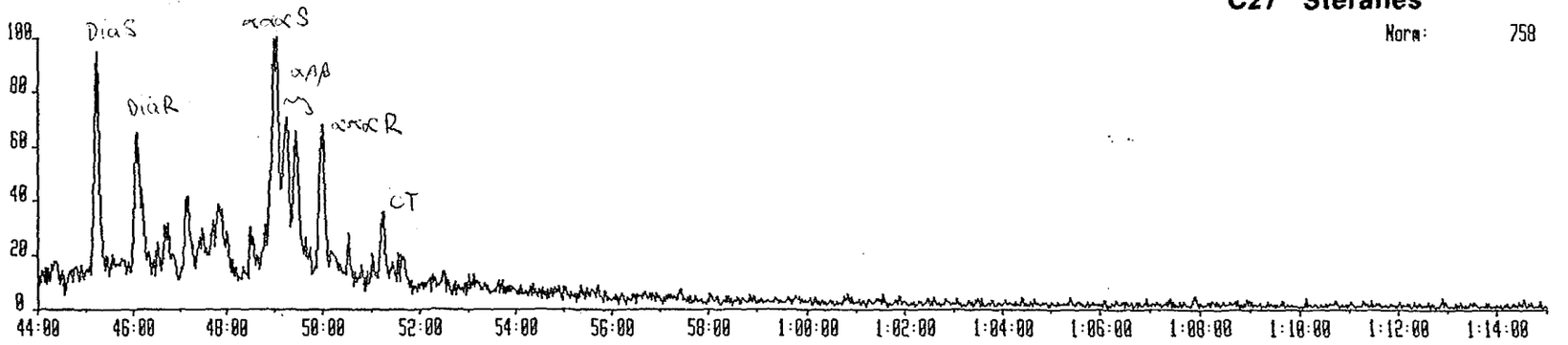

3JU15C 15-JUN-93 Sir:Reaction 78-E Sys: ALLTERPC
Sample 5 Injection 1 Group 2 Mass 414.4230 414.4230->231.2120
Text: #795 C-17 ROCK EXTRACT SATS 0.2/100 = 1 mg + 100 ng STD

C30 Ring A-Methyl Steranes

Norm: 1692

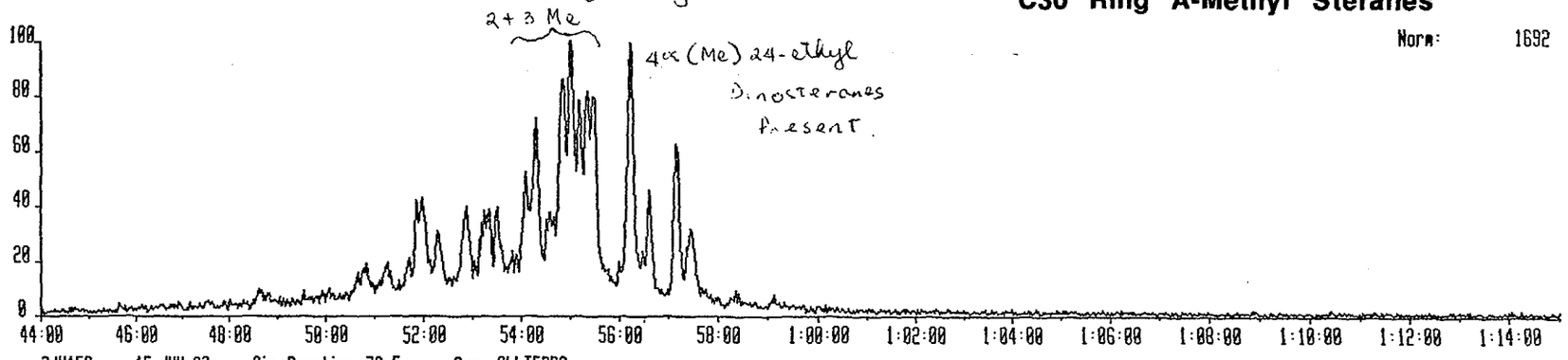

3JU15C 15-JUN-93 Sir:Reaction 78-E Sys: ALLTERPC
Sample 5 Injection 1 Group 2 Mass 389.4105 389.4105->234.2324
Text:

Internal Standard

Norm: 1569

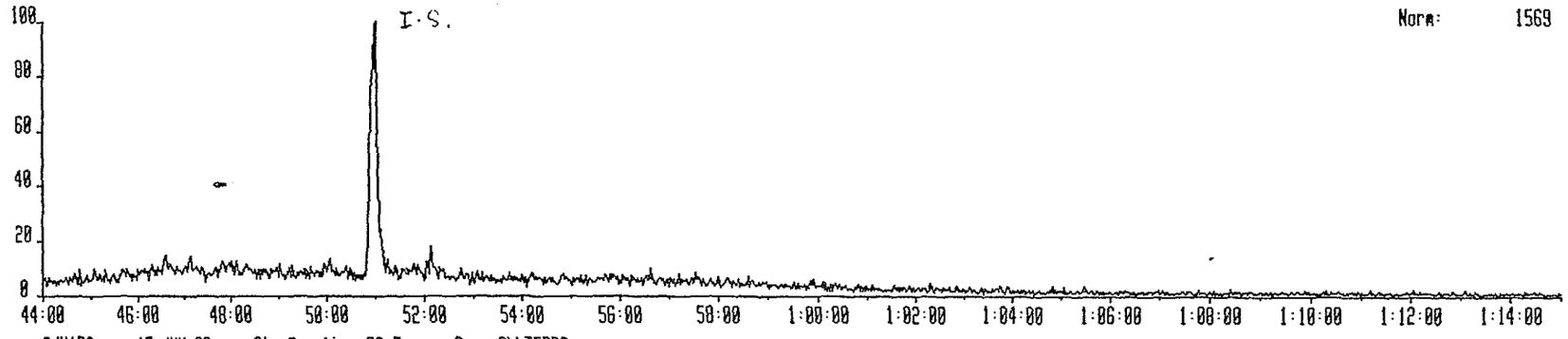

3JU15C 15-JUN-93 Sir:Reaction 78-E Sys: ALLTERPC
Sample 5 Injection 1 Group 2 Mass 412.4060 412.4060->369.3400
Text:

C30 Bicadinanes

Norm: 18929

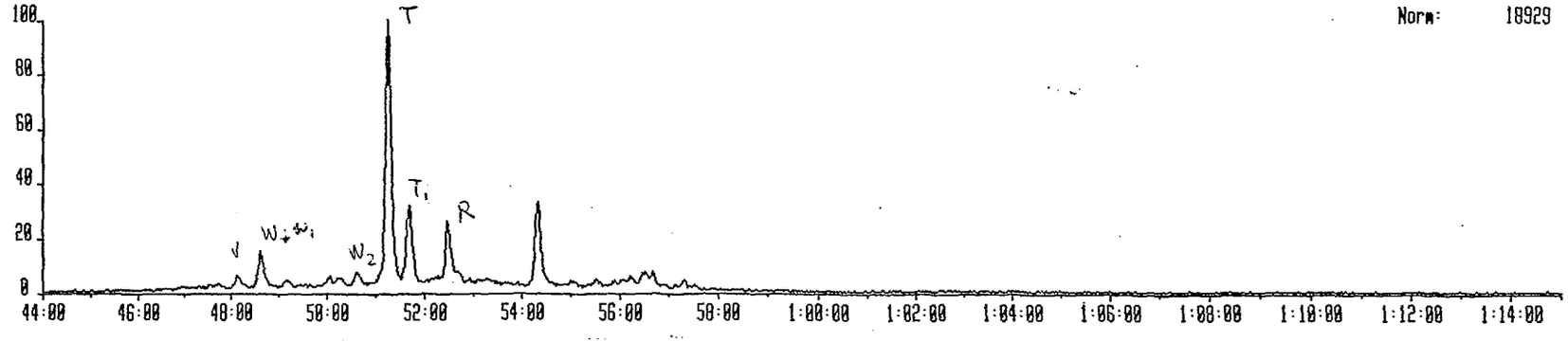

3JU15C 15-JUN-93 Sir:Reaction 70-E Sys: ALLTERPC
Sample 5 Injection 1 Group 2 Mass 426.4230 426.4230->383.3550
Text:#795 SATS C-17 ROCK EXTRACT 0.2/100 = 1 NG + 100 NG STD.

C31 Methyl Bicadinanes

Norm: 28849

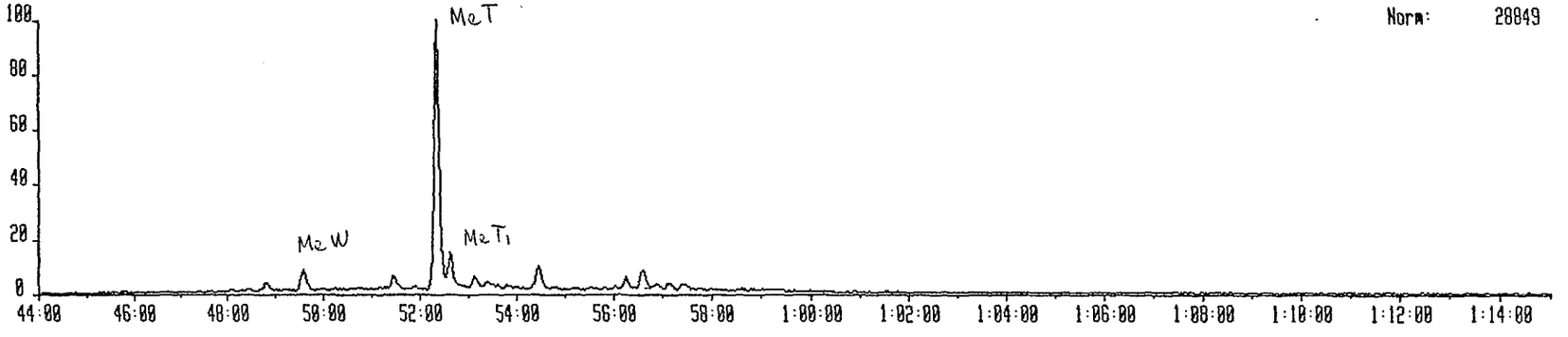

3JU16A 16-JUN-93 Sir:Magnetic 70-E Sys: MPI2
Sample 5 Injection 1 Group 2 Mass 178.0782
Text:#795 AROMS C-17 ROCK EXTRACT 1:200

Phenanthrene

Norm: 363

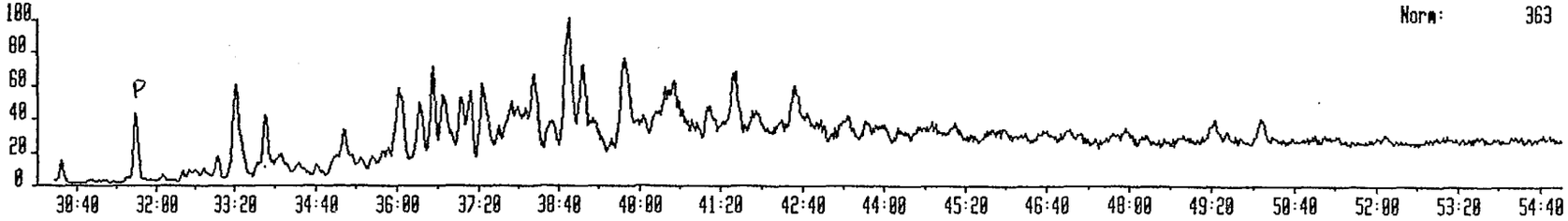

3JU16A 16-JUN-93 Sir:Magnetic 70-E Sys: MPI2
Sample 5 Injection 1 Group 2 Mass 192.0930
Text:#795 AROMS C-17 ROCK EXTRACT 1:200

Methyl Phenanthrene

Norm: 176

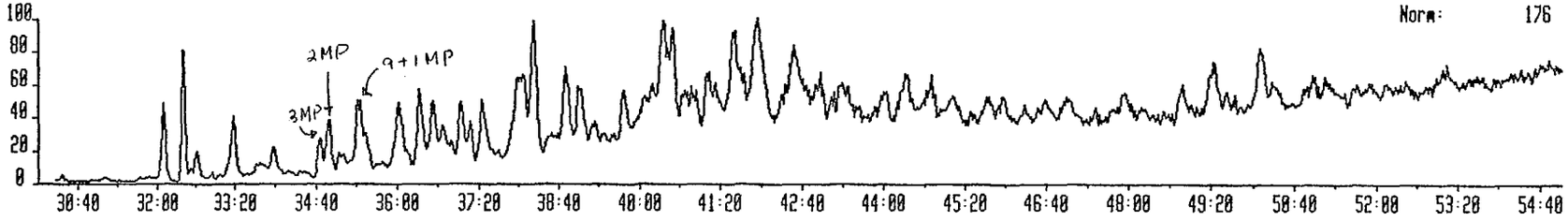

3JU16A 16-JUN-93 Sir:Magnetic 70-E Sys: MPI2
Sample 5 Injection 1 Group 2 Mass 206.1000
Text:#795 AROMS C-17 ROCK EXTRACT 1:200

Dimethyl Phenanthrene

Norm: 1503

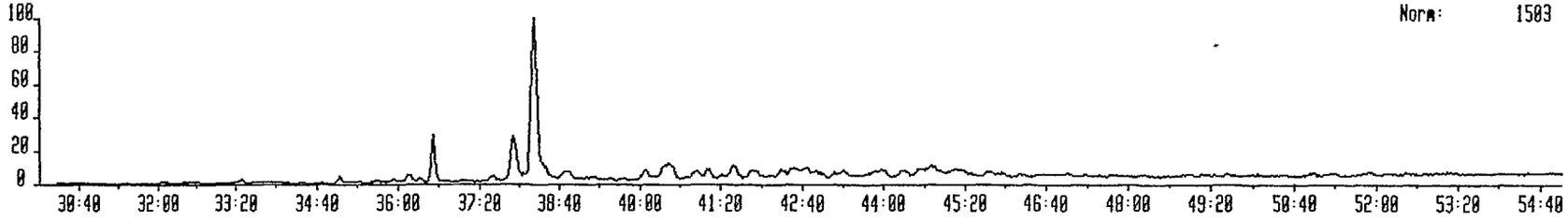

3JU16A 16-JUN-93 Sir:Magnetic 70-E Sys: MPI2
Sample 5 Injection 1 Group 2 Mass 219.1000
Text:#795 AROMS C-17 ROCK EXTRACT 1:200

Retene
(not detected)

Norm: 486

APPENDIX 5

DIRECT HYDROCARBON DETECTION IN BOTTOM WATERS OF THE OFFSHORE PHILIPPINES

by

D. T. Heggie[1], D. Evans[1], E. N. Reyes[2],
C. S. Lee[1], J. H. Bishop[1], J. B. Willcox[1], and D. Lowe[3]

1 Australian Geological Survey Organisation, Canberra, ACT, Australia
2 Department of Energy, Energy Research Laboratory, Manila, Philippines
3 National Inst. of Water & Atmospheric Research, Lower Hutt, New Zealand

ABSTRACT

Approximately 5000 line km of geochemical (direct hydrocarbon detection or DHD), gravity, bathymetric and 2750 line km of seismic data were collected from four offshore areas of the Philippines that are potentially prospective for petroleum. These areas are the Ragay Gulf, Tayabas Bay, North east Palawan Shelf and Cuyo Platform.

Many anomalous bottom-water concentrations of saturated light hydrocarbons (C_1 through C_4) were detected in the Ragay Gulf, which are more than ten-fold typical background concentrations. Bottom-water anomalies are local features detectable over distances of three to twenty kilometres, and were found to exist as 20 to 80 m thick plumes near the base of the local thermocline. The $\delta^{13}C$ signature of the methane in these anomalies varies between -37.8$^{o}/_{oo}$ and -51.3^{o}/oo, and these data when combined with radiocarbon contents of methane, which all showed <20% modern carbon, are indicative of a fossil and thermogenic origin for migrating hydrocarbons.

Many of the strong DHD anomalies identified in the Ragay Sub-basin were found near the flanks of the Alabat-Burias High. These observations, and consideration of the depths of burial of potential source rock horizons suggest that hydrocarbons are being generated in the depocentres of the Bondoc and Ragay Sub-basins and migrating into identified leads on the flanks of the Alabat-Burias High. Consideration of the chemical compositions of DHD anomalies and the depths of burial of potential source rock horizons in the Ragay Gulf suggest that the Ragay Sub-basin is more condensate-to-liquids prone than is the Bondoc Sub-basin.

The location of the bottom-water anomalies appears to be related to sub-surface features identified on seismic sections including half grabens, normal faults, diapirs and possible carbonate platforms. Several of these features are associated with closed structural highs. The results suggest that previously identified prospects known as B1 and B2 in the Bondoc Sub-basin, and R1 and R2 in the Ragay Sub-basin are charged with hydrocarbons. The same applies to new leads identified in other areas of the Bondoc and Ragay Sub-basins and the Alabat-Burias High.

Moderate-to-weak DHD anomalies were detected in Tayabas Bay close to major regional features- the Tayabas Bay Fault and the Bondoc Point Flower Structure.

In the Northeast Palawan Shelf, a weak anomaly was found to coincide with a broad low relief anticline at Middle Miocene unconformity level. There were no distinct anomalies found over the Cuyo Platform although a very weak contoured anomaly was found to be associated with a structural closure southwest of Manamoc Island.

CONTENTS

INTRODUCTION **9**

BOTTOM-WATER GEOCHEMICAL EXPLORATION METHOD **12**
Data collection

SURFACE GEOCHEMICAL RESULTS AND DISTRIBUTION OF BOTTOM-WATER ANOMALIES **14**
Northeast Palawan Shelf and Cuyo Platform
Tayabas Bay and Ragay Gulf

ORIGIN AND SOURCE OF LIGHT HYDROCARBON ANOMALIES **26**
Molecular Composition of Light Hydrocarbon Anomalies: the Cross-Plot Model of Hydrocarbon Origin and Source
Carbon Isotopic Composition of Bottom-Water Methane Anomalies in Ragay Gulf

THE RELATIONSHIP BETWEEN BOTTOM-WATER DHD ANOMALIES AND SUB-SURFACE GEOLOGY WITH IMPLICATIONS FOR HYDROCARBON EXPLORATION **39**
A Reconnaissance-Scale Comparison of Cuyo Platform, Northeast Palawan Shelf, Tayabas Bay and Ragay Gulf
Prospect-Scale Exploration: Northeast Palawan and Cuyo Platform
Prospect-Scale Exploration: Tayabas Bay and Ragay Gulf
Conceptual Model of Hydrocarbon Generation, Migration, and Entrapment in the Ragay Gulf

CONCLUSIONS **56**

REFERENCES **58**

TABLES

Table 1 Direct Hydrocarbon Detection data collected from the offshore Philippines.

Table 2 Summary of bottom-water anomalies discussed in the text from various structural elements identified in the Ragay Gulf.

Table 3 Median methane, ethane and propane concentrations, $\delta^{13}C$ composition of methane, calculated Bernard parameter, structural element and the tow-fish depth (m) of samples collected for isotopic analysis.

Table 4 Radiocarbon compositions of methane, median methane concentrations and mean sample depth for select methane anomalies from different areas of the Ragay Gulf, Philippines

Table 5 Identified hydrocarbon Leads and the predominant chemical composition of DHD anomalies in the Ragay Gulf..

FIGURES

Figure 1a Map of the Tayabas Bay and Ragay Gulf areas showing the density of combined DHD and seismic data coverage. The survey lines discussed here are highlighted. The inset shows the survey areas in the Philippines.

Figure 1b Map of the survey lines on the Northeast Palawan Shelf and the Cuyo Platform.

Figure 2 Schematic of the Direct Hydrocarbon Detection (DHD) equipment installed on the *Rig Seismic* for the survey.

Figure 3 Map of Ragay Gulf, showing (a) the locations of DHD anomalies and associated survey lines, bathymetry, locations of vertical profiles and gas samples for isotopic analyses, (b) the major structural elements of Ragay Gulf with the geochemical /seismic lines discussed in the text, the locations of geochemical anomalies, and closed structures and diapirs identified from seismic data.

Figure. 4 Total hydrocarbons (THC), methane, ethane, ethylene and propane versus DHD shotpoint for survey lines: (a) 109/59 in the Bondoc Sub-basin; (b) 109/34 in the northwestern part of Ragay Sub-basin (c) 109/39P1 which traverses (east-west) the southeastern Ragay Sub-basin and the Alabat-Burias High (d) 109/58 in the southeastern Ragay Sub-basin, crossing (north-south) onto the Alabat-Burias High.

Figure 5 Depth profiles in the water column of (a) temperature (b). total hydrocarbons (THC) and methane (c) ethane, propane and ethylene, for vertical profile vp109/070 from over the Ragay Sub-basin.

Figure 6 Depth profiles in the water column of (a) temperature (b). total hydrocarbons (THC) and methane (c) ethane, propane and ethylene, for vertical profile vp109/076 from over the Bondoc Sub-basin.

Figure 7 Cross-plot model of methane versus hydrocarbon wetness, showing the general decrease in wetness with increasing methane for gas-prone thermogenic or biogenic gas mixtures. Liquids-prone sources are indicated by increasing wetness with increasing methane. Gas-condensate sources fall between the dry gas and liquids-prone trends.

Figure 8 The cross-plot model of percent hydrocarbons wetness and methane content for all survey lines discussed in the text.

Figure 9 Methane versus percent hydrocarbon wetness for survey lines shown in (a) Bondoc Sub-basin (b) Ragay Gulf Sub-basin (northwestern part) (c) the Alabat-Burias High and the Ragay Sub-basin (southeast) (d) the southeast Ragay Sub-basin.

Figure 10 Methane vs ethane; methane vs propane and methane vs butane for those survey lines shown in (a) Bondoc Sub-basin (b) Ragay Gulf Sub-basin (northwestern part).

Figure 11 Methane vs ethane; methane vs propane and methane vs butane for those survey lines shown in (a) the Alabat-Burias High and the Ragay Sub-basin (southeast) (b) the southeast Ragay Sub-basin.

Figure 12 Carbon isotopic composition of methane versus the Bernard parameter (C_1/C_2+C_3) for Ragay Gulf samples (the Bernard Model).

Figure 13 Geochemical contour maps of (a) methane > 10 ppm; (b) propane >0.05 ppm from the Ragay Gulf.

Figure 14 Combined seismic and DHD data from survey line 109/62 in the Bondoc Sub-basin. This line intersects both 109/59 and 109/40 in the northern sector near the strong anomaly.

Figure 15 Combined seismic and DHD data from (a) survey line 109/59 in the Bondoc Sub-basin. This line intersects 109/62 at sp 1229 (shown); (b) survey line 109/40 which intersects 109/62 at sp 1171.

Figure 16 Combined seismic and DHD data from survey line 109/34 in the north-western Ragay Gulf, Ragay Sub-basin. This line intersects 109/35 where this same anomaly was detected (data not shown).

Figure 17 Combined seismic and DHD data from the southeastern Ragay Gulf, Ragay Sub-basin (a) survey line 109/58; (b) survey line 109/42.

Figure 18 Combined seismic and DHD data from the southeastern Ragay Gulf, Ragay Sub-basin (a) survey line 109/39P1; (b) survey line 109/33; (c) survey line 109/41.

Figure 19 Combined DHD/seismic survey line 109/50 from the southern part of Ragay Sub-basin.

Figure 20 A schematised east-west cross-section of the Ragay Gulf (in the vicinty of survey line 109/58) showing the comparative thicknesses and depths of burial of the potential source rock horizons (the Middle Miocene-Vigo Formation and the Late Oligocene-Early Miocene Panaon Limestone). Also shown are the approximate percent hydrocarbon wetness values of the major anomalies found in each of the areas discussed in this text and plotted in their approximate structurally equivalent (not necessarily geographic) positions. Potential hydrocarbon migration pathways are shown with arrows.

INTRODUCTION

The offshore Philippines is a frontier area for petroleum exploration. Four areas of the Philippines - Ragay Gulf, Tayabas Bay, Cuyo Platform and the Northeast Palawan Shelf - which were ranked as having fair to good hydrocarbon potential according to a World Bank Report (1986), were recently surveyed by the Australian Geological Survey Organisation (AGSO) and the Philippines Deptartment of Energy (DOE) under funding from the Australian International Development and Assistance Bureau (AIDAB) (Figs.1a and 1b).

The Ragay Gulf and Tayabas Bay areas (Fig. 1a) are similar geologically, being part of the Southeast Luzon Basin and composed of Oligocene to Holocene clastics and carbonates deposited in shallow to deep marine environments. The deepest grabens contain up to 9 km of Tertiary sediments. The major regional structures and sediment thicknesses have been defined from approximately 4000 line km of seismic data and 11,000 line km of aeromagnetic data (World Bank Report, 1986). In the absence of any offshore exploration wells, the petroleum potential of the Ragay Gulf and Tayabas Bay areas has been assessed on the basis of onshore geology and well information from the Bondoc and Bicol Peninsulas, where several exploration wells have been drilled to depths of about 2100 m. Thermal generation of hydrocarbons onshore is indicated by small oil and gas flows in several of these wells, and numerous oil and gas seeps (World Bank Report, 1986). The Ragay Gulf and Tayabas Bay areas were ranked second after the now-producing Northwest Palawan Shelf, as being frontier areas with fair-to-good potential for oil and minor gas accumulations (World Bank Report, 1986).

The Northeast Palawan Shelf and Cuyo Platform (Fig. 1b) are located on the eastern side of northern Palawan (inset to Fig. 1a)., and developed as part of a continental rift basin formed when the Kalayaan-Calamian Microplate drifted from the South China continental margin during the Late Oligocene through Middle Miocene times (Hamilton, 1979). The Late Mesozoic and Tertiary marine clastic/carbonate section has a thickness of over 10 km, of which the Tertiary fill probably accounts for as much as 4 to 5 km. Limited seismic and some aeromagnetic data (Bosum et al, 1971) have been obtained from both of these areas. No exploration wells have been drilled in the Cuyo Platform, despite the fact that hydrocarbon discoveries were recently made on the nearby Northwest Palawan Shelf. Three exploration wells have been drilled in the Northeast Palawan Shelf. No hydrocarbon shows were recorded in Roxas-1 (1979) or Paly-1 (1981), but Dumaran-1 (1979) encountered gas shows over a 1000 m interval in non-reservoir conglomerates. The World Bank Report (1986) ranked this region fifth, being a frontier area with fair to good potential for gas and minor oil deposits.

While potential source, reservoir and seal rocks are believed to exist in the Ragay Gulf and possibly the Tayabas Bay areas, there had been no direct evidence for the thermal generation of hydrocarbons offshore, prior to the AGSO/DOE survey. Similarly, it has been speculated that Mesozoic source rocks exist in the Cuyo Platform and Northeast Palawan areas (World Bank Report, 1986). Surface geochemical techniques were therefore used to further evaluate these areas, both in a reconnaissance sense by seeking evidence for the thermal generation of hydrocarbons within the deeply buried sediments offshore, and at a local scale, by testing previously identified potential prospects in the Ragay Gulf for hydrocarbon charge.

The technology for measuring dissolved hydrocarbon concentrations in bottom-waters of the continental shelf has been available for more than a decade (Schink et al., 1971;

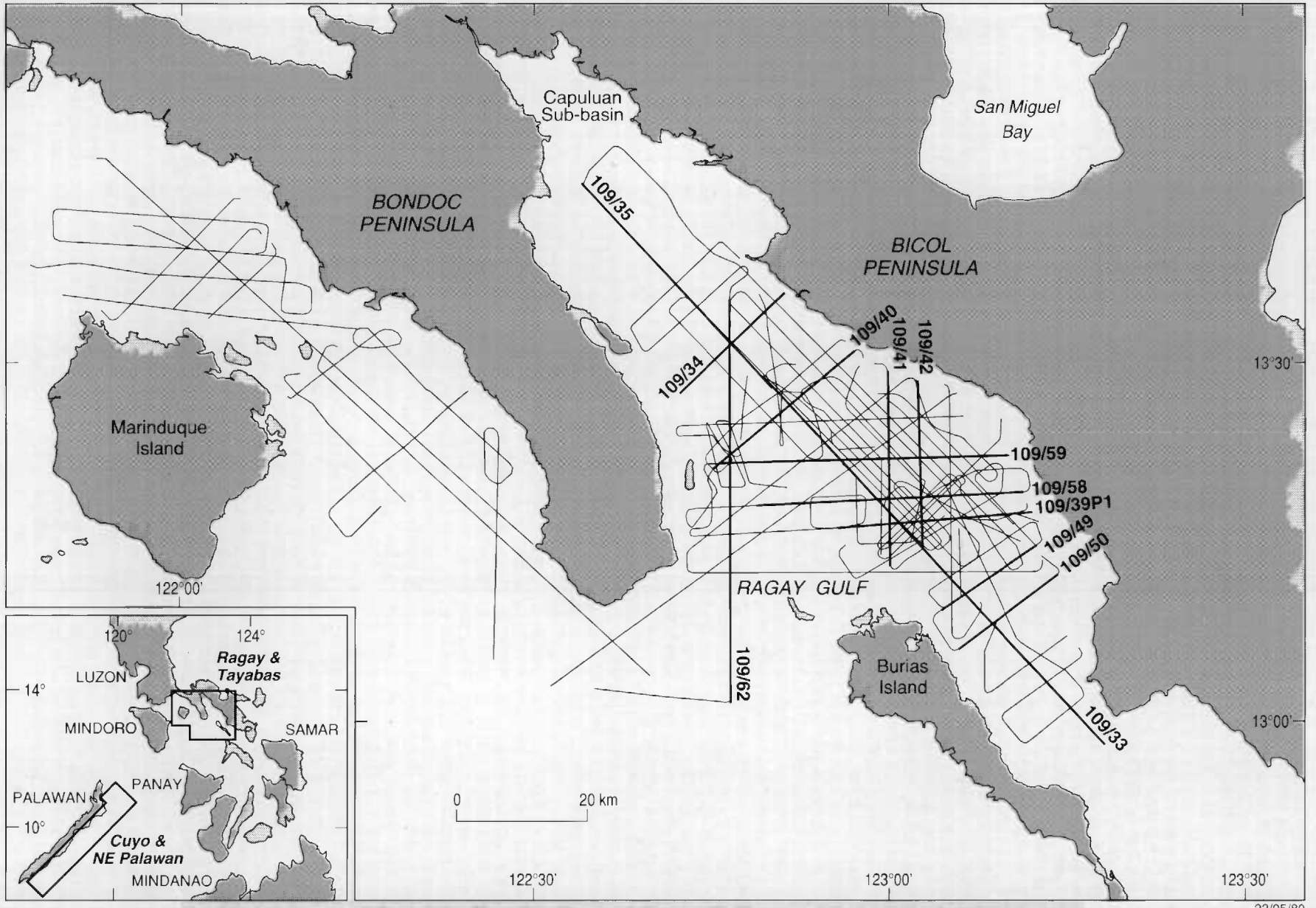

Figure 1a Map of the Tayabas Bay and Ragay Gulf areas showing the density of combined DHD and seismic data coverage. The survey lines discussed here are highlighted. The inset shows the survey areas in the Philippines.

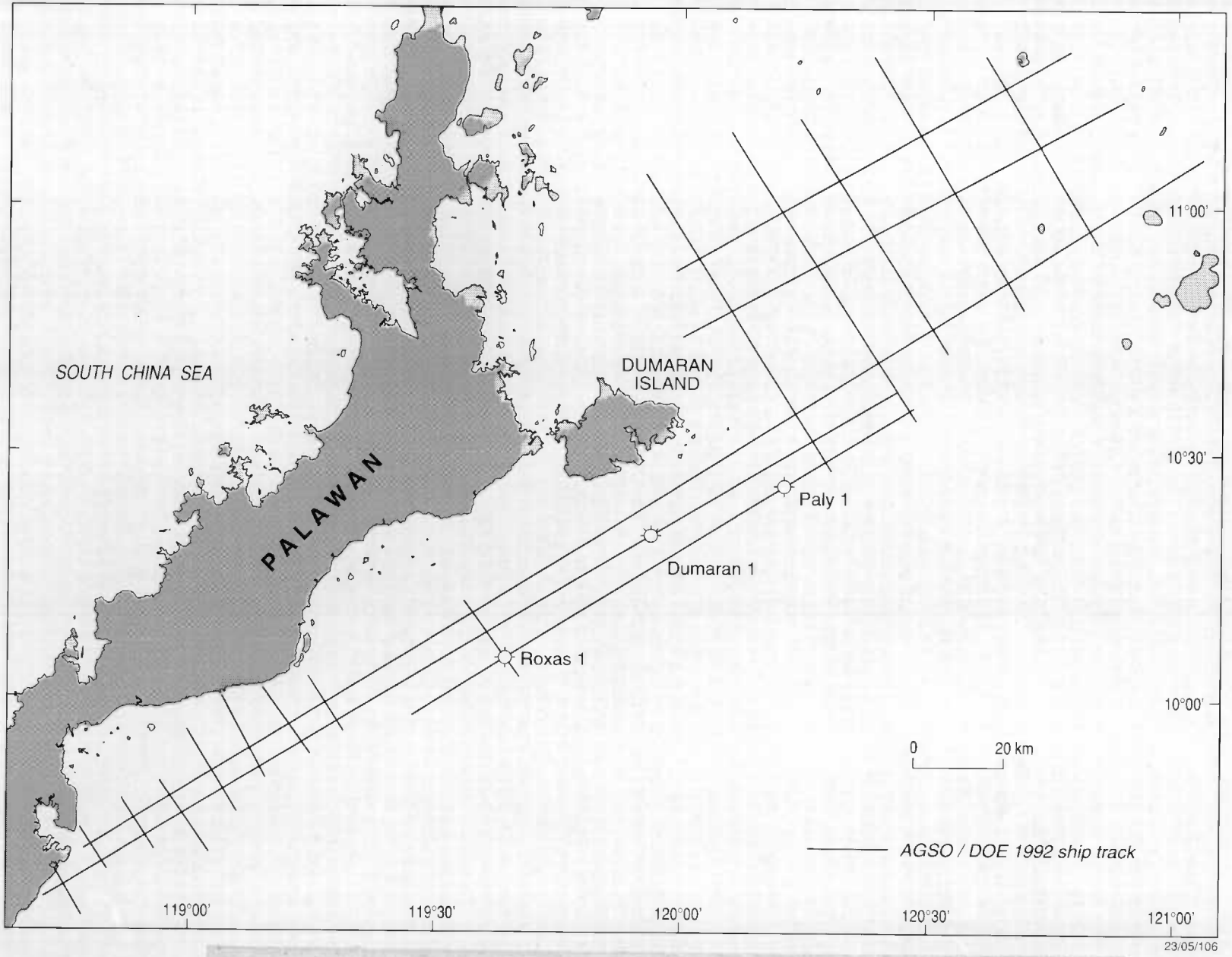

Figure 1b Map of the survey lines on the Northeast Palawan Shelf and the Cuyo Platform.

Sigalove and Pearlman, 1975; Sackett, 1977). However, these surface geochemical techniques, which use a submerged tow-fish to gather samples for continuous light hydrocarbon analyses, have not been widely accepted by the offshore geoscientific community, in part because the results of surveys are not usually widely available for scrutiny and evaluation. Schiener (1985) has commented upon the use of surface geochemical techniques, including 'sniffer' technology in the North Sea, while Sigalove (1985) has discussed bottom-water geochemical data from the Gulf of Mexico, offshore California and elsewhere. An initial assessment of the use of surface geochemical techniques around Australia, based upon 15,000 line km of data collected by the Australian Geological Survey Organisation (AGSO), has been presented by Heggie et al. (1991a) and Heggie et al. (1991b).

The surface geochemical objectives of this survey included the following:

1. To seek evidence of thermogenic hydrocarbon generation in the sediments underlying the Ragay Gulf, Tayabas Bay, Northeast Palawan Shelf and the Cuyo Platform, and hence to encourage further exploration by reducing risks in these areas.

2. To determine the origin (thermogenic or biogenic) of any light hydrocarbon anomalies in bottom-waters.

3. To predict light hydrocarbon sources - either source beds from which hydrocarbons are migrating directly to the surface, or hydrocarbon accumulations (oil, gas or condensate) from which hydrocarbons are escaping to the surface.

4. To test previously identified potential prospects in the Ragay Gulf for evidence of hydrocarbon charge, and to seek new exploration leads and prospects.

5. To examine the relationship(s) between hydrocarbon generation and migration by relating the surface expressions of hydrocarbon seepage (bottom-water anomalies) to geology.

6. To examine oceanographic and other dispersal processes of light hydrocarbon bottom-water anomalies.

To achieve these objectives, bottom-water DHD data were collected simultaneously with seismic reflection, gravity, and magnetic data by the AGSO research vessel *Rig Seismic* in the Ragay Gulf, Tayabas Bay, Northeast Palawan Shelf and Cuyo Platform (Lee and Ramsay, 1992; Galloway et al., 1992). Many bottom-water geochemical anomalies were found in the Ragay Gulf, with fewer and apparently less significant anomalies detected in the other survey areas. The geochemical data are presented in their entirety in Evans et al. (1992), and a preliminary overview of survey results is given in Lee et al. (1992). This manuscript provides a summary of the DHD results from all four survey areas, but the bulk of the discussion concerns the Ragay Gulf where most DHD anomalies were found.

BOTTOM-WATER GEOCHEMICAL EXPLORATION METHOD

The technique used on the *Rig Seismic* involved towing, close to the seafloor, a submerged tow-fish which continuously pumps seawater into a geochemical laboratory. Light C_1 to C_8 hydrocarbons were extracted and measured in the laboratory by gas chromatography, a technique referred to as Direct Hydrocarbon Detection (DHD). The configuration of the equipment is shown schematically in Figure 2. The details of its deployment on the *Rig Seismic* are summarised in Heggie et al. (1991a) and Heggie et al. (1991b). DHD data were acquired concurrently with seismic data, and linked to the

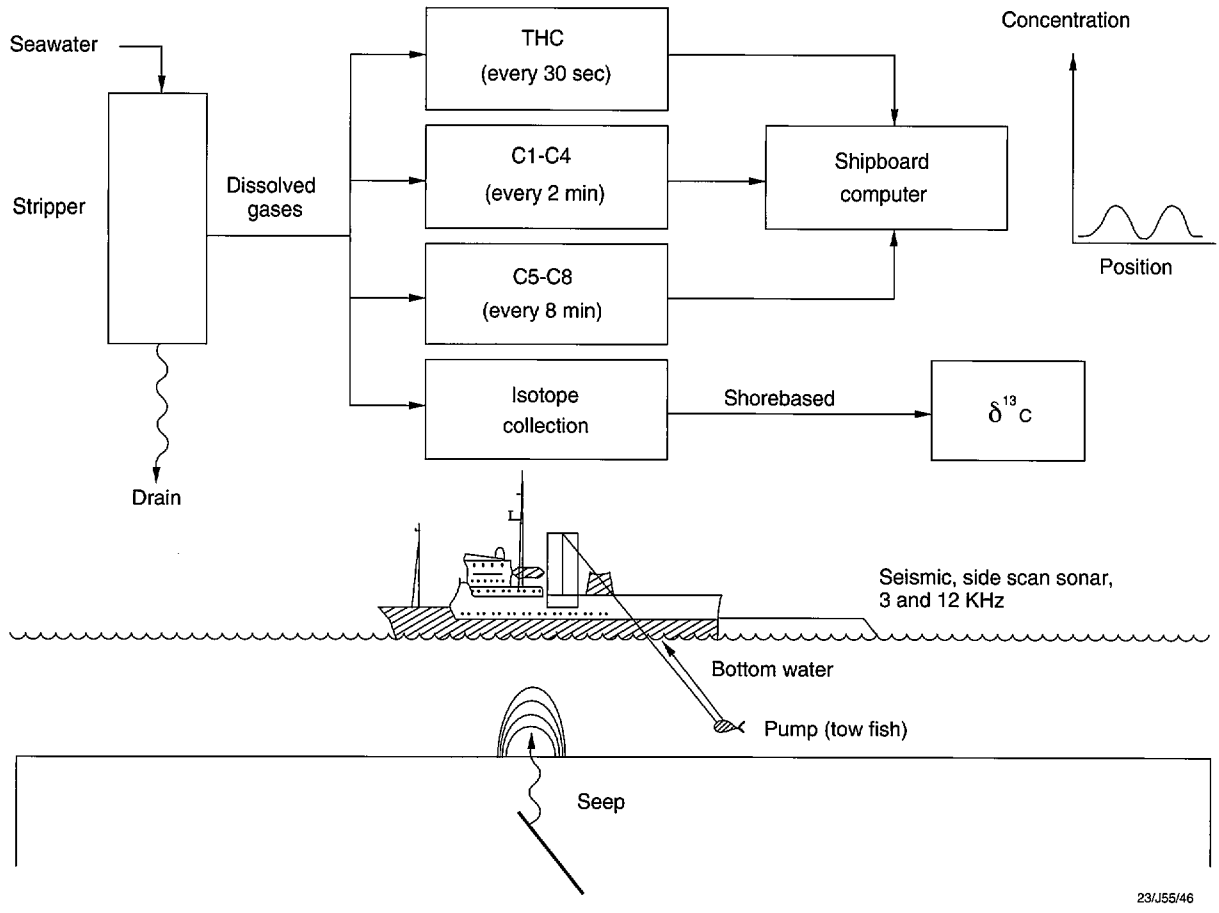

Figure 2 **Schematic of the Direct Hydrocarbon Detection (DHD) equipment installed on the *Rig Seismic* for the survey.**

shipboard navigation system. All DHD data were recorded and displayed continuously so that any hydrocarbon anomalies in the water column could be easily recognised, and gas samples for isotopic analyses could be collected if appropriate. Tow-fish altitude above the seafloor (echo sounder), and differential global positioning system (DGPS) navigation data were also displayed in the laboratory. Detector sensitivity is less than 0.010 parts per million (ppm v/v) in the stripped headspace sample. Gas chromatograph calibrations were conducted on a daily basis and were consistently reproducible within 5 percent for the entire program; system blanks were less than 2 ppm for methane and 0.010 ppm for C_{2+} compounds (ethane, propane and the butanes). The final data were corrected for the travel time of seawater from the tow-fish intake to the laboratory. This correction is essential if DHD are to be compared directly with seismic data. Because of variations in the flow-rate of seawater through the hollow umbilical connector, corrections in the travel time led to uncertainties of less than 0.5 km when aligning DHD and seismic data.

Data Collection

Approximately 5000 line-km of DHD data were acquired during the survey. This included 2750 line km of DHD data acquired simultaneously with seismic data from all survey areas. In the Ragay Gulf, 950 line km were collected with seismic during daylight hours, while another 2410 line km of DHD data only were collected at night when seismic operations could not be conducted (Table 1). The density of DHD coverage for Ragay Gulf and Tayabas Bay is shown in Figure 1a. Nine vertical profiles of hydrocarbon concentration in the water column were measured in the Ragay Gulf. The density of combined DHD and seismic coverage in the Northeast Palawan Shelf and Cuyo Platform is shown in Figure 1b. All geochemical data from Tayabas Bay (490 line km), Northeast Palawan Shelf (580 line km), and Cuyo Platform (730 line km) were acquired simultaneously with seismic data (Table 1).

When significant bottom-water anomalies were detected, some flowing gas stream from the gas extractor was diverted from the gas chromatographs to be collected and stored over water in amber glass bottles. These samples were subsequently analysed for carbon isotopic composition of the methane component at the New Zealand National Institute of Water and Atmospheric Research. Methane was separated from extracted seawater gases (nitrogen, oxygen and carbon dioxide), and converted to carbon dioxide. Isotopic abundances were then measured by mass spectrometry (Lowe et al. 1991). The carbon isotopic composition of methane was calculated from: $\delta^{13}C_1$ sample($^o/_{oo}$) = $[(R_{sample}/R_{standard}) - 1] \times 1000$, where $R = {}^{13}C/{}^{12}C$, using the Pee Dee Belemnite, PDB standard. Selected samples were converted to graphite and analysed for their radiocarbon content using techniques described in Lowe et al. (1987)

SURFACE GEOCHEMICAL RESULTS AND DISTRIBUTIONS OF BOTTOM-WATER ANOMALIES

Many bottom-water anomalies were found during this survey and were classified according to a simple scheme. Strong anomalies were defined as those with hydrocarbon concentrations more than ten-fold higher than typical background concentrations, moderate anomalies as those with hydrocarbon concentrations that are five-to-tenfold above typical background concentrations, and weak anomalies as those with hydrocarbon concentrations two-to-fivefold above background. Typical background levels of hydrocarbons were found to be: total hydrocarbons (THC) 8-10 ppm; methane (C_1) 3-5 ppm; ethane (C_2), and propane (C_3) less than 0.05 ppm; and butanes below the detection limit of less than 0.01 ppm.

Table 1. Direct Hydrocarbon Detection data collected from the offshore Philippines

Survey Area	Number of survey lines	Line-km of data
Ragay Gulf	47 (plus 9 vertical profiles)	3360 DHD total (950 line-km DHD and seismic 2410 line-km DHD only)
Tayabas Bay	9	490 line-km DHD and seismic
NE Palawan Shelf	12	580 line km DHD and seismic
Cuyo Platform	8	730 line km DHD and seismic

Northeast Palawan Shelf and Cuyo Platform

The North east Palawan Shelf comprised three areas - Honda Bay, an area of rugged sea floor topography with water depths mostly between 100m and 2000m, the Roxas area with water depths generally less than 500m and the Paly/Dumaran area which was surveyed in water depths between about 100 m and 2000 m. Some weak, local, DHD anomalies were found. Anomalous total hydrocarbon concentrations were generally less than 25 ppm, compared to typical local background concentrations of 10-12 ppm. Similarly, anomalous methane levels were up to 15 ppm, compared to background levels of 3 to 5 ppm typical of open marine environments. A local THC anomaly associated with the Dumaran-1 location is probably the result of gas leakage from the abandoned exploration well. Elsewhere, broad, weak to moderate variations in methane and ethane concentration appear to be unrelated to variations in biogenic ethylene, suggesting that a seafloor source exists for the hydrocarbons (Evans et al., 1992).

The Cuyo Platform is an area of relatively shallow water (40 to 120 m) with only minor topographic relief. No distinct DHD anomalies were detected, although background levels of methane were generally elevated over much of the survey area (4 to 8 ppm compared to typical open marine background levels of 3 to 5 ppm).

Tayabas Bay and Ragay Gulf

Several weak to moderate anomalies in THC, methane, ethane and propane were detected in Tayabas Bay (Evans et al., 1992). Total hydrocarbon concentrations were measured up to 80 ppm, or about five-fold typical local background concentrations (15-20 ppm), and methane concentrations were measured up to 23 ppm, or about four-fold typical background levels. Local background concentrations of light hydrocarbons were somewhat elevated over typical open marine background levels. Water depths in the survey area vary from 100 to 2000 m, and many anomalies appear to be related to the depth of the DHD tow-fish. No vertical profiles of hydrocarbon concentration were measured in Tayabas Bay, but the distinctive vertical distributions of hydrocarbons noted in Ragay Gulf suggest that DHD anomalies related to variations in the depth of the DHD tow-fish, could be explained by the fact that hydrocarbon anomalies are trapped as plumes near the base of a stratified layer of the water column.

The Ragay Gulf survey was conducted in water depths of 20 and 600 m. More than 130 anomalies were detected, and many of these were in the 'strong'category, with hydrocarbon concentrations exceeding typical background concentrations by more than an order of magnitude. Several survey lines from Ragay Gulf have been selected to illustrate the nature and extent of various light hydrocarbon anomalies.

The combined DHD/seismic data lines discussed below are highlighted on Figures 1a and 3. All lines chosen have significant anomalies near the intersection with other seismic/DHD lines, and because these data were collected often several days apart, they demonstrate the persistence and general reproducibility of strong or moderate bottom-water anomalies. Figure 3a is a map of Ragay Gulf showing generalised bathymetry and locations of seismic/DHD lines, vertical DHD profiles, and gas sampling sites, together with the approximate extent of geochemical anomalies. Structural elements of Ragay Gulf and locations of DHD anomalies, diapirs, and structures with closure identified from seismic data, are shown in Figure 3b. The key structural elements pertinent to the discussion below include the Bondoc Sub-basin in the western part of Ragay Gulf, the Ragay Sub-basin to the east, and the Alabat-Burias High which separates them.

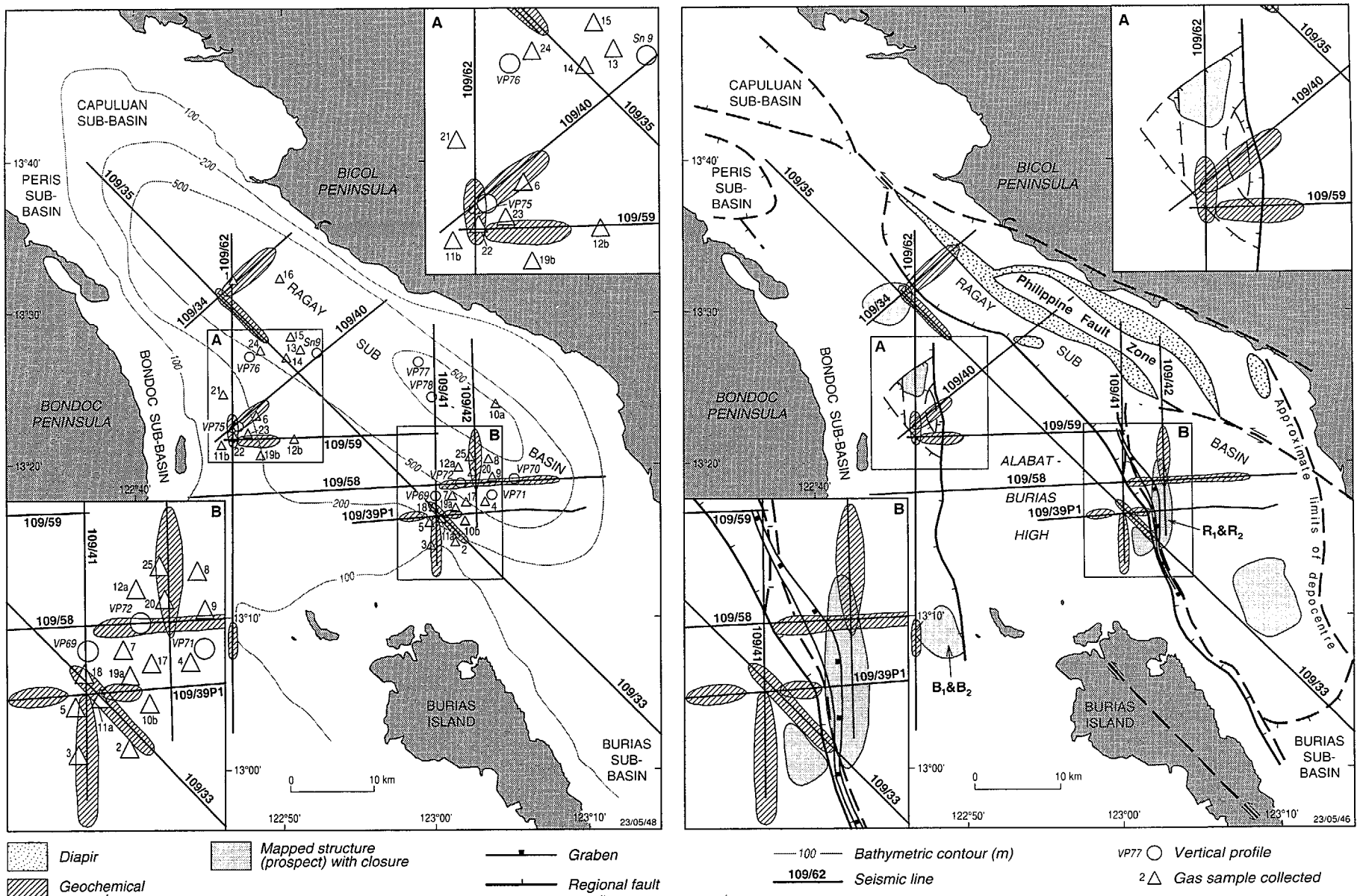

Figure 3 Map of Ragay Gulf, showing (a) the locations of DHD anomalies and associated survey lines, bathymetry, locations of vertical profiles and gas samples for isotopic analyses, (b) the major structural elements of Ragay Gulf with the geochemical /seismic lines discussed in the text, the locations of gechemical anomalies, and closed structures and diapirs identified from seismic data.

In the following discussion, geochemical data from one key line from each area selected for discussion (Ragay Sub-basin; Bondoc Sub-basin, the flank of the Alabat-Burias High with the south eastern Ragay Sub-basin, and the northwestern Ragay Sub-basin) are illustrated in Figure 4. These examples are presented to demonstrate the nature and extent of bottom-water anomalies detected, and to illustrate the systematic differences in chemical composition between anomalies in different parts of the survey area. The geochemical anomalies from the survey lines discussed here are summarised in Table 2.

Bottom-water anomalies: Bondoc Sub-basin, western Ragay Gulf. Seismic lines 109/40, 109/59 and 109/62 intersect in the western part of Ragay Gulf (Figs. 1 and 3). THC and methane reach values greater than 150 ppm (Fig. 4a), at the western end of survey line 109/59 (Figs. 1a and 3). These high concentrations are located near a strong anomaly noted on line 109/40, (Fig. 3). The anomaly on 109/59 is about 7 km wide, but total hydrocarbons remained higher than typical background values over a distance of about 20 km. Weak ethane and propane anomalies were found over most of this survey line, but the elevated concentrations are accompanied by elevated levels of the biogenic hydrocarbon, ethylene. These unsaturated hydrocarbons are the product of recent biosynthesis, and the low levels of ethane are considered to be co-produced with ethylene and unrelated to seepage of thermogenic hydrocarbons (Fig. 4).

Several bottom-water anomalies were found over the Bondoc Sub-basin (Table 2), each comprising significant increases in methane, with trace increases in ethane and occasional trace increases in propane and butane.

Bottom-water anomalies: Ragay Sub-basin, northwestern Ragay Gulf. There is one very distinctive anomaly on line 109/34 in the northwestern Ragay Sub-basin (Fig. 4b). It is characterised by high THC and methane concentrations (> 80 ppm) and trace increases of ethane (<0.07 ppm, about two-fold background; Fig. 4b). The anomaly was detected in the deep-water part of the Ragay Sub-basin (water depth > 500 m), over a distance of about 8 km.

Bottom-water anomalies: flank of the Alabat- Burias High within the Ragay Sub-basin, southeastern Ragay Gulf. Two strong anomalies in close proximity are evident on an east-west oriented line 109/39P1 in central Ragay Gulf (Figs. 3 and 4c). Methane concentrations rise from background (approximately 5 ppm), to levels greater than 60 ppm in both anomalies. One anomaly (sp 50-60), is accompanied by elevated levels of ethane and propane, about an order of magnitude above background levels (Fig. 4c), and a significant increase in butane, and is located near the boundary of the Ragay Sub-basin with the Alabat-Burias High (Fig. 3). This anomaly is coincident with one detected on line 109/33, which was surveyed three days earlier. The other THC and methane anomaly on line 109/39P1 (sp 60-75) is accompanied by only a trace increase in ethane (less than two-fold background). It is located further west, directly over the Alabat-Burias High, and is close to an anomaly on line 109/41 surveyed approximately twenty-four hours later.

All anomalies detected in this area, although in close proximity to each other, are of different molecular compositions. Significant increases in saturated hydrocarbons ethane and propane above background are not accompanied by increases in unsaturated hydrocarbons ethylene or propylene. The increases in the ethane and propane noted in Figure 4c are coincident with a significant seafloor topographic feature with relief of approximately 100 m. Similarly, the generally elevated ethylene values were located on the shallow side of this feature and the rapid decrease in ethylene is associated with an increasing water depth. These horizontal variations in hydrocarbon concentration can, in

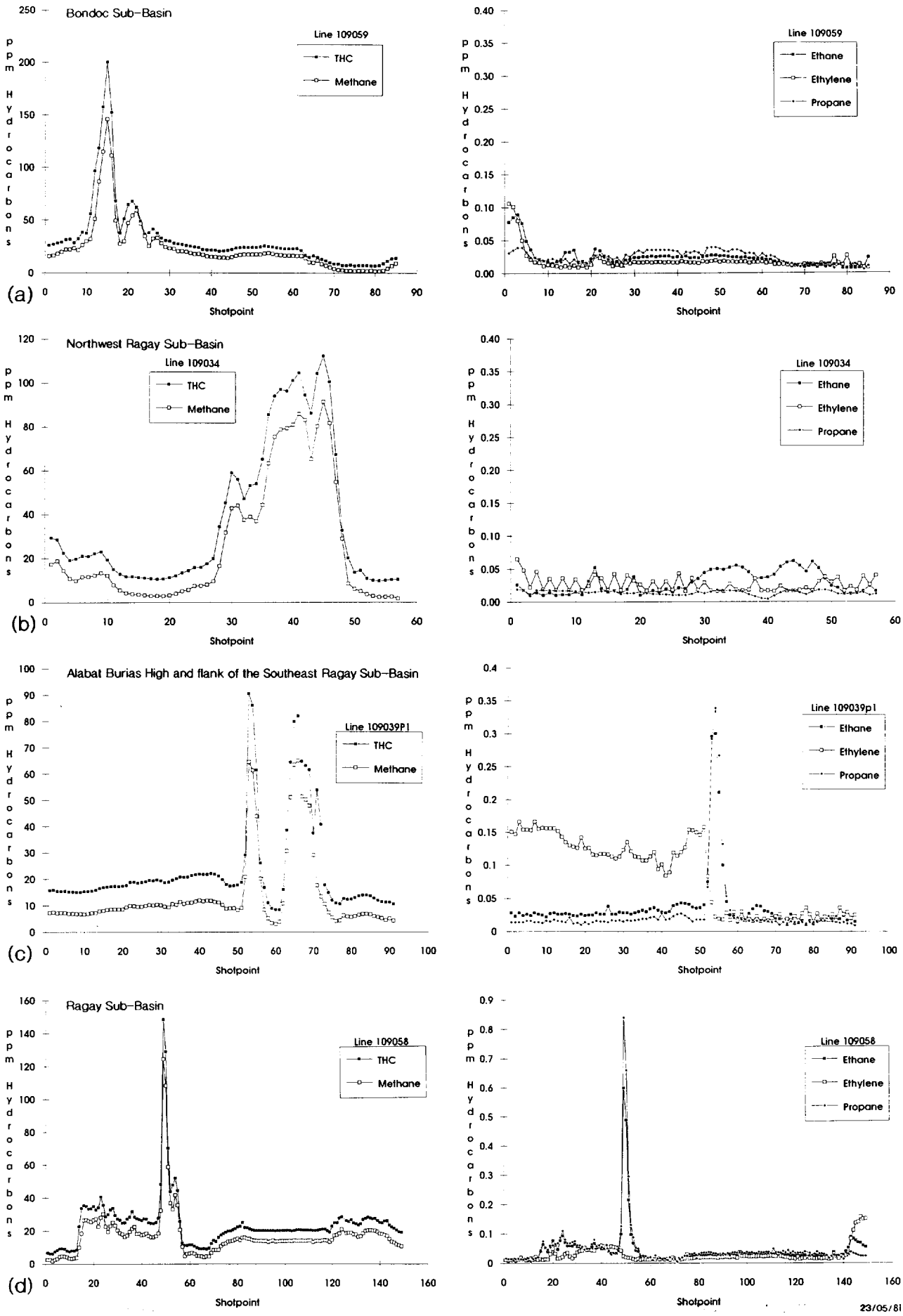

Figure. 4 Total hydrocarbons (THC), methane, ethane, ethylene and propane versus DHD shotpoint for survey lines: (a) 109/59 in the Bondoc Sub-basin; (b) 109/34 in the northwestern part of Ragay Sub-basin (c) 109/39P1 which traverses (east-west) the southeastern Ragay Sub-basin and the Alabat-Burias High (d) 109/58 in the southeastern Ragay Sub-basin, crossing (north-south) onto the Alabat-Burias High.

Table 2. Summary of the bottom-water anomalies discussed in the text from various structural elements identified within the Ragay Gulf

Area	Bottom-water light hydrocarbon anomalies
Bondoc Sub-basin:	
Bondoc Sub-basin 109/40	THC, methane near 200 ppm, ethane <0.05 ppm, propane <0.03 ppm.
Bondoc Sub-basin 109/59	THC (>200 ppm), methane (>50 ppm), ethane and propane <0.05 ppm
Bondoc Sub-basin 109/62	THC (>100 ppm), methane (>80 ppm), ethane and propane <0.05 ppm in the anomaly in the north. THC and methane >50 ppm, ethane <0.01 ppm in the anomaly to the south.
Bondoc Sub-basin 109/73	THC, methane (>200 ppm), ethane & propane <0.05 ppm.
Bondoc Sub-basin 109/74	THC & methane >100 ppm, ethane & propane <0.05 ppm.
North westernern Ragay Sub-basin and Alabat-Burias High:	
Ragay Sub-basin 109/34	THC, methane >80 ppm, ethane <0.07 ppm, propane <0.03 ppm.
Alabat-Burias High 109/35	Two anomalies, THC, methane >20 ppm, ethane <0.15 ppm, propane <0.05 ppm. One anomaly is near that discussed on 109/34, while the other is far to the north and not discussed.
South eastern Ragay Sub-basin and Alabat-Burias High:	
Ragay Sub-basin 109/39P1	Two strong anomalies; one with THC, methane >60 ppm, ethane and propane >0.3 ppm, butane >0.1 ppm located on the flank of the Ragay Sub-basin. The other anomaly, with THC, methane >60 ppm, ethane & propane <0.05 ppm is located over the Alabat-Burias High.
Alabat-Burias High 109/41	THC, methane >120 ppm, ethane and propane <0.01 ppm.
Alabat-Burias High 109/33	Two anomalies, one with THC, methane >60 ppm, ethane and propane >0.2 ppm, butane >0.05 ppm was located on the structural high but near the flank of the Ragay Sub-basin.. The other with THC, methane >30 ppm with ethane <0.07 ppm was located to the north, near that anomaly identified on 109/35 above.
Ragay Sub-basin 109/69.	THC, methane >200 ppm, ethane & propane > 0.35 ppm.

Table 2. continued

Ragay Sub-basin:	
Ragay Sub-basin 109/42	THC (>90 ppm), methane (>50 ppm), ethane and propane >0.1 ppm, butane >0.05 ppm
Ragay Sub-basin 109/58	THC and methane >120 ppm, ethane (0.6 ppm), propane (>0.8 ppm), butane (>0.2 ppm)
Ragay Sub-basin 109/70	THC >100 ppm, methane >80 ppm, ethane and propane near 0.4 ppm, butane >0.1 ppm
Ragay Sub-basin 109/79.	THC >350 ppm, methane >200 ppm, ethane and propane > 1 ppm, butane >0.3 ppm
Ragay Sub-basin 109/49 109/50	THC (23 ppm), methane (<15 ppm), ethane and propand <0.04 ppm)

part, be explained by the vertical distribution of hydrocarbons in the water column (Figs. 5 and 6). The contrasting saturated and unsaturated hydrocarbon distributions highlight the different processes controlling their distributions in continental shelf waters, and the potential application of utilising saturated/unsaturated hydrocarbon abundances to indicate whether hydrocarbons are of biogenic or thermogenic origin.

Hence, on the flank of the Ragay Sub-basin and over the Alabat-Burias High, anomalies of two distinctly different compositions exist. One anomaly-type has significant methane, ethane, propane and elevated butane, while the other anomaly-type has significant methane with only a minor increase in ethane and no significant increases in propane or other hydrocarbons (Table 2).

Bottom-water anomalies: Ragay Sub-basin, southeastern Ragay Gulf. Survey line 109/58 trends east-west, is approximately 70 km in length, and shows one very distinct anomaly over the Ragay Sub-basin (Figs. 3 and 4d), which overlaps another strong anomaly on line 109/42 (Table 2; Fig. 3). THC concentrations increase from background values (< 10 ppm) to values near 40 ppm, and thereafter to concentrations greater than 150 ppm. Methane concentrations similarly increase to highest concentrations above 120 ppm. These concentrations are more than an order of magnitude above typical background concentrations and represent 'strong' anomalies. THC and methane values remain elevated (above typical background) for much of this line and are accompanied by elevated ethane, propane and butane concentrations. Both ethane and propane concentrations exceed 0.6 ppm, nearly fifty-fold typical background values. Within this anomaly, propane concentrations exceed ethane concentrations, and butane concentrations rise significantly above background (<0.01 ppm) to values in excess of 0.2 ppm. As noted above there are no increases in the biogenic hydrocarbons ethylene and propylene associated with the strong ethane and propane anomalies. Hence, in the south eastern sector of the Ragay Sub-basin bottom-water anomalies are predominantly methane with significant quantities of ethane, propane and butanes (Table 2).

Vertical Profiles of Hydrocarbons in the Water Column of the Ragay Gulf. Nine vertical profiles of light hydrocarbon distributions in the water column were measured in the Ragay Gulf (Evans et al., 1992). Two examples of vertical profiles are illustrated here, and the distinctions between the molecular compositions of anomalies noted above is also evident in the vertical profiles. Vertical profile VP109/70 (Fig. 5) was measured over the Ragay Sub-basin near the flank of the Alabat-Burias High in a water depth of 164 m (Fig. 3a. Temperature and conductivity (data not shown) systematically decrease with increasing water depth to the seafloor indicating a stratified water column, and there is a noticeable change in the vertical temperature gradient below 120 m depth. Total hydrocarbons (THC), methane, ethane, and propane values are low in surface waters and increase rapidly below about 120 m depth, with maxima about 10 m above the seafloor. The highest THC concentrations are about 70 ppm, methane 55 ppm, ethane 0.2 ppm, and propane near 0.25 ppm. These vertical distributions of the saturated hydrocarbons suggest that hydrocarbons are emanating from the seafloor to form a plume about 20 m in thickness (Fig. 5b). Concentrations of the unsaturated hydrocarbon ethylene decreases systematically from above 0.3 ppm in surface waters to less than 0.05 ppm at depths below 150 m. Propylene varies similarly to ethylene, but these data are not shown. The distribution of ethylene is thus depth-dependent, as is temperature.

Vertical profile VP 109076 (Fig. 6) was measured the Bondoc Sub-basin, western Ragay Gulf, in a water depth of 274 m, near the intersection of lines 109/62 and 109/40 (Fig. 3).

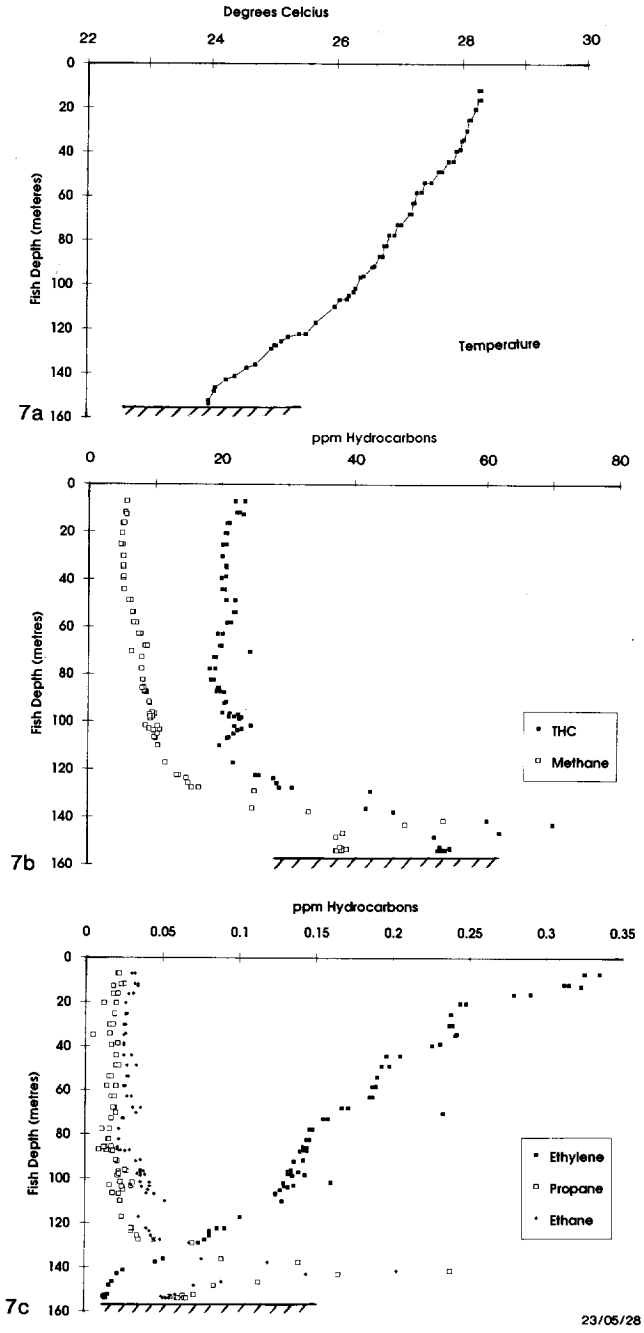

Figure 5 Depth profiles in the water column of (a) temperature (b). total hydrocarbons (THC) and methane (c) ethane, propane and ethylene, for vertical profile vp109/070 from over the Ragay Sub-basin.

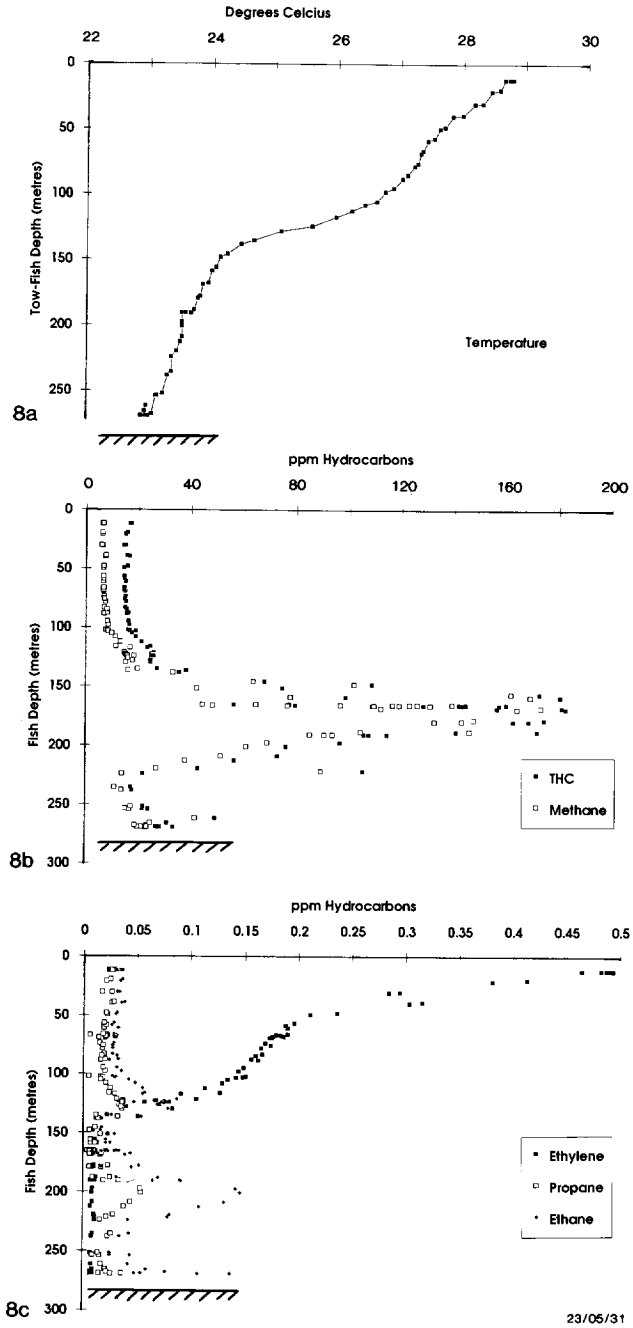

Figure 6 Depth profiles in the water column of (a) temperature (b). total hydrocarbons (THC) and methane (c) ethane, propane and ethylene, for vertical profile vp109/076 from over the Bondoc Sub-basin.

Temperature decreases systematically with increasing water depth, with the steepest temperature gradient between depths of about 100 and 150 m (Fig. 6a), below which there is a significant change. These data suggest a stratified, 'two-layer' water column; with a surface layer extending to about 150 m water depth overlying a relatively well mixed zone.

Concentrations of total hydrocarbons(>180 ppm), methane (>90 ppm), ethane and propane are highest between about 150 m and 220 m (Fig. 6b,c) in an 80 m thick plume, the top of which is near the base of the steepest temperature gradient. The saturated hydrocarbon concentrations increase systematically below about 230 m to the seafloor at 274 m water depth. Ethylene concentrations decrease from about 0.5 ppm near the surface to less than 0.03 ppm at 150 m, and then remain constant below that depth. Propylene concentrations vary similarly.

The contrasting depth profiles of saturated and unsaturated hydrocarbons in these profiles indicate that their vertical distributions are controlled by different processes. Unsaturated hydrocarbons are produced microbially near the surface (Primrose and Dilworth, 1976; Claypool and Kvenvolden, 1983),whereas saturated hydrocarbons, present in high concentrations in near bottom-waters, are indicative of a seafloor source.

Interesting contrasts in these profiles are evident in the comparative concentrations of methane, ethane and propane. Data from VP109/70 (Ragay Sub-basin, southeastern Ragay Gulf) show relatively high concentrations of methane (>50 ppm) ethane (>0.2) and propane (> 0.2 ppm), with methane/(ethane+propane) ratios being about 100. In contrast, ethane and propane concentrations in VP 109/76 over the Bondoc Sub-basin are less than 0.15 ppm at methane concentrations of greater than 170 ppm, giving methane/(ethane+propane) ratios of nearly 1000. The elevated C_{2+} hydrocarbon concentrations relative to methane in the southeastern Ragay Sub-basin, as compared to other parts of the Ragay Sub-basin and the Bondoc Sub-basin is an important feature and is discussed below in terms of the predicted hydrocarbon source for these anomalies.

Vertical profile data indicate that DHD anomalies are in the form of plumes, up to about 80 thick, with maximum concentrations generally being found at depths between 120 m and 220 m. While it is beyond the scope of this report to discuss how these plumes were formed, modelling of these data (Radlinski and Leyk, personal communication), indicate that plumes are unstable features formed as a result of periodic effluxes of dissolved hydrocarbons from the seafloor being trapped within a stratified water column. The hydrocarbon plume results from different mixing dynamics between a relatively stagnant layer, near the base of the thermocline, and more dynamic top and bottom layers from which hydrocarbons are eroded away by combinations of horizontal and vertical mixing.

These observations have implications for the use of DHD techniques. First, when surveying shelfal areas in temperate regions, where the water column hydrography may vary seasonally, surveys should be conducted when the water column is stratified (and not well-mixed), because hydrocarbon seepage will be preserved in a bottom-layer. Second, when surveying in relatively deep waters, where the water depth exceeds the depth of the seasonal thermocline, the DHD tow-fish should be set at a depth near the base of the stratified layer, rather than close to the seafloor, because anomalies resulting from seepage persist in this layer for longer periods than in deeper water closer to the seafloor (Radlinski and Leyk, personal communication).

ORIGIN AND SOURCE OF LIGHT HYDROCARBON ANOMALIES

In the context used here, the genetic 'origin' of naturally occurring light (C_1 through C_4) hydrocarbons refers to the distinction between thermogenic and biogenic hydrocarbons. The 'source' of thermogenic hydrocarbons refers to the nature of hydrocarbons- dry-gas, gas-condensates or liquids- emanating from petroleum source rocks or reservoirs.

Thermogenic hydrocarbons are produced by the effect of heat on organic matter buried to depths of several kilometres in sedimentary basins (e.g. Hunt, 1979; Tissot and Welte, 1984). The products of these reactions which are of interest in DHD methods include methane and the higher saturated hydrocarbons (C_2 through C_8). Thermogenic hydrocarbons may migrate, either from source rocks or from reservoirs, through fractures and pore spaces in the overlying sedimentary strata to escape into the overlying water column, resulting in bottom-water thermogenic anomalies.

Biogenic hydrocarbons, in contrast, are produced microbially and photochemically in seawater (Claypool and Kvenvolden, 1983). The vertical distributions of hydrocarbons shown in Figures 5 and 6 are unusual, although similar profiles, principally for methane, have been measured in seawater (Scranton and Brewer, 1977; Burke et al., 1983; Owens et al., 1991). However, the methane distributions cited above, result from microbial degradation of organic matter in the water column. In addition, during early diagenesis, methane and minor quantities of both saturated and unsaturated hydrocarbons are produced by the activities of microbial organisms during aerobic and anaerobic destruction of organic matter in the top few tens of metres of sediments (Hunt, 1979; Claypool and Kvenvolden, 1983 and references cited therein). These compounds produced *in-situ* generally occur in low concentrations as background hydrocarbons in seawater (Claypool and Kvenvolden, 1983). However, high concentrations of biogenically-produced hydrocarbons may accumulate in shallowly buried sediments and seep into the overlying water, resulting in biogenic bottom-water anomalies (Brooks et al., 1974; Bernard et al., 1976).

In some offshore areas, hydrocarbons from other sources could be introduced into the marine environment. These may be of a thermogenic character such as ship oil spills, refined petroleum products used in industrial processes, or formation waters from existing petroleum production platforms; or of a biogenic origin such as hydrocarbons resulting from microbial degradation of urban sewage. However, because there are no petroleum production nor refining facilities in the Bondoc and Bicol Peninsulas, the possibility that light hydrocarbon anomalies are derived from anthropogenic sources can probably be discounted. The anomalies detected in the Ragay Gulf therefore could be produced from one or more of the following processes: (1) in-situ biogenic production in the water column associated with metabolic oxidation of contemporary organic matter derived from sinking particulates or resuspended from surficial sediments; (2) biogenic production within the near-surface sediments and migration of the light hydrocarbons into bottom-waters; (3) thermogenic production in the underlying, deeply buried sediments with migration by some unknown mechanism into the overlying water. The following discussion examines these possibilities.

Molecular Composition of Light Hydrocarbon Anomalies: the Cross-Plot Model of Hydrocarbon Origin and Source

One model that we have been investigating to examine both the origin and source of anomalies is a plot of methane concentration versus percent hydrocarbon wetness

(percent wetness = [sum(C_2+C_3+C_4)/Sum(C_1+C_2+C_3+C_4)] x100). The rationale behind this plot (Fig. 7) is that hydrocarbons of different origins (thermogenic or biogenic), and sources (dry - gas, gas-condensate and oil), can be distinguished on the basis of differences in their light hydrocarbon molecular composition (Hunt, 1979; Tissot and Welte, 1984; Claypool and Kvenvolden, 1983). In this model, background hydrocarbons plot in a narrow range towards the left origin (low concentrations), while end-member source hydrocarbons derived from oil-prone, gas-condensate or dry-gas source rocks or reservoirs plot to the right (high concentrations, Fig. 7).

As the hydrocarbons in bottom-waters represent mixtures of background (low) and source (high) concentrations, the trends between the end-members in these plots are indicative of the source of the hydrocarbons comprising the anomalies. For example, when the percent hydrocarbon wetness increases with increasing methane concentration, the trend indicates that the anomaly was probably derived from a gas-condensate or oil-prone source. In contrast, increasing methane concentrations, coupled with decreasing percent hydrocarbon wetness, suggest that the anomaly was derived from a 'dry' gas of either a thermogenic or biogenic origin. The model cannot distinguish between 'dry' biogenic and gas-prone thermogenic anomalies. Carbon isotope (e.g. Fuex,1977; Bernard et al., 1977) and molecular compositional data are required to discriminate between these anomaly types.

Combined cross-plots, from the Ragay Gulf data, of percent hydrocarbon wetness and methane for survey lines presented in Figure 4 and Table 2, are shown in Figure 8. The same data, separated according to location within the major structural elements are shown in Figure 9. There are two main trends evident in the data. One trend of increasing methane concentration with decreasing hydrocarbon wetness is seen in data from most lines, but is most strongly developed in lines from the Bondoc Sub-basin, the north western part of the Ragay Sub-basin and the Alabat-Burias High (Figs. 8 and 9). Methane concentrations increase up to values of about 250 ppm and percent hydrocarbon wetness values decrease from typical 'background' values (about 0.5 percent), to values less than 0.1 percent. This trend indicates that hydrocarbon anomalies are derived from a 'dry' gas source - either a biogenic gas produced microbially, or a thermogenic gas produced by the action of heat on a 'gas-prone' source rock. These trends of decreasing percent hydrocarbon wetness with increasing methane have not been observed in cross-plots of DHD from around the Australian continental margin (Heggie et al., 1991a,b).

Another trend in Figures 8 and 9, shows increasing percent hydrocarbon wetness with increasing methane concentration. Data from this trend indicate methane increasing up to 250 ppm (background methane about 3 ppm), while percent hydrocarbon wetness increases from background values (approximately 0.5 percent), to values approaching about 1.5 percent. This trend is well developed in lines from the Ragay Sub-basin, and is also evident in the data from the Alabat-Burias High and the flank of the Ragay Sub-basin (Fig. 9). This trend is not developed in the data from the Bondoc Sub-basin nor the northwestern Ragay Sub-basin (Fig. 9). These trends of increasing (albeit weakly) wetness with increasing methane indicate that hydrocarbons are derived from a condensate-prone source rock or reservoir, or perhaps from oil-associated gases at depth. There are no data from Philippines hydrocarbon accumulations to calibrate this model, but DHD data from the Petrel gas-condensate discovery in the Bonaparte Gulf, northwestern Australia, indicate wetness values of 2 to 8%, at methane concentrations of up to 400 ppm. In contrast, different trends were found in oil/gas sourced bottom-water anomalies detected in the Gippsland Basin, Australia, with wetness values approaching 30 percent at methane

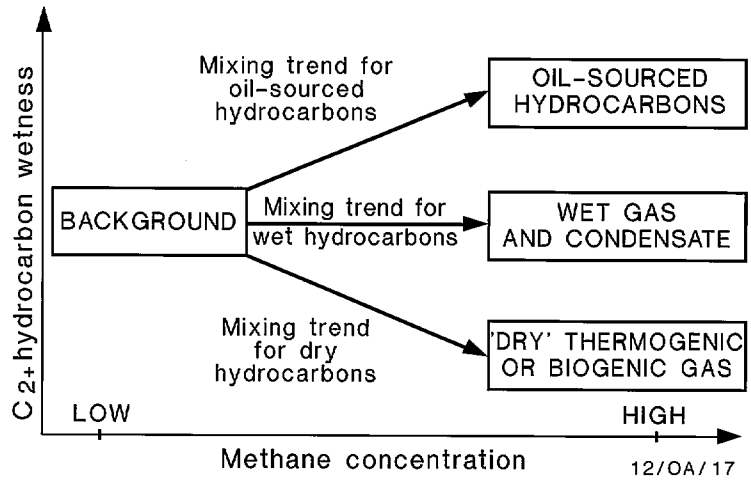

Figure 7 Cross-plot model of methane versus hydrocarbon wetness, showing the general decrease in wetness with increasing methane for gas-prone thermogenic or biogenic gas mixtures. Liquids-prone sources are indicated by increasing wetness with increasing methane. Gas-condensate sources fall between the dry gas and liquids-prone trends.

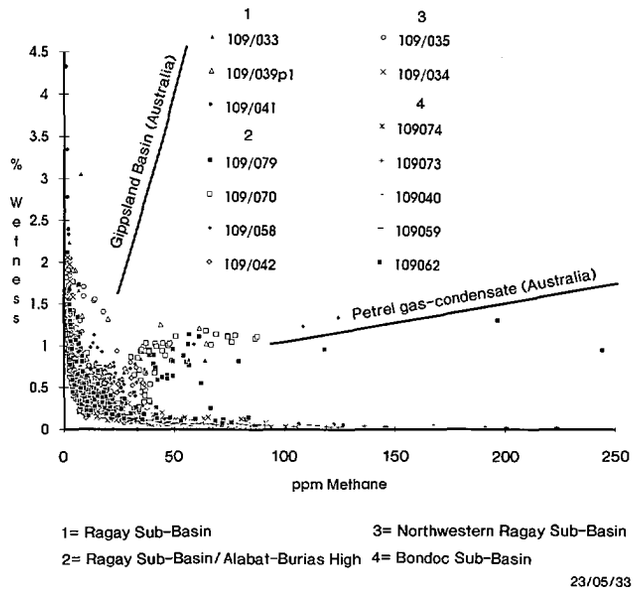

Figure 8 The cross-plot model of percent hydrocarbons wetness and methane content for all survey lines discussed in the text.

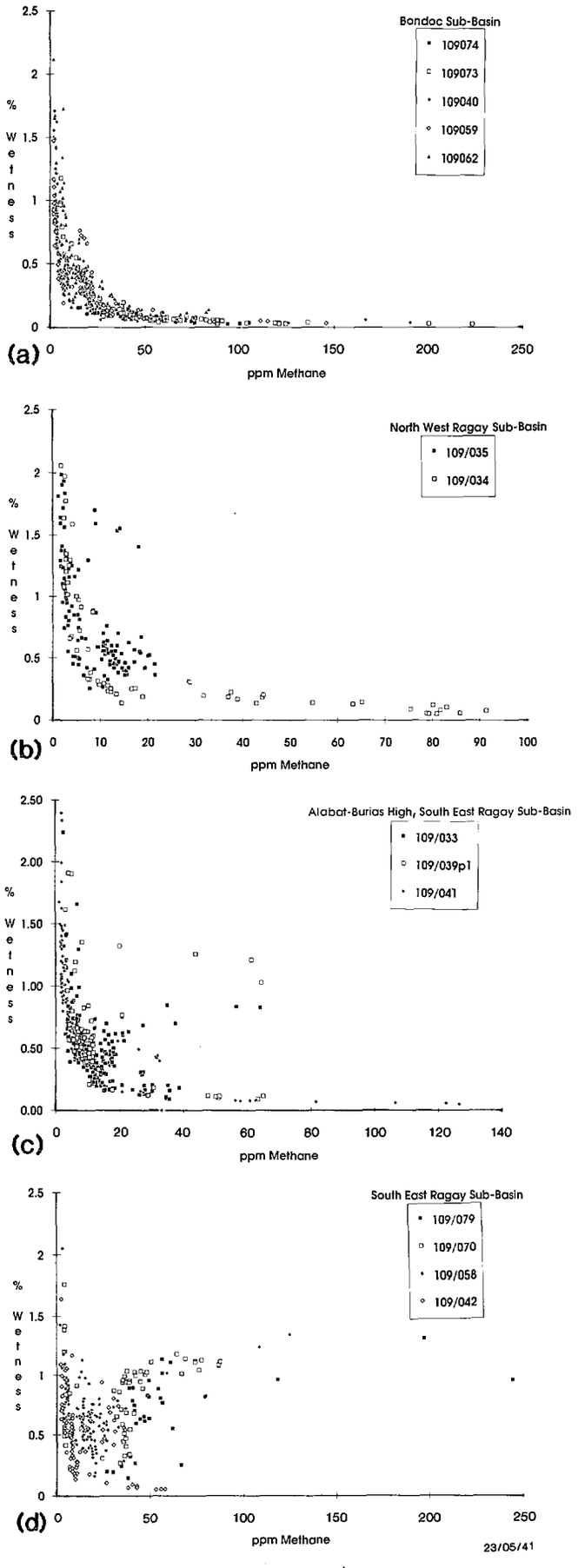

Figure 9 Methane versus percent hydrocarbon wetness for survey lines shown in (a) Bondoc Sub-basin (b) Ragay Gulf Sub-basin (northwestern part) (c) the Alabat-Burias High and the Ragay Sub-basin (southeast) (d) the southeast Ragay Sub-basin.

concentrations of about 100 - 200 ppm (Heggie et al., 1991a,b). These trends from Australian gas-condensate (Petrel) and oil-gas (Gippsland Basin) accumulations are superimposed on Figure 8.

There exists a third trend in the data of increasing wetness (up to about 5 %; Fig. 8), at low methane concentrations (< 10 ppm) which, according to the cross-plot model of Figure 7, indicates a strong 'oil-prone' hydrocarbon source. This trend is evident to some degree in all areas (Fig. 9). However, the interpretation of this trend in terms of hydrocarbon source is problematic and must be treated with caution. For example on line 109/33, wetness values of up to three percent are associated with significant increases in ethane but no increases in methane. The anomalous ethane however, is accompanied by elevated levels of ethylene (a biogenic hydrocarbon), and the ethane, in this case, is probably co-produced biogenically with ethylene and therefore has no significance for hydrocarbon exploration. In other instances increased wetness results from small and occasional increases in ethane, or other saturated hydrocarbons, unaccompanied by increases in other hydrocarbons (e.g. survey line 109/41; Evans et. al. 1992). When disparate data points such as these are combined on this type of cross-plot they appear as a single trend line - but they are not indicative of seepage from the seafloor nor a bulk hydrocarbon source.

The existence of two primary sources of hydrocarbons, of different molecular compositions, which produce the bottom-water anomalies, is more clearly shown in the cross-plots of methane versus ethane, propane and butane (Figs. 10 and 11). Data from the Bondoc Sub-basin and northwestern Ragay Sub-basin predominantly indicate trace increases in ethane, with no significant changes in propane or butane as methane increases from background to values up to 250 ppm. In these anomalies the methane/ethane ratio is greater than 1000, based upon ethane values generally less than 0.05 ppm at methane concentrations of 100 ppm (Fig. 10).

In distinct contrast to these data above, data from near the junction of the Alabat-Burias High with the flank of the Ragay Sub-basin, and also data from within the Ragay Sub-basin proper (Fig. 11), indicate two trends of increasing ethane and propane with increasing methane. In one trend the methane/ethane ratio is comparable to that in the previous data (>1000), while another trend shows methane/ethane, and methane/propane ratios of about 250. Data from the southeastern Ragay Sub-basin show that the dominant trend is of increasing methane, ethane, propane and butane with methane/ethane and methane/propane ratios of about 250, and a methane/butane ratio of about 750.

Cross-plots of the molecular compositional data therefore indicate the presence of thermogenic hydrocarbons sourced from a condensate or perhaps a liquid-prone hydrocarbon source in the southeast Ragay Sub-basin. Relatively 'dry' hydrocarbons were also identified predominantly in the Bondoc Sub-basin, the northwestern part of Ragay Sub-basin and near the Alabat-Burias High, but the molecular compositional data alone are not sufficient to distinguish 'dry' thermogenic gas from biogenic gas.

Carbon Isotopic Composition of Bottom-Water Methane Anomalies in Ragay Gulf

Twenty-five gas samples containing anomalous concentrations of light hydrocarbons were sent to the New Zealand National Institute of Water and Atmospheric Research Limited (NIWAR) for carbon isotope analysis of the methane gas component. Insufficient sample was available from the extracts to determine the carbon isotopic composition of C_{2+} hydrocarbons.

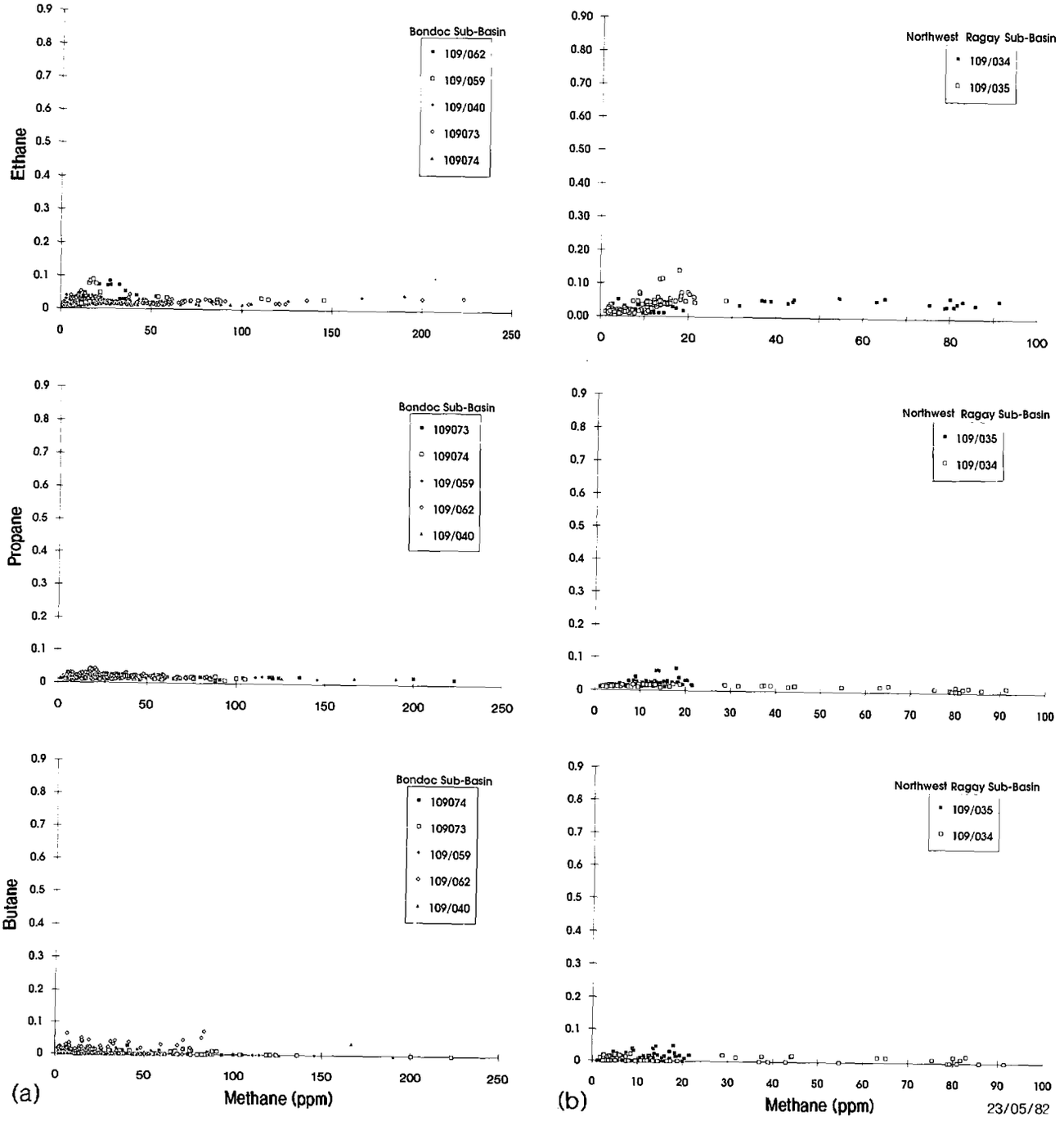

Figure 10 Methane vs ethane; methane vs propane and methane vs butane for those survey lines shown in (a) Bondoc Sub-basin (b) Ragay Gulf Sub-basin (northwestern part).

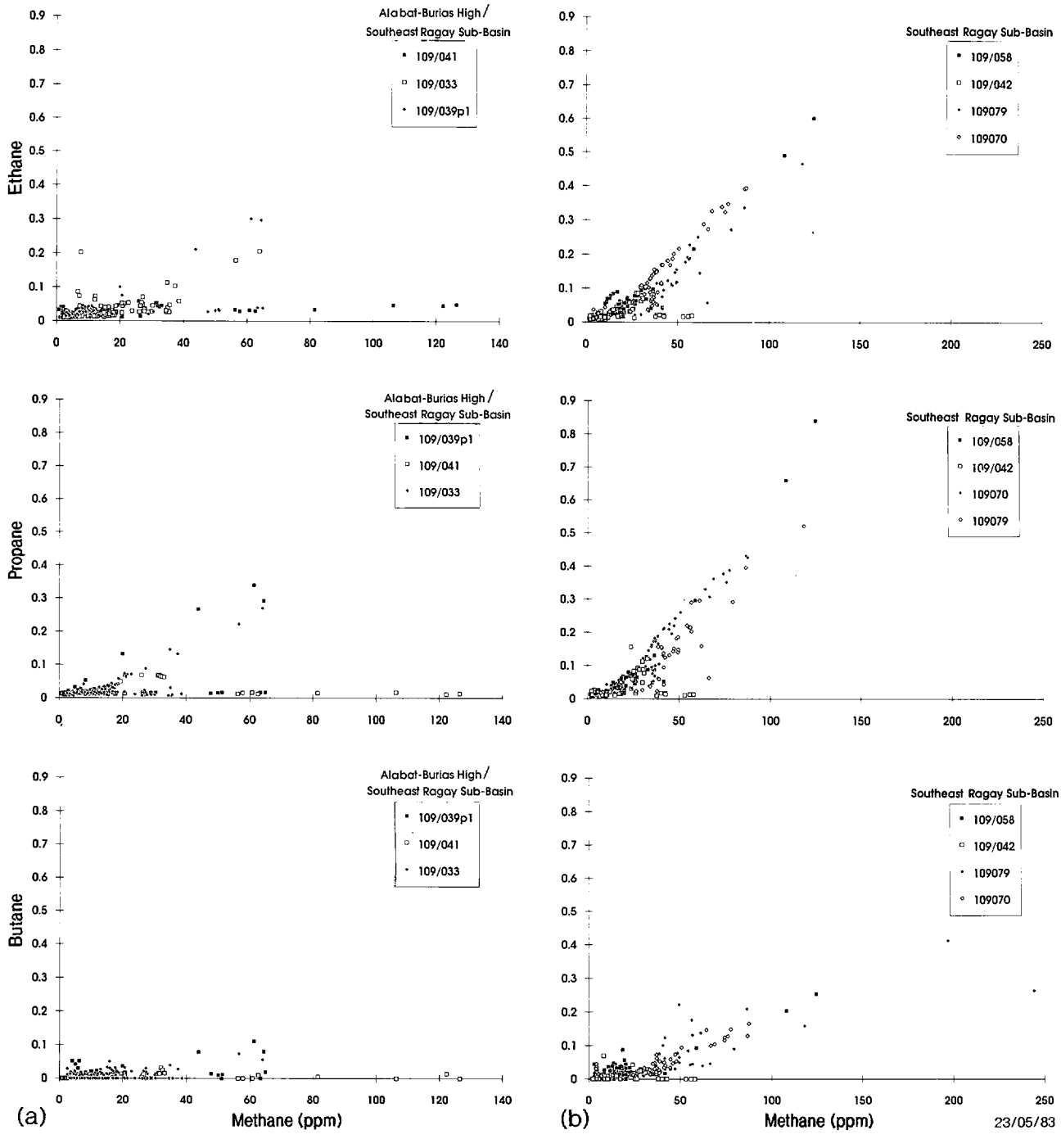

Figure 11 Methane vs ethane; methane vs propane and methane vs butane for those survey lines shown in (a) the Alabat-Burias High and the Ragay Sub-basin (southeast) (b) the southeast Ragay Sub-basin.

Table 3 lists the median methane, ethane and propane concentrations, the carbon isotopic composition, the Bernard parameter (C_1/C_2+C_3), and the tow-fish depth for the samples collected. The major structural elements these samples were collected from, according to Fig. 3, is also listed. Selected samples were analysed for the radiocarbon content of the methane (Table 4). The radiocarbon content distinguishes methane derived from recent as opposed to fossil organic matter (Bernard et al., 1976; Oremland et al., 1987). The data for nine samples collected in the Ragay Gulf indicate that methane in most samples was derived from fossil carbon, with modern carbon contents generally less than 7 percent. One sample collected from over the Bondoc Sub-basin had a pMC (percent modern carbon) of 16.2 % and indicates a small contribution of contemporary methane. Collectively, these data exclude the possibility that the anomalous hydrocarbon concentrations are derived primarily from in-situ biogenic processes in the water column, including degradation of contemporary organic matter in near-surface sediments. Hence, the anomalous hydrocarbons are derived from deeply buried sediments.

The $\delta^{13}C$ isotopic composition of the methane gas component of the Ragay samples range from -57.3 to -37.8 $^{o}/_{oo}$. A frequency distribution analysis of $\delta^{13}C_1$ values indicates clusters of $\delta^{13}C$, with the most abundant values being found between -42.5 to -41.5 $^{o}/oo$ and, -48.5 to -47.5 $^{o}/_{oo}$ respectively, with one sample (collected from over the Bondoc Sub-basin) having a $\delta^{13}C_1$ of -57.3$^{o}/_{oo}$. These data indicate methane in these samples is primarily of thermogenic origin, based upon an empirical cut-off between thermogenic and biogenic gases at about -60 $^{o}/_{oo}$ (Fuex, 1977; Bernard et al., 1977; Schoell, 1983), and more recent data (Whiticar et. al., 1986), which indicates that the carbon isotopic signature of biogenic methane in marine sediments is consistently lighter (ie., more negative) than -60$^{o}/_{oo}$.

These data are plotted with the calculated Bernard Parameter ($BP = C_1/[C_2+C_3]$) in Figure 12. The Bernard model of genetic classification of gases was assembled from seep gases in the Gulf of Mexico (Bernard et al., 1976; Bernard et al., 1977), and has been used to interpret the genetic origin of methane gas from a wide variety of different environments (e.g., Claypool and Kvenvolden, 1983; Schoell, 1984 a,b; Oremland et al., 1987; Schiener et al. 1985).

Fifteen samples from the Philippines (109/1 through 5, 7 through, 12, 17, 19, 20, 25), have a BP less than 1000 and $\delta^{13}C_1$ between -49 and-39 o/oo, while nine samples (109/6, 13 through 15, 9, 18, 21, 22, 24) were found to have Bernard parameters greater than 1000 and $\delta^{13}C_1$ between -52 and -38 $^{o}/_{oo}$. One sample has a BP greater than 3000 and a $\delta^{13}C_1$ of -57.3o/$_{oo}$ and, while isotopically thermogenic, lies closer to the biogenic field defined by Bernard et al. (1977), than any other sample. There is also a systematic geographical distribution of the molecular abundances of these samples, with all samples from the Bondoc and northwestern Ragay Gulf areas having Bernard parameters greater than 1000, while those from the southeastern Ragay Gulf and within the Alabat-Burias High had generally lower Bernard parameters (see discussion below).

The isotopic composition of thermogenically-produced methane reflects both the organic matter type and maturation, and is not fractionated on migration (e.g., Fuex, 1977; Reitsema et al., 1981; Schoell, 1983 and references therein). However, microbial effects in the underlying near-surface sediments or in seawater, notably both aerobic and anaerobic oxidation of biogenic methane gas are processes which may result in fractionation of the methane isotopes (e.g., Barker and Fritz, 1981; Coleman et al., 1981; Oremland and DesMarais, 1983; Whiticar and Faber, 1986; Burke, R.A. jr and Sackett,

Table 3. Median methane, ethane and propane concentrations, $\delta^{13}C$ composition of methane, calculated Bernard parameter, structural element and the tow-fish depth (m) of samples collected for isotopic analysis

Sample No	C_1	C_2	C_3	$\delta^{13}C$	C_1/C_2+C_3	Area	D (m)
109/06	50	0.015	0.014	-50.20	1724	B	200
109/21	61	0.024	0.013	-51.30	1648	B	210
109/22	59	0.020	0.019	-49.10	1512	B	185
109/23	190	0.037	0.021	-57.30	3275	B	182
109/24	120	0.035	0.021	-48.30	2143	B	192
109/01	60	0.053	0.012	-41.70	923	NWR/ABH	185
109/13	72	0.019	0.011	-47.80	2400	ABH/NWR	159
109/14	65	0.015	0.011	-46.70	2500	ABHNWR	74
109/15	55	0.015	0.010	-40.60	2200	ABH/NWR	140
109/16	70	0.011	0.009	-47.00	3500	ABH/NWR	149
109/04	30	0.150	0.100	-42.80	120	SER	115
109/07	40	0.080	0.080	-46.50	250	SER	178
109/08	45	0.025	0.019	-48.80	1022	SER	175
109/09	75	0.275	0.290	-46.70	132	SER	136
109/10	47	0.800	0.850	-38.80	28	SER	155
109/17	60	0.230	0.240	-43.00	127	SER	155
109/20	57	0.200	0.210	-46.10	139	SER	153
109/25	38	0.041	0.044	-49.10	447	SER	140
109/02	40	0.200	0.150	-40.70	114	ABH/SER	100
109/03	38	0.047	0.055	-40.60	372	ABH/SER	160
109/05	45	0.031	0.015	-41.80	978	ABH/SER	170
109/12	45	0.150	0.160	-43.40	145	ABH/SER	190
109/18	390	0.100	0.020	-37.80	3250	ABH/SER	167
109/19a,b	70	0.100	0.110	-44.80	333	ABH-SER/B(m)	167
109/11a,b	40	0.043	0.042	-48.50	470	SER-ABH/B(m)	164

NWR=North western Ragay Sub-basin; SER=South east Ragay Sub-basin; B=Bondoc Sub-basin; ABH=Alabat-Burias High; m=mixed sample from different Sub-basins.

Table 4. Radiocarbon compositions of methane, median methane concentrations and mean sample depth for select methane anomalies from different areas of the Ragay Gulf, Philippines.

Sample No	Area of Collection	Mean sample depth (m)	Median methane (ppm)	$\delta^{13}C$ (o/oo)	^{14}C (pMC)
109/17	Ragay Sub-basin (VP71;72)	155	60	-43.0	5.6 +/- 1.6
109/03	Alabat-Burias High	160	38	-40.6	1.8 +/- 1.8
109/09	flank of the Alabat-Burias high and Ragay Sub-basin	136	75	-46.7	1.1 +/- 1.1
109/18	flank of the Alabat-Burias High and Ragay Sub-basin (VP 69)	167	390	-37.8	0.6 +/- 0.2
109/14	north western Ragay Sub-basin	74	65	-46.7	7.0 +/- 1.5
109/06	Bondoc Sub-basin	200	50	-50.2	1.2 +/- 1.2
109/23	Bondoc Sub-basin (VP 75)	182	190	-57.3	2.0 +/- 0.5
109/24	Bondoc Sub-basin (VP 76)	192	120	-48.3	16.2 +/- 1.1

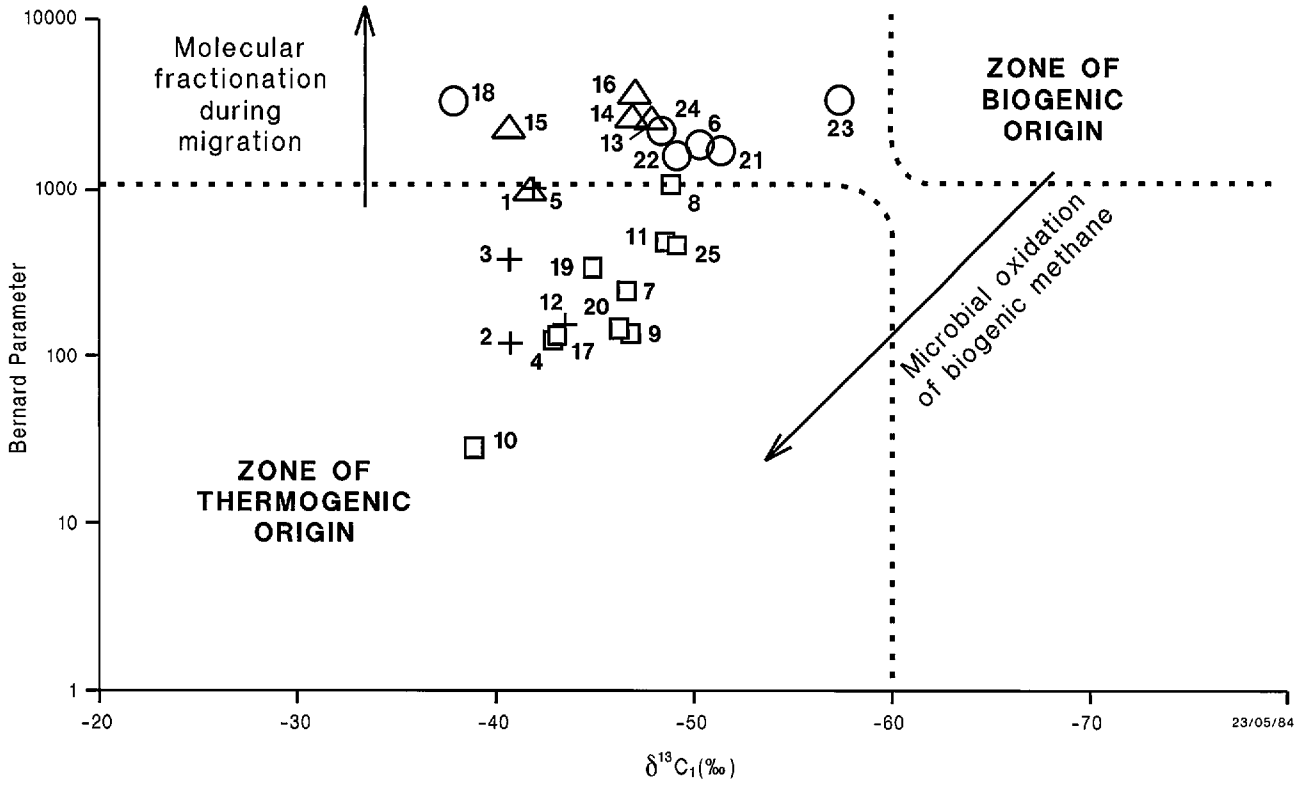

Figure 12 Carbon isotopic composition of methane versus the Bernard parameter (C1/C2+C3) for Ragay Gulf samples (the Bernard Model).

1986; Whiticar and Faber, 1986; Alperin et al., 1988), such that residual biogenic methane may appear to be thermogenic. The radiocarbon content of nine samples (109/17; 03; 09; 18; 14; 06; 23 and 24) rules out the possibility of an oxidised contemporary biogenic methane component in the samples. Aerobic oxidation in the water column of migrated palaeo-biogenic methane from the underlying sediments or, migration of residual palaeo-biogenic methane, which has escaped anaerobic oxidation in the sediments, and migrated into bottom-waters could potentially complicate our interpretation of a thermogenic origin for bottom-water anomalies in the Ragay Gulf. Oxidation of migrated biogenic methane from the sediments cannot be ruled-out unequivocally, and its potential effect on the isotopic composition of methane and the calculated Bernard parameter is illustrated in Figure 12. There is no evidence of methane oxidation. In fact the isotopic compositions of methane in Table 3 are similar to those measured on a gas sample taken from an exploration well on the Bondoc Peninsula, which had an isotopic composition of -45.26^{o}/oo (Cortez and Murray, 1993). Furthermore, the measured vertical distributions of methane in the water column, noted earlier, can be explained by differences in physical mixing processes Radlinski and Leyk (personal communication), and consumption of methane by oxidation in the water column is not required to explain these vertical methane distributions. Collectively, these data, when considered with the sub-surface geology (see below) indicate (1) a systematic distribution of the molecular compositions of anomalies between different structural elements in the Ragay Gulf and (2) significant faults in the near-surface sediments providing hydrocarbon migration conduits from potential source rocks and reservoir horizons into bottom-waters, and favour an interpretation that the isotopic compositions of the methane are relatively 'artifact free' indicators of a thermogenic origin for bottom-water anomalies in the Ragay Gulf.

Methane is the predominant hydrocarbon (>99%) in all anomalies, and while all samples in Table 3 appear isotopically to be thermogenic, there is a wide range (30 to >3000) in the relative abundances of methane/(ethane+ propane) - the calculated Bernard parameter. Mixing of biogenic (unoxidised) hydrocarbons with thermogenic hydrocarbons results in significant changes in the carbon isotopic composition of methane towards more negative $\delta^{13}C$ (biogenic) values, but causes little change in the Bernard parameter value (Bernard et al., 1977), and cannot explain the Philippines data. Oxidation of palaeo-biogenic methane, a process which results in a decrease of the Bernard parameter and a shift in the carbon isotopic composition to less negative values (thermogenic; Fig. 12), is a process which we cannot unequivocally rule out in the Philippines seep samples - although the available data suggest that methane oxidation is not important. The large variation in molecular abundances in the light hydrocarbons, and a consistent thermogenic isotopic composition of methane measured in samples from the Ragay Gulf, therefore reflect either the relative maturity of the source rocks within the areas surveyed, different kerogen source(s) (gas-prone vs oil-prone) between different areas, fractionation of the C_{2+} hydrocarbons during migration, or perhaps combinations of both source and migration effects (Bernard et al., 1976; 1977; Reitsema et al., 1981; Schoell, 1983; Schoell, 1984a,b).

THE RELATIONSHIP BETWEEN BOTTOM-WATER DHD ANOMALIES AND SUB-SURFACE GEOLOGY WITH IMPLICATIONS FOR HYDROCARBON EXPLORATION

Reconnaisance-Scale Comparison of the Cuyo Platform, Northeast Palawan Shelf, Tayabas Bay and the Ragay Gulf.

Most bottom-water anomalies from the Rig Seismic survey were found in the Ragay Gulf. Thirty two of these were strong (> ten-fold background levels), and more than one hundred were moderate-to-weak. No strong anomalies were found in the other survey areas although several weak-to-moderate, weak, isolated and spatially limited anomalies were detected in the Tayabas Bay, Northeast Palawan Shelf and Cuyo Platform. Based upon an assessment of both the number and strength of bottom-water anomalies detected in these areas, the Ragay Gulf would appear to be the most prospective area for hydrocarbons. However, this interpretation is overly simplistic, and must be qualified by the fact that hydrocarbons from sub-surface accumulations can only migrate to the seafloor, and into bottom-waters if adequate migration pathways are present. The possibility that the other areas surveyed are prospective for petroleum hydrocarbons cannot be ruled out if these areas are geologically well-sealed and hydrocarbons cannot migrate to the seafloor (see below). This is an important caveat in predicting prospectivity based solely upon the number and strength of bottom-water anomalies between survey areas and must be emphasised.

Prospect Scale Exploration: Northeast Palawan Shelf and Cuyo Platform

Selected geochemical parameters were contoured and overlain with structural elements maps to investigate the relationship between DHD anomalies and the sub-surface geology, particularly to assist in identifying potential hydrocarbon prospects. Because of limited data in the Cuyo Platform, Northeast Palawan Shelf and Tayabas Bay, as compared to the Ragay Gulf, the DHD contours are not tightly constrained and the interpretation is equivocal. We have chosen therefore to report observations of correlations between geochemical contours and structural elements, without offering a conclusive interpretation.

When the DHD data were contoured and compared to structure contour maps of the Northeast Palawan Shelf, the following observations were made:

(1) Within the Roxas survey area, weak anomalies in total hydrocarbons and methane were found to coincide with the Roxas Lead, a broad, low relief anticline at Middle Miocene unconformity level. (2) Anomalies in total hydrocarbons, methane and C_{2+} hydrocarbons were found over the site of Dumaran-1, an exploration well which was plugged and abandoned after encountering non-commercial hydrocarbons. These anomalies probably result from a 'leaky' well-head. (3) A weak anomaly in methane was found near the site of the Paly-1 exploration well. This well encountered only traces of gas, and no significance is attached to this anomaly. However, weak anomalies of C_{2+} hydrocarbons (ethane+propane) and the ratios of ethane/ethylene and propane/propylene were found about 10 km to the northwest of Paly-1 in an area characterised by normal faulting of the Base Tertiary horizon. (4) Within the Honda Bay area, weak anomalies in the C_{2+} hydrocarbon contours (ethane+propane) were found approximately 4 km south of the Honda Bay Lead, a structural high identified at the Top Cretaceous horizon.

Within the Cuyo Platform, some very weak anomalies in total hydrocarbons and methane were noted in close proximity to stratigraphic highs, and one very weak anomaly was found directly above a structural closure southwest of Manamoc Island.

Prospect Scale Exploration: Tayabas Bay and Ragay Gulf

Despite the fact that relatively few DHD anomalies were detected in Tayabas Bay, and anomalies were generally weak to moderate (ie, less than five-fold typical background concentrations), it was noted that the local background of total hydrocarbon (10-30 ppm) and methane (approximately 6-8 ppm) in this area were generally somewhat higher than typical open-marine background concentrations (2-5 ppm for methane).

The following observations were made on the comparison between the structure map of the base of the Vigo Shale/seismic green horizon (which is the regional seal and possibly a hydrocarbon source rock), and the overlay of contoured DHD values. (1) Several anomalies were found in fairly close proximity (< 10 km) to the Tayabas Bay Fault, a major regional fault of recent (Late Pliocene to present) development. (2) Two anomalies in total hydrocarbons and methane were also found adjacent to the margin of the Bondoc Point Flower Structure, a major compressive feature also of recent origin (see section on Tayabas Bay structure in Volume 1, Part 2). These anomalies also showed elevated contours of the ethane/ethylene and propane/propylene ratios, which suggest that they may be non-biogenic in origin although the C_{2+} hydrocarbon concentrations were generally low. (3) Two anomalies in THC and methane were also found in the east of the Tayabas Bay, directly over the 'kitchen' area of the Bondoc Sub-basin. (4) Several anomalies were noted in the north of the region near the Mabio Lead, which is outside of the main part of the Bondoc Sub-basin. The cross-plot of hydrocarbon source (noted earlier) shows a trend of near-constant hydrocarbon wetness with increasing methane content up to about 22 ppm, or about four times the typical background concentration for this area. These data suggest that a condensate-prone hydrocarbon source may be present at depth.

Within the Ragay Gulf, contours of methane concentration greater than 10 ppm (about twice background) are shown in Figure 13a. There are three general areas of tightly clustered contours where highest methane concentrations are about 250 ppm. These include areas near the intersection of lines 109/34 and 109/33 (Figs. 1a and 3), encompassing the flank of the Alabat-Burias High and the northern Ragay Sub-basin; near the intersections of survey lines 109/62, 59 and 40 in the Bondoc Sub-basin (Figs. 1 and 3); and near the intersections of lines109/58, 109/42 and 109/39P1, 109/33 and 109/41 over the Alabat-Burias High and the southeast Ragay Sub-basin. These anomalous zones of methane concentration all correlate closely with closed geological structures, indicating that the structures have been, or are presently being charged with hydrocarbons and are currently leaking.

Some of these structures were identified on earlier seismic data (World Bank Report, 1986), most notably those labelled R1 and R2 where several strong anomalies are clustered (Figs. 3 & 13). There is no distinct clustering of contours around B1 and B2 on Figure 13, probably because of the sparseness of data in this area, but a distinct anomaly is evident to the south of Line 109/62 (Fig. 3 &14; see below). New closed structures mapped using the AGSO seismic data include ones in the northern part of the Bondoc Sub-basin; in the northwest of Ragay Sub-basin over the flank of the Alibat-Burias High; and in the far southeast Ragay Sub-basin. The structures in the northern parts of the Bondoc and Ragay Sub-basins are also associated with strong bottom-water anomalies.

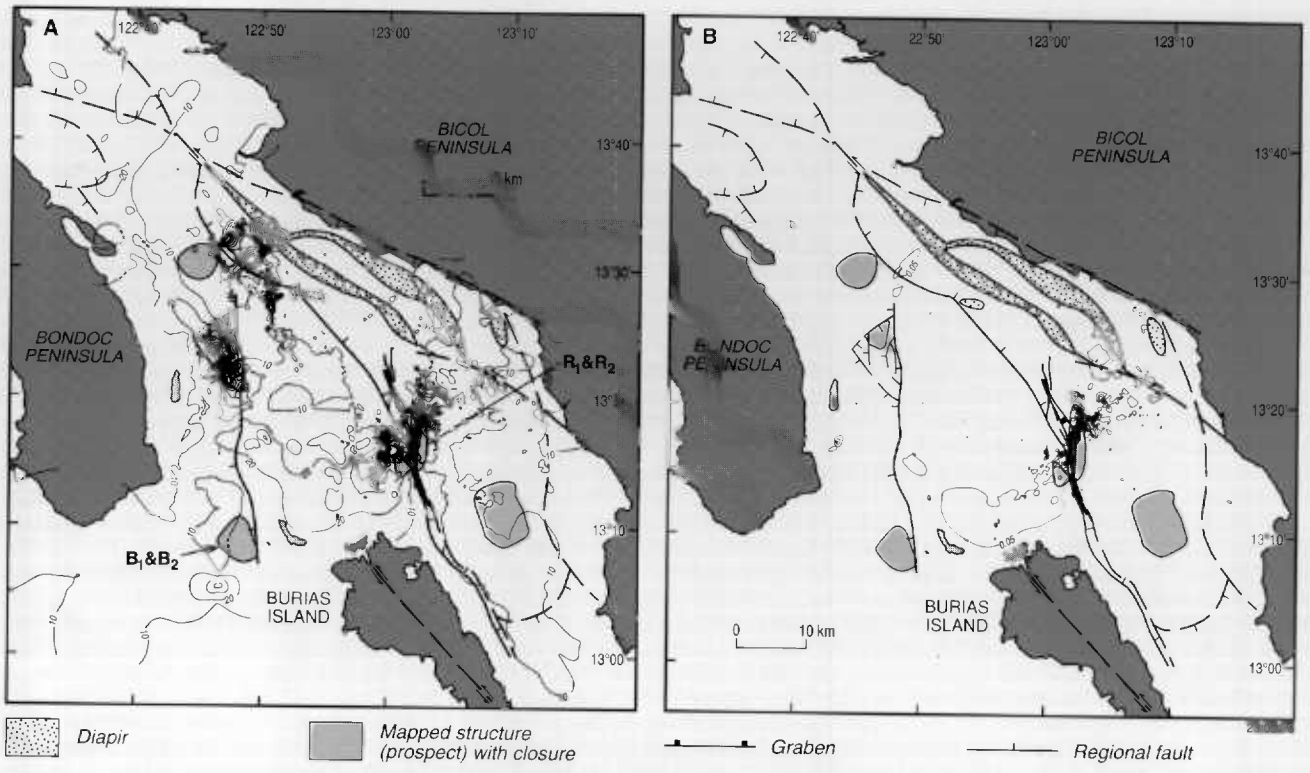

Figure 13 Geochemical contour maps of (a) methane > 10 ppm; (b) propane >0.05 ppm from the Ragay Gulf.

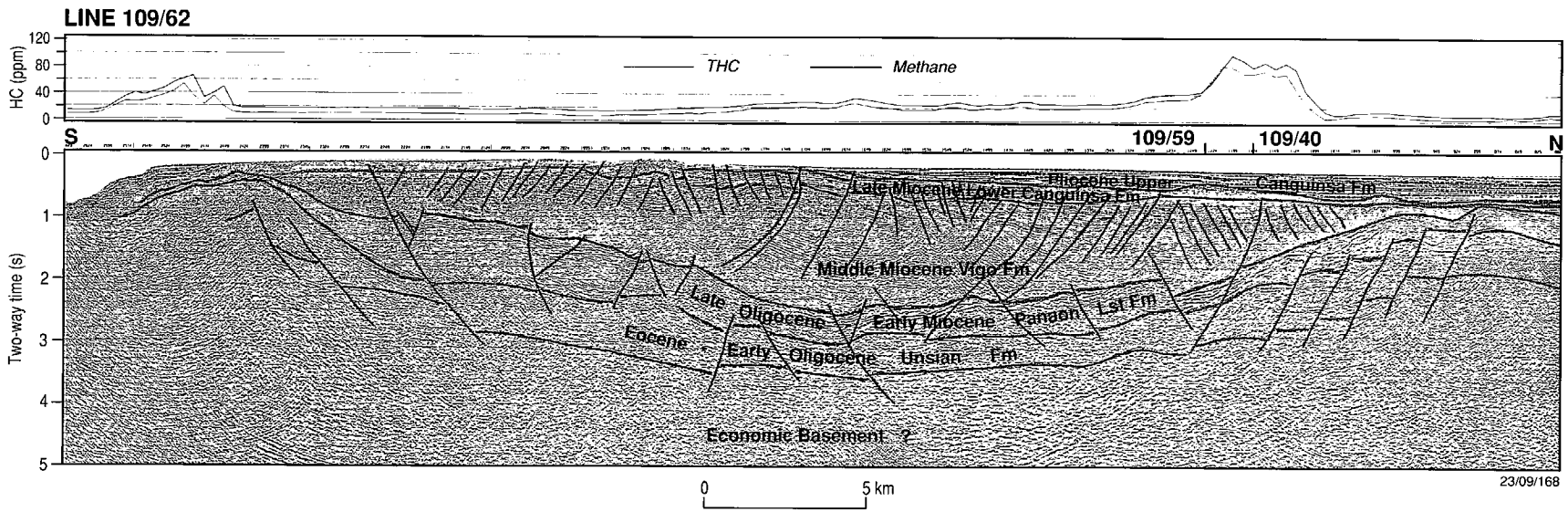

Figure 14 Combined seismic and DHD data from survey line 109/62 in the Bondoc Sub-basin. This line intersects both 109/59 and 109/40 in the northern sector near the strong anomaly.

However, in contrast, there is no obvious correlation between methane contours and the identified structure on Figure 13a in the far southeastern Ragay Sub-basin. This large structure, tentatively identified as a carbonate build-up, has only weak methane anomalies (< five-fold background), which are evident on lines 109/49 and 109/50. The significance of these weak anomalies associated with this structure are discussed below, but the seismic profiles suggest this structure may be relatively well-sealed, limiting hydrocarbon leakage from the reservoir into bottom-waters.

Contours of propane concentrations are shown in Figure 13b. In contrast to the methane contour plot, elevated levels of propane were found trending to the northeast over only part of the southeast Ragay Sub-basin and the Alabat-Burias High. The location of this trend suggests that the southeast sector of the Ragay Sub-basin is more condensate-to-liquids prone than the Bondoc Sub-basin or the northwest Ragay Sub-basin where no strong propane anomalies were found.

The following discussion relates bottom-water DHD anomalies to identifiable sub-surface geological features, and develops a conceptual model of hydrocarbon generation, migration and entrapment in the Ragay Gulf. The DHD anomalies, for purposes of identification, are referred to by the name of the hydrocarbon lead (mapped, described and named by Lee et al., Volume 1, Part 1; Table 5).

Bondoc Sub-basin. Two strong DHD anomalies were detected near the northern and southern flanks of the Bondoc Sub-basin, in the portion of the basin to the east of the Bondoc Peninsula (Figs. 3 & 14). In this area, the sub-basin is bounded by a structured platform, the Alibat-Burias High (Fig. 15). The Bondoc Sub-basin/Alibat-Burias High boundary is the East Bondoc Fault, which is interpreted as a compressional wrench-fault system. In north-south section, the Bondoc Sub-basin depocentre contains more than 5 km of sediments (3.5 sec. two-way time) overlying economic basement (Fig. 14). The oldest sequences in the basin are the Eocene-Early Oligocene Unisan Formation and the Late Oligocene-Early Miocene Panaon Limestone Formation, which appear to have been structured by normal faults. These are overlain by the Middle Miocene Vigo Formation, which onlaps the older sequences and appears to be a megasequence associated with rapid basin subsidence and development. The thickness of the Vigo Formation on Line 109/62 is comparable to that on the Bondoc Peninsula, where about 4700 m was recorded in outcrop.

Major deformation and uplift in the Bondoc Sub-basin took place in the late Middle Miocene. This is expressed as basin inversion, particularly along the Bondoc Peninsula, and is presumably a result of compressional wrenching of the basin fill created by left-lateral movement on basin boundary faults. This inversion is clearly evident on Line 109/62 (Fig. 14) where the Vigo Formation is affected by wrench faults, and has been uplifted and thrust over the basin margins, and then strongly eroded.

Arena DHD Anomaly The southern DHD anomaly on 109/62 is associated with prospects B1 and B2 (Figs. 3 & 13), previously identified in the World Bank Report (1986), and lies about 5 km south of the 'Arena Lead' as defined by Lee et al. (Volume 1, Part 1). The lead comprises several largely fault-dependent closures at the Top Panaon Limestone level, and possible buildups on the late Middle Miocene erosional surface. Overall, the structure is complex and associated with inversion of the southern flank of the basin. Several deep-seated faults and decollment planes may have provided migration conduits from source rocks within a kitchen area in the east Bondoc depocentre.

Table 5. Identified hydrocarbon Leads and the predominant chemical composition of DHD anomalies

Lead	Structural element	DHD anomaly
Gorda	Bondoc Sub-basin	'dry'
Arena	Bondoc Sub-basin	'dry'
San Narciso	flank of Alabat-Burias High and Ragay Sub-basin	'dry'
Anima Sola	Ragay Sub-basin	'wet'
Apud	Ragay Sub-basin	unpredictable

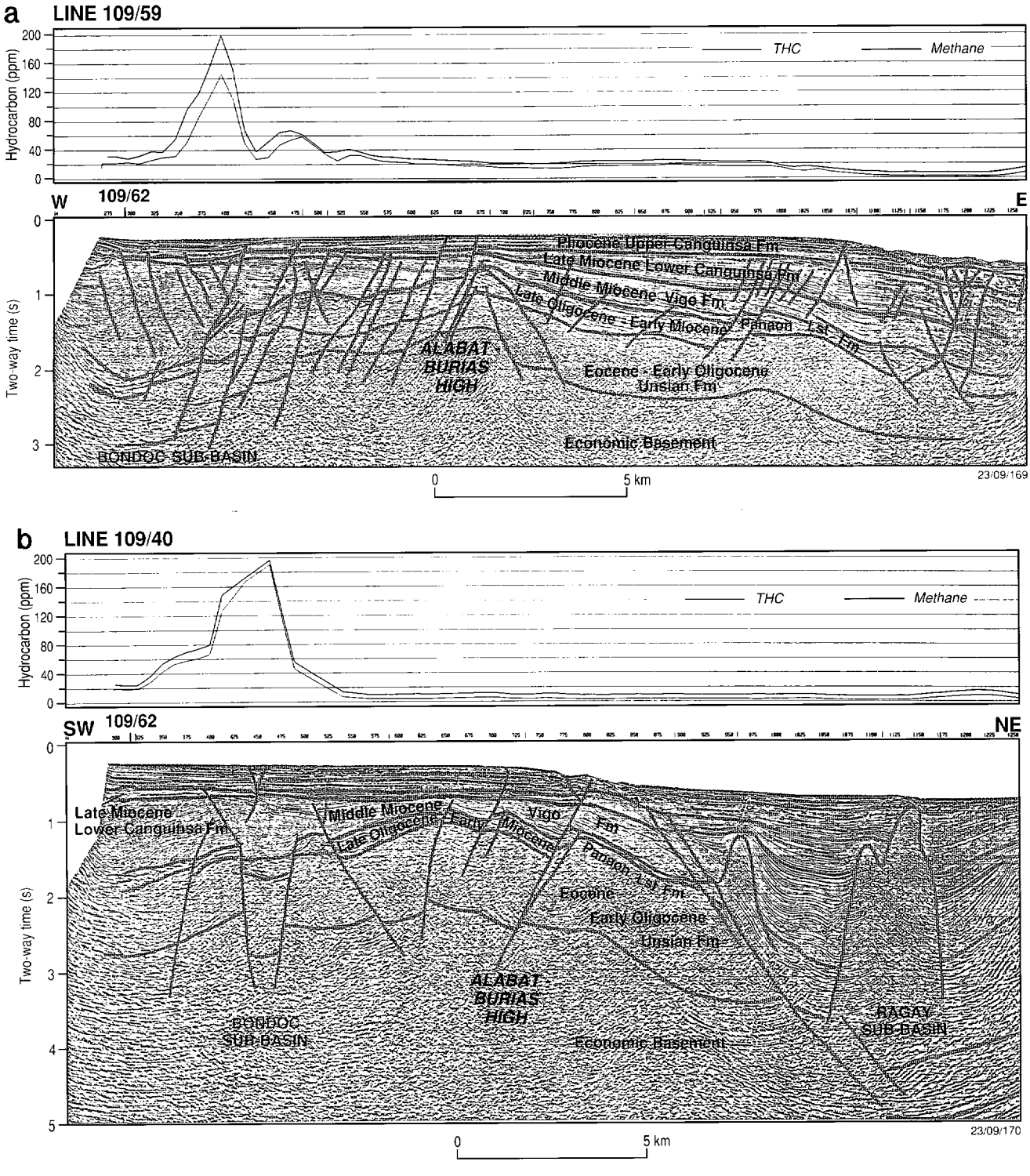

Figure 15 Combined seismic and DHD data from (a) survey line 109/59 in the Bondoc Sub-basin. This line intersects 109/62 at sp 1229 (shown); (b) survey line 109/40 which intersects 109/62 at sp 1171.

Gorda DHD Anomalies Anomalies to the north (see inset A of Fig. 4) were recorded on three intersecting lines (109/62;59;40; Figs 3, 14 & 15) near a closed structure mapped from the current AGSO seismic data, termed the 'Gorda Lead' by Lee et. al (Volume 1, Part 1). The anomalies are not directly over the structure, but are offset to the south where many minor faults are seen to extend close to the seafloor, providing potential pathways for escaping light hydrocarbons. An alternative explanation for the offset of the bottom-water anomalies and the structure is that the structural closure may be larger than mapped, and that the anomaly marks the location of a spill-point of a trap fully charged with hydrocarbons. It is also possible that the anomalies are associated with small unmapped structural traps charged with hydrocarbons along the northern boundary of the sub-basin.

Deep-seated faults separating the Bondoc Sub-basin from the Alabat-Burias High, and a relatively deeply buried (>2 secs) section of Panaon Limestone and thick Vigo Formation are characteristic of this part of the Bondoc Sub-basin (Fig. 15a). Major faults intersect source and reservoir intervals and penetrate close to the seafloor. At the southwest end of Line 109/40, up dip from Line 109/59, there are horst and graben structures which are bounded by faults intersecting potential source and reservoir horizons and providing possible hydrocarbon migration pathways to the seafloor. Strong anomalies detected on these lines are within the Bondoc Sub-basin and on the flank of the Alabat-Burias High, but there is no evidence for significant light hydrocarbon anomalies over the Alabat-Burias High proper (Fig. 15). These data suggest that hydrocarbons generated in the relatively deeply-buried potential source rock intervals (Middle Miocene Vigo Formation and Late Oligocene-Early Miocene Panaon Limestone) migrated towards traps on the flank of the Alabat-Burias High.

Five samples from the Gorda Lead anomalies were collected during the survey for isotopic analysis of the methane component. The radiocarbon content of three of these samples indicated a modern carbon content of less than 17%, and a predominantly fossil source of methane. The $\delta^{13}C$ of methane in the anomalies varies between -48.3 $o/_{oo}$ and -57.3 $o/_{oo}$, demonstrating the anomalies to be thermogenic, although one sample is close to the empirical distinction between thermogenic and biogenic methane (Fuex, 1977; Bernard et al., 1977; Schoell, 1983; Whiticar et al., 1986). All gas samples collected here for isotopic analyses are characterised by methane/[ethane+propane] ratios of greater than 1500, and represent a relatively 'dry' gas. Cross-plots for anomalies on lines 109/62,59 and 40 show a trend of decreasing hydrocarbon wetness with increasing methane and thus indicate 'dry' sources for these anomalies (Fig. 9).

The seismic and surface geochemical data jointly suggest a petroleum play which combines the Middle Miocene Vigo and older formations as potential source rocks with Late Oligocene to Early Miocene Panaon Limestone or equivalent carbonates as reservoirs, sealed by shales of the Vigo and Canguinsa Formations. Other potential reservoirs are the sands and conglomerates of the Vigo and Canguinsa Formations.

Ragay Sub-basin. The Ragay Sub-basin is a north to northwest-trending depocentre which extends for about 80 km along the eastern edge of Ragay Gulf. It contains similar sequences to those in the Bondoc Sub-basin, with a comparable total thickness of sediment. The main differences are that the potential source rock section, the Vigo Formation is generally thinner, whereas the Panaon Limestone is considerably thicker. The Ragay Sub-basin, like the Bondoc Sub-basin, is bounded by complex wrench zones - the Anima Sola Fault separating it from the Alabat-Burias High to the west, and the

Legaspi Lineament with its associated diapirs to the northeast (Fig. 3). The two sub-basins probably share a common history.

Within the Ragay Sub-basin and on the flank of the Alabat-Burias High there are four clearly identified leads which correlate broadly with DHD anomalies. These are shown in Figure 3 and include the 'San Narciso Lead', near the intersection of seismic lines 109/34 and 109/35 in the northwest; the 'Anima Sola Lead' on seismic lines 109/39P1, 109/42 and 109/58; an Alabat-Burias High lead to the west and south of the Anima Sola Lead in an area near the intersection of seismic lines 109/39P1, 109/33 and 109/41; and the 'Apud Lead' on seismic lines 109/49 and 109/50 in the far southeast.

San Narciso DHD Anomalies The strong anomaly detected on Line 109/34 which trends northeast across the area (Figs 3 & 16) is a distinctive feature. The elevated THC and methane concentrations on this line are detectable over a distance of about 8 km, and are positioned over a graben-like feature, bounded to the southwest by a wrench fault system which appears to have been active from the Eocene to the late Middle Miocene, and to the northwest by a complex fault zone which is associated with possible mud/shale diapirism (interpreted from the very low seismic interval velocities recorded in this area). The total sediment infill of the graben is of the order of 5 km (4.2 sec. reflection time). The potential source horizons, the Panaon Limestone and the Vigo Formation, are buried at depths ranging from 900 to 3600 m (0.7 to 2.9 sec.TWT). Faulting associated with the graben boundaries and the diapirs provides potential migration pathways for hydrocarbons to the seafloor. The highest THC concentration was found almost directly above where a major fault near the northeast boundary intersects the seafloor. The up-dip terminations of seismic horizons, against the flanks of the diapir/fault zone, may provide potential hydrocarbon traps. Molecular compositional data for this anomaly shows a strong trend of decreasing hydrocarbon wetness with increasing methane (up to about 100 ppm), and thus a 'dry' gas source for the hydrocarbons is predicted (Fig. 9).

A major bounding wrench-fault separates this part of the Ragay Sub-basin from the Alabat - Burias High. A DHD anomaly was detected over the Alabat-Burias High just south of the San Narciso Lead, on Line 109/35 near its intersection with the western end of Line 109/34 (Fig. 3). The molecular composition of this anomaly is mixed as it plots on trend lines (Fig. 9b) of both decreasing and increasing percent hydrocarbon wetness values with increasing methane (to about 30 ppm). However, the trend of increasing wetness with increasing methane is only weakly developed. Potential source rocks on the Alabat-Burias High are too shallow to have attained maturity and hydrocarbons were probably derived from deeply buried source horizons in the graben to the east, as evidenced by the anomaly on line 109/34. It is possible that hydrocarbons migrated to the area via the San Narciso Lead.

Five samples collected for isotopic analysis of the methane component had $\delta^{13}C$ contents between -41.7°/oo and -47.8°/oo, indicating a thermogenic origin. Methane/[ethane+propane] ratios ranged between about 900 and 3500 (Evans et al., 1992). These data suggest a relatively 'dry' thermogenic gas source for the anomalies, and are in agreement with that predicted from the cross-plot model (Fig. 9).

Anima Sola DHD Anomaly Another group of strong DHD anomalies in the Ragay Sub-basin were found at the intersection of AGSO Lines 109/42 and 58 (inset B, Fig. 3). A strong and extensive anomaly is evident on Line 109/42, over a distance of approximately 8 km (Fig. 17a), and is nearly coincident with one on Line 109/58 (Fig. 17b). The anomaly is associated with a prominent, largely fault-dependent closure along the central

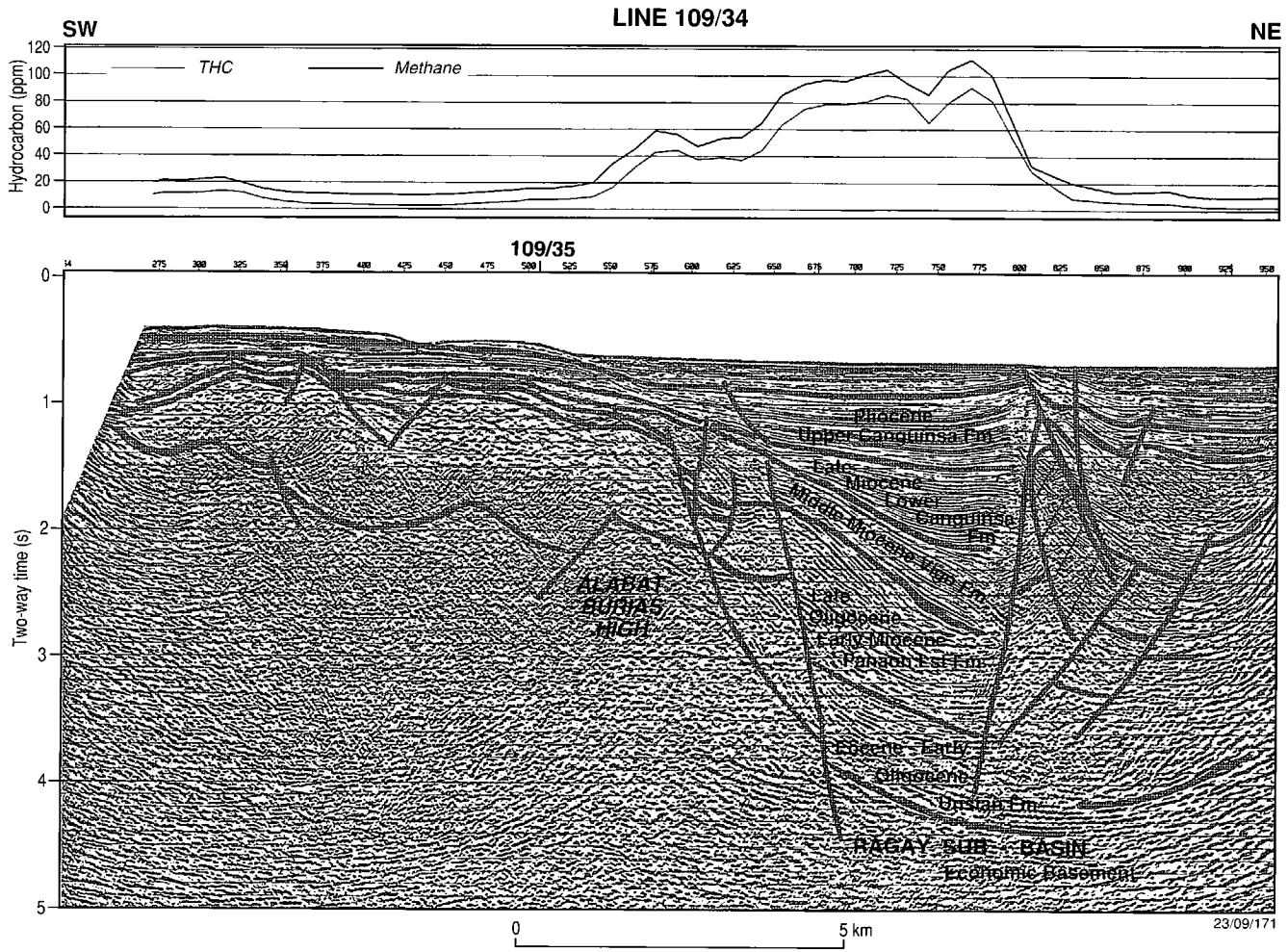

Figure 16 Combined seismic and DHD data from survey line 109/34 in the north-western Ragay Gulf, Ragay Sub-basin. This line intersects 109/35 where this same anomaly was detected (data not shown).

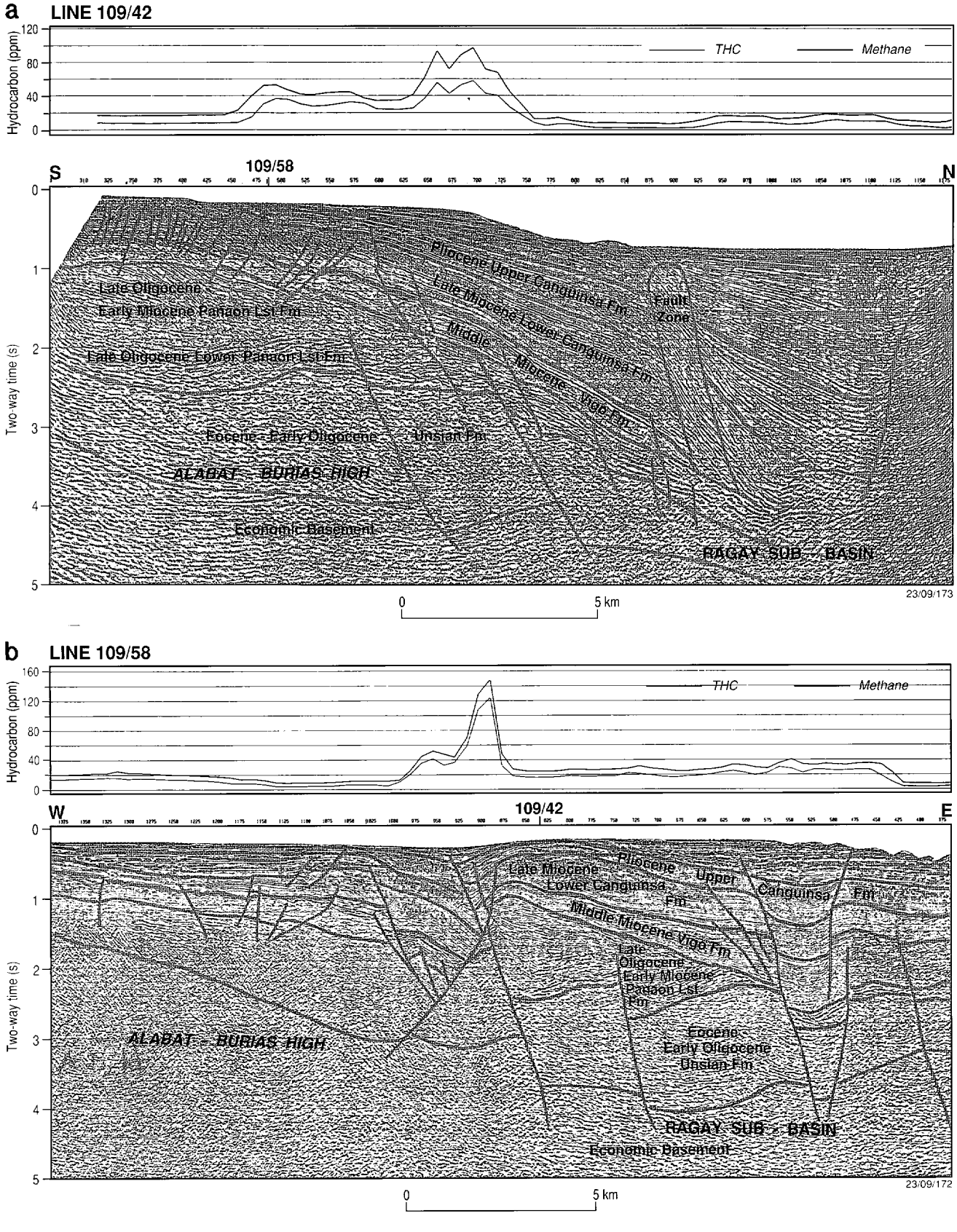

Figure 17 Combined seismic and DHD data from the southeastern Ragay Gulf, Ragay Sub-basin (a) survey line 109/58; (b) survey line 109/42.

western side of the sub-basin (Fig. 3) which Lee & others (Volume 1, Part 1) have termed the Anima Sola Lead. The Anima Sola structure is a large north-trending, compressional wrench-related, anticline/horst with about 3 km of east-west horizontal closure, and over 20 km of north-south closure along the trend of the Anima Sola Fault system which bounds it to the west. The structure has a vertical fault-independent closure of perhaps 200 to 300 m, but a fault-dependent closure as large as 700 to 900 m.

Line 109/58 shows a strong THC and methane anomaly, evident for about 4 km over the seafloor, directly above and to the west of the main wrench-fault system. Here, several smaller faults cut through the Late Miocene Canguinsa Formation and appear to extend almost to the seafloor (Fig. 7b). The Late Oligocene-Early Miocene Panaon Limestone and the Middle Miocene Vigo Formation are again the most likely source rocks. The Panaon Limestone is particularly thick in the Anima Sola structure (calculated at 1800 m), but quite thin to the east under the basinal axis. The Panaon Limestone sequence, as mapped by Lee et al. (1992), would thus appear to have been deposited in a major half-graben which was inverted mainly in the Late Miocene. The bounding fault to the west was reactivated by wrenching to produce the Anima Sola Fault system. The Panaon Limestone source lies at depths of 800 to 2500 m in the area of the structure, but is considerably deeper under the basinal axis (Fig. 10a). The Middle Miocene Vigo Formation, which is about 400 m thick in the Anima Sola structure, generally thickens towards the basinal axis, and its depth of burial ranges from 600 to 1700 m in the structure, to about 4000 m in the depocentre (Fig. 17b). The Anima Sola structure clearly lies up dip of the main Ragay Sub-basin depocentre and could be charged via lateral migration along the strata and vertical migration through fault conduits. There is also a likelihood of hydrocarbon migration from smaller depocentres lying to the west of the main structure (Fig. 17b).

The anomaly on 109/58 is associated with the northern part of the Anima Sola Lead (see inset B to Fig. 3), identified from the current seismic data, and also as prospects R1 and R2 from earlier data (World Bank Report, 1986). The coincidence of bottom-water anomalies and a closed sub-surface structure are indicative of hydrocarbon charge. Further east on Line 109/58, generally elevated levels of THC (up to 40 ppm), over distances of ten to twelve kilometres, were found over the Ragay Sub-basin and a small graben bounded by faults that extend to the seafloor. Notably, no anomalies were detected to the west over the Alabat-Burias High (Fig. 17b). Cross-plots (Fig. 9) show a dominant trend of increasing hydrocarbon wetness with increasing methane (up to about 250 ppm). The anomaly on line 109/58 and others in the area (Fig. 9) have some of the highest concentrations of C_{2+} hydrocarbons measured on the survey, with ethane and propane abundances sometimes exceeding 1 ppm (compared to background concentrations of approximately 0.02 ppm). This indicates a gas-condensate to liquids prone hydrocarbon source at depth. A weak trend of decreasing wetness with increasing methane (to about 70 ppm) was found for data from Line 109/58 over the Alabat-Burias High.

Samples collected for isotopic analysis of the methane component had $\delta^{13}C$ values between -38.8o/$_{oo}$ and -49.1o/$_{oo}$, indicating a thermogenic origin. Methane/(ethane+ propane) abundances varied between 1022 and 28, with most samples being less than 450. These data are consistent with the cross-plot model of hydrocarbon source above, and are in sharp contrast to those from the Bondoc Sub-basin (Arena and Gorda Leads), the northwestern Ragay near the diapirs to the east, and the San Narciso Lead on the flank of

the Alabat-Burias High where methane/(ethane + propane) abundances were consistently greater than 1000 and up to 3500. The Anima Sola Lead is associated with the only significant anomalies in the propane contour map (Fig. 13b).

Alabat-Burias High (southeast) Anomalies Four DHD anomalies were identified over the eastern flank of the Alabat-Burias High, two on line 109/39P1, and one each on 109/41 and 109/33 (Fig. 4). THC concentrations in excess of 80 ppm were measured in the two anomalies on line 109/39P1 (Fig. 18a). The anomaly to the east has abundant methane with significant amounts of ethane and propane (Table 2) and hydrocarbon wetness values exceeding 1%. It is located over a 'negative flower structure' associated with a wrench zone which separates two provinces (Fig. 18a). The anomaly is associated with the western edge of the Anima Sola Lead and the other relatively 'wet' anomalies with high propane concentrations (Fig. 13b). The other anomaly on 109/39P1, comprises abundant methane (approximately 60 ppm), but only trace ethane and no anomalous propane. It is located on the Alabat-Burias High itself, directly over a feature at about 600 m depth which has been interpreted as a possible carbonate platform, as indicated by a high amplitude reflector and an underlying chaotic seismic reflection character. This platform appears to lie within the Late Miocene Lower Canguinsa Formation (Fig. 18a). Faulting which extends through the near-surface sediments at both anomaly locations provide potential hydrocarbon migration pathways to the seafloor from a kitchen area within the flanking Ragay Sub-basin.

A strong anomaly was detected on Line 109/33 over about 8 km, in a position almost coincident with the relatively 'wet' anomaly described above (Figs. 3 & 18b), and over the southern edge of the Anima Sola Lead (Fig. 3). Data from lines 109/39P1 and 109/33, were collected nearly three days apart, which demonstrates that the anomalies are reproducible, at least over short time scales. The anomaly comprises moderate amounts of ethane, propane and butane and is consistent in molecular composition with other anomalies associated with the Anima Sola Lead. Data from 109/33 predominantly plot on the trend line of increasing hydrocarbon wetness with increasing methane (Fig. 9), thus indicating a gas-condensate to liquids hydrocarbon source.

Line 109/41, intersects lines 109/33 and 39P1 (Figs. 3 & 18c) and similarly shows a strong anomaly with THC greater than 180 ppm and methane greater than 130 ppm, but with only trace levels of ethane and propane. This line trends north-south and the anomaly is more clearly seen to be over the Alabat-Burias High and away from the influence of kitchen areas within the Ragay Sub-basin. The relatively 'dry' character of the anomaly is similar to that found on line 109/39P1 (Fig. 18a), and also the 'dry' component of the mixed anomaly found on line 109/33 (Figs. 3, 9 & 18b).

Cross-plots of hydrocarbon wetness versus methane from these lines show two trends (Fig. 9). One trend, observed in data from lines 109/33 and 109/39P1 shows increasing hydrocarbon wetness with increasing methane content associated with anomalies on the flank of the Alabat-Burias High near the Anima Sola Lead. This trend indicates a gas-condensate or liquids-prone source for hydrocarbons in the anomalies. The other trend, observed in data from lines 109/39P1, 109/33 and 109/41 over the Alabat-Burias High, shows decreasing hydrocarbon wetness with increasing methane, indicative of a 'dry' source of hydrocarbons. Samples collected for isotopic analysis from the Alabat-Burias High and its eastern flank all have $\delta^{13}C$ values between -37.80°/oo and -41.80°/oo indicating a thermogenic origin. The methane/[ethane+propane] ratios however varied over a wide range between 14 and 3250, with three samples having values less than 500

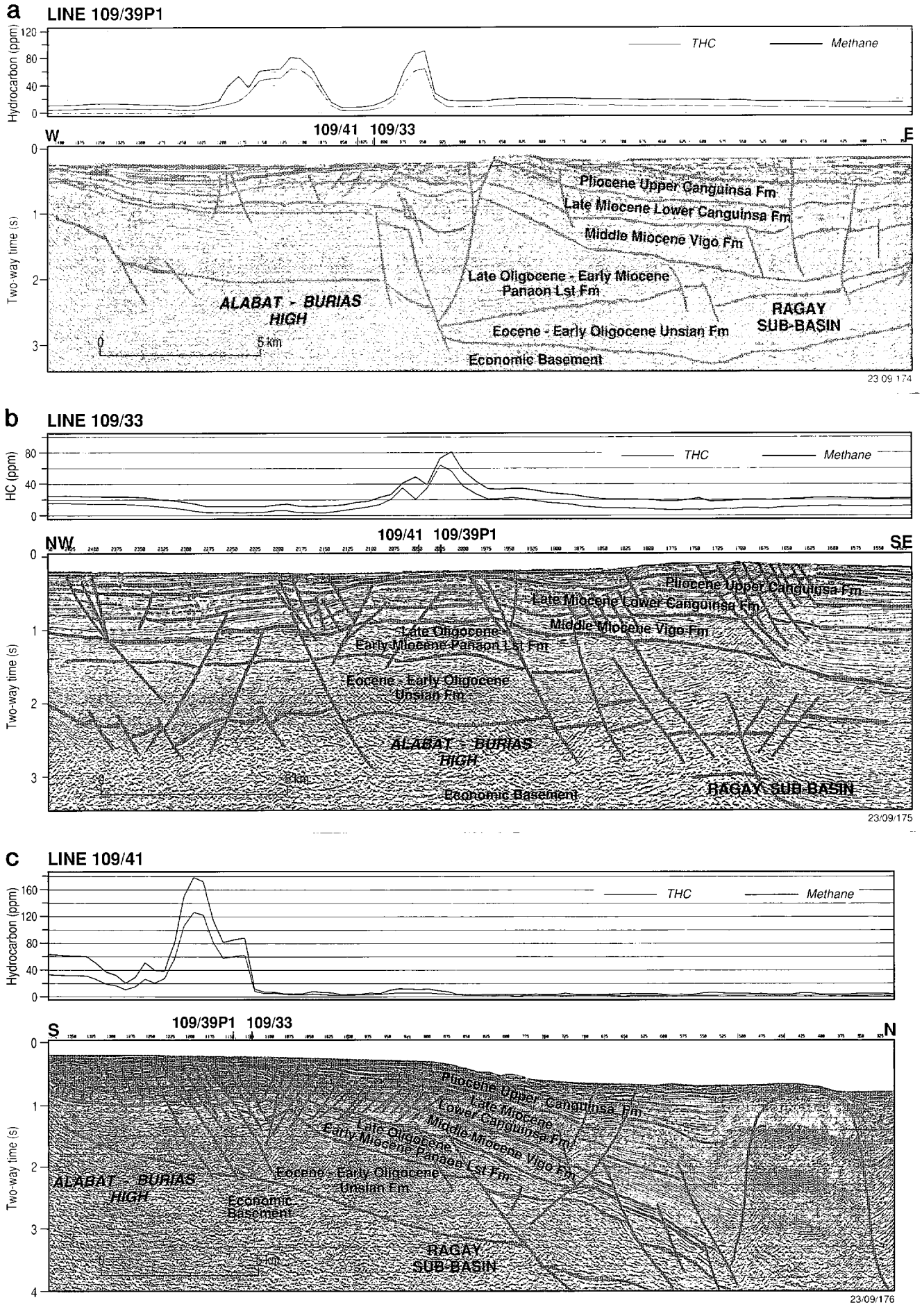

Figure 18 Combined seismic and DHD data from the southeastern Ragay Gulf, Ragay Sub-basin (a) survey line 109/39P1; (b) survey line 109/33; (c) survey line 109/41.

and two samples greater than 1000. These data are consistent with cross-plot data suggesting that anomalies over the Alabat-Burias High are of a mixed geochemical signature.

Apud Anomaly Within the southern part of the Ragay Sub-basin there is evidence of very weak but extensive DHD anomalies which might have been dismissed as insignificant, but which are possible indicators of hydrocarbon entrapment. These anomalies contrast sharply with the relatively strong features described above. As an example, lines 109/49 and 109/50 in the far southern part of Ragay Gulf (Fig. 3) showed evidence of very weak anomalies of less than three times the background concentration (Table 2). On Line 109/50, total hydrocarbons and methane increased from a background of about 16 ppm and 7 ppm respectively to concentrations of about 25 and 15 ppm. This very weak anomaly could be detected over a distance of 7 to 10 km and, from a data set of many strong anomalies, would not normally have been identifed as significant. The anomaly is dominated by methane and analysis of the data indicate a poorly defined trend of decreasing hydrocarbon wetness with increasing methane, suggesting a 'dry' gas source. However, it must be pointed out that for weak anomalies, the prediction of hydrocarbon source is speculative.

The anomaly is associated with a distinct, wrench-related, horst-type, structure of about 5 km extent (Fig. 19), with bounding faults which intersect the potential Panaon Limestone and Vigo Formation source horizons and thus provide viable migration pathways to the reservoir, the Late Miocene Lower Canguinsa Formation. However, this structure is apparently well sealed, with little evidence of significant faulting in the post Canguinsa sequences extending to the seafloor. This situation may have restricted hydrocarbon migration from the reservoir to bottom-waters. The significance of this observation for surface geochemistry, is that weak anomalies which are often overlooked when evaluating data, may be significant in detecting potential hydrocarbon habitats. Hence, the apparent strength of bottom-water anomalies is not necessarily an indicator of sub-surface prospects, and weak anomalies, detectable with high quality DHD data may be significant.

Conceptual Model of Hydrocarbon Generation, Migration and Entrapment in the Ragay Gulf

The preceding discussion has highlighted some correlations between the chemical compositions of anomalies and their locations within the structural elements of the Ragay Gulf. Figure 20 is an east-west cross-section taken from Lee et al (Volume 1, Part 1) of the Ragay Gulf, in the vicinity of survey line 109/58. This shows the Alabat-Burias High separating the Bondoc Sub-basin in the west and the Ragay Sub-basin in the east. Superimposed on the cross-section are the dominant wetness values of bottom-water anomalies found in the different sub-basins. The following observations can be made:

(1) Within the Bondoc Sub-basin, the potential source rock intervals - the Late Oligocene to Early Miocene Panaon Limestone and the Middle Miocene Vigo Formation - are buried at depths of about 4 km and 3 to 3.5 km respectively. Molecular compositions of the anomalies are dominated by high methane with only traces of ethane and propane, (methane/[ethane+propane] ratios >1500), thus indicating a 'dry' gas source. These observations are consistent with hydrocarbon generation from gas-prone or deeply buried source rocks in the Bondoc Sub-basin, and migration eastwards and up dip on to the flank of the Alabat-Burias High. Hydrocarbons there may be trapped in Panaon Limestone or equivalent carbonate reservoirs and sealed by shales of the Vigo and Canguinsa

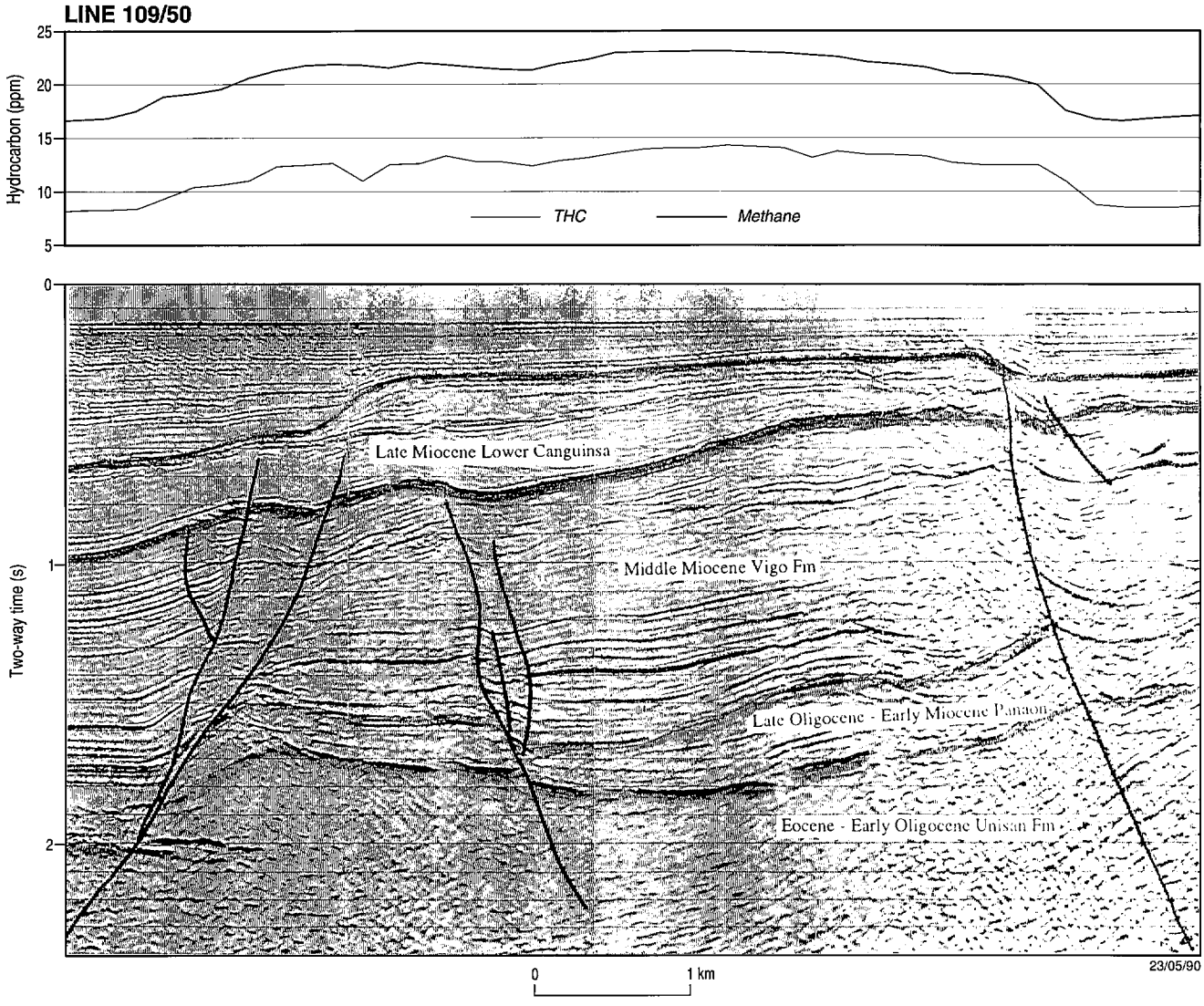

Figure 19 Combined DHD/seismic survey line 109/50 from the southern part of Ragay Sub-basin.

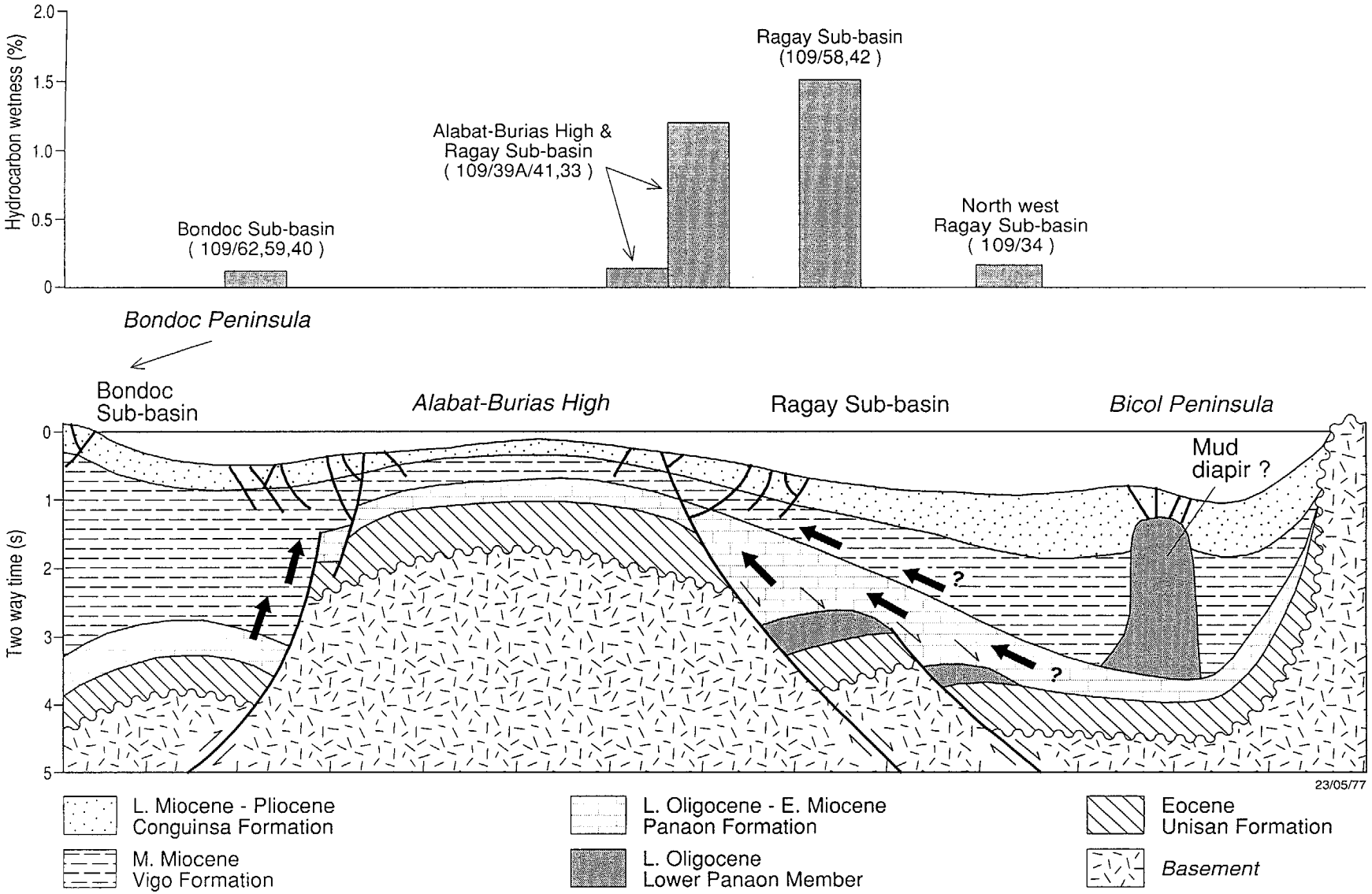

Figure 20 A schematised east-west cross-section of the Ragay Gulf (in the vicinty of survey line 109/58) showing the comparative thicknesses and depths of burial of the potential source rock horizons (the Middle Miocene-Vigo Formation and the Late Oligocene-Early Miocene Panaon Limestone). Also shown are the approximate percent hydrocarbon wetness values of the major anomalies found in each of the areas discussed in this text and plotted in their approximate structurally equivalent (not necessarily geographic) positions. Potential hydrocarbon migration pathways are shown with arrows.

Formations. Other potential reservoirs are sands and conglomerates of the Vigo and Canguinsa Formations.

(2) The anomalies detected over the Alabat-Burias High, particularly those on the eastern flank adjacent to the Ragay Sub-basin, were of a mixed chemical composition. Potential source rocks within the Alabat-Burias High are probably too shallow to have attained maturity, and hydrocarbons may have migrated from kitchen areas in the eastern Ragay Sub-basin. The relatively 'wet' anomalies in the sub-basin are consistent with a gas-condensate or liquids prone source in the Vigo Formation or Panaon Limestone, with lateral migration up-dip onto the Alabat-Burias High. The relatively 'dry' anomalies found over the Alabat-Burias High probably originate from either deeply-buried source rocks or gas-prone kerogen sources at comparatively shallow depth. A further possible explanation involves fractionation effects during migration, similar in concept to that for 'deep' migration described by Schoell (1983). Migrating 'dry' gas strips C_{2+} hydrocarbons from shallower source or reservoir horizons, such that the migrating gas mixture becomes progressively enriched in C_{2+} compounds.

(3) The southeastern Ragay Sub-basin, in contrast to the Bondoc Sub-basin, is characterised by relatively wet anomalies with methane/(ethane+propane) ratios of less than 500 and as low as 30. Potential source rocks - the Vigo Formations and the Panaon Limestone - are buried to shallower depths than they are in the Bondoc Sub-basin. This is the most probable explanation for the wet anomalies, although it is possible that source rocks in the Ragay Sub-basin are more gas-condensate to liquids prone than in the Bondoc Sub-basin.

(4) Predominantly dry anomalies were detected in the northwestern Ragay Sub-basin. This can be explained by the late maturity of potential source rocks which are buried to depths of more than 3.5 km, as in the Bondoc Sub-basin.

CONCLUSIONS

(1) Numerous light hydrocarbon anomalies were detected in the Ragay Gulf, many of which were more than an order of magnitude above typical background concentrations. Some anomalies near line intersections were resurveyed several days after first being detected, demonstrating that anomaly measurements are repeatable. Most anomalies are local features, being detected for distances of between 3 and 20 km over the seafloor.

(2) Analysis of the radiocarbon and isotopic composition of methane in the anomalies from Ragay Gulf indicates that anomalies are of thermogenic origin. The anomalies were found to be of two different chemical compositions, as indicated by a cross-plot model of percent hydrocarbon wetness versus methane content. Relatively 'dry' anomalies were identified comprising predominantly methane and only trace amounts of ethane and propane, with hydrocarbon wetness values of less than 0.2%. In contrast relatively 'wet' anomalies were found containing abundant methane and moderate amounts of ethane, propane and butane, having hydrocarbon wetness values of greater than 1%.

(3) Strong anomalies in the Ragay Gulf were found on the western flank of the Alabat-Burias High adjacent to the Bondoc Sub-basin, and on the eastern flank of the Alabat-Burias High adjacent to the the Ragay Sub-basin. Two different types of anomaly were detected in the Ragay Gulf. The Bondoc Sub-basin and the northwestern Ragay Sub-basin, where potential source rocks are buried to depths of more than 3 km, are characterised by relatively 'dry' geochemical anomalies. In contrast, the southeastern

Ragay Sub basin, where potential source rocks are considerably shallower, is characterised by relatively 'wet' anomalies. Anomalies detected over the Alabat-Burias High have both 'dry' and 'wet' characteristics.

(4) Anomalies were observed to be coincident with sub-surface features including half grabens, deep-seated faults, diapiric intrusions and possible carbonate platforms, several of which form stuctural closures. All strong anomalies (i.e. those more than ten times the background concentration) were associated with faulting that intersects potential source and reservoir horizons and extends close to the seafloor, providing hydrocarbon migration pathways from sub-surface hydrocarbon accumulations into bottom-waters.

(5) Comparison of DHD anomaly contours with seismic data suggests that previously identified prospects known as B1 and B2 (Arena lead) in the Bondoc Sub-basin and R1 and R2 in the Ragay Sub-basin are charged with hydrocarbons. Furthermore, new prospects associated with DHD anomalies were identified in other areas of the Bondoc Sub-basin (Gorda Lead), the Ragay Sub-basin (Anima Sola and Apud Leads) and the Alabat-Burias High (San Narciso Lead).

(6) Many strong DHD anomalies identified in the Ragay Sub-basin were found near the flanks of the Alabat-Burias High. These observations and consideration of the depths of burial of potential source rocks suggest that hydrocarbons are being generated in depocentres of the Bondoc and Ragay Sub-basins and are migrating towards leads identified on the flanks of the Alabat-Burias High.

(7) Consideration of the chemical composition of DHD anomalies and the depths of burial of potential source rock horizons in the Ragay Gulf, suggest the Ragay Sub-basin is more condensate-to-liquids prone than is the Bondoc Sub-basin.

(8) DHD anomalies were also detected in the Tayabas Bay, although these were generally weak-to-moderate and considerably fewer in number than those found in the Ragay Gulf. However, some anomalies were found within 10 km of the Tayabas Bay fault, a major regional fault of Late Pliocene to Recent development, and two anomalies in total hydrocarbons and methane were found adjacent to the Bondoc Point Flower Structure, a major compressive feature also of recent origin. Two anomalies in THC and methane were found in the east of Tayabas Bay, directly over the 'kitchen' area of the western Bondoc Sub-basin.

(9) DHD data from the Northeast Palawan Shelf showed few distinct and extensive anomalies. However, the Dumaran-1 exploration well was clearly identified on hydrocarbon -contour plots, as were the Paly-1 and Roxas-1 wells although these were only identified by very weak methane anomalies in the vicinity of the exploration wells. Within the Roxas survey area, a weak anomaly was found to coincide with the Roxas Lead, a broad, low relief anticline at Middle Miocene unconformity level. A weak ethane+ propane anomaly was found approximately 4 km to the south of the Honda Bay Lead, a closed structure identified at Top Cretaceous level.

(10) There were no distinct anomalies found over the Cuyo Platform, although the local background hydrocarbon levels appeared to be generally higher than those measured elsewhere. A very weak anomaly was found to be associated with the Manamoc Lead, a structural closure to the southwest of Manamoc Island.

REFERENCES

Alperin, M.J., Reeburgh, W.S and Whiticar, M.J., 1988. Carbon and hydrogen isotope fractionation resulting from anaerobic methane oxidation. *Global Biogeochemical Cycles*, 2, 279-288.

Barker, J.F. and Fritz, P., 1981. Carbon isotope fractionation during microbial methane oxidation. *Nature*, 293, 289-291.

Bernard, B. B., Brooks, J. M. and Sackett, W. M., 1976. Natural gas seepage in the Gulf of Mexico. *Earth and Planetary Science Letters*, 31, 48-54.

Bernard, B.B., Brooks, J.M. and Sackett, W.M., 1977. A geochemical model for characterisation of hydrocarbon gas sources in marine sediments. *In: 9th Offshore Technology Conference, Houston, Texas,* OTC 2934, 435-438.

Bosum W., Fernandez, J., Kind, E. and Terdro, C., 1971. Aeromagnetic survey of the Palawan-Sulu offshore area of the Philippines. *UNECAFE, CCOP Technical Bulletin*, 6, 141-90.

Brooks, J. M. Gormly, J. R and Sackett, W. M., 1974. Molecular and isotopic composition of two seep gases from the Gulf of Mexico. *Geophysical Research Letters*, 1, 213-29.

Burke, R.A. jr., Reid, D.F., Brooks, J.M. and Lavoie, D.M., 1983. Upper water column methane geochemistry in the eastern tropical North Pacific. *Limnology and Oceanography*, 28, 19-31.

Burke, R.A. jr and Sackett, W.M., 1986. Stable Hydrogen and carbon isotopic compositions of biogenic methane from several shallow aquatic environments. In: *ACS Symposium Series No. 305. Organic Marine Geochemistry* (ed. M. L. Sohn), the American Chemical Society.

Claypool G. E. and Kvenvolden, K. A., 1983. Methane and other hydrocarbon gases in marine sediment. *Annual Review of Earth and Planetary Science*,11, 299-327.

Coleman, D.D., Risatti, J.B. and Schoell, M., 1981. Fractionation of carbon and hydrogen isotopes by methane-oxidising bacteria. *Geochimica et Cosmochimica Acta*, 45, 1033-1037.

Cortez, E. and Murray, A., 1993. New hydrocarbon geochemistry of oil and gas seeps from Bondoc and Bicol, SE Luzon Basin. Unpublished Report Australian Geological Survey Organisation, Canberra, Australia.

Evans, D., Heggie, D.T., Bishop, J.H., Reyes, E.N. and Lee, C.S., 1993. Light hydrocarbon geochemistry in bottom-waters of the Philippines continental shelf, Rig Seismic Survey 109. *Australian Geological Survey Record*, 1992/92.

Fuex, A. N., 1977. The use of stable carbon isotopes in hydrocarbon exploration. *Journal of Geochemical Exploration* 7, 155-188.

Galloway, M. C., Lee, C.S. and Rillera, F. G., 1992. Australian *R/V Rig Seismic* survey of the Philippines: a precursor to renewed exploration. *9th Offshore South east Asia Conference Reprints*, 715-719.

Hamilton, W., 1979. Tectonics of the Indonesian region. *US Geological Survey Professional Paper*, 1078, 345p.

Heggie, D.T., O'Brien, G. W., Bickford, G.P., Bishop, J.H. and Hartman, B., 1991a. Direct Hydrocarbon Detection in bottom-waters of the Australian continental margin: application to offshore hydrocarbon exploration. *Petroleum Exploration Society Australia Journal*, 19, 75-91.

Heggie, D.T., O'Brien, G. W., Bickford, G.P. and Bishop, J.H., 1991b. Surface geochemistry and offshore hydrocarbon exploration on the Australian continental margin: a status report. In: Aribert-Christ, R. P. et al., eds, Technical papers presented at the *First Offshore Australia Conference*, held in Melbourne 25-27 November, 1991, Australian Exhibition Services., Melbourne, Australia.

Hunt, J. M., 1979. *Petroleum Geochemistry and Geology*, Freeman & Co, San Francisco., 617p.

Lee, C. S., Trinidad, N. D. and Galloway, M. C., 1992. A preliminary result for the Ragay Gulf survey: stratigraphy, seismic and geochemistry. Proceedings of the Plenary Session on the Geo-energy Technical Papers, Geological Society of the Philippines, 23p.

Lee, C. S. and Ramsay, D., 1992. Philippines Marine Seismic Survey Project Cruise Report. *Bureau of Mineral Resource, Australia Record*, 1992/49, 69p.

Lowe, D. C., Brenninkmeijer, C.A.M., Tyler, S.C. and Dlugokencky, E.J., 1991. Determination of the isotopic composition of atmospheric methane and appliction in the Antarctic. *Journal of Geophysical Research*, 96, 15,455-15,467.

Lowe, D.C. and Judd, W.J., 1987. Graphite target preparation for radiocarbon dating by accelerator mass spectrometry. *Nuclear Instrumentation Methods of Physical Res*earch, B28, 113-116.

Oremland, R.S. and DesMarais D., 1983. Distribution, abundance and carbon isotopic compositions of gaseous hydrocarbons in Big Soda Lake Nevada: An alkaline, meromictic lake. *Geochimica et Cosmochimica Acta*, 47, 2107-2114.

Oremland, R. S., Miller, L. G., and Whiticar, M. J., 1987. Sources and flux of natural gases from Mono Lake, California. *Geochimica et Cosmochimica Acta*, 51, 2915-2929.

Owens, N.J.P., Law, C.S., Mantoura, R.F.C., Burkill, P.H. and Llewellyn, C.A., 1991. Methane flux to the atmosphere from the Arabian Sea. *Nature*, 354, 293-296.

Primrose, S. B. and Dilworth, M. J., 1976. Ethylene production by bacteria. *Journal of General Microbiology*, 93, 177-181.

Reitsema, R.H., Lindberg, F.A. and Kaltenback, A. J., 1978. Light hydrocarbons in Gulf of Mexico water: sources and relation to structural highs. *Journal of Geochemical Exploration*, 10, 139-151.

Reitsema, R. H., Kaltenback, A. J. and Lindberg, F.A., 1981. Source and migration of light hydrocarbons indicated by carbon isotopic ratios. *American Association of Petroleum Geologists Bulletin*, 65, 1536-1542.

Sackett, W. M., 1977. Use of hydrocarbon sniffing in offshore exploration. *Journal of Geochemical Exploration*, 7. 243-254.

Schiener, E.J., Stober, G. and Faber, E., 1985. Surface geochemical exploration for hydrocarbons in offshore areas - principles, methods and results. In: Thomas, B.N. et al (eds), *Petroleum geochemistry in exploration of the Norwegian Shelf*. Norwegian Petroleum Society, Graham and Trotman Ltd, London, 223-238.

Scranton, M.I. and Brewer, P. G., 1977. Occurrence of methane in the near-surface waters of the western subtropical North-Atlantic. *Deep-Sea Research*, 24, 127-138.

Schink, D. R., Guinasso, N. L. Jr., Sigalove, J. J. and Cima, N. E., 1971. Hydrocarbons under the sea - a new survey technique. *3rd Annual Offshore Technology Conference*, Houston, Texas, OTC 1139, 1-15.

Schoell, M., 1983. Genetic classification of natural gases. *American Association of Petroleum geologists Bulletin*, 67, 2225-2238.

Schoell, M., 1984a. Recent advances in petroleum isotope geochemistry. *Organic Geochemistry*, 6, 635-663.

Schoell, M., 1984b. Stable isotopes in petroleum research. *Advances in petroleum geochemistry*, 1, 215-245.

Sigalove, J. J. and Pearlman, M. D., 1975. Geochemical seep detection of offshore oil and gas exploration. *7th Annual Offshore Technology Conference, Preprints*, 95-102.

Sigalove, J.J., 1985. Geochemical identification of resource potential. *Oil and Gas Journal*, March 18, 164-168.

Tissot, B. P. and Welte, D. H., 1984. *Petroleum Formation and Occurrence*. Springer-Verlag, New York., 697p.

Whiticar, M.J. and Faber, E., 1986. Methane oxidation in sediments and water column environments - isotope evidence. *Organic Geochemistry*, 10, 759-768.

Whiticar, M. J., Faber, E. and Schoell, M., 1986. Biogenic methane formation in marine and freshwater environments: CO2 reduction vs acetate fermentation-isotope evidence. *Geochimica et Cosmochimica Acta*, 50, 693-709.

World Bank Report, 1986. Sedimentary Basins of the Philippines : Their Geology and Hydrocarbon Potential. *A 12-volume Special Report to the Bureau of Energy Development*, Robertson Research Australia Pty. Ltd., and Flower Doery Buchan Pty. Ltd.

7 Colour Figures

APPENDIX 6

PALYNOLOGICAL ANALYSIS OF SAN FRANCISCO-1 AND KATUMBO CREEK-1, BONDOC SUB-BASIN, LUZON ISLAND

by

A. D. Partridge[1]

1 School of Earth Sciences, La Trobe University, Bundoora, Victoria, Australia

ABSTRACT

Twenty samples comprising a composite section, of Early Miocene (or possibly latest Oligocene) to Pleistocene age, from the wells San Francisco-1 and Katumbo Creek-1 have been analysed by palynology with the aim of improving the age datings, correlations and the understanding the evironment of deposition of the Neogene sequence in the Bondoc Sub-basin being investigated by the Philippines Seismic Survey Project. The samples were also analysed for their thermal maturation based on spore-pollen colour (or carbonisation) and a visual estimate of kerogen types was made to aid the organic geochemical evaluation of the sequence to determine hydrocarbon source potential.

The samples comprise two core and 10 cuttings samples from San Francisco-1 between 300-6860 ft covering a sequence of Middle Miocene to Pleistocene in age and 8 cuttings samples from Katumbo Creek-1 between 4700-6400 ft representing a sequence of possible Late Oligocene, but more likely Early Miocene to earliest Middle Miocene age. These ages are based on the analysis of planktonic foraminifera.

Because of the low sample size (average <7 grams/sample) the recovery of palynological residues was low to very low from a majority of samples. This combined with overall low palynomorph concentrations in the residues, and their generally poor preservation in samples below 3000 ft, has meant that the diversity of the palynomorph assemblages could only be partially recorded. In particular the miospore marker taxa for the standard palynological zonation schemes used in the Southeast Asian Cenozoic (eg. Germeraad *et al.*, 1968; Morley, 1978, 1990) where so rarely recorded that they are of little practical biostratigraphic value in these wells.

Overall the palynological assemblages from the Miocene were dominated by fungal spores, fruiting bodies and other fungal remains (average >66% of total palynomorph count) whilst the two Pliocene/Pleistocene samples were dominated by monolete spores (average >42%). Marine palynomorphs are represented by chitinous microforaminiferal tests and dinoflagellate cysts. Although recorded in nearly all samples they are never abundant or diverse enough to be of immediate biostratigraphic value.

No clear age correlation of the Neogene sequence in these two wells could be made to established palynological zonations due mainly to difficulties caused by low yields, low palynomorph concentrations, rarity or absence of established spore-pollen index species and rarity and low diversity of dinoflagellates. Palynology nevertheless has potential to improve local correlation within the Bondoc Sub-basin by utilising the rich assemblage of fungal spores and fruiting bodies recorded as well as some of the characteristic monolete fern spores found. When and if these are recorded in other basins in Southeast Asia they may have potential for regional age dating.

The palynological assemblages are interpreted to represent predominantly marine environments in which sediments derived overwhelmingly from terrestrial sources are deposited at relatively high depositional rates. The palynological assemblages are broadly similar but of relatively low diversity compared to other tropical sequences. This is interpreted to imply the regional diversity is diluted by local palynomorphs as a by-product of the relatively high depositional rates. No estimate of palaeobathymetry can be made from the palynology assemblages nor can it be determined from the two sequences examined how far offshore the depositional sites are located.

The kerogen analysis shows the particulate organic matter in the samples is dominated by terrestrially derived kerogen which would traditionally be interpreted as a gas prone source. However as much of the kerogen is also biodegraded to form more amorphous like kerogen significant oil source potential is indicated. The maturation analysis based on spore-pollen colour further suggests the section below about 3500 ft in both wells would be mature enough to have been, or currently be, generating hydrocarbons.

CONTENTS

INTRODUCTION..... 7

SAMPLE PREPARATION..... 8

PALYNOMORPH YIELDS..... 12

CHARACTER OF PALYNOLOGY ASSEMBLAGES..... 12

PALYNOLOGICAL ZONATION AND AGE..... 15

PALAEOENVIRONMENT..... 17

KEROGEN TYPES AND MATURATION..... 18

CONCLUSIONS AND RECOMMENDATIONS..... 22

REFERENCES..... 24

APPENDIX 1 Palynomorph Species List
APPENDIX-2 Catologue List - San Francisco-1
APPENDIX-3 Catologue List - Katumbo Creek-1

PLATE 1 Fungal Fruiting Bodies
PLATE 2 Fungal Spores
PLATE 3 Monolete Spores
PLATE 4 Trilete Spores
PLATE 5 Pollen
PLATE 6 Marine Palynomorphs
PLATE 7 Interpreted Modern Contaminants in Cuttings

San Francisco-1 Palynomorph Range Chart
Katumbo Creek-1 Palynomorph Range Chart

INTRODUCTION

This report concerns an initial or reconnaissance palynological analysis of the age and environment of deposition and visual kerogen analysis of the Neogene sequence in the onshore portion of the Bondoc Peninsula in southeast Luzon Island. The analysis is based on 12 samples from San Francisco-1 between 300-6860 ft covering a sequence from the Middle Miocene to Pleistocene and 8 samples from Katumbo Creek-1 between 4700-6400 ft representing a sequence of possible Late Oligocene to earliest Middle Miocene age.

The study is part of the Philippines Marine Seismic Survey Project, a co-operative venture between the Australian Geological Survey Organisation and the Philippine Office of Energy Affairs funded by the Australian International Development Assistance Bureau. Reviews of the project are provided by Chao-Shing Lee *et al.* (1992) and Galloway *et al.* (1992).

The potential for palynology to provide new information to the project which could have exploration significance was initially discussed at meetings with Dr Chao-Shing Lee and Dr Malcolm C. Galloway on 11 November 1992. A review of the palaeonological data available to the project at that time showed that ages were mostly based on planktonic foraminifera which were presented as single page summaries of either zones or first and last appearance datums. Subsequently a foraminiferal range chart was provided from San Francisco-1. This showed the foraminiferal analysis was based on 132 cuttings samples at 50 ft intervals between approximately 200-6600 ft. A total of 43 species of planktonic foraminifera and a restricted list of 7 species of benthonic foraminifera were recorded. Average diversity was less than 6 species of planktonic foraminiferal per sample. Environmental interpretations were based on these foraminiferal assemblages and associated lithological data. Other palaeontological data also appears to have been used for the environmental interpretation but the fossil species are not recorded. Overall, this appears to be a reasonably comprehensive micropalaeontological analysis of San Francisco-1. However, well correlations based on this data show only moderate agreement with the lithological and log correlations. The lack of distinct lithological contrast and distinctive markers on the electrics log has proved to be a troubling feature of the basin (Galloway, in prep.).

Against this background palynology was suggested as an alternative biostratigraphic tool which might generate new ideas, and the project was outlined in a letter (18 November 1992). It was proposed to study a limited number of samples over the Neogene sequence penetrated in selected wells to test the possibility that one of several palynomorph groups would provide useful biostratigraphic correlations. In particular dinoflagellate cysts were to be targeted as they have been demonstrated to be extremely useful in Mesozoic and Cenozoic near-shore marine to non-marine sequences.

Prior to the study it was stressed that the published palynological zonations for Southeast Asia were based on spores and pollen and typically rely on only a relatively few spore-pollen taxa with recorded stratigraphic significance. The individual zones also cover longer time intervals than the equivalent planktonic foraminiferal zones. The most recent discussions of the spore-pollen zonations are by Morley (1990) and Watanasak (1990). In other works Poumot (1989) provides examples of more detailed environmental correlations that can be obtained by palynomorph counts, whilst van Gorsel (1988, p.279) hints at more refined zonations as yet unpublished. To the north of the Philippines

considerable palynological work has been done on basins in China and under the continental shelf of the South China Sea. Unfortunately the published literature is mostly in Chinese and has not yet been translated into English. It is also difficult to obtain and has not been comprehensively reviewed for this project. The principal references referred to during this study are Sun Xiang-jun *et al.* (1981) and He Cheng-quan & Li Peng (1981) on the northern South China Sea; and Song Zhi-cheng (1988), Song Zhi-cheng & Zhong Bi-zhen (1984) and Zhu Zunghao *et al.* (1985) all concerning sequences from mainland China. In general these papers deal with palynological successions which contain spore-pollen assemblages derived from more temperate floras.

In summary the study proposed to record and document all palynomorphs groups in the samples that could have biostratigraphic and environmental significance besides just spores and pollen. It was anticipated dinoflagellate cysts, algae, fungal spores and hyphae, microforaminiferal liners or inner tests and scolecodonts could give age or environmental information.

SAMPLE PREPARATION

The samples were received on 12 May 1993, and shipped to Laola Pty Ltd in Perth for processing to prepare both kerogen and oxidised slides. The former slides were for determination of organic types and maturation, the latter to better concentrate the palynomorph assemblages.

Tables-1 & 2 provide the basic data on the samples. A minimum of 1.6 grams to a maximum of 13.7 grams of sample were provided from the cuttings and slightly higher 13.6 to14.3 grams of sample were provided from the two core samples. The eight cuttings from Katumbo Creek-1 averaged a low 4.2 grams per sample. The ten cuttings from San Francisco-1 averaged 7.6 grams and the two core samples 13.9 grams.

The quality of the samples was poor to fair. In San Francisco-1 some of the cuttings were distinctly bimodal in grain size suggesting the possibility of a significant caved fraction whilst others were contaminated by modern plant fragments and seeds which may have been drilling mud additives. This modern contamination was removed from the samples by flotation prior to processing. Nevertheless, some contamination from modern plant materials was recorded in the palynological slides. The Katumbo Creek-1 cuttings were all very fine grained (most <1mm) and because of this it was difficult to evaluate if they were significantly contaminated.

In the palynological preparation procedures the initial breakdown of the sediment was by acid treatment using dilute HCl, then by concentrated HF which was followed by density separation using Zn Br_2 solution to float off the released organic matter from any remaining undigested mineral matter. Kerogen slides were then prepared and the remaining residue oxidised using Schulze solution followed by treatment with dilute NH_4OH. The residues were then filtered (sieved) to increase the concentration of palynomorphs prior to the preparation of the oxidised slides.

TABLE 1 Basic Sample Data San Francisco-1

Sample Type	Depth (Feet)	Sample	Cuttings Grain-Size	Lithology
Cuttings	300-20		Clumped indet.	Gluggy claystone.
Cuttings	900-10		1-3mm	Lt. grey fossiliferous lst 60%, med. grey claystone 40%.
Cuttings	1700-10		70%<1mm 30%>1mm	Brown-grey clay-siltstone 90%, lt. grey-white limestone 10%.
Cuttings	2020-30		60%<1mm 40% 2-4mm	Fine matrix of clay to sand 60%, mixed with grey shale splinters 40% which may be caved.
Cuttings	2500-10		1-5mm evenly distributed	Grey-brown silt-claystone.
Core-1	2909		Large pieces	Lt. brown claystone.
Core-2	3907.5		Large pieces	Med. grey brown claystone with carbonaceous flecks <3%.
Cuttings	4560-70		<1-3mm	Mixed lithic and quartz <35% sandstones.
Cuttings	4970-80		Bimodal <1mm and 1-3mm	Mostly fine lithic sandstone <60%, siltstone/claystone 30% (possibly caved) and 10-20% contamination comprising modern seeds and plant material.
Cuttings	5520-25		70% 1-5mm	Med. grey lithic sandstone 80%, claystone 20%.
Cuttings	6390-95		90%<2mm	Mixed lithic sst, clayst, siltstone similar to above with 10% modern plant contamination.
Cuttings	6860-65		30% 2-7mm rest <2mm	Claystone 60%, lt. grey sandstone 30% and modern plant contamination >10%.

TABLE 2 Basic Sample Data Katumbo Creek-1

Sample Type	Depth (Feet)	Sample	Cuttings Grain-Size	Lithology
Cuttings	4700-20		All <1mm	Mixed lithic sandstone 50%, shale/claystone 50%.
Cuttings	5000		Most <0.5mm	Very fine lithic sandstone.
Cuttings	5390		<1mm	Mostly claystone >70%, minor lithic sandstone.
Cuttings	5740		0.5-1.5mm	Dark grey shale 90% with probably caved white limestone 5% and lithic sandstone 5%.
Cuttings	5910		<1mm	Claystone 50%, lithic sandstone 50%.
Cuttings	6240		<1mm	Shale 70%, quartz sand 20%, white limestone 10%.
Cuttings	6340		<1.5mm	Grey shale 75%, mixed sands 20%, white lst 5% with trace <1% of carbonaceous or coaly grains.
Cuttings	6400		<1mm	Shale 65%, lithic sands 20%, light grey-white lst 15%.

TABLE 3 Basic Palynomorph Data for San Francisco-1

Sample Type	Depth (feet)	Residue Yield	Palynomorph Concentration	Preservation	Comment
Cuttings	300-20	Very low	Moderate	Fair-good	Sample very small
Cuttings	900-10	Low	Low	Fair-good	Small sample.
Cuttings	1700-10	High	High	Fair-good	Probably contaminated
Cuttings	2020-30	High	High	Fair-good	Probably contaminated.
Cuttings	2500-10	High	Moderate	Fair-good	Moderate contamination
Core-1	2909	High	Low-moderate	Poor-good	Dominated by fungii.
Core-2	3907.5	High	Low	Poor-fair	Dominated by fungii.
Cuttings	4560-70	Low	Moderate	Poor-fair	Yield low due to sandy lithology
Cuttings	4970-80	High	Low	Poor	Dominated by fungii.
Cuttings	5520-25	High	Low	Poor-good	Light spore-pollen probably contaminants.
Cuttings	6390-95	High	Low	Poor	Fossils sparse in oxidised slides.
Cuttings	6860-65	High	Low	Poor	Dominated by fungii.

TABLE 4 Basic Palynomorph Data for Katumbo Creek-1

Sample Type	Depth (feet)	Residue Yield	Palynomorph Concentration	Preservation	Comment
Cuttings	4700-20	Very low	Very low	Poor	Sample very small.
Cuttings	5000	Very low	Low	Poor	Unfavourable lithology.
Cuttings	5390	Low	Very low	Poor	Sample very small.
Cuttings	5740	High	Moderate	Poor-Fair	Good yield from dominant lithology even though sample small.
Cuttings	5910	Very low	Low	Poor	Unfavourable lithology.
Cuttings	6240	Low	Low	Poor	Largest sample in well but yield poor.
Cuttings	6340	Very low	Low	Poor	Preservation becoming a problem.

PALYNOMORPH YIELDS

Organic residue yields, concentration of palynomorphs on the slides and their state of preservation are summarised on Tables-3 & 4. From San Francisco-1 good yields were obtained from the majority of samples except for the two shallowest cuttings from which only minimal sample was available, and the cuttings at 4560-70 ft whose low yield reflects its predominantly quartz sandstone lithology. In marked contrast the yields from Katumbo Creek-1 were all very low with all samples (except for cuttings at 5740 ft) yielding only one or two slides. These low yields are no doubt a result of the low average initial sample weight combined with the fine grain size of the samples which would have biased the samples to those lithologies leaner in kerogen and palynomorphs. It is suspected the better shale lithologies have been partially washed out of these samples. The yields of individual samples is reflected in the number of palynological slides produced and these are catalogued in Appendixes 2 & 3.

CHARACTER OF PALYNOLOGY ASSEMBLAGES

All samples were found to be dominated by terrestrially derived kerogen and terrestrial palynomorphs and all have a relatively consistent character. The species assemblages identified in the samples are presented on the accompanying range charts for San Francisco-1 and Katumbo Creek-1. Eight of the better assemblages were also counted to provide more reliable estimates of the relative abundances of the major palynomorph categories (Table-5).

The dominant terrestrial palynomorphs were **fungal spores, fungal fruiting bodies** and fragments of **fungal hyphae.** Next most common were **fern spores,** particularly a high diversity of monolete types (see Plate 3), then **angiosperm pollen** followed by **gymnosperm pollen.**

The commonest marine palynomorphs are **microforaminiferal inner tests** which occur in low numbers in the majority of samples and are more abundant in the kerogen slides. Because their organic walls are considered to be made of **chitin** rather than **sporeopollenin** (Traverse 1988, p.8) they are partly or wholly removed from the oxidised slides by the harsher chemical treatment. The next most common marine palynomorphs are **dinoflagellates cysts** which are represented by from 1 to 5 recorded specimens per slide. The commonest species are *Polysphaeridium zoharyi* (Rossignol), *Eocladopyxis peniculata* Morgenroth and *Lingulodinium machaerophorum* (Deflandre & Cookson) all of which have long ranges extending beyond the age limit of the sections under study. The rarest marine palynomorph is the record of a **scolecodont** at 5910 ft in Katumbo Creek-1.

The spore-pollen species so far recorded in Appendix 1 are only a partial list of the total diversity. The main references used for taxa identification are Germeraad *et al.* (1968), Khan (1976), Morley (1978, 1982, 1990), Muller (1968), Playford (1982) and Thanikaimoni *et al.* (1984). The assemblages recorded can be divided into two components.

Table-5: Palynomorph Percentages from Counts on Selected Samples

	SAN FRANCISCO-1								KATUMBO CREEK-1
	300-20 ft Cuttings	900-10 ft Cuttings	2020-30 ft Cuttings	2500-10 ft Cuttings	2909 ft CORE-1	3907.5 ft CORE-2	4560-70 ft Cuttings		5740 ft Cuttings
PALYNOMORPHS									
Trilete spores-smooth	6.4%	18.2%	3.6%	1.3%	2.5%	5.1%	2.7%		0.8%
Trilete spores-ornamented	12.7%	4.0%	1.4%	1.3%	3.1%	1.7%	2.7%		4.8%
Monolete spores-smooth	43.6%	19.2%	4.3%	5.2%	7.4%	3.4%	3.6%		2.4%
Monolete spores-ornamented	13.6%	9.1%	2.1%	1.3%	0.6%		2.7%		4.0%
SPORES %	**76.4%**	**50.5%**	**11.4%**	**9.0%**	**13.6%**	**10.2%**	**11.6%**		**12.1%**
Bisaccate pollen	1.8%		7.9%	3.4%			2.7%		
Cupressacites sp.			28.6%	9.4%			5.4%		1.6%
Other gymnosperms	0.9%	1.0%	0.7%	0.4%					
GYMNOSPERM POLLEN %	**2.7%**	**1.0%**	**37.1%**	**13.3%**			**8.0%**		**1.6%**
Triporate pollen			14.3%	7.7%			10.7%		2.4%
Tricolp(or)ate pollen	0.9%		10.7%	4.7%	4.3%		4.5%		0.8%
Other angiosperms		8.1%	0.7%	1.7%	3.7%		3.6%		0.8%
ANGIOSPERM POLLEN %	**0.9%**	**8.1%**	**25.7%**	**14.2%**	**8.0%**		**18.8%**		**4.0%**
TOTAL SPORES & POLLEN COUNT	**88**	**59**	**104**	**85**	**35**	**6**	**43**		**22**
Fungal spores	9.1%	18.2%	11.4%	15.0%	50.6%	45.8%	36.6%		38.7%
Fungal fruiting bodies	1.8%	5.1%	1.4%	1.3%	5.6%	3.4%	0.9%		6.5%
Fungal setae		2.0%	2.9%	2.6%	0.6%		3.6%		1.6%
Fungal hyphae & other fragments	2.7%	4.0%	8.6%	44.6%	21.0%	40.7%	18.8%		35.5%
Total Fungal Remains %	**13.6%**	**29.3%**	**24.3%**	**63.5%**	**77.8%**	**89.8%**	**59.8%**		**82.3%**
TOTAL FUNGAL REMAINS COUNT	**15**	**29**	**34**	**148**	**126**	**53**	**67**		**102**
MICROPLANKTON	2.7%	5.1%	1.4%		0.6%				
MICROFORAMINIFERAL LINERS	3.6%	6.1%					1.8%		
TOTAL COUNT	**110**	**99**	**140**	**233**	**162**	**59**	**112**		**124**

Firstly, there is a group of species which are frequent to common in the assemblage and which appear to range throughout most of the stratigraphic section studied but are either not adequately documented or have long unhelpful stratigraphic ranges. Examples of species not described or poorly known are: *Distaverrusporites* sp. A, *Clavatosporis* spp., *Cyclophorusisporites* spp. and *Polypodiidites* spp. The latter three species groups are similar to the diversity of monolete spores illustrated by Song Zhi-Chen & Zhong Bi-Zhen (1984). Examples of species with stratigraphic ranges known to extend well beyond the stratigraphic limits of the interval being studied include: *Foveotriletes lacunosus*, *Spinozonocolpites baculatus* and *Zonocostites ramonae.*

Secondly, there are a number of stratigraphically significant species which so far have only been found in one or a couple of samples. Examples are:

SPECIES	AFFINITY	LOCATION
Echiperiporites estelae	(=*Malvaceae*)	San Francisco-1 at 6860-65 ft
Florschuetzia levipoli	(= *Sonneratia caseolaris*)	San Francisco-1 at 900-10 ft
Malvacearupollis papuensis		San Francisco-1 at 900-10 ft and at 6390-95 ft
Pellicieroipollis sp.	(= *Alangium griffithii*)	San Francisco-1 at 2500-10 ft
Polypodiidites usmensis	(= *Stenochlaena palustris*)	San Francisco-1 at 900-10 ft, 6390-95 ft, and caved in Katumbo Creek-1 at 6340 ft

Although these species have considerable value for local and regional correlation they are too rare in the sections being studied to confidently use them for biostratigraphic correlation.

The fungal spores and fruiting bodies and fragments of fungal hyphae are both diverse and common in all samples and offer additional potential for local correlation and age dating primarily because of their consistent occurrence. Total fungal remains in the counts range from 13% to 90% with an average >66% (Table 5). Even though some of the counts contain a high proportion of fungal hypae and other fragments the spores and fruiting bodies are conspicuous in all samples. Of particular note is the abundance of fungal remains in the two core samples compared to the cuttings. This marked difference is supportive evidence for interpreting a significant component of the pollen in the cuttings as derived from cavings or mud contamination as discussed below. Notwithstanding the abundance of fungal remains, aside from illustration and description of some species in the Chinese literature (eg. Zhu Zunghao *et al.* 1985) I am not aware of their application to biostratigraphy in Southeast Asia. The species listed on Appendix 1 are an initial selection of forms identified and photographed from San Francisco-1 and Katumbo Creek-1 (Plates 1 & 2). They are classified according to the form-genera recognised by Elsik (in prep.) some of which are still informally named. Individual species have mostly not yet been named so the forms identified are given code numbers with the following prefixes:

FS = Fungal spore
FB = Fungal fruiting bodies
FH = Fungal hyphae.

A feature of the fungal assemblages is the diversity of **microthyriaceous fruiting bodies.** Their abundance, between 1%-6.5%, and consistent occurrence in nearly all samples is extremely unusual based on my past experience. According to Elsik (1978) modern forms are mainly tropical and their distribution correlates with forest areas with >1000 mm (>40 inches) precipitation per year. Their stratigraphic ranges are mostly Paleocene and younger and they hitherto have not been used for palynological zonation and age dating.

Both wells contain a group of gymnosperm and angiosperm pollen species which because they are of lighter in colour (ie. less carbonised) than the other palynomorphs (and most of the kerogen) in the cuttings are interpreted as derived from either down hole cavings or contamination from a lignite based drilling mud additive. Selected species are shown as a separate block on each range chart and in Plate 7. For San Francisco-1 the species concerned are numbered 59-68, and for Katumbo Creek-1 numbered 46-51. In San Francisco-1 the colour difference is only discernible below 3000 ft. Also three of the species, *Alnipollenites verus, Betulaceoipollenites* sp. and *Lacrimapollis pilosus* are recorded from the core samples. The proposition of derivation from a lignite based drilling mud additive is uncertain as nearly all of the species have been recorded in publications on the Southeast Asian microfloras. The one exception illustrated is perhaps *Sequoiapollenites* (Plate 7, fig.D) which has affinities to the modern *Sequoia* which is better known by its common name of Californian Redwood. The uncertainty concerning the derivation of these pollen affects the age assignment as *Alnipollenites verus* and *Cupressacites* sp. (= *Inaperturopollenites dubius* of Watanasak 1990) are considered to be important marker speices. Of the samples counted the cuttings from San Francisco-1 at 2020-30 ft, 2500-10 ft and 4560-70 ft are suspected to be the most affected by contamination based on the abundance of *Cupressacites* (5% to 29%) and bisaccate pollen (mostly *Pinuspollenites* spp.). This interpretation of significant contamination of the cutting can only be resolved by further palynological work on either core or outcrop samples in the Bondoc Sub-basin.

PALYNOLOGICAL ZONATION AND AGE

The palynological zonation schemes in current use in Southeast Asia either published or referred to in unpublished petroleum exploration company reports are all largely based on the seminal work of Germeraad, Hopping & Muller (1968). They erected a set of pantropical zones recognised from the Caribbean, West Africa (Nigeria) and Borneo/Sarawak. Three additional local zones were defined in the Oligocene to Pleistocene of Borneo/Sarawak based on evolutionary changes in the pollen form-genus *Florschuetzia* which was shown to have unambiguous affinities to the modern *Sonneratia* mangrove. Improvements and additions to the palynological zonation since 1968 have most recently been reviewed by Morley (1990). The changes have seen additional marker taxa utilised and the more recent trend to detailed counts of the assemblages to recognise "quantitative events" in the palynological succession. The zonation is based on spores and pollen from vascular terrestrial plants primarily from coastal mangrove floras. However, as emphasised by Watanask (1990) detailed descriptions of the zones, including systematic palynology and photomicrography are still lacking. Further, in the published literature and available unpublished reports little use has been made of the biostratigraphic potential of either dinoflagellate cysts or the abundant fungal microfossils which also occur through the successsion.

Unfortunately application of even a modified version of the above "standard" zonation to the composite Miocene to Pleistocene sequence in Katumbo Creek-1 and San Francisco-1 is not possible due to the rarity of the key marker taxa. In particular, recognising the zones in the Miocene relies principally on finding specimens of and recognising the evolutionary changes in the pollen form-genus *Florschuetzia*. However, in the present study *Florschuetzia levipoli* was the only species recorded and then only from the one sample in San Francisco-1 at 900-10 ft, much younger than its diagnostic first appearance. Other accessory index species with restricted ranges in the Miocene (eg. Morley 1978, fig. 2; 1990, fig.2) because they are mostly derived from the same mangrove environments as *Florschuetzia* are similarly either very rare or not recorded in this study.

Watanasak (1990) had a similar problem when studying Miocene palynological assemblages from both marine and non-marine basins in Thailand. His study which extends over a latitude range of 8°N to 20°N is perhaps more applicable to the Bondoc Sub-basin at 13°N than the basins in Malaysia, Borneo and Indonesia between 10°N and 10°S where most of the palynological work seems to have been concentrated. To overcome the lack of spore-pollen derived from mangrove floras in non-marine and intermontane basins Watanasak (*ibid.*) erected two new zones SIAM 1 (late Oligocene to basal early Miocene) and SIAM 2 (Early Miocene) defined on pollen found in montane floras. Diagnostic ranges relevant to the Bondoc Sub-basin are the last apperance of *Alnipollenites verus* defining the top of zone SIAM 2 and the common occurrence of *Inaperturopllenites dubius* (= *Cupressacites* sp. herein) through zone SIAM 1. However, both these species would appear to extend into younger strata in San Francisco-1 based on the foraminiferal age dating. A further complication is the suspicion that both these species may wholly or partly be contaminants in the cuttings samples (see p. 10). Differences in local extinction points for these "montane" pollen types is not however unexpected as both have affinities to plants growing in more temperate regions today. Their extention into tropical regions in the past is a complex interplay of climatic change, presence of suitable mountain habitats and availability of long range dispersal mechanisms (prevailing winds or rivers draining mountain ranges). The range charts in Sung Xiang-jun *et al.* (1981) also indicate longer ranges for thse types in the norther portion of the South China Sea.

Even though **none** of the established zones can be recognised the overall spore-pollen assemblages in San Francisco-1 and Katumbo Creek-1 are consistent with the Neogene ages derived from the foraminiferal dating. Because all the assemblages appear to be of high diversity, notwithstanding the limitations of low yields, poor preservation and probable contamination in the cuttings, the microfloras should be able to provide a **local zonation** for the Bondoc Sub-basin. It is premature however to attempt to erect such a zonation based on the limited set of samples, from essentially only a single composite section, as analysed in this study.

Concerning the marine palynomorphs none of the limited number of recorded species on the range charts and in Appendix 1 are particularly age diagnostic although all are consistent with the ages suggested by the foraminifera. Further, because of the rarity of the dinoflagellates it is unlikely they will be much practical use in establishing a local zonation to correlate between wells in the Bondoc Sub-basin. It should also be noted that the brackish to fresh-water species of *Bosedinia* spp. and *Granodiscus* sp. described by

Cole (1992) from the South China Sea were not found. This probably reflects a different environment of deposition as well as the younger age of most of the section.

The remaining significant group with potential are the fungal spores and fruiting bodies which are abundant and diverse throughout the section studied. To date these have not been consistently recorded or adequately documented in Southeast Asia to be of much biostratigraphic use. Of the form-genera identified the known stratigraphic ranges of *Mediaverrusporonites* and *Tetraploa* would indicate a Miocene or younger age.

PALAEOENVIRONMENT

The **occurrence in all samples** of either or both microforaminiferal inner tests and dinoflagellate cysts is consistent with the foraminiferal analysis which suggests that the sequences in both wells have been deposited in predominantly inner to middle neritic marine environments. However, it should be stressed that the marine palynomorphs are rare compared to the terrestrial palynomorphs and this is considered to reflect **dilution** of the marine components by the influx of terrestrial kerogen with its fern spores, pollen and fungi obviously coming from a nearby land mass. This dilution partly reflects the occurrence of highly productive tropical vegetation on the adjacent land and partly the high average rates of deposition of the formations on the Bondoc Peninsula. In San Francisco-1 the average depositional rate is >425 ft/million years (>130 m/m.y.) whilst in Katumbo Creek-1 over the sample interval (where the age control is less certain) it ranges from 110-150 ft/m.y. (33-45 m/m.y.)

The dilution of marine dinoflagellate cysts in neritic sediments deposited under high depositional rates is an empirical observation based on experience from a number of basins and ages. As a comparison a typical depositional rate for a palynological assemblage containing >50% dinoflagellate cysts would be <50 ft/m.y. (<20 m/m.y.).

Given that the foraminiferal analyses, supported by the palynology, indicates that the sequence sampled in both wells are marine it is surprising that mangrove pollen are so rare. Pollen species representative of the lower delta plain mangrove/saltmarsh environments (Morley 1990, fig.9) in order of frequency of occurrence are *Lacrimopollis pilosus* (= *Brownlowia* pollen); *Spinozonocolpites baculatus* (= *Nypa* palm); *Zonocostites ramonae* (= *Rhizophora* pollen) and *Florschuetzia levipoli* (= *Sonneratia* pollen). *Lacrimopollis pilosus* also shows similarity to pollen of the genus *Pentace* whose ecological distribution extends from swamps to low altitude evergreen forests (Thanikaimoni *et al.* 1984, p.38) and thus may not indicate mangrove environments in this instance. Also missing or poorly represented in the assemblages are spore-pollen typical of the freshwater swamps on the upper delta plains (Morley 1990, fig.9), or open forests of the alluvial plain (Poumot 1989, fig.2). In fact the bulk of the spore-pollen assemblages appear more typical of hinterland fluvial (abundant spores; Poumot *ibid*, p.441), rainforest (abundant fungii) and montane (abundant gymnosperm pollen) environments.

Two factors appear to be involved here to account for the nature of the spore-pollen assemblages. The first is that in the Bondoc Sub-basin there was not developed in the Neogene the broad coastal plain with large deltas supporting abundant mangroves as was certainly the case in Borneo/Sarawak. Instead it is suggested the land had more topographic relief which would have restricted the mangrove environments to narrow strips along the palaeoshorelines. Such a limited areal extend for both upper and lower coastal plain environments would explain the under-representation of spore-pollen from

these environments in the samples. The second factor that may be acting on the palynomorph assemblages is the **neves** effect (Traverse 1988, p.413). Where there are coastal plain and delta environments spore-pollen representative of these environments are typically most abundant close to the strand line while those derived from the more distant hinterland become **relatively** more abundant in more distal marine environments. High abundances gymnosperm pollen which are more bouyant in water and therefore transported further are generally typical of the action of the neves effect. The dominance of hinterland pollen types in the samples, which are marine based on other criteria, can be taken as weak evidence for a distal marine depositional environment somewhat remote from the palaeoshoreline. The palynological data can provide no further information on the likely palaeobathymetry aside from of this indication of a possible distal marine environment.

Negative evidence to support the above conclusions is the absence of coal beds in the wells examined and apparently from the Bondoc Sub-basin. The palynological assemblages recorded indicate a highly productive tropical vegetation growing under high humidity, high rainfall which could be expected to develop peats provided the appropriate environment was present for both deposition and preservation. The absence of coals supports limited coastal plain environments in the basin.

KEROGEN TYPES AND MATURATION

Kerogen or particulate organic matter types determined from a visual estimate of percentage abundance and the level of the maturation of the samples are provided on Tables 6 & 7.

The kerogen types nomenclature used is a modified version of the classification of Masran & Pocock (1981) whilst maturation is determined in terms of the Thermal Alteration Index of Staplin (1977). The visual estimates of the percentage volume of each kerogen type is made on the unfiltered kerogen slide. For some samples so little residue was recovered that only a filtered kerogen slide was prepared, and for these samples the kerogen types are biased towards the coarser components. Usually this is reflected in an increase in the percentage of semi-opaque structured terrestrial kerogen.

The kerogen in both wells is dominated by the **biodegraded terrestrial** category with averages of 34% and 47.5% (in San Francisco-1 and Katumbo Creek-1 respectively). This type represents terrestrially sourced organic material which has undergone micro-biological breakdown by the action of bacterial and fungal decay. The next most common kerogen type is the **amorphous kerogen** group with average percentages of 31% and 22%. Although recorded as undifferentiated most belong to the sub-categories of **granular-bacterial** and **structureless amorphous**. As there is no significant abundance of the yellow-amber or "fluffy" sub-types of amorphous recorded it is believed that a significant proportion of the undifferentiated amorphous recorded may represent further breakdown of the biodegraded terrestrial kerogen. Only a single speciment of the algae *Pediastrum* was recorded in San Francisco-1 at 5520-25 ft, whilst *Botryococcus* the other algae typically associated with amorphous kerogen was not recorded. It is therefore suggested that amorphous kerogen derived from these brackish to fresh-water algal precursors is insignificant. Based on the palaeoenvironmental setting suggested for both wells marine amorphous kerogen should be present. However the only confidently identified marine kerogen types are the microforaminiferal inner tests and dinoflagellate cysts which although present in nearly all samples comprise less than 0.1% of the total

kerogen based on the visual estimates. If any of the amorphous kerogen is derived from other marine precursors it cannot be identified by the morphological criteria seen using a light microscope.

The third most abundant category is **structured terrestrial** which is morphologically subdivided between laminar, cellular and semi-opaque angular and has average percentages of 28% and 24%. Laminar refers to planar pieces of kerogen such as cuticle. Cellular is applied to three dimensional pieces of kerogen with well preserved (ie. not biodegraded) plant structures. Semi-opaque is applied to darker, thicker and blockier pieces of kerogen which are too dark to differentiate cellular structure but are clearly translucent, particularly along their edges. All these types are considered to be derived from terrestrial "woody" plants.

Noteworthy because of its absence, as a significant component, is the charcoal group representing oxidised terrestrial woody materials which can be produced by processes of fire, or recycling and oxidation of woody materials at surface temperatures, or by reworking of kerogen which has been matured (metamorphosed) through burial. The absence of these charcoal types is consistent with high rates of deposition. It is noteworthy that no reworked palynomorphs were recorded.

Amongst the palynomorphs only fungal remains occurred in greater than 1% abundance by volume. Their abundance is consistent with the dominance of biodegraded kerogen as well as the provenance of most of the kerogen from tropical "rainforest" vegetation.

Another feature of all samples with unfiltered kerogen slides is the abundance of tiny pyrite crystals mostly in the size range of 0.1 to 3 microns in diameter. These are evenly disseminated through the amorphous kerogen and irregularly distributed throughout most of the other kerogen types. The pyrite is estimated to represent between 5%-20% of the total volume of the kerogen residue, but is excluded as a percentage of the kerogen types.

Overall the dominance of terrestrial versus marine or algal kerogen would suggest a gas prone source, but the pervasive breakdown of the land derived kerogen to biodegraded terrestrial and probably further to undifferentiated amorphous kerogen may indicate significant oil source potential. Although it has long been speculated within the oil exploration companies that "biodegradation" can result in better oil source potential this has not to my knowledge been demonstrated by experimentation nor are there any published papers which adequately analyse this problem.

The kerogen maturation, expressed as T.A.I. (Thermal Alteration Index) values, ranges from 1.5 to 2.5 in San Francisco-1 and 2.3 to 2.5 in Katumbo Creek-1. In the cuttings samples the T.A.I. values recorded range over 0.2 of a unit. This is considered to reflect the presence of some cavings in all the cuttings samples. According to Staplin (1977) values above 2.4 would be mature for oil generation. This would suggest that the section below about 3500 ft (1050 m) in both wells could be mature enough to have been, or currently be, generating hydrocarbons.

TABLE 6 Kerogen Analysis San Francisco-1

Depth (feet)	TAI	Kerogen Types							Total	%P	M
		1.	2.	3.	4.	5.	6.	7.			
300-20	1.5-2.0	40	14	tr	1		35	10	100	20%	X
900-10	1.5-1.7	20	14	1	5	20	20	20	100	20%	X
1700-10	2.0-2.2	60	9	1	5	5		20	100	5-10%	X
2020-30	2.1-2.2	55	25	tr	5			15	100	10%	X
2500-10	2.1-2.3	30	50	tr	5	5		10	100	10%	
2909	2.3	20	50	tr	10			20	100	20%	X
3907.5	2.4	35	40	tr	10	5		10	100	10%	X
4560-70	2.1-2.3	20	35	tr	5			35	100	10%	X
4970-80	2.3-2.4	20	40	tr	5	5	10	20	100	10%	X
5520-25	2.4-2.5	15	40	tr	3		7	35	100	10%	X
6390-95	2.4-2.5	30	45	tr	5			20	100	20%	X
6860-65	2.4-2.5	25	50	tr	5			20	100	20%	X
	Average	**31**	**34**		**5**	**3**	**6**	**20**			

Abbreviations

T.A.I. = Thermal Alteration Index

Kerogen Types

1. = Amorphous undifferentiated
2. = Biodegraded Terrestrial
3. = Spores & Pollen
4. = Fungal spores, fruiting bodies and hypae
5. = Structured Terrestrial - Laminar
6. = Structured Terrestrial - Cellular
7. = Structured Terrestrial = Semi-Opaque

%P = % Pyrite as proportion of kerogen residue
M = Microforaminiferal inner tests
X = Present
tr = trace

TABLE 7 Kerogen Analysis Katumbo Creek-1

Depth (feet)	T.A.I.	Kerogen Types							Total	%P	M
		1.	2.	3.	4.	5.	6.	7.			
4700-20	2.3-2.5	2	30	1	4	3		60	100	<5%	
5000	2.4-2.5	10	55	tr.	10			25	100	10%	X
5390	2.3-2.5	30	50	tr	5		5	10	100	20%	X
5740	2.3-2.5	40	35	tr	5	5	5	10	100	10%	X
5910	2.3-2.5	35	45	tr	10			10	100	15%	
6240	2.3-2.5	40	45	tr	10			5	100	10%	X
6340	2.3-2.5	17	60	tr	3			20	100	<5%	X
6400	2.4-2.5	5	60	tr	5			30	100	1%	X
	Average	**22.4**	**47.5**		**6.5**	**1**	**1.3**	**21.3**			

Abbreviations

T.A.I. = Thermal Alteration Index

Kerogen Types

1. = Amorphous undifferentiated
2. = Biodegraded Terrestrial
3. = Spores & Pollen
4. = Fungal spores, fruiting bodies and hypae
5. = Structured Terrestrial - Laminar
6. = Structured Terrestrial - Cellular
7. = Structured Terrestrial = Semi-Opaque

%P = % Pyrite as proportion of kerogen residue
M = Microforaminiferal inner tests
X = Present
tr = trace

CONCLUSIONS AND RECOMMENDATIONS

The 20 samples analysed for palynology from San Francisco-1 and Katumbo Creek-1 have provided only a reconnaissance review of the Neogene sequence in the Bondoc Sub-basin. The main results are:

1. The Neogene sequence in the Bondoc Sub-basin contains diverse palynological assemblages with significant potential for use in **local correlation** and determination of environments.

2. Abundant and diverse fungal spores and fungal fruiting bodies and spores and pollen derived from terrestrial vascular plants are likely to be the most useful palynomorphs for establishing a local palynological zonation.

3. Marine palynomorphs although present throughout the sequence analysed were comparatively rare and of only low diversity. Unless present in more abundance and diversity in unsampled environments they are unlikely to have any practical application for local or regional biostratigraphic correlation but could provide important information for the interpretation of environments.

4. To erect a reliable local zonation for the Bondoc Sub-basin will require detailed work on many more samples. It is anticipated that it would require analysis of hundreds rather than tens of samples to achieve a reliable and sophisticated zonation in the basin which would be able to compete with and improve on the available foraminiferal age dating and zonation.

5. Because of the identification of contamination in the cuttings from either cavings or drilling mud additives the next palynological study should target outcrop sequences or wells containing cores or sidewall cores which can be sampled for palynology. This approach would be the quickest route to developing reliable local stratigraphic ranges for the palynomorphs.

6. Because of the rarity, in the samples analysed, of the index taxa derived from coastal mangrove floras the established spore-pollen zonations which are based on the *Florschuetzia* lineage and used widely in Southeast Asia could not be identified. It is unlikely that more samples or more detailed analysis of individual samples would significantly alter this observation. Thus, the best approach to successfully applying palynology in the Bondoc Sub-basin is to erect a local zonation.

7. Although the two well sections analysed were mostly, if not entirely, deposited in marine environments the rarity of microplankton and comparatively low abundance and moderate to low diversity of calcareous microfossils requires explanation. It is interpreted as due to dilution of the marine fossils by the rapid deposition of predominantly terrestrially derived sediments. The adjacent landmass is envisage to consist of abundant unconsolidated volcano-clastic sediment cloaked with a diverse tropical rainforest vegetation. Northern temperate montane forests were developed at higher altitudes on the volcanoes in the hinterland whilst the coastline appears to have had only a narrow fringe of coastal mangrove vegetation.

8. Analysis of kerogen extracted by palynological processing shows a dominance of terrestrial derived organic matter types which are currently interpreted as predominantly a gas prone source. The speculation that biodegradation of the kerogen may cause a change to more oil prone source types could be tested by **elemental analysis** of any

remaining kerogen residues to determine hydrogen index. The equipment to perform this analysis is now available through Laola Pty Ltd.

9. Maturation determinations based on kerogen analysis suggests sections below about 3500 ft in the wells examined from Bondoc Sub-basin could be mature enough to have commenced generating hydrocarbons.

REFERENCES

CHAO-SHING LEE, TRINIDAD, N.D. & GALLOWAY, M.C., 1992. A preliminary result of the Ragay Gulf Survey: Stratigraphy, seismic and geochemistry. *Geological Society Philippines, Plenary Session on Geo-energy, Technical Papers, Makati Manila*, 11 Dec. 1992, 1-8, 8 figs.

COLE, J.M., 1992. Freshwater dinoflagellate cysts and acritarchs from Neogene and Oligocene sediments of the South China Sea and adjacent areas. In *Neogene and Quaternary Dinoflagellate cysts and Acritarchs*, Head, M.J. & Wrenn, J.H., eds, American Assoc. Stratigraphic Palynologists Foundation, Dallas, 181-196.

ELSIK, W.C., 1978. Classification and geological history of the microthyriaceous fungi. *IV Int. Palynol. Conf., Lucknow (1976-77) 1*, 331-342.

ELSIK, W.C., in prep. Fossil fungal palynomorphs.

ELSIK, W.C. & JANSONIUS, J., 1974. New genera of paleogene fungal spores. *Canadian J. Bot. 52* (5), 953-958.

GALLOWAY, M.C., CHAO-SHING LEE, & RILLERA, F.G., 1992. Australian RV *Rig Seismic* Survey of Philippines - A precursor to renewed exploration? *Offshore South East Asia, 9th Conference & Exhibition World Trade Centre Singapore*, 1-4 Dec. 1992, 5p.

GALLOWAY, M.C., in prep. Stratigraphy of Bondoc Peninsula.

GERMERAAD, J.H., HOPPING, C.A. & MULLER, J., 1968. Palynology of Tertiary sediments from tropical areas. *Rev. Palaeobot. Palyno. 6* (3-4), 189-348.

HE CHENG-QUAN & LI PENG, 1981. 2. Dinoflagellates and Acritarchs. In *Tertiary palaeontology of North Continental Shelf of South China Sea*, Hou You-tang *et al.* eds., Guandong Science & Technology Press, 59-72, pls.31-35 (in Chinese).

KHAN, A.M., 1976. Palynology of Tertiary sediments from Papua new Guinea. I. New form genera and species from Upper Tertiary sediments. *Aust. J. Bot. 24*, 753-781.

MASRAN, Th. C. & POCOCK, S.A.J., 1981. The classification of plant derived particulate organic matter in sedimentary rocks. In *Organic Maturation Studies and Fossil Fuel Exploration*, J. Brooks, editor, Academic Press Inc. (London) Ltd, 145-175.

MORLEY, R.J., 1978. Palynology of Tertiary and Quaternary sediments in Southeast Asia. *Proc. 6th Ann. Conv,. Indonesian Petr. Assn.*, 255-276.

MORLEY, R.J., 1982. Fossil pollen attributable to *Alangium* Lamarck (Alangiaceae) from the Tertiary of Malesia. *Rev. Palaeobot. Palyno. 36*, 65-94.

MORLEY, R.J., 1990. Tertiary stratigraphic palynology in Southeast Asia; current status and new directions. *Keynote address at the Geological Society of Malaysia Petroleum Geology Seminar, Kuala Lumpur, Nov. 27-28.* 1-41, 13 figs.

MULLER, J., 1968. Palynology of the Pedawan and Plateau Sandstone Formations (Cretaceous-Eocene) in Sarawak, Malasia. *Micropaleontology 14*, 1-37, 5 pls.

PLAYFORD, G., 1982. Neogene palynomorphs from the Huon Peninsula, Papua New Guinea. *Palynology 6*, 29-54.

POUMOT, C., 1989. Palynological evidence for eustatic events in the tropical Neogene. *Bull. Centres Rech. Explor. - Prod. Elf-Aquitaine 13* (2), 437-453.

SONG ZHI-CHEN, 1988. Late Cenozoic palyno-flora from Zhaotong, Yunnan. *Mem. Nanjing Inst. Geol. Palaeont. Acad. Sinica No. 24*, 1-52.

SONG ZHI-CHEN & ZHONG BI-ZHEN, 1984. Tertiary spore-pollen assemblages from Jinggu, Yunnan. *Bull. Nanjing Inst. Geol. & Palaeont., Acad. Sinica 8*, 1-53, 15 pls (in Chinese).

STAPLIN, F.L., 1977. Interpretaton of thermal history from color of particulate organic matter - a review. *Palynology 1*, 9-18.

SUN XIANG-JUN, LI MING-XING, ZHANG YI-YONG, LEI ZUO-QI, KONG ZHAO-CHEN, LI PENG, OU QI & LIU QI-NA, 1981. 1. Spores and Pollen. In *Tertiary palaeontology of North Continental Shelf of South China Sea*, Hou You-tang *et al.* eds., Guandong Science & Technology Press, 1-58, pl.1-30 (in Chinese).

THANIKAIMONI, G., CARATINI, C., VENKATACHALA, B.S., RAMANUJAM, C.G.K. & KAR, R.K., 1984. Selected Tertiary angiosperm pollen from India and their relationship with African Tertiary pollens. *Inst. Fr. Pondichéry, Trav. Sect. Sci. Tech. 19*, 1-92, 72 pls.

TRAVERSE, A., 1988. *Palaeopalynology*. Unwin Hyman Ltd, Boston, 1-600.

Van GORSEL, J.T., 1988. Biostratigraphy in Indonesia: methods, pitfalls and new directions. *Proc. Indonesian Petr. Assn. 17th Ann. Conv.*, 275-300.

WATANASUK, M., 1990. Mid Tertiary palynostratigraphy of Thailand. *Jour. S.E. Asian Earth Sci.* 4(3), 203-218.

ZHU ZUNGHAO, WU LIYU, XI PING, SONG, ZHICHEN & ZHANG YIYONG, 1985. A research on Tertiary Palynology from the Qaidam Basin, Qinghai Province. *The Petroleum Industry Press*, 1-297, 62 pls (in Chinese).

Appendix 1: Palynomorph Species List

Fungal Spores and Hyphae

Desmidiospora sp. FS4

Dicellaesporites spp.

Dyadosporonites sp. FS2

Echisporonites sp. FS5

Fractisporonites spp.

Fusiformisporites sp. FS6

Hypoxylonites sp. FS7

Inapertisporites sp. FS8

Inapertisporites spp.

Involutisporonites spp.

Linearium sp. FS9

Mediaverrusporonites sp. FS1

Multicellaesporites sp. FS3

Partitiosporonites spp.

Pluricellaesporites sp. FS12

Polyadosporites sp. FS 10

Polyadosporites sp. FS 11

Poridicellaesporonites sp. FS 13

Psiladisporonites spp.

Retidisporonites sp. FS 14

Tetraploa spp.

Tetraseptites spp.

Fungal Fruiting Bodies

Actinopelte sp. A (=FB5)

Actinopelte sp. B

Callimothalus sp. FB9

Microthallites sp. FB1

Microthallites sp. FB2

Microthyriacites sp. FB6

Phragmothyrites sp. FB3

Phragmothyrites sp. FB4

Phragmothyrites sp. FB10

Setaesporonites sp. FB7

Spores and Pollen

Alnipollenites verus Potonié 1934

Baculatisporites papuanus Khan 1976

Betulaceoipollenites sp. (= modern *Betula*)

Clavatosporis sp. A

Cupresaccites sp.

Cyathidites sp. (small)

Cyathidites sp. (large)

Cyclophorusisporites sp. A.

Distaverrusporites sp. A

Echinosporis sp.

Florschuetzia levipoli Germeraad *et al.* 1968

Foveotriletes lacunosus Partridge *in* Stover & Partridge 1973

Lacrimapollis pilosus Venkatachala & Rawat 1973

Laevigatosporites major (Cookson) Krutzsch 1959

Laevigatosporites ovatus Wilson & Webster 1946

Lygistepollenites florinii (Cookson & Pike) Stover & Evans 1974

Matonisporites mulleri Playford 1982

Momipites sp. (= modern *Carya*)

Monoporites sp.

Pellicieroipollis sp. A (= modern *Alangium griffithii*)

Pinuspollenites spp.

Podocarpidites spp.

Polypodiaceoisporites papuanus (Khan 1976) n. comb.

Polypodiaceoisporites retirugatus Muller 1968

Polypodiaceoisporites spp.

Polypodiidites sp. (large verrucae)

Polypodiidites sp. (small verrucae)

Polypodiidites usmensis (van der Hammen) Hekel 1972

Polypodiisporites foveoirregularis Khan 1976

Sequoiapollenites sp. (= modern *Metasequoia*)

Spinozonocolpites baculatus Muller 1968

Stereisporites sp.

Tricolporites spp.

Trilobosporites sp.

Zonocostites ramonae Germeraad *et al.* 1968

Dinoflagellate Cysts, Acritarchs and Other Palynomorphs

Eocladopyxis peniculata Morgenroth 1966

Lejeunecysta sp.

Lingulodinium machaerophorum (Deflandre & Cookson) Wall 1967

Oligosphaeridium sp.

Operculodinium centrocarpum (Deflaundre & Cookson) Wall 1967

Pediastrum sp.

Polysphaeridium zoharyi (Rossignol) Bujak *et al.* 1980

Pseudoschizaea sp.

Selenopemphix sp. cf. *S. brevispinosa* Head *et al.* 1989

Spiniferites spp.

Microforaminiferal inner tests

Scolecodonts

Appendix-2

Catologue List - Palynology Slides from San Francisco-1

Prepared By: A.D. Partridge

Date: 23 August 1994

Sample Type	Depth (ft)	Depth (m)	Slide Description
Cuttings	300-320	91-98	Kerogen slide K1 filtered/unfiltered fractions.
Cuttings	900-910	274-277	Kerogen slide K2 filtered/unfiltered fractions.
Cuttings	900-910	274-277	Oxidised slide 2 (1/4 cover slip).
Cuttings	1700-1710	518-521	Kerogen slide K1 filtered/unfiltered fractions.
Cuttings	1700-1710	518-521	Kerogen slide K2 (1/2 cover slip).
Cuttings	1700-1710	518-521	Oxidised slide 2.
Cuttings	1700-1710	518-521	Oxidised slide 3.
Cuttings	1700-1710	518-521	Oxidised slide 4.
Cuttings	1700-1710	518-521	Oxidised slide 5.
Cuttings	2020-2030	616-619	Kerogen slide K1 filtered/unfiltered fractions.
Cuttings	2020-2030	616-619	Kerogen slide K2 filtered (1/2 cover slip).
Cuttings	2020-2030	616-619	Oxidised slide 2.
Cuttings	2020-2030	616-619	Oxidised slide 3.
Cuttings	2020-2030	616-619	Oxidised slide 4.
Cuttings	2020-2030	616-619	Oxidised slide 5.
Cuttings	2500-2510	762-765	Kerogen slide K1 filtered/unfiltered fractions.
Cuttings	2500-2510	762-765	Kerogen slide K2 filtered (1/2 cover slip).
Cuttings	2500-2510	762-765	Oxidised slide 2.
Cuttings	2500-2510	762-765	Oxidised slide 3.
Cuttings	2500-2510	762-765	Oxidised slide 4.
Cuttings	2500-2510	762-765	Oxidised slide 5.
Core 1	2909	886.7	Kerogen slide K1 filtered/unfiltered fractions.
Core 1	2909	886.7	Kerogen slide K2 filtered (1/2 cover slip).
Core 1	2909	886.7	Oxidised slide 2.
Core 1	2909	886.7	Oxidised slide 3.
Core 1	2909	886.7	Oxidised slide 4.
Core 1	2909	886.7	Oxidised slide 5.
Core 2	3907.5	1191.0	Kerogen slide K1 filtered/unfiltered fractions.
Core 2	3907.5	1191.0	Kerogen slide K2 filtered (1/2 cover slip).
Core 2	3907.5	1191.0	Oxidised slide 2.
Core 2	3907.5	1191.0	Oxidised slide 3.
Core 2	3907.5	1191.0	Oxidised slide 4.
Core 2	3907.5	1191.0	Oxidised slide 5.
Cuttings	4560-4570	1390-1393	Kerogen slide filtered/unfiltered fractions.
Cuttings	4970-4980	1515-1518	Kerogen slide K1 filtered/unfiltered fractions.
Cuttings	4970-4980	1515-1518	Kerogen slide K2 filtered (1/2 cover slip).
Cuttings	4970-4980	1515-1518	Oxidised slide 2.
Cuttings	4970-4980	1515-1518	Oxidised slide 3.
Cuttings	4970-4980	1515-1518	Oxidised slide 4.
Cuttings	4970-4980	1515-1518	Oxidised slide 5 (1/2 cover slip).
Cuttings	5520-5525	1682-1684	Kerogen slide filtered/unfiltered fractions.
Cuttings	5520-5525	1682-1684	Kerogen slide K2 filtered (1/2 cover slip).
Cuttings	5520-5525	1682-1684	Oxidised slide 2.
Cuttings	5520-5525	1682-1684	Oxidised slide 3.
Cuttings	5520-5525	1682-1684	Oxidised slide 4.
Cuttings	5520-5525	1682-1684	Oxidised slide 5.

Appendix-2 cont...
Catologue List - Palynology Slides from San Francisco-1

Sample Type	Depth (ft)	Depth (m)	Slide Description
Cuttings	6390-6395	1948-1949	Kerogen slide filtered/unfiltered fractions.
Cuttings	6390-6395	1948-1949	Kerogen slide K2 filtered (1/2 cover slip).
Cuttings	6390-6395	1948-1949	Oxidised slide 2.
Cuttings	6390-6395	1948-1949	Oxidised slide 3.
Cuttings	6390-6395	1948-1949	Oxidised slide 4.
Cuttings	6390-6395	1948-1949	Oxidised slide 5.
Cuttings	6860-6865	2091-2092	Kerogen slide filtered/unfiltered fractions.
Cuttings	6860-6865	2091-2092	Kerogen slide K2 filtered (1/2 cover slip).
Cuttings	6860-6865	2091-2092	Oxidised slide 2.
Cuttings	6860-6865	2091-2092	Oxidised slide 3.
Cuttings	6860-6865	2091-2092	Oxidised slide 4.

Appendix-3
Catologue List - Palynology Slides from Katumbo Creek-1

Prepared By: A.D. Partridge
Date: 23 August 1994

Sample Type	Depth (ft)	Depth (m)	Slide Description
Cuttings	4700-4720	1433-1439	Kerogen slide filtered (1/2 cover slip).
Cuttings	5000	1524.0	Kerogen slide filtered/unfiltered fractions.
Cuttings	5000	1524.0	Oxidised slide 2 (1/4 cover slip).
Cuttings	5390	1642.9	Kerogen slide filtered/unfiltered fractions.
Cuttings	5390	1642.9	Oxidised slide 2 (1/4 cover slip).
Cuttings	5740	1749.6	Kerogen slide filtered/unfiltered fractions.
Cuttings	5740	1749.6	Kerogen slide K2 (1/2 cover slip).
Cuttings	5740	1749.6	Oxidised slide 2.
Cuttings	5740	1749.6	Oxidised slide 3.
Cuttings	5740	1749.6	Oxidised slide 4.
Cuttings	5740	1749.6	Oxidised slide 5.
Cuttings	5910	1801.4	Kerogen slide filtered/unfiltered fractions.
Cuttings	6240	1902.0	Kerogen slide filtered/unfiltered fractions.
Cuttings	6240	1902.0	Oxidised slide 2 (1/2 cover slip).
Cuttings	6340	1932.4	Kerogen slide filtered (1/4 cover slip).
Cuttings	6400	1950.7	Kerogen slide filtered (1/4 cover slip).

DESCRIPTION OF PHOTOGRAPHIC PLATES

PLATE 1: Fungal Fruiting Bodies

A. *Actinopelte* sp. A (=FB5).
Katumbo Creek-1 at 5000 ft. Slide K1/11.9, 89.5; F93/5.

B. *Actinopelte* sp. B.
San Franciso-1 at 4970-80 ft. Slide 2/15.5, 96.8; F93/9. Scale as for A.

C. *Callimothalus* sp. FB9.
San Francisco-1 at 2020-30 ft. Slide 3/20.5, 91.4; F93/8. Scale as for A.

D. *Microthallites* sp. FB1.
San Francisco-1 at 2909 ft. Slide 4/4.4, 94.9; F92/4.

E. *Microthallites* sp. FB1.
San Francisco-1 at 900-10 ft. Slide K/8.5, 89.8; F93/2. Scale as for D.

F. *Phragmothyrites* sp. FB3.
San Francisco-1 at 2020-30 ft. Slide 2/10.1, 83.8; F93/8.

G. *Phragmothyrites* sp. FB3.
San Francisco-1 at 2909 ft. Slide 4/7.6, 78.5; F93/4.

H. *Phragmothyrites* sp. FB10.
San Francisco-1 at 6860-65 ft. Slide 2/7.8, 93.8; F93/10.

I. *Microthyriacites* sp. FB6.
San Francisco-1 at 1700-10 ft. Slide K1/13.2, 85.9; F93/5.

J. "*Setaesporonites*" sp. FB7.
San Francisco-1 at 5520-25 ft. Slide K1/8.5, 94.3; F93/5.

K. *Phragmothyrites* sp. FB4.
San Francisco-1 at 2909 ft. Slide 4/12.0, 92.8; F93/4.

L. *Microthallites* sp. FB2.
San Francisco-1 at 2909 ft. Slide 5/2.5, 94.8; F93/4.

PLATE 2: Fungal Spores

A. *Mediaverrusporonites* sp. FS1
San Francisco-1 from core-1 at 2909 ft. Slide 4/12.8, 91.6; F93/4-2.

B. *Mediaverrusporonites* sp. FS1
San Francisco-1 at 2500-10 ft. Slide 2/19.8, 103.4; F93/9-4.

C-D. *Multicellaesporites* sp. FS3
San Francisco-1 from core-1 at 2909 ft. Slide 5/4.8, 97.3; F93/4-31.

E. *Multicellaesporites* sp. FS3
San Francisco-1 from core-1 at 2909 ft. Slide 5/6.1, 93.2; F93/4-25.

F. *Hypoxylonites* sp. FS7
San Francisco-1 from core-2 at 3907.5 ft. Slide 2/17.6, 81.4; F93/4-16.

G. *Hypoxylonites* sp. FS7
Katumbo Creek-1 at 5740 ft. Slide 3/4.2, 102.3; F93/10-18.

H. *Hypoxylonites* sp. FS7
Katumbo Creek-1 at 5740 ft. Slide 2/18.6, 116.0; F93/10-19.

I. *Tetraploa* sp.
San Francisco-1 at 4970-80 ft. Slide K2/13.4, 90.2; F93/9-23.

J. *Poridicellaesporonites* sp. FS13
San Francisco-1 from core-1 at 2909 ft. Slide 4/12.2, 103.8; F93/4-1.

K. *Involutisporonites* sp.
San Francisco-1 at 2500-10 ft. Slide 2/18.3, 98.8; F93/9-3.

L. *Tetraseptites* sp.
San Francisco-1 at 2020-30 ft. Slide 2/4.8, 90.5; F93/8-15.

M. *Tetraseptites* sp.
San Francisco-1 at 4560-70 ft. Slide K/22.8, 86.2; F93/9-18.

N. *Fractisporonites* sp.
San Francisco-1 from core-1 at 2909 ft. Slide 5/7.2, 96.8; F93/4.

O. *Dyadosporonites* sp. FS2
San Francisco-1 from core-1 at 2909 ft. Slide 5/13.8, 85.9; F93/4-19.

P. *Inapertisporites* sp. FS8
San Francisco-1 at 2020 ft. Slide K2/2.8, 104.0; F93/2-7.

Q. *Striadiporites* sp. cf. *S. sanctaebarbarae* Elsik & Jansonius 1974
San Francisco-1 at 1700-10 ft. Slide 3/7.8, 82.2; F93/8-11.

R. *Retidisporonites* sp. FS14
San Francisco-1 at 900-10 ft. Slide 2/13.0, 105.1; F93/2-8.

S. *Linearium* sp. FS9
San Francisco-1 from core-1 at 2909 ft. Slide 4/8.2, 80.6; F93/4-9.

T-U. *Echisporonites* sp. FS5
San Francisco-1 from core-1 at 2909 ft. Slide 5/22.3, 113.2; F93/4-15.

V-W. *Desmidiospora* sp. FS4
San Francisco-1 from core-2 at 3907.5 ft. Slide 5/21.6, 100.6; F93/5-2.

X. *Fusiformisporites* sp. FS6
San Francisco-1 from core-1 at 2909 ft. Slide 5/7.3, 88.7; F93/4-24.

Y. *Pesavis tagluensis* Elsik & Jansonius 1974
San Francisco-1 at 1700-10 ft. Slide 3/5.2, 87.6; F93/8-9.

Z. *Polyadosporites* sp. FS10
San Francisco-1 from core-1 at 2909 ft. Slide 4/11.9, 94.1; F93/4-5.

PLATE 3: Monolete Spores

A. *Polypodiidites* sp. (small verrucae)
San Francisco-1 at 1700-10 ft. Slide 3/4.9, 95.6; F93/8.

B. *Polypodiidites* sp. (small verrucae)
San Francisco-1 from core-2 at 3907.5 ft. Slide 2/4.8, 98.2; F93/9.

C. *Polypodiidites* sp. (large verrucae)
San Francisco-1 at 4970-80 ft. Slide 2/2.3, 101.9; F93/9.

D. *Polypodiidites* sp. (large verrucae)
San Francisco-1 at 300-20 ft. Slide K/17.1, 88.7; F93/2.

E-F. *Clavatosporis* sp. A
San Francisco-1 at 1700-10 ft. Slide K2/8.8, 95.8; F93/2.

G-H. *Clavatosporis* sp. B
San Francisco-1 from core-2 at 3907.5 ft. Slide 5/21.4, 106.8; F93/5.

I. *Cyclophorusisporites* sp. A
Katumbo Creek-1 at 5910 ft. Slide K/13.8, 106.5; F93/6.

J. *Cyclophorusisporites* sp. A.
San Francisco-1 at 6860-65 ft. Slide K2/7.3, 92.2; F93/10.

K. *Cyclophorusisporites* sp. A
San Francisco-1 at 5520-25 ft. Slide K1/10.6, 93.1; F93/5.

L-M. *Cyclophorusisporites* sp. B
San Francisco-1 from core-2 at 3907.5 ft. Slide K1/14.1, 75.9; F93/9.

N. *Laevigatosporites ovatus* Wilson & Webster 1946
San Francisco-1 from core-1 at 2909 ft. Slide 5/19.3, 95.7; F93/4.

O-P. *Polypodiisporites foveoirregularis* Kahn
San Francisco-1 from core-1 at 2909 ft. Slide 5/10.2, 92.9; F93/4.

Q-R. *Echinosporis* sp.
Katumbo Creek-1 at 5000 ft. Slide K/20.5, 79.9; F93/5.

S. *Echinosporis* sp.
Katumbo Creek-1 at 6240 ft. Slide K/1.8, 87.3; F93/6.

T. *Echinosporis* sp.
San Francisco-1 at 6860-65 ft. Slide K2/19.8, 105.3; F93/10.

PLATE 4: Trilete Spores

A-B. *Polypodiaceoisporites papuanus* (Kahn 1976) n. comb.
San Francisco-1 at 1700-10 ft. Slide 3/16.5, 117.4; F93/8-13.

C-D. *Polypodiaceoisporites* n.sp.
San Francisco-1 at 2020-30 ft. Slide 2/8.5, 82.9; F93/8-18.

E-F. *Polypodiaceoisporites* n.sp.
San Francisco-1 at 2500-10 ft. Slide 2/12.5, 79.8; F93/9-6.

G. *Foveotriletes lacunosus* Partridge *in* Stover & Partridge 1973.
San Francisco-1 from core-1 at 2909 ft. Slide 5/6.7, 86.8; F93/4-23.
Scale as for H-I.

H-I. *Foveotriletes lacunosus* Partridge *in* Stover & Partridge 1973.
Katumbo Creek-1 at 5740 ft. Slide 4/10.3, 100.9; F93/6-21.

J-K. Trilete spore gen. et. sp. indent.
San Francisco-1 from core-1 at 2909 ft. Slide 5/6.9, 87.3; F93/4-20.

M-O. *Distaverrusporites* sp. A.
San Francisco-1 from core-1 at 2909 ft. Slide 4/15.6, 88.2; F93/4-11.

P-R. *Distaverrusporites* sp. A.
Katumbo Creek-1 at 5000 ft. Slide K/18.9, 92.4; F93/6-1.

T. *Stereisporites* sp.
San Francisco-1 from core-2 at 3907.5 ft. Slide 4/3.3, 111.6; F93/5-1.
Scale as for X.

U. *Cyathidites* sp. (small variety)
San Francisco-1 from core-2 at 3907.5 ft. Slide 5/17.9, 113.8; F93/5-6.
Scale as for X.

V-W. *Polypodiaceoisporites* sp.
San Francisco-1 from core-1 at 2909 ft. Slide 5/15.3, 97.8; F93/5-8.

X. *Trilobosporites* sp.
San Francisco-1 at 2020-30 ft. Slide K2/16.8, 111.2; F93/2-3.

PLATE 5: Pollen

A-B. *Spinozonocolpites baculatus* Muller 1968
San Francisco-1 at 900-10 ft. Slide K1/5.2, 81.8; F93/5-21.

C. *Lacrimapollis pilosus* Venkatachala & Rawat 1973.
San Francisco-1 from core-1 at 2909 ft. Slide 5/7.6, 96.9; F93/4-37.

D. *Lygistepollenites florinii* (Cookson & Pike) Stover & Evans 1974
San Francisco-1 at 300-20 ft. Slide K/19.7, 85.5; F93/2-16.

E-F. *Pellicieroipollis* sp. A (= *Alangium griffithii*)
San Francisco-1 at 2500-10 ft. Slide K1/17.7, 89.9; F93/5-13.

G-H. *Zonocostites ramonae* Germeraad *et al.* 1968
San Francisco-1 from core-1 at 2909 ft. Slide 5/18.8, 82.5; F93/4-17.

I-J. *Tricolporites* sp. (=*Avicennia*)
San Francisco-1 from core-1 at 2909 ft. Slide 5/7.2, 96.8; F93/4-33.

K. *Betulaceoipollenites* sp.
San Francisco-1 from core-1 at 2909 ft. Slide 5/12.9, 100.9; F93/5-10.

PLATE 6: Marine Palynomorphs

A. *Lejeunecysta* sp.
San Francisco-1 from core-1 at 2909 ft. Slide K1/7.8, 76.3; F93/9-10.

B. *Eocladopyxis peniculata* Morgenroth 1966
San Francisco-1 from core-1 at 2909 ft. Slide K2/2.2, 99.8; F93/9-8.

C. *Polysphaeridium zoharyi* (Rossignol) Bujak *et al.* 1980.
San Franscico-1 at 900-10 ft. Slide 2/15.1, 99.5; F93/2-9.

D. *Oligosphaeridium* sp.
San Francisco-1 at 4970-80 ft. Slide 2/6.2, 97.8; F93/9-22.

E. *Selenopemphix* sp. cf. *S. brevispinosa* Head *et al.* 1989.
San Francisco-1 from core-1 at 2909 ft. Slide K1/12.2, 80.2; F93/9-11.

F. *Selenopemphix* sp. cf. *S. brevispinosa* Head *et al.* 1989.
San Francisco-1 from core-1 at 2909 ft. Slide K1/2.8, 95.2; F93/9-12.

G. *Selenopemphix* sp. cf. *S. brevispinosa* Head *et al.* 1989.
San Francisco-1 at 1700-10 ft. Slide K1/11.9, 85.8; F93/5-18.

H-I. *Spiniferites* sp.
San Francisco-1 at 6390-95 ft. Slide K2/17.9, 108.2; F93/10-16.

J. Microforaminiferal inner test.
San Francisco-1 at 2020-30 ft. Slide K2/12.2, 110.0; F93/2-5.

K. Scolecodont.
Katumbo Creek-1 at 5910 ft. Slide K/17.5, 85.1; F93/6-23.

PLATE 7: Interpreted Modern Contaminants in Cuttings

A. *Podocarpidites* sp.
San Francisco-1 at 2500-10 ft. Slide 2/11.2, 103.4; F93/9-5.

B. *Cupressacites* sp.
San Francisco-1 at 1700-10 ft. Slide 3/17.3, 102.9; F93/8-3.

C. *Cupressacites* sp.
San Francisco-1 at 1700-10 ft. Slide 3/10.0, 88.9; F93/8-4.

D. *Sequoiapollenites* sp.
San Francisco-1 at 1700-10 ft. Slide 3/14.3, 88.0; F93/8-5.

E. *Pinuspollenites* sp.
San Francisco-1 at 5520-25 ft. Slide 2/18.8, 93.2; F93/10-1.

F-G. *Momipites* sp.
San Francisco-1 at 2020-30 ft. Slide 3/20.7, 89.3; F93/9-1.

H. *Betulaceoipollenites* sp.
San Francisco-1 at 1700-10 ft. Slide 3/6.6, 88.1; F93/8-10
Scale as for F-G.

I. *Alnipollenites verus* Potonié 1934.
San Francisco-1 at 1700-10 ft. Slide 3/11.8, 97.2; F93/8-7.
Scale as for F-G.

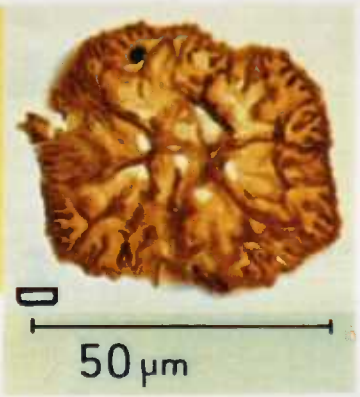

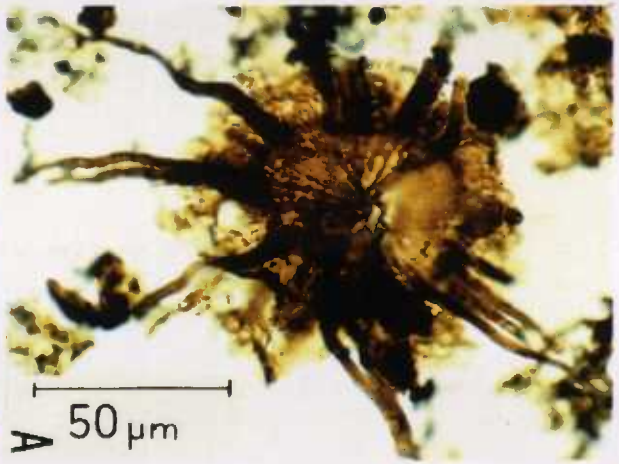

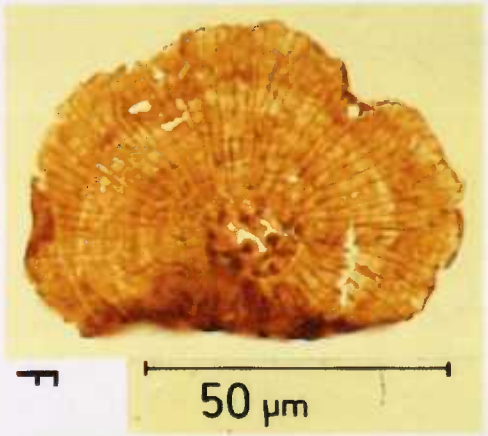

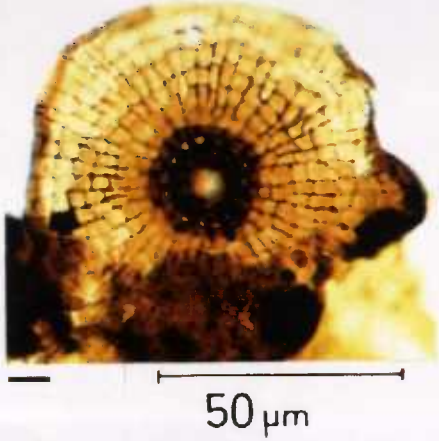

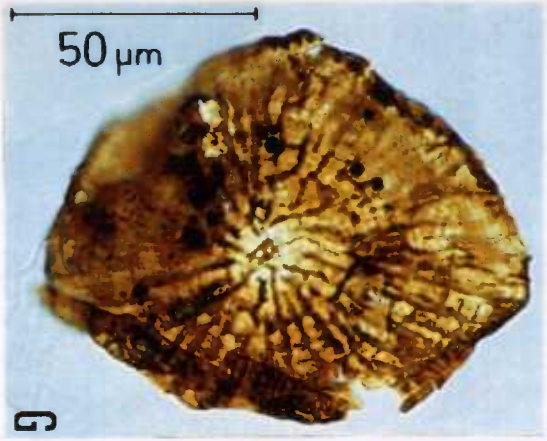

PLATE-1

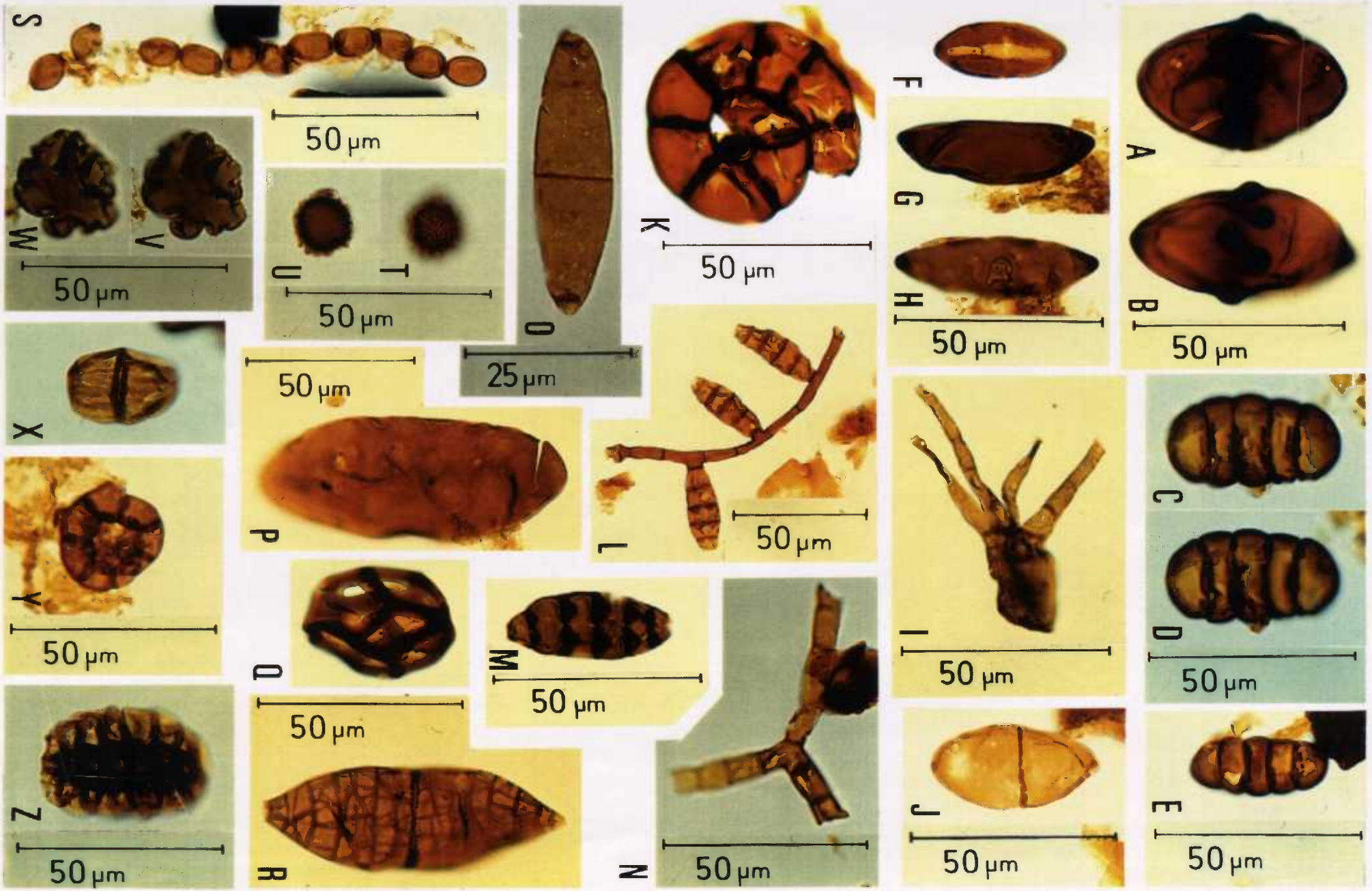

PLATE-2

PLATE-3

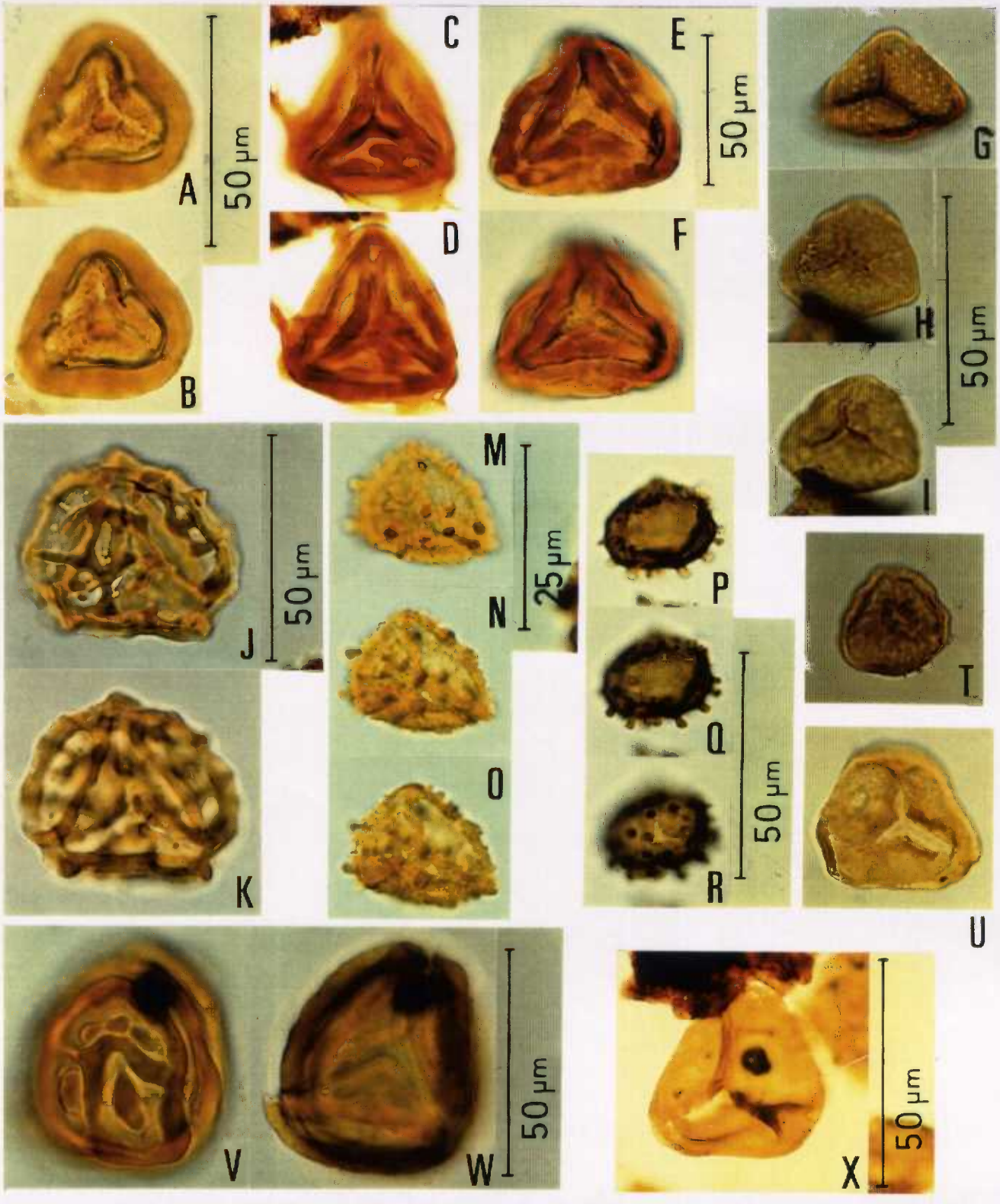
A
B
C
D
E
F
50 µm
G
H
I
50 µm
J
K
50 µm
M
N
O
25 µm
P
Q
R
50 µm
T
U
V
W
50 µm
X
50 µm

PLATE-5

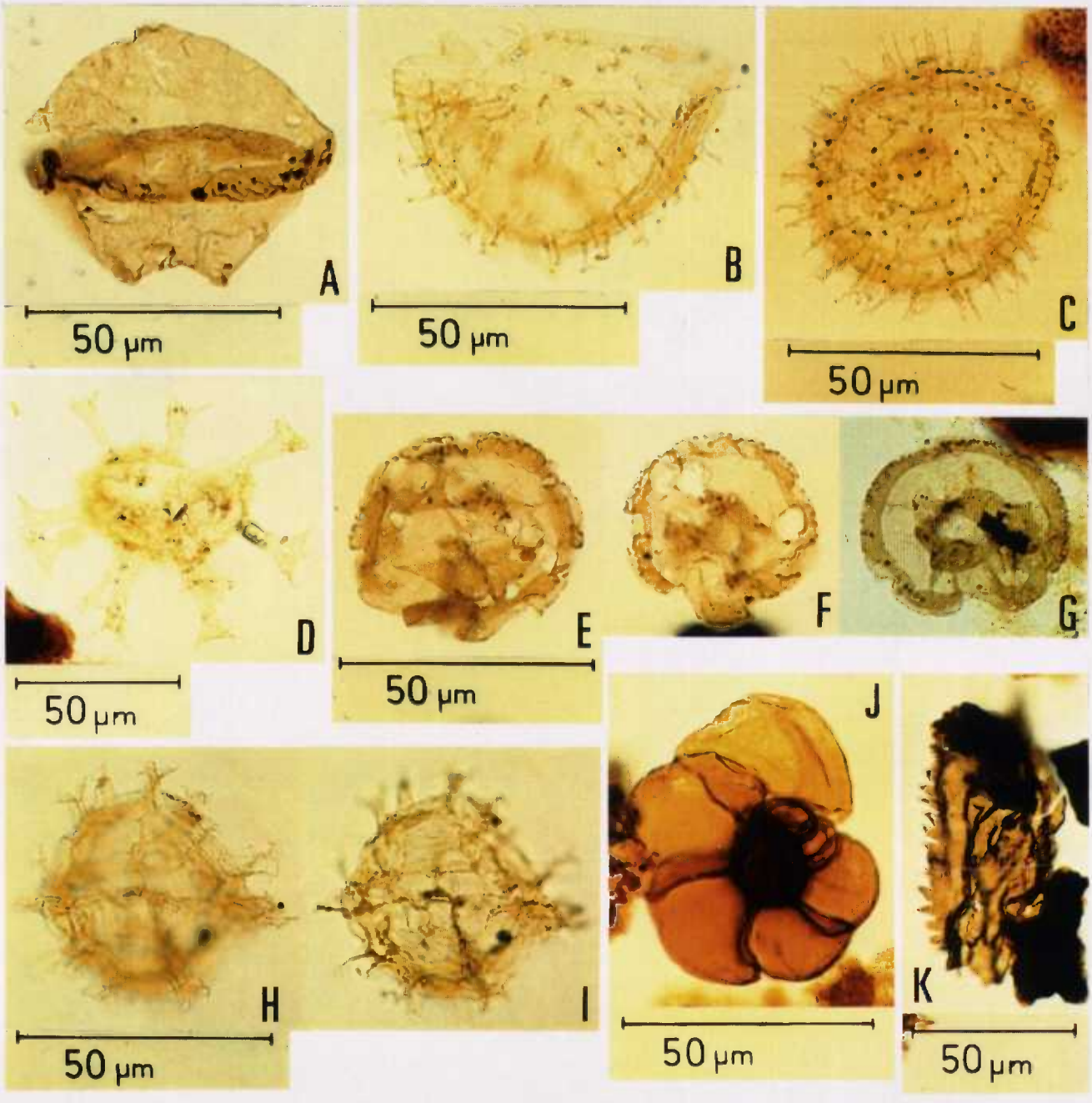

SAN FRANCISCO-1 PALYNOMORPH RANGE CHART

ANALYSIS BY: ALAN D. PARTRIDGE
DATE: 14 NOVEMBER 1993

Format: Relative Abundance By Highest Appearance

Key to Symbols

M = MODERN CONTAMINATION
D = CAVED CONTAMINATION
I = SINGLE SPECIMEN
R = RARE <1%
F = FREQUENT >1% TO <5%
C = COMMON >5% TO <20%
A = ABUNDANT >20%
? = Questionably Present
. = Not Present

SPECIES LOCATION INDEX

CHART
COLUMN SPECIES

19	ACTINOPELTE SP. A
35	ACTINOPELTE SP. B
62	ALNIPOLLENITES VERUS
51	BACULATISPORITES PAPUANUS
63	BETULACEOIPOLLENITES SP.
16	CALLIMOTHALUS SP. FB9
52	CLAVATOSPORIS SP. A
64	CUPRESSACITES SP.
45	CYATHIDITES SPP. (large)
37	CYATHIDITES SPP. (small)
46	CYCLOPHORUSISPORITES SP. A
21	DESMIDIOSPORA SP. FS4
30	DICELLAESPORITES SPP. 7.28
58	DISTAVERRUSPORITES SP. A
34	DYADOSPORONITES SP. FS2
53	ECHINOSPORIS SP.
33	ECHISPORONITES SP. FS5
1	EOCLADOPYXIS PENICULATA
47	FLORSCHUETZIA LEVIPOLI
57	FOVEOTRILETES LACUNOSUS
24	FRACTISPORONITES SPP. 7.68
26	FUSIFORMISPORITES SP. FS6
22	HYPOXYLONITES SP. FS7
27	INAPERTISPORITES SP. FS8
25	INAPERTISPORITES SPP. 7.1
31	INVOLUTISPORONITES SPP. 7.58
65	LACRIMAPOLLIS PILOSUS
38	LAEVIGATOSPORITES MAJOR
39	LAEVIGATOSPORITES OVATUS
8	LEJEUNECYSTA SP.
4	LINGULODINIUM MACHAEROPHORUM
40	LYGISTEPOLLENITES FLORINII
55	MATONISPORITES MULLERI
23	MEDIAVERRUSPORONITES SP. FS1
12	MICROTHALLITES SP. FB1
17	MICROTHALLITES SP. FB2
15	MICROTHYRIACITES SP. FB6
66	MOMIPITES SP.
61	MONOPORITES SP.
32	MULTICELLAESPORITES SP. FS3
10	OLIGOSPHAERIDIUM SP.
7	OPERCULODINIUM CENTROCARPUM
28	PARTITIOSPORONITES SPP. 7.57
9	PEDIASTRUM SP.
18	PHRAGMOTHYRITES SP. FB10
20	PHRAGMOTHYRITES SP. FB3
13	PHRAGMOTHYRITES SP. FB4
59	PINUSPOLLENITES SPP.
60	PODOCARPIDITES SPP.
56	POLYPODIACEOISPORITES PAPUANUS
41	POLYPODIACEOISPORITES SPP.
42	POLYPODIIDITES SP. (large verrucae)
43	POLYPODIIDITES SP. (small verrucae)
48	POLYPODIIDITES USMENSIS
44	POLYPODIISPORITES FOVEOIRREGULARIS
5	POLYSPHAERIDIUM ZOHARYI
2	PSEUDOSCHIZAEA SP.
6	SELENOPEMPHIX SP.
67	SEQUIOPOLLENITES SP.
14	SETAESPORONITES SP. FB7
11	SPINIFERITES SPP.
49	SPINOZONOCOLPITES BACULATUS
68	STEREISPORITES SP.
36	TETRAPLOA SPP. 7.62
29	TETRASEPTITES SPP. 7.56
54	TRICOLPORITES SPP.
50	ZONOCOSTITES RAMONAE
3	microforaminiferal inner tests

R9404139

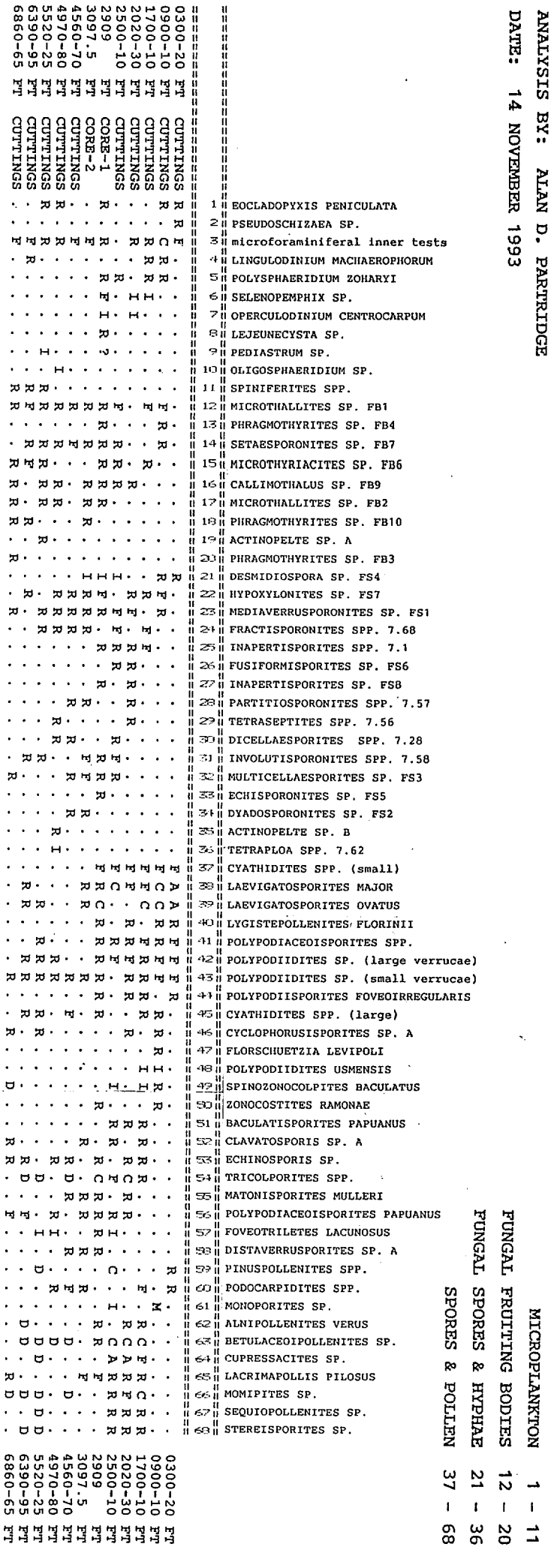

MICROPLANKTON 1 - 11
FUNGAL FRUITING BODIES 12 - 20
FUNGAL SPORES & HYPHAE 21 - 36
SPORES & POLLEN 37 - 68

PLATE-7

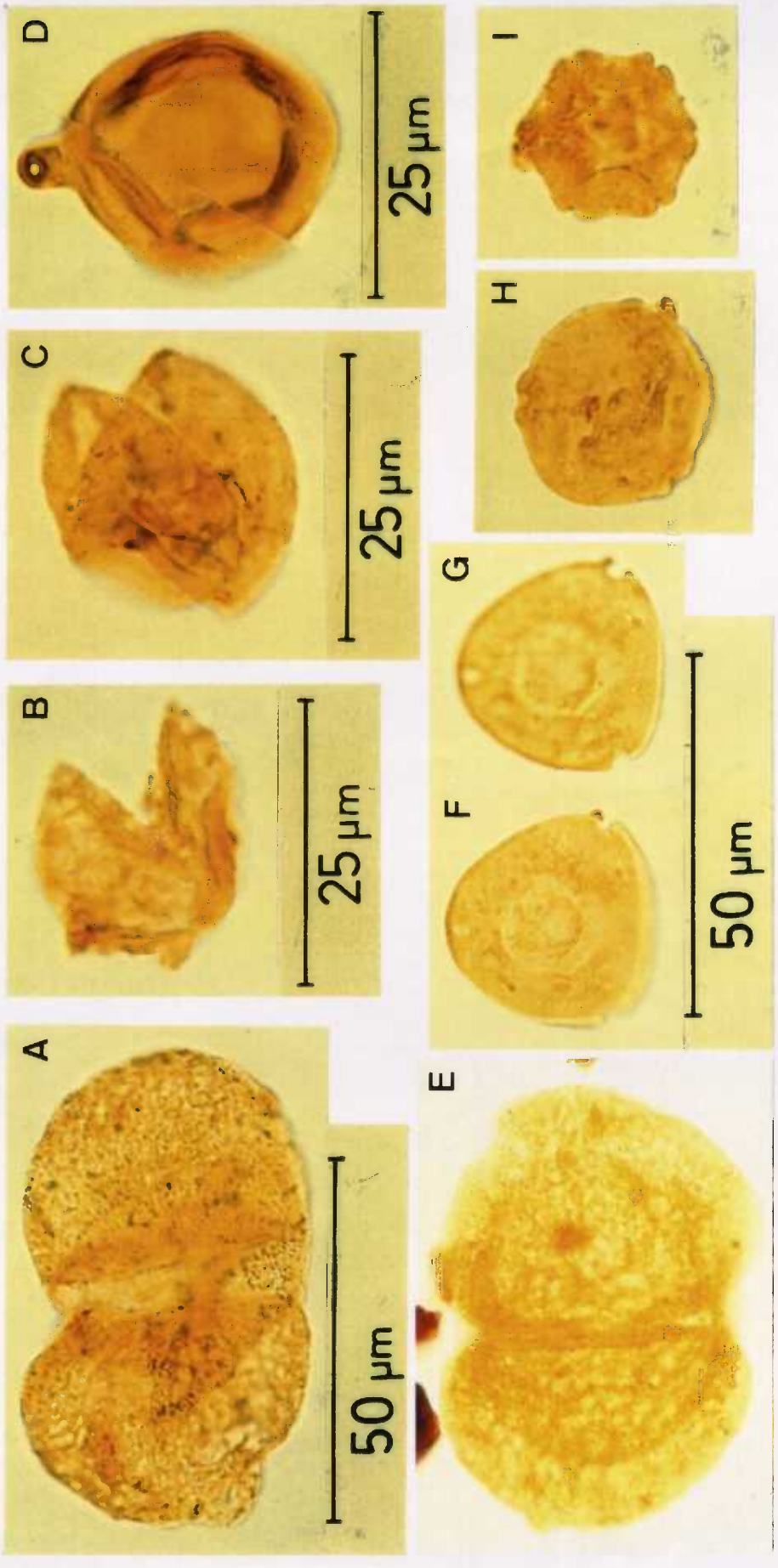

KATUMBO CREEK-1 PALYNOMORPH RANGE CHART

ANALYSIS BY: ALAN D. PARTRIDGE

DATE: 14 NOVEMBER 1993

Format: Relative Abundance By Highest Appearance

Key to Symbols

M = MODERN CONTAMINATION
D = CAVED CONTAMINATION
I = SINGLE SPECIMEN
R = RARE <1%
F = FREQUENT >1% TO <5%
C = COMMON >5% TO <20%
A = ABUNDANT >20%
? = Questionably Present
. = Not Present

SPECIES LOCATION INDEX

CHART COLUMN	SPECIES
9	ACTINOPELTE SP. A
23	ACTINOPELTE SP. B
51	ALNIPOLLENITES VERUS
36	BACULATISPORITES PAPUANUS
48	BETULACEOIPOLLENITES SP.
12	CALLIMOTHALUS SP. FB9
37	CLAVATOSPORIS SP. A
47	CUPRESSACITES SP.
40	CYATHIDITES SPP. (large)
33	CYATHIDITES SPP. (small)
41	CYCLOPHORUSISPORITES SP. A
24	DESMIDIOSPORA SP. FS4
16	DICELLAESPORITES SPP. 7.28
42	DISTAVERRUSPORITES SP. A
22	DYADOSPORONITES SP. FS2
38	ECHINOSPORIS SP.
17	ECHISPORONITES SP. FS5
7	EOCLADOPYXIS PENICULATA
43	FOVEOTRILETES LACUNOSUS
18	FRACTISPORONITES SPP. 7.68
25	FUSIFORMISPORITES SP. FS6
19	HYPOXYLONITES SP. FS7
26	INAPERTISPORITES SP. FS8
20	INAPERTISPORITES SPP. 7.1
27	INVOLUTISPORONITES SPP. 7.58
45	LAEVIGATOSPORITES MAJOR
34	LAEVIGATOSPORITES OVATUS
2	LEJEUNECYSTA SP.
3	LINGULODINIUM MACHAEROPHORUM
21	MEDIAVERRUSPORONITES SP. FS1
10	MICROTHALLITES SP. FB1
13	MICROTHYRIACITES SP. FB6
49	MONOPORITES SP.
28	MULTICELLAESPORITES SP. FS3
32	PARTITIOSPORONITES SPP. 7.57
14	PHRAGMOTHYRITES SP. FB10
15	PHRAGMOTHYRITES SP. FB4
50	PINUSPOLLENITES SPP.
44	POLYPODIACEOISPORITES PAPUANUS
35	POLYPODIIDITES SP. (large verrucae)
39	POLYPODIIDITES SP. (small verrucae)
46	POLYPODIIDITES USMENSIS
4	POLYSPHAERIDIUM ZOHARYI
29	PSILADISPORONITES SPP. 7.40
5	SELENOPEMPHIX SP.
11	SETAESPORONITES SP. FB7
6	SPINIFERITES SPP.
30	TETRAPLOA SPP. 7.62
31	TETRASEPTITES SPP. 7.56
1	microforaminiferal inner tests
8	scolecodont

		4700-20 FT CUTTINGS	5000 FT CUTTINGS	5390 FT CUTTINGS	5740 FT CUTTINGS	5910 FT CUTTINGS	6240 FT CUTTINGS	6340 FT CUTTINGS	6400 FT CUTTINGS
1	microforaminiferal inner tests	R	R	R	R	R	R	R	R
2	LEJEUNECYSTA SP.	.	.	.	.	.	R	R	R
3	LINGULODINIUM MACHAEROPHORUM	.	.	.	.	.	R	R	R
4	POLYSPHAERIDIUM ZOHARYI	.	.	.	.	.	R	R	R
5	SELENOPEMPHIX SP.	.	.	.	.	.	R	R	R
6	SPINIFERITES SPP.	.	.	.	.	.	R	R	R
7	EOCLADOPYXIS PENICULATA	.	.	.	.	.	R	R	R
8	scolecodont	.	.	.	.	.	I	R	R
9	ACTINOPELTE SP. A	.	.	.	.	.	.	R	R
10	MICROTHALLITES SP. FB1	.	.	.	.	.	F	R	R
11	SETAESPORONITES SP. FB7	R	R	R	R	R	R	R	R
12	CALLIMOTHALUS SP. FB9	.	.	.	.	.	R	R	R
13	MICROTHYRIACITES SP. FB6	.	.	.	.	.	R	R	R
14	PHRAGMOTHYRITES SP. FB10	.	.	.	.	.	R	R	R
15	PHRAGMOTHYRITES SP. FB4	.	.	.	.	.	R	R	R
16	DICELLAESPORITES SPP. 7.28	.	R	.	.	.	R	R	R
17	ECHINSPORONITES SP. FS5	.	.	.	.	.	R	R	R
18	FRACTISPORONITES SPP. 7.68	.	.	.	.	.	R	R	R
19	HYPOXYLONITES SP. FS7	.	.	.	.	.	R	R	R
20	INAPERTISPORITES SPP. 7.1	.	.	.	.	.	.	.	R
21	MEDIAVERRUSPORONITES SP. FS1	.	.	.	.	.	F	R	R
22	DYADOSPORONITES SP. FS2	.	.	R	.	.	.	R	.
23	ACTINOPELTE SP. B	.	.	.	R	R	.	.	.
24	DESMIDIOSPORA SP. FS4	.	.	.	.	I	R	.	.
25	FUSIFORMISPORITES SP. FS6	.	.	.	.	R	R	.	.
26	INAPERTISPORITES SP. FS8	.	.	.	.	R	R	.	.
27	INVOLUTISPORONITES SPP. 7.58	.	.	R	.	R	R	.	.
28	MULTICELLAESPORITES SP. FS3	.	.	.	.	R	R	.	.
29	PSILADISPORONITES SPP. 7.40	.	.	.	.	R	R	.	.
30	TETRAPLOA SPP. 7.62	.	.	.	.	R	R	.	.
31	TETRASEPTITES SPP. 7.56	.	.	R	.	R	R	.	.
32	PARTITIOSPORONITES SPP. 7.57	.	R	R	R	.	.	.	.
33	CYATHIDITES SPP. (small)	.	.	.	.	R	.	.	R
34	LAEVIGATOSPORITES OVATUS	.	R	R	.	R	R	R	R
35	POLYPODIIDITES SP. (large verrucae)	.	.	R	.	R	R	R	R
36	BACULATISPORITES PAPUANUS	.	.	.	.	R	R	R	R
37	CLAVATOSPORIS SP. A	.	R	F	.	C	.	F	.
38	ECHINOSPORIS SP.	R	.	F	.	R	.	R	.
39	POLYPODIIDITES SP. (small verrucae)	.	.	.	R	R	.	R	.
40	CYATHIDITES SPP. (large)	R	.	.	.	R	R	.	.
41	CYCLOPHORUSISPORITES SP. A	.	.	.	R	R	R	.	.
42	DISTAVERRUSPORITES SP. A	.	.	F	.	R	R	.	.
43	FOVEOTRILETES LACUNOSUS	.	.	R	.	F	.	.	.
44	POLYPODIACEOISPORITES PAPUANUS	.	.	F	.	R	.	.	.
45	LAEVIGATOSPORITES MAJOR	.	.	R	.	.	.	.	.
46	POLYPODIIDITES USMENSIS	.	D	.	.	.	.	.	.
47	CUPRESSACITES SP.	.	.	.	.	D	D	.	.
48	BETULACEOIPOLLENITES SP.	D	D	D	.	D	D	.	.
49	MONOPORITES SP.	.	.	.	.	D	D	.	.
50	PINUSPOLLENITES SPP.	.	.	D	.	.	.	.	.
51	ALNIPOLLENITES VERUS	.	.	.	.	.	.	.	.
		4700-20 FT CUTTINGS	5000 FT CUTTINGS	5390 FT CUTTINGS	5740 FT CUTTINGS	5910 FT CUTTINGS	6240 FT CUTTINGS	6340 FT CUTTINGS	6400 FT CUTTINGS

MICROPLANKTON 1 - 8

FUNGAL FRUITING BODIES 10 - 15

FUNGAL SPORES & HYPHAE 16 - 32

SPORES & POLLEN 33 - 51